TechnologyReview

EDITED AT THE MASSACHUSETTS INSTITUTE OF TECHNOLOGY MAY/JUNE 1994 $3.75

COLD FUSION HEATS UP

- Computer Simulations in the Courtroom
- Crops That Resist Chemicals
- Car Talk's Tom Magliozzi on Civilizing the Highways
- Reinventing Big Business: The Dark Side of Lean and Mean
- A Global New Deal for Jobs and Wages
- A View from the White House

By Edmund Storms

WARMING UP TO COLD FUSION

FIVE years have passed since two chemists working at the University of Utah announced a startling result: they had built a simple, room-temperature laboratory device that generated more energy in the form of heat than was fed into it as electricity. The researchers—Stanley Pons of the University of Utah and Martin Fleischmann of the University of Southampton in England—attributed this heat to a nuclear fusion reaction.

The claim ignited a scientific controversy not seen for a hundred years. Fusion had been known to occur only in stars and thermonuclear bombs; attempts to harness it for energy had been limited to systems that heat hydrogen fuel to extremely high temperatures using complex and expensive equipment.

Fusion requires the joining together of two atomic nuclei, both of which have a positive electric charge and so repel each other strongly. Scientists had thought that only by making the nuclei extremely energetic could they overcome this electrostatic repulsion, sometimes called the "coulombic barrier" (a coulomb is a unit of electrical charge). "Hot fusion" does this by ripping the electrons off atoms of the two heavy forms of hydrogen—deuterium and tritium—at very high temperature, thereby creating a cloud of ions, or plasma. Huge magnets generate fields that hold the plasma together long enough for some of the nuclei to crash into each other and fuse. This fusion reaction creates tritium and helium nuclei, as well as a shower of neutrons and gamma radiation.

But despite decades of work and great expense, hot fusion has yet to produce more energy than needed to heat the fuel and power the magnets. So the notion that a tabletop apparatus at room temperature could produce significant amounts of fusion energy raised hopes among many people for a more easily realizable energy source.

Pons and Fleischmann's experiment—the basic model for much of what has been done since—is based on electrolysis. An electrode pair consisting of a strip of palladium surrounded by a coil of platinum wire is immersed in a container of "heavy water"—that is, water in which deuterium takes the place of ordinary hydrogen. (Deuterium is a commonly occurring form of hydrogen that has one neutron in its nucleus in addition to the one proton that all forms of hydrogen have. Deuterium atoms undergo fusion reactions; ordinary hydrogen atoms do not.) A salt, typically lithium deuterhydroxide, is dissolved in the heavy water to make it more conductive. When a voltage is applied to the electrodes, an electrical current flows through the liquid and causes the heavy water to decompose into its constituent atoms: deuterium migrates to and dissolves in the palladium electrode and oxygen is released as a gas at the platinum electrode. As deuterium builds up in the palladium, it supposedly undergoes the fusion reaction. The palladium's atomic lattice captures the energy released by the reaction and the metal heats up.

Heat is not the only evidence for cold fusion. Many experiments have also produced tritium (the radioactive isotope of hydrogen, with two neutrons along with the lone proton that all hydrogen has) and helium; both tritium and helium are known to be produced only by nuclear reactions. Researchers have also detected neutrons with the 2.54-megaelectron-volt (MeV) energy level characteristic of the neutrons produced by the fusion of two deuterium nuclei, as well as neutrons with other unexpected energies.

In the wake of Pons and Fleischmann's report, dozens of laboratories around the world eagerly tried to duplicate the results. Most failed, and scientists and the general public grew skeptical. But the significance of these negative results, especially by certain well-known institutions such as Caltech and MIT in the United States and Harwell in Britain, has been exaggerated.

In some cases, the conditions those studies used are now known to prevent the cold fusion effect. MIT researchers, for example, used an experimental apparatus that was open to the humid Massachusetts air and therefore subject to contamination by ordinary water, which has since been found to inhibit the cold fusion effect. Also, early experimenters used commercially available palladium without regard for its condition; it is now known that most off-the-shelf palladium samples do not meet the special conditions required for cold fusion. Some labs also used inappropriate equipment to look for heat. Experimenters at both Caltech and Harwell, for example, used heat-measuring techniques that have since been shown to be insensitive to small amounts of excess energy. Moreover, on the few occasions that the MIT and Harwell labs did observe a small amount of excess heat, the researchers attributed the readings to experimental error and ignored them.

If the validity of the effect rested only on results reported during the first year after the initial claims by Pons and Fleischmann, this strange diversion from routine science would have joined "n-rays," polywater, and other excesses of the imagination. But enough reputable researchers have now published findings, produced from a broad enough range of experimental approaches, that it has become difficult to doubt that something is going on outside the explanations offered by conventional physics.

What is happening might be fusion; it might not

EDMUND STORMS, a chemist living in Santa Fe, N.M., recently retired as a researcher at the Los Alamos National Laboratory. He has published extensively on materials used in high-temperature nuclear reactors, and has been conducting research on cold fusion since 1989.

Some cold-fusion experiments have reportedly produced power densities higher than those of uranium-fueled fission reactors.

be. But to dismiss the claims as the result of experimental error or fraud is no longer appropriate. Regardless of admitted conflict with accepted theory, these results strongly support the conclusion that a new class of phenomena, which I call chemically assisted nuclear reactions, has been discovered. Given the enormous scientific and economic importance of this work if it turns out to be valid, it is prudent to examine the data with an open mind.

Accumulating Evidence: Tritium

Many cold fusion experiments have produced tritium (the radioactive isotope of hydrogen) and helium, both of which can be produced only by nuclear reactions. A group at Texas A&M University, for example, has produced in electrolytic cells quantities of tritium about one thousand times those found in normal heavy water. Heat is sometimes detected during the production of tritium and neutrons; sometimes it is not. The Bhabha Atomic Research Centre (BARC) in Bombay, India, has produced tritium at several thousand times background levels, using a variety of electrode materials, including alloys of palladium and titanium.

At the Los Alamos National Laboratory, Thomas Claytor and Dale Tuggle have produced tritium in various ways. In one method, they applied a voltage to a deuterium-filled cell containing alternating electrodes of palladium and silicon. The electric discharge between the electrodes has repeatedly generated 20 billion atoms of tritium per hour. More recently, the Los Alamos group has obtained even higher production rates by sending pulses of current through the palladium rather than applying a voltage through the gas. Apparently, one key may be to induce a sudden change in temperature. The amount of tritium in the materials was measured before each study was begun, each system was completely sealed from the environment, and tritium production was monitored continuously during the studies.

Some skeptics contend that the tritium found in these experiments either is in the palladium to begin with or enters the cell from the environment. Closer examination of the results shows that this is improbable. In the Texas A&M work, for example, turbulence from vibration or the addition of heavy water caused tritium production to stop temporarily—an effect that is inconsistent with contamination.

My own studies of the behavior of dissolved tritium in palladium cast further doubt on the likelihood that tritium is present in the metal to begin with. I have found that during normal electrolysis, almost all the dissolved tritium (more than 99 percent) leaves the metal as

a gas; very little tritium initially present in the palladium appears in the electrolyte solution, which is where the "anomalous" tritium is being found in the cold fusion experiments. Furthermore, the tritium begins to leave the platinum electrode immediately after electrolysis begins, and one-half is gone between 12 and 24 hours later. Anomalous tritium, on the other hand, takes many days to appear and the appearance is sudden.

What about environmental contamination? Tritium is rare but not absent in the normal environment. Studies at Los Alamos show that if tritium does enter a cell from the environment, it begins to accumulate immediately and at a roughly constant rate. But anomalous production of tritium starts only after many hours of electrolysis and frequently occurs in bursts. In some cases, the amounts produced are so large that if the tritium had originated in the environment, the required concentrations would pose a health hazard and be easily detected by laboratory monitoring systems. High tritium concentrations do occur occasionally in some areas of laboratories. But such "hot spots" typically occur in places—unlike the sealed cell of a typical cold fusion experiment—where environmental tritium can easily concentrate.

A third possibility, raised most prominently by journalist Gary Taubes, is that proponents of cold fusion have deliberately added tritium to the cells, actions that would of course constitute scientific fraud. But numerous positive results reported at many laboratories worldwide make this assertion an unlikely explanation of all results.

While the presence of tritium provides evidence that a nuclear reaction is occurring, it also raises questions. According to conventional understanding, the fusion of two deuterium nuclei should produce significant amounts of gamma radiation as well as neutrons and tritium. But in cold fusion work, gamma radiation, if detected at all, occurs at very low levels. And tritium and neutrons are found in the wrong amounts and with the wrong energies.

When tritium is produced in conventional fusion, for example, it normally has enough energy to fuse with any deuterium nuclei that might be present. This reaction produces neutrons with a characteristic energy of 14 MeV, as well as high-energy helium-3 nuclei. (In helium-3, two protons in the nucleus are accompanied by one neutron instead of the two neutrons found in the more common helium-4.) The absence of 14-MeV neutrons and helium-3 when tritium is produced by the cold fusion effect shows that the tritium is born without enough energy to fuse with deuterium. Where does the energy released from the nuclear reaction go, then, if not into neutrons or tritium? Energy apparently transfers directly from the nuclear reaction to the atomic lattice of the metal where it is manifest as heat. This effect, which is at odds with current theory, has never before been observed.

Tritium detection also provides evidence that

Experiments that use crack-free palladium and follow the proper procedures now routinely produce heat, nuclear products, or both.

nuclear reactions other than fusion can occur in the environment of a cold fusion cell. Researchers at Bhaba, for example, recently reported producing tritium in a cell containing not heavy water but rather normal water, in which was dissolved either lithium carbonate or potassium carbonate. The ordinary hydrogen nuclei (that is, naked protons) that make up normal water do not fuse with one another, even under "hot fusion" conditions. The tritium in these experiments is therefore most likely to originate in nuclear reactions between protons and the dissolved lithium or potassium nuclei.

Accumulating Evidence: Excess Heat

A variety of experimental designs continue to produce heat output exceeding the electrical input. Several studies have produced excess energy thousands of times larger than any known chemical (that is, non-nuclear) reaction could produce. In some experiments, the power "density," in watts per cubic centimeter of palladium, exceeds those found in uranium-fueled nuclear fission reactors.

Excess heat in the experiments by Pons and Fleischmann, who have continued their work in France with support from the Japanese company Technova, has reached levels that cause water in the electrolytic cells to boil. These scientists claim that when they applied 37.5 watts to a cell as electric power, it produced 144 watts of excess power as heat—enough to raise the temperature of the palladium electrode to several hundred degrees. And the cells have produced excess energy at a comparable level for many hours after the applied power is turned off. No oxygen is allowed into the cells during this time, ruling out the possibility that the energy results from the reaction of deuterium with oxygen—that is, ordinary chemical combustion.

Dozens of examples reporting such excess energy have now been published. Francesco Celani at Italy's Frascati National Laboratory has reported producing heat levels that exceed electrical energy input by as much as 7.5 percent for many weeks, with bursts to 25 percent. Akito Takahashi of Osaka University measured up to 130 watts of excess power (an average of 70 percent) using special palladium produced by Tanaka Metals. The excess heat increased over several months, and the cells also produced a small amount of tritium and neutrons. In my own attempts to replicate the Osaka experiments, using the same palladium source, I produced 7.5 watts—20 percent more power than I put into the cell.

An inability to replicate results continues to frustrate many cold fusion researchers (and bolster skeptics' disbelief that the phenomenon is real). Bor Liaw and colleagues at the University of Hawaii, for example, produced up to 1,500 percent excess energy using a molten salt electrolyte. Because the lithium-potassium-chloride electrolyte is at 400 degrees C, this energy could be more useful than that generated in a heavy-water cell. However, Liaw has been unable to duplicate this one tantalizing experiment.

Critics of cold fusion work have questioned the validity of such measurements. Some maintain that because the water in the cells is not stirred, temperature gradients could account for the unusual readings. In fact, active stirring is not necessary: as long as enough current is applied to the cell, the gas that bubbles out of the water does the mixing. Nevertheless, recent studies have corrected for this possible source of error by actively stirring the cells or by using a type of heat-measuring system—that is, a calorimeter—that temperature gradients do not affect.

Another charge concerns a lack of control studies. Such studies would, for example, replace the cell's heavy water with normal water or replace the palladium with platinum. Because it is extremely unlikely that the hydrogen in ordinary water would undergo fusion, any anomalous heat from a normal-water cell would suggest that the effect has some other, less spectacular source—such as experimental error or a chemical (that is, non-nuclear) process.

But many such control studies have now been carried out, and no one so far has claimed excess heat in a palladium/normal-water or a platinum/heavy-water cell. Skeptics have complained, however, that these control studies run for too brief a time, since the active cold fusion cells run for months. To rule out the possibility that the anomalous results arise from random error, these critics say, the controls should run for the same duration. This presents a problem: to address such concerns, researchers would have to devote a significant fraction of time and funding to waiting for possible errors to show up rather than to understanding the nature of the effect. As a compromise, experimenters run control cells for a shorter time and take great pains to make the calorimeters stable.

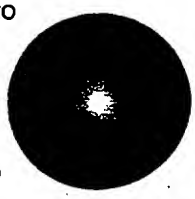

The demand for long-term control cells reflects results from the early cold fusion experiments, which produced heat or nuclear products in occasional bursts. More recent work has achieved steady output. Once a cell turns on, it typically stays on for many days.

Skeptics who accept the data on excess heat nevertheless assert that it originates not from any nuclear process but from some hitherto unknown chemical reaction. But no evidence from any study has been reported to support various speculated chemical sources. If a novel chemical reaction is the source of this power, significant quantities of some chemical product must be present in the cell, yet no such products have been observed. Moreover, many distinct and novel chemical reactions would be required to explain the excess-heat observations in a the variety of chemical environments that have now been studied.

One reason that cold fusion has been so difficult to accept is that the experiments are so hard to replicate. Many experienced researchers, attempting to follow exactly the methods described in published studies, have, until recently, produced little or no evidence for a nuclear reaction. But scientists are starting to solve the puzzle of why some cells work and some do not.

An important requirement for producing heat, for example, now appears to be palladium largely free of microscopic cracks. Deuterium apparently escapes from any cracks too fast for a critical concentration to build up. Michael McKubre and co-workers at SRI International, as well as researchers at several other laboratories, have shown that the larger the ratio of deuterium to palladium in the electrode, the greater the heat.

The presence of surface impurities is also important to produce the required deuterium content. McKubre's first experiments, which were successful, used pyrex containers for the cell. When he changed to Teflon, the cell did not work. Further investigation revealed the apparent reason: aluminum and silicon atoms from the pyrex migrated to the palladium surface and allowed the deuterium to build up to higher concentrations.

McKubre's studies also identified another criterion for producing excess heat. His work, which have now been supported by at least four other laboratories, indicates that the electrical current entering the cell must exceed a threshold of at least 150 milliamperes per square centimeter of palladium. For experiments using large pieces of palladium, this can mean a very large overall current. Many experimenters have failed to produce anomalous effects because they have not applied enough current to their cells.

Several experiments have shown that the nature and timing of the electrical input to a cell significantly affects the chances of its success. Heat is more likely to be produced when the electrical current is repeatedly "ramped" from a high to lower level or briefly pulsed to high values. Applying certain microwave frequencies is also beneficial. Moreover, for reasons still unknown, electrolysis must continue for several days before the cell "turns on" and begins to generate excess heat. Many of the early efforts to reproduce the effect failed at least partly because the researchers did not stick with them long enough. Experiments that use crack-free palladium and follow the proper procedures now routinely result in excess heat, nuclear products, or both.

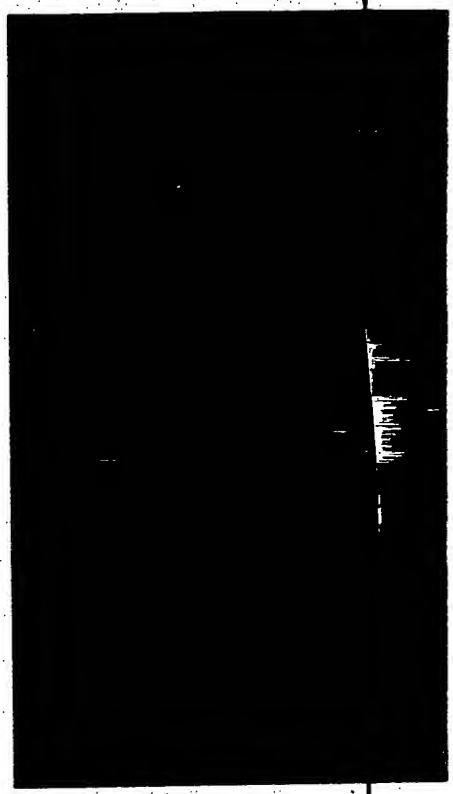

Heat might be arising from nuclear reactions other than fusion, as well. At least 10 different laboratories have measured significant excess energy coming from light-water cells using nickel, rather than paladium, as the cathode, and in which is dissolved a carbonate of one of the so-called alkali metals (lithium, sodium, potassium, or rubidium). Experiments by Robert Bush and Robert Eagleton at California Polytechnical University and by Reiko Notoya at Hokkaido University in Japan suggest that this heat arises from a transmutation reaction: a proton enters the nucleus of the dissolved metal to give the next higher element in the periodic table. Potassium, for example, is proposed to take up a proton to produce calcium, and rubidium is similarly transformed into strontium. Researchers have detected calcium and strontium at levels that suggest this transmutation is occurring.

Accumulating Evidence: Helium

One of the products of the fusion of two deuterium atoms is helium, which with its two protons is the next element up on the periodic table. Many experiments have produced measurable helium. Hawaii's Liaw, for example, found significant helium in the palladium in his heat-producing experiments with a molten-salt elec-

trolyte. Workers at Texas A&M also detected normal helium-4 in the palladium after tritium was produced. However, no effort was made to measure heat during this study. Q.F. Zhang and colleagues at the University of Science and Technology in Chengdu, China, have detected helium-4 in titanium rods that produced excess heat in an electrolytic cell. They saw no helium when excess heat was absent, suggesting a link between the two.

the atmosphere, Miles and Bush repeated the experiment using steel flasks and obtained similar results while also showing that the diffusion rate of helium through glass was too small to account for the observed amounts. Apparently, most of the generated helium resides in the gas, rather than in the electrodes where researchers have mainly been looking.

When helium forms during fusion, two particles are condensed into one. The laws of physics require that in

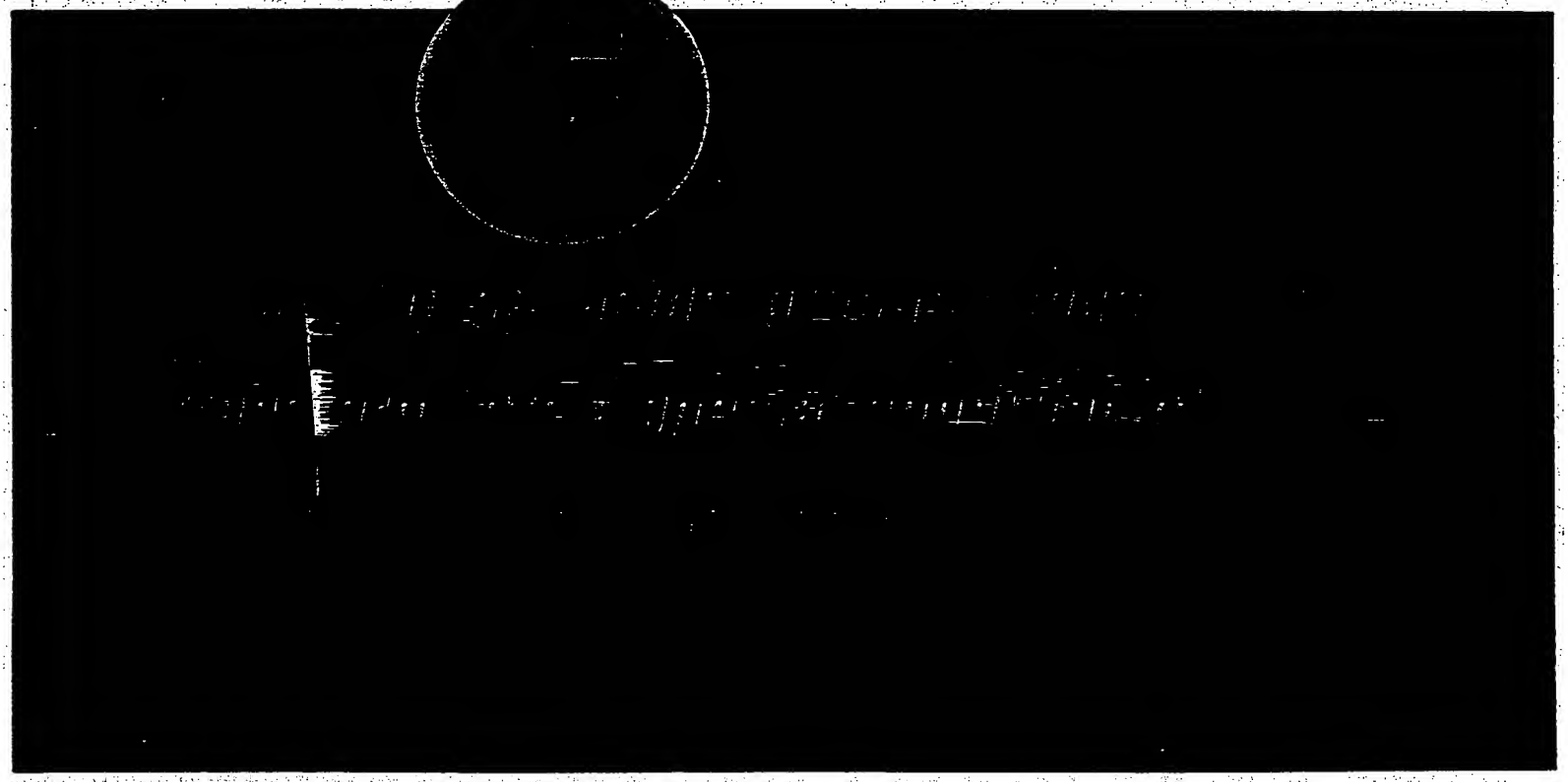

Skeptics have complained that cold-fusion experiments have produced too little helium; if the heat measured truly has nuclear origin, they contend, far more helium should be detected. The helium found in the palladium after the Hawaii experiments, for example, while significant, could account for only 10 percent of the large amounts of excess energy that this work generated.

Recent work has whittled away at this objection. Melvin Miles and Benjamin Bush of the Naval Air Warfare Center at China Lake, Calif., for example, have measured helium in the gas emitted by electrolytic cells and have measured helium levels 90 percent of those needed to account for the measured heat. Since these scientists found no helium when using normal water in the cell instead of deuterium-bearing heavy water, the heat appears to be nuclear in origin. When critics suggested that the helium entered the glass collection flasks from

any interaction between particles, momentum (the product of mass and velocity) must be conserved. In hot fusion, a 24-MeV gamma ray is emitted to satisfy this conservation requirement. No gamma rays with this energy are observed in cold fusion.

The most probable reason, I believe, is that the material has transformed into a special condition that enables the atomic lattice to absorb most of the nuclear energy being generated. If we assume that the material in this condition has a similar ability to absorb nuclear radiation applied from outside, a straightforward experiment could test this hypothesis. One could irradiate the material with gamma radiation, which easily penetrates ordinary palladium. When this special condition exists, the material should block some of the gamma rays; the portion of gamma radiation absorbed should correspond to the amount of the material that has switched to the fusion-enabling condition.

Evidence for this special condition does exist. Experiments by Yan Kucherov and co-workers at Russia's Scientific Industrial Association (LUCH) in Podolsk produced an electrical discharge in low-pressure deuterium, using palladium as one of the electrodes. Heat was accompanied by an unusual form of gamma radiation. Gamma rays ordinarily fan out in all directions from their source. In this case, the radiation emerged from the palladium in tightly focused beams. Such beams suggest the existence within the metal of reflection planes with much closer spacing than normally exist in the atomic lattice. Such planes might be owing to an unusual, tightly bound electron structure.

Much of the evidence for cold fusion has come from techniques alien to nuclear physics, such as electrolysis and the precise measurement of heat. But in the past several years, researchers have been producing cold fusion results using the tools of nuclear physics, such as high-energy ion beams.

Toshiyuki Iida and co-workers at Osaka University, for example, bombarded palladium and titanium samples with energetic deuterium nuclei. During this bombardment, the cell emitted a variety of ions with energies consistent with conventional fusion between two deuterium nuclei. This was in itself unremarkable, and could be explained as "hot" fusion, as high-energy deuterons in the beam slammed into those that had already taken up residence in the metal. But defying expectations, emission of energetic ions continued from the palladium target for many hours after the implantation beam was turned off. The Osaka group also detected high-energy helium nuclei. Such observations suggest that fusion—cold fusion—continues in the material even without the presence of a high-energy beam.

A trail of evidence for cold fusion comes from work by Jirohta Kasagi and co-workers at Tohoku University in Japan. Kasagi bombarded titanium deuteride with 150-kiloelectron-volt deuterons. When the deuterium content of the titanium deuteride was high enough, the experiment produced protons with energies up to 17.5 MeV. These energetic protons are thought to result from the fusion of deuterium and helium-3. It is the helium-3 that provides evidence for cold fusion.

In theory, helium-3 could arise in two ways. One is from the "hot" fusion of the energetic deuterium nuclei with the deuterium contained in the metal. But the helium-3 is found in isolated pockets within the titanium, which is inconsistent with this explanation. If the helium were formed in hot fusion, it is unlikely to diffuse through the material, as is required for the build-up in pockets. More likely is that the helium-3 is a product of the radioactive decay of tritium, which was produced within the metal in a cold fusion process. The tritium thus formed could, unlike helium, easily migrate

None of the proposed explanations for cold fusion accounts for the full range of experimental observations.

through the material and accumulate in pockets, where it would decay into helium-3. (Hydrogen is well known to accumulate in regions of high stress within a metal.)

Attempting an Explanation

Many aspects of the cold fusion effect are now reproducible if known procedures are used. Palladium, when reacted with enough deuterium, apparently converts to a special condition of matter in which various nuclear reactions—including deuterium-deuterium fusion—can occur despite the repulsive force of the two positively charged nuclei. These reactions can be made to proceed rapidly enough to produce measurable heat.

But any explanation for the cold-fusion phenomenon must answer some fundamental questions. What is the mechanism that allows positively charged atomic nuclei to overcome the coulombic barrier and join together? How is the significant energy unleashed by a nuclear reaction transferred directly to a material, instead of departing the scene in the form of energetic particles and radiation? Finally, why does cold fusion occur when a material is in a special condition of matter, akin to the state of superconductivity that some materials enter at low temperatures? What is this special condition that occurs in palladium and some other materials when they are infused with high concentrations of deuterium?

Scientists have published several dozen models, ranging from highly analytical approaches to pictorial representations, to explain these events. Most theories address only the problem of overcoming the coulombic barrier—how it is possible for nuclei to overcome their natural repulsion for each other without an infusion of massive amounts of energy from the outside. A sampling follows:

oNEUTRON TRANSFER. According to this theory, the nuclear reactions that occur are not fusion but rather involve the transfer of a neutron from one nucleus to another. Neutrons have no charge and can therefore enter a nucleus and initiate a reaction without having to acquire enough energy to overcome a barrier. While this approach removes the coulombic barrier problem, it cannot explain all the nuclear reactions that appear to have taken place in various experiments. Furthermore, it raises the question of why so few neutrons are seen leaving the material; if even a small fraction of the neutrons leaving one nucleus are not captured by another nucleus, a great many neutrons should emanate from the material.

oSCREENING OF THE NUCLEAR CHARGE BY ELECTRONS. The high concentration of negatively charged electrons in a metal might partially offset the positive nuclear charge. However, electrons in materials ordinarily do not have enough energy to completely mask the nuclear charge. Therefore, unless the electrons can achieve much higher energy states than are presently known, this is unlikely to be the only process.

oRESONANCE. Some nuclear processes are known to occur when the reactants have an energy level that matches a characteristic value, known as a resonance. Such resonance levels may be far below the energy ordinarily required to initiate the reaction. Among a large number of deuterium nuclei at room temperature, then, a few might possess such a resonant energy, permitting them to undergo reactions that would seem to be off-limits. While appealing, this theory falters on lack of evidence; physicists have never detected such a low-energy resonance for deuterium-deuterium fusion. Also, if such a resonance does exist, it must operate only in the special environment created by cold fusion cells. Otherwise, fusion would occur all the time.

oHIDDEN HIGH VOLTAGES. According to this theory, cracks in the material generate a large voltage that accelerates deuterium ions briefly to energies that can produce normal "hot" fusion. The problem with this explanation is that the radiation detected from cold fusion is different from that known to be generated in hot fusion. Also, while this process might partly account for fusion, it does not explain the other nuclear reactions.

oFUSION INVOLVING MORE THAN TWO DEUTERONS. This proposal is consistent with the observed need for a high deuterium concentration in the metal, and with the observed energy of some emitted nuclear products. However, it cannot explain the other nuclear reactions nor all of the observed energies. Also, this theory says nothing about how such multinucleus fusion reactions might be initiated; in particular, the puzzle of how the coulombic barrier is overcome remains.

oUNUSUAL TUNNELING PROCESSES. Conventional nuclear theory recognizes processes that allow a small fraction of charged particles to "tunnel" through the coulombic barrier. Tunneling is a logical consequence of the quantum-mechanical principle that it is impossible to know a particle's location and momentum simultaneously. However, according to our understanding of this phenomenon, while low-energy nuclei may tunnel through the barrier at a rate to account for the observed neutrons, the rate would be too slow to account for tritium or heat.

oA NOVEL CHEMICAL EFFECT. Randell Mills, of HydroCatalysis Power in Lancaster, Pa., has proposed that excess heat results neither from nuclear fusion nor from a conventional chemical reaction but rather when the electrons in hydrogen drop to a lower energy state than has been previously thought as it forms a two-hydrogen "dihydrino" molecule. This theory offers a possi-

ble explanation for some of the excess heat that several labs have detected in nickel/light-water cells. But the explanation cannot account for any of the nuclear products (neutrons, tritium, and helium) that often accompany heat in heavy-water cells. Moreover, studies using sealed calorimeters have failed to observe the expected pressure increase that would result from the buildup of the hypothesized dihydrino gas.

A NEW MODEL OF NUCLEAR STRUCTURE. Maybe our current understanding of the nucleus is wrong, or at least incomplete. An explanation of cold fusion might then invoke new nuclear particles or new types of nuclear interactions.

Theoreticians are nowhere near a consensus on which of these explanations are most likely to contribute to our ultimate understanding of the phenomenon. None of the proposed explanations accounts for the full range of experimental observations. Many of the theories do not offer predictions that can be quantitatively checked.

Nevertheless, a workable theory is crucial if we ever hope to apply cold fusion. It will be important to develop an understanding of the special condition of matter in which these nuclear reactions occur. For example, what is the crystal structure of the material when it is in this phase? What other characteristics will it exhibit? How can it be created and then modified to trigger a variety of nuclear reactions? Such questions will need to be answered before the phenomenon can be made to occur reproducibly and at high levels—an essential requirement if the effect is to be used to produce energy on an industrial scale.

Is Science Dropping the Ball?

Early investigations of all new phenomena tend to be incomplete, prone to error, and difficult to reproduce. Further scientific investigations require money; the more complex the phenomenon, the more money is required. But dollars tend to flow toward research with a clear chance of success. Thus many potentially important ideas never receive enough funding to enable scientists to understand them.

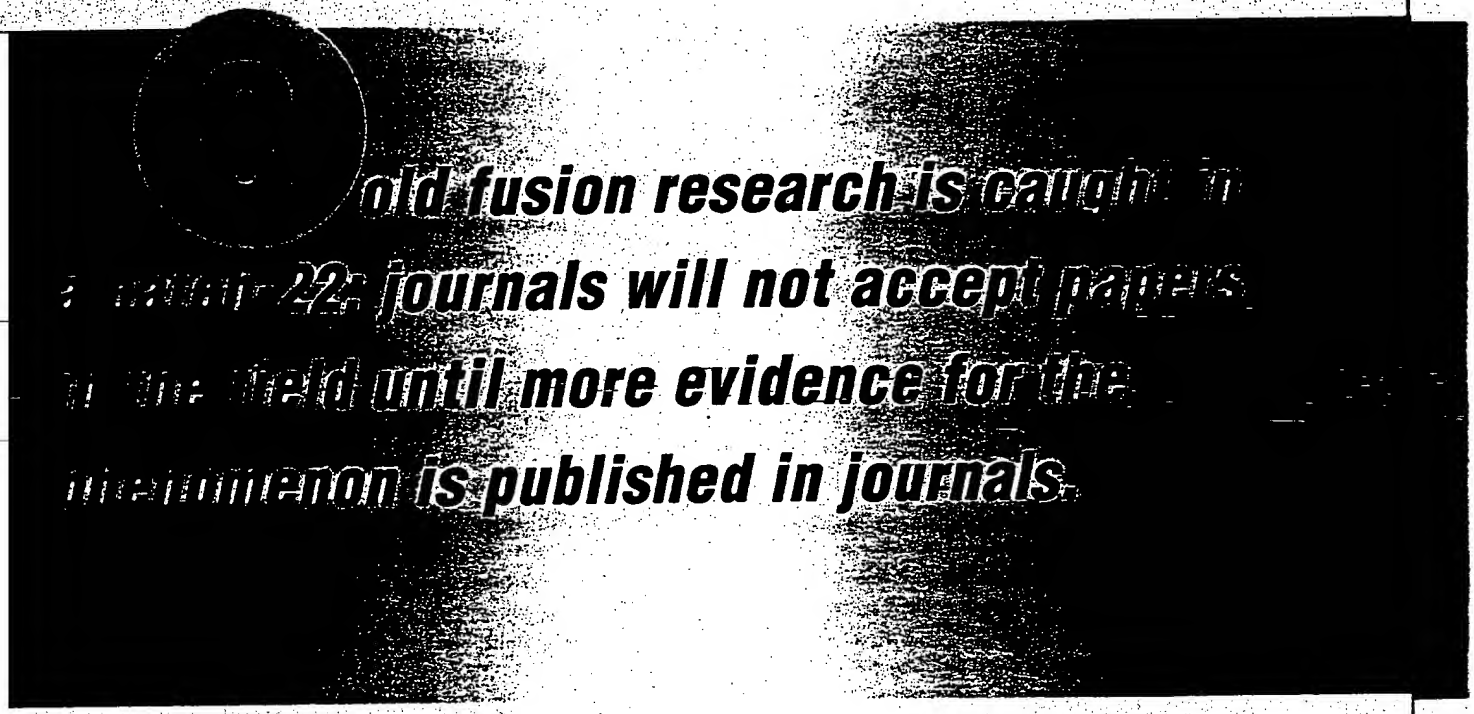

To a large extent, this is the case with cold fusion. Skeptics maintain that the effect is not real and that funds should therefore not be wasted on studying it. Rather than invest a little money on the possibility that they might be wrong, skeptics actively try to turn off support. The U.S. Department of Energy is not funding research on cold fusion, nor, for the most part, are other federal agencies. The patent office has stopped issuing patents related to this field. Fortunately, a few imaginative and courageous organizations are backing U.S. cold fusion work—most conspicuously the Electric Power Research Institute and, more recently, ENECO, a company based in Salt Lake City that has begun to fund research at a number of labs. ENECO has also invested heavily in buying up rights to the cold fusion patents that do exist.

The advance of scientific knowledge rests on the

idea that before work is judged valid it must be evaluated by, and reproduced by, other scientists. While these procedures have kept science from making too many mistakes, they can also stifle new ideas. It is now virtually impossible to publish positive cold fusion results in certain journals because the editors or their chosen peer reviewers are convinced that the effect is bogus. This creates a catch-22: the journals will not accept papers until more papers published in such journals show evidence for the effect.

The cold fusion effect is one of the most intriguing scientific puzzles of this century. Its ultimate practicality is still open to question, but practical worth does not always follow immediately upon discovery of a scientific phenomenon. Superconductivity, for example, was first observed in 1911 and languished as an unexplained laboratory curiosity for most of this century; today we have magnetic resonance imaging systems that rely on superconducting magnets. Einstein predicted the basic principle of a laser before 1920; decades later, we have supermarket checkout scanners, compact discs, and fiber-optic communications.

The comparison of cold fusion with these technologies is not exact. The theory of lasers was well accepted for decades before anyone figured out how to build one. Superconducting effects were consistently observed in the lab for decades before physicists were able to explain it. So far, cold fusion falls short on both fronts: experimental evidence is difficult to replicate and a theoretical underpinning is absent. It is up to scientists of all disciplines to perform the experiments and devise the theories that will transform cold fusion from laboratory scale phenomenon into something of lasting value.■

Some Lessons from 3 Years of Electrochemical Calorimetry

Michael E. MELICH
Physics Department Naval Postgraduate School
Monterey, California 93943-5000 USA

Wilford N. HANSEN
Physics Department Utah State University
Logan, Utah 84322-4415 USA

Abstract

An analysis of the time series data from the 16 Harwell FPH electrochemical cells is being conducted. Using generally accepted calorimetric principles and detailed numerical analysis, the behavior of "cold fusion" output data is used to estimate the instrumental sensitivity and the time varying accuracy of the results of the experiments. In Harwell's D_2O Cell 3 there are more than ten time intervals where an unexplained power source or energy storage mechanism may be operating. A comparison to a previous analysis of Pons and Fleischmann data is made.

Introduction

With the cooperation of Harwell and its research team, Williams et al[2], we have obtained copies of the digital data, laboratory notebooks, and other records of the 1989 Harwell electrochemical calorimetry experiments on "cold fusion". With this information we have been able to explore the characteristics of their experimental design and their data thereby developing insight into the quality of the experimental results. These results are briefly compared to results of Hansen's [1] similar analysis of Pons and Fleischmann data.

Conclusions

- Characterizing the Instruments. Harwell's extensive variations in the timing and magnitude of the calibration heater power and the electrochemical current/voltage pose a robust test of models of the electrochemical calorimetry instrument.
- Experimental Protocol and Interpretability. The regularity of the experimental protocol used by Pons and Fleischmann as reported at ICCF2 by Hansen[1] produces significantly less ambiguity in interpretation of experimental results than those used by Harwell.
- Extractable Information. Regression techniques for estimating parameters in mathematical models can be applied to the Harwell data to extract more information than presented by Williams et al [2].
- Reliability of Data Sets. Not all operating regimes captured in the Harwell data can be described by the available models. However, performance over extensive time intervals are well described and can be used to accurately estimate heat transfer coefficients, anomalous power values, and experimental uncertainty.

FRONTIERS OF COLD FUSION

• Anomalous Power in Cell 3. Heavy water Cell 3 showed a marked temperature rise on more than ten occasions while its light water control Cell 4 showed no such rise. The power required to generate these increased temperatures is 100-200 mW. The input power to the cell was generally less than 1500 mW. The calorimetric error during these periods was approximately 1%.

Data Screening and Parameter Estimation

We have found in studying the Harwell data from their FPH cells that the accuracy to which they can be analyzed varies greatly from cell to cell and within a given cell. We have found that an effective way of finding "good" regions, i.e., those with small fluctuations in the estimated parameters, for analysis is to calculate the conductive heat transfer coefficient Kc using a "sliding" window of , say, ten points(30 min), which is moved over the entire time history of the cell. For this the excess heat, Qf, is temporarily assumed to be zero.

Plots of such running Kc values are shown in Figure 1a for heavy water Cell 5 and in Figure 1b for light water Cell 14. Cell 14 is obviously much better behaved

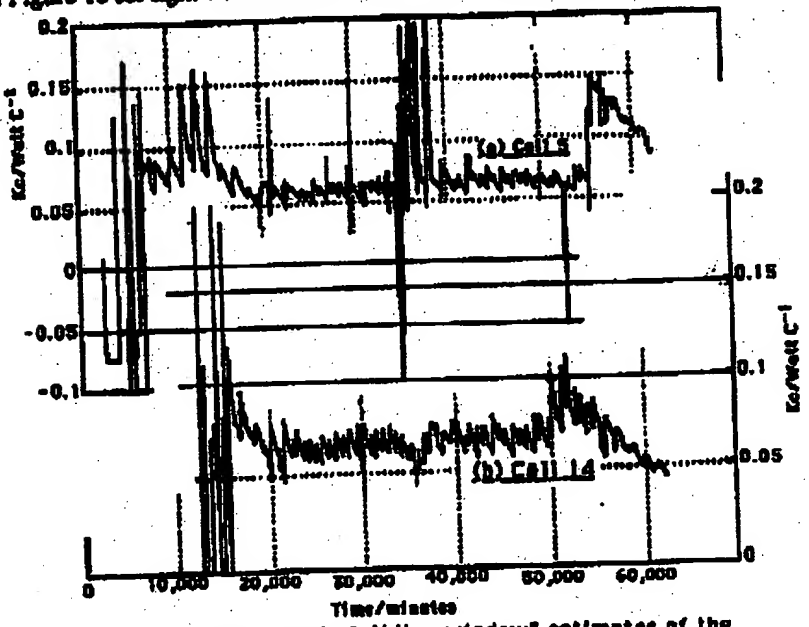

Figure 1. Thirty minute "sliding window" estimates of the conductive heat transfer coefficent for: (a) 41 days of operation of D_2O Cell5; (b) 36 days of operation of H_2O Cell 14.

than Cell 5. Ideally, Kc should remain constant. The large change with electrolyte height, the "tidal effect", is easily understood. The tidal variations and especially the wild gyrations are simply due to poor cell design and function.(Effects on performance and virtual elimination of the tidal variations in Pons and Fleischmann redesigned cells is described in Hansen[1].) Fortunately there is an abundance of FPH data, including many calibration pulses of known power. Sometimes the equations(Pons and Fleischmann equations are used here) don't fit the large changes in current and heater power, presumably because stirring ceases to be adequate or some other control breaks down. These regions become obvious from a study of

Subsequent to Cell 3's rapid temperature rise at 13,918 minutes it experiences a sequence of over 10 similar increases during the next 9 days. Throughout these anomalous increases in temperature in Cell 3, Cell 4 behaves "normally", i.e., it suffers no unexplained pulses of energy. Our initial estimate of the power associated with these anomalous temperature increases is 100-200 mW. The electrolytic current was under 300 mA and the potential was less than 5 V. There are calibration pulses which occur during these events. Further analysis of this data is warranted and underway.

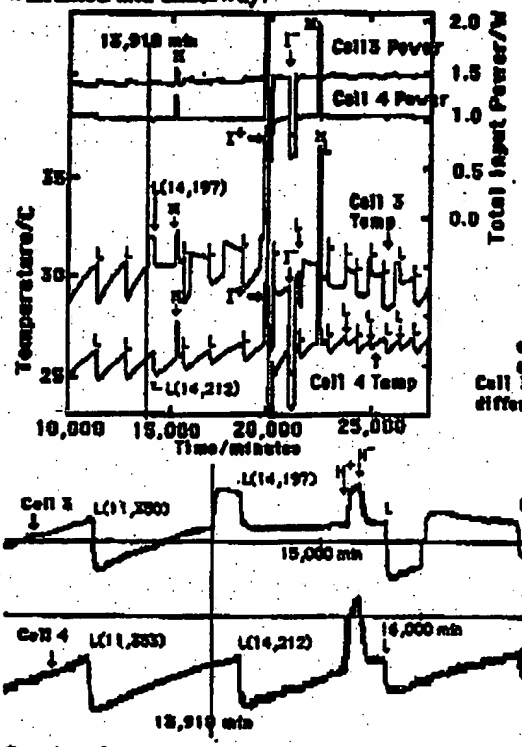

Figure 2. Temperature and total externally supplied input power for D_2O Cell 3 and H_2O over a 13 day period. L= liquid addition; H= heater pulse; I= electrolytic current change. +=increase; -=decrease.

Lower chart is an expansion of the temperature time series around the time 13,918 where Cell 3 shows a rise in temperature different from Cell 4.

List of Symbols/Nomenclature

Kc - Conductive heat transfer coefficient, W/degree C

Kr - Radiative heat transfer coefficient, W/degree C^4

Qf - Excess Heat, W

Points - Data point set, collected every three minutes in Harwell experiments

T(14,198) - Temperature at time 14,198 since starting time of Harwell experiments, may not be from starting time of particular Cell

L; L(19,128) - Liquid addition; at the particular indicated minute, e.g., 19128 minutes

References

1. Hansen, W.N., 1992, *Proceedings of the II Annual Conference on Cold Fusion. Vol. 33 of the Conference Proceedings*, The Italian Physical Society, Bologna, p.491

2. Williams, D.E., et al, *Nature*, 342 (1989), 375

apparent Kc behavior. But where Kc is somewhat misbehaved the fit is good and a non-zero Qf would show up clearly.

These observations are illustrated in the Figure 1 and Table 1. Cell 14 is fairly well behaved from data point 5,500(18,850 min) out to 15,800(49,750 min). The many pulses and current gyrations in this region are well accommodated by the equations. In Cell 5, however, there are several regions where a reasonable fit cannot be achieved. It is simply fruitless to attempt fits in these regions. The data are faulty. Fits can still be had in good regions.

Table 1 shows the results of least squares optimization over various time intervals with simultaneous fitting of Kc and Qf. By choosing regions with calibration pulses and by avoiding a few bad regions, Qf can be determined to within about 0.01 watts. This is an order of magnitude better than the original analysis of these data presented by Williams[2].

Table 1. Estimated Kc and Qf for H_2O Cell 14. ($Kr = 5x10^{-10}$ watts deg^{-4})

Time/minutes	Kc/Watts C^{-1}	Qf/ Watts
18,850-21,850	0.0659	-0.0072
20,500-23,350	0.0676	0.0028
23,350-25,350	0.0649	0.0091
29,350-32,350	(Failed to converge,	no good calibration pulse.)
33,850-36,850	0.0766*	0.0621*
38,350-41,350	0.0688	-0.0093
18,850-35,350	0.0682	0.0143
18,850-62,350	0.0698	0.0064
41,350-62,350	0.0757**	0.0205**

* Suspect estimates, see Figure 1.

** Data beyond 50,350 min is suspect, yet the estimate for average Qf is within 2% of zero.

Anomalous Power in Cell 3

Harwell Cells 1, 2, 3, and 4 were wired in series to a constant current source. Odd numbered cells had D_2O, even numbered cells H_2O. The Pd cathode of 6mm diameter by 10 mm length was in 0.1 molar NaOD in Cell 3 and 0.1 molar NaOH in Cell 4. Figure 2 shows a section of time series data covering the period 10,000 minutes to 30,000 minutes. The data collection started at 2,350 minutes and a 198 mA current was first applied at 2,632 minutes.

Compare the behavior of the temperature and input power traces for Cell 3 with those of Cell 4 starting at time 13,918 min, where the Cell 3 voltage jumps by 80 mV(not shown) and its temperature begins a much faster rise. The temperature rise is halted with the refilling of Cell 3 at time 14,197 min, which produces a voltage increase of 26 mV, while Cell 4 is refilled at 14,212 min producing a voltage drop of 39mV. The temperature change for Cell 3, T(14,197) - T(13,918) = 31.84 - 30.47 = 1.37 C; compare to Cell 4, T(14,212) - T(13,918) = 26.16 - 25.96 = 0.20 C. That is, over the same nearly 3 hour interval with the same electrical current in the same bath but with different electrolytes, Cell 3 experienced a 1.37/.20 = 6.85 greater temperature rise than Cell 4.

FUSION facts

A Monthly Newsletter Providing Factual Reports On Cold Fusion Developments

ISSN 1051-8738 • University of Utah Research Park • Copyright 1992

Fusion Facts Now Reports on Both Cold Fusion and Other Enhanced Energy Devices.

VOLUME 4 NUMBER 2 FUSION FACTS AUGUST 1992

CONTENTS FOR AUGUST 1992

ERRATA

Due to problems with our collator, some copies of *Fusion Facts* for July 1992 were sent without pages 5 & 6. We have enclosed an extra page 5 & 6, in case your copy was defective. Our apologies.

A. *COLD FUSION ATTRACTING INVESTORS*

Shortly after the University of Utah announcement of the discovery of cold fusion (by Professors Pons and Fleischmann, March 23, 1989), Hal Fox confidently predicted it would take only two years to commercialize. The professors and Fox both have been critized. However, Pons and Fleischmann were right (cold fusion is real), Hal Fox was wrong (commercialization is taking longer).

Sometime later, *Fusion Facts* defined that 300% excess heat is a suitable measure for a device to have commercial potential. The rationale is: high-cost electrical energy is being supplied and lower-cost heat energy is being generated. The ratio of cost is about three to one (e.g., electric power cost versus natural gas cost.) Several experimental teams are obtaining results that are close to 300% excess heat in both Pd and Ni electrochemical cells. Cold fusion, therefore, is finally showing commercial potential. In addition, the recent announcement by MITI and the more favorable press reception given to Takahashi's work and to its replication (see NEW MEXICO, this issue) has generated increased interest in the funding of cold fusion projects.

Since the Pons-Fleischman announcement other key events have been: 1) replication by over 200 laboratory groups in more than 25 countries; 2) evidence that the nuclear reactions produced tritium about a million times more than neutrons; 3) demonstration of the importance of a high D/Pd loading ratio; 4) discovery of the importance of resonance conditions; 5) discovery and replication of light-water excess heat experiments; 6) verification of effects predicted by models; 7) successes using Pd/Ag alloys; 8) determination that ^{4}He is a nuclear byproduct of cold fusion; 9) announcement and international replication of the Takahashi experiment; 10) discovery of many anomalies that mark cold fusion as a new science; and 11) refusal of a few scientists to recognize the validity of peer-reviewed, widely-replicated, experimental evidence.

"I'll believe it when I read it in the *Wall Street Journal*," was the comment of a businessman sitting next to me on an airplane trip in the U.S. in 1990. In the early days of cold fusion, a news release to the *Wall Street Journal* or to the *New York Times* and to similar publications would be checked for believability with "friends" at Princeton, Harvard, Yale, MIT, Columbia, and sometimes Cal Tech and receive a rather negative reception. The fact that replication of the early work in cold fusion was not easy and that nearly all of the "important" schools had tried and failed to reproduce significant positive results led to the belief among many scientists that it was a "Utah Effect." Positive reports were dismissed as errors or delusions. Skeptics refused to read the peer-reviewed literature. Therefore, corporations showed little interest in cold fusion and none in funding development work.

Thanks to the continued efforts of many (about 200 - 300) dedicated scientists around the world, research work in cold fusion continued; professional meetings were held; papers were prepared, peer-reviewed, and published; and the news gradually spread that cold fusion was real but not fully understood. Several valiant editors have provided a forum for cold fusion. Chief among these are *Fusion Technology*, *21st Century Science and Technology*, *Nuovo Cimento*, the *Journal of Electroanalytical Chemistry*, and this newsletter. Among the non-technical press, the *Wall Street Journal* has been fair in its presentations.

Serious treatment of the reality of cold fusion began to increase shortly after the Second Annual Conference on Cold Fusion held in Como, Italy, June-July (1991). The replication of both light-water electrochemical cells and of the Takahashi experiment during 1992 (and still continuing) has spurred a gradually increasing interest in cold fusion by sophisticated investors. One of the foremost and far-sighted groups has been the Electrical Power Research Institute in the United States (an estimated $3 million spent). Modest funding of cold fusion has been achieved in Spain, Italy, the former USSR, India, Taiwan, China, and Japan. In terms of international patents filed, Japanese entities have filed about one-half of the patent applications.

In the United States, at least three government energy laboratories and another three or four Department of Defense laboratories are still doing some work in cold fusion. All have published positive results. In terms of on-going work in cold fusion in universities in the United States, Texas A&M; Cal Poly - Pomona; Univ. of Hawaii; and the University of Utah all have some modest funded programs. Limited, private research work is being done at an estimated six other U.S. universities and colleges. In addition, several (an estimated ten) U.S. corporations are carrying on with small-scale research and development programs.

At least six funding groups are seriously considering the funding of further development of cold fusion. Several large corporations are considering funding local university groups who have made significant developments in cold fusion. A few entrepreneurs are working in the area. A few large corporations are funding or planning to fund cold fusion research. The Fusion Information Center (Salt Lake City, Utah), publishers of *Fusion Facts*, and *Fusion Briefings*, have had the privilege of helping its callers save many thousands of dollars in research funds by providing direct linkages between corporate R&D managers and research groups who were already working in similar fields but not known to those who called the Center for information. We are pleased to be able to provide this modest service to subscribers involved in the development of cold fusion.

The Salt Lake City, Utah based Fusion Information Center (FIC) will continue to help provide released database information with its subscribers in its continuing efforts to speed the progress of cold fusion. FIC must honor the confidences that are from time-to-time entrusted to us. However, to be forthright with our readers and callers, we announce that FIC has a vested interest in Fusion Energy Applied Technology [FEAT], Inc. FEAT is a Utah company dedicated to the commercialization of cold fusion.

FIC will do its best to make recommendations to its callers about other companies who are also interested in developing cold fusion energy systems. FIC can only share information that it receives and is permitted to share. If you have any ventures in enhanced energy systems, FIC will be pleased to receive such information and handle such news as being "for publication" or "for verbal referrals only." *Fusion Facts* is willing to publish advertisements from both entrepreneurs and funding entities if you will contact our office.

In summary, the new science of cold fusion is approaching that stage at which development of commercial applications makes both scientific and commercial sense. Regardless of the fact that there are still many scientists and engineers who are, as yet, unconvinced of the reality of the new science of cold fusion, there are dramatic developments that have laid the basis for commercialization of this new science. Some of these experimental results are still pending publication. As fast as we can obtain permission to share the latest work with you, you will read the summary in *Fusion Facts*.

NEWS RELEASE - CLUSTRON SCIENCES CORP.

On Agust 10, 1992, we received a Press Release from Dr. Eugene Mallove and Russell George concerning the funding of Clustron Sciences Corporation by Venture America, located in the Washington, D. C. area. The

There was an announcement by a certain Charles Martin here before the Santa Fe conference but he then withdrew the claim later on and said that it was false. So I think we do get it [the recognition that Hal Fox omitted and apologizes for.]

Anyway, no hard feeling about your statement but I do want to make clear that we do believe that our Santa Fe announcement of the ratio was the first time this very vital piece of information was brought out.

Sincerely, /s/ J. O'M. Bockris

An apology from Hal Fox: *Fusion Facts* has often cited Bockris et al., at Texas A&M as being the first after Pons and Fleischmann to produce cold fusion in a laboratory. As you can see from reading the nominations from Peter Glück, he had more wits than I did. Dr. Bockris: With this apologize, *Fusion Facts* hereby, belatedly, present you with the **FIRST REPLICATORS AWARD. As Peter states, you are one of our heroes. For the sake of historical accuracy, we are pleased to be informed about the branching ratio. I had forgotten that the unexpected branching ratio came up at the Santa Fe conference.** Thanks for your help in keeping an accurate report on these important items.

Note: Dr. Bockris also shared with us a letter which he sent to *Nature* in answer to the ridiculous comments made in *Nature* about the absence of tritium measurements at Texas A&M. See *Nature*, Vol 357, 25 June 1992, page 635, "Out, out brief candle..." and our comments about this article in *Fusion Facts*, July 1992, page 10. If *Nature* refuses to print Professor Bockris' correction to their misleading article, *Fusion Facts* will, with Bockris' permission, share his letter with you.

LETTER FROM CHINA

Dear Mr. Fox,

Thank you for your recent issue of *Fusion Facts*, which conveys the important message about the MITI investment. . . . I am still trying to recruit volunteers on my campus for the experimental study of light-water "excess heat." . . . We are interested in Takahashi's experiment also. We are expected more messages about the duplication of Takahashi's experiment in *Fusion Facts*.

/s/ Li, Xing Zhong

[We are always pleased to exchange news with our friends abroad. Prof. Li also pointed out the collating error in our July issue. The correction is being mailed to everyone with this issue. We apologize for our error. Ed.]

LETTER FROM MINNESOTA

Wanted: Better Texts for Oldsters

In trying to both do experiments, and "educate the stone" (this writer's head) I have been reading "Quantum Mechanics" and "Solid State Physics" texts the last three years. I find that there is a marked lack of QM texts which work out examples in their entirety in the text. I did find a wonderful QM text by W. Greiner. It is titled Theoretical Physics 1, and Dr. Greiner does go into great detail in working out the equations. I'm looking for a similar text in Solid State Physics. I'm familiar with Kittle and Ashcroft and with Mermin, neither of which are very involved when it comes to working out examples in the text. ("The Proof is left as an exercise for the reader...," is the classic comment made throughout Kittle and Ashcroft's texts. I don't need that, I'm too old for that nonsense. If someone has done the work already--I'm not going to re-invent the wheel.") Last: does anyone have any papers/info on the so-called "muon-catalyzed" cold fusion? I'm curious if anyone knows the lifetime of a "muon" in a solid state matrix. As I understand it, muons in "free space" reactions can catalyze several hundred fusions before being "consumed." Perhaps if their lifetime is orders of magnitude longer in the solid state, and if fusion reactions themselves can liberate muons, our "cold fusion" might be a natural extension of that phenomenon. But I speak out of ignorance, not knowledge, and would appreciate help in this realm.

Yours, /s/ Mark D. Hugo

Note to Mark: Jones and Rafelski did some of the original work in muon-catalyzed cold fusion and there has been a periodic conference on the subject for several years. In a recent summary publication [Rafelski et al., "Cold fusion: muon-catalyzed fusion," *Jrnl of Physics B: Atomic, Molecular and Optical Physics*, Vol 4, 1991, pp 1469-1516, 115 refs.] the authors present a topical overview of muon-catalyzed fusion. In the concluding remarks is the following sentence: "However, as highlighted in this survey, it is generally believed that MuCF is already close to the limits posed by a combination of practical approaches with fundamental laws of physics, and hence further improvement is exceedingly difficult." The last two sentences of this massive "topical review" states the following: "While the chances of success are probably remote, the furor generated by the reports of *cold fusion* show the general appreciation for the importance of unconventional directions in the search for clean fusion energy. It is from this perspective that we must look upon *cold, muon-catalyzed fusion.*" This paper was reviewed in the June 1991 issue of *Fusion Facts*. Ed.

H. REEXAMINATION OF A KEY COLD FUSION EXPERIMENT: "PHASE-II" CALORIMETRY BY THE MIT PLASMA FUSION CENTER

By Dr. Mitchell R. Swartz, January 14, 1992, revised July 16, 1992. (c) M. Swartz 1992 JET Technology, Weston, Ma. 02193

EDITOR'S NOTE: *Fusion Facts* was asked to publish this information after it had been peer-reviewed. Although this article is longer than we normally publish, it covers an important aspect of the history of the development of cold fusion. We strongly believe that scientists have the right to reject or accept other scientific work based on its merits. We completely reject the right of any scientific group to be immune from criticism regardless of their institution. When a widely circulated peer-reviewed publication is found to be faulty, then we believe that a professional criticism of the work deserves publication. The following article carefully evaluates an MIT paper that has been widely cited (especially by the U.S. Patent Office) as "proof" that cold fusion is not real. As a former worker in the Lincoln Labs, I have great love and respect for MIT, the institution, and regret the events that have led to Dr. Mallove's resignation and to the need for the publication of this article by Dr. Swartz. *Fusion Facts*, will, of course, provide space for a reply to this article from Albagli, et al. Hal Fox, Ed.

1.0 INTRODUCTION: ASYMMETRIC CURVE TRANSFORM

In the Spring of 1989, electrochemically-induced excess enthalpy reactions using palladium filled with deuterons from heavy water [1] were initially reported to be very difficult to reproduce. Because of those difficulties cold fusion incorrectly connotes a "failed" technology in the minds of many scientists -- even as a positive literature supporting the phenomenon grows. Experimental papers now involve palladium, titanium, and possibly nickel, with the chief product being excess heat [2,3]. Other products released include tritium [4,5], sparse neutrons [6,7,8], helium[4] [9], and possibly heavy elements [10].

Many skeptics [11] cite the published Phase-II data from the Massachusetts Institute of Technology Plasma Fusion Center (MIT PFC [12]). Despite increasing evidence for cold fusion from labs in France, Japan, and Italy, the work-in-progress within the United States declined precipitously by late 1989 and has remained virtually non-existent, in part because of the publication of the Plasma Fusion Center Phase-II data, and the widespread press which it received.

By 1991, scientific criticisms of the PFC data and techniques appeared. The data was criticized as being faulty with respect to its thermal calculations and conclusions [13]. More criticism accrued over differences between an in-house report (July 10, 1989) and the later (July 13, 1989) prepublication report [14]. The most serious complaint has involved alleged "shifting" of the heavy water excess power curves [15].

What follows is an independent examination to both determine if there was a curve "shift," and whether the same method of data conversion was applied equally to the light and heavy water curves. This optical imaging study of the PFC Phase-II curves has revealed many curves purported by the PFC to represent the same experiment. Table 1 sorts them out into several types [see figure 1].

Section 1 is an overview of the PFC Phase-II curve catalog, and presents two measurements of the second baseline shift removed from Type 2 D_2O excess power curve to obtain the prepublication Type 3 (and publication Type 3_B [12]) curves. Section 2 presents a critical analysis of the Phase-II methodology which is revealed to be insensitive to steady state ("d.c.") excess heats. More valid processing of the Phase-II data suggests excess heat may have been produced after 48 hours in the range suggested by Fleischmann and Pons experiment [1].

1.1 EXPERIMENTAL: IMAGE PROCESSING

The curves reported by the PFC (for both heavy and light water) were captured using image scanners including the raw heater power curves, the preliminary excess power curves (July 10, 1989), later "averaged" curves (July 13, 1989 - ref. [16]), the *J. Fusion Energy* published curves [12], and the March 10, 1992 Memo curves (later published in the PFC May 1992 Appendix [17]).

A Prime Option Scanner [400 dots per inch] was used. The images were stored as 16 bit data files, bitmapped by an Amiga 3000UX onto at least 1240 by 2100 pixels. To facilitate comparison, images were colorized (Professional Art Department (tm), [ASDG]) to enable unambiguous superposition of the different curves by applying each as a brush (Deluxe Paint IV (tm), [Electronic Arts]).

To accurately superimpose the curves, each was put in registration using rules at indicated power and time tics. Proportional control and careful alignment allowed each set of curves to be matched, superimposed, and recaptured. Some of the figures (Figure 2) thus demonstrate two sets of numbers along one axis consistent with the technique.

1.2 RESULTS: ASYMMETRIC ALGORITHM

Figure 1 shows how the Type 2 curve was already shifted once from the raw data (Type 1 curves). The Type 3

curve (composed of dots in the July 13, 1989 manuscript [16]) was reported to be a time average of the original data. The published curve (Type 3_B [12]) is nearly identical to the (dotted) Type 3 curve [14] and differs only in that the heavy water curve darkens locally between some groups of data points.

Figure 2 shows the matched and superimposed excess heat curves taken from the July 10, and 13, 1989 manuscripts. The upper set is for the light water (cell A). The lower set is for heavy water (cell B). For each set both the July 10, 1989 data (continuous curve in black) and the July 13th prepublication "averaged" data (gray dots) are shown. The two continuous curves (Type 2 from the July 10, 1989 manuscript) have high frequency components.

Examination of the light water curves (Figure 2, upper pair) reveals a very good correlation between the July 10th (Type 2) and the twice-processed (July 13th, Type 3) prepublication curves. This implies there was a negligible (second) baseline subtraction for the light water data.

In contrast, the two heavy water curves (Figure 2, lower pair) have a poorer correlation which imply a significant second baseline subtraction. Almost none of the twice-processed data points overlap the July 10th data beyond 30 hours. The Type 3 curve also appears too wide on its left hand side.

1.3 RESULTS: DERIVATION OF THE CURVE SHIFT

An attempt was made to determine what algorithm(s) were used to process the July 10th D_2O curve (once-processed Type 2) to create the prepublication curve (twice-processed Type 3). First, a temporal averaging for the heavy water July 10, 1989 curve was derived. Figure 3 shows three sets of curves. The upper set shows both the low-pass ("time averaged") curve and the PFC heavy water Type 2 (July 10, 1989) curve from which it was obtained. Next various linear baseline shifts were effected upon the low-pass D_2O curve, and are shown in the mid and lower portions of figure 3.

For simplicity, a linear model was used to determine the transformations used, i.e., Type 2 + [A+(B*t)]---> Type 3. A and B are the linear terms for that second baseline shift. A has the units of watts; and B has the units of watts/second.

Several curves were derived using various A and B parameters. The middle set of curves in figure 3 are the superposition of the low-pass curve with four linear baseline shifts [A=0]. The published heavy water data of the PFC is also shown as the darkest dots. The darker gray continuous curve (with the greatest time-varying baseline shift) shows the superposition of A=0 and B= -158 nanowatts/second upon the low-pass curve.

The lower set of curves in figure 3 show the superposition of the low-pass curve with various fixed (non time-varying) baseline shifts [B=0]. The published [12] Type 3 data points are again shown as the darkest dots. The darker gray continuous curve (with the greatest fixed baseline shift) shows the effect of A = -59 milliwatts and B=0 superimposed upon the low-pass curve.

It is important to consider that the published curves for heavy water [Type 3 or 3_B] are too thick on their left hand side. Because the possibility of superimposed points added to a linear transformation cannot be excluded, it is unclear which values of A and B produce the best fit.

Notwithstanding the above, the transformation used to change the Type 2 (7/10/89) to Type 3 (7/13/89) D_2O curve was approximately:

fixed baseline shift [A=] -9.6 milliwatts, and
time varying shift [B=] -94 nanowatts/second.

To determine the actual energy subtracted from the July 10, 1989 curves, the integrals under the power curves were measured. Then using the duration of the experiment, the average excess power subtracted was derived. For the heavy water this derived power was about 30 milliwatts (+/- 15%) in the time beyond 18 hours. The light water curve was characterized by an average power baseline subtraction of 0.3 milliwatts. In summary, this analysis demonstrated that either a relative D_2O/H_2O excess power was measured, or that an asymmetric (second) treatment of the data was used after July 10, 1989, that is, the light and heavy water data were processed differently.

1.4 RESULTS: ARTIFACTUAL POINTS

Some of the points in the published D_2O curves appear to be possible artifact, of two varieties. Points A and A' in figure 4 are one variety. These points are arbitrarily positioned along what was purported in the published paper to have been "intentionally introduced as a time calibration mark." It is not clear either how the locations of points A and A' [in Type 3 and Type 4 curves, respectively] were chosen, or why the published temperature curve [12] changed at that time.

A second variety of possible artifact concerns the apparent higher density cluster of points on the D_2O curve between 18 and 25 hours [figures 2, 3, and 4]. The PFC publication [12] indicates that dots were the result of a time "average(d) over 1-h(our) blocks."

The upper set of curves in figure 4 are the Type 3 D_2O and H_2O curves, one above the other to facilitate examination. Gray dots were located over each data point

to facilitate a count within a forty (40) hour period for these curves. Although less than 42+/-1 dots were expected, for the D_2O curve the number of dots exceeds 45. Although differences in sampling rate could account for the number, it would not account for the unusual thickness of the published heavy water curve on its left side.

These observations of artifacts were reported to the PFC in February 1992. The March 10, 1992 PFC memo presented two "new" curves to "correct" this matter [17]. One new curve (Type 4) is examined in the mid and lower sets of curves in figure 4. The mid set of curves compares one published curve (Type 3, dark dots) to the post-publication-3/10/1992 (Type 4) curve. The two curves have been normalized, put in registration, and superimposed. The only change is that in the 3/10/92 memo, the Type 4 curve had the symbol "[ ]." For easier identification, a solid gray dot has been placed between each pair of brackets.

At least three published data points [labelled "i," "ii," and "iii"] are missing from the Type 4 curve. Most notably absent is data point "iii," the expected opposite superior half of the "incidental" points: "A" and "A'."

The mid set of curves in figure 4 also compares data points A (Type 3) and A' (Type 4). Point A' appears shifted toward the baseline. This is examined further in the lower set of curves in figure 4 which have been normalized and are in registration for comparison. The times are hours and the power (vertical axis) is watts. One published curve [Type 3 (PFC/JA-89-34)] is on the right hand side and is gray colored. The data from the July 10, 1989 curve [Type 2] is also shown on the right side, located slightly higher (black continuous curve). The Type 4 curve is on the left hand side.

The magnitude of the "data" point shift [A to A'] is +24 milliwatts. This point shift is one of a number of changes used to optically identify and distinguish this Type 4 curve.

1.5 ANALYSIS: EVAPORATION FROM D_2O SOLUTION

Why was a second baseline subtracted from the D_2O curve after July 10, 1989? The PFC has said that the "shift for the heavy water data came as a result of a computer subtraction designed to compensate for water evaporation [15]." Could increased solvent loss for D_2O actually impose a need for a greater "baseline shift"? Albagli [12] states that the temperatures of the two solutions were similar. However, temperature curve imaging indicates that the H_2O experiment was operated at a higher (1 degree Centigrade) temperature.

Given that the D_2O solution was at a lower temperature than the H_2O solution, and given that for each temperature the vapor pressure of D_2O is less than H_2O [deuterium oxide melting point (STP) is 3.82 Centigrade, its boiling point is 101.4C] more evaporation must have occurred for the light water. Therefore, the baseline subtraction should have been less for the D_2O experiment.

There is another reason why less baseline subtraction should have been used for the D_2O data. The PFC data itself indicates that evaporation was a minor source of solvent loss, because the calculated thermoneutral potentials were quite close to their theoretical values [13]. Therefore most solvent loss occurred by electrolysis. Such solvent loss would be greater for the H_2O solution again because such electrolysis is, in fact, used to commercially isolate heavy water due to light water's tendency to form gas by electrolysis first.

In summary, putative differential excess solvent loss for heavy water is not a reasonable explanation for the asymmetric algorithm used to shift the 7/10/1989 D_2O curve.

1.6 ANALYSIS: EFFECT OF CURVE SHIFT

"This equation (P_x+P_h = constant) allows the unknown power, P_x, to be determined. If P_x increases, then the feedback control system of the calorimeter reduces P_h to maintain T_c constant [12]." Therefore any potential curve shift would hide part, or all, of any measured excess heat.

Furthermore, unless stated otherwise, readers presumed that baseline shifts were the same for the H_2O and D_2O, and based upon careful calibration experiments. "(T)he data for the H_2O curve ... was taken at the time of the 1989 experiments, and in the exact same way that the data was obtained for the D_2O curve [19]."

1.7 SUMMARY OF SECTION 1

In summary, Table 1 lists the different curves which have been purported by the PFC to be the results of a single Phase-II heavy water experiment in 1989. Neither baseline data from before the experiment, nor calibration data concerning the putative heat loss versus solution height, nor the solution volume during the experiment, have been released or provided. Given these limitations, the following optical assignments remain presumptive.

Type 1 curves are the raw heater power data. The best experimental graph is 1_D. A baseline shift of about 900 nanowatts/second was applied to the Type 1 curve to get the Type 2 curve. A second 94 nanowatts/second shift was applied after July 10, 1989 to generate prototype 3. The superposition of additional points, not present in

either the Type 1 or Type 2 curves, completes the transformation to the Type 3 curve (7/13/89).

The Type 4 curve (which appeared March 1992 [17, 18]) has one of the published "data" points moved 24 milliwatts. Other questioned "data" points are missing. In the "newest" curve [Type 5] all of the questioned "data" points have vanished.

2.0 INTRODUCTION: SENSITIVITY OF THE PHASE-II METHODOLOGY

The March 10, 1992 PFC memo states they "first subtract(ed) the baseline drift [so that] any onset of anomalous heating would appear as an excursion from zero." That memo and the subsequent Appendix [17] explored various linear curves [derived by uncertain fit over varying portions of the data] used to produce baseline shifts.

Given the widespread reports confirming cold fusion phenomena [2,3,4,5,7,8,9,10] and the recent release of the PFC Phase-II methodology [17], it is reasonable to evaluate the technique. The following analysis determined whether the Phase-II method was sensitive to excess enthalpy characterized by a ramp and step function, including the presence of a changing baseline.

2.1 ANALYSIS: CAN THE PHASE-II METHODOLOGY DETECT EXCESS POWER

Figure 5 shows five sets of curves. Each set has three curves derived from three hypothetical "successful" experiments wherein excess enthalpy occurred at time T. Each set of three curves is labelled a, b, and c, and is the result of "operations" used to process the first set of curves in the upper left of the figure.

These hypothetical curves (labelled with lower case nonsubscripted letters) should not be confused with the several curves of figure 1 such as Type 3_B curve (note upper case subscript).

In figure 5, curve 1a is the first hypothetical heater power curve, with a slow "turn-on" of excess heat at time T. An expected delay to onset is reasonable. As was noted in the March 10, 1992 PFC memo "(t)he level of excess heat .... was claimed to appear after an initial 'loading period' of some hours or days."

Curve 1a is initially stable (flat baseline) but then decreases as the hypothetical excess heat increases. The shift occurs because the heater requires less input power to maintain the same temperature.

One complexity is that the baseline of the heater power curve, prior to a "successful" experiment, may not be flat. Such baseline drift could be due to electrolysis loss (which might increase the thermal diffusion pathlength to the environment) or evaporation or other reasons. For the second hypothetical experiment (curve 1b) there was the same change in excess heat at time T, but superimposed upon an intrinsic baseline drift. Curve 1c is the hypothetical experiment wherein at time T a step function occurs rather than a ramp function.

The following analysis demonstrates why it is critically important to notice that a linear regression fit can be made to either the entire curve, or to the baseline prior to the onset of excess power. Figure 5 presents these two methods. Curve sets 2 (with 4) and 3 (with 5) show each method.

On the left of figure 5, curves 2a, 2b, and 2c show the derivations of excess heat using regression fits made to the initial portions of the heater power curves prior to the onset of excess enthalpy. Such linear fits made using only the experimental data prior to the hypothetical onset of excess heat are labeled Y_{HT} (for "true" linear regression fits) to distinguish them from the curves Y_{HF} (for "false" linear regression fits). Y_{HT} curves are fit to the curve prior to the onset of excess enthalpy, whereas the Y_{HF} curve are fit to the entire data curve (including the excess enthalpic portion). The "truth" and "falsity" of each method will be apparent now.

Curves 4a, 4b, 4c show the result of deriving the true excess power: $P_{XT} = Y_{HT} - P_H$. Curves 5a, 5b, and 5c show the "falsely derived" excess power using the linear regression fits made to the entire curve: $P_{XF} = Y_{HF} - P_H$. The fundamental value of each method can be seen by comparing each matched pair of Curves 4a with 5a, then 4b with 5b, and then 4c with 5c. The P_{XT} curves do qualitatively reveal the excess enthalpies which were postulated in this gendanken "successful" experiment. On the right side of figure 4, curves 5a, 5b, and 5c, the P_{XF} curves, confirm that the flawed technique masks the excess heat even in every hypothetical "successful" case.

Note also that the P_{XT} curves (4a, 4b, 4c) correctly derive that the excess heats began at time T. However, in the P_{XF} curves (5a, 5b, 5c) there is only a breakpoint at time T, and the presence of excess heat is not clearly revealed. In the P_{XF} curves there appears a surge of "excess" heat, a narrow impulse, at the initiation of the hypothetical excess heat. It is interesting that reexamination of the PFC heavy water published curves (Types 3 and 3_B) reveals a similar pattern, a possible "signature" of excess heat detected by the Phase-II methodology.

In summary, the algorithm used in the Phase-II experiment is flawed because it hides any constant excess heat. Efforts using such an insensitive methodology are doomed a priori. Critical data analysis requires careful

measurement of the baseline drift before the turn-on of any putative excess heat. Perhaps additional heavy water should not have been added to the solution soon after the experiment started, but should have tried to obtain the best possible initial baseline, which may be lacking in Types 3, 3b, 4 and 5 curves.

2.2 ANALYSIS: REEXAMINATION OF THE PHASE-II D_2O CURVES

Given the asymmetry of the curve shifts for the heavy and light water experiments, it is thus important to consider if there actually was excess power in the D_2O experiment. The PFC paper [12] does give hints of excess power. First,

"(w)hen enough solvent was added to the D_2O cell to compensate for that lost to electrolysis at the end of the 100 h period shown in Figure 6, Ph (the heater power) returned to within 20% of its original value."
[Albagli et al., J. of Fusion Energy, 9, 133 (1990)]

That 20% discrepancy in heater power, used to heat the same volume of fluid has been suggested as corroborating evidence that the heavy water cell produced excess heat [14].

Noninski [13] examined these thermal matters and calculated that as much as 2 watts per cm^3 palladium of excess power was generated over 60 hours for the heavy water.

The optical analysis and integral derivations of subtracted energy from the D_2O curve, as discussed above, indicate approximately 400 milliwatts per cm^3 generated for the 9 cm by 0.1 cm diameter cathode.

Because of the flawed Phase-II methodology and these facts, the Phase-II D_2O experiment was reexamined using the initial baseline drift on the Type 1_D curve. A calibrated excess power curve [P_{XT}, the "true" corrected excess power] for the Phase-II D_2O experiment was derived. It is listed as Type 6 in Table 1 and shown in the upper portion of figure 6. The average excess power derived by this method is 62 milliwatts (+/- 34 milliwatts).

This derived value of excess heat is on the order of the measured difference between the Type 2 and Type 3 curves. It is qualitatively similar to the value expected for a "successful" experiment [1,12]. The time of apparent turn-on of excess heat in the derived Type 6 curve is also close to the expected time cited [12].

2.3 ANALYSIS - THERMAL PATHLENGTH LOSS

The PFC Appendix [17] indicates that the Phase II system was calibrated during the experiment by adding 5 cc of D_2O at t=14 hours. The D_2O-air interface was described as located at L+x(t) from the top of the calorimeter. The Appendix purports without supporting evidence that because a 1/(L+x(t)) term dominates the thermal losses it produces a linear baseline drift of the heater power curve.

The Appendix [17] claims that such linearization follows because x is close to 0.0, and so 1/(L+x(t)) can thus be approximated as: $1-(x/L)+(x^2/L^2)$ and so there supposedly results a linear baseline drift.

But is x/L really close to zero under open conditions wherein solvent losses include both evaporation and electrolysis [0.2 amperes]? Use of the Faraday and the dimensions provided in Albagli [12] and the Appendix [17] indicate that the approximation was inappropriate before the experiment was over.

However, just suppose that it were appropriate to remove some baseline shift. Removing the baseline based upon a linear regression from data taken after the experiment begins simply eliminates any steady state signal. As figure 4 shows, the effect is not merely a baseline correction, but is the removal of the entire time-invariant signal.

Therefore, a correct method was made to determine the calibrated excess power using appropriate mathematics for the baseline correction. A series of curves was generated using the actual postulated 1/(L+x(t)) thermal resistive pathlength, instead of the improper linearization. The model consisted of two thermal loss paths, one fixed and one varying. The ratios of the two thermal losses are shown in the lower set of parametric curves in figure 6. When the Type 1_D curve is plotted upon the initial corresponding baseline-shift/thermal-loss curve [with an estimated 55% (+/- 20%) of heat exiting through the variable path] the difference (gray area) would be the calibrated excess heat for D_2O.

This derivation is similar to the excess heat derived optically and shown in the upper curve in figure 6. The parametric-baseline subtraction method appears to have more sensitivity to excess heat.

2.4 CONCLUSIONS and SUMMARY

The light water curve was published by the PFC essentially intact after the first baseline shift, whereas the heavy water curve was shifted a second time. The cells were matched [12], and solvent loss would be expected to be greater for H_2O.

The Phase-II methodology is flawed because it masks a constant [steady-state] excess heat. Furthermore this paradigm fails to use either the true baseline drift, and

may avoid the first 15% of the D_2O curve in Types 3, 3_B, 4, and 5 curves.

What constitutes "data reduction" is sometimes but not always open to scientific debate. The application of a low pass filter to an electrical signal or the cutting in half of a hologram properly constitute "data reduction," but the asymmetric shifting of one curve of a paired set is probably not. The removal of the entire steady state signal is also not classical "data reduction."

In the May 1992 Appendix, the PFC retroactively claims its "systematic" errors now total 100 to 400 milliwatts, implying an insensitivity of >30 kilojoules.

Much current skepticism of the cold fusion phenomenon was created by the PFC paper's reporting "failure-to-reproduce" [12] as opposed to its later claimed "too-insensitive-to-confirm" experiments [17]. Because it may be the single most widely quoted work used by critics of cold fusion to dismiss the phenomena, the paper should have clarified all "data" points and the methodology used. Apparent curve proliferation, volatile points, asymmetric curve shifts, combined with an impaired methodology have needlessly degraded the sensitivity, and believability, of the Phase-II calorimetry experiment.

REFERENCES

1. M. Fleischmann, S. Pons, "Electrochemically Induced Nuclear Fusion of Deuterium," *J. Electroanal. Chem.*, 261, 301 (1989).

2. J.O'M. Bockris, G.H. Lin, N.J.C. Packham, "A Review of the Investigations of the Fleischmann-Pons Phenomena," *Fusion Technology*, 18, 11, (1990).

3. E.F. Mallove, "Fire from Ice: Searching for the Truth behind the Cold Fusion Furor," John Wiley, New York, (1991).

4. M. Srinivasan, "Nuclear Fusion in an Atomic Lattice: An Update," *Current Science*, 143, (1991).

5. E. Storms, C. Talcott, "Electrolytic Tritium Production," *Fusion Technology*, 17, 680, (1990).

6. S.E. Jones, E.P. Palmer, et al., "Anomalous Nuclear Reactions in Condensed Matter," *J. Fusion Energy*, 9, 199, (1990).

7. D. Gozzi, P.L. Cignini, et al., "Nuclear and Thermal Effects During Electrolytic Reduction of Deuterium at Palladium Cathode," *J. Fusion Energy*, 9, 241 (1990).

8. H.O. Menlove, M.M. Fowler, et al., "Measurement of Neutron Emission from Ti and Pd in Pressurized D2 Gas and D_2O Electrolysis Cells," *J. Fusion Energy*, 9, 495, (1990).

9. B.F. Bush, J.J. Lagowski, M.H. Miles, G.S. Ostrom, "Helium Production During the Electrolysis of D_2O in Cold Fusion Experiments," *J. Electro. Chem.*, 304, 271, (1991).

10. T. Matsumoto, K. Kurokawa, "Observation of Heavy Elements Produced During Explosive Cold Fusion," *Fusion Technology*, 20, 323, (1991).

11. The United States Patent Office is reported to rely upon Albagli et al., (12) to reject all patent applications involving cold fusion or even those inventions capable of working in the "cold fusion environment."

12. D. Albagli, R. Ballinger, V. Cammarata, X. Chen, R.M. Crooks, C. Fiore, M.P.J Gaudreau, I. Hwang, C.K. Li, P. Linsay, S.C. Luckhardt, R.R. Parker, R.D. Petrasso, M.O. Schloh, K.W. Wensel, M.S. Wrighton, "Measurement and Analysis of Neutron and Gamma-Ray Emission Rates, other Fusion Products, and Power in Electrochemical Cells Having Pd-Cathodes," *J. of Fusion Energy*, 9, 133 (1990).

13. V.C. Noninski, C.I. Noninski, "Comments on 'Measurement and Analysis ... Cathodes," *Fusion Technology*, 19, 579-580 (1991).

14. Complaint to President C. M. Vest, Massachusetts Institute of Technology, Cambridge MA from Dr. Eugene Mallove (August 1991).

15. C. Anderson, "Cold fusion tempest at MIT," *Nature*, 353, (1991). Also, Majorie Hecht, "A Case Study of Fudging," *21st Cent. Sci & Tech.*, Fall 1991, Vol 4, No. 3. page 54.

16. D. Albagli, R. Ballinger, et al., "Measurement and Analysis ... Pd Cathodes," PFC/JA-89-34 [July 1989].

17. S.C. Luckhardt, "Technical Appendix to D. Albagli, et al., *J. Fusion Energy*, 1990, Calorimetry Error Analysis," MIT Report PFC/RR-92-7, (May 1992).

18. It remains difficult to interpret Types 4 and 5 curves because although the regression coefficients used to shift the raw experimental data curve (?Type 1_D) were listed to five (5) decimal places, no mention was given of the many coefficients of fit, or as to why the first about 18 hours of data may have been left off the linearization scheme.

19. Personal communication [August 30, 1991] from Prof. R. Parker to the author.

ACKNOWLEDGMENTS:

The author is grateful to many people for their support, information and/or discussions provided during the preparation of this manuscript including Drs. S. Baer, E. Mallove, I. Straus, D. Towne, and at MIT Profs. P. Hagelstein, P. Morrison, R. Parker, L. Smullin, M. Zahn, and President C. Vest.

TABLE 1 : SIX TYPES OF CURVES FOR D_2O EXPERIMENT

The PFC Phase-II D_2O data has been displayed several ways since July 10, 1989. This table lists known curves of that single experiment, including the five Types reported by the PFC.

#	CODE	DUR'N [HRS]	CONT/ DOTS	INCID PTS	QUEST PT	?ASYM SHIFT	? PT SHIFT	BLS nW/s	DOCUMENT [DATE]	ASSIGNMENT
1	1	0-98	CONT	n.a.	n.a.	n.a.	n.a.	n.a.	7/10/89	Raw data
2	1_B	0-98	CONT	n.a.	n.a.	n.a.	n.a.	n.a.	JFE 90	Published
3	1_C	0-80	CONT	n.a.	n.a.	n.a.	n.a.	n.a.	9/1991	Memo 1991
4	1_D	0-98	CONT	n.a.	n.a.	n.a.	n.a.	n.a.	3/10/92	Best?
5	1_E	13-98	CONT	n.a.	n.a.	n.a.	n.a.	n.a.	5/92	PFC/RR-92-7
6	2	0-98	CONT	n.a.	n.a.	?	n.a.	900	7/10/89	Memo 7/10/89
7	3	18-98	DOTS	+++	+++	yes	n.a.	994	7/13/89	Memo 7/13/89
8	3_B	18-98	DOTS	+++	++++	yes	n.a.	994	JFE 90	Published
9	4	18-98	DOTS	+	gone	yes	yes	994	3/10/92	3/10/92,5/92
10	5	18-98	DOTS	gone	gone	yes	gone	994	3/10/92	Memo 3/10/92
11	6	18-98	CONT	n.a.	n.a.	n.a.	n.a.	yes	Fig.6	Calibrated

CODE - TYPE. Type 1 has five graphs, shown in figure 1. They are nearly identical with various portions clipped or removed. Curve 1_D may be the best raw data curve released to date.

DUR'N - Duration of Experimental Time shown in graph. Clipping often occurs at >80 hours or 0-16 hours.

CONT - Continuity. Continuous (CONT) or binned samples (DOTS).

INCID(ental) Points - Points from experimenter-created glitch.

QUEST(ionable) Points - Points beyond the raw data curve.

?ASYM(metric) SHIFT - Is there a second shift of the curve beyond the first baseline shift.

? P(oint) SHIFT - Is there movement of point "A" to "A'."

BLS (Baseline Shift) - Is there any baseline shift?. Quantities are nanowatts per second.

n.a. Not Applicable.

ASSIGNMENTS BY TYPE

Type 1 are the raw data (heater power curves) which have been released several forms, which appear to be identical.

1_D - BEST PROBABLE RAW EXPERIMENTAL DATA - continuous.

1_C - PROBABLE RAW EXPERIMENTAL DATA - continuous,
Identical to 1_D; clipped at circa 80 hours.

Types 2 and 3 are the previously released 7/10 and 7/13/89 excess power curves. Type 3_B was published [12], and is slightly different from Type 3, but not enough to warrant a new category.

2 - FIRST-SHIFTED BASELINE [July 10, 1989 curve]
Continuous [shift circa -900 nanowatts/second].

3 - SECOND-SHIFTED BASELINE [July 13, 1989 curve]
Sampled data [shift circa -990 nanowatts/second].

3_B- PUBLISHED D_2O CURVE - Figure 5b in J. Fusion Energy (9, 199)

Types 4 and 5 [March 10, 1992 PFC memo] were derived using various regression fits [although given to five significant figures, the correlation coefficients were not presented].

4 - NEW SHIFTED BASELINE [Fig. 5 in 3/10/1992 Memo]
Sampled data : one incidental point missing; the other shifted 24+ milliwatts; other minor differences.

5 - NEWEST SHIFTED BASELINE [Fig. 9 in March 10, 1992 Memo]
All incidental and questioned points missing.

6 - CALIBRATED DERIVATION OF EXCESS HEAT
Correction based upon initial slope of Phase-II data. The Type 6 curve is shown in Figure 6.

Figure 1 - FIVE TYPES OF PHASE-II D_2O CURVES

These are nine different graphs available regarding a single MIT PFC Phase-II heavy water experiment in 1989. Five types are distinguishable. The four graphs on the left side (Types 1, 1_B, 1_C, and 1_D) are nearly identical with various portions clipped at 80+ hours or 0-16 hours. Types 2 and 3 are the July 10, and 13, 1989 curves. Type 3_B was in J. Fusion Energy [9, 133 (1990)]. Types 4 and 5 appeared March 10, 1992.

TYPE 1: RAW DATA [7/10/89] AND CONGENERS

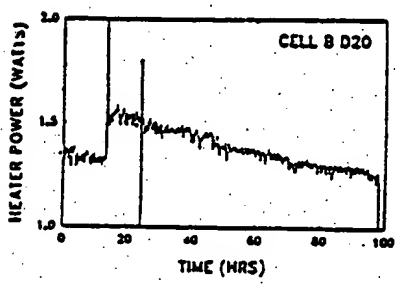

TYPE 1_B [J.F.Energy '90]

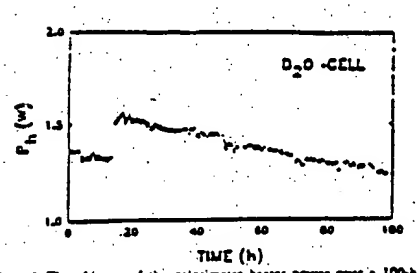

Fig. 6. Time history of the calorimeter heater power over a 100-h

TYPE 1_C [circa 9/91]

TYPE 1_D [3/10/92]

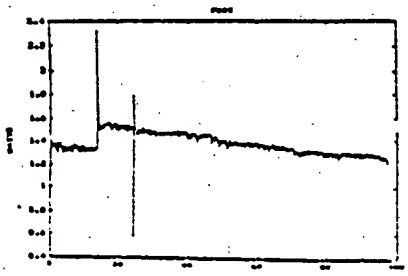

TYPE 2: FIRST SHIFTED CURVE [7/10/89]

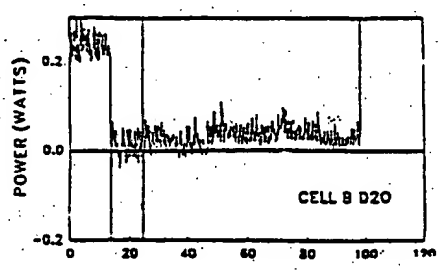

TYPE 3: SECOND SHIFTED CURVE [7/13/89]

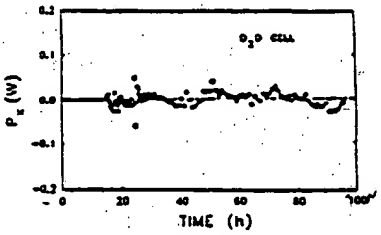

TYPE 3_B [J. Fus. Energy '90]

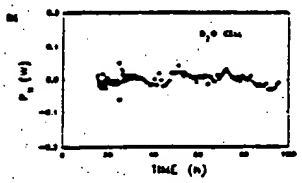

TYPE 4 [3/10/92; +24 milliwatt shift]

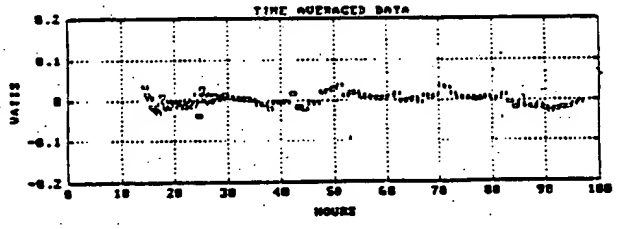

TYPE 5 [3/10/92; "cleansed"]

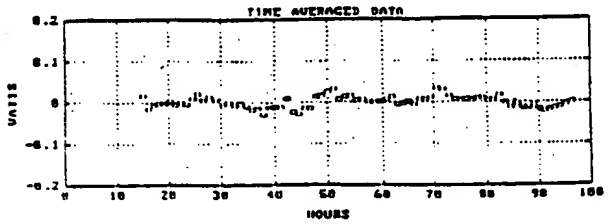

Figure 2 - ASYMMETRIC CHANGES IN JULY 1989

These are composite curves of the MIT PFC Phase-II data [after Albagli et al. (1989, 1990)]. The upper are light water (H_2O) and the lower are heavy water (D_2O). The continuous dark curves are from July 10, 1989 [Type 2]. The curves composed of gray dots are from the July 13, 1989 PFC Report JA-89-34 [Type 3].

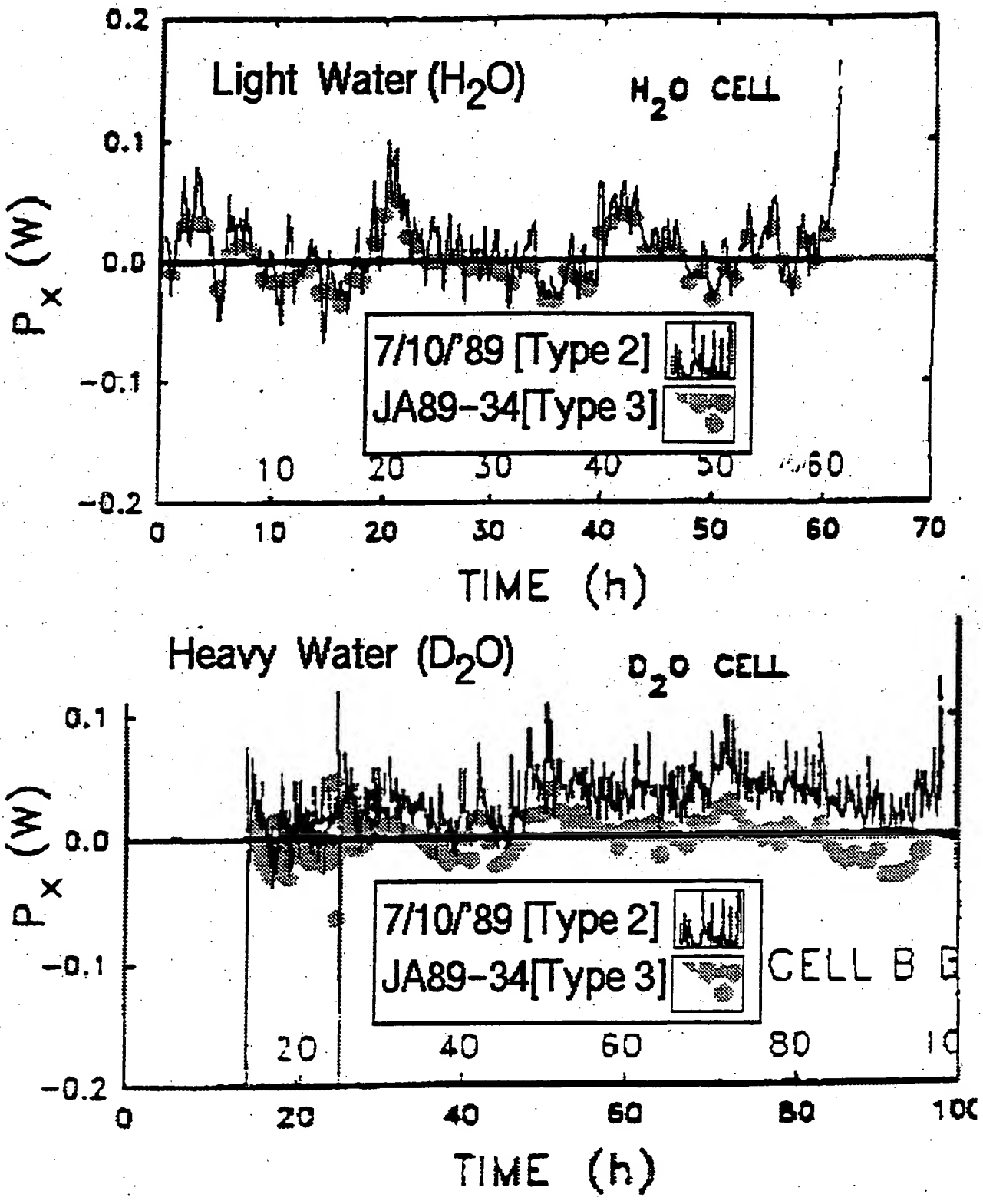

Figure 3 - LINEAR CHANGES TO THE PHASE-II D_2O TYPE 2 CURVE

The upper section shows a Phase-II D_2O Type 2 curve (continuous high frequency) which is superimposed upon a low-pass [time-average] curve (light grey curve).

The mid and lower sections show the Type 2 curve, with the low-pass curve upon it, and the published curve [J. Fusion Energy (1990), Type 3_B] in black with its characteristic thicker line and accompanying dots. Also shown are linear displacements of the low-pass curve. In the midsection, four time-varying fits [A=0] are shown; whereas in the lower section three fixed baseline shifts [B=0] can be seen (in varying shades of grey).

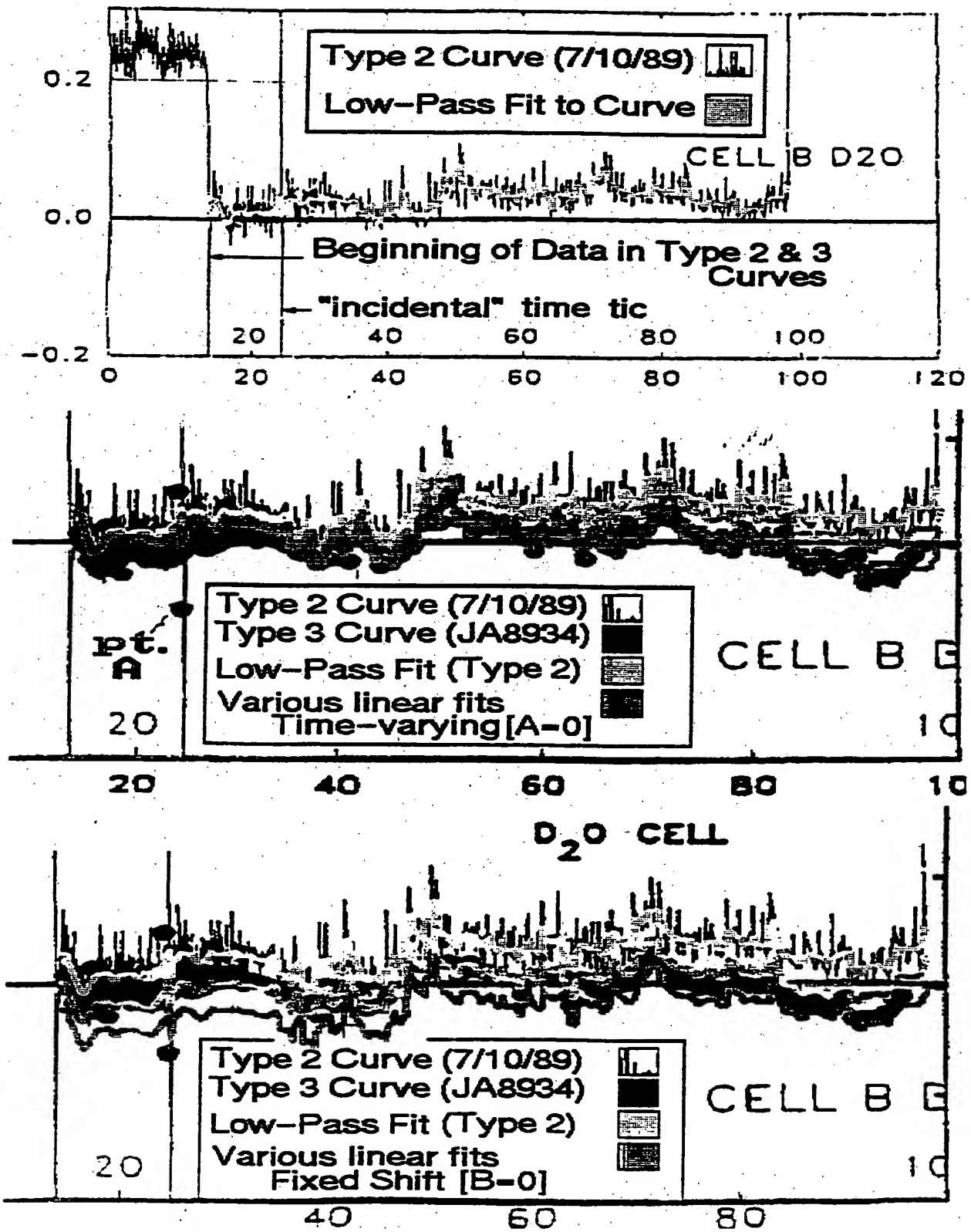

Figure 4 - EXAMINATION OF TYPES 2, 3, AND 4 CURVES

These three sets of curves examine some of the PFC D_2O curves.
Upper: Two curves enable a count of data points in 40 hours.
Mid : Disappearance of points occurs in Type 3 -> Type 4.
Lower: Shifted point (A) drifts by 24 milliwatts.

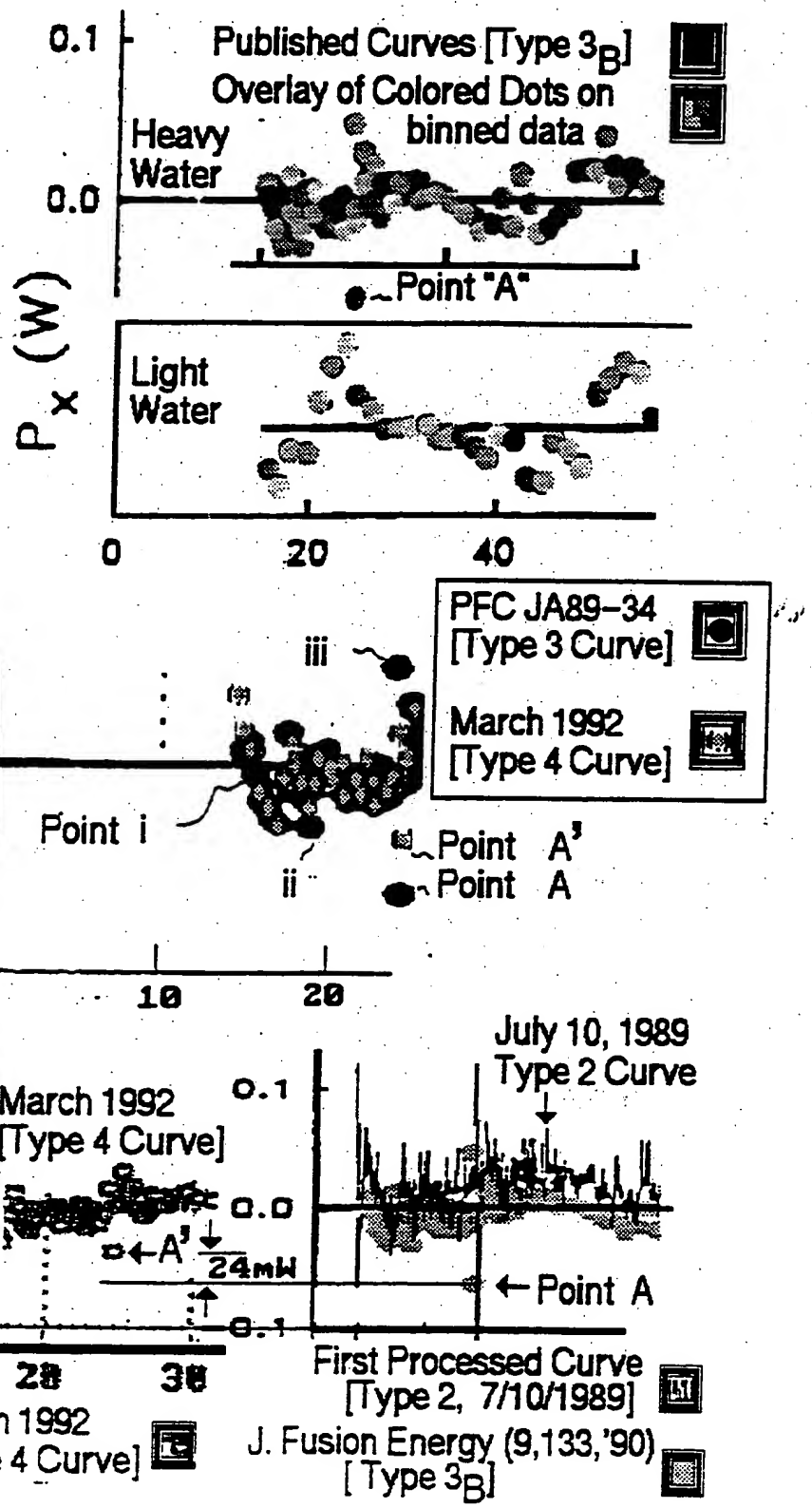

Figure 5 - HYPOTHETICAL EXAMINATION OF BASELINE SUBTRACTION

These three thought-experiments involve hypothetical "successful" experiments which produce excess heat. The impact of that heat upon the input power heater curves (1a, 1b, 1c) is to produce decreases characterized by ramp functions (1a and 1b) and a step function (1c). Two heater power curves (1b, 1c) have additional baseline drift. These three curves are treated by either of two methods (either curve sets 2 or 3) to produce the respective derived excess heat curves (sets 4 or 5).

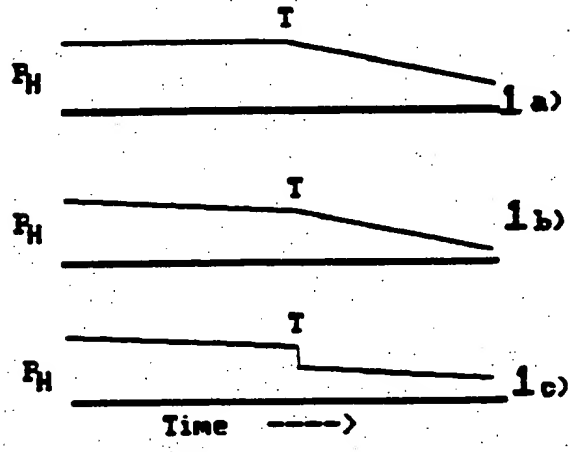

HYPOTHETICAL SUCCESSFUL EXPTS

GENDANKEN EXPERIMENT
TO INVESTIGATE
BASELINE-SUBTRACTION
PARADIGMS USED
TO EVALUATE
EXCESS ENTHALPY
EXPERIMENTS

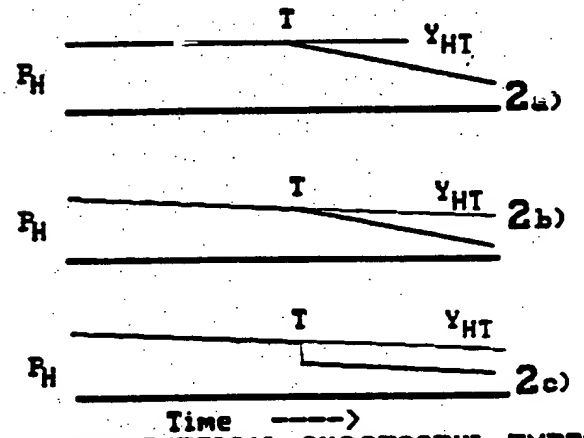

HYPOTHETICAL SUCCESSFUL EXPTS
'TRUE' REGRESSION FIT [Y_{HT}]

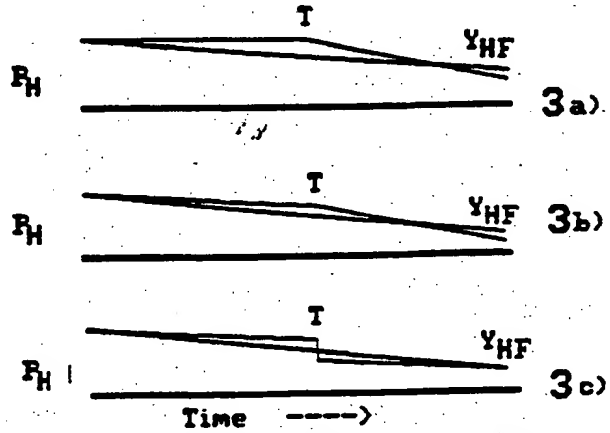

HYPOTHETICAL SUCCESSFUL EXPTS
'FALSE' REGRESSION FIT [Y_{HF}]

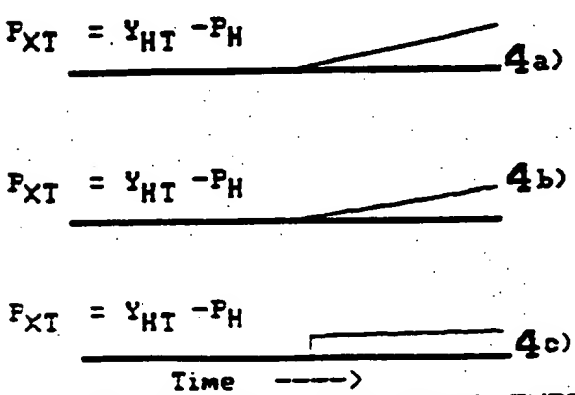

HYPOTHETICAL SUCCESSFUL EXPTS
'TRUE' REGRESSION FIT [Y_{HT}]

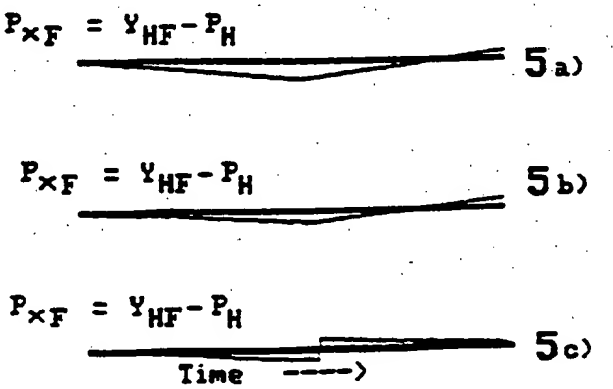

HYPOTHETICAL SUCCESSFUL EXPTS
'FALSE' REGRESSION FIT [Y_{HF}]

Figure 6 - CORRECTED EXCESS HEAT FOR PHASE-II D_2O EXPT.

These are the derived excess heats obtained by two alternative methodologies.
Upper: Derived using the initial baseline correction technique.
Lower: Derived using the varying thermal pathlength model.

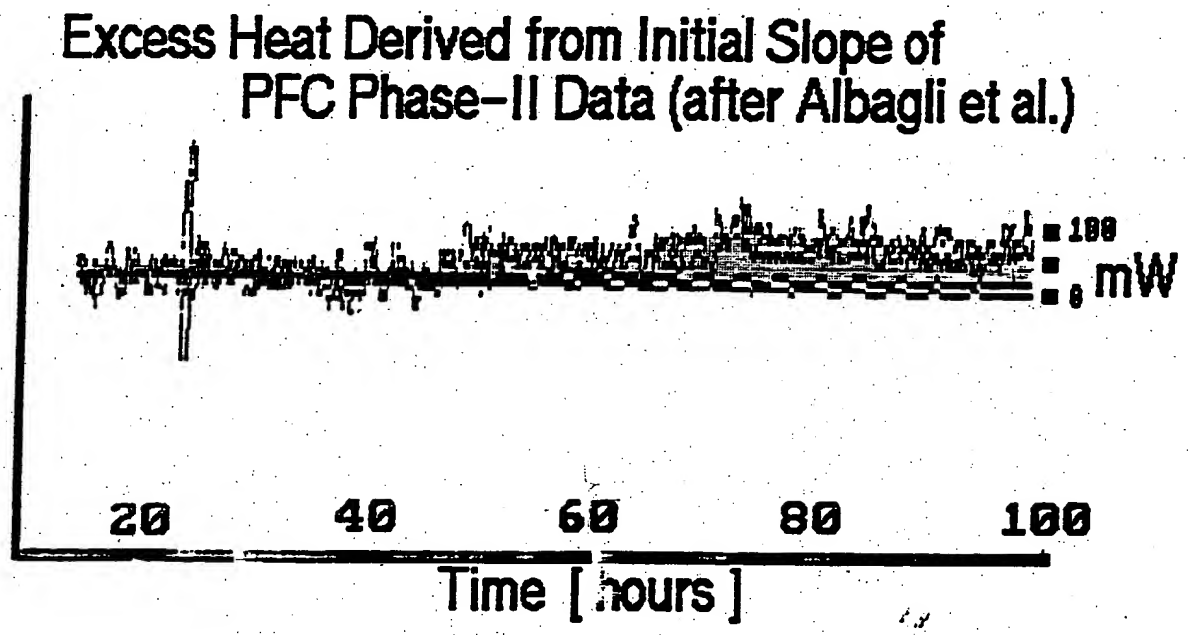

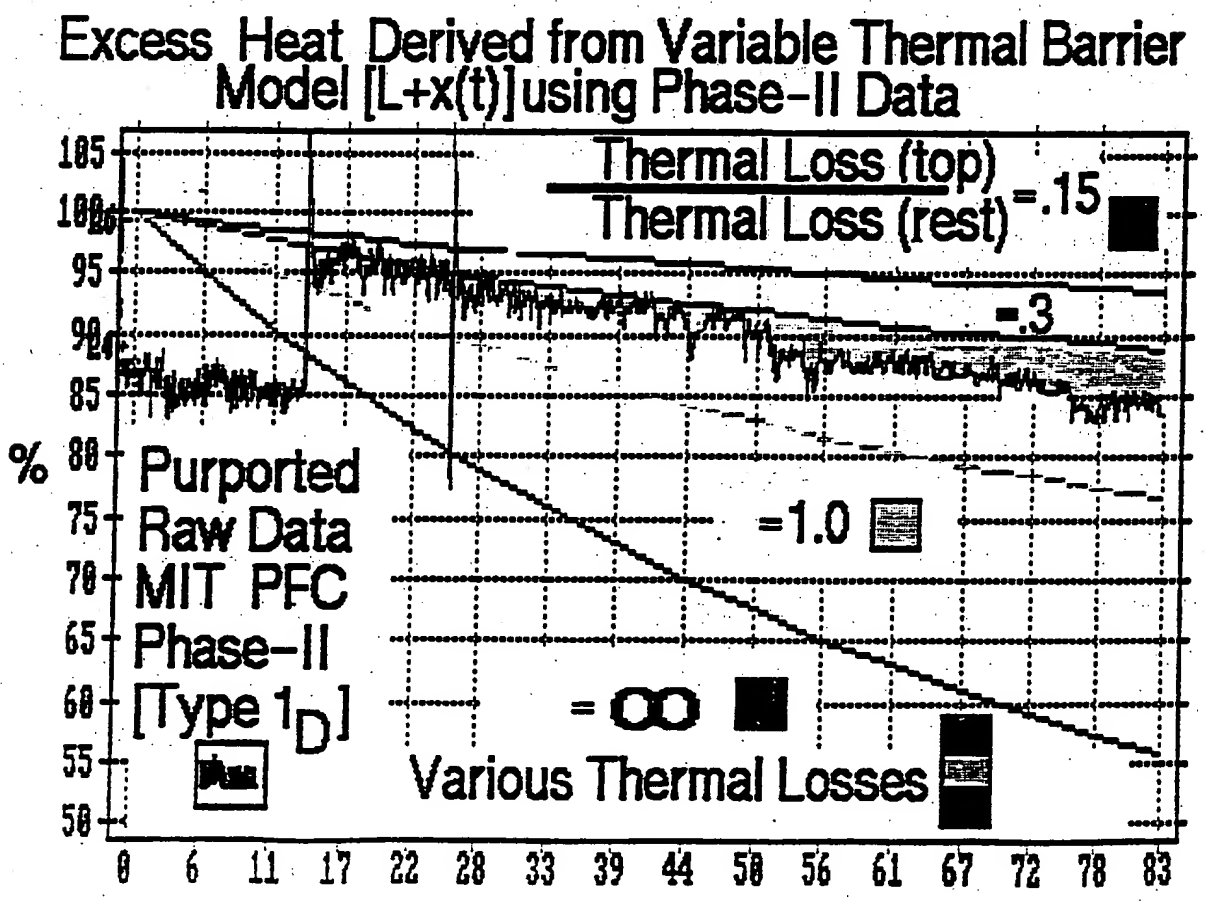

2ND Annual CONFERENCE PROCEEDINGS

T. Bressani, E. Del Giudice, G. Preparata, Editors, VOLUME 33 - THE SCIENCE OF COLD FUSION, Conf. Proceedings, published by Societa Italiana di Fisica, 46 figs, 528 pages.
Orders should be sent to:
Societa Italiana di Fisica, Redazione
Via L. Degli Andalo, 2
40124 Bologna, BO, ITALY

Price is 110,000 Lira. Send U.S. $90 for surface mail or U.S. $110 for expedite by air mail. Make checks payable to the Societa Italiana di Fisica.

NEW FROM FUSION FACTS - Fusion Briefings

Fusion Briefings presents an overview of what is happening in the areas of research, business, patents, and the companies involved with cold fusion. Designed for the manager who needs to be aware of cold fusion development, but does not require all of the technical details, Fusion Briefings lets him track the developments that will have the most impact on his business.

Fusion Briefings is airmailed to you for only $49.00 for twelve issues. Single issues are $5.00 per issue. Mention to us that you saw this notice and we will send you a free complimentary copy.

NEW BOOK AVAILABLE - Impact Studies

"Fusion Impact Studies" (Second Edition) is now being published. Available to FF subscribers for $15.00. Updated with new statistical information and graphs to illustrate and support the information, "Fusion Impact Studies" is a timely resource book detailing the impact that enhanced energy systems will have on eight industries and the government.

Fusion Facts Subscription Office

P.O. Box 58639
Salt Lake City, UT 84158
Phone: (801) 583-6232
FAX: (801) 583-6245

Street Address: 505 Wakara Way
Salt Lake City, UT 84108

***FUSION FACTS* Each Issue Mailed First Class.**

12 ISSUES.....	$ 345
36 ISSUES.....	$ 900

***FUSION FACTS* SINGLE ISSUES**

CURRENT ISSUES EACH.....	$ 35
3 MONTHS OR OLDER ISSUES EACH...	$ 10

SUBSCRIPTION REQUEST

For your convenience you can order by phoning (801) 583-6232, or FAX (801) 583-6245, or use the Mail.

Send *Fusion Facts* to:

NAME:_____

COMPANY:_____

PO BOX, DEPT:_____

CITY:_____

STATE_____ZIP_____

We accept VISA or MASTER CARD
Send check or money order with order and receive one extra issue free. Make checks payable to *Fusion Facts*.

PREMIER ISSUE • Welcome to the Water-Fuel Age

"COLD FUSION"

A Wayne Green Publication

May 1994 Vol.1 No.1

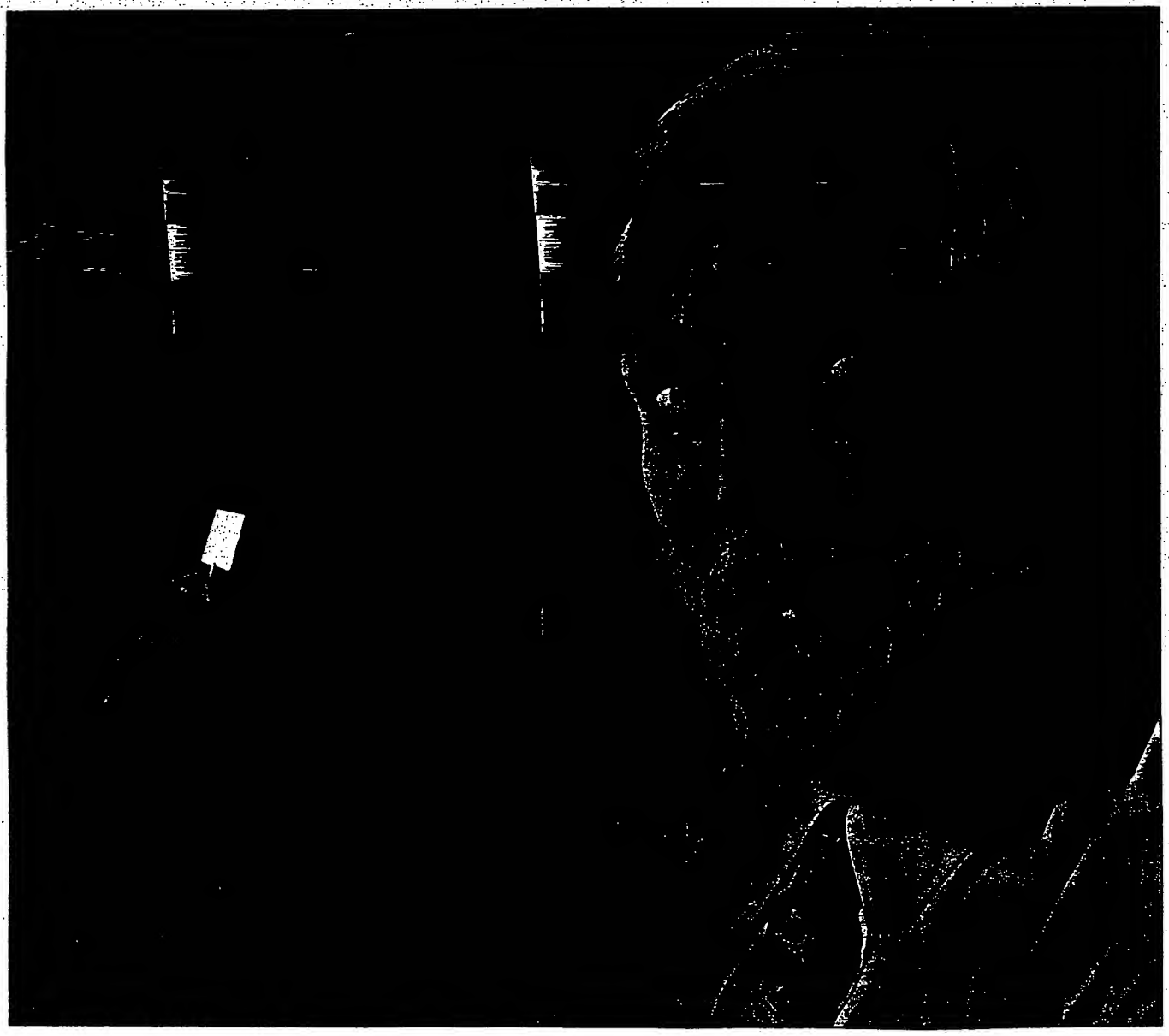

After 34 Years at Los Alamos, Dr. Edmund Storms now pioneers cold fusion research. p. 43

U.S. $10.00
Canada $13.00

05

Table of Contents

Features

Columns

Departments

Premier Issue, May 1994

About our cover

Free-lance photographer Eric Swanson of Santa Fe, New Mexico, shot this portrait of Dr. Edmund K. Storms who is holding one of the palladium cathodes that were used in his successful cold fusion experiments. Dr. Storms carried out his cold fusion work at the Los Alamos National Laboratory, and continues to be a pioneer in the field.

"COLD FUSION" Magazine

Volume 1, No.1, May 1994

Publisher
Wayne Green
Vice President
James Kendrick
Associate Publisher
John Grow, Sr.
Editor
Eugene F. Mallove, Sc.D.
Managing Editor
Stuart Norwood
Contributing Editors
Lawrence P.G. Forsley
Jed Rothwell
Dr. Mitchell R. Swartz
Christopher Tinsley
Editorial Assistant
Chris Aubert
Circulation Manager
Harvey Chandler
To Subscribe: 1-800-234-8458
Graphic Arts Manager
Linda Drew
Graphic Designer
Pamela J.Veenstra
Graphic Services
FilmWorks, Inc., Hancock, NH
UltraScan, Hudson, NH

"Cold Fusion" Magazine (ISSN 1074-5610) is published monthly by Wayne Green Inc., 70 Route 202 North, Peterborough, NH 03458. Subscription price: $98 U.S., $122 foreign. POSTMASTER: Send address changes to "Cold Fusion", PO BOX 4926, Manchester NH 03108.

"Cold Fusion" Magazine
70 Route 202 North
Peterborough, NH 03458
(603) 924-0058
(800) 677-8838
Fax (603) 924-8613
To subscribe, call: 1-800-234-8458

EUGENE F. MALLOVE
SC.D.

Why "*Cold Fusion*"?

Dennis Cravens, working with equipment that cost him less than $5,000, much of it from Radio Shack and the local hardware store, has been doing what lots of well-known scientists claim is totally impossible—he's producing "cold fusion" excess heat, and he's been doing it in a lab that he set up in his garage in Vernon, Texas.

Dennis is a professor of chemistry and physics at Vernon Regional Junior College, and he's by no means alone in his success with this new technology. Hundreds of researchers around the world—at universities, national laboratories, and some of the largest corporations in the world—have confirmed the claims of scientists Martin Fleischmann and Stanley Pons. On March 23, 1989 at the University of Utah, they said that their research had shown something very mysterious was happening when an electrical current was passed between a palladium and a platinum electrode in a solution of heavy water and lithium salt. They were getting more power out as heat than they were putting in as electricity.

When they added up all the excess energy their cell had produced, the amount was so large that it could not be explained by a mere chemical reaction—of any kind. The process became known as "cold fusion," for the lack of a better explanation, and because Fleischmann and Pons were using the very same deuterium form of hydrogen that scientists with billion-dollar machines were using to try to create practical *hot* nuclear fusion at temperatures of millions of degrees.

Dennis Cravens doesn't have a $30 million dollar a year budget like the hot fusion laboratory at MIT in Cambridge, Massachusetts, the Plasma Fusion Center, or the Princeton Plasma Physics Laboratory in New Jersey, where new results often capture headlines—even though the hot fusioneers have never produced *a single watt* of excess energy. (If and when the hot fusioneers do achieve excess energy, it will be with a blast of lethal neutron radiation that will have to be tamed.) Professor Cravens' work is completely and deliberately ignored by the U.S. government, even though major Japanese corporations have embraced this upstart technology.

Cravens has already accomplished what the hot fusioneers have never done and will never do with their $500 million a year program. He gets more heat energy out of his tiny liquid cells with palladium or nickel electrodes than he puts in as electrical energy—and he gets it with no radiation. You can read about his experiments in this issue, and—if you are then bubbling over with enthusiasm about "cold fusion"—you may want to try them yourself. He'll point the way.

Something new under the sun

Water as fuel? Pollution-free power? How can unlimited power from water be real, when scientific officialdom supposedly investigated the Fleischmann and Pons claims and found them without merit back in 1989? More to the point, why are some scientists ridiculing anyone who even *suggests* investigating "cold fusion?" Where does all this excess heat in the opposition to cold fusion come from? Is it intellectual arrogance on the part of some scientists and the fear of pack journalists that they may have to eat crow?

Any student of history will tell you that following many major breakthroughs in science and technology, the pioneers were ridiculed by the establishment, often with the enthusiastic support of the news media. Nothing has changed. Did the media cover last December's Fourth International Conference on Cold Fusion on Maui, which was sponsored by the Electric Power Research Institute? If they had, you would have seen cover stories on *Newsweek* and *Time*.

The Maui conference showed, as had the previous international conference in Nagoya, Japan in October, 1992, that hundreds of researchers around the world are achieving the same astonishing results in an increasing variety of reproducible, solid experiments. Unlike the hot fusion people, "cold fusion" researchers aren't trying to mimic the nuclear reactions inside stars, which occur at millions of degrees. So what is this "cold fusion?" Is it a new form of nuclear energy or something else even more remarkable that *seems* like nuclear energy, because it gives out so much continuous power—far more, apparently, than can be explained by chemistry. Yes, there is something new under the Sun, only it doesn't work like the Sun!

If this technology develops as the pioneers in the field expect, within a few years we will be seeing the beginning of the end to our dependence on oil, coal, and natural gas—and the end of much environmental pollution. This new low-cost power source may change the world far more than the automobile, the airplane, the telephone, or the computer. The predictions are that this new process—in all its variants—will provide lower cost power than hydroelectric generators, photovoltaics, wind-driven generators, and nuclear power plants. The generators should be small, light, and inexpensive enough to power cars, homes, and aircraft. Formidable industries stand to lose if they are unable to

adapt to the expected rapid development of cold fusion energy.

Water as fuel?

It sounds crazy until you stop to think about it. Sure, for thousands of years we knew we could get energy out of matter through chemical reactions—ordinary fire does that with wood and fossil fuels. Then in the 1930s and 40s we learned how to split the nuclei of uranium atoms to get fission power and the atomic bomb. Soon thereafter, scientists developed the even more powerful hydrogen bomb, which gets energy out of matter by uniting—fusing—forms of hydrogen nuclei. Now science and technology are confronted with what is indisputably another way of getting energy out of matter, a gentler way of tapping it: "cold fusion." Though its detailed mechanism remains unexplained, there is simply no longer any doubt that cold fusion works. To deny the scientific evidence for cold fusion—as many have attempted—is to stand science on its head: to suggest that past "accepted theory" can legitimately falsify thousands of experiments that appear to contradict that theory.

Because of "cold fusion", the world as we know it is about to end.

This is very good news. The fossil fuel age, the Oil Age, will in all probability begin to end during the waning years of the 20th Century, and we intend to be the herald of this process. After five years of controversy and neglect, an astonishing discovery—"water as fuel"—has begun to blossom around the world. "Cold fusion," Utah's "miracle or mistake" of the spring of 1989, turned out to be a real phenomenon after all. Hence this magazine: the world's first devoted exclusively to "cold fusion" and possibly the world's first to have mysterious quotation marks in its name! We do know what we are talking about—excess energy; we just don't know exactly what causes it! Our cold fusion theorist friends have plenty of ideas, and they will be telling you about them in our pages.

Cold fusion has now reached a critical stage in which improved communications will play a key role. The field is in ferment and expanding explosively. In one of history's classic ironies, the 1989 announcement of "excess energy from water" in a relatively simple table-top experiment—possibly by a heretofore unknown form of nuclear energy—occurred less than 12 hours before the Exxon Valdez caused a massive oil spill into the waters off the coast of Alaska. There was an initial media hoopla over the cold fusion story, but the press then lost interest as it became more difficult to discern the truth amid claims and counter-claims of angry chemists and physicists. With few exceptions, journalists bought the notion that cold fusion was nothing but hot air. "Pathological science" became the common insult, as few noticed that *pathological skepticism* about a new phenomenon was the real problem. Contrary to the media's perception, cold fusion never died and was certainly never disproved; it simply went underground as groups of courageous scientists in over a dozen countries mounted a concerted effort to understand and reproduce the mysterious phenomenon. Thanks to their hard work, it has survived.

Where does all this excess heat in the opposition to cold fusion come from? Is it intellectual arrogance on the part of some scientists and the fear of pack journalists that they may have to eat crow?

Scientists in laboratories around the world are closing in on an explanation. Some cold fusion researchers suggest that the nuclei of hydrogen isotopes participate in heretofore unknown nuclear reactions within the confines of metal atomic lattice structures leading to virtually radiationless nuclear energy. Others say that cold fusion manifests as very faint low-level nuclear reactions, but that its more important aspect for technology—the prodigious heat evolution, which is far beyond known chemistry—comes from a new type of "super-chemistry," which affects not the nucleus but the outermost part of an atom, its electron "cloud."

Whatever nature's long-hidden secret that allows us to use water as fuel, cold fusion phenomena are real beyond any reasonable doubt. Excess power production and low-level nuclear effects have been convincingly demonstrated and made substantially reproducible with a remarkable variety of techniques. Moreover, laboratory cold fusion experiments have begun to exhibit astonishingly high levels of power intensity, surpassing in small volumes the powers found even in fission nuclear reactors—many kilowatts per cubic centimeter, but without associated radiation.

Is cold fusion about to be commercialized?

Yes, indeed! The Japanese Ministry of International Trade and Industry (MITI) has launched a massive "New Hydrogen Energy" program to do just that. It is conservatively estimated that Japanese corporations are already spending $90 million/year on cold fusion, a figure sure to increase dramatically as practical prototype devices emerge in the next few years—or months. In the U.S., where anti-cold fusion sentiment has been particularly intense, the Electric Power Research Institute, the $500-million/year research arm of the electric utility industry, continues its cold fusion R&D program. Last December it organized the Fourth International Conference on Cold Fusion, which was held on Maui. Other entrepreneurial cold fusion companies are springing up in the U.S. This corporate involvement is perhaps the most important reason we decided that the time was ripe for *"Cold Fusion."*

Wayne Green, our New Hampshire publisher, whose magazines helped accelerate the personal computer and other

technology revolutions, says that a publication in a new technology area serves three purposes: "It speeds up technical development by providing faster and better communications between the researchers and developers in the new field; it not only helps attract new people to the field, it enables them to get up to speed much faster than they could waiting for books to be published; and, probably of even greater importance, a publication makes it possible for entrepreneurs to provide products to help the new field grow. It makes a new industry develop faster."

There you have it, our mission: to accelerate the "cold fusion" revolution by disseminating the truth about scientific and technological developments in what will surely be one of the most significant technology upheavals in history. We will publish the latest discoveries and findings in a manner that can be understood by a broad spectrum of people. Our intended audience is not restricted to scientists and engineers, though we will certainly aim to provide these experts with timely and challenging material that will help them in their work. "Cold Fusion" will also explore the spectacular changes in store for civilization in the coming energy revolution—technological, as well as economic, social, and political.

We will also expose the strange politics of opposition to cold fusion, both past and present, which has so hamstrung research on the phenomenon. Part of that role will be to comment on how cold fusion is or is not being treated in the news media. We promise that our magazine will expose the numerous instances in which the media have ignored the facts, disparaged honest research, and stood science on its head.

Since the parallel is so striking, it is worth recalling what happened to two American inventors whose initial success occurred just over 90 years ago. On December 17, 1903, Wilbur and Orville Wright realized an age-old dream when they launched the world's first successful heavier-than-air flying machine. For five years, their millennial accomplishment went largely ignored by the scientific establishment and the major media, even though the brothers Wright made no secret of their invention. For years leading up to a dramatic demonstration at Fort Myer, Virginia, they tested their aircraft in full view of commuters on an interurban railroad near Dayton, Ohio. Yet for five years the Wrights were considered cranks by U.S. government bureaucrats who refused to take them seriously! So, in search of support the Wrights took their invention to France.

Formidable industries stand to lose if they are unable to adapt to the expected rapid development of cold fusion energy.

A few years ago, two other scientist-inventors, one American and one British, took another millennial invention to France: "cold fusion." Drs. Pons and Fleischmann are now working on cold fusion energy technology in the well-equipped Japanese-financed IMRA Europe S.A. laboratory near Nice, France. They left behind the scientific bigotry against their discovery that was unleashed in the U.S. The Japanese consortium of industrial giants has given them research funding. Meanwhile, in hundreds of other laboratories the world over, researchers explore an astonishing array of physical phenomena that stem from the original discovery of the cold fusion pioneers. It has been five years since the announcement in Utah, and the "Fort Myers of cold fusion" approaches—the demonstration of prototype technology.

Like flight, which we take for granted today, "cold fusion" will some day be taken for granted. But only five years into the Cold Fusion Age, as we launch *"Cold Fusion"* Magazine, we can hardly imagine anything nearly as exciting and pregnant with virtually infinite possibilities.

Our pages will offer much more than theories on the frontiers of science. In the exciting months to come, "Cold Fusion" will feature some of the most knowledgeable people in the world writing about what the cold fusion revolution is likely to mean for the world. How will cold fusion energy begin to replace the existing energy infrastructure? What will cold fusion automobiles be like, and the "cold fusion home"? What about the impact of water-fuel energy on agriculture, financial markets, geopolitics, and the environment? These will be a continuing focus of this magazine, in addition to detailed reports about the ongoing science, technology, and business of cold fusion. We expect that you will be thrilled with what future issues bring to you.

...bout the editor ...

"Cold Fusion" Editor Dr. Eugene F. Mallove brings to the magazine broad experience in high technology engineering with Hughes Research Laboratories, TASC (The Analytical Science Corporation), Jaycor Systems Division, Northrop Precision Products Division, and MIT Lincoln Laboratory. Since 1991, Dr. Mallove has worked as a consultant to U.S. corporations conducting and planning R&D in cold fusion. He is the author of three science books for the general public, including the Pulitzer-nominated book on cold fusion, "Fire from Ice: Searching for the Truth Behind the Cold Fusion Furor" (John Wiley & Sons, 1991). He has taught science journalism at MIT and at Boston University; he was Chief Science Writer at the MIT News Office when cold fusion erupted. Prior to that, he was a top science writer and broadcaster with the Voice of America in Washington, DC, and also wrote science and technology articles for magazines and newspapers, including MIT *Technology Review* and *The Washington Post*. Dr. Mallove holds a Doctoral Degree (Sc.D.) in Environmental Health Sciences (Air Pollution Control Engineering) from Harvard University, and a Master of Science Degree (SM, 1970) and Bachelor of Science Degree (SB, 1969) in Aeronautical and Astronautical Engineering from the Massachusetts Institute of Technology.

"It is beyond serious dispute any more that anomalous amounts of energy are being produced from hydrogen by some unknown reaction...Now, please fasten your seatbelts. After these modest daydreams, I want to really stretch your imaginations."

2001: The Coming Age Of Hydrogen Power...

And the Dawn of a New Era

by Arthur C. Clarke

Fellow of King's College, London
Chancellor, International Space University
Chancellor, University of Moratuwa

What follows is Arthur C. Clarke's memorable address at the Pacific Area Senior Officer Logistics Seminar (PASOLS) in March, 1993 at the Hilton in Colombo, Sri Lanka. Among the audience were Adm. Larson, Commander In Chief of the Pacific Fleet, Lt. Gen. Stackpole of the Marines, and leading officers of the military forces from many other countries, including Australia, India, Japan, Korea, Russia, the Philippines, Sri Lanka, and others.

Admiral Larson, Lieutenant General Stackpole, Major General Abayaratna, distinguished guests, I'm very happy to be here today, even though I should really be in Washington this week. All my friends will be gathered in the Uptown Theatre to celebrate the 25th anniversary—I can't believe it—of 2001: A Space Odyssey.

Now, that movie provides a very good example of how difficult it is to predict the future. You may recall that in the film we showed the Bell system and PAN-AM—well, they've both gone, long before 2001. But I'm happy to see that the Hilton, which we also showed in 2001, is still here, though not yet in orbit!

This proves how impossible it is to predict social and political developments: Who could have imagined what's happened in Europe during the last few years? However we can, to some extent, anticipate technological developments, by observing what's going on in science and engineering. But the problem there is predicting when things will happen, even though one can be quite certain that they will.

A good example is provided by my 1945 paper on communications satellites, which I imagined would be large, manned space-stations. When I wrote that, World War II was still in progress, and I was working on Ground Controlled Approach Radar, which had the then enormous number of something like a thousand vacuum tubes in it, at least one of which would blow everyday.

So it was impossible to believe, back in 1945, that TV relay stations could operate without a staff of engineers changing tubes and checking circuits. But of course, the transistor and the solid-state revolution came along within a few years, and what I'd assumed would have to be done by large manned stations could be achieved by satellites the size of oil drums. So everything I imagined would be done around the end of the century happened decades in advance.

I'm going to say very little about communications satellites and the communications revolution, because you are all very familiar with what's happened here. Essentially anything we want to do in this area can now be done. And satellites have not only transformed communications, but meteorology and navigation. You all know what the GPS (Global Positioning System) did during Desert Storm. However, the satellites I have always been particularly interested in are what I call "Peacesats," the reconnaissance satellites largely responsible for the Cold War never becoming a hot one, ones which created a transparent world, and vastly reduced the threshold of uncertainty. But I won't say any more about satellites, because (if I may be allowed a commercial) I've just written a whole book about them, How The World Was One.

So now I want to change the subject completely, to something perhaps even more important than the communications revolution. But first I'd like to mention a bit of forgotten history.

In December, 1903, Orville and Wilbur staggered off the ground in North Carolina, and made the first controlled flight in a heavier-than-air machine. As a result, the North Carolina state motto is "First in Flight," which you military men may well think a rather unfortunate choice of words.

Yet for five years, Washington didn't believe that the Wright brothers had actually flown—because everybody knew it was impossible. Leading scientists were then still writing papers proving it couldn't be done. Not until the Wrights went to France and started giving public demonstrations did the boys in the War Department say, "My goodness, these things really can fly. Perhaps they may even be useful for reconnaissance. We'd better look into it." And they did—five years late.

Physics Letters A 170 (1992) 265–272
North-Holland

PHYSICS LETTERS A

Nuclear product ratio for glow discharge in deuterium

A.B. Karabut, Ya.R. Kucherov and I.B. Savvatimova
Scientific Industrial Association LUTCH, 24 Zhelesnodoroznaja Street, 142100 Podolsk, Moscow Region, Russian Federation

Received 24 September 1992; accepted for publication 28 September 1992
Communicated by J.P. Vigier

New results for glow discharge in deuterium calorimetry are presented. In separate experiments a heat output five times exceeding the input electric power was observed. The result for the charged particle spectrum measurement is presented. Charged particles with energies up to 18 MeV and an average energy of 2–4 MeV were seen. Beams of gamma-rays with energies of about 200 keV and a characteristic X-ray radiation were registered. The summed energy of the registered products is three orders short of the values needed to explain the calorimetric results.

1. Introduction

After the known work of Fleishman and Pons on neutron and excessive heat registration at heavy water electrolysis [1] many attempts to reproduce this result were reported [2].

In our experiments we used a low voltage electric discharge at a low deuterium pressure. This approach is much more suitable for X-ray and charged particle registration because the detectors can be placed in the discharge chamber itself. In our previous work we saw an excessive heat, a correlation of the heat release values with the neutron flux change and we measured the neutron flux by various methods including silver foil activation [3]. By measuring the gamma spectrum we found a radioactive isotope formation, we measured the neutron spectrum in which neutrons with an energy up to 17 MeV could be seen, and achieved reproducibility of the effect [4].

Our next work was devoted to the prolongation of the nuclear reaction, an increase of the excessive heat values and an increase of the measured parameters: X-ray and gamma-ray spatial distribution, charged particle registration, etc.

As methods using electronics are not immune for electric pick-ups we tried to use independent methods wherever this was possible – activation, tracks, photoemulsion, for absolute nuclear product flux measurements. We also performed spectral measurements after the discharge switch-off, allowing one to improve the reliability of the results.

Complex measurements of the fluxes and the energy spectra of the neutrons, gamma emission, X-rays and charged particles allowed us, putting aside the nature of the effect, to compare the heat release and the energy carried by the nuclear reaction products.

2. Experimental

The experimental device (fig. 1) consisted of vacuum chambers with diameters of 1.5×10^{-1} and 2×10^{-1} m and a volume of 10^{-2} m^3. The vacuum system allowed a residual pressure of $\sim10^{-3}$ Pa. The gas fill system was supplied with multi-stage gas purification cells. The cathode assembly consisted of a quartz insulated thin-walled stainless steel holder with a molybdenum heat collector at the end. The heat collector has channels for cathode thermocouples. The cathode sample is placed on the collector and fastened with an Al_2O_3-insulated cap. Usually the cathode sample (cathode) was in the form of a foil 10^{-4}–10^{-3} m thick with an area of $\sim10^{-4}$ m^2. As a cathode we used various materials, such as metals, alloys and ceramics. All excessive heat results and the largest nuclear product fluxes were achieved with specially treated palladium. The anode assembly

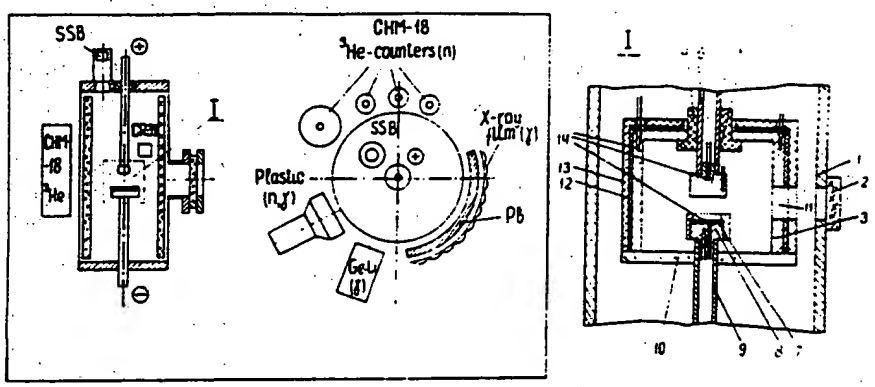

Fig. 1. Experimental device. (I) Calorimeter design. (1) Vacuum chamber, (2) inspection window, (3) heat collector, (4) insulator, (5) anode, (6) anode holder, (7) cathode sample, (8) cathode holder, (9) thin-walled holder, (10) quartz plate, (11) inspection window, (12) aluminium oxide insulation, (13) screening insulation, (14) thermocouples.

consisted of a quartz insulated thin-walled molybdenum tube holder with thermocouple channels and a massive molybdenum end. In the chamber's upper flange an appendix was made for silicon surface barrier detectors (SSB). The chamber had a quartz inspection window. In separate experiments the insulating quartz tube or the calorimeter were inserted into the discharge chamber. X-ray films or photoemulsion cassettes, CR-39 detectors and various screens could be inserted into the chamber. All other detectors for neutron and gamma-quantum registration were placed outside the chamber (see fig. 1).

The typical deuterium pressure in the chamber was 3–10 Torr, the discharge voltage 100–500 V and the discharge current 10–100 mA. We used both transformer-based and thyristor-based electric power stabilizers for the electric feed.

3. Calorimetry

We used the same heat-loss-type calorimeter as described in ref. [3]. The calorimetric insert is shown in fig. 1.

We used W–Re thermocouples in the cathode and the anode and electrically insulated CC thermocouples in the heat collector. The thermocouples were the standard type used for nuclear reactor thermometry, providing a better than 1% accuracy. The signal from the thermocouples was registered with KCII-4 automatic registrators, providing a 0.5% accuracy and a reaction time of 0.1 s. The electric discharge current and voltage were registered with the same registrators, thus providing discharge power measurements with ~1% accuracy.

The calorimeter calibration was done in hydrogen and in deuterium, using a "worn-out" palladium cathode (with no neutron or gamma emission). The latter approach allowed us to eliminate the difference in heat conductivity of hydrogen and deuterium. We used two approaches to measure the heat: the calorimeter integral efficiency and the heat loss curves for the calorimeter elements. The former is much easier to process and the latter is more accurate, but requires the use of three calibrations for every calorimeter element instead of one integral. For interesting cases we processed the results both ways.

The amount of heat measured by the calorimeter consists of an input electric energy $Q_{el} = IV\tau$ (I is the current, V the voltage, τ the discharge glow time) and an excessive heat Q_n. We measure this heat as a sum of elements: $Q_m = \sum Q_i$, where

$$Q_i = C_i M_i \Delta T_i .$$

Here C_i, M_i, ΔT_i are, respectively, the heat capacity, the mass and the temperature difference for the cathode, the anode and the heat collector.

4. Integral efficiency method

The heat release in the calorimeter consists of Q_{el}, resulting from the electric discharge glow, and the excessive heat from the nuclear reaction Q_n (if such

a thing exists). Then the measured heat Q_m is

$$Q_m = (Q_n + Q_{el})\eta(Q),$$

where $\eta(Q)$ is the calorimeter efficiency, depending on the measured heat. When $Q_n = 0$ we can write

$$\eta(Q) = Q_m / Q_{el}.$$

It is evident that $\eta < 1$, because in the quasi-stationary regime Q_{el} exceeds Q_m by an amount equal to the conductive losses of the cathode and the anode holders and the convective losses. The thermal radiation losses are small due to the calorimeter design and the small heat collector temperature ($T \lesssim 100°C$).

If we assume the heat registration to be independent of the physical nature of the heat source, which is quite reasonable because in our experiments the neutron and gamma emission which can leave the calorimeter is relatively small (usually less than 10^{-5} W), then by measuring $\eta = \eta(Q)$, Q_m and Q_{el} we can determine Q_n:

$$Q_n = Q_m/\eta - Q_{el}.$$

So the calorimeter calibration consists in measuring $\eta = \eta(Q_m)$ with regimes close to real experiment.

5. Heat loss method

At every given moment for every calorimeter element (cathode, anode and heat collector) the input power is compensated by an element temperature change $W = \partial Q/\partial\tau$, where $Q = CM\Delta T$. When the discharge is switched off every element temperature has a corresponding heat loss power (conductive and convective losses). Thus by measuring the cooling curve one can define the heat loss power for each temperature and the calibration consists in measuring $W_{losses} = W_{losses}(T)$ for each calorimeter element.

A multiple calibration processing both methods showed a reproducibility of the calibration with an accuracy of ~4% in the interval of absorbed heat 100–1000 J and of 10% at 5 kJ. The degradation of the accuracy with temperature is supposedly related with the instability of the convective flows in the chamber with increasing heat gradient. These values by far exceed all other experimental errors and define the accuracy of the measurements.

As an example fig. 2 shows the change of the electric energy Q_{el}, the measured heat Q_m and the real heat Q corrected for the time. Figure 3 shows the change of the electric power and the excessive power with time. This curve is obtained by differentiating the curve in fig. 2.

The best result of 78 calorimetric experiments is a 33 W excessive power at a 500% efficiency ϵ, where

$$\epsilon = (Q_m - Q_{el})/Q_{el}.$$

Without special means the average values for the excessive heat time and the efficiency are 20 min and

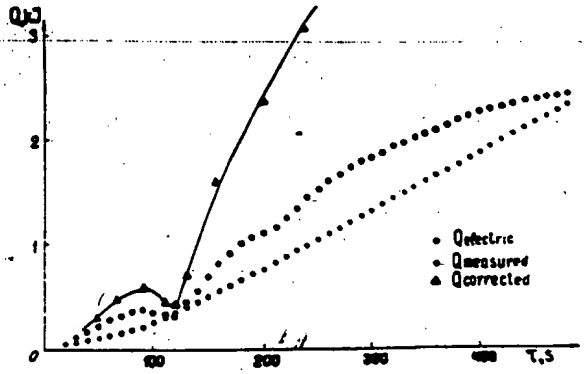

Fig. 2. Time dependence of the amount of heat in the calorimeter. Q_{el} is the electric discharge heat, Q_m the heat measured by the calorimeter, $Q_{cor} = Q_m/\eta$, with η the calorimeter efficiency.

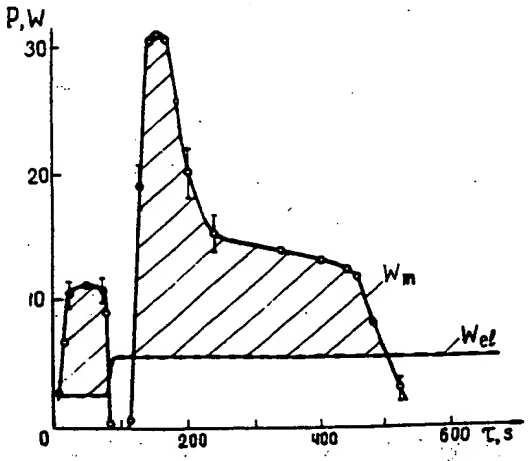

Fig. 3. Time dependence of the power released in the calorimeter. W_m is the power measured by the calorimeter, Q_{el} the electric power.

50%. We solved the duration problem but high efficiency values are still sporadic.

We must note that the excessive heat correlates with the neutron flux change but not with its value. We also must note that most of the excessive heat is released at the cathode, sometimes more than 90% of the total amount of heat.

The amount of excessive heat we can measure with a passable accuracy is about 6 kJ, which is much more than one can get from chemical reactions, even if one would burn all the deuterium in oxygen (a 10^6 times higher O_2 concentration is needed for that), which would give only 800 J.

6. Charged particle registration

To measure charged particles we used a silicon surface barrier detector of DKD and DKP type with a thickness of 25 to 509 μ and an energy resolution of 25–50 keV. The efficiency of the counters in the used geometry was about 10^{-5}. The cosmic and natural radioactivity background was less than one count per hour. We used various degrading foils, from 6 μ $(C_2H_2)_n$ to 50 μ beryllium. Earthed brass grids with 2 μ aluminium foils were used to protect the detectors from electric pick-ups. Still the results obtained during the discharge glow are disputable. But as we can often see a signal for a few minutes after the discharge switch-off, spectrometry at this time is much more reliable. 4.58 and 5.16 MeV alpha particles from ^{235}U and ^{239}Pu isotopes were used to calibrate the measuring channel, consisting of an AMUR amplifier and an AMA-3 multiscaler. The charged particle spectrum is shown in fig. 4. Energies up to 18 MeV can be seen. A degrading foil is not the best method for particle type definition, but the 3.5 MeV peak are alphas, the whole region with $E > 10$ MeV corresponds to particles with an atomic number $A \geq 4$ and the 12 and 16 MeV peaks are probably alphas.

Energetic alpha particles were probably observed in the first experiments with charged particle registration [5].

In the first publication where CR-39 polycarbonate detectors were used to detect charged particles during deuterated metal thermocycling [6] a significant amount of charged particles was found though the type of particles was not defined.

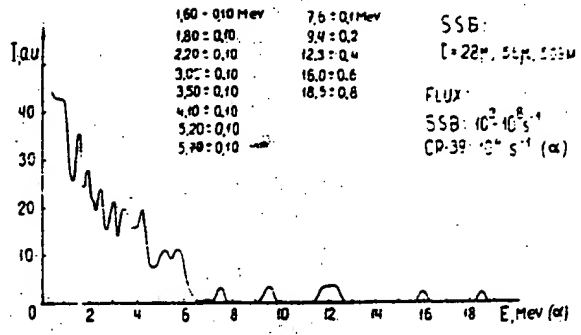

Fig. 4. Charged particle energy spectrum, measured after the discharge switch-off. Calibration was done with alpha particles.

In collaboration with the team from the Moscow Physico-Engineering Institute, using ^{239}Pu-calibrated CR-39 plates placed in the discharge chamber, alpha particle tracks with a density of 2×10^5 cm^{-2} were found, corresponding to a 10^5 s^{-1} emission from the cathode and roughly corresponding to the SSB results. The average energy (4–5 MeV) is also consistent with the average energy from the measured spectrum (2–4 MeV). The photographs of the ^{239}Pu-treated and discharge treated standardly developed CR-39 plates are shown in fig. 5. About 10^2 neutrons per second were registered in this experiment.

7. Gamma-quantum registration

In the previous experiments [4] we used various scintillation detectors with various efficiency but a low energy resolution. Later we used mainly a liquid-nitrogen cooled Ge–Li DGDK-50 detector with a 1.6 keV resolution at the 1332 keV gamma-line energy and a measuring range up to 10 MeV. The detector efficiency in our geometry was $\sim 10^{-3}$ for the 511 keV gamma line.

The measuring procedure consisted in a constant gamma-background monitoring before the experiment, measurements during the experiment and for about one week after the experiment. The spectrum goes back to its initial state in 3–5 days (for the Pd cathode). Numerous radioactive isotope lines can be seen. In accordance with previous measurements most of the rhodium isotopes can be seen at the palladium cathode. Some strange isotopes, such as ^{86m}Sr

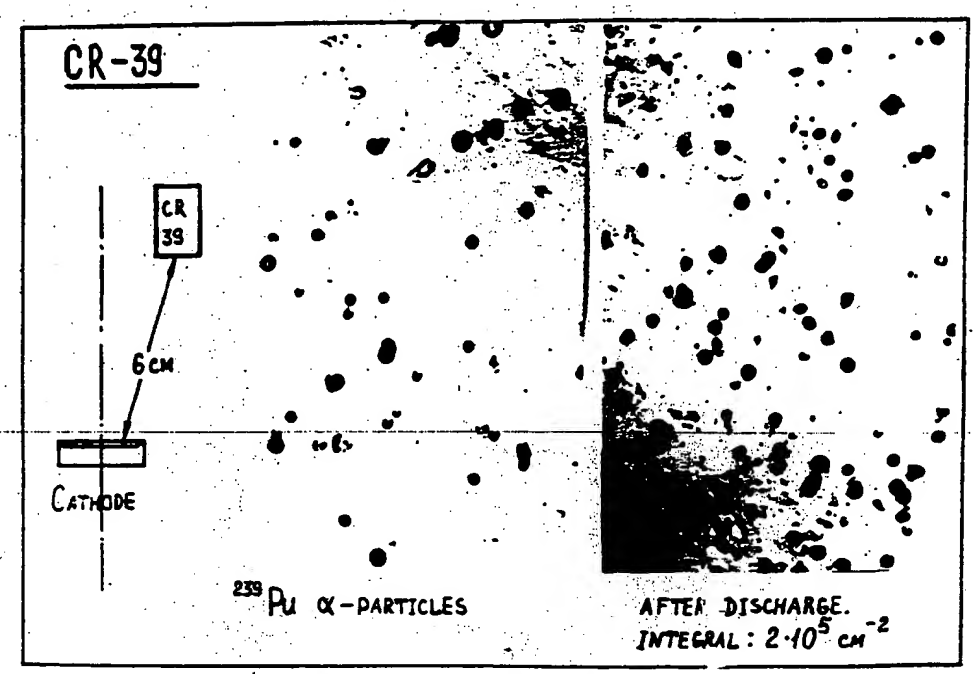

Fig. 5. Scheme of the CR-39 detector plate placement in the discharge chamber. The left photo plate is irradiated with ^{239}Pu alpha particles; the right photo plate is irradiated in the discharge chamber.

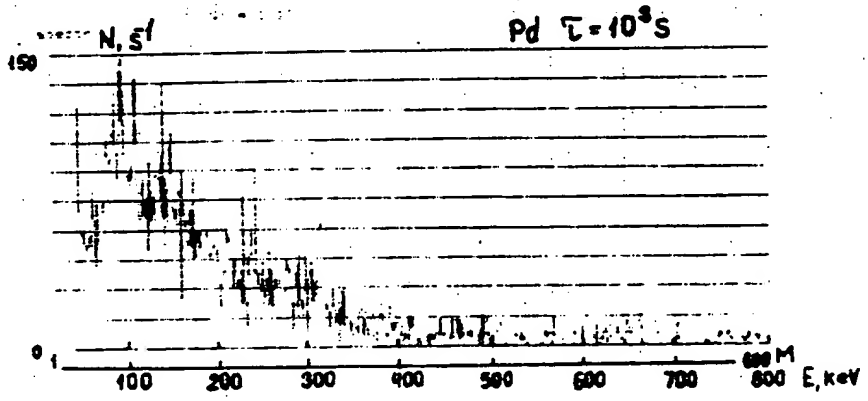

Fig. 6. Energy spectrum of gamma radiation from the discharge chamber with a palladium cathode.

can also be seen. The experimental gamma spectrum for the Pd cathode is shown in fig. 6. We must note that the ≈5 MeV gamma-line intensity is very low, eliminating d–p reactions. An abbreviated list of gamma lines for the Pd cathode is given in table 1.

To determine the spatial distribution of the gamma emission we used RT-1V X-ray films with lead screens. It appeared that gamma emission exists in the form of spatially uniform emission and narrow beams. Beams have two modifications, with smaller and larger angular divergence. A photo of these beams at a distance of 0.5 m is shown in fig. 7. Judging from the attenuation by lead films in most of the beams the gamma-quantum energy is about 200 keV, though some of them have a higher energy. Most of the beams can be found in the cone 45°–60° with the

Table 1
Abbreviated list of gamma lines for the Pd cathode.

keV	Isotope	keV	Isotope
51	^{104m}Rh ($T_{1/2}$=4.4 min)	188	^{109m}Pd ($T_{1/2}$=4.7 min)
78	^{104m}Rh	190	
84		195	
88		210	
97	^{104m}Rh	230	^{85m}Sr
102		240	
108		265	
120		280	
129	^{103m}Rh?	295	
142		305	^{103}Rh ($T_{1/2}$=35 h)
148		320	^{103}Rh
151	^{85m}Sr ($T_{1/2}$=70 min)	335	
175			

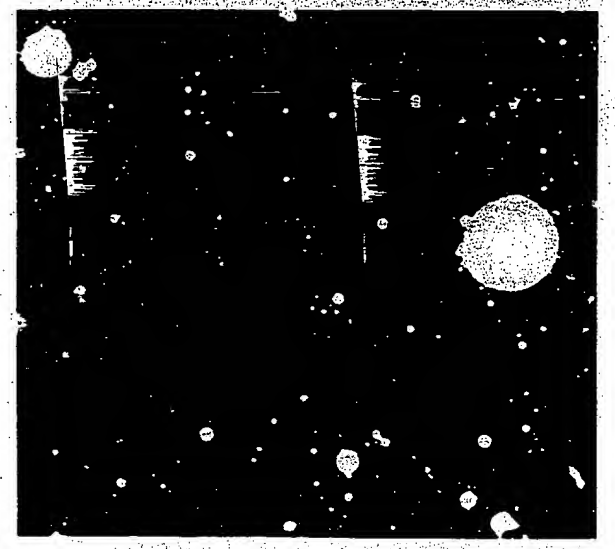

Fig. 7. Photo of gamma beams on an X-ray film with a 2 mm lead screen.

cone axis coinciding with the discharge chamber axis.

Using the same X-ray film with aluminium and lead screens X-rays with diffraction spots can be seen (fig. 8). Most of this radiation lies in the range 5–20 keV. As the intensity of this radiation is rather high some of it can be detected with the same Ge-Li detector. The characteristic X-ray lines of palladium can be clearly seen around 20 keV. The X-ray intensity was evaluated by densitometry of the exposed films.

Fig. 8. X-ray diffraction s pots on an X-ray film placed in the discharge chamber in a lead cassette with a 0.5 mm aluminium window.

8. Nuclear product intensity ratio

Using the above described methods, a table of the detector type, the detector efficiency, the sensitivity and the measuring error can be constructed. We must note that the measuring error has nothing to do with the physical error, which in the case of charged particles can be very high, depending on the type and the energy of the particle and the distance from the cathode surface to the reaction area. The average energy based on the spectrum measurements can also be placed in this table (table 2).

The intensity ratios of the gamma quanta, neutrons, charged particles and X-rays averaged over a few experiments look like

$$I:I_n:I_{c.p.}:I_{xr}$$
$$=1:(10^{-5}\text{–}10^{-2}):(10^{-1}\text{–}10^{2}):(10\text{–}10^{2})\,.$$

If we take the average energy from the table, the energy transfer ratio for the products will look like

$$E:E_n:E_{c.p.}:E_{xr}=1:(10^{-3}\text{–}1):(1\text{–}10^{3}):(1\text{–}10)\,.$$

If we take the extremal values in the last ratio the charged particles are transmitting 10^6 times more energy than the neutrons, still 3–4 orders short of the

Table 2

Product type	Detector type	Efficiency	Range (s^{-1})	Error (%)	Average energy	Note
neutrons	CHM-18 (^{3}He)	10^{-1}	>10	~20	5–7 MeV	
gamma-rays ($E>30$ keV)	DGDK-50 (Ge–Li)	10^{-3}	$>10^2$	~50	~200 keV	
charged particles	DKD, DKP (SSB)	$\sim 10^{-5}$	$>10^2$	~50	2–4 MeV	
X-rays ($E<30$ keV)	Ge–Li, XR-films	integral	$\sim 10^4$	~65	15–20 keV	X-ray film densitometry

values allowing one to explain the calorimetric results.

9. Cathode material change

A more detailed paper on the material science aspects will follow this one but some of the results concerning the subjects of the present paper will be noted. The palladium cathode after the work in the discharge chamber at temperatures up to 400°C was etched from the back side and analyzed with a high resolution transmitting electron microscope. A lot of small size "bubbles" with dimensions of 100–1000 Å and density 10^{20} m^{-3} can be seen to a depth of 1000–10000 Å. Such pictures (fig. 9) are characteristic of bombardment at temperatures higher than half of the melting point (750°C) with high-energy deuterons. Some of the cathodes together with the reference samples were analyzed at the Rockwell International Laboratory (Oliver's group). A small increase in the ^{3}He concentration and a large increase in the ^{4}He (4–100 times) concentration was found in the discharge treated samples. This is the third independent evidence of ^{4}He presence in the nuclear reaction.

After the experiments the cathode samples were autoradiographed with degrading foils. Some tritium was found along with the high energy particle traces, equivalent to 0.5 MeV betas. The high-energy component disappears in about one week after the discharge switch-off.

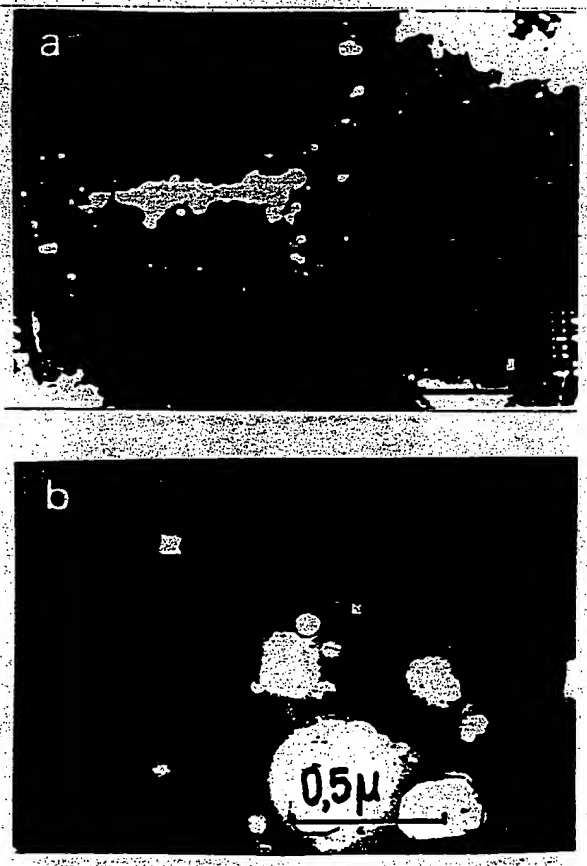

Fig. 9. Transmitting electron microscope photos of a palladium cathode at a distance of ~2000 Å from the cathode surface. (b) is in the central zone of (a).

10. Conclusion

Many new questions arise with the latest results. The trigger mechanism of the nuclear reaction still remains unclear. As we already pointed out charged

particles with a good portion of alphas are found in quantities 3–4 orders short of those needed to explain the excessive heat. We did not measure the electron flows in our work and this still leaves the possibility of K-electron capture with a radioactive isotope formation with a consequent beta decay with large energy release. A more plausible scenario is that the main mass of the charged particles does not leave the cathode. This leaves us with two possibilities: either they have a small energy or they are heavy. Judging from the transmitting microscopy results most of the cathode material damage takes place at a depth of 1000–10000 Å from the surface. If this is the region were the nuclear reaction takes place most of the alphas must have an energy less than 1 MeV. Palladium fission products even with a high energy will have small paths in the cathode material and the alphas can be by-products. Anyway, the calorimetric results are promising by themself.

Acknowledgement

We are happy to express our thanks to Drs. A.D. Kurepin, B.Ya. Guzovsky, V.N. Chernikov, Professors L.N. Permiakov, I.I. Fedik and R.Ya. Kucherov for their help in this work.

References

[1] M. Fleishmann and S. Pons, J. Electroanal. Chem. 261 (1989) 301.
[2] E. Storms, Fusion Technol. 20 (1991) 433.
[3] A.B. Karabut, Ya.R. Kucherov and I.B. Savvatimova, Cold fusion observation at gas discharge device cathode, in: Nuclear Energy in Space Conference, Obnisk, USSR, 15–19 May 1990.
[4] A.B. Karabut, Ya.R. Kucherov and I.B. Savvatimova, Fusion Technol. 20 (1991) 924.
[5] F.E. Cecil and H. Liu, private communication.
[6] S.Y. Dong et al., Fusion Technol. 20 (1991) 330.

***

IMPROVED CALCULATIONS INVOLVING ENERGY RELEASE USING A BUOYANCY TRANSPORT CORRECTION

Mitchell Swartz
JET Energy Technology, Inc. [1]

ABSTRACT

Measurement of energy release in the evaluation of fusion systems may rely upon flow calorimetric systems susceptible to Bernard instability which may have inadvertently impacted the calorimetry. Such thermal-driven convection can produce the appearance of "excess heat", or a magnified excess heat, because of unanticipated thermal-driven mass transfer. A semiquantitative correction to enthalpic calculations is suggested after separation of the observed Power output ($P_{derived}$) into two terms, the actual power out (P_{out}) and a second bouyancy-flow-related error term (P_{error}).

DISCUSSION

Measurement and documentation of energy release are critical in the evaluation of fusion, or other putative over-unity systems. Reliance upon flow calorimetric systems are being increasingly used by some to detect enthalpic changes secondary to putative nuclear reactions in condensed phases [1,2,3,4,5]. The equation used to derive the estimated power output, and therefore the presence of any excess heat involves the applied fluid flow, the specific heat of the water, and the temperature differential. Although this equation may be dimensionally correct, it does not appear to be always valid for low flow rates [6], such as in certain cases where Bernard instability [7,8] may inadvertently have an impact upon the calorimetry. Previously qualitatively examined has been the time-varying distribution of temperature in a quasi-one-dimensional model, for both horizontal and vertical flow calorimetry, both with and without convection [6]. There can be thermal redistribution in a vertical system with the addition of upward thermal-driven convection, driven by thermal-induced buoyancy instability. As a result, there can be shift of the isothermal lines away from the intrinsic symmetry exhibited by horizontal flow calorimetric systems with zero applied convective flow, producing the appearance of "excess heat", or a magnified excess heat, even in the absence of applied convection. Thus, the quoted efficiencies of energy generated by classical calculation may not be correct. There may be an apparent error "signal" for zero flow because of the thermal instability which can create mass transfer. This brief note suggests a semiquantitative correction for the enthalpic calculations using a first order term for heat transport secondary to buoyant forces generated by unstable thermal inhomogeneities.

If η_B is the ratio of heat transported by the buoyant forces to all of the heat transported including that by the applied solution convection, then the Q1D model of heat and mass transfer [6] indicates that what is generally correct for horizontal calorimetric systems may not be correct for vertical systems, when the non-dimensional number ($= \eta_B$) is significantly greater than zero.

The buoyant heat flow ratio, η_B, in real systems may also depend upon other non-dimensional factors including the Archimides non-dimensional number, which is the ratio of the buoyant force to the viscous force, and possibly the Rayleigh non-dimensional number, which is the ratio of gravity to thermal conductivity.

For this simplification, we suggest the separation of the observed Power output ($P_{derived}$) into two terms, the actual power out (P_{out}) and a second buoyancy-flow-related error term (P_{error}). Because the total observed signal -- the delta-T in the face of the applied convention ($v_{convection}$) and incidental thermal buoyant convection ($v_{buoyancy}$) -- results from their combined velocity, then to zeroth order one can write

$$P_{observed} = P_{out} + P_{error} = C_p * \Delta T * V_{total} \cong C_p * \Delta T * (V_{convection} + V_{buoyancy}) \quad \text{(eq. 1)}$$

The error term is thus first order on the non-dimensional ratio η_B .

$$P_{error} \approx C_p * \Delta T * V_{total} * \eta_B \quad \text{(eq. 2)}$$

We assume that η_b is small and therefore $V_{total} \approx V_{convection}$. This is also an approximation because the chain rule from calculus, and consideration of possible coolant redistribution, suggest that there are other higher order terms also potentially arising from the impact of the buoyant flow.

$$\frac{\delta P_{error}}{\delta_{\eta_B}} \approx (C_p * \Delta T * V_{total}) + [C_p * V_{total} * \eta_B * \frac{\delta \Delta T}{\delta \eta_B}] \quad \text{(eq. 3)}$$

Thus, the second term in the equation, involving $\frac{\delta \Delta T}{\delta \eta_B}$, may depend upon several additional factors involving at least the to al tank volume just outside the reac or (or capacity of the thermal control) and the actual input temperature boundary condition.

Ignoring in this approximation the terms of higher order, and using the approximations above, the linear correction to the observed power becomes corrected as

$$P_{corrected} \approx P_{observed} - (C_p * \Delta T * V_{convection} * \eta_B) \quad \text{(eq. 4)}$$

Thus, a more accurate estimate of purported over-unity power gain (π) could be directly derivable, from the correction to first order, as

$$\pi_{corrected} = \pi_{observed} * (1 - \eta_B) \quad \text{eq. 5)}$$

Since the submission of this manuscript, the correction technique of subtracting for the buoyant uplift in flow calorimetric systems has been experimentally applied independently by Dr. Barry Merriman and P. Burchard [9]. In that system, the correction is taken as a direct calibration to set the null signal. Based on this paper, it may also be possible to semiquantitatively derive both terms in some systems.

In summary, the extent of any such reported 'excess heat' may be inflated, if the information was collected with a vertical flow calorimetric system, without confirmatory calibrations under low to moderate flow conditions where the non-dimensional number (η_B) is not trivial. Equations 4 and 5 offer semiquantitative corrections to the observed calculations of present verticle flow calorimetric systems used to investigate heat producing reactions in the condensed phase. These can be used even in the presence of buoyant flow in vertical flow calorimetric systems, using a linear correction based upon the measured, or estimated, values of η_B.

REFERENCES

1. R.D. Armstrong, E.A. Charles, I. Fells, L. Molyneux, M. Todd, "Some Aspects of Thermal Energy Generation During the Electrolysis of D_2O using a Palladium Cathode," *Electrochim. Acta*, vol 34 (1989), p 1319.
2. L. Bertalot, F. De Marco, A. De Ninno, A. La Barbera, F. Scaramuzzi, V. Violante, P. Zeppa, "Study of Deuterium Charging in Palladium by the Electrolysis of Heavy Water Heat Excess Production," *Nuovo Cimento*, vol 15 D (1993), p 1435.
3. D. Cravens, "Flowing Electrolyte Calorimetry," Proceedings of 5th International Conference on Cold Fusion, pp 79-86 (1995).
4. M.C.H. McKubre, S. Crouch-Baker, R.C. Rocha-Filho, S.I. Smedley, F.L. Tanzella, T.O. Passell, J. Santucci, "Isothermal Flow Calorimetric Investigations of the D/Pd and H/Pd Systems," *J. Electroanal. Chem.*, vol 368 (1994), p 55.
5. O.A. Velev, R.C. Kainthla; "Heat Flow Calorimeter with a Personal-Computer-Based Data Acquisition System," *Fusion Technol.*, vol 18 (1990), p 351.
6. M. Swartz, " Potential for Positional Variation in Flow Calorimetric Systems," *Journal of New Energy*, vol 1, pp 126-130 (1996)
7. J. Melcher, Continuum Electromechanics, MIT Press, Cambridge, pp 10.13-10.18 (1981).
8. S. Chandrasekhar, Hydrodynamic and Hydromagnetic Stability, Clarendon Press, Oxford, 9-75 (1961).
9. B. Merriman, P. Burchard, "An Attempted Replication of the CETI Cold Fusion Experiment," http://www.math.ucla.edu/~barry/CF/reportcover.html (1996)

JET Energy Technology, Inc.
P.O.Box 81135
Wellesley Hills, MA 02181

The influence of conductivity on neutron generation process in proton conducting solid electrolytes.

A.L. Samgin, A.N. Baraboshkin, I.V. Murigin,
S.A. Tsvetkov, V.S. Andreev, S.V. Vakarin.

Institute of High-Temperature Electrochemistry
Russian Academy of Science, Ekaterinburg, RUSSIA, 620219.

Abstract

It is mentioned, that the nature and the mechanism of conductivity and the existence of multilayered structures with different conductivity types in solids appears to be the additional critical conditions of abnormal y increased rate of nuclear-electron reactions in solid state-deuterium system.

Introduction

Anomalous nuclei-electron phenomena, including cold fusion process, accompanied with neutrons or gamma-quantum generation are observed in solids, which have different conductivity nature: metals[1,2], oxide bronzes[3], KH_2PO_4-type segnetoelectrics[4], heavy ice[5], solid proton conducting electrolytes[6]. Therefore the investigations of phase transformation influence on the process of neutron generation, resulted conductivity mechanism change or even the conductivity type transformation are very important.

In this paper we tried to look over the anomalous nuclear effects from the protonic conductivity point of view. Actually all the materials from the papers listed before are protonic conductors. This papers, except the works on the base of metals, one would think with quite different materials are unificated on the base of deuteron conducting electrolytes. It's true, that heavy ice, KH_2PO_4 in paraelectric phase are low-temperature protonic conductors, with relatively small electric conductivity. In ice the proton is moving along a chain of H_2O. It is characteristic, that KH_2PO_4 - crystal is low-temperature protonic conductor, with intrinsic structures irregularities having the spasmodically conductivity change during phase transformation at definite temperatures. Oxide bronzes of transition metals are one of the type of superionic crystals with high protonic mobility and oriented movement along channels in the lattice. Finally, some high-temperature solid electrolytes possesses large deuteronic conductivity. Quick deuteronic transport at temperatures in range of 600°-900° C is possible to them, but the spasmodically conductivity change didn't observed.

Results and discussion

Among the following electrolytes the last ones with perovskite-like structure have high protonic conductivity in deuterium atmosphere and as for perovskite-proton conductive electrolytes on the base of doped $SrCeO_3$ - it's especially significant, that the proton conductivity in them is not mask over the conductivity background on the other ions. Moreover, the proton nuclei in them is transported as an individual particle- H^+ ion. That's so, on the base of criteria of appreciable protonic conductivity it is possible to determine (as experimentally revealed) the class of materials, optimal to nuclei-electronic phenomena investigations. In this case the only difference in above mentioned experiments will be the way of external energy admission to deuterons. It takes place during mechanical distortion of heavy ice, segnetoelectric-superionic conductor phase transformation in KH_2PO_4 crystal, hydrogen gas saturation of near-surface structures in oxide bronzes in which the spatial conductivity channels are made by electrochemical treatment, and during long strontium cerate electrolysis.

Let us mention, that with the criteria described above some other conditions, which are necessary to cold fusion existence, have a good corellation. We'll note two of them:

- first-the formation during deuterium saturation of solids with nonlinear properties in strongly nonequilibrium conditions of local zones with sufficiently increased deuteron to lattice atoms ratio (at the first time this hypothesis was spoken out by Tsarev V. et al[8]. The theoretical basis of this effect during electrolysis and from the gas-phase satu ation was made in our previous paper[7]);
- second-the high transport speed and the oriented nuclei movement. Since the proton conductivity is calculated from proton concentration and proton mobilities and suggested spatial or energy channel existence, the view on current problem seems to be correct.

Another important feature for anomalous nuclei effect's investigations in deuterium-solid system is the problem of making clear the question of phase boundary and heterostructures with different conductivity types role. In dependence of stoichiometry composition oxide bronzes possess both metal and semiconductor conductivity type. In paper[3] before deuterium intercalation the stretching of sodium ions took place. Decreasing of alkali metal concentration and the replacement of such atoms by hydrogen isotopes near the surface resulted in the formation of thin layer with semiconductor conductivity type. To obtain neutron generation the removal of sodium ions took place[2]. The hypothesis of formation of regions with dielectrical properties in Pd was already discussed[8]. The additional factor is the electrical current which flow throe phase boundary during electrolysis. This peculiarities of conductivity nature may also related with mechanism which have "a common origin" in "electromagnetic current behavior in dense media" and in the process of "capillary fusion" in special structures with channels".

In our experiments with barium and strontium cerate the correlation between neutron generation and the sample's conductivity was observed.

Detailed description of experimental method and apparatus was presented in ref[4] (in paper presented on the Fourth International Conference on Cold Fusion, December 6-9, 1993, Hyatt Regency Maui, Lahaina, Hawaii). The sample was made as a heterostructure

from a doped strontium cerate ceramics or barium cerate ceramics disk covered with porous metallic electrodes. The cell's construction and the installation which the sample was placed on, permits to make both gas pumping out and electrolysis with increased deuterium pressure with the sample's heating or cooling in the same time (fig.1).

During definite time the sample was under electrolysis treatment at temperature 750° C after which thermocycling was made in temperature range from 800° till 400° C with electrolysis in the same time (the typical change of temperature and electrolysis current presented on fig.).

At this process some single neutron bursts which prolonged a few seconds were observed, when the electrolysis was conducted more then twenty four hours. They were detected both in process of increasing the sample's temperature and during electrolysis current rasing and at the sample's temperature decreasing.

Neutron emission only observed at temperatures related to high sample's protonic conductivity. In the case of the highest deuterium pressure in cell (3 atm.) and the sample's thermocycling without electrolysis it was founded the sample's reduction accompanied turning the sample blackening. As the result of the reduction process is change the sample's conductivity to n-type electronic conductivity. A neutron emission usually is over when reduction process is completed and it suppose to be related to type of conductivity change from electronic/cationic to pure electronic. This phenomena was observed both on barium and on strontium cerate.

Deuteron conductivity of the high temperature electrolyte based on the doped strontium cerate is changing as an exponential function. During this conductivity change initiated by temperature change of the ceramic sample with predetermined speed was discovered enough intensive neutron burst. It was correlated with strictly specified ceramic temperature which was measured by thermocouple placed near the sample at 3 mm distance. These neutron burst where reproduces in three times on the same sample during the experiments before it's degradation (fig. 3). On fig.3 it is shown the most severe first burst, every following burst had the obviously expressed damping nature as the temperature raise near the sample's surface accompanied the appearance of neutron impulses. On the same fig. it is shown the spontaneous deuterium gas pressure change in cell. The excess of pressure and temperature are correlated in time with neutron bursts.

We compared the results of the analysis of the sample before and after saturation by deuterium during electrolysis and thermocycling in the increased temperatures. It was discovered the an existence of unmovable structure changes. The sample's degradation is reflected in the simultaneous neutron burst decreasing and further cessation it's emission.

Conclusions

Our experiments have shown the main condition of a neutron emission is an existence of ion (proton) conductivity in cerate channels. Appearance of an electron conductivity with reduction of ceramic resulted by neutron emission cessation.

Obviously the nature and mechanism of conductivity and the existence of multilayered heterostructures with different conductivity type are an additional critical condition of essential increasing of speed and the intensity of electron-

nuclei reactions in solid state/deuterium system.

Acknowledgments

This research was sponsored by ENECO (USA) and partially was supported by Russian Foundation of Fundamental Researches (RFFR).
Authors express their gratitude to Dr. Oleg Finodeyev (ENECO) and A. Cherepanov (IHTE) for their assistance to prepare this papers.

References

1. M. Fleischmann and S. Pons. "Electrochemically induced nuclear fusion of deuterium". Electroanal. Chem. Vol. 261, p. 301 (1989).

2. S.E. Jones, E.P. Palmer, J.B. Czirr et al. "Observation of cold nuclear fusion in condensed matter". *Nature*. Vol.338., N 6218, p. 737 (1989).

3. K. Kaliev, A. Baraboshkin, A. Samgin et al. "Reproducible Nuclear Reactions during Interaction of Deuterium with Oxide Tungsten Bronze. Phys. Lett. A. Vol. 172, p.199 (1993); *Frontiers Science*, Series No. 4, *Tokyo Proc. of ICCF-3:* Universal Academy Press, 1992, pp. 241-244.

4. A. Lipson, D. Sakov, U. Kalinin et al. Pisma v zhyrnal tekhnicheskoi fiziki. Vol. 18, N 16, p. 52 (1992) (in Russian).

5. V. Kluev, A. Lipson, Yu. Topornov et al. Pisma v zhyrnal tekhnicheskoi fiziki. Vol. 12, p. 1333 (1986) (in Russian).

6. A. Samgin, A. Baraboshkin, V. Andreev et al. "Neutron generation in the solid protonic conductors with perovskite-type structure". Paper N2.7, presented at the ICCF-4, Hawaii (December 1993).

7. A. Samgin, V. Tsidilkovski and A. Baraboshkin. "On the possible formation of regions with high hydrogen isotope concentration at nonlinear diffusion in transition metals". Proc. All-Union Workshop "Chemistry and Technology of Hydrogen". Zarechny, USSR. November 1991, p.30; Paper presented at ICCF-3, Japan, Abst. of ICCF-3, p.39 (October 1992).

8. V. Tsarev. "Cold fusion". Uspekhi fizicheskih nauk. Vol. 160, p. 1 (1990) (in Russian); "*Cold Fusion Researches in Russia*". *Frontiers Science*, Series No. 4, *Tokyo Proc. of ICCF-3*, Universal Academy Press, 1992, p. 341-351.

9. J. Vigier. "New Hydrogen Energies in Specially Structured Dense Media: Capillary Chemistry and Capillary Fusion". *Frontiers Science*, Series No. 4, *Tokyo Proc. of ICCF-3*, Universal Academy Press, 1992, p. 325-336.

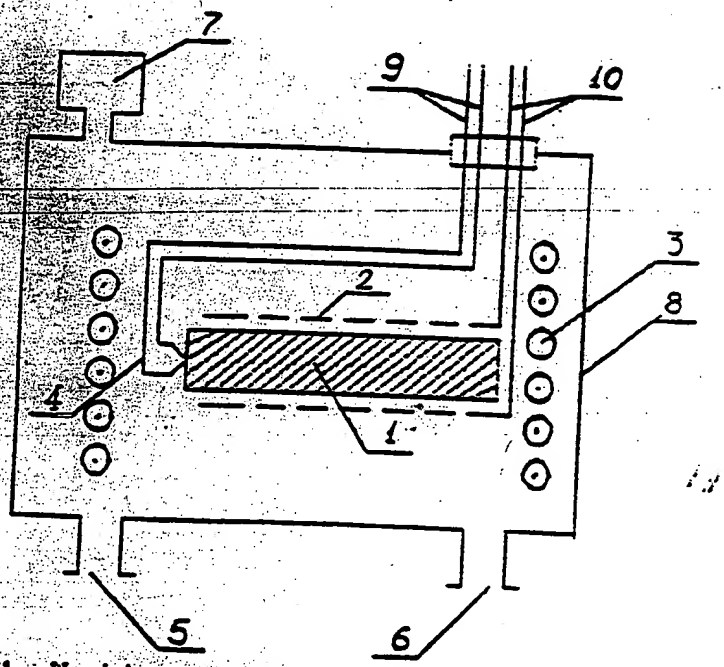

1. Working element.
2. Sample's porous cover.
3. Cylindrical heater.
4. Thermocouple.
5. ... to the vacuum pump system.
6. Deuterium flow.
7. Vacuum gage.
8. Vacuum cell
9. ... to temperature gage.
10. Current lead to the sample.

High-temperature electrolysis cell with solid electrolytes.

fig 1

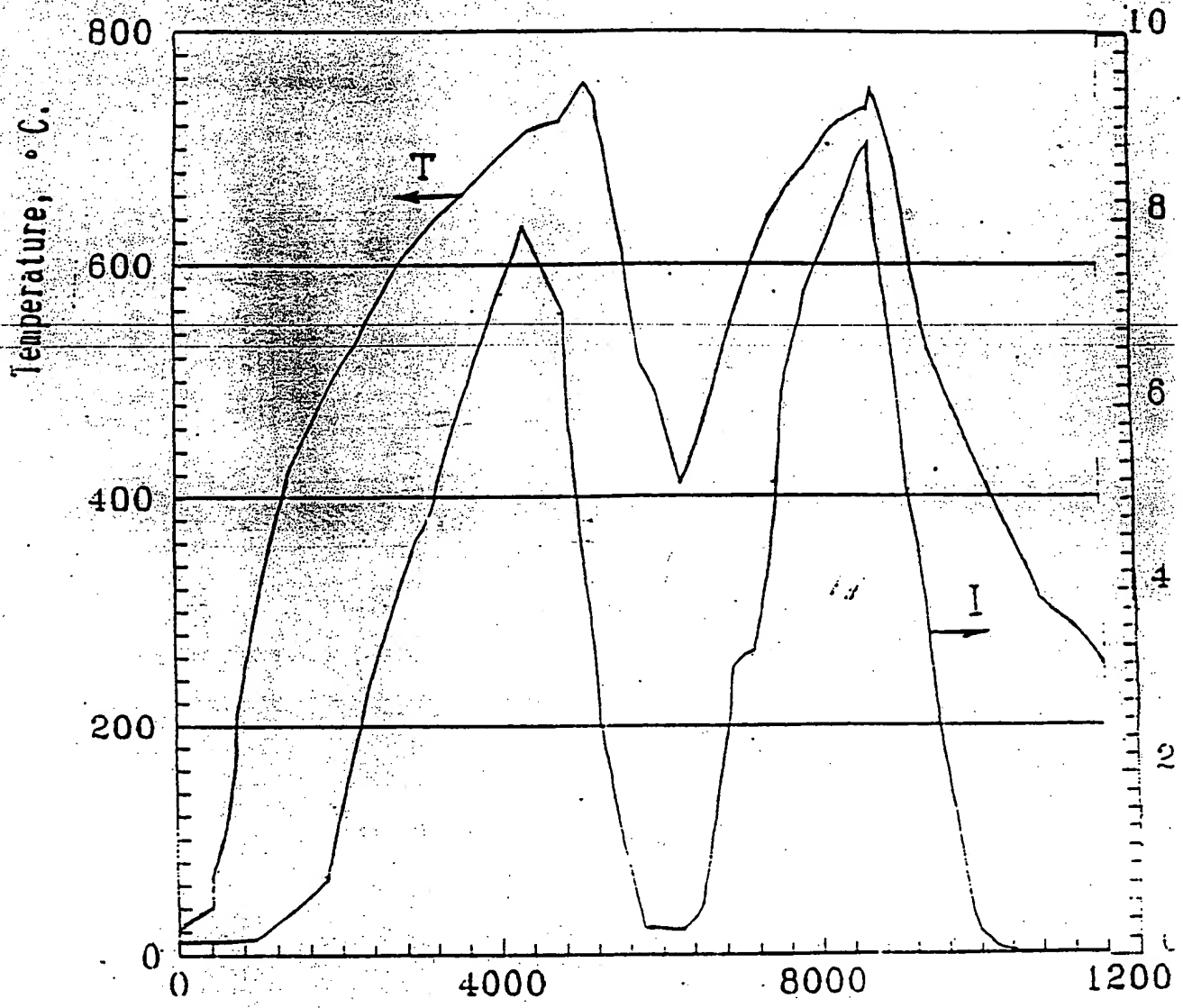

Dependence temperature and current at termocycling

fig 2

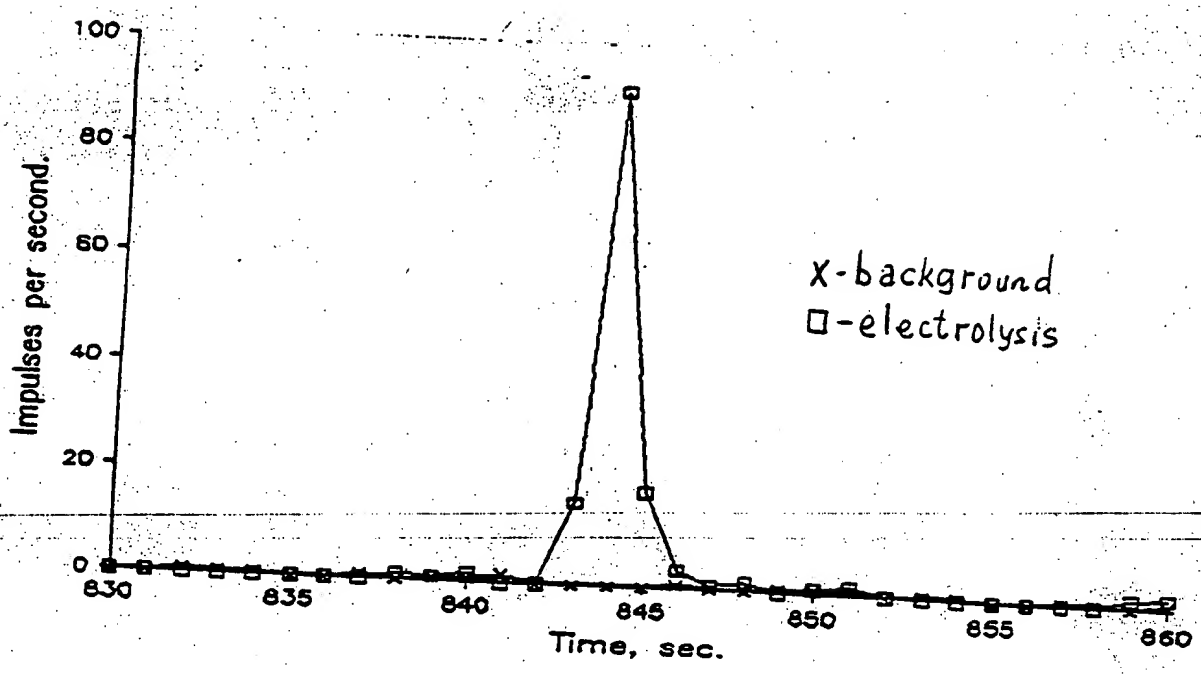

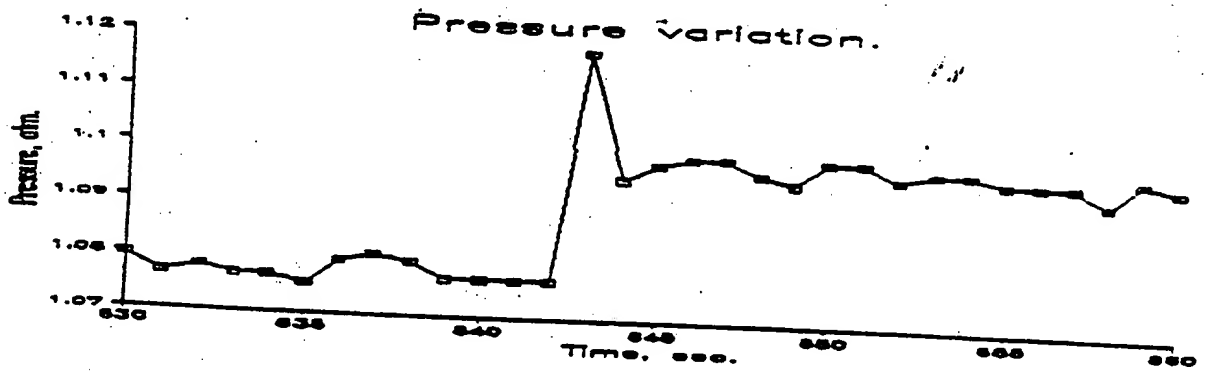

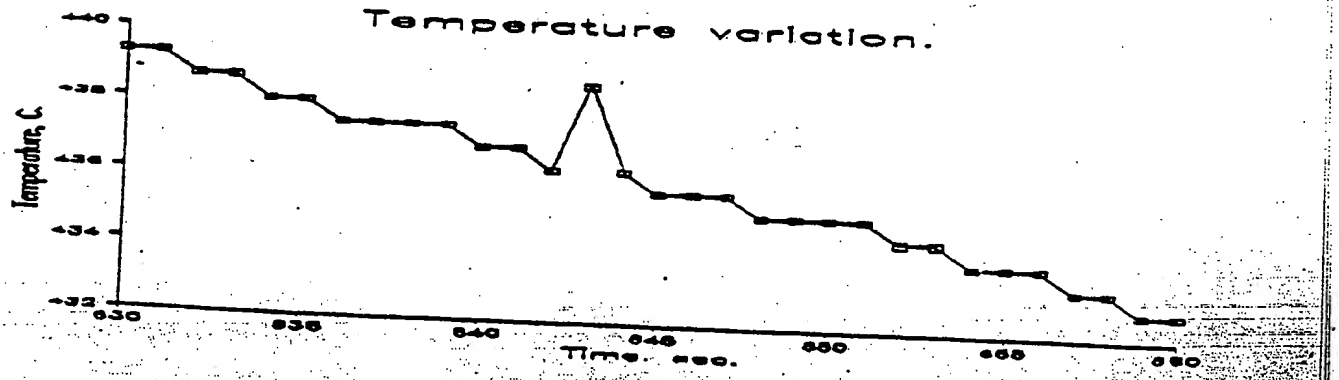

Neutron burst during solid electrolyte thermocycling and electrolysis.

LATTICE-INDUCED ATOMIC AND NUCLEAR REACTIONS

Peter L. Hagelstein
Massachusetts Institute of Technology
Research Laboratory of Electronics
Cambridge, Massachusetts 02139
(617) 253-0899

ABSTRACT

A new theory for a variety of atomic and nuclear reaction mechanisms resulting from the decay of a highly excited lattice is introduced.

In our previous work on neutron transfer reactions, we found that large energy transfer between a lattice and nuclei could occur through the frequency shift of a highly excited continuum phonon mode across a band gap that is caused by the neutron transfer. Here, we generalize the energy transfer mechanism to include impurity continuum phonon modes due to the presence of vacancies; processes that change the number of vacancies can in principle stimulate the transfer of energy with the lattice.

A consequence of this is that a metal hydride lattice with host vacancies that has very high excitation of gap-jumping phonon modes will be unstable against decay by a variety of atomic and nuclear processes. Coulomb-induced recoil reactions of nuclei with electrons and nearby nuclei that cause vacancy production are found to occur with very high predicted reaction rates.

A lattice with a large number of highly excited phonon modes that can decay sequentially will most likely decay with a "burst" of emitted decay products, as a high order multi-step quantum process. A theory for this type of high-order decay is outlined.

The predictions of this theory may apply to many of the anomalous phenomena claimed to occur in experiments performed on metal deuterides, including neutron production, tritium production, gamma emission and host lattice activation.

I. INTRODUCTION

Nearly five years have passed sinced the initial announcement by Pons and Fleischmann[1] of the observation of what they and others have termed "cold fusion." During this time, a wide variety of claims have been made for the observation of anomalous phenomena of one sort or another in PdD, in TiD_2,[2-5] in other metal deuterides,[6,7] and now also in metal hydrides.[8-10] Perhaps most important, if true, is the claimed observation of excess heat; the heat production reported is sufficiently large that if real, it would not be attributable to chemical or other atomic effects.[11] Many in the field hope that this effect, believed to be due to yet unknown nuclear reactions, will eventually be harnessed to provide a new clean source of energy for mankind.

The scientific community has long since grown immune to any reports of such claims. In a sense, the field of "cold fusion" has been judged, the data weighed and found wanting, and the field sentenced to oblivion. The cause: experiments that seem not to be reproducible, data that may suffer from either systematic errors or poor signal to noise ratio, no consistent effect that appears in all experiments, and no compelling theoretical reason to believe that anything anomalous should happen at all. No obvious progress has been made during the past year in effecting a basic change in attitude.

Our research in the area takes as its premise the possibility that some of the experimental results are in fact correct, and seeks to address the question as to what physical mechanisms, if any, could be responsible. Our studies have led us to consider numerous potential nuclear reaction pathways, focussing on possible enhancements in reaction rates that might be brought about by the atomic environment. Due to the large energy required to cause anything nuclear to happen, it is crucial in any such candidate theory for a clear and obvious energy transfer mechanism to be present that is capable of transferring such large energy.

Recently, such a mechanism was identified in the case of reactions that involve neutron transfer.[12] The basic idea is to generate a very large number of phonons into a small number of continuum phonon modes, and then shifthe frequency of these phonon modes by transferring a neutron to or from a nucleus in the lattice. The total energy transfer through this mechanism is

$$\Delta E = n\hbar\delta\omega \qquad (1.1)$$

where $\delta\omega$ is the frequency shift, and where where n is the number of phonons present in the frequency-shifting modes.

To arrange for a continuum phonon mode to change its resonant frequency can be accomplished in certain materials that possess an impurity phonon band separated

from other phonon modes by a finite band gap; a neutron transfer process that changes the number of impurity atoms also causes a change in the number of impurity phonon modes, which implies that a small number of phonon modes must jump the band gap. To arrange for a large number of phonons to be in a small number of phonon modes essentially implies the presence of a phonon laser.

Recently we have proposed the generalization of this mechanism to a much wider class of processes, some of which are nuclear and some of which are atomic. The key observation is that an impurity band can be due to the presence of vacancies, which implies that mechanisms that alter the number of vacancies of a certain type can in principle cause a large energy transfer to occur.

For example, in a metal deuteride that possesses a large band gap between the acoustic and optical phonon branches, it may occur that impurity bands for those deuterium atoms near a vacancy will form within the band gap. In PdH, for example, the basic hydrogen occupation of octohedral sites persists in lattice cells with a Pd vacancy;[13] we assume that the same is true in PdD. Deuterium atoms next to a Pd vacancy see a softer potential, and consequently oscillate at a lower frequency, than deuterium atoms not next to a vacancy. The frequency of this type of defect vacancy band is presently unknown; we will make the anzatz in this work that these modes in fact lie within the band gap in the case of the metal deuteride PdD (see Figure 1). A change in the number of vacancies will result in a change in the number of vacancy phonon modes; new vacancy modes are formed from the lowest modes above the band gap, which jump down to join the vacancy impurity band.

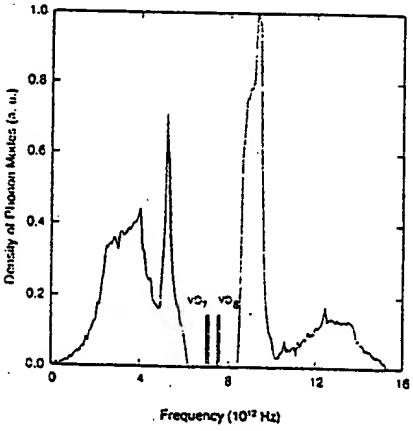

Figure 1: Density of states in PdD (based on the force constants of Ref. 14), augmented with proposed vacancy impurity bands (VD_7 and VD_8). VD_8 indicates modes due to cells with 8 deuterons around a Pd vacancy; VD_7 indicates modes due to 7 deuterons around a Pd vacancy.

In a metal hydride that works in the way ou above, the generation of a very large number of ph in "gap-jumping" phonon modes results in an uns system that will decay through any mechanism tha duces an additional vacancy. For example, the Cou interaction between an electron and a nucleus can in a fast ejected electron, as long as the recoil is suff to irreversibly displace the nucleus; in this case the tion energy is supplied by the lattice through frequ shifting a large number of phonons, which is caus the reaction. Coulomb interactions between neighb nuclei can cause recoil capable at lower energy of ing nuclei and causing phonon mode jumps. In the that the lattice transfers a very large amount of en nuclear decay channels become available.

In what follows, we will outline briefly the basic th for anomlous energy transfer from the lattice, and review results for various decay channels. Although straightforward to compute reaction rates using Fe Golden Rule, we find that the rates predicted in this are much too large for the processes to occur inde dently; Fermi's Golden Rule breaks down. Conseque if the processes occur at all, they must occur in b as coupled reactions. The generalization of the th to describe coupled reactions is straightforward form but leads to formulas fo reaction rates that appe be difficult to evaluate; we propose a method to ex numerical results from these formula.

II. LATTICE-INDUCED FAST ELECTRON PROD TION

The decay of a highly-excited atomic or nuclear tem by Coulomb-mediated fast electron production is known; in the atomic system the process is known a toionization, or Auger decay; in the nuclear system, process is known as internal conversion. A molecule a very high level of vibrational excitation could in pr ple decay through electron ejection, although the au is not aware of any examples where this has been served. The decay of a highly excited lattice by fast tron ejection as a direct process has not been descr previously.

A lattice with a highly-excited gap-jumping mode be able to decay by electron ejection, as long the r is sufficiently great for a vacancy to be produced. A example, we consider lattice decay through ejection K-shell electron, in a lattice with very great excita of the lowest optical phonon modes. The electron re in this case must be sufficiently strong to permane dislodge the nucleus. Our goal in what follows here describe a theory for this process that includes expli the energy transfer from the lattice, the Coulomb in

action between electron and nucleus, and the resulting nuclear recoil.

In perhaps the simplest possible model for such a decay process, we start with Fermi's Golden Rule

$$\Gamma = \frac{2\pi}{\hbar}\sum_f \sum_{\mathbf{k}} |<\Psi_i|\hat{V}|\Psi_f>|^2 \delta (I_K + \hbar^2|\mathbf{k}|^2/2m_e + E_f^{(L)} - E_i^{(L)}) \quad (2.1)$$

In this formula, the phonon operator $\hat{V}$ is the Coulomb potential between the nuclei and the K-shell electrons

$$\hat{V} = \sum_j \sum_{j'} \frac{Ze^2}{|\mathbf{r}_{j'} - \hat{\mathbf{R}}_j|} \quad (2.2)$$

where $\mathbf{r}$ refers to the electron coordinate, and where the nuclear center of mass coordinates $\hat{\mathbf{R}}_j$ are taken to be lattice phonon operators. The summations are over all final lattice states f and final electron momenta $\mathbf{k}$. Energy conservation is constrained between the initial lattice energy and final lattice plus electron energy; I_K is the K-shell electron binding energy.

The individual matrix elements that occur in Fermi's Golden Rule rate formula

$$M = <\Psi_i|\hat{V}|\Psi_f> \quad (2.3)$$

approximately factor into parts that can be individually identified with Coulomb exchange, recoil, and frequency-shifting of phonon modes, as we will argue below. To do so, we will use the Born approximation for the free electron, and the Born-Oppenheimer approximation for the lattice nuclear motion.

For the computation of an individual matrix element, the initial and final state wavefunctions are taken to be product wavefunctions that are built up from lattice wavefunctions $\Psi^{(L)}$ and single electron orbitals ϕ as follows:

$$\Psi_i = \Psi_i^{(L)} \phi_{1s}(\mathbf{r} - \hat{\mathbf{R}}_j) \quad (2.4)$$

$$\Psi_f = \Psi_f^{(L)} \phi_{\mathbf{k}}(\mathbf{r}) \quad (2.5)$$

This form of initial and final state wavefunctions is appropriate for a rate involving a single electron transfer; had we started with a more complicated many-electron wavefunction, we would find that only one orbital at a time contributes to the total rate. We must keep the total lattice wavefunction at this point, since the vibrational energy that is transferred in the process is not localized.

The integration over an electron coordinate at site j yields

$$\int \phi_{1s}^*(\mathbf{r} - \mathbf{R}_j) \frac{Ze^2}{|\mathbf{r} - \hat{\mathbf{R}}_j|} \phi_{\mathbf{k}}(\mathbf{r}) d^3\mathbf{r} = V(\mathbf{k}) e^{i\mathbf{k}\cdot\hat{\mathbf{R}}_j} \quad (2.6)$$

where

$$V(\mathbf{k}) = Ze^2 \left[\frac{N_{1s}}{V}\right]^{\frac{1}{2}} \left[\frac{Z^3}{\pi a_0^3}\right]^{\frac{1}{2}} \frac{4\pi}{|\mathbf{k}|^2 + (Z/a_0)^2} \quad (2.7)$$

assuming a nonrelativistic $1s$ hydrogenic orbital and a plane-wave $e^{i\mathbf{k}\cdot\mathbf{r}}/\sqrt{V}$ continuum orbital; the number of $1s$ electrons in the K-shell orbital at site j is N_{1s}.

The matrix element for a Coulomb exchange that occurs at site j can now be written as

$$M = V(\mathbf{k}) <\Psi_i^{(L)}|e^{i\mathbf{k}\cdot\hat{\mathbf{R}}_j}|\Psi_f^{(L)}> \quad (2.8)$$

The definitions of the phonon modes may differ between the initial and final lattice states, so that some care must be taken in analyzing this matrix element. In our previous work on energy transfer in the case of neutron capture reactions,[15] we found that correct answers could be obtained most simply by taking equation (2.8) to be defined as involving integrations over nuclear center of mass coordinates

$$M = V(\mathbf{k}) <\Psi_i^{(L)}(\{\mathbf{R}\})|e^{i\mathbf{k}\cdot\mathbf{R}_j}|\Psi_f^{(L)}(\{\mathbf{R}\})> \quad (2.9)$$

temporarily dispensing with carats to indicate phonon operators. Considering all terms to be functions of center of mass coordinates removes any such problems because the center of mass coordinates themselves are invariant during Coulomb exchange. The nuclear center of mass coordinates can be expressed in terms of the initial state and final state phonon mode amplitudes q_m through

$$\mathbf{R}_j = \mathbf{R}_j^{0,i} + \sum_m \mathbf{u}_m^{(i)}(j) q_m \quad (2.10)$$

$$\mathbf{R}_j = \mathbf{R}_j^{0,f} + \sum_m \mathbf{u}_m^{(f)}(j) q_m \quad (2.11)$$

where $\mathbf{u}_m^{(i)}(j)$ and $\mathbf{u}_m^{(f)}(j)$ are the lattice displacement vectors for the initial and final lattices.

We need to recast the matrix element M in terms of phonon mode amplitudes in order to analyze frequency-shifting effects. Changing over to phonon amplitudes leads to

$$M = V(\mathbf{k}) C <\Psi_i^{(L)}(\mathbf{q}_i)|e^{i\mathbf{k}\cdot\mathbf{R}_j}|\Psi_f^{(L)}(\mathbf{q}_f)> \quad (2.12)$$

The normalization coefficient C is required since the initial and final state phonon amplitudes may not be equivalent. Due to this inequivalence, the matrix element is very difficult to compute in its present form; we would be able to make further progress if we could express Ψ_f in terms of $\mathbf{q}_i$.

As a consequence of the invariance of the center of mass coordinates during Coulomb exchange, there exists a linear relationship between the initial and final state mode amplitudes. From equations (2.10) and (2.11), it is possible to compute individual final state phonon amplitudes in terms of initial state phonon amplitudes; the resulting relation can be summarized as

$$\mathbf{q}_f = \mathbf{A} \cdot \mathbf{q}_i + \mathbf{b} \qquad (2.13)$$

in the case of a harmonic lattice. This problem is well known in the case of electronic transitions in polyatomic molecules; this relation between initial and final state phonon amplitudes is called a Duschinsky transformation.[16]

Our goal of obtaining the final state wavefunction in terms of the initial state coordinates is accomplished through the use of the Duschinsky operator $e^{-i\hat{S}_D}$,[17] which has the property

$$e^{-i\hat{S}_D}\psi(\mathbf{q}_i) = \psi(\mathbf{A} \cdot \mathbf{q}_i + \mathbf{b}) = \psi(\mathbf{q}_f) \qquad (2.14)$$

We may use this to rewrite the matrix element M as

$$M = V(\mathbf{k}) < \Psi_i^{(L)}(\mathbf{q}_i)|e^{i\mathbf{k}\cdot\hat{\mathbf{R}}_j}e^{-i\hat{S}_D}|\Psi_f^{(L)}(\mathbf{q}_i) > \qquad (2.15)$$

once again using carats to indicate phonon operators.

There exists a very large number of phonon modes in a macroscopic lattice, but only a few modes can undergo a significant frequency shift during the creation of a single vacancy. Although the frequency-shifting modes will be involved in the recoil, recoil effects will be dominated by the vast majority of the modes that do not undergo any significant frequency shift. This suggests that a separation between recoil effects and frequency-shifting would be a reasonably good approximation, leading to

$$M \approx V(\mathbf{k}) < \Psi_i^{(L)}(\mathbf{q}_i)|e^{-i\hat{S}_D}|\Psi_f^{(L)}(\mathbf{q}_i) >_{m^*} \times < \Psi_i^{(L)}(\mathbf{q}_i)|e^{i\mathbf{k}\cdot\mathbf{R}_j}|\Psi_f^{(L)}(\mathbf{q}_i) >_m \qquad (2.16)$$

where $< \cdots >_m^*$ denotes an average over the gap-jumping modes, and where $< \cdots >_m$ denotes an average over non gap-jumping modes. This result perhaps exhibits most cleanly the physics involved in the proposed decay of a highly excited lattice by electron emission; the Coulomb exchange between nucleus and electron results in ... energy transfer of the lattice comes about through ... quency shifts in a small number of phonon modes; ... the vacancy production required for energy transfe... occur is a simple recoil effect.

The reaction rate for a transition at site j is then g... by

$$\Gamma_j = \frac{2\pi}{\hbar}\sum_{f,\mathbf{k}}|V(\mathbf{k})|^2| < \Psi_i^{(L)}(\mathbf{q}_i)|e^{-i\hat{S}_D}|\Psi_f^{(L)}(\mathbf{q}_i) >_m$$

$$\times | < \Psi_i^{(L)}(\mathbf{q}_i)|e^{i\mathbf{k}\cdot\mathbf{R}_j}|\Psi_f^{(L)}(\mathbf{q}_i) >_m |^2$$

$$\times \delta(I_K + \hbar^2|\mathbf{k}|^2/2m_e + E_f^{(L)} - E_i^{(L)}) \quad (...$$

It is convenient to introduce a function that keeps tra... the probability that an energy transfer ϵ occurs, giv... recoil momentum $\mathbf{k}$. Such a function may be conveni... defined through

$$p_{j,\mathbf{k}}(\epsilon) = \sum_f | < \Psi_i^{(L)}(\mathbf{q}_i)|e^{-i\hat{S}_D}|\Psi_f^{(L)}(\mathbf{q}_i) >_{m^*} |^2$$

$$| < \Psi_i^{(L)}(\mathbf{q}_i)|e^{i\mathbf{k}\cdot\mathbf{R}_j}|\Psi_f^{(L)}(\mathbf{q}_i) >_m |^2 \delta(\epsilon + E_f^{(L)} - E_i^{(L)}) \quad (...$$

This function may be used to develop a perhaps ... intuitive version of the decay rate, given by

$$\Gamma_j = \sum_{\mathbf{k}}\int p_{j,\mathbf{k}}(\epsilon)\Gamma_{j,\mathbf{k}}(\epsilon)d\epsilon \qquad (...$$

with

$$\Gamma_{j,\mathbf{k}}(\epsilon) = \frac{2\pi}{\hbar}|V(\mathbf{k})|^2\delta(I_K + \hbar^2|\mathbf{k}|^2/2m_e - \epsilon) \quad (...$$

These formulas suggest a point of view in which ... exists a probability p of transferring an energy ϵ fron... lattice, and that energy transfer drives a reaction ... a partial rate that may be computed essentially wit... consideration of lattice effects.

The computation of $p_{j,\mathbf{k}}(\epsilon)$ is of course in general ... complicated. As defined, this function is proporti... to a lineshape function that might be associated wi... process that has an associated recoil and that modifie... underlying phonon mode structure. The recoil tern... itself is generally computed by evaluating contribut... from 0,1,...,n-phonon pieces; the mode-matching ph... is usually treated in perturbation theory. In the ca... a thermal lattice, this function would result in a ra... standard few-meV wide line that is perhaps shifted ... few-meV. However, if there exist highly excited ph...

modes that jump a band gap as a result of modifications to the lattice due to recoil, then the function must shift in energy by an amount $n\delta\omega$ for each mode that jumps, as would a line profile under corresponding circumstances.

In general, there will be a probability that sufficient recoil will occur to cause a gap jumps, as well as a probability that the recoil is insufficient to cause gap jumps. In this case, the function $p_{j,\mathbf{k}}(\epsilon)$ will have two pieces – one that gives energy transfer, and one that does not. Of course, if no energy transfer occurs due to gap-jumping, then the energy transfer from the lattice from thermal recoil effects alone will be too small to drive any of the reactions that we consider below. Consequently, our interest is focussed only on the part of $p_{j,\mathbf{k}}(\epsilon)$ that corresponds to situations where gap-jumping occurs. Mathematically, the probability $p_{j,\mathbf{k}}(\epsilon)$ will be of the form

$$p(\epsilon) = |T|^2 p_{jump}(\epsilon - \sum n\hbar\delta\omega) + (1-|T|^2)p_{no\ jump}(\epsilon) \tag{2.21}$$

where $|T|^2$ is the probability that the recoil was sufficient to cause a jump, and where $p_{jump}(\epsilon)$ and $p_{no\ jump}(\epsilon)$ are complicated functions of energy whose precise shapes will be of little concern to us, as long as $p_{jump}(\epsilon)$ is narrow compared to the energy transfer $\sum n\hbar\delta\omega$. In what follows, we will discuss this further. Given that $p_{no\ jump}(\epsilon)$ is of no interest in computing reaction rates for anomalous processes, we will neglect it henceforth.

We have computed previously the line shape for lattice energy transfer as a function of ϵ in the case of neutron capture,[12] under conditions where there was no direct recoil (in this case, the energy transfer occurs through a mass change rather than through the creation of a vacancy). We found that the probability for energy transfer in the case of a single gap-jumping phonon mode initially in a number state was a shifted Gaussian

$$\sum_f |<\Psi_i^{(L)}(\mathbf{q}_i)|e^{-iS_D}|\Psi_f^{(L)}(\mathbf{q}_i)>_{m^*}|^2 \sim e^{-\beta(\epsilon - n<\hbar\delta\omega>)^2} \tag{2.22}$$

where ϵ is the actual energy transfer from the lattice, and $n<\hbar\delta\omega>$ is the expectation value of the energy transfer. The line is narrow; $\beta^{-1} \sim n<(\hbar\delta\omega)^2>$. The spread is due to the range of frequencies of the final-state modes into which a single gap-jumping mode projects.

Perhaps more relevant (since it is not clear how to excite a phonon mode to a number state) is the probability distribution in the case of a highly excited gap-jumping continuum phonon that is initially in a classical state. A classical state $|\alpha>$ can be constructed from number states, and it is well known that a Poisson distribution is produced:[18]

$$|\alpha> = e^{-|\alpha|^2/2}\sum_n \frac{\alpha^n}{\sqrt{n!}}|n> \tag{2.23}$$

which leads to

$$|<n|\alpha>|^2 = e^{-|\alpha|^2}\frac{|\alpha|^{2n}}{n!} \tag{2.24}$$

A highly excited classical state is well approximated by a shifted Gaussian around the mean number of phonons $<n>=\alpha^2$; in this case the variance is

$$<\Delta n^2> = <(n-<n>)^2> = <n>$$

For an energy transfer of 1 MeV, on the order of 10^8 or more phonons must be present, which implies a narrow probability distribution $\sqrt{<\Delta n^2>}/<n> \sim 10^{-4}$. Consequently, both for number states and for classical states, it will be an excellent approximation to take

$$p(\epsilon) \approx \delta(\epsilon - \sum_{m^*} <n_{m^*}><\hbar\delta\omega_{m^*}>) \tag{2.25}$$

Here we must extend our analysis to include recoil effects in the probability function. In the case of electron ejection the recoil is relatively weak, and the essential effect that occurs is that the transfer of energy is prevented unless the recoil energy is sufficiently strong to permanently dislodge the nucleus.

For most of the values of the lattice energy transfer ϵ that are of potential interest, the recoil momentum is sufficiently great that a vacancy is created with certainty. An accurate calculation of the recoil matrix element requires a model for inter-nuclear potentials in the lattice, and is beyond the scope of this work. In essence, a nucleus that recoils must overcome a potential barrier to land in a new and inequivalent site in order to satisfy the requirement that the phonon modes be irreversibly changed. We assume that the energy of the vacancy plus displaced nucleus lies at an energy E_d relative to the initial configuration, that the barrier energy is E_b, and that the potential barrier is adequately modeled by a parabola over a distance d

$$V_b(x) = E_b - \frac{1}{2}\alpha x^2 \tag{2.26}$$

with $V_b(\pm d/2) = E_d$. We then obtain an estimate of the efficiency for tunneling for $E_d < E_r < E_b$ to be

$$\sum_f |<\Psi_i^{(L)}(\mathbf{q}_i)|e^{i\mathbf{k}\cdot\mathbf{R}_j}|\Psi_f^{(L)}(\mathbf{q}_i)>_m|^2 = |T(\mathbf{k})|^2$$

$$\Gamma \approx \exp\left\{-\frac{\pi}{2}\frac{(E_b - E_r)}{\sqrt{(E_b - E_d)(\hbar^2/2Md^2)}}\right\} \quad (2.27)$$

where E_r is the recoil energy of the Pd nucleus $\hbar^2|\mathbf{k}|^2/2M$. For $E_r < E_d$, a vacancy is not created, and we take $T = 0$; for $E > E_b$ we assume that the decay occurs freely, and $|T|^2 = 1$.

We have found that the frequency-shift of gap-jumping phonon modes leads ultimately to the appearance of an isolated system reaction rate evaluated at an anomalous energy transfer ϵ; the recoil effects primarily cuts off the reaction rate at low energy. Precisely where this cut-off occurs as a function of lattice energy transfer depends strongly on the details of the chemical environment in the vicinity of the nucleus, details that are not easily available at present. The parabolic tunneling model presented here allows us to obtain predictions given "reasonable" estimates of the excitation energies and barriers.

These approximations lead to an estimate of the reaction rate per nucleus given by

$$\Gamma_j = \Gamma_0(\Delta E_L)\ |T(\mathbf{k})|^2 \quad (2.28)$$

where the lattice energy transfer is

$$\Delta E_L = \sum_{m^*} < n_{m^*} >< \hbar\delta\omega_{m^*} > \quad (2.29)$$

and where the rate $\Gamma_0(\epsilon)$ is obtained by summing over $\mathbf{k}$ to yield

$$\Gamma_0(\epsilon) = \frac{2\pi}{\hbar}|V(\mathbf{k})|^2\rho(E_f) \quad (2.30)$$

where $\mathbf{k}$ is evaluated at $\hbar^2|\mathbf{k}|^2/2m_e = \epsilon - I_K$. Inserting expressions for $V(\mathbf{k})$ and for $\rho(E_f)$, we obtain

$$\Gamma_0(\epsilon) = \frac{24N_{1s}}{\pi Z}\frac{I_H}{\hbar}\left[\frac{\epsilon}{I_H}\right]^{\frac{1}{2}}\frac{1}{[1+(\epsilon/Z^2I_H)]^2} \quad (2.31)$$

where I_H is 13.6058 eV.

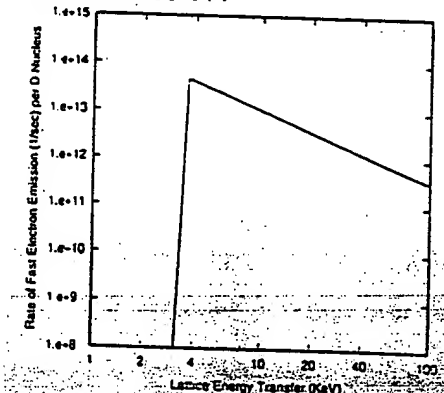

Figure 2: Predicted fast electron emission rate from deuterons as a function of lattice energy transfer.

Results for K-shell ejection from deuterium and fr Pd in PdD are shown in Figures 2 and 3. The thresh for emission of fast electrons occurs when the recoil ener of the nucleus becomes equal to the barrier energy vacancy creation; this occurs in the nonrelativistic lir at

$$\Delta E = 1835\ A\ E_d \quad (2.$$

In the case of Pd vacancy production, we have used E_d $6eV$ and $E_b = 10eV$ as our "reasonable" estimates energies required to irreversibly create a vacancy. the case of deuterium, we have selected the paramet $E_=0.7eV$, $E_b = 1.0eV$ and $d = 1a_0$; while the excitati to nearby octohedral or tetrahedral sites will occur wi energies below 0.3eV, 1 eV should be sufficient to mc the deuterium to a more remote local. Relativistic fc mulas have been used to estimate the recoil energy in t Figures.

It should be noted that the phonon modes that jun a band gap are different for these two processes. We ha discussed gap-jumping in the case of Pd vacancy creatic above; this process should occur with strong excitatic of the lowest optical phonon modes. In the case of de terium vacancy creation, we rely on a postulate set isolated vacanc impurity modes that correspond to cel with different numbers of deuterons in the vicinity of host metal vacancy.

The decay rates per nucleus for these processes a seen to be very large, consequently the total lattice deca rates will be so great that it must be questioned unde what conditions the model will be valid. We will examir this question in the following section.

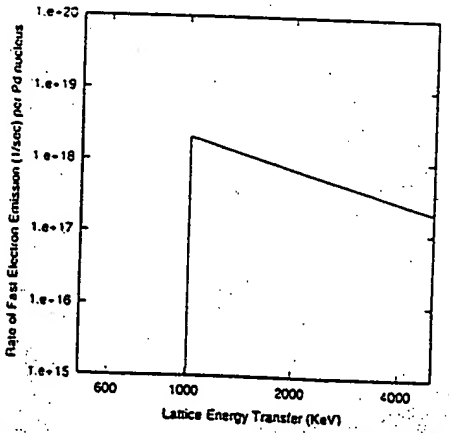

Figure 3: Predicted fast electron emission rate fron Pd nuclei as a function of lattice energy transfer.

III. COUPLED REACTIONS

The reaction rate estimates presented in the last sec tion indicates that a lattice with very highly excited gap jumping phonon modes will decay by fast electron emis

out very rapidly. The characteristic decay rates can be greater than 10^{10} sec^{-1} per nucleus, which if correct, would perhaps imply a total lattice decay rate between 10^{25} and 10^{30} sec^{-1} for the total volume over which the phonon modes extend; these total rates are much too fast to be physical.

Towards the resolution of this problem, there are a number of issues that must be considered. For example, if the lattice decay rate is so fast, then it becomes problematic how the lattice could have been so highly excited originally. In the process of exciting the gap-jumping modes, a fast decay should have occured once sufficient excitation was present to enable Coulomb decay to occur at all at much slower rates. Under these conditions, the theory described in Section II would apply, and no inconsistencies would be present.

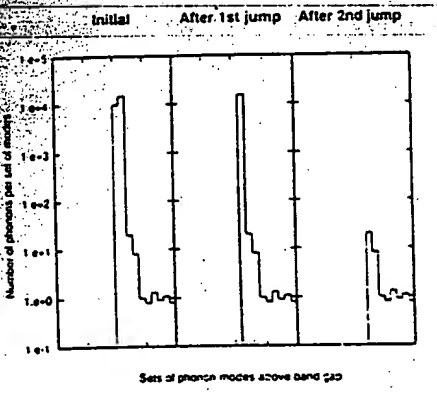

Figure 4: Pictorial of phonon mode excitation near the band gap before and after gap-jumping.

The situation becomes very much more interesting under conditions where the initial moderately-excited modes jump the gap to reveal new gap-jumping modes that are much more highly excited. When downward gap-jumping occurs, it is the lowest phonon modes above the gap that actually jump (see Figure 4). If several jumps occur in succession, it is always the lowest modes that jump in any specific reaction; consequently, phonon modes are stripped away from the bottom in sequence, much like the peeling of an onion.

Under such conditions, it can no longer be argued that the phonon population could not have built up without provoking a fast Coulomb decay; highly excited modes that are shielded from the gap by unexcited modes are free to build up to very high levels, as illustrated in Figure 5. Nevertheless, we would be certain that if the resulting rate estimate when these modes did finally jump, were on the order of 10^{25} to 10^{30} sec^{-1}, that rate estimate must be in error.

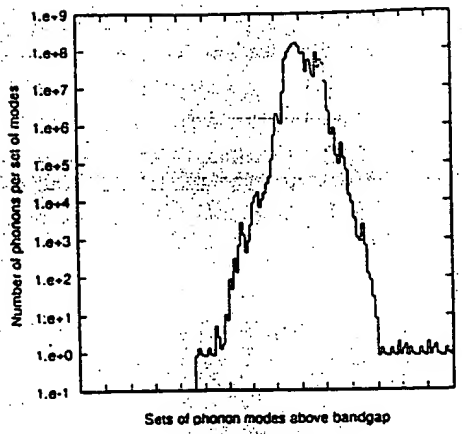

Figure 5: Pictorial of high phonon mode excitation that is shielded from the band gap by modes with low excitation.

The resolution to this problem is that the two reactions would become coupled together in the Raman sense, and reaction rates must be computed using a theory which fundamentally treats the processes as coupled. The mechanisms that would produce very high phonon populations would however likely not result in such high selectivity as to produce just one or two reactions, rather it is more-likely that 10^5 to 10^8 phonon modes would cause reactions at a time. Consequently, we require a theory for bursts of large numbers of reactions.

The starting point for our discussion is the expression for a single isolated event from the last section, recast as

$$\Gamma_j = \frac{2\pi}{\hbar}\sum_{\mathbf{k}}|V(\mathbf{k})|^2\int d\epsilon\, p_{j,\mathbf{k}}(\epsilon)\delta(I_K+\frac{\hbar^2|\mathbf{k}|^2}{2m_e}-\epsilon) \quad (3.1)$$

Taking the probability function to be sharply peaked in energy, we obtain

$$\Gamma_j = \frac{2\pi}{\hbar}\sum_{\mathbf{k}}|V(\mathbf{k})|^2|T(\mathbf{k})|^2\delta(I_K+\frac{\hbar^2|\mathbf{k}|^2}{2m_e}-\overline{n}\hbar\overline{\delta\omega}) \quad (3.2)$$

We have used $\overline{n}\hbar\overline{\delta\omega}$ for $\sum_{m'} < n_{m'} >< \delta\hbar\omega_{m'} >$, as the spread will be similar for gap jumping modes.

In the case of two coupled reactions, we obtain

$$\Gamma_{j_1,j_2} = \frac{\pi}{\hbar}\sum_{\mathbf{k}_1}\sum_{\mathbf{k}_2}\left|\frac{V(\mathbf{k}_1)V(\mathbf{k}_2)T(\mathbf{k}_1)T(\mathbf{k}_2)}{I_K+\frac{\hbar^2|\mathbf{k}_1|^2}{2m_e}-\overline{n}_1\hbar\overline{\delta\omega}_1-i\hbar\gamma}\right.$$
$$\left.+\frac{V(\mathbf{k}_2)V(\mathbf{k}_1)T(\mathbf{k}_2)T(\mathbf{k}_1)}{I_K+\frac{\hbar^2|\mathbf{k}_2|^2}{2m_e}-\overline{n}_1\hbar\overline{\delta\omega}_1-i\hbar\gamma}\right|^2$$
$$\times\delta(2I_K+\frac{\hbar^2|\mathbf{k}_1|^2}{2m_e}+\frac{\hbar^2|\mathbf{k}_2|^2}{2m_e}-\overline{n}_1\hbar\overline{\delta\omega}_1-\overline{n}_2\hbar\overline{\delta\omega}_2) \quad (3.3)$$

The interaction matrix element is now composed of two terms, as is appropriate for a second order process. The relative phases between the various matrix elements will generally be random; when averaged over all pairs of sites in the lattice, the interference terms will not contribute due to cancellation. Consequently, it is of interest to focus on a site-averaged version of the decay rate

$$\overline{\Gamma}_{fi} = \frac{2\pi}{\hbar}\sum_{\mathbf{k}_1}\sum_{\mathbf{k}_2}\frac{|V(\mathbf{k}_1)V(\mathbf{k}_2)T(\mathbf{k}_1)T(\mathbf{k}_2)|^2}{(I_K+\frac{\hbar^2|\mathbf{k}_1|^2}{2m_e}-\overline{n}_1\hbar\overline{\delta\omega}_1)^2+\hbar^2\gamma^2}$$

$$\delta(2I_K+\frac{\hbar^2|\mathbf{k}_1|^2}{2m_e}+\frac{\hbar^2|\mathbf{k}_2|^2}{2m_e}-\overline{n}_1\hbar\overline{\delta\omega}_1-\overline{n}_2\hbar\overline{\delta\omega}_2) \quad (3.4)$$

To obtain the total decay rate, this formula must be summed over all pairs of nuclei in a domain in which the highly excited phonon modes exist.

Further generalization to larger numbers of coupled reactions is straightforward; we obtain

$$\overline{\Gamma}_N = \frac{2\pi}{\hbar}$$

$$\sum_{\mathbf{k}_1\cdots\mathbf{k}_N}\frac{|V(\mathbf{k}_1)T(\mathbf{k}_1)|^2\cdots|V(\mathbf{k}_N)T(\mathbf{k}_N)|^2}{\prod_j^{N-1}\left[\left[jI_K+\sum_i^j(\frac{\hbar^2|\mathbf{k}_i|^2}{2m_e}-\overline{n}_i\hbar\overline{\delta\omega}_i)\right]^2+\hbar^2\gamma^2\right]}$$

$$\times\delta(NI_K+\sum_j^N\frac{\hbar^2|\mathbf{k}_j|^2}{2m_e}-\sum_j^N\overline{n}_j\hbar\overline{\delta\omega}_j) \quad (3.5)$$

This formula, summed over all sets of N nuclei in the domain of the highly excited phonon modes, would give the decay rate for an N-particle "burst".

The appearance of such high order matrix elements in the calculation of reaction rates is rare in the literature. A currently active area of research wherein high order matrix elements are calculated routinely is the area of laser-induced multi-photon ionization.[19] A number of methods have proven to be successful in these calculations, including Floquet theory coupled with R-matrix methods,[20] and time-dependent Hartree-Fock theory.[21] These types of methods could be used in the present case with some modifications.

It is possible that reliable rates for the present problem could be obtained using a method of steepest descents. The basic idea is as follows: The largest total decay rates would be obtained in the limit that all of the individual steps were resonant; however, many of the transitions will likely take place off of resonance if an adequate degree of phonon excitation is not present — this would be especially true of the earliest decays, which were postulated above to be at best marginal. As a result, excitatio ergy must be borrowed from those phonon modes are well above threshold in order for decays to occur sufficient recoil to cause phonon modes to jump th in cases where the phonon excitation is marginal.

Consequently, it should be possible to select a timum set of decay energies $\{|\mathbf{k}|^2\}$, subject to the straint that overall energy conservation be mainta that would give the largest possible value for the pro inside the summation of equation (3.5). This opti would likely have many decays occuring on reson with as few decays as possible loaning energy to t decays that are marginal or forbidden. Away from optimum selection of decay energies, there would be contribution to the summations; the reduction in the tribution would by definition be second order away the optimum, and this could be evaluated algebrai using Gaussian integrations.

These arguments imply the following approxima scheme. Define the variational function

$$I[\mathbf{k}_1\cdots\mathbf{k}_N] =$$

$$\frac{|V(\mathbf{k}_1)T(\mathbf{k}_1)|^2\cdots|V(\mathbf{k}_N)T(\mathbf{k}_N)|^2}{\prod_j^{N-1}\left[\left[jI_K+\sum_i^j(\frac{\hbar^2|\mathbf{k}_i|^2}{2m_e}-\overline{n}_i\hbar\overline{\delta\omega}_i)\right]^2+\hbar^2\gamma^2\right]}$$

$$-\lambda(NI_K+\sum_j^N\frac{\hbar^2|\mathbf{k}_j|^2}{2m_e}-\sum_j^N\overline{n}_j\hbar\overline{\delta\omega}_j) \quad ($$

where λ is a Lagrange multiplier. Compute the optin distribution of decay energies through

$$\frac{\partial}{\partial k_i}I[\mathbf{k}_1\cdots\mathbf{k}_N]\Big|_{\{\mathbf{k}\}_0}=0 \quad ($$

Next, develop a Gaussian model around the optimum of decay energies

$$J(\mathbf{k}_1\cdots\mathbf{k}_{N-1}) = J_0e^{-(\mathbf{k}-\mathbf{k}_0)^T\cdot\mathbf{G}\cdot(\mathbf{k}-\mathbf{k}_0)} \quad ($$

where we have adopted a notation $\mathbf{k}$ for a very large ve composed of all individual components for $\mathbf{k}_1\cdots\mathbf{k}_N$ the optimum for the momenta is now denoted by $\mathbf{k}_0$. partial sum $J(\mathbf{k}_1\cdots\mathbf{k}_{N-1})$ is defined by

$$J(\mathbf{k}_1\cdots\mathbf{k}_{N-1}) =$$

$$\sum_{\mathbf{k}_N}\frac{|V(\mathbf{k}_1)T(\mathbf{k}_1)|^2\cdots|V(\mathbf{k}_N)T(\mathbf{k}_N)|^2}{\prod_j^{N-1}\left[\left[jI_K+\sum_i^j(\frac{\hbar^2|\mathbf{k}_i|^2}{2m_e}-\overline{n}_i\hbar\overline{\delta\omega}_i)\right]^2+\hbar^2\gamma^2\right]}$$

$$\times\delta(NI_K + \sum_j^N \frac{\hbar^2|\mathbf{k}_j|^2}{2m_e} - \sum_j^N \bar{n}_j\hbar\delta\bar{\omega}_j) \quad (3.9)$$

The matrix G is obtained by matching second derivatives around the optimum. Finally, the total decay rate is computed using

$$\bar{\Gamma}_N = \frac{2\pi}{\hbar}\sum_{\mathbf{k}_1}\cdots\sum_{\mathbf{k}_{N-1}} J_0 e^{-(\mathbf{k}-\mathbf{k}_0)^T\mathbf{G}(\mathbf{k}-\mathbf{k}_0)} \quad (3.10)$$

taking advantage of algebraic Gaussian integration formulas.

We have not carried out any computations for the rates of "bursts" yet with this model; this project is left for future work. There is little question that the excitation of many low-lying modes will result in decays that occur through bursts, and in principle we will be able to estimate rates for the bursts, either with the formulas presented above or through other routes. It is of interest to inquire as to what distribution of decay products would be expected within a burst, assuming that more than one possible decay channel occurs. The theory for bursts presented above is readily generalized in the case of multiple decay channels, with little change in essential physics. The distribution of decay products would be determined in principle by performing sets of burst rate calculations with slightly different sets of decay channels around whatever set of decay channels maximizes the total burst rate.

As these models have not yet been studied, we cannot say at this point with certainty what distribution of decay products should be expected in general. Nevertheless, the appearance of each individual decay process occurs in the total burst rate formula through terms that are very much like those that occur in the single-event version of Fermi's Golden Rule rate. One might postulate that the burst rate fraction f_j for a single decay channel could be estimated by computing the ratio of the single-event rate with the total of all possible single-event rates for all available decay channels dependent on the same phonon modes

$$f_j = \frac{\Gamma_j}{\sum_i \Gamma_i} \quad (3.11)$$

Such a formula might be useful in a "low rate" limit, corresponding to the I^n dependence observed for n-photon absorption in the low intensity regime. Whereas the multiphoton rates saturate at high I, a non-perturbative treatment of the bursts would likely show "saturation effects". In this limit, a weak channel competing with a stronger channel would have a lower fraction f_j, but it is not clear at this point by how much. In the sections that follow, lacking more precise tools to quantify reaction rates, we will continue to calculate Fermi's Golden Rule rates for the various channels as single events, keeping in mind that these estimates are only qualitative indicators of actual rates and fractions.

IV. DEUTERON ACCELERATION AND NEUTRON PRODUCTION

Another dominant decay mechanism for a lattice that possesses very highly excited gap-jumping phonon modes is Coulomb-induced nucleus-nucleus recoil. For example, if two Pd nuclei in PdD recoil off of each other with 50 eV energy input from the lattice, at least two Pd vacancies will be created; depending on the details of the outcome, this process could self-consistently lead to energy transfer from the lattice caused by highly excited optical phonon mode jumping a band gap to increase the number of "vacancy" optical phonon models.

Perhaps the most interesting example of this process is lattice decay by deuteron recoil off of other nuclei, for the reason that fast deuterons produced in this way could in principle fuse with other deuterons in the lattice resulting in dd-fusion neutrons at 2.45 MeV. We have estimated decay rates for deuteron-deuteron recoil as a function of lattice energy, and used these rates to estimate neutron production rates; the results are quite interesting, and are not inconsistent with some of the experimental claims for the production of neutrons.

Fermi's Golden Rule applied to lattice-induced deuteron-deuteron recoil gives rise to the following rate estimate

$$\Gamma = \frac{2\pi}{\hbar}\sum_{f,\mathbf{K}} |<\Psi_i|\hat{V}|\Psi_f>|^2\delta(2I_D + \frac{\hbar^2|\mathbf{K}|^2}{2\mu} + E_f^{(L)} - E_i^{(L)}) \quad (4.1)$$

where I_D is the binding energy of a deuteron, $\hbar^2|\mathbf{K}|^2/2\mu$ is the relative kinetic energy of the two deuterons that have recoiled away from each other, and the potential $\hat{V}$ is the Coulomb interaction

$$\hat{V} = \sum_{j<j'} \frac{e^2}{|\hat{\mathbf{R}}_j - \hat{\mathbf{R}}_{j'}|} \quad (4.2)$$

The arguments of Section II can be used here when the energy transfer from the lattice is dominated by the frequency shift of highly excited gap-jumping phonon modes. We focus on the matrix element in the case of the recoil of two specific neighboring deuterons, in which case the Coulomb matrix element can be written in terms of phonon amplitudes

$$<\Psi_i|\hat{V}_{j,j'}|\Psi_f> = <\Psi_i(\mathbf{q}_i)|\hat{V}_{j,j'}e^{-iS_D}|\Psi_f(\mathbf{q}_i)> \quad (4.3)$$

where the Duschinsky operator takes into account modifications in the phonon mode structure. As before, the matrix element separates approximately into a piece responsible for the primary energy transfer, and a piece containing the majority of non-gap-jumping phonon modes that are involved in the recoil process

$$< \Psi_i(q_i)|\hat{V}_{j,j'}e^{-iS_D}|\Psi_f(q_i) > \approx$$

$$< \Psi_i(q_i)|e^{-iS_D}|\Psi_f(q_i) >_{m^*} < \Psi_i(q_i)|\hat{V}_{j,j'}|\Psi_f(q_i) >_m \quad (4.4)$$

The initial and final states $\Psi_i(q_i)$ and $\Psi_f(q_i)$ have the same energy, and total energy is conserved in this type of recoil reaction. Following the arguments of the last two sections, the Duschinsky matrix element will be sharply peaked around an energy transfer of $< n >< \hbar\delta\omega >$ for the m^* phonon modes that jump the gap. Because of energy conservation, this energy becomes available for the local Coulomb repulsion between two nuclei. We obtain

$$\Gamma_{j,j'} = \frac{2\pi}{\hbar}\sum_f\sum_{\mathbf{K}}| < \Psi_i(q_i)|e^{-iS_D}|\Psi_f(q_i) >_{m^*} |^2$$

$$| < \Psi_i(q_i)|\hat{V}_{j,j'}|\Psi_f(q_i) >_m |^2\delta(2I_D + \frac{\hbar^2|\mathbf{K}|^2}{2\mu} + E_f^{(L)} - E_i^{(L)}) \quad (4.5)$$

which evaluates approximately to

$$\Gamma_{j,j'} = \frac{2\pi}{\hbar}\sum_f\sum_{\mathbf{K}}| < \Psi_i(q_i)|\hat{V}_{j,j'}|\Psi_f(q_i) >_m |^2$$

$$\delta(2I_D + \hbar^2|\mathbf{K}|^2/2\mu - < n >< \hbar\delta\omega >) \quad (4.6)$$

This formula assumes that the recoil is sufficiently great to insure that deuterons are truly irreversibly removed from their cells so that the m^* phonon modes jump a bandgap. Our neglect of the tunneling factor in this formula will mean that our results will be valid only for an energy transfer exceeding 2-3 eV.

The local Coulomb repulsion matrix element is strongly dependent on the local chemical environment, since a large recoil can only occur when the deuterons are close together. Focusing on the interesting case of large momentum transfer, we have approximated the relative probability amplitudes of deuterons in the lattice using the molecular D_2 ground state wavefunction:

$$< \Psi_i(q_i)|\hat{V}_{j,j'}|\Psi_f(q_i) >_m \approx < \Psi_{D_2}(\mathbf{r})|\frac{e^2}{|\mathbf{r}|}|\Psi_{\mathbf{K}}(\mathbf{r}) > \quad (4.7)$$

In this formula, the final state $\Psi_{\mathbf{K}}(\mathbf{r})$ represents a c
ciated molecule with a relative momentum betwee
deuterons of $\hbar$K. This type of approximation has
used by many authors to provide molecular estimat
dd-fusion rates thought to be relevant to the proble
fusion rates in PdD. While the applicability of this ty
model in the case of fusion reactions may be question
it is very likely a much better approximation in the
of recoil, since the recoil matrix element samples p
space at larger inter-deuteron separations; the recoil
trix elements appear to be far less sensitive to varia
in the potential.

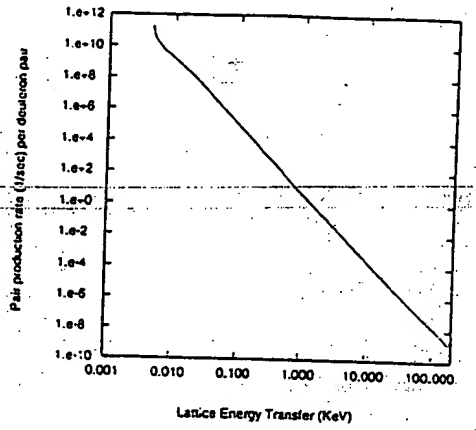

Figure 6: Decay rate per deuteron pair for latt
induced Coulomb recoil.

It was convenient for us to evaulate the reaction r
using a coupled-channel model, which is an improvem
over the approximations discussed above. In this mo
the unperturbed ground state radial wavefunction
computed by solution of the unperturbed radial Schrod
equation

$$EP_o(r) = -\frac{\hbar^2}{2\mu}\frac{d^2}{dr^2}P_o(r) + V(r)P_o(r) \quad (4$$

using the parameterization[22]

$$V(r) = e^{-\alpha r}\left[\frac{e^2}{r} - b\right] \quad (4$$

with $\alpha = 0.886/a_0$ and $b = 2.630I_H$. The continu
channel was computed using

$$\frac{\hbar^2|\mathbf{K}|^2}{2\mu}P(r) = -\frac{\hbar^2}{2\mu}\frac{d^2}{dr^2}P(r) + V(r)P(r) + \frac{e^2}{r}P_o(r) \quad (4.1$$

subject to the boundary condition

$$P(r) \longrightarrow f(\mathbf{K})e^{i|\mathbf{K}|r} \quad (4.1$$

The decay rate is obtained by integrating the outwa
flux over a sphere at large r; this results in

$$\Gamma_{j,j'} = \frac{\hbar|\mathbf{K}|}{\mu}|f(\mathbf{K})|^2 \qquad (4.12)$$

The results of this calculation are shown in Figure 6.

Predicted by this theory are fast deuterons that can in principle fuse with neighboring deuterons. Taking the results of the deuteron-deuteron recoil calculation discussed above, we combined the production rate of fast deuterons with the neutron yield (including the energy loss of the deuterons on the host palladium nuclei) to produce an estimate of the *dd*-fusion neutron rate. The results are shown in Figure 7. Keeping in mind the discussion of Section 3, this process will compete with fast electron production at lattice transfer energies above a few kilovolts, which will have the ultimate effect of essentially eliminating this channel. In metal hydrides with deeper deuteron potentials (such as TiD_2), this competition will be put off to higher lattice transfer energy, resulting in larger neutron production rates.

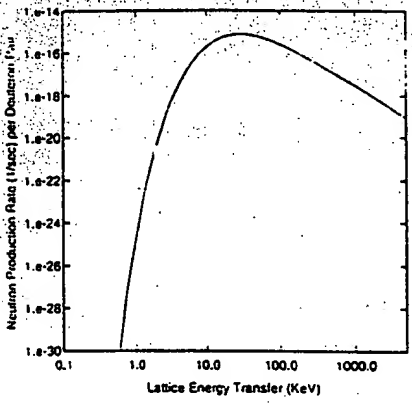

Figure 7: Production rate of *dd*-fusion neutrons from deuteron-deuteron recoil followed by fusion.

For completeness, we estimated reaction rates for the rare process in which the Coulomb exchange causes the two initial recoiling deuterons to fuse with each other. The resulting rate is observed to increase by about thirty orders of magnitude over the ground state D_2 fusion rate, but in our calculations did not compete with the deuteron-other-deuteron fusion rate given above.

V. LATTICE-INDUCED BETA DECAYS

We have thus far discussed the decay of a highly excited lattice through atomic decay channels. The lattice may also decay through available nuclear channels, subject to the constraints discussed above, and in competition with other open channels such as electron recoil. In this section, we examine lattice-induced reactions mediated by the weak force.

The basic theory for lattice-induced electron capture reactions and beta decays follows immediately from the theory outlined in Sections 2 and 3. The Fermi's Golden Rule estimate for a lattice-induced decay is

$$\Gamma = |T(\mathbf{k})|^2\Gamma_0(\Delta E_L) \qquad (5.1)$$

where $|T|^2$ is the probability that the recoil is sufficient to irreversibly create a vacancy, and where $\Gamma_0(\Delta E_L)$ is the rate computed assuming that an energy ΔE_L is transferred from the lattice. We have computed lattice-induced decay rates according to this estimate based on the $f\tau$ theory discussed in Ref. 23.

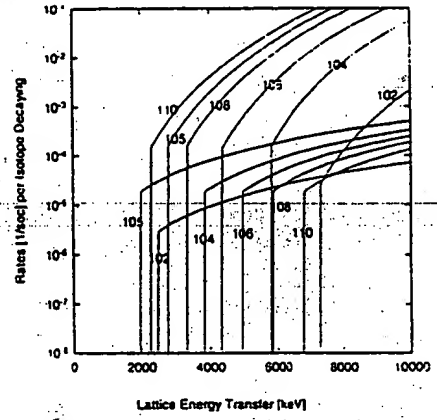

Figure 8: Lattice-induced electron capture and beta decay rates for the Pd nuclei. Curves that continue to rise are e^- decay; curves that are lower are electron capture.

As a function of lattice energy transfer, the first decay to occur is electron capture from ^{105}Pd to ^{105}Rh. This may be interesting, in that the first two excited states of ^{105}Rh occur at 129.6 KeV and at 149.1 KeV; emission at these energies is claimed to have been observed in glow discharge experiments at Luch. Gamma lines produced by the decay of ^{105}Rh back to ^{105}Pd have also been claimed in these experiments.[7] In Figure 8 is shown estimates of the lattice-induced electron capture rates and beta decay rates for the stable Pd nuclei.

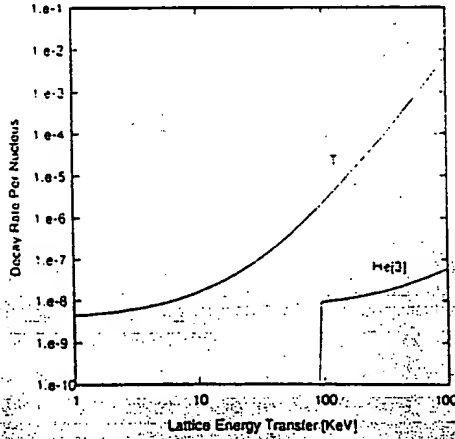

Figure 9: Lattice-enhanced tritium beta decay; lattice-induced ^{3}He electron capture to make tritium.

Isotopes that are already unstable against beta decay can decay more rapidly with extra energy input from the lattice. We studied the enhancement of the beta decay of ^{107}Pd to ^{107}Ag through this mechanism. As expected, no enhancement occurs until the recoil becomes sufficiently great to cause a vacancy to be formed. With the model of Section 2, this does not occur until about 950 KeV. At this energy, one would expect to observed characteristic gamma emission from excited ^{107}Ag at 93 KeV.

Tritium decay can be enhanced through this type of mechanism, and lattice-induced electron capture on ^{3}He can in principle produce tritium, although precisely which vacancy impurity bands ^{3}He decay would involve is not clear at this point. The rates for these processes are shown in Figure 9.

VI. LATTICE-INDUCED ALPHA DECAY

If the energy transfer is sufficiently great, alpha decay becomes an available decay channel. The analysis of lattice-induced alpha decay is particularly simple, in that the decay always provides sufficient recoil for local vacancy formation. We have calculated the rate for lattice-induced alpha decay of Pd nuclei; the results are shown in Figure 10. The first isotope to decay as a function of energy is ^{102}Pd; energy transfers in excess of about 5 MeV are required for this process.

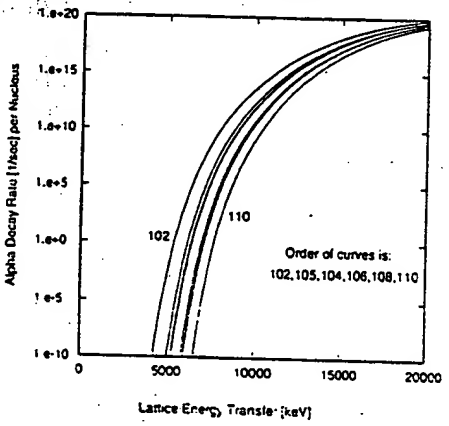

Figure 10: Lattice-induced alpha decay of the Pd isotopes.

Larger energy transfers can lead to more complicated decay channels; for example, proton and neutron decays turn on near 10 MeV lattice energy transfer. We have examined reaction rates for a wide variety of fission decay channels; these will be discussed further elswhere. Qualitatively, the rates for these decays go something like those for alpha decay, but require significantly more energy; from 20 MeV to more than 50 MeV of energy transfer will lead to a wide range of open lattice-induced fission channels. At such large energy transfer where alpha and fission decay processes are allowed, these reactions are predicted to be the dominate decay channels.

VII. DISCUSSION AND CONCLUSIONS

We have presented a new theory for lattice-in reactions, which a predicted to be driven by high cited gap-jumping phonon modes. The reaction n nisms discussed in this work were motivated by the recent claimes of observations of anomalies in Pd other metal deuterides, and in metal hydrides.

At low energy transfer, the dominant lattice mechanisms are the Coulomb-mediated nucleus-n recoils; in the case of deuteron-deuteron recoils, *dd*- at low levels is predicted. The reaction rates com for this process are of the correct order of magnitude consistent with the claimed experimental neutron sion, at low lattice energy transfer below that at fast electron decay channels open.

Fast electron emission through Coulomb induce coil is predicted to be a dominant process, at lattic ergy transfer where the nuclear recoil is strong enou vacancy creation. There are currently relatively fe ports of the observation of fast electrons in cold fusio priments. Fast electron emission is predicted starti relatively low energy transfer (a few KeV) from deu recoil, and at energies starting near 1 MeV for recoil Pd. In the case of the stable Pd isotopes, this pr competes with all beta decay reactions.

We have studied neutron transfer reaction mechan elsewhere[12,24,25] as a route to heat production. Alth we have examined neutron transfers from ^{105}Pd to with an energy mismatch of 156 KeV, a more recent ysis suggests that this reaction will be suppressed d selection rules affecting the Pd transition. There are candidate reactions that are perhaps more promising ative to the selection rules: neutron transfer from ^{29} ^{29}Si (producing ^{28}Si and ^{30}Si) at 2.14 MeV; and neu transfer from ^{30}Si to ^{10}B at 845 KeV. In the case of light water experiments, neutron transfer from ^{62}N ^{29}Si has a mismatch of 12 KeV.

The generation of high phonon densities has not been addressed. We are considering seriously the p bility that D_2 desorption from the metal deuteride in face produces phonon gain when exothermic. In the of PdD, the desorption is exothermic at high loading which is correlated well with the proposed requirem of high PdD loading for heat production in Pons Fl chmann experiments. The quantum theories that h been developed for desorption[27,28] certainly contain the essential physics for optical phonon gain, altho this appears not to have been realized yet in the desc tion literature. We will discuss this further elsewhere.

ACKNOWLEDGMENTS

The author would like to acknowledge support from EPRI and from the EE & CS Department at MIT. This work was stimulated by discussions with Y. Kucherov, I. Savvatimova, and A. Karabut. The author would like to thank S. Kaushik, L. Smullin and Y. Fukai for many valuable conversations.

REFERENCES

1. S. Pons, M. Fleishmann and M. Hawkins, *J. Electroanal. Chem* **261** 301 (1989).
2. S. Jones, E. P. Palmer, J. B. Czirr, D. L. Decker, G. L. Jensen, J. M. Thorne, S. F. Taylor and J. Rafelski *Nature* **339** 737 (1989).
3. M. C. H. McKubre, S. Crouch-Baker, A. M. Riley, S. I. Smedley and F. L. Tanzella, *Frontiers of Cold Fusion*, Proceedings of the Third International Conference on Cold Fusion, Ed. H. Ikegami, Nagoya, Oct. 1992; p. 5.
4. F. O. Menlove, M. M. Fowler, E. Garcia, A. Mayer, M. C. Miller, R. R. Ryan and S. E. Jones, *Fusion Tech.* **9** 215 (1990).
5. T. N. Claytor, D. G. Tuggle and S. F. Taylor, *Frontiers of Cold Fusion*, Proceedings of the Third International Conference on Cold Fusion, Ed. H. Ikegami, Nagoya, Oct. 1992; p. 217.
6. F. Lanza, V. Bertolini, E. Vocino, E. Parnisari, and C. Ronseco, *The Science of Cold Fusion*, Ed. T. Bressani, E. Del Guidice, and G. Preparata, Conf. Proc. Vol. 33, Italian Physical Society, Bologna, 1992; p. 151.
7. A. B. Karabut, Ya. R. Kucherov, I. B. Savvatimova, *Phys. Lett. A* **170** 265 (1992).
8. R. L. Mills and S. P. Kneizys, *Fusion Tech.* **20** 65 (1991).
9. R. Notoya and M. Enyo, *Frontiers of Cold Fusion*, Proceedings of the Third International Conference on Cold Fusion, Ed. H. Ikegami, Nagoya, Oct. 1992; p. 421.
10. M. Srinivasan, A. Shyam, T. K. Sankaranarayanan, M. B. Bajpai, H. Ramamurthy, U. K. Mukherjee, M. S. Krishnan, M. G. Nayar and Y. P. Naik, *Frontiers of Cold Fusion*, Proceedings of the Third International Conference on Cold Fusion, Ed. H. Ikegami, Nagoya, Oct. 1992; p. 123.
11. S. Pons and M. Fleischmann *Phys. Lett. A* **176** 118 (1993).
12. P. Hagelstein, *Fusion Tech.* **23** 353 (1993).
13. Y. Fukai and N. Okuma, *Jpn. J. Appl. Phys.* **32** L1256 (1993).
14. A. Rahman, K. Skold, C. Pelizzari and S. K. Sinha, *Phys. Rev. B* **14** 3630 (1976).
15. P. Hagelstein, presented at ICAME'93; proceedings to appear in *Hyperfine Interactions*.
16. F. Duschinsky, *Acta Physicochimica U.R.S.S* **7** 551 (1937).
17. T. R. Faulkner and F. S. Richardson, *J. Chem. Phys.* **70** 1201 (1979).
18. R. Loudon, *The Quantum Theory of Light*, Clarendon Press, Oxford, (1973).
19. G. Mainfray and C. Manus, *Rep. Prog. Phys.* **54** 1333 (1991).
20. M. Dorr, M. Terao-Dunseath, J. Purvis, C. J. Noble, P. G. Burke and C. J. Joachain, *J. Phys. B* **25** 2809 (1992).
21. A. L'Huillier, P. Balcou, S. Candel, K. J. Schafer, and K. C. Kulander, *Phys. Rev. A* **46** 2778 (1992).
22. A. A. Frost and B. Musulin, *J. Chem. Phys.* **22** 1017 (1954).
23. P. Marmier and E. Sheldon, *Physics of Nuclei and Particles*, Academic Press, New York (1969).
24. P. Hagelstein, *Frontiers of Cold Fusion*, Proceedings of the Third International Conference on Cold Fusion, Ed. H. Ikegami, Nagoya, Oct. 1992; p. 297.
25. P. Hagelstein and S. Kaushik, presented at the Fourth International Conference on Cold Fusion, Maui, 1993.
26. Y. Fukai, *Frontiers of Cold Fusion*, Proceedings of the Third International Conference on Cold Fusion, Ed. H. Ikegami, Nagoya, Oct. 1992; p. 265.
27. Z. W. Gortel, H. J. Kreuzer and R. Teshima, *Can. J. Phys.* **58** 376 (1980).
28. J. Harris, *Surface Sci.* **221** 335 (1989).

THE ROLE OF HYDROGEN ION BAND STATES IN COLD FUSION

Scott R. Chubb and Talbot A. Chubb
Research Systems, Inc.
5023 N. 38th St.
Arlington, VA 22207
(703)536 4427

ABSTRACT

Quantum diffusion studies of hydrogen (H) and deuterium (D) inside and on the surfaces of transition metals indicate that both H and D may occupy wave-like band states (H and D ion band states) analogous to the electron band states that are responsible for making metals conductors. When these wave-like ion band states become occupied, fusion involving $D+D \rightarrow {}^4He$ without emission of gamma rays or other high energy by-products can occur, provided a number of conditions are met. We have previously identified and used these conditions to predict a number of important experimental results that were subsequently observed. In part 1 we examine the underlying justification for believing that ion band state occupation can lead to nuclear reaction. We show that under suitable conditions associated with the underlying electronic structure, ion band state occupation may lead to wave function overlap between a small number of indistinguishable D^+. These conditions appear to be met as $x \rightarrow 1$ in PdD_x. Then, ion-ion correlation effects that result from coulomb repulsion, which normally inhibit overlap, are not present in the ground state wave function, provided the number of indistinguishable ion band state deuterons is very much less than the total number (N_{cell}) of unit cells in the crystal, and the crystal is sufficiently large: $N_{cell} > 10^8$. In part 2, we examine the implications of the ion band state fusion scenario, including a summary of important selection rules and reactions which follow as a result of the restrictions that are implied by the physical limit in which the theory applies.

I. INTRODUCTION

Acceptance of cold fusion as a real phenomenon by the mainstream physics community has been delayed mainly for two reasons: 1) a refusal of physicists to believe that the coulomb barrier that normally prevents nuclear reactions at room temperature can be overcome in the solid state environment, and 2) a belief that γ-ray and high energy particle emission must inevitably accompany the release of nuclear energy. The cold fusion community for the most part bases its belief in cold fusion on the evidence for the reality of the cold fusion heat effect. Nonetheless, it shares with the larger physics community a belief that mainstream physics cannot overcome the coulomb barrier problem and cannot provide radiationless emission. This paper presents an alternate view, based on ordinary quantum mechanics, that explains not only how the coulomb barrier can be overcome in a radiationless manner and why this can be done using the procedure developed by Fleischmann and Pons[1], but also why this procedure leads to unexpected products, modes of energy release, and other effects that have been observed. The underlying ideas behind this alternative view are closely tied to the known electronic properties and structure of palladium deuteride PdD, and the governing rules of bound (as opposed to unbound) systems, and known effects associated with periodic order and the exchange of identical particles.

In the resulting picture, cold fusion is the result of a relatively small number of D^+ occupying wave-like (Bloch function) band states. Once this happens, as a result of the behavior of indistinguishable particles, these wave-like D^+ ions are free to overlap each other and fusion can occur. An important point is that the D^+ become delocalized as a result of occupying these states. The associated nuclear reactions also become distributed. This leads to different, distributed modes of interaction, in which the effects of periodic order and particle indistinguishability alter the relevant forms of reaction. From the underlying physics, it follows that in these distributed, transistor-like (as opposed to vacuum tube-like) modes of interaction, high energy particle and γ-ray emissions are not to be expected. Also, the underlying

assumption that D^+ ion band state occupation should occur becomes valid in the limit that $x \rightarrow 1$ in PdD_x.

In the paper, we first examine what we believe to be the most compelling experimental evidence in support of excess heat. Then, using a concrete example, we explain the underlying logic, based on system energy minimization, behind our conclusion that the quantum mechanics of bound systems can potentially alter particle-particle overlap in a manner that may significantly affect the possibilities for nuclear reaction. We also explain why energy minimization precludes the possibility of nuclear fusion between chemically bound D or in D_2 molecules, but that the same principle can be used to demonstrate that under suitable circumstances nuclear reaction can occur between D^+ ions within a sufficiently large, periodically-ordered solid as a result of ion band state occupation. In the remainder of the paper we examine the underlying implications and conditions associated with ion band state occupation and interaction, including a summary of the important restrictions and selection rules associated with potential ion band state mediated nuclear reactions.

II. PART 1: UNDERPINNINGS OF EXCESS HEAT COLD FUSION THEORY

A. Evidence for Excess Heat

Before exploring the theoretical aspects of cold fusion, we briefly consider the evidence for the reality of cold fusion heat. There have been many observations of excess heat in electrochemical system experiments. Among the hardest to refute are the observations of Fleischmann and Pons during temperature excursion events in which water in their electrolytic cell boils away.[1] The energy balance observed in their temperature-increase event published in *Phys. Lett. A* is:

- Heat of vaporization of 47 cc D_2O: 102500 J in 10-minute boil-dry period
- Concurrent electrolysis power input: 22500 J
- Missing heat (cold fusion): 80000 J

The missing heat corresponds to 197 eV per Pd atom, which exceeds by a factor of 20 the value possible from stored chemical energy. The only mainstream physics possibility is that the heat was derived from the nuclear potential.

B. Why Ion Band State Matter Avoids the Coulomb Barrier: Guiding Principle

There is considerable common ground among physicists concerning the principles of physics, and the requirements of a successful theory of the cold fusion heat effect. A successful theory must explain how the coulomb barrier is overcome and why fusion is radiationless. For nuclear reaction to occur there must be wave function overlap of the feedstock components and also wave function overlap with the product. There is also agreement that in free space this overlap can be explained by scattering theory, which provides transient overlap calculable from Gamow theory. On the other hand there does not seem to be an equal acceptance as to how one properly proceeds in applying the principles of physics to bound systems. It is worthwhile emphasizing that we believe that the governing principles of bound systems (as opposed to those of unbound systems) provide the appropriate framework for understanding cold fusion and that this fact has been largely ignored.

The applicable rules of physics for ground state bound systems are that 1) the overlap and other system properties are fully contained in the system wave function that minimizes total system energy, 2) the wave function is constrained by the natural boundary conditions of the environment, and 3) the rules of boson or fermion exchange symmetry (or anti-symmetry) that have been found to apply differently to sets of distinguishable and non-distinguishable particles must be included in an appropriate manner. These principles underlie the physics of atoms and molecules. They are the basis of atomic physics and quantum chemistry. The energy-minimizing wave functions have particle-particle avoidance terms, called correlation terms, which can be, but need not be required to restrict a specific particle A from being present at a point in space when particle B is present. In bound systems near room temperature the amplitude of these particle-particle avoidance terms is determined by the energy minimization process. An important point is that in bound systems, system energy is constrained to be finite. For this reason, energy minimization principles always apply (often with unexpected results), and can be used to determine the ground state and lowest excited states. In unbound systems, such as plasma, the energy is not constrained to be finite. In this case the use of scattering theory and the associated quantum mechanics is the more appropriate approach for determining system dynamics.

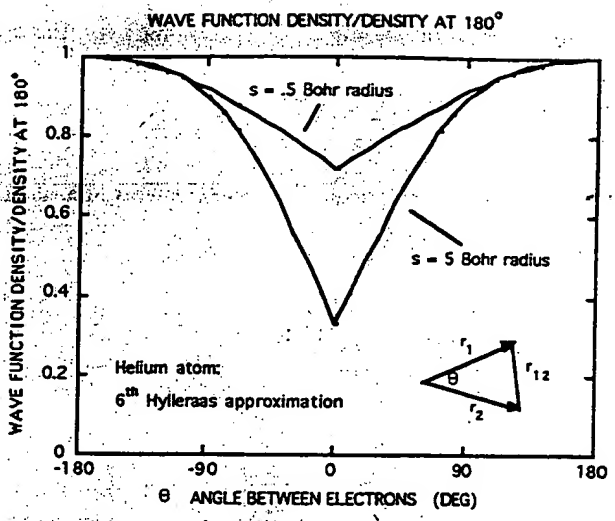

Fig. 1 Amplitude of helium ground state 2-electron wave function on the surfaces of 2 spheres for which s = constant. Values have been normalized with respect to the peak values, which occur when the 2 electrons are on opposite sides of the nucleus. Nature uses a cusp at $r_{12} = 0$ to compensate for the infinite electrostatic potential existing at this condition. The values at $\theta=0$ measure the degree of electron-electron ovelap. If the electrons had the nuclear properties of deuterons, they would fuse.

C. The Helium Atom as an Example of a Bound Physical System

A good example of the physics of bound systems is provided by the calculation of the 2-body wave function that describes the 2 electrons of the ground state helium atom.[2] The Schroedinger equation for the helium atom (simplified by taking the nuclear mass as infinite) is

$$-\hbar^2/2m_e[\nabla_1^2 + \nabla_2^2]\Phi_s(r_1,r_2) + [e^2/r_{12} - 2e^2/r_1 - 2e^2/r_2]\Phi_s(r_1,r_2) = E\,\Phi_s(r_1,r_2)$$

where E is the ground state energy of the 2-electron spatial wave function $\Phi_s(r_1,r_2)$ for the zero-spin state, and $r_{12} = |r_1 - r_2|$. $\Phi_s(r_1,r_2) \propto \Phi_1(r_1)\Phi_2(r_2) + \Phi_2(r_1)\Phi_1(r_2)$ is symmetric with respect to interchange of r_1 and r_2. In this equation the $-\hbar^2/2m_e[\nabla_1^2 + \nabla_2^2]\Phi_s$ term represents the kinetic energy of the electrons, and the $[e^2/r_{12} - 2e^2/r_1 - 2e^2/r_2]\Phi_s$ term represents the potential energy. The $e^2/r_{12}\,\Phi_s$ term is the 2-electron coulomb repulsion term which results in correlated avoidance behavior by the two electrons.

The variational method was used by Hylleraas[3] to determine a sequence of 2-electron wave functions of increasingly better accuracy. Making use of the elliptical symmetry of the problem he reduced the six independent configurational coordinates of the 2 electrons that appear in the Shroedinger equation, namely r_1 and r_2, to three independent elliptic coordinate variables s, *t*, u derived therefrom. He also made use of the symmetric spatial exchange symmetry of indistinguishable fermions with anti-parallel spins, which requires that candidate solutions be even functions of variable *t*. His third approximation is

$$\Phi_s = e^{-1.82\,s/b}\,[1 + 0.29\,u/b + 0.13\,t^2/b^2] \quad ,$$

where

$$s = |r_1| + |r_2| \quad ,$$

$$t = |r_1| - |r_2| \quad ,$$

$$u = r_{12} = |r_1 - r_2| = (|r_1|^2 + |r_2|^2 - 2|r_1||r_2|\,\mathrm{Cos}\theta)^{1/2}, \text{ and}$$

b = Bohr radius of hydrogen = 0.53 Å .

Consider what the Hylleraas solution tells us abou particle-particle overlap in bound particle systems. The Hylleraas solution is dominated by the exponential decrease in $|\Phi_s|$ with the mean distance of the 2 electrons from the nucleus, i.e., with s/2. To explore the electron-electron avoidance behavior we study the

Hylleraas 6th approximation solution[3] on the surface of a sphere of fixed radius, i.e. s is fixed and $t=0$. A plot of the variation of the amplitude of Φ_s with respect to the central angle θ between the 2 electrons as viewed from the nucleus is given in Fig. 1. The wave function amplitude goes through a minimum at q=0, which corresponds to the point $r_{12}=0$. The wave function amplitude has been normalized to its value at $q=180^o$, which corresponds to the 2 electrons being on opposite sides of the nucleus. Since the wave function amplitude at these two points is not much different, the figure shows that the 2 electrons of the helium atom have substantial overlap; in other words, if the electrons had the fusion capability of deuterons, they would fuse.

D. Wave Equation Singular Points

The behavior of the 2 electrons of the helium atom is an illustration of the more general behavior of particles in bound systems. The more general Schroedinger equation for electrostatically interacting particles in an external potential V_{ext} is

$$[-\hbar^2/2m \sum_i \nabla_i^2 + \sum_{i,j} e^2/r_{ij} + V_{ext}] \Phi_s(r_1,r_2,..r_N) = E\, \Phi_s(r_1,r_2,..r_N)$$

where $r_{ij} = |r_i - r_j|$.

The e^2/r_{ij} terms in the wave equation go to ∞ at $r_{ij}=0$. However, because the system is bound, the eigenvalue E is always finite (and less than zero). This means that both the right and left sides of the equation must remain finite. (For unbound systems, E need not remain finite.) This means that at $r_{ij}=0$, because $e^2/r_{ij} \rightarrow \infty$ either $\Phi_s(r_1,r_2,..r_N) = 0$ or $\sum \nabla_i^2 \Phi_s = \infty$. In the latter case $\Phi_s(r_1,r_2,..r_N)$ has a discontinuous derivative at $r_{ij}=0$, i.e. the wave function has a cusp at $r_{ij}=0$. In practice Nature (i.e. energy minimization) makes use of both possibilities. If the kinetic energy terms $-\hbar^2/2m \sum \nabla_i^2 \Phi_s(r_{ij})$ dominate the energy balance, Nature uses cusp solutions; if the potential energy terms dominate, Nature zeroes the wave function at $r_{ij}=0$. However, the situation for nuclei in molecules is different than for electrons in the helium atom. For nuclei in deuterated molecules m is the deuteron mass m_D, instead of the electron mass m_e used in the He solution. This reduces the importance of the kinetic energy terms by a factor of 3700. This reduction makes the potential energy term dominant. Energy minimization (in which D^+-D^+ separation is included as a variational parameter) zeroes the wave function and no fusion is possible. (This condition also applies to any possible interstitial D_2 configuration.)

Since interstitial occupations of a metal lattice by D_2 are unable to fuse, the cold fusion heat observations require that the D be in some other configuration. We now show that when D^+ is in a delocalized Bloch-function configuration, overlap can occur and fusion becomes possible.[4]

E. Bound State Systems Containing Band State Ions

The physics of bound solid state systems depends on the same laws as the physics of molecules. If one considers a Bloch state D^+ population in a microscopic crystal resembling an atom cluster, no D^+-D^+ overlap can occur because the potential energy coulomb repulsion term in the wave equation dominates the kinetic energy term in determining the magnitude of the correlation terms in the wave function, just as it does in normal D_2 molecules. On the other hand, Bloch states have the important property that their amplitudes are periodic functions of the underlying lattice. This means that in a periodically ordered lattice, if the band state D^+ ions are spread out over successively larger crystal sizes, i.e. if N_{cell} is increased, the amplitude of each single particle wave function decreases, and the importance of the wave equation coulomb repulsion potential terms decreases relative to the importance of the kinetic energy terms. As shown below, this behavior means that wave function overlap occurs and fusion becomes possible.

To pursue our argument let us first look at the potential energy reduction that occurs as a result of introducing nodes or cusps into the wave function in order to reduce the amplitude of the wave function when $r_{ij}=0$. The particle-particle avoidance interaction reduces system potential energy by ΔE_{pot}

$$\Delta E_{pot} = 1/2 \iint e^2 |\Phi_{corr}(r)|^2 |\Phi_{corr}(r')|^2/|r-r'|\, dr\, dr' - 1/2 \iint e^2 |\Phi(r)|^2 |\Phi(r')|^2/|r-r'|\, dr\, dr'$$

where within the many-body wave function

Φ is a single particle Bloch function without correlation terms, and

Φ_{corr} is a correlated single particle function that also possesses Bloch function symmetry but is derived with r_{ij} avoidance terms (which results in dimples: nodes or cusps).

The particle-particle avoidance increases system kinetic energy by ΔE_{ke}

$$\Delta E_{ke} = \hbar^2/2m_D \int \nabla\Phi^*_{corr} \nabla\Phi_{corr}\, dr - \hbar^2/2m_D \int \nabla\Phi^* \nabla\Phi\, dr$$

where

$\nabla\Phi$ is the gradient of the wave function without correlation terms, and

$\nabla\Phi_{corr}$ is the gradient of the correlated wave function with r_{ij} avoidance terms (nodes or cusps).

With increasing N_{cell} both $|\Phi|^2$ and $|\nabla\Phi|^2$ decrease as $1/N_{cell}$. Since on a per unit cell basis $\Delta E_{pot} \propto |\Phi|^4$, ΔE_{pot} decreases as $1/N_{cell}^2$. In contrast, $\Delta E_{ke} \propto |\Phi|^2$. Then, at large N_{cell} it follows that ΔE_{ke} dominates ΔE_{pot}. This resulting dominance of kinetic energy over potential energy in the part of the wave equation controlling particle-particle avoidance means that total energy is minimized in a similar manner to the way kinetic eneregy dominance leads to energy minimization and overlap of the electrons of the ground state helium atom. As a result the many-particle energy-minimizing wave function has only a small amount of correlation wave function curvature, and has a shallow cusp at $r_{ij}=0$, i.e. particle-particle overlap is almost complete.

As discussed in the next paragraph D^+ ion band state fusion energy is released in a distributed fashion. The comparison between the D^+ ion band state picture including nuclear energy release and the situation involving the balance between kinetic energy and coulomb repulsion between electrons in the helium atom is especially meaningful provided the distributed nuclear energy release per unit cell is of the order of the characteristic D^+ vibration energies, which are in the 0.01 to 0.1 eV range. Since the distributed nuclear energy release $= 23.8\ MeV/N_{cell}$, this requirement is that $N_{cell} >\sim 10^8$. Since the kinetic energy term in the wave equation relative to the potential energy term is reduced by the order of 10^4 in going from the electrons in the helium atom to D in the D_2 molecule, the value $N_{cell} = 10^8$ is much greater than that needed to meet the requirement for D^+-D^+ overlap. Thus with $N_{cell} = 10^8$, the essential overlap requirement for D^+-D^+ fusion is satisfied.

F. Why Ion Band State Fusion Is Radiationless

We now consider why D^+ ion band state fusion produces no γ-rays or energetic particles. Interaction between band state occupations makes only a small amount of nuclear energy available in each unit cell. This is because, when both the reactants and products of the potential nuclear reaction occupy band states, only a small fraction of each reactant and product is located in each unit cell, meaning that only a small amount of each reaction occurs in each unit cell. In contrast, high energy particle and γ-ray emission requires concentration of the available energy into a small volume. At the near room temperature conditions used in cold fusion studies concentration of the available energy into a single unit cell by incoherent or coherent processes is statistically impossible because of the large entropy cost associated with accomplishing this process.

G. Where the Energy Goes

The small amounts of energy made available in each unit cell by the 2-$D^+_{band} \rightarrow {}^4He^{++}_{band}$ reaction should be able to excite phonons, either thermally (through residual electron-ion interaction), or at the boundaries of the lattice where periodic order is lost. The large density of states that is provided by these processes is responsible for making the nuclear reactions irreversible. At low temperature, phonon generation occurs primarily at the boundaries of the crystal lattice, where periodic order is lost. In these regions, the electron-ion interaction is dominated by the requirement that the "spill-out" dipole layer associated with electrons near the surface and the surface ion band states adjust themselves in a manner that is consistent with Gauss's law and the applied electric field. (In the surface region, as opposed to the bulk, it is possible for a net distribution of charge to be present because there exists a net electric field flux into and out of this region.)

Although this readjustment process is dominated by the behavior of the electrons and the associated electron-ion interaction, it is possible to identify a prospective ground state ion configuration in the surface region that is consistent with the arrangement of electrons. In particular, at the surface, although three dimensional periodic order is lost, at low temperature, it is plausible (depending on loading conditions) that two dimensional order (defined by the lattice structure in planes parallel to the surface) will be present. Then, the same kinds of ion band state (as well as electron band state) considerations apply except that Bloch symmetry in this case applies only in directions parallel to the surface. In directions normal to the surface, each wave function is smoothly matched onto the appropriate solutions of the Schroedinger equation. The result of this construction is that each bulk-like (electron or ion) band state smoothly matches onto a surface state which possesses two dimensional Bloch symmetry in the surface region (whe

the net electric field flux is non-vanishing), and exponentially decays in directions normal to the surface, in a manner similar to the exponential decays that occur in all negative kinetic energy region solutions associated with the bound state Schroedinger equation.

In the extreme low temperature limit it is plausible that the dominant phonons will result from extreme long wavelength acoustical phonons in which large portions of the bulk lattice effectively resonate with respect to each other. This is because these phonons, which can be generated through small fluctuations in the electrostatic zero (by the average value of the chemical potential), 1) are the most sensitive to the smallest variations in charge in the surface region, and 2) can also result from the large density of states associated with intermediate "horizontal" (or Umklapp) processes, in which the lattice (or a large portion of the lattice) effectively recoils as a whole. An additional possibility is that long wavelength optical phonons will be generated through the volumetric stress associated with each fusion. Although it might appear that the possible modes of energy release associated with these optical phonon processes would occur with higher energies (and temperatures) than the ones associated with long wavelength acoustical phonons, each fusion includes an effective softening of the ion band state in the zero-point motion of the ion band state material (owing to the larger mass of the $^4He^{++}$ product).

H. Ion Band State Matter as a Matter Field within a Host Lattice

Limitations on cold fusion possibilities are determined in major part by limitations on allowed final state wave functions. To the extent that the coulomb barrier terms in the many-body wave function have vanishing amplitude, the ion band state approximates a non-relativistic quantized matter field[5] restricted to a finite volume V_{xtal}. For a D^+ band state population the quantum of mass is 2 AMU, i.e. the matter content of the field can only increase or decrease in discrete steps of 2 AMU. Within the matter field there is concurrent action at a distance, as required to resolve the Einstein, Podolsky, and Rosen[6] argument against the completeness of quantum mechanics. An important point is that the ion band state picture only makes sense if the ion bands remain occupied for a sufficiently long period of time relative to the required time necessary for nuclear reaction to proceed. For this to occur, each nucleus that occupies such a state must effectively dissociate from its own electron (as well as the remaining electrons) over a time scale that is short with respect to times associated with electrostatic processes, but long relative to nuclear process time scales. This requirement places important constraints associated with the underlying electronic structure on the kinds of environments where ion band state matter will form in a manner that will allow for appreciable nuclear reaction to occur.

The physical system includes the crystal interior lattice, the crystal surface boundary region where periodic order is lost, the interior D^+ ion band state matter field, and the matter field's surface stress region within which the band state matter wave function transitions into a decaying exponential, associated with the negative kinetic energy region outside the solid. The final state consists of bulk-like ion band state $^4He^{++}$, which, depending on the temperature and degree of crystalline order in the surface region, may match onto any of a variety of functional forms in the surface region. In the extreme low temperature limit, as mentioned above, the ion band states can match onto localized surface states provided adequate crystalline order is present in planes parallel to the surface. An interesting point about this case is that these ion band surface states in principle can couple coherently to electron surface states (occupied by the host electrons as well as by the injected electrons that accompany the ion band state D^+) in a manner that could preserve Bloch symmetry in planes parallel to the surface. The significance of this form of coupling is that neutral or ionized ^4He could be ejected from the solid in a coherent manner, leading to a Bragg-like diffraction pattern, reminiscient of the diffraction patterns that are observed in low-energy ^4He scattering experiments. In all cases, the large strain energies (and propensity for cracking, etc.) associated with multiple occupation of a unit cell by either D or He in a non-ion-band-like form, inhibit the final state $^4He^{++}$ from occupying or coupling to non-ion-band-state ^4He in bulk regions. This is the justification for the prediction that we made[4,7] prior to the experimental measurements[8,9] that the ^4He product should be found primarily at low energy and in regions outside heat-producing electrodes.

I. The Reaction Process

In the above picture there is no intermediate observable state between ejection of a normal $^4He^{++}$ product and annihilation of 2 deuterons in the matter field. The normal astrophysical factors affecting fusion rate apply. The $D^+ + D^+ \rightarrow {}^4He^{++}$ reaction would be restricted only by the requirement for anti-parallel spins, which, in most cases, reduces the reaction rate by a factor of 3. This last reduction factor would be reduced in a situation in which band state D^+ is preferentially prepared so that spin populations of opposite spin are equally occupied. An

interesting point is that by introducing a constant magnetic field **H** (or a constant magnetic field **H** accompanied by a perpendicular oscillating magnetic field, as in standard NMR measurements), it is possible to enhance both 1) spin allignment in directions parallel to **H** and 2) anti-alligment of spins in directions perpendicular to the field. It is also interesting to note that the creation of $^4He^{++}$ in ion band state form provides a source for reducing magnetism (since $^4He^{++}$ is non-magnetic while the feedstock ion band state D^+ is magnetic) in a delocalized manner that preserves periodic order. We have also shown[4,10] that for low $^4He^{++}$ concentrations, the fusion rate is proportional to the concentration of final state $^4He^{++}$. As discussed below, it also is true that reductions in periodic order inhibit fusion. Together these observations suggest that the process of creating $^4He^{++}$, which is enhanced by preferentially preparing the feedstock D^+ in a form in which equal populations of anti-parallel states are occupied, may help to preserve both crystalline and magnetic order in a manner that may further enhance the fusion process.

As discussed in section III, the above picture conforms to the requirement of Born-Oppenheimer separability of the fast nuclear reactions with respect to the slower electrostatic interactions that affect only the center-of-mass coordinates. The nuclear/zero-point-motion volume ratio V_{nuc}/V_{zp} enters in as described in our 1991 *Fusion Technology* paper[4]. In contrast, reactions of the type H^+-H^+ going to a deuteron by electron capture or positron emission with emission of a neutrino would probably be excessively slow due to the required weak force interaction.

III. PART 2: D^+ ION BAND STATE FUSION

A. Exotic Situation, Not Exotic Physics

The arguments presented above show that cold fusion is not the result of exotic physics; instead it is mainstream physics applied to an exotic situation that can only occur inside condensed matter. It is the result of the formation of exotic types of compounds, wave-like occupations of energy bands, which become allowable when chemical thermodynamic conditions support their formation. We have suggested several types of compounds that could include such ion band state occupations, namely, $PdD_{1+\delta}$, AgD_δ or NiD_δ. However, the designation $PdD_{1+\delta}$ should not be taken too literally. Although it describes conditions that might allow ion band state formation at low temperature, some D^+ ion band state occupation will occur in PdD_x wi $x<1$ even at low temperature. The cause of su occupations is the entropy term in the chemical potenti associated with occupation of a fixed number of interstiti sites.[11] This term forces the chemical potential for absorption to become infinitely positive before the val $x=1$ is reached. Equally important, at finite temperatu some occupation of the band state would occur at x even if the entropy term were not included. (Band st occupations are only required to occur over some fini lifetime that is considerably shorter than the typical tim scales associated with the dominant thermodynam processes. Band state occupations occur only over a fin volume V_{xtal}, where V_{xtal} can be a sub-volume of t entire crystal.) The temperature dependence of excess h production reported by Storms[12] suggests an energy activation of ~15 kcal/mol for populating the heat relea state, which we assume to be the band state. The prop designation for the palladium deuteride that suppo fusion is $PdD_{1-\eta+\delta}$, where $\eta(T) << 1$.

The exotic character of the D^+ band state matter st is shown in par by the very small concentration of io required for t e production of measurable he Calculations ind cate that an occupation density of ~10 band state D^+/unit cell is sufficient to explain observ heating rates. Moreover, there are limitations on the t end values of x that are compatible with heat productio A population of $\delta > 10^{-3}$ may be sufficient to for occupation of the Pd tetrahedral interstitial sites in PdD which may destroy the periodic order needed for pow production. The range in values of x that correspond these δ limits may be quite restricted. The drop resistivity observed by McKubre[13] in PdD_x once exceeds ~0.73 is a qualitative measure of lattice ord Only the portion of D absorbed into Pd that increas ordering is important to the band state fusion proce Hydrogen uptake measurement of x can sometimes misleading since other non-productive means containment of D exist, e.g. filling of interstic occupations of tetrahedral sites in octahedrally load metal, and possibly some kind of LiD:Pd alloyir Another important factor affecting ion band st formation in the different metals is host electron structure.

B. Experimental Evidence for the Existence of Ba State Hydrogen

Although D^+ ion band state matter may be consider exotic, 2-dimensional ion band state matter is known be present in H and D adsorptions on the surfaces transition metals. This idea has been used to explain t

vibrational spectra dependence on H- and D- coverage in the adsorptions of H and D on Cu(110) and Ni(100).[14,15] Ion Band State occupation potentially can be used to explain the huge diffusion lengths of D and H in many metals.

C. Role of Electronic Structure

An important aspect of ion band state occupation and the implications of ion band state occupation to cold fusion, that we have not emphasized in the past, is the role of electronic structure. Normal chemistry at room temperature inherently favors neutrality (or approximate neutrality). It is well known that this is true in the solid state and this fact has been the cornerstone for understanding a large number of the cohesive, chemical, and electronic properties of solids. For this reason D^+ ion band states can become occupied and ion band state mediated fusion can occur only if specific conditions associated with the underlying electronic structure are fulfilled. 1) Sufficient periodic order must be present for a sufficiently long period of time. 2) Deuterium and host electrons must dissociate from D^+ band-state matter on time-scales that are long compared with those required for fusion through nuclear self-interaction. 3) D^+ band-state matter must distribute itself in a sufficiently diffuse manner as a result of interactions with the host lattice.

In the case of Pd and PdD, we know from neutron diffraction experiments[16] the structure of PdD, the presence of crystalline order, the location of the D, and its characteristic zero-point motion radius, which is relatively large (~0.2Å). We know from the excellent agreement between a number of first-principles ab initio electronic structure calculations[17] and photoemission experiments[18] even some of the more delicate aspects of the associated electronic structure of both Pd and PdD, to a fair level of precision. Thermodynamic modeling[11], and electronic structure calculations in particular, show that in PdD_x as x is increased from values below 0.7 to unity, chemical bonding involves important hybridization between bonding 4d states and anti-bonding 5s states provided by the Pd.

In the case of the $PdD_{1+\delta}$ that we have suggested is relevant to cold fusion, within the bulk, in each unit cell the concentration (=δ) of ion band state D^+ is balanced by an equal concentration of electrons (which also occupy band states). The assumptions that both the D^+ and the electrons may fractionally occupy band states in this manner is not only consistent with the known laws of solid state physics, it is consistent both with thermodynamics[11] and with the electronic structure calculations[17]. In particular, Wicke and Brodowsky[11] have summarized the behavior of the chemical potential with respect to changes in D-loading. Their figure 3.11 shows that large lattice strain energy costs are associated with D-occupation of a Pd unit cell when x is small, from which one concludes that huge lattice strain energy costs would be associated with D-occupation of a unit cell by more than one D in the limit that $x \to 1+\delta$ in PdD_x. This result essentially is tied to the dominant Pd-to-H bonding-anti-bonding features associated with the 4d-5s hybridization identified by Papaconstantopoulos et al.[17].

An important point is that it follows from a minor generalization of local density theory[19] (which provides the basis of these calculations) that, when δ is sufficiently small, as D is loaded into PdD to form $PdD_{1+\delta}$, the energy associated with the accompanying additional concentration (δ) of electrons is minimized provided 1) these electrons fractionally occupy the lowest unoccupied states (immediately above the PdD Fermi level), and 2) variations in electronic structure associated with these fractional occupations do not alter the density of ion band state deuterons. Although it is not rigorously necessary to impose these last two constraints, it does follow rigorously that they provide a means of constructing a self-consistent local density approximation method for determining the ion band states in the limit in which δ becomes infinitesimally small. This minimization of electronic energy requires that the added D^+ be in a band state.

Additional results of Papaconstantopoulos et al.[17] suggest that variations in electronic structure associated with fractionally occupying new states immediately above the Fermi energy E_F of PdD probably would not appreciably affect the ion band state densities that we have used previously[20], nor would the densities differ importantly from those that would result from self-consistent local density approximation calculations carried out in this fashion. These earlier ion band state calculations were carried out using minimum uncertainty wave packets of a characteristic size defined by the known[16] zero-point motion volume of D in PdD. Papaconstantopoulos et al.[17] have shown that, as a result of the 4s-5d hybridization discussed above, near E_F electron occupation involves anti-bonding 5s-like states primarily in regions in the vicinity of Pd ion cores, and only a very small (~0.1 e), predominantly s-like electronic charge is found in the vicinity of the octahedral-site zero-point-motion volume in which deuteron cores are known to bind to the solid.

Both results indicate that effectively D^+ ions do dissociate from host electrons on time-scales that are large

enough to allow for fusion to occur. In particular, in ref. 21, we have used the minimum uncertainty packets mentioned above to determine meaningful bounds on the electrostatic ion-ion self-interaction, which we find to be ~ 10^{-17} second. This value, which is the rate-limiting effect associated with the coulomb repulsion between potentially interacting D^+, is much smaller than the time-scales (~10^{-14} s) associated with the 10's of meV bandwidths characteristic of the coupling between D^+ and electrons in PdD. This value is also considerably larger than the typical time-scales (~10^{-22} s) associated with nuclear self-interaction.

It is worthwhile noting in passing that it is possible to consider generalizations of the above picture associated with relaxing the restriction (implied by local density theory) requiring that variations in ion band state density become independent of variations in electron band state density. This restriction applies rigorously for the ground state wave functions provided electron-ion-band-state correlation effects are not present that could lower system energy. Although in the extreme low ion concentration limit, these correlation effects must become unimportant, it is possible that, at finite ion band state concentrations, electron-ion pairing mechanisms could lower system energy in a manner similar to the way pairing between electrons through phonon coupling to the lattice lowers system energy in the formation of Cooper pairs. Waber[21] has identified this possibility and suggested potential nesting features in the Fermi surface associated with the fractionally occupied electronic states that could trigger these forms of correlation.

D. Transistor vs Vacuum Tube Thinking

To visualize the cold fusion process one must adopt a different mode of thinking relative to that employed in hot fusion and conventional nuclear physics. In hot fusion one thinks in terms of collisions between randomly moving ions. These collisions are analogous to the electron-electron collisions that electrons undergo in the electron cloud surrounding the hot filament of a vacuum tube. To visualize the cold fusion process one must switch from thinking about the localized discrete particles encountered in "vacuum tube thinking" to thinking in terms of the collective action of the delocalized wave-like "particles" existing in semiconductors, i.e. to "transistor thinking". Once an individual D occupies an ion band state, it no longer is located in any specific unit cell. It is located everywhere. This is analogous to the behavior of electrons in metals. Potential interactions and modes of interaction are altered dramatically. More importantly, the coulomb barrier idea of particle-particle Gamow theory is replaced by the correlation properties of the many-b wave function.

E. How Ion Band State Nuclear Reactions Occur

The physics of collectively interacting wave-like i has substantial implications with respect to poten nuclear interactions. Under the rules of solid s physics, cold fusion can occur as a transformation wavelike deuterium into wavelike ^{4}He. As previo discussed[4,7,10], the energy release from transformation involves no high energy concentration, no high energy particles are emitted. The nuc interactions are governed by a self-consistent, n relativistic quantum field theory that we have na Lattice Induced Nuclear Chemistry (LINC)[7]. LIN based on ordinary non-relativistic quantum field theor it should apply to an indistinguishable collection of band state D (also called a Bose Bloch condens corresponding to the small band state concentrations D^+ associated with the $PdD_{1+\delta}$, AgD_δ, and N compounds. Energy is minimized through eliminatio lattice stress and by the occupation of uncorrelated m body wave functions that are constructed from si particle ion band states. The resulting potential nuc reactions preserve the requirement that the location both the potentially reactive D and the reaction prod cannot be determined on the time-scales associated maintaining periodic order.

F. Born-Oppenheimer Separability and Selec Rules of LINC

Through LINC, transistor-like (i.e., distributed s state-like) as opposed to vacuum tube-like (colli dominated) rules about particle overlap and trans become valid. The mathematical basis for this is pro by the underlying assumption of LINC and its react reactions and overlap can occur provided the domi electrostatic interactions are between the lattice an center of mass of potentially nuclearly reactive nucl and not between the individual nucleons. This limi occur when amplitudes of the ion-ion correlation ter the many-body wave function become small, and pro the time-scales for nuclear reaction are very much sl than those associated with electrostatic interaction.

When the time-scales for particular nuclear proc are very different than those associated with the moti the nucleus within an applied electrostatic field, it becomes appropriate to write the wave function c nucleus as the product of a rapidly varying functior describes the motions of the individual nucleons w

the nucleus relative to the center of mass r_{cm} multiplied by a more slowly varying function that describes the center of mass motion of the nucleus with respect to the applied electrostatic potential. This factorizing of the wave function is referred to as Born-Oppenheimer separability. This assumption holds rigorously provided the time-scales associated with the center of mass motion and the motions of the individual nuclei always remain very different. This representation applies to the initial state provided the center of mass motion of each D^+ is well-described by a band state. Expressed in terms of the separation coordinates of the protons and neutrons in p-n pairs (r_n-r_p), the wave function of each deuteron is given by

$$\Phi(r_n, r_p) = \Psi_{nuc}(r_n - r_p)\, \Psi_{band}(r_{cm}) \quad ,$$

where Ψ_{nuc} is the rapidly varying nuclear wave function that describes the probabilty amplitude of finding a proton or neutron within a small volume centered about the center of mass, and r_n and r_p respectively are the locations of the proton and neutron.

The assumption of LINC is that this form of Born Oppenheimer separabilty applies rigorously as a function of time in all multi-particle fluctuations (governed by the underlying field theory) that are consistent with the requirements that the nuclear and electrostatic time scales associated with these fluctuations remain very different. This means that at any time during the reaction the final state must be representatable in a Born-Oppenheimer separable form:

$$\Phi(r_1,\ldots,r_m) = \Psi_{nuc}(r_1 - r_{cm},\ldots,r_m - r_{cm})\, \Psi_{band}(r_{cm}) \quad ,$$

where $\Psi_{nuc}(r_1 - r_{cm},\ldots,r_m - r_{cm})$ now describes the nuclear (multiple-nucleon) wave function. In refs. 7 and 10, we have derived important selection rules associated with this constraint. In particular, the constraint automatically rules out a large number of potential reactions. This is because the constraint is only meaningful provided 1) zero-point motions of the center of mass of potentially reacting nuclei are sufficiently large both during and subsequent to the reactions, and 2) these center of mass motions must remain independent from the motions of the individual nucleons at all times during the reaction.

Because nuclear reactions between closely separated nucleons are always independent of the absolute location of the center-of-mass, there exists an important symmetry which insures that the final state representation is meaningful since it preserves this symmetry. Because of the requirement that the zero-point motions of the center of mass must be sufficiently large, the limitations of the representation are closely tied to the underlying electronic structure. Using reasonable wave functions, based on known values of zero-point motion for D in PdD_x, we have estimated in refs. 7 and 20 suitable bounds for the electrostatic self-interaction and nuclear self-interaction, where we have shown that separability can be expected to apply for a ^4He product.

Perhaps of greater significance is the following: The assumption that Born-Oppenheimer separability must be maintained in the final state and during all intermediate states involving multi-particle fluctuations associated with band state overlap leads to an important selection rule. Beginning from a state consisting entirely of D^+ ion band states, the many-nucleon portion of the final-state-wave function $\Psi_{nuc}(r_1 - r_{cm},\ldots,r_m - r_{cm})$ must be formed exclusively from unbroken proton-neutron pairs.

As we have shown in ref. 10, this rule is based on rigorous requirements associated with constraining the governing field theory so that the nuclear and band state wave functions evolve independently from each other. We have demonstrated this using the defining constraints of canonical quantization (using Poisson Brackets) associated with the problem of constructing a field theory that maintains Born-Oppenheimer separability starting from an initial state consisting of ion band state D^+. We have previously used the terminology[7,20] "bosons in and bosons out" to refer to the resulting selection rule that proton-neutron pairs cannot be broken.[20]

The presence of unpaired proton-neutron pairs, or of unpaired protons or neutrons, in the initial state requires that this rule be modified. In ref. 10, we have discussed these modifications. The resulting selection rules and reactions associated with LINC, both when either unpaired protons and neutrons are and are not present, are summarized below.

G. Many-body Wave Function

The initial state many-body wave function is constructed from a summation of terms. Each term consists of a product of all of the single deuteron wave functions in which each deuteron is assigned a specific location. The summation imposes the required particle-exchange symmetry, ensuring that the many-body wave function describes indistinguishable bosons. Because of Born-Oppenheimer separability, automatically, the summation of terms can be factored into a product

consisting of a single factor derived from a subproduct of the localized wave functions (Ψ_{nuc}) multiplied by a sum of terms associated with the slowly-varying band state D^+ many-body function. (Because of Born Oppenheimer separability, the effects of particle exchange symmetry of the entire many-body function appear only through the many-body band state wave function.) Band state D^+ matter has magical properties that are implicit because of the exchange symmetry that is embodied in the many-body band state wave function. Because each single particle band state wave function has Bloch function symmetry, when the many-body band state wave function becomes occupied, the lattice strain (associated with injection of non-band state D into the host) vanishes. For this reason, this function minimizes system energy in crystals that are sufficiently large, when the number of band-state D^+ is much less than the total number of unit cells, and the band state D^+ remain uncorrelated.

This many-body wave function can also be written in a "vacuum tube-like" form, based on a particle-like (Wannier state) representation[4]. The resulting description is characterized in a manner involving particle-like occupations (involving whole numbers of D^+), in which each occupation is transient and possesses a finite lifetime Δt. Specifically, $\Delta E \cdot \Delta t \sim h$, $\Delta t \sim 10^{-16}$ s. The particle-aspect of the matter field's behavior is shown in the Wannier form (analogous to an inverse Fourier transform) of the many-body bosonic wave function.[4]

$$\Psi(\epsilon_p, r) = (1/N_D!)^{1/2} \sum_{\{r_m\}} (1/N_{cell})^{N_B/2} \times \left\{ \prod_{m=1}^{N_D} \sum_{s=1}^{N_{cell}} \Phi_s(r_m) \exp(i k_p \cdot R_s) \right\}$$

Here $\{r_m\}$ means the sum is over all products in which distinct pairs of particles are exchanged. All terms are of the form

$$\Phi_{121}(r_{11}) \cdot \Phi_{61}(r_{77}) \cdot \Phi_{18214}(r_{480}) \cdot \Phi_{2107}(r_{396}) \cdots \Phi_{97}(r_{11}) \cdots$$

Each term contains N_D factors, where N_D is the number of deuterons in the many-body band state. There are $N_D! \, (N_{cell})^{N_D}$ terms in the wave function. In the many-body wave function the deuteron index never repeats, but the unit cell index may repeat. The expansion contains terms that correspond to zero, single, double, triple, etc. occupations of specific unit cells. existence of multiple occupation terms reveals that D^+, or D^+-D^+-D^+, etc. overlap can occur. In other w the algebraic properties of the many-body wave fun imply that overlap occurs. The underlying reason this becomes possible is that in the localized, Wan representation, occupation of an individual site become short-lived. Another way of understanding point is that in the "usual" (or vacuum tube) wa looking at deuterons, they appear to be long-l particles, while if a collection of them occupy ion states, this particle (i.e., Wannier state) picture breakdown because the lifetime of a "particle" at individual location can become very short. Underlyin resulting overlap process is this question of lifetim the lifetime for electrostatic overlap (as a result o band state occupation) is considerably longer at a la site in this "particle-like" representation than comparable "particle-like" lifetime associated with nu decay, nuclear reaction can occur. As a result, a varie reactions become possible.

H. The 2-body Reaction

The number of double occupations of unit exceeds the number of triple occupation by the factor where δ is the number of band state ions per unit Since δ may of the order of 10^{-6}, 2-body interaction expected to dominate. All the reactions inv delocalized D^+ ions and proceed as volume distrib interactions. The first reaction step is a rever coalescence of p-n pairs

$$2D^+ \rightleftarrows {}^4He^{++*}$$

The reaction is made irreversible by excitation of lattice

$${}^4He^{++*} + \text{lattice} \rightarrow {}^4He^{++} + \text{lattice}^*$$

Helium is ejected from the lattice either as a neutral surface species

$${}^4He^{++} \rightarrow {}^4He^{++}_{surface}$$

$${}^4He^{++}_{surface} + 2\,e \rightarrow {}^4He_{surface} \uparrow$$

or (as discussed above), at low temperature, possibly Bragg scattered neutral atom or ion. The species in it are delocalized configurations (Bloch states). The sur ejection of He was predicted[4,7] before being observ In the 2-body reaction overlap of p-n pairs allows nuc

fusion $2D \rightarrow {}^4He$. (As little as 0.3 ppm of wavelike D^+ may be needed to produce 600 W/cc.)[4]

I. Multiple- and Mixed-body Reactions

Other interactions between band states include[10] the three body reactions

$$3D^+ \rightarrow {}^4He^{++} + D^+$$

and

$$2D^+ + {}^1H^+ \rightarrow {}^3H^+ + {}^1H^+\downarrow {}^1H^+\uparrow$$

where the small arrows indicate the relative directions of nuclear spin. The latter reaction requires occupation of both deuteron and protium band states, and has been suggested as a possible tritium-creating band state side reaction. In all the reactions energy release is distributed over the lattice, only a small amount occurs in each unit cell. (As applied to a proposed "normal" water reaction, concentrations of 10^{-7} D/Pd and 10^{-3} H/Pd may be adequate to produce claimed heat.)

IV. PREDICTIONS

Predictions made before experimental verification include the requirement for ~1:1 D/Pd ratio (McKubre et al., Kunimatsu et al.)[22,23], no appreciable radiation or neutrons (many groups), and primay products being heat and low-energy ^{4}He in the outgases (Miles et al., Yamaguchi and Nishioka).[8,9] Cracking, overloading, and other processes that cause loss of periodic order should impede cold fusion heat release.

Other predictions include: Reactions are fractional, involving infinitesimal energy release in each unit cell. Energy is transferred to the lattice through coupling to phonons, excitation of high frequency sound modes, inelastic scattering of products with host electrons, etc.. Lattice disintegration terminates heat generation. High energy particle release may occur if periodic order is lost suddenly. Optimal heating occurs when lattice disintegration is minimized, with energy release occurring dominantly through extreme long-wave phonons caused by release of products in regions where periodic order is lost. Reaction products are distributed at surfaces, near cracks, at interfaces, and in the out-gases. At low temperature, lattice termination and motion may induce nuclearly mitigated near-surface stresses, leading to the potential for surface isotopic anomalies (Rolison effect). We interpret these anomalies to be the result of stress imbalance and not a direct nuclear isotope reaction. At sufficiently low temperature, if a single crystal is used, outgassing products (primarily ^{4}He) will distribute themselves in the form of a Bragg diffraction pattern. Also, we find[4,10] that fusion rate is proportional to the concentration of final state ion-band-state $^4He^{++}$, suggesting that the reaction possibly has a "self-triggering" mechanism, possibly consistent with a number of run-away heating episodes that seem to have been observed[1]. We also find[10] that steady-state power density should be proportional to current density.

V. CONCLUSIONS

There is experimental evidence for cold fusion which is difficult to explain away. The poor repeatability is understandable in view of the nonequilibrium chemistry required for creating $PdD_{1+\delta}$ and the problem of cracking due to differential expansion during D loading. There exists a quantum mechanics rationale by which release of fusion energy in a solid can occur without production of energetic particles. This energy release requires the presence of delocalized wavelike D^+ and involves a volume distributed reaction.

REFERENCES

1. M. Fleischmann and S. Pons, *Phys Lett. A.* **176**, 118 (1993); see p. 128.

2. F. Seitz, *The Modern Theory of Solids* (McGraw-Hill, New York, 1940), pp. 227-234.

3. E. A. Hylleraas, Zeit. f. Phys. **54**, 347 (1929).

4. T. A. Chubb and S. R. Chubb, *Fusion Technology.* **20**, 93 (1991).

5. P. Roman, *Advanced Quantum Theory*, (Addison-Wesley, Reading,MA 1965), pp.63-90.

6. A. Einstein, B. Podolsky, and N. Rosen, *Phys. Rev.*, **47**, 777 (1935).

7. S. R. Chubb And T. A. Chubb, "Lattice Induced Nuclear Chemistry", *AIP Conference Proc.*, **228**, titled *Anomalous Nuclear Effects in Deuterium/Solid Systems*, Eds. S. E. Jones, S. Scaramuzzi, and D. Worledge, p. 691 (1991).

8. M. H. Miles and B. F. Bush in *Frontiers of Cold Fusion*. H. Ikegami, Editor, (Universal Academy Press, Tokyo, 1993), p. 189.

9. E. Yamaguchi and T. Nishioka, in *Frontiers of Cold Fusion*. H. Ikegami, Editor, (Universal Academy Press, Tokyo, 1993), p. 179.

10. S. R. Chubb and T. A. Chubb, *Fusion Technology*. **24**, 403 (1993).

11. E. Wicke and H. Brodowsky, in *Hydrogen in Metals II*, p. 73., G. Alefield and J. Volkl, Eds., Springer , Berlin (1978).

12. E. Storms, "Some Characteristics of Heat Production Using the 'Cold Fusion' Effect", *ICCF4 Notebook*, p. C 2.6 (1993).

13. M.C.H. McKubre, Presentation at ICCF4 in Maui, December 1993.

14. M. J. Puska, J. R. M. Nieminen, M. Manninen, B. Chakraborty, S. Holloway, and J. K. Norskov, *Phys. Rev. Lett.*, **51**, 1081 (1983).

15. C. Astaldi, A. Bianco, S. Modesti, and E. Tosatti, *Phys. Rev. Lett.*, **68**, p. 90, (1992).

16. G. Nelin, "A Neutron Diffraction Study of Palladium Hydride", *Phys. Status Solidi*, **45**, 527 (1971).

17. D. A. Papaconstantopoulos, B. M. Klein, J. S. Faulkner, And L. L. Boyer, "Coherent-potential-approximation calculations for PdH_x", *Phys. Rev. B*, **18**, 2784 (1978). A. C. Switendick, "Electronic Energy Bands of Metal Hydrides - Palladium and Nickel Hydride", *Ber. Bunsenges. Phys. Chem.*, **76**, 535 (1972).

18. T. Riesterer, J. Osterwalder, And L. Schlapbach, "Inverse photoemission from $PdH_{0.65}$", *Phys. Rev. B*, **32**, 8405 (1985). D. E. Eastman, J. K. Cashion, And A. C. Switendick, "Photoemission Studies of Energy Levels in the Palladium-Hydrogen System", *Phys. Rev. Lett.*, **27**, 35 (1971).

19. P. C. Hohenberg and W. Kohn, *Phys. Rev. B*, **138**, 864 (1964). W. Kohn and L. J. Sham, *Phys. Rev. A*, **140**, 1133 (1965).

20. S. R. Chubb And T. A. Chubb, "Quantum Mechanics of 'Cold' and Not-So-Cold' Fusion," *Proc. First Annual Cold Fusion Conf.*, Salt Lake City, Utah, March 28-31, 1990, p. 119 (1990). S. R. Chubb and T. A. Chubb, "Fusion Within a Solid through Solid State Effects: The Grand Identity Crisis," *Proc. EPRI-NSF Workshop on Anomalous Effects in Deuterated Metals, Oct. 16, 1989*, (ed. Schneider, Electric Power Research Institute), p. 29-1 (1993).

21. J. T. Waber and M. de Llano, "Cold Fusion as Bose Condensation in a Fermi Sea", in this Proceedings.

22. M. C. H. McKubre, S. Crouch-Baker, A. M. Rice, S. I. Smedley, and F. L. Tanzella in *Frontiers of Cold Fusion*. H. Ikegami, Editor, (Universal Academy Press, Tokyo, 1993), p. 5.

23. K. Kunimatsu, N. Hasegawa, A. Kubota, N. Ikeda, M. Ishikawa, H. Akita, and Y. Tsuchida, in *Frontiers of Cold Fusion*. H. Ikegami, Editor, (Universal Academy Press, Tokyo, 1993), p. 31.

This paper is not a part of the foregoing conference.

POTENTIAL FOR POSITIONAL VARIATION IN FLOW CALORIMETRIC SYSTEMS

Mitchell Swartz
(c) JET TECHNOLOGY

February 10, 1996

Although many aspects of calorimeters have been discussed, including issues of potential problems with the thermometry (i.e. thermocouples, thermistors and thermometers, as well as electrical grounding and crosstalk, thermal mixing and sensor positioning problems), the potential impact of the positional effects of the flow calorimetry has not been mentioned. The positional orientation refers to the direction of the flow, and not to the orientation of any temperature probes therein. Despite the reported advantages for flow calorimetry in detecting enthalpy from putative fusion reactions, these studies theoretically suggest that there may be effects from positional variational in the calorimetry of such flow systems. Rather than 'ease of calibration' usually touted for such systems, it is suggested that calibration may be more complicated for vertical flow calorimetric systems. In the absence of additional calibration, it may be critical to keep semiquantitative calorimeters horizontal.

One recent series of reports using vertical flow calorimetry [1,2,3,4] involves the *CETI* microspheres, reported to use a few percentages of the metal of other systems. The microspheres have multilayer metallic coats and are used as a distributed electrode bed. The cell is 10 cm long, 2.5 cm in diameter, and contains 1 to 40 ml of beads. Electrolyte percolates through, removing the heat, and exits from the top. The flow causes a temperature gradient. The observed delta-T, between the top and bottom is in the range of 1.5 to 20C (flow rates is 1.0 - 1.5 liters per minute, with the water circulated by a magnetic impeller pump, total power consumption ~85 watts). At the ICCF5, the *CETI* cell was reported to have an input of 0.14 watts and a peak excess of 2.5 watts, a ratio of 1:18. At SOFE '95, the *CETI* cell had 0.06 watts input and 5 watts peak output, a ratio of 1:83. At Power-Gen, the ratio reportedly ranged from 1:1000 to 1:4000.

There have been several complaints regarding the *CETI* demonstrations in relation to recombination, flow measurement, and heat ejection [3]. Assuming the thermometry is correct, it is instructive to closely examine the calorimetry using a computer model representing heat and mass transfer. The equation used to derive the output, and therefore the presence of any excess heat involves the flow, the specific heat of the water, and temperature differential. Although this equation may be dimensionally correct, it may not be valid for low flow rates in certain cases discussed below. The role of the Bernard instability [5] has not been previously mentioned, even though it may have inadvertently impacted the calorimetry [4].

The following describes the result of a quasi-one-dimensional (Q1D) analysis which further examined the impact of the flow orientation, with respect to the gravitational field, during flow calorimetry. The model generated to test the hypothesis examined convection, conduction, and gravity-thermal instabilities. Figures 1 through 4 show four groups of curves which show the time-varying distribution of temperature

in such a quasi-one-dimensional model. The four groups of curves represent horizontal and vertical flow calorimetry, both with and without convection. In each graph, the spatial distribution of heat (in one dimension) is represented as a single curve. There is one curve for each point in time. There is heat input from a single point source - at midposition along the x-axis - during the entire time subtended by each series of curves. The earliest curves, in each group, are those closest to the x-axis where the heat arise out of the central point source. Thus the dynamics can be followed from the graphs generated for the model.

After the heat enters at the midposition along the x-axis it can be redistributed by thermal conduction, by convection and by redistribution secondary to the changes in specific gravity resulting from the temperature changes (as with the Bernard instability). Radiative loss is not considered in this simplified model. The first group of curves in Fig. 1, which is labeled "Horizontal Flow - Thermal Diffusion" to indicate that the flow is horizontal to the Earth's surface and that thermal diffusion is included. Fig. 1 shows both the midline exogenous heat component and a slow thermal diffusion away from the point-source of heat. The velocity is zero; that is, there is no convection. The second group of curves, Fig. 2, show the impact of convection upon the spatial distribution of heat. This figure shows how the redistribution of heat is used in typical flow calorimetry to generate a temperature gradient, from a sampling of which a calculation is made to determine the output heat (energy). The two groups of curves, Figs. 3 and 4, labeled "Vertical Flow" represent the output from a vertical system, both with and without the addition of upward convection. The extreme along the x-axis away from the point source of heat input, previously 'right' and 'left' in Figs. 1 and 2, are now 'top' and 'bottom' in Figs. 3 and 4. Upon examination of the curves on the lower left, gravity is observed to now play a role in the distribution of the warmed water. It is saliently obvious that because the thermal-driven buoyancy which also leads to the Bernard instability -- where hot water rises due to its lower specific gravity -- the curves in Fig. 3 do shift in position away from the symmetry exhibited by horizontal flow calorimetric systems <u>even in the absence of convection</u> (compare to Fig. 1). There may be, for such conditions, an apparent "signal" for zero flow because of the thermal instability, which simulates the effect of flow (the group of curves in Fig. 3; compare to the group of curves in Fig. 2). The addition of convection produces additional contribution to the heat shift in the vertical flow system (Fig. 4), quite similar to that which it does for horizontal systems (Fig. 2).

One observation from the model is that the boundary condition from zero to negligible flow conditions is different for the horizontal and vertical flow calorimetric systems. It is important to consider that generally, quoted efficiencies of energy generated from putative over-unity devices are calculated assuming the standard equation is always correct. Another salient observation resulting from this theoretical Q1D study is that simple equations which apply for horizontal calorimetric systems may not be strictly applicable for vertical flow calorimetric systems for low flow conditions. But which?

We now define η_B as the ratio of heat transported by the buoyant forces to the heat transported by solution convection.

$$\eta_B \equiv \frac{\text{heat transported by boyant forces}}{\text{heat transferred by solution convection}}$$

This Q1D model of heat and mass transfer has indicated that what is generally correct for horizontal calorimetric systems, may not be correct for vertical systems, when the non-dimensional number ($=\eta_B$) is significantly greater than zero. Any apparent amplification of the 'excess heat' (if any, and there does appear to be some) would be greatest at the low levels. Increased flow makes the positional error less important. As a corollary, any false excess heat, or excess heat magnification, should also reduce with increased flow.

In summary, thermometry may not be the only rate limiting factor for obtaining high-quality information from flow calorimeters if the non-dimensional number η_B {defined as the ratio of heat transfer by buoyancy to the heat transfer by convection} is greater than zero. η_B, in a real system where viscosity, turbulence, and other parameters play a role, depends upon other non-dimensional factors including the Archimedes non-dimensional number which is the ratio of the buoyant force to the viscous force, and possibly the Rayleigh non-dimensional number, which is the ratio of gravity to thermal conductivity. Studies are underway to explore this. It is also proposed that a simple test of the theory would be to build a rotatable flow cell with a resistive heat element, perhaps mounted on a goniometer for any system to check sensitivity. This hypothesis, and Q1D model of heat and mass transfer, do not imply that such systems do not exhibit 'excess heat.' But rather that any such reported 'excess heat' parameters may be inflated, if the information was indeed collected with a vertical flow calorimetric system, in the absence of confirmatory calibrations under low to moderate flow conditions where the non-dimensional number (η_B) is not trivial.

REFERENCES

[1] D. Cravens, "Flowing Electrolyte Calorimetry," Proceedings of 5th International Conference on Cold Fusion, 79-86 (1995).

[2] H. Fox, "Dramatic Cold Fusion Demonstration Seen By Hot Fusion Scientists," *Fusion Facts*, vol. 7, number 4, 1-4 (1995).

[3] M. Jones, "Some Simple Calculations Assuming 42 Cubic Feet per Minute," posted on sci.physics.fusion; excerpts in *Cold Fusion Times*, vol. 4, number 1, 6-8 (1996).

[4] M. Swartz, "Elementary Survey of CETI Microsphere Demo." *Cold Fusion Times*, vol. 4, number 1, 7-9 (1996).

[5] S. Chandrasekhar, "Hydrodynamic and Hydromagnetic Stability," Clarendon Press, Oxford, 9-75 (1961)

[6] J. Melcher, "Continuum Electromechanics," MIT Press, Cambridge, 10. 13-10. 18 (1981)

The author is most grateful to Gayle Verner, Hal Fox, Horace Heffner, Mark Hugo, Jed Rothwell, Barry Merriman and Profs. Louis Smullin and Keith Johnson of MIT and the staff of JET Technology and Fusion Information Center for helpful comments and assistance during the development of this model and the preparation of this manuscript.

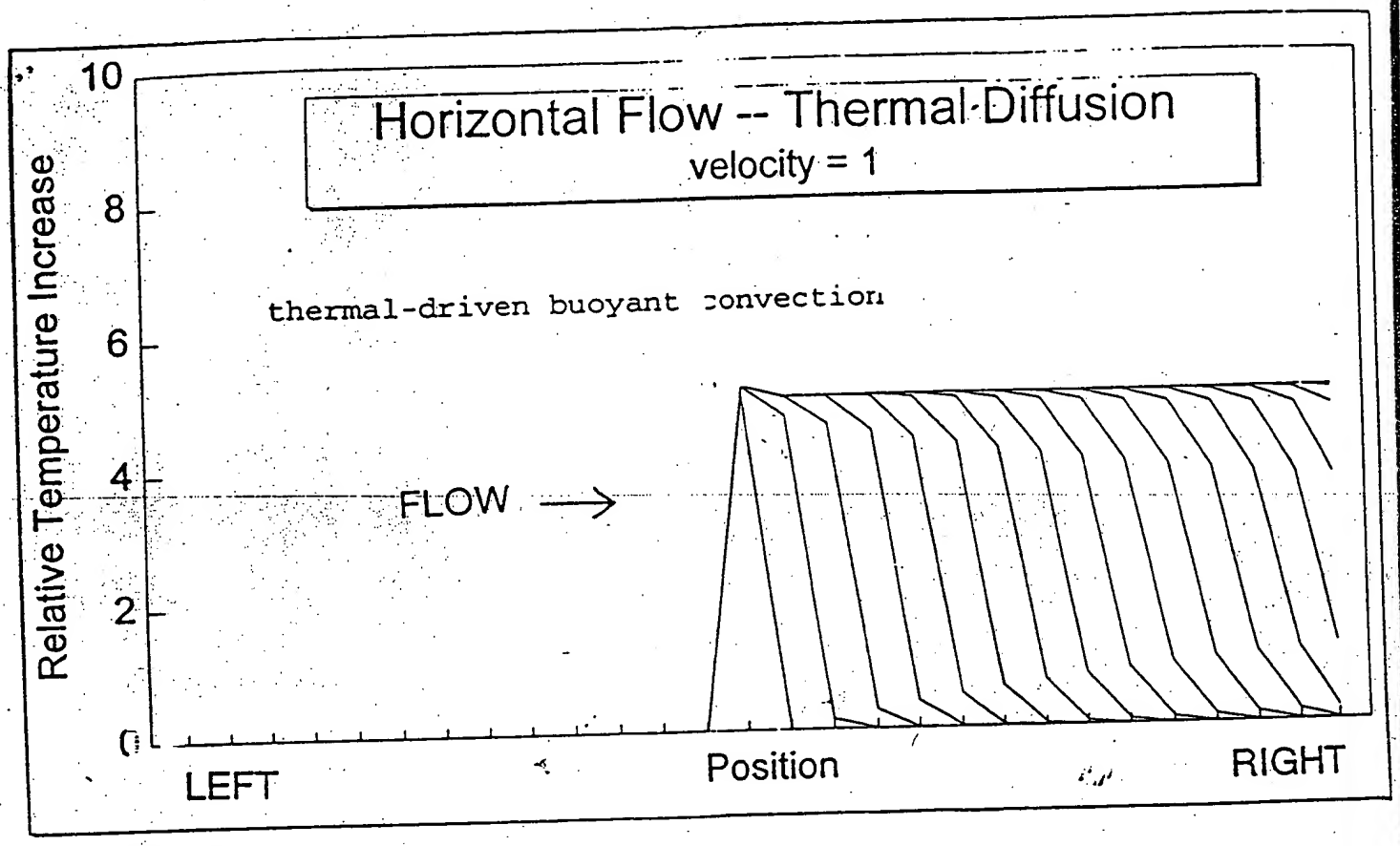
Horizontal Flow -- Thermal-Diffusion
velocity = 1
thermal-driven buoyant convection
FLOW
Relative Temperature Increase
10
8
6
4
2
0
LEFT
Position
RIGHT

FIG. 3

FIG. 4

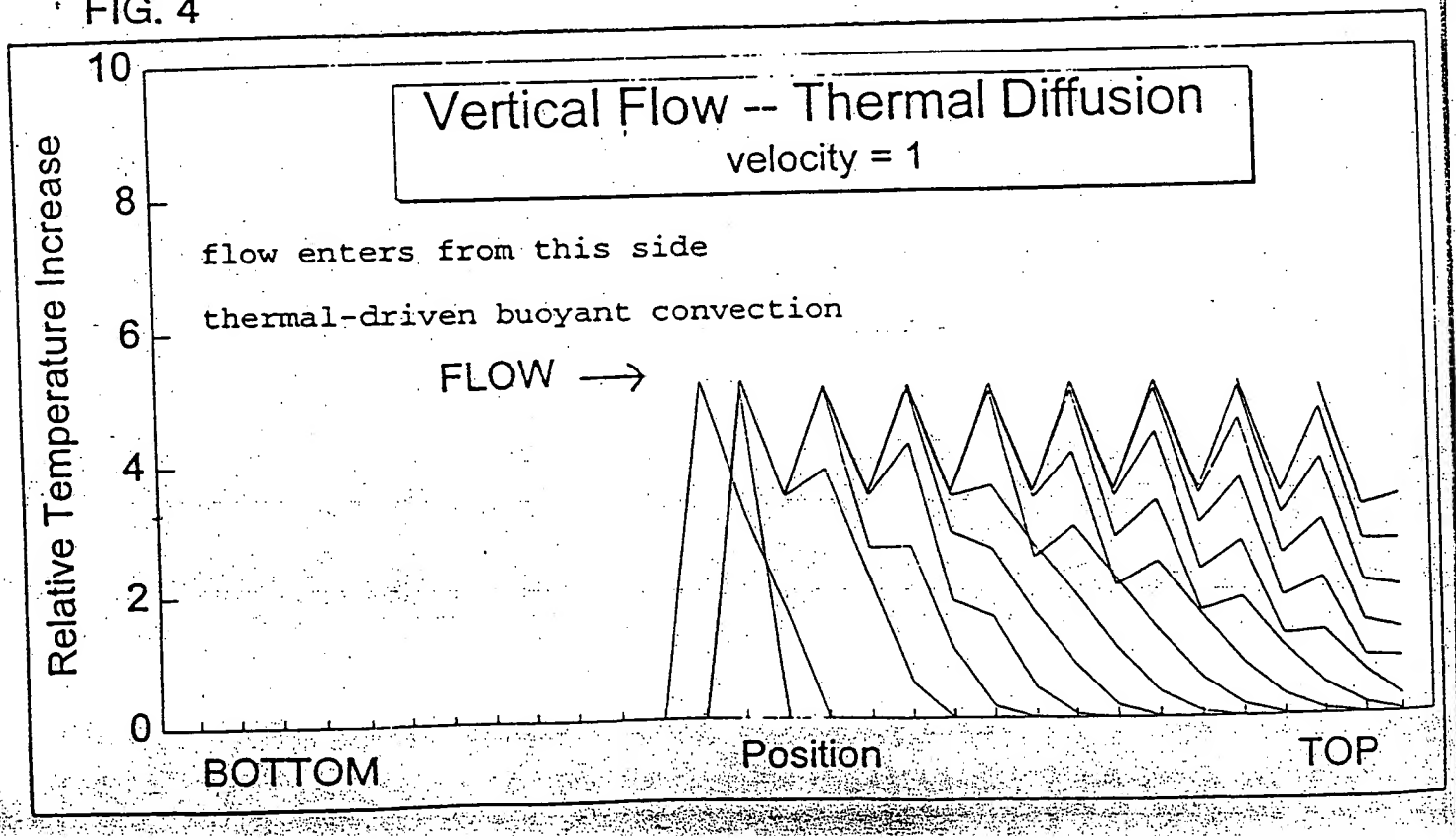
Vertical Flow -- Thermal Diffusion
velocity = 1
flow enters from this side
thermal-driven buoyant convection
FLOW
Relative Temperature Increase
10
8
6
4
2
0
BOTTOM
Position
TOP

CODEPOSITION OF PALLADIUM AND DEUTERIUM

NUCLEAR REACTIONS IN SOLIDS

KEYWORDS: heavy water electrolysis, quasi-one-dimensional model of isotopic loading, nonequilibrium loading ratio

MITCHELL R. SWARTZ
JET Energy Technology, Inc., P.O. Box 81135, Wellesley Hills, Massachusetts 02181

Received March 30, 1995
Accepted for Publication August 15, 1996

The quasi-one-dimensional model of isotope loading into a material relates the loading flux, the electric order/thermal disorder ratio, and other physical issues. The theoretical nonequilibrium deuteron/palladium ratio at the surface of a palladium electrode, previously shown to depend on the loading flux ratio, is corrected both for intrapalladial diffusion of the loaded deuterons and for secondary changes in electrode volume, possibly explaining the often considerable time elapsed until the onset of the desired reactions.

INTRODUCTION

Several hurdles remain in the successful utilization of the cold fusion phenomena.[1] Most important is the improved characterization and preparation of palladium of sufficient integrity into which to successfully load[2] and activate[3] the isotopic fuel—deuterium. Adequate loading ($\lambda_{D,Pd}$) must occur despite major difficulties involving the loading flux ratio,[2] the electric order/thermal disorder ratio, and other physical issues.[2,4,5] Additional difficulties include the often considerable time elapsed until the onset of the desired reactions.[1]

MODEL

The quasi-one-dimensional (Q1D) model of isotope loading[2,4,5] has enabled the cathode deposition of ions to be investigated using nonequilibrium calculations.[6] In the absence of significant convection, the flux of each species (here deuterium and palladium cations) results from diffusion down concentration gradients and electromigration drift.[5,7] The coupled equations follow (see Nomenclature on p. 129):

$$J_D = -B_D * \frac{d[D(z,t)]}{dz} - \mu_D * [D(z,t)] * \frac{d\Phi}{dz} \qquad (1)$$

and

$$J_{Pd} = -B_{Pd} * \frac{d[Pd(z,t)]}{dz} - \mu_{Pd} * [Pd(z,t)] * \frac{d\Phi}{dz} \qquad (2)$$

The mathematical solution for the time rate of change of the deuterium in any given volume is determined by these fluxes and Gauss's theorem. Deuteron and palladium entry to the cathode is electron limited. Three components of the deuteron flux are considered at the cathode. The first flux component is the entry of deuterons into the bulk of palladium J_e. The second flux component is the volume loss of deuterons secondary to gas evolution J_g. The third flux component is caused by those deuterons lost to all putative fusion reactions J_{fus}. The palladium flux at the cathode is simpler because of the absence of palladium gas formation. The mathematical solutions are determined both by the boundary conditions and by conservation of mass for both species. There is assumed conservation of deuterons with the exception of a loss J_{fus} to all putative fusion reactions.[4] However, J_{fus} is extremely small compared with most loading rates or gas-evolving reactions.[2]

By assuming that the fluxes are first order on the local concentrations of available material, then the first-order reaction rates of deuteron loading/gas evolution and fusion ΣK_i and palladium deposition K_{Pd} are definable, enabling a possible solution. In the steady state, the initial coefficient $[A_{0,D}]$ of the final spatial distribution of deuterons at the pericathodic interface has been derived[2,4,6]

$$A_{0,D} = \frac{[D_{init}] * \left\{\left[\left(\frac{qE}{2k_BT}\right) - \left(\frac{\sum K_i}{2 * B_D}\right) * L_c\right]\right\}}{\left(\exp\left\{\left[\left(\frac{qE}{2k_BT}\right) - \left(\frac{\sum K_i}{2 * B_D}\right) * L_c\right]\right\} + \left[\left(\frac{qE}{2k_BT}\right) - \left(\frac{\sum K_i}{2 * B_D}\right) * L_c\right] - 1\right)} \quad (3)$$

As discussed,[2] this finding was augmented by the initial coefficient $[A_{0,Pd}]$ of the final spatial distribution for palladium that is electrodeposited on the cathode in codeposition:

$$A_{0,Pd} = \frac{[Pd_{init}] * \left\{\left[\left(\frac{qE}{2k_BT}\right) - \left(\frac{K_{Pd}}{2 * B_{Pd}}\right) * L_c\right]\right\}}{\left(\exp\left\{\left[\left(\frac{qE}{2k_BT}\right) - \left(\frac{K_{Pd}}{2 * B_{Pd}}\right) * L_c\right]\right\} + \left[\left(\frac{qE}{2k_BT}\right) - \left(\frac{K_{Pd}}{2 * B_{Pd}}\right) * L_c\right] - 1\right)} \quad (4)$$

The ratio of Eqs. (3) and (4) did show that the use of codeposition of palladium from palladium salts in a deuteron-containing solution[2,3,7] can be used to attain a much more rapid onset of (at least local) full loading. Thus, the initial coefficient of the deuteron/palladium ratio at the surface of a palladium electrode with the full inclusion of palladium cation codeposition[2,7] has been discussed[2]:

$$A_{0,D/Pd} = \frac{\left(\exp\left\{\left[\left(\frac{qE}{2k_BT}\right) - \left(\frac{K_{Pd}}{2 * B_{Pd}}\right) * L_c\right]\right\} + \left[\left(\frac{qE}{2k_BT}\right) - \left(\frac{K_{Pd}}{2 * B_{Pd}}\right) * L_c\right] - 1\right) * [D_{init}] * \left\{\left[\left(\frac{qE}{2k_BT}\right) - \left(\frac{\sum K_i}{2 * B_D}\right) * L_c\right]\right\}}{\left(\exp\left\{\left[\left(\frac{qE}{2k_BT}\right) - \left(\frac{\sum K_i}{2 * B_D}\right) * L_c\right]\right\} + \left[\left(\frac{qE}{2k_BT}\right) - \left(\frac{\sum K_i}{2 * B_D}\right) * L_c\right] - 1\right) * [Pd_{init}] * \left\{\left[\left(\frac{qE}{2k_BT}\right) - \left(\frac{K_{Pd}}{2 * B_{Pd}}\right) * L_c\right]\right\}} \quad (5)$$

This loading ratio has indicated the possibility of sufficient loading very close to the electrode surface with a time constant related to the relaxation of palladium from the solution onto the cathode. If a minimal loading ratio is required for the desired cold fusion reactions, then the maneuver would be an important control point of these reactions. This is shown in Fig. 1, which presents the derived peak local loading ratio based on these assumptions, with and without codeposition. The loading ratio is shown for a range of electrical ordering energies.

However, except for the relaxation time interval, Eq. (5) indicates that this generation of loading sufficiently would be nearly instantaneous, which is simply not observed. Therefore, we have now corrected Eq. (5) (and the volumes to which it refers) both for observed intrapalladial diffusion of the loaded deuterons and for the secondary changes in electrode volume.

The first-order diffusion rate was included for its impact on the local surface concentration, thereby calculating the local depletion secondary to internal redistribution in the bulk metal. Within the metal, the deuteron diffusion has been considered by several models. Anharmonic effects,[8] optical and acoustic phonon spectra, material defects, grain boundary dislocations, and fissures[9] all influence the deeper loading of the metal. These mechanisms may lead to a relative decrease in the surface concentrations of deuterons and thus the local surface loading ratio. The local loading ratios were derived using the simple redistribution mechanisms, with the understanding that the actual three-dimensional mechanisms are what actually accounts for the phenomena. The diffusivities are such (Table I) that only the term for the hydrogen isotope appears to be important to first order. The volume change, albeit small, was also included in the final calculation.

TABLE I

Diffusivities of Materials in Palladium

Substance	Deuterium (cm^2/s)	E_a (kJ/mol)	References
Hydrogen	0.0029 to 0.0053	22.2 to 22.8	See Oriani,[10] Chemical
Deuterium	0.0027	19.8 to 20.5	Rubber Company Hand-
Tritium	0.0048	39.4	book,[11] and Swartz[12]
Palladium (self-diffusion)	0.00001	266	

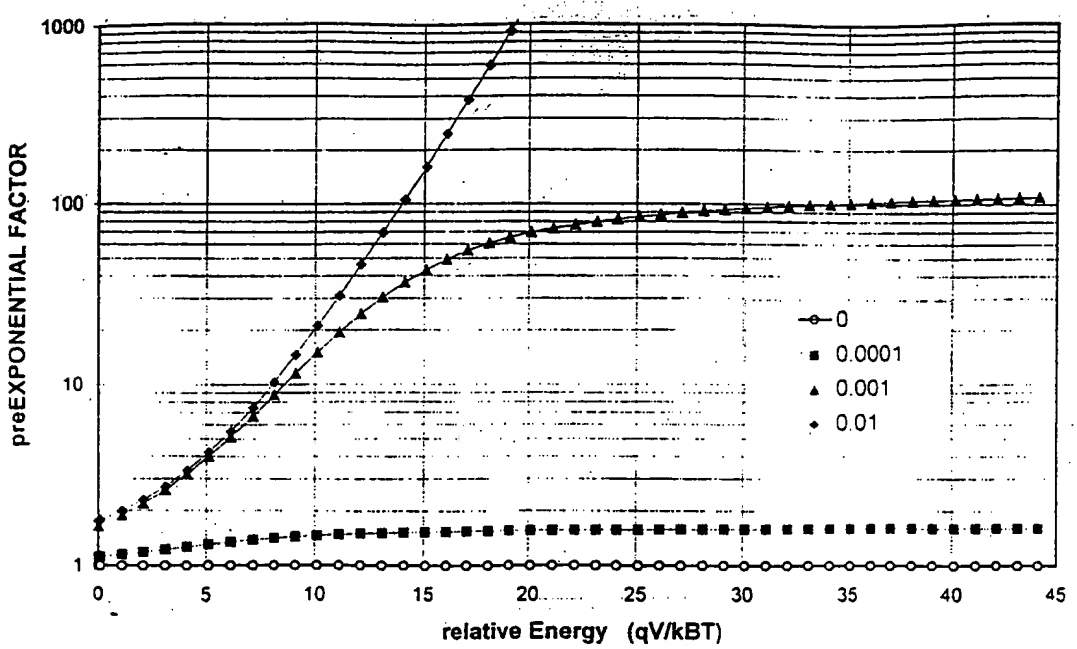

Fig. 1. Preexponential peak local loading ratio: These four curves are the derived preexponential factor for the peak local loading ratios both with (solid circles, triangles,-squares) and without (open circles) codeposition. The preexponential factor is shown for a range of electrical ordering energies in units of electrical energy compared with kinetic energy $k_B T$. The three codeposition curves are for 0.1, 1, and 10 mA. The diffusivity of the palladium ions in solution is estimated as 10% that of the deuterium ion itself.

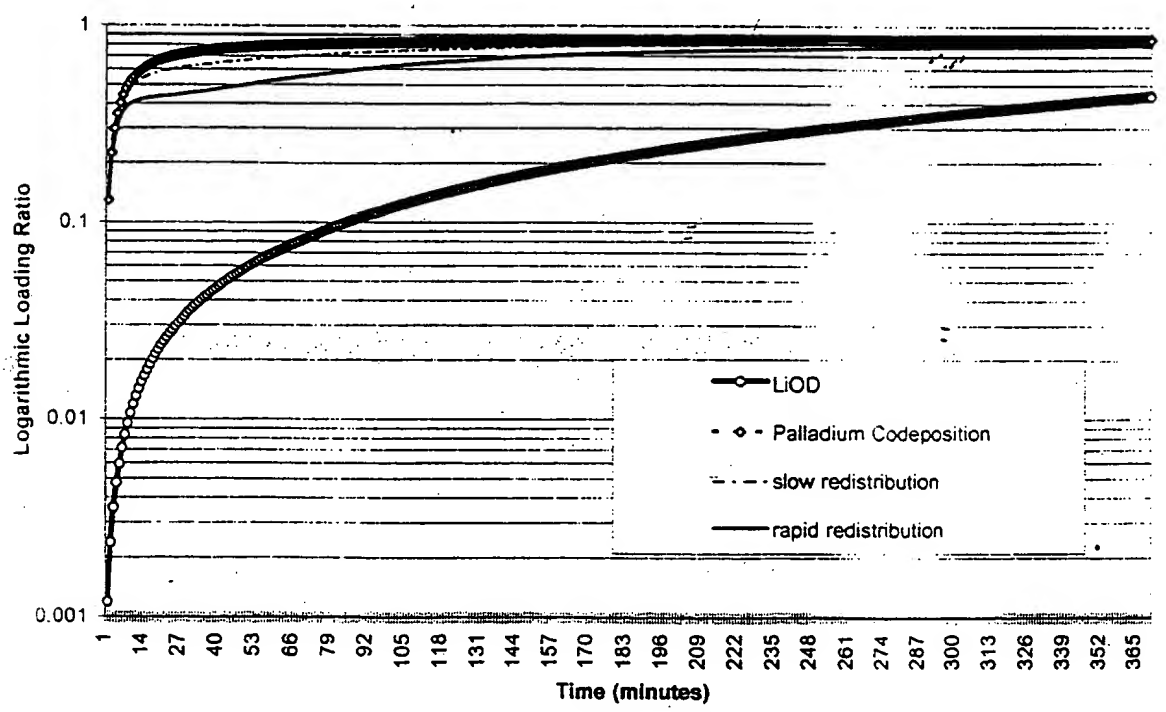

Fig. 2. Theoretical peak local deuteron loading and the impact of codeposition: These curves show the theoretical peak local and average deuteron/palladium loading ratios for four types of experimental arrangements. Four curves are shown. The lowest curve is for ordinary cold fusion electrolysis with LiOD as the solution. The upper three curves are for systems where palladium cations are also codeposited with the deuterons onto the palladium. The theoretical peak loading ratios are shown as a function of time. The top curve is pure codeposition and does not include redistribution within the palladium cathode. The two curves below it represent slow and faster internal redistribution. The model assumes solution and cathode volumes of 100 and 0.5 cm^3, an electric current of 200 mA, and faradic efficiencies of 0.35 and 0.61 for palladium and deuterium, respectively.

INTERPRETATION

The result of the calculations is shown in Fig. 2. Four curves are shown. The lowest curve is for ordinary cold fusion with LiOD. The upper three curves are for palladium cations codeposited with the deuterons onto the palladium. The theoretical peak loading ratio is shown as a function of time. Assuming that the reaction occurs when the loading factor approaches one, the values in Fig. 1 have been compared with independent tests of Pd,D codeposition on the cold fusion phenomena,[1] which confirm that the decrease of the time of onset of successful cold fusion reactions may be <1 h (Ref. 13). The impact of the internal diffusion in the electrode is to bring the calculations in fair approximation with what is observed. From a materials point of view, the observed turn-on time constant for the desired reactions with codeposition in such reactions[2,7,13] appears to be consistent with the rapid internal diffusion rate for deuterons within the palladium, probably related to the anharmonic[8] and other[9] unique characteristics of the loaded material.

SUMMARY

In summary, the theoretical nonequilibrium deuteron/palladium ratio at the surface of a palladium electrode, previously shown to depend on the loading flux ratio, is now corrected both for intrapalladial diffusion of the loaded deuterons and for the secondary changes in electrode volume. Comparison with experimental data suggests yet another application and further confirmation[14] of the Q1D model of isotopic fuel loading into a material.

NOMENCLATURE*

A	= area (cm^2)
$A_{0,D}$	= initial coefficient of spatial distribution, deuterium ion (mol/cm^3)
$A_{0,Pd}$	= initial coefficient of spatial distribution, palladium (mol/cm^3)
B_D	= diffusivity of deuterium ions (cm^2/s)
B_{Pd}	= diffusivity of palladium (cm^2/s)
$[D]_{init}$	= initial deuteron ion concentration (mol/cm^3)
$[D(z,t)]$	= deuteron ion concentration (mol/cm^3)
E	= electric field intensity (V)
E_a	= activation energy (J)
F	= faraday (96 484.56 C/mol)
I	= electrical current (A)
J_c	= deuteron flux entering cathode (mol/cm^2·s)
J_f	= deuteron flux entering cathode to fusion reactions (mol/cm^2·s)
J_g	= deuteron flux evolving to gas (mol/cm^2·s)
J_{Pd}	= palladium flux onto cathode (mol/cm^2·s)
K_{Pd}	= first-order palladium flux rate onto cathode (cm/s)
$\sum K_i$	= first-order deuteron flux rate to all fusion, gas, and loading reactions (cm/s)
k_B	= Boltzmann constant (J/K)
L_c	= length of cell (cm)
$[Pd]_{init}$	= initial palladium concentration (mol/cm^3)
$[Pd(z,t)]$	= palladium concentration (mol/cm^3)
q	= electric charge (C)
T	= temperature (K)
Δt	= time increment (s)
Greek	
$\lambda_{D,Pd}$	= loading ratio (nondimensional)
μ_D	= electrophoretic mobility deuterium ion (cm^2/V·s)
μ_{Pd}	= electrophoretic mobility palladium (cm^2/V·s)
Φ	= potential = −V (voltage)

*In this paper, deuterium D represents atomic heavy hydrogen and is to be distinguished from both diatomic heavy hydrogen D_2 and the deuteron d. At the electrode, intermolecular deuteron transfer occurs from the aqueous phase to the metallic electrode. This may occur in combination with an asymmetric infrared vibration. In this paper, for simplicity, the deuterons contained in the aqueous phase are represented by the symbol D. This is consistent both with what is done conventionally with protons (i.e., pH), because deuterium is contained as paired deuterons covalently bound to oxygen as heavy water, and at the electrodes, where after a two-phase process (involving adsorption of deuterons), diatomic deuterium gas D_2 forms.

Also for these approximations, tritium and mixed species[12] are ignored at the cathode. As a final simplicity, in the equations, symbols for vectorial components and electric charge are not explicitly shown, although these are used to derive both the equations and their mathematical solutions. Hence, the deuterium ion should have a superscript +, to formally distinguish it from monoatomic un-ionized deuterium.

ACKNOWLEDGMENT

The author thanks G. Verner for her very helpful comments and suggestions in the development of this manuscript.

REFERENCES

1. M. FLEISCHMANN and S. PONS, "Electrochemically Induced Nuclear Fusion of Deuterium," *J. Electroanal. Chem.*, 261, 301 (1989); see also M. FLEISCHMANN, S. PONS,

M. W. ANDERSON, L. J. LI, and M. HAWKINS, "Calorimetry of the Palladium-Deuterium-Heavy Water System," *J. Electroanal. Chem.*, **287**, 293 (1990); see also M. FLEISCHMANN and S. PONS, "Calorimetry of the Pd-D_2O System: From Simplicity Via Complications to Simplicity," *Phys. Lett. A*, **176**, 118 (1993).

2. M. R. SWARTZ, "Quasi-One-Dimensional Model of Electrochemical Loading of Isotopic Fuel into a Metal," *Fusion Technol.*, **22**, 296 (1992).

3. M. R. SWARTZ, "Catastrophic Active Medium Hypothesis of Cold Fusion," *Proc. 4th Int. Conf. Cold Fusion*, Maui, Hawaii, December 1994, Vol. 4, Electric Power Research Institute and the U.S. Office of Naval Research (1994).

4. M. R. SWARTZ, "Isotopic Fuel Loading Coupled to Reactions at an Electrode," *Fusion Technol.*, **26**, *4T*, Part 2, 74 (1994).

5. M. R. SWARTZ, "Generalized Isotopic Fuel Loading Equations," *Cold Fusion Source Book, Int. Symp. Cold Fusion and Advanced Energy Systems*, Minsk, Belarus, May 1994, H. FOX, Ed. (1994).

6. M. R. SWARTZ, "Charge Transfer to Methemoglobin and Oxygen Using Methylene Blue, Light, and Electricity," Massachusetts Institute of Technology, Cambridge, Massachusetts (1984).

7. M. R. SWARTZ, "Systems to Increase the Efficiency, Control, Safety, and Energy Utilization of Electrochemically Induced Fusion Reactions," S.N. 07/339,976 (Apr. 1989).

8. K. H. JOHNSON, "Jahn-Teller Symmetry Breaking and Hydrogen Energy in γ-PdD—Storage of the Latent Heat of Water," *Cold Fusion Source Book*, p. 75 (1994).

9. M. R. SWARTZ, "Catastrophic Redistribution of Isotopic Fuel in the Solid State," *Fusion Technol.* (submitted for publication).

10. R. A. ORIANI, "The Physical and Metallurgical Aspects of Hydrogen in Metals," *Fusion Technol.*, **26**, *4T*, Part 2, 235 (1994).

11. C. HODGEMAN et al., *Handbook of Chemistry and Physics*, Chemical Rubber Company, Cleveland, Ohio (1973).

12. M. SWARTZ, "Possible Deuterium Production from Light Water Excess Enthalpy Experiments Using Nickel Cathodes," *J. New Energy*, **3**, 68 (1996).

13. S. SZPAK, P. A. MOSIER BOSS, and J. J. SMITH, "On the Behavior of Pd Deposited in the Presence of Evolving Deuterium," *J. Electroanal. Chem.* **302**, 225 (1991); reviewed by S. FAILE and J. JONES, *Fusion Facts*, H. FOX, Ed., Fusion Information Center, Salt Lake City, Utah (May 1991); see also S. SZPAK, C. J. GABRIEL, J. J. SMITH, and R. J. NOWAK, "Electrochemical Charging of Pd Rods," *J. Electroanal. Chem.*, **309**, 273 (1991).

14. M. R. SWARTZ, "Consistency of the Biphasic Nature of Excess Enthalpy in Solid State Anomalous Phenomena with the Quasi-One-Dimensional Model of Isotope Loading into a Material," *Fusion Technol.*, **31**, 63 (Jan. 1997).

Mitchell R. Swartz (BS, 1971; MS, EE, and ScD, 1984, electrical engineering, Massachusetts Institute of Technology; MD, Harvard University, 1978) is a research scientist at JET Energy Technology, Inc., where he is responsible for the development of improved materials for isotopic fuel loading. He is also a research engineer at the Massachusetts Institute of Technology, where he contributes to the investigation of the impact of ionizing radiation on materials and continues his own investigations of phonon/material interactions and other changes during loading. His clinical specialties are the interaction of radiation and materials for the treatment of cancer and viral infections and the use of nuclear medicine in the better delineation of solid neoplastic tumors.

PHUSONS IN NUCLEAR REACTIONS IN SOLIDS

NUCLEAR REACTIONS IN SOLIDS

KEYWORDS: *isospin restrictions, phonon coupling, Bose condensate*

MITCHELL R. SWARTZ *JET Energy Technology*
16 Pembroke Road, Weston, Massachusetts 02193

Received August 21, 1995
Accepted for Publication May 7, 1996

An explanation is given for the anomalous branching ratio in solids based on Boson-cooperative removal of the $^4He^*$ energy prior to decay by two-body fission. Facilitated by isospin restrictions that limit conventional pathways, the excess heat is driven by the reconfiguration to the more tightly bound ^4He ground state. A temperature rise occurs as well-mixed acoustical and optical phonons are unable to carry off all the local momentum and excess energy of the reactions. Four-vector analysis indicates conservation of energy, which suggests the use of a fusion quantum of energy delivered to the lattice's phonon cloud: a phuson. Special relativistic considerations indicate that the phonon cloud subtends ~450 to 800 unit cells and can couple with de-excitation times >0.1 fs. Thus, commensurate levels of neutrons and gammas are not required because of unique isospin and energy restrictions that facilitate the alternate Bose-cooperative pathway leading from the excited state.

INTRODUCTION

Conventional deuteron-deuteron (*d-d*) fusion remains elusive because electrostatic repulsion[1-3] makes close approach unlikely until the requisite few Fermi separation, which exists only for kinetic energies ≥0.1 MeV or temperatures 50 to 100 million K. Nonetheless, laboratories in over 15 countries[4,5] have reported replication of nonplasma ("cold") fusion[6] using heavy water alkaline solutions with a platinum anode and palladium cathode. Such D-Pd systems produce excess heat and nuclear products only when the cathode is loaded[7,8] to an atomic ratio greater than ~0.85 (Fig. 1). Under such conditions, excess power ratios of 300 to 1000%, peak energy densities of 1 to 15 MJ/cm^3 palladium, and peak power densities of 100 to 2000 W/cm^3 palladium have been reported. The excess enthalpy exceeds any chemical explanation.

The chief products of cold fusion in addition to excess heat[6,7] are helium[9,10] (^{4}He) and very low level tritium.[11-14] Helium-4 has been shown to be linked to the production of excess heat by palladium and heavy water (12 σ above background) when metal flasks were used to prevent diffusion in from the ambient.[10] Such careful experiments yield $2.0^{=0.5} \times 10^{11}$ ^{4}He/W·s, which is ~30% of the ash expected for a nuclear process. Tritium production is infrequent, but when it is present, it is ~100 000 times greater than neutron production. The neutrons are produced at peak levels ~2 to 3 times

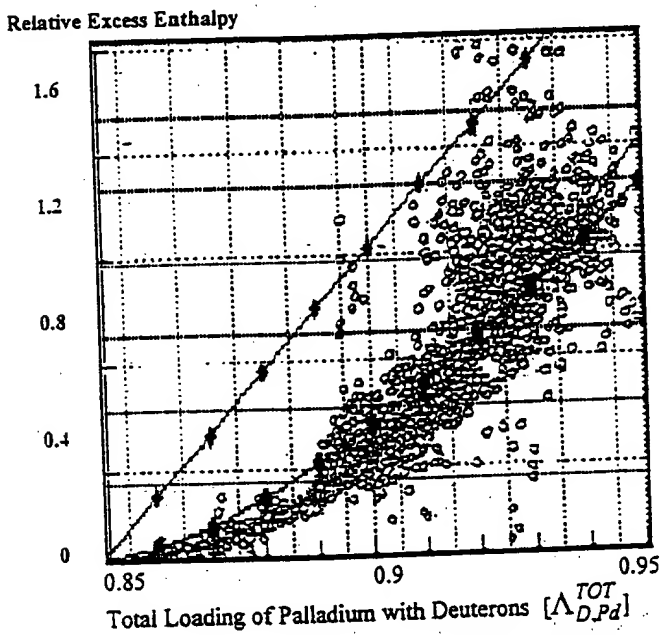

Fig. 1. Form factor of matrix element of fusion matched to excess power-loading curve (Pd-D). The scatter points (open data symbols) are the relative output from a palladium/heavy water electrolysis system.[8] An inflection in the output as a function of loading begins at loadings equal to 0.85 D/Pd. The three calculated probability curves are superimposed (linear, 1.5 power, and quadratic) as a function of total loading.

background.[15,16] Autoradiography[13,17] has documented low-level ionizing radiation in the photoelectric range emanating from some active electrodes, consistent with either a nuclear source of ^{4}He or secondary X-ray excitation of surrounding atoms.

Given such extensive data,[4–17] it appears that either the Coulomb barrier is soft in the fully loaded solid state or there is an alternate pathway or frame of reference that does not involve the simple collision of two particles. The latter has been a natural reflex since nuclear fusion was first achieved by irradiation of a deuterium target by high-energy deuterons derived from a cyclotron 60 yr ago. The Coulomb barrier approach has been examined by many hypotheses, including tunneling facilitated by screening electrons,[18–20] by changes in the effective mass of both the electrons[21,22] and the deuterons,[23] deuteron energy fluctuations,[24,25] and hypothesized coherent screening.[26] Other lattice factors able to increase the likelihood of possible fusion include the deuteron band structure.[27] Bloch-symmetric Bose-Bloch condensates,[28,29] plasmon exchange,[30] additional electron screening,[31] the increased effective mass of the deuterons due to polarons,[32] anharmonic and nonlinear effects,[33] catastrophic phenomena,[34,35] and tight orbits (with orbital energies of ~50 kV) produced by spin-spin and spin-orbit couplings between antiparallel proton-electron magnetic moments.[36] However, as Tajima et al.[19] and others[23] have shown, screening factors alone may not be sufficient to explain the observations.

We suggest a second pathway of fusion involving not a unidimensional collision of two particles but rather the stereoconstellation of the fully loaded metal acting in a cooperative fashion and consistent with the findings. The final product occurs via a simultaneous Bose-Einstein cooperative reaction of a cluster of phonons (the phuson) with de-excitation of the excited helium (^{4}He*). If loaded sufficiently, the material may under appropriate conditions produce effects on the nuclei contained therein. This material effect cannot be along conventional thinking because the tunneling probability increases markedly only when the *d-d* internuclear distance drops below ~0.7 Å (Ref. 19), but within the crystalline metal, at low loadings to moderate, the average internuclear deuteron separation distance in palladium is larger than diatomic D_2O (Ref. 37). Although good data for the highest loading states are pending, the phuson hypothesis offers an explanation for even closer *d-d* approach through coupled phonon interactions combined with Jahn-Teller displacements.

When examining cold fusion solid-state systems, most preliminary analyses may ignore two unique features of this system.[34,35] The first feature is the impact of the electrical charging of the cathode to a high loading and negative voltage, which is an ~100 molar deuteron concentration and ~1000 molar electron population. These assist the deuterons in approaching each other and are added by the processes now discussed. The second feature, also ignored in simplifications, is the phonons and the intraelectrode deuteron flux, which are important because the latter is proportional to the tunneling matrix element,[19] which may offer a pathway for phonon-assisted tunneling,[38] and together they may further facilitate close approach. The intramaterial deuteron flux[34,35] can be aided by phonons,[39,40] increases with temperature,[41] differences in phases,[42] and grain-boundary formation.[43] It is propelled by sudden catastrophic desaturation with positive feedback arising from the saturation-temperature relationship of the metal and also from diffusive-focusing effects, observed for transition metals.[43] Other reactions available for activation energy include collisions,[34] polaron formation and drift, both optical and acoustic phonon generations, lattice deformation and fracture,[35] anharmonic motions driven by the Jahn-Teller displacement,[33] the latent heat of water,[33] diatomic deuterium formation[44] (7 to 9.4 eV/atom), and any potential fusion reactions. For either 0.048 or 7.0 eV (the energies associated with phonon and with deuteron recombination to diatomic deuterium), a lattice width of ~200 to 1000 lattice sites could provide adequate energy (by volume) required to penetrate the Coulomb barrier to form ^{4}He. Also, catastrophic redistribution, which accounts in part for some of the local astronomic fugacities,[6,43] may produce unusually close *d-d* separations in an active medium capable of rapid desorption of deuterons with the recruitment potential of even more deuterons.[35] Let us assume it is possible that the material offers an opportunity for fusion. How can the anomalous branching ratio be explained?

ANOMALOUS BRANCHING RATIO

The anomalous branching ratio is perhaps more problematic than the anomalous heat. Since 1989, this great discrepancy between the neutron and tritium production rates (Table I) in cold fusion compared with those in conventional plasma fusion systems has been a key to the "knee-jerk" dismissal of this scientific field. The energy release Q_T by the fusion of two deuterons flows by several pathways including emission of a 24-MeV gamma ray. In plasma systems, the fusion of two deuterons yields mainly neutrons and tritium by two reactions that have similar probabilities[4]; this ratio is the branching ratio. Helium-4 generation requires coupled reactions[45] and is rarely a product in plasma fusion (~1 per 10 million fusion events). All of the plasma pathways have the emission of a high-energy ionizing photon in common. In contrast, neither gamma nor neutron emission characterizes the cold fusion phenomena. Instead, ^{4}He is generated, coupled to the production of significant excess heat, in amounts ~30% of that expected. The following discussion focuses on the de-excitation side and suggests an explanation for this lack of plasma-type reaction products. This explanation is based on a novel method from

TABLE I

Select Energy Levels and Pathways of ^{4}He*

Configuration		Energy (MeV)	Branching Ratio	
			Cold Fusion	Hot Fusion
	$2n^0 + 2p$	28.30		
	$d + n^0 + p$	26.07		
Deuterons	$d + d$	23.82		
^{3}He, neutron	$^3\text{He} + n^0$	20.58	? (negligible)	0.5
^{4}He first excited state	^{4}He	20.20		
Triton, proton	$t + p$	19.82	1/10 000 000	0.5
^{4}He ground state	^{4}He	0	0.3	1/1 000 000

removal of the excited state alpha (^{4}He*) energy before it decays by two-body fission.

Figure 2 is the relevant energy diagram that shows the lower two excited states in helium's singlet isospin manifold.[46] Table I lists the lower helium nuclear states, their energy (in mega-electron-volts), and quantum numbers for total angular momentum, parity, and isospin. Several excited states with mega-electron-volt separations are located 20 MeV above the ground state of ^{4}He (defined as zero energy). These excited states couple with two deuterons and can provide other decay configurations (Tables I and II). The critical first excited nuclear state (^{4}He*) is energetically located below the *d-d* ground state, and the quantum electrodynamic selection rules[26,29,45–47] limit how ^{4}He* can decay. This is the key point because it limits de-excitation and creates a relatively long-lived ^{4}He* state. Electric dipole moment transitions are technically forbidden. Therefore, any conventional decomposition through ^{4}He* is neither possible nor observed at low temperatures. In contrast, in hot fusion systems, sufficient energy is provided to both perturb and mix the nuclear states past the restriction and thereby create either tritium + proton or (by rising to a higher level [see Table I]) ^{3}He + neutron. Instead, there can occur a phonon-coupled de-excitation[16,19] (with phuson energy transfer) that is not forbidden because it does not involve an electric dipole moment[26,29,45,47] but does conserve isospin, momentum, and energy. The excess heat is transferred to the phonon cloud through the periodic lattice by the reconfiguration of the ^{4}He* to its ground state with the collapse of the entire system through the strong force as the linear momentum is conserved. This phonon bath of the lattice conserves momentum and energy (*vide*

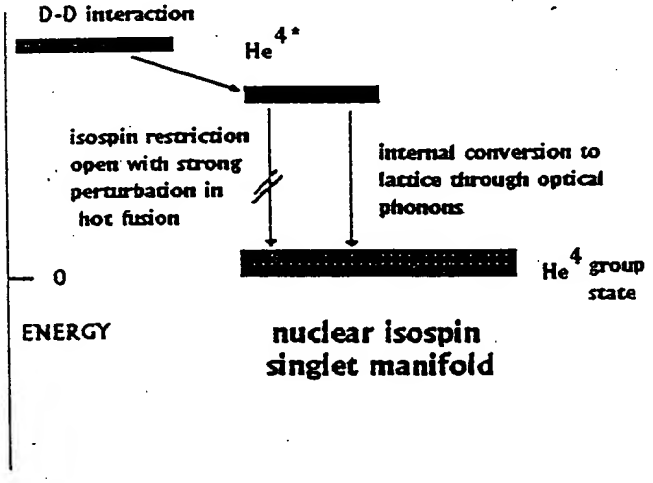

Fig. 2. Simplified energy diagram of two lowest helium nuclear states. This is a simplified energy level diagram showing the lowest excited nuclear state in the isospin singlet manifold and the helium ground state. The upper level (^{4}He*) receives energy and momentum from the *d-d* state (which may involve more than a classical two-body system). Helium-4* waits de-excitation. (See Tables I and II.)

TABLE II

Helium Nucleus Energy States

State	Energy (MeV)	Total Angular Momentum (J)	Parity (π)	Isospin (T)	Criteria $E < d$-d Isospin Conserved
	25.95	1	−	1	No
	25.28	0	−	1	No
	24.25	1	−	0	No
	23.64	1	−	1	No
	23.33	2	−	1	No
Third	21.84	2	−	0	[a]
Second	21.01	0	−	0	[a]
First	20.21	0	+	0	[a]
Ground	0	0	+	0	[a]

[a]States below $d + d$.

infra). The temperature rise occurs as the well-mixed acoustical and optical phonons become unable to carry off all the momentum and excess energy produced by the reactions.

But, is there evidence for such coupling? Yes, there could be with the Mossbauer effect–type of coupling. This means not that cold fusion proceeds through the Mossbauer effect but rather that the effect demonstrates that the lattice is coupled through S-orbitals to nuclei. The salient point is that the nuclear isospin restriction for ^{4}He* de-excitation enables the vicinal phonon ensemble to compete effectively and thus allow fusion reactions to proceed in the unique fully loaded metals. Such energy transfer to the phonon cloud (with phuson energy transfer) is consistent with the observed branching ratios. The analysis of the nuclear levels and their de-excitation pathways is consistent with the finding that helium accounts for about one-third of the ash. These pathways and their relative probabilities also explain the observed unique branching ratio, including why neutrons are not observed. Tritium, created from an energy state that is located below ^{4}He*, does remain an unlikely product but is of a very low likelihood because of the electric dipole. If such a nuclear-phonon cloud pathway were not available, then even with sufficient energy to overcome the softened Coulomb barrier, the tiny population of ^{4}He* would saturate and end all such reactions.

We have suggested that phonons can handle the conservation of energy and momentum and energy in the de-excitation of ^{4}He*. We now show that ^{4}He* has a nonforbidden de-excitation pathway for energy flow (E: $^4\text{He}^* \leftarrow \Psi^{\gamma}_{d\text{-}d}$) that couples to the interstitial-loaded crystalline lattice's optical phonons, which provides conservation of both isospin and energy, and is also consistent with causality as required by special relativity. This (E: $^4\text{He}^* \leftarrow \Psi^{\gamma}_{d\text{-}d}$) pathway explains why neutrons are not seen in the observed unique branching ratio. The ^{4}He* level is energetically below the d-d ground state at this system temperature. Any decomposition through a level above the ^{4}He* energy level is therefore not possible, and not observed. Tritium, created from an energy state that is located below, remains an unlikely possibility because of the electric dipole and isospin restrictions.

GAMMA-STATE NUCLEAR-LATTICE COUPLINGS

Any analysis of the boundary conditions on the material side must begin with the unique group VIII transition elements densely loaded with minute interstitials. Unlike most metals[48] characterized by low solubility (~one deuteron/10 000 metal atoms), the deuteron solubility in palladium is quite large. Full loading (Λ_d^{TOT}) is the *sine qua non* to the desired reactions, and only when the loading is nearly complete do the phenomena begin (Fig. 1). This may be a requirement for decorating the gamma sites.[33,35] Thus, it is prudent that the total loading must be distinguished from gamma-site loading because the latter does not even occur until the loading approaches 0.85. Gamma loading, the critical parameter, may be approximately derived through the Heaviside function:

$$\Lambda^{\gamma}_{D,Pd} \approx \left(\frac{\Lambda^{TOT}_{D,Pd} - 0.85}{0.15} \right) \times u_{-1}(\Lambda^{TOT}_{D,Pd} - 0.85) \quad . \quad (1)$$

In palladium, two phonon bands result from the small mass of the deuteron in the transition metal.[49] The acoustic phonons are from the palladium, and the optical phonons arise from the low molecular weight hydrogen nuclei.[34,35,50] Optical phonons[39] in the loaded PdD lattice have energies ~32 to 48 mV with significant zero-point motions.[51,52] Reactions can couple to these phonons by shifts in the phonon frequency:

$$\Delta E = nh\delta\omega \quad . \quad (2)$$

The phonon spectra have been hypothesized to permit a nonionizing radiation pathway to satisfy the energy and momentum conservation requirements. This is reasonable because experimental results indicate that most of the products are nonionizing phonons, and therefore they must be included in any analysis.

We assume that the electrode has adequate gamma-site[33,35,53–55] decoration. The lattice wavefunction involves the interstitial deuterons and electron wavefunctions.[49] Given the separate sites,[35] we modify the Hagelstein wavefunction by the separation of the deuteron wavefunction (in each state therein) from the acoustic (palladium) lattice. The (L) refers to the lattice, and the (d-d) refers to the loaded deuterons, and this is only shorthand because the reaction may involve many more than two deuterons:

$$\Psi^f = \psi_{(L)}\phi_K(r) = \Psi^{Pd}_{(L)}\Psi^{\alpha}_{(d\text{-}d)}\Psi^{\beta}_{(d\text{-}d)}\Psi^{\gamma}_{(d\text{-}d)}\phi_K(r) \quad . \quad (3)$$

Consistent with the data, the relevant optical phonon cloud arises in $\Psi^{\gamma}_{d\text{-}d}$. This phonon cloud is unique because its strong entropic and anharmonic components, already showing anomalies from the inverse isotope effect, may enable de-excitation of ^{4}He*. Such internal conversion would account for the observed branching ratios as discussed earlier by avoiding de-excitations associated with electric dipole transitions. If such a nuclear-phonon cloud pathway were not available, then the tiny population of ^{4}He* would saturate that level and end such reactions. In hot fusion systems, sufficient energy is provided to perturb and mix the states past the restriction and thereby create either tritium + proton or [by rising to a higher level (see Tables I and II)] ^{3}He + neutron.

Each watt of excess heat requires ~10^{12} to 10^{13} fusion event/s out of a total sample population of perhaps ~10^{20} to 10^{22} candidate nuclei. Therefore, a very small fraction of the interstitial population is involved at any time. Weak couplings that link the lattice to the nuclei

through S-orbital coupling exist, as demonstrated in other systems by Mossbauer spectroscopy.

SPECIAL RELATIVITY

Causality arguments consistent with special relativity must be considered. First, it is important to consider the lifetime of the excited state. From the uncertainty principle, we can derive the expectation of that state based on the energy width of the energy emitted. It is not infrequent in this field to confuse E with ΔE, but this should not occur because to do so yields an incorrectly very short derived half-life:

$$\Delta E \times \Delta \tau \cong \frac{h}{2\pi} \quad . \tag{4}$$

But, can the half-life be in the range required? We can compare lifetimes to other nuclei that are better known and will do so for alpha decays and Mossbauer-associated nuclei. Corroboration of the de-excitation time can be estimated from the width of the output in the frequency domain, where Γ is the natural line width using the uncertainty principle. Consider alpha decay in the range observed for some of the cold fusion data. Such alpha decay involves the emission of monoenergetic electrons (e.g., ^{238}Pu), and those 4- to 6-MeV alpha particles have half-lives of ~86 yr. The nuclei with Mossbauer nuclear resonance states (Table III) are also consistent with half-lives being of adequate length to transfer the energy from the ^{4}He* state. The timescales of de-excitation may be on the order of nanoseconds.[30] Table III contains additional examples. These half-lives range from about a few nanoseconds (^{40}K) to almost 100 nanoseconds (^{57}Fe). So there is reason to believe that an adequate half-life of the excited state is available.

Second, we proceed to calculate the special relativistic and four-vector limitations imposed on the energy and momentum transfer from the first excited nuclear state of helium (^{4}He*). It is important to note that the sum of the phonon energies (in two disparate spectra: acoustic and optical) in the phonon ensemble [the precursor to a possible Bose-Einstein cooperative reaction (?condensation)] postulated here is equal to the energy between ^{4}He* and its ground state. Thus, it is postulated that there is a quantum of energy (phuson) that satisfies energy and momentum considerations. Calculations below indicate that the phuson involves a phonon cloud subtending ~450 to 800 unit cells. Any putative fusion release energy on the mega-electron-volt scale at a single location has a possibility for spreading the released energy among the lattice sites coupled by the cone angle subtended by a (virtual) photon during the de-excitation time of ^{4}He*. Photon propagation speeds cover substantial numbers of lattice sites during this cone-angle analysis. The size of the maximal recruitment from the surrounding lattice depends on the interaction radius r_{DE} determined by the speed of light c:

$$r_{DE} = (c \times \tau_{DE}) \quad . \tag{5}$$

Therefore, the number of lattice cells (UC) involved in a single event, coupled through the Bose-Einstein phuson complex, is

$$N_{sites}(r_{DE}) = \frac{(c \times \tau_{DE})^3}{(V_{unitcell})} \quad . \tag{6}$$

Special relativistic considerations[16] indicate that the phonon cloud subtends ~450 to 800 unit cells. Quantum mechanical considerations using gamma-phase analysis and a wavevector approach have concluded that there are a sufficient number of phonons available to account for a coherent energy transfer to the lattice during the de-excitation of ^{4}He* provided that the de-excitation time is >0.5 fs. We now calculate the magnitude of the putative phuson that couples to the phonon cloud. Third is the energy transfer time on the order of a phonon cycle time. Yes, if one considers that in these cases of low-atomic-weight nuclei in group VIII metals that there are acoustic phonon spectra as well, then there is adequate time for coupling.

TABLE III

Mossbauer Nuclear Resonance States

Isotope	Transition Energy, $E_2 - E_1$ (keV)	Half-Life, $T_{1/2}$ (ns)	Natural Line Width, 2Γ (mm/s)
^{40}K	29.4	4.26	2.18
^{57}Fe	14.41	97.81	0.19
^{57}Fe	136.46	8.7	0.23
^{61}Ni	67.4	5.06	0.8

GAMMA-STATE MATRIX ELEMENT INCLUDING PHONON TERMS

If one considers the available lattice sites, the ensemble does have a sufficient number of phonons available to account for energy transfer to the lattice during the de-excitation of ^{4}He* (Fig. 2) provided that the de-excitation time is >0.5 fs:

$$E_{ensemble} = N_{sites}(r_{DE}) \times \frac{phonons}{UC} \times \frac{energy}{phonon}$$

$$= \frac{(c \times \tau_{DE})^3}{(V_{unitcell})} \times (\Lambda_{D,Pd}^{TOT} \times 8) \times 40 \text{ meV} \quad . \tag{7}$$

The matrix element **M** must include Coulomb exchange, acoustic and optical recoil in all modes, and the energy from D_2 formation and H_2O latent heat, which are ignored in this simplification:

$$\mathbf{M} = \langle \Psi^f | \hat{V} | \Psi^i \rangle \quad . \tag{8}$$

With consideration of Fermi's golden rule and the phonons, the tunneling probability is

$$\Gamma = \frac{2\pi}{h} \times \sum_f \sum_k |\langle \Psi^f_{^4\mathrm{He}.(L)'} | \hat{V} | \Psi^i_{d\text{-}d.(L)'} \rangle|^2 \times \delta\left[I_k + \frac{h^2|k|^2}{8\pi \times m_e} + E^f_{(L)} - E^i_{(L)} \right] , \tag{9}$$

where $\hat{V}$ is the phonon operator acting through the Coulomb potential between the nuclei and the K-shell electron, acting over each f'th location, which may in fact be the gamma sites alone:

$$\hat{V} = \sum_j \sum_{j'} \frac{Z \times e^2}{|r_{j'} - \hat{R}_j|} \quad . \tag{10}$$

Switching from center-of-mass (c.m.) coordinates during the Coulomb exchange to reciprocal space[49] enables the use of the Duschinsky operator $e^{-i\hat{S}_o}$, and the matrix element becomes

$$\mathbf{M} = \langle \Psi^f(q_i) | e^{ik \cdot R_j} e^{-i\hat{S}_o} | \Psi^i(q_i) \rangle \quad . \tag{11}$$

Not all modes need to be involved in the energy transfer. Hagelstein[49] has demonstrated that well-defined modes with nontrivial probabilities $[p_{j,k}(\epsilon)]$ may account for transferring energy to the lattice. For each potential (j'th) site, this becomes

$$\Gamma_j = \sum_k \int p_{j,k}(\epsilon) \times \Gamma_{j,k}(\epsilon)\, d\epsilon \tag{12a}$$

and

$$p_{j,k}(\epsilon) = \frac{2\pi}{h} |\hat{V}(k)|^2 \times \delta\left(I_k + \frac{h^2|k|^2}{2\pi \times m_e} + \epsilon \right) \quad . \tag{12b}$$

Equations (12) require summation over all moments, but given the observations (Fig. 1) and Hagelstein's simplified probability density coupling rate,[45,49] we qualitatively examined the case where the optical phonon density is proportional to the phonons arising from the gamma sites. We approximate that the optical phonon density is proportional to the gamma-site loading:

$$\Theta_N \sim f_\Theta \times [D_{\gamma-phase}]_{Pd} = f_\Theta \times [Pd] \times \left[\frac{(\Lambda^{TOT}_{D.Pd} - 0.85)}{0.15} \right] . \tag{13}$$

The fusion probability is proportional to the square of the wavefunction, also proportional to $\Lambda^{\gamma}_{D.Pd}$,

$$[\Psi^{\gamma}_{(d\text{-}d)}]^2 \propto \left[\frac{(\Lambda^{TOT}_{D.Pd} - 0.85)}{0.15} \right]^2 . \tag{14}$$

Thus, the matrix element has two terms reflecting the gamma-state loading. The fusion probability should be proportional to the square of the gamma-state loading:

$$\Gamma \propto \Theta_N \times [Pd] \times \left[\frac{(\Lambda^{TOT}_{D.Pd} - 0.85)}{0.15} \right] \cong f_\Theta \times \left\langle [Pd] \times \left[\frac{(\Lambda^{TOT}_{D.Pd} - 0.85)}{0.15} \right] \right\rangle^2 \equiv f_\Theta \times \langle [Pd] \times (\Lambda^{\gamma}_{D.Pd}) \rangle^2 \quad . \tag{15}$$

This calculated expression is shown in Fig. 1 superimposed over the measured data. It has fairly good agreement with the curvature of the data comprising the observed data for palladium and heavy water.

In summary, nuclear isospin restriction for ^{4}He* de-excitation enables the vicinal phonon ensemble to compete effectively and thus allow the fusion reactions to proceed. Sufficient ^{4}He* can undergo de-excitation with the energy drained off by the ensemble of phonons. The excess heat is transferred to the phonon cloud on a coherent basis by the reconfiguration of the ^{4}He* to its ground state. The final outcome is ground-state ^{4}He with the collapse of the entire system through the strong force as the linear momentum is conserved by internal conversion. Well-mixed phonon pools herald the collapse as excess enthalpy. The temperature rise occurs as the acoustical and optical phonons become unable to carry off all the momentum and excess energy of the reactions. The need for commensurate levels of neutrons and gamma radiation apparently does not stand for this unique case because of isospin restrictions, the availability for transfer to the phonon cloud, and the absence of the strong perturbations of hot fusion.

COOPERATIVE BOSE-EINSTEIN ENERGY AND MOMENTUM TRANSFER

We have analyzed the ^{4}He* nonelectric dipole de-excitation pathway and are proposing a novel idea of bose condensation involving the phonons. Swartz suggested phonon amplification using the cold fusion process, and Schwinger first publicly suggested phonons in the cold fusion process itself. Here the role of phonons is further developed to include coupling to the lattice and a proposed process involving cooperativity. The phuson hypothesis ends in a Bose-Einstein cooperative dispersion of energy by the phonons distributing what was the energy

located in the helium-excited state. In fact, this is reasonable not only because of the lifetime, and energy, considerations (*vide supra*), but it is consistent with hot fusion systems, where for deuterium and tritium fusion ($Q_T \sim$ 17.6 MeV), the kinetic energy of the ^{4}He* and the neutrons (for that case) are transferred through the gas to the surrounding materials if the density of the gas is approximately $>10^{-5}$ atm, permitting continued fusion reactions to proceed (nuclear ignition).

In solid-state fusion systems, the density is more favorable for any such transfer. Following the loading itself,[53-55] solid-state fusion may represent a two-stage process that couples ^{4}He* to the interstitial-loaded crystalline lattice's optical phonons. The net effect is a cooperative energy transfer to the phonon cloud via the crystalline lattice's unique phonon entropic and anharmonic properties (heralded by the inverse isotope effect). The incremental energy and momentum change that flows to the phonon cloud, when coupled to the nucleus, is called a phuson:

$$\Psi^{\gamma}_{(d\text{-}d\text{-}d\text{-}d\text{-}d\text{-}d)} \rightarrow \Psi^{\gamma}_{(\text{He}\text{-}d\text{-}d\text{-}d\text{-}d)} + {}^4\text{He}^* + \Sigma\Theta$$
$$\rightarrow \Psi^{\gamma}_{(\text{He}\text{-}d\text{-}d\text{-}d\text{-}d)} + {}^4\text{He} + (\Sigma\Theta)^* \quad , \quad (16)$$

where $\Psi^{\gamma}_{(d\text{-}d\text{-}d\text{-}d\text{-}d\text{-}d)}$ represents the loaded palladium wavefunction and includes the gamma notation to explicitly denote the requirement to fill the gamma states (loadings greater than ~0.85). The "*d-d-d-d-d-d*" subscript reminds us that this is a process in a three-dimensional solid involving much more than two deuterons. The "He-*d-d-d-d*" subscript follows the generations of the desired reactions. The terms $\Sigma\Theta$ and $\Sigma\Theta^*$ represent the phonon cloud and its excited state activated by the phuson.

FOUR-VECTOR ANALYTIC REDUCTION

The four vectors relate the momenta (p_i; $i = x,y,z$) and energy (E), and have been used in this field to examine the putative role of *ab initio* negative pion mesons.[56] The following four-vector analysis begins in the c.m. frame of reference between the deuterons:

$$P(i) = \left[p_x, p_y, p_z, \left(\frac{E}{c}\right)\right]$$
$$= \left\{0,0,0,\left[\frac{\sum_k (h\Theta_k)}{c} + \frac{2m_d \times c^2}{c}\right]\right\} . \quad (17)$$

We follow the phonon cloud and generated helium in the c.m. frame of reference.

The final four vectors become

$$P(f) = \left\{0,0,0,\left[\frac{\sum_k (h\Theta^*_k)}{c} + \frac{(m_{^4\text{He}} \times c^2)}{c}\right]\right\} . \quad (18)$$

The scalar-dot products and binomial expansion are used. The only real (logical) solution reduces to the conservation of energy equation involving mass-energy equivalence:

$$\sum_k (h\Theta^*_k) - \sum_k (h\Theta_k) \equiv h \times \sum_k (\Delta\Theta^*_k)$$
$$= C^2 \times (2m_d - m_{^4\text{He}}) . \quad (19)$$

SUMMARY

Given a source of ^{4}He*, that state can undergo de-excitation with the energy drained off by the ensemble of phonons, as they themselves undergo a Bose-Einstein cooperative reaction, possibly a condensation. The excess heat is driven by a reconfiguration of the helium nucleus from the less tightly bound ^{4}He* configuration to the more tightly bound ground state, with a temperature rise occurring as the well-mixed acoustical and optical phonons are unable to carry off all the local momentum and excess energy of the reactions. The magnitude of the energy transfer is consistent both with general relativity and, through the size of the lattice over which such transfer reacts, special relativity. A four-vector analysis indicates this is consistent with conservation of energy, which suggests the use of a fusion quantum of energy delivered to the lattice's phonon cloud: a phuson. Special relativistic considerations indicate that the phonon cloud subtends ~450 to 800 unit cells and that the de-excitation times ought be >0.1 fs. The need for commensurate levels of neutrons and gammas apparently does not stand for this unique case because isospin and energy restrictions facilitate alternate pathways involving the phonons, both intrinsic and generated, to handle the de-excitation of the excited state.

ACKNOWLEDGMENTS

The author thanks I. Straus, P. Hagelstein, M. Zahn, S. Baer, G. Verner, D. Blue, and B. Ahern for their helpful comments and suggestions on the development of this model and the staff of JET Energy Technology for their support.

REFERENCES

1. M. RABINOWITZ, Y. E. KIM, V. A. CHECHIN, and V. A. TSAREV, "Opposition and Support for Cold Fusion," *Trans. Fusion Technol.*, **26**, *4T*, Part 2, 3 (1994).

2. H. HORA et al., "Screening in Cold Fusion Derived from D-D Reactions," *Phys. Lett. A*, 175, 138 (1993).

3. G. H. MILEY, *Fusion Energy Conversion*, American Nuclear Society, La Grange Park, Illinois (1976).

4. H. FOX and M. SWARTZ, "Progress in Cold Nuclear Fusion—Metanalysis Using an Augmented Database," presented at 5th Int. Conf. Cold Fusion, Monaco, April 9–13, 1995.

5. M. SWARTZ, "Metanalysis of the Cold Fusion Literature," *Fusion Technol.* (submitted for publication).

6. M. FLEISCHMANN and S. PONS, "Electrochemically Induced Nuclear Fusion of Deuterium," *J. Electroanal. Chem.*, **261**, 301 (1989); see also M. FLEISCHMANN and S. PONS, Erratum, *J. Electroanal. Chem.*, **263**, 187 (1989); see also M. FLEISCHMANN, S. PONS, M. W. ANDERSON, L. J. LI, and M. HAWKINS, "Calorimetry of the Palladium-Deuterium-Heavy Water System," *J. Electroanal. Chem.*, **287**, 293 (1990).

7. M. FLEISCHMANN and S. PONS, "Calorimetry of the Pd-D_2O System: From Simplicity Via Complications to Simplicity," *Phys. Lett. A*, **176**, 118 (1993); see also M. FLEISCHMANN and S. PONS, "Some Comments on the Paper 'Analysis of Experiments on Calorimetry of LiOD/D_2O Electrochemical Cells,'" *J. Electroanal. Chem.*, **332**, 33 (1992).

8. M. McKUBRE, "The Complex New Science of Cold Fusion," *Fusion Facts*, Vol. 5, No. 4, p. 13 (Oct. 1993).

9. M. H. MILES, R. A. HOLLINS, B. F. BUSH, J. J. LAGOWSKI, and R. E. MILES, "Correlation of Excess Power and Helium Production During D_2O and H_2O Electrolysis Using Palladium Cathodes," *J. Electroanal. Chem.*, **346**, 99 (1993).

10. M. H. MILES and B. F. BUSH, "Heat and Helium Measurements in Deuterated Palladium," *Trans. Fusion Technol.*, **26**, *4T*, Part 2, 156 (1994).

11. F. G. WILL, K. CEDZYNSKA, and D. C. LINTON, "Tritium Generation in Palladium Cathodes with High Deuterium Loading," *Trans. Fusion Technol.*, **26**, *4T*, Part 2, 209; see also "Reproducible Tritium Generation in Electrochemical Cells Employing Palladium Cathodes with High Deuterium Loading," *J. Electroanal. Chem.*, **360**, 161 (1993).

12. M. SRINIVASAN et al., "Tritium and Excess Heat Generation During Electrolysis of Aqueous Solutions of Alkali Salts with Nickel Cathode," *Frontiers of Cold Fusion*, H. IKEGAMI, Ed., *Proc. 3rd Int. Conf. Cold Fusion*, Tokyo, Japan, October 21–25, 1992, Universal Academy Press, p. 123.

13. M. SRINIVASAN, *Curr. Sci.*, 143 (1991).

14. E. STORMS and C. TALCOTT, "Electrolytic Tritium Production," *Fusion Technol.*, **17**, 680 (1990).

15. D. GOZZI et al., *J. Fusion Energy*, **9**, 241 (1990).

16. H. MENLOVE et al., *J. Fusion Energy*, **9**, 495 (1990).

17. M. McKUBRE, "Horizon," Prod. D. Cadbury, British Broadcasting Corporation film (1994).

18. G. PREPARATA, "Some Theories of 'Cold' Nuclear Fusion: A Review," *Fusion Technol.*, **20**, 82 (1991).

19. T. TAJIMA, H. IYETOMI, and S. ICHIMARU, "Influence of Attractive Interaction Between Deuterons in Pd on Nuclear Fusion," *J. Fusion Energy*, **9**, 437 (1990).

20. R. H. PARMENTER et al., *Proc. National Academy Science*, Vol. 87, p. 8652, National Academy of Science (1989).

21. T. MATSUMOTO, "'Nattoh' Model for Cold Fusion," *Fusion Technol.*, **16**, 532 (1989).

22. C. WALLING and J. SIMONS, "Two Innocent Chemists Look at Cold Fusion," *J. Phys. Chem.*, 93, 4693 (1989).

23. M. RABINOWITZ and D. H. WORLEDGE, "An Analysis of Cold and Lukewarm Fusion," *Fusion Technol.*, **17**, 344 (1990).

24. Y. E. KIM, R. A. RICE, G. S. CHULICK, and M. RABINOWITZ, "Cluster-Impact Fusion with Cluster Beams," *Mod. Phys. Lett. A*, **6**, 2259 (1991).

25. R. A. RICE, G. S. CHULICK, and Y. E. KIM, "Effect of Velocity Distribution and Electron Screening on Cold Fusion," *Proc. 1st Annual Conf. Cold Fusion*, Salt Lake City, Utah, March 28–31, 1990, p. 185, National Cold Fusion Institute (1990).

26. J. SCHWINGER, "Cold Fusion: A Hypothesis," *Z. Naturforsch. A*, **45**, 756 (1990).

27. M. R. SWARTZ, U.S. Patent 07/339 976 (1989).

28. T. A. CHUBB and S. R. CHUBB, "Bloch-Symmetric Fusion in PdD_x," *Fusion Technol.*, **17**, 710 (1990).

29. T. A. CHUBB and S. R. CHUBB, "Ion Band States: What They Are, and How They Affect Cold Fusion," *Cold Fusion Source Book, International Symposium on Cold Fusion and Advanced Energy Systems*, 75-83, H. FOX, Ed., Minsk, Belarus (May 1994).

30. M. BALDO, R. PUCCI, and P. F. BORTIGNON, "Relaxation Toward Equilibrium in Plasmon-Enhanced Fusion," *Fusion Technol.*, **18**, 347 (1990).

31. H. EZAKI, M. MORINAGA, and S. WATANABE, "Hydrogen Overpotential for Transition Metals and Alloys and Its Interpretation Using an Electronic Model," *Electrochim. Acta*, **38**, 557 (1993).

32. R. W. BUSSARD, "Virtual-State Internal Nuclear Fusion in Metal Lattices," *Fusion Technol.*, **16**, 231 (1989).

33. K. H. JOHNSON, "Jahn-Teller Symmetry Breaking and Hydrogen Energy in γ-PdD 'COLD FUSION' as Storage of the Latent Heat of Water," *Cold Fusion Source Book, International Symposium on Cold Fusion and Advanced Energy Systems*, 84-89, H. FOX, Ed., Minsk, Belarus (1994).

34. M. SWARTZ, "Catastrophic Redistribution of Isotopic Fuel in the Solid State," *Fusion Technol.* (submitted for publication); see also M. SWARTZ, "Hydrogen Redistribution by Catastrophic Desorption in Select Transition Metals," *J. New Energy*, **1**, 4 (1997) (to be published).

35. M. R. SWARTZ, "Catastrophic Active Medium Hypothesis of Cold Fusion," *Proc. 4th Int. Conf. Cold Fusion*, Lahaina, Maui, Hawaii, December 6–9, 1993, Vol. 4 (1994).

36. J.-P. VIGIER, "New Hydrogen Energies in Specially Structured Dense Media: Capillary Chemistry and Capillary Fusion," *Phys. Lett.* (to be published).

37. S. H. WEI and A. ZUNGER, "Instability of Diatomic Deuterium in fcc Palladium," *J. Fusion Energy*, 9, 367 (1990).

38. A. PUSCH, W. FENZL, and J. PEISLL, "Hydrogen in Niobium Under Pressure," *J. Less-Common Met.*, 172–174, 709 (1991).

39. H. TEICHLER, "Theory of Hydrogen Hopping Dynamics Including Hydrogen-Lattice Correlations," *J. Less-Common Met.*, 172–174, 548 (1991).

40. H. R. SCHOBER and A. M. STONEHAM, "Diffusion of Hydrogen in Transition Metals," *J. Less-Common Met.*, 172–174, 538 (1991).

41. C. A. HAMPEL, *Rare Metals Handbook*, Reinhold Publishing Company, New York (1954).

42. H. ZUCHNER and T. RAUF, "Electrochemical Measurements of Hydrogen Diffusion in Intermetallic Compound LaNi5," *J. Less-Common Met.*, 172–174, 611 (1991).

43. R. V. BUCUR, "Interaction of Hydrogen with the Microstructure in Pd and Pd77Ag23," *Proc. 2nd Int. Conf. Cold Fusion*, Cumo, Italy, T. BRESSANI et al., Ed., Italian Physical Society (1991); see also G. L. POWELL, J. R. KIRKPATRICK, and J. W. CONANT, "Surface Effects in the Reaction of H and D with Pd-Macroscopic Manifestations," *J. Less-Common Met.*, 172–174, 867 (1991); see also H. H. UHLIG, *Corrosion and Corrosion Control*, John Wiley & Sons, New York (1971).

44. R. SEITZ, "Fusion in from the Cold?" *Nature*, 339, 185 (1989).

45. M. R. SWARTZ, "The Other Side of the Coulomb Barrier," *Phys. Lett. A* (submitted for publication).

46. W. E. MEYERHOF, *Elements of Nuclear Physics*, McGraw-Hill Book Company, New York (1957).

47. R. BASS, "LINT: A Semi-Classical Quantized Theory of Lattice Induced Nuclear Transmutations," *Cold Fusion Source Book, International Symposium on Cold Fusion and Advanced Energy Systems*, H. FOX, Ed., p. 32, Minsk, Belarus (1994).

48. C. J. SMITHELL, *Metals Reference Book*, Butterworths Scientific, London (1949).

49. P. L. HAGELSTEIN, "Coherent Fusion Theory," *J. Fusion Energy*, 9, 451 (1990); see also P. HAGELSTEIN and S. KAUSHIK, "Neutron Transfer Reactions," *Proc. 4th Int. Conf. Cold Fusion*, Lahaina, Maui, Hawaii, December 6–9, 1993, Vol. 1; see also P. HAGELSTEIN, "Lattice-Induced Atomic and Nuclear Reactions," *Trans. Fusion Technol.*, 26, *4T*, Part 2, 461 (1994).

50. C. R. A. CATLOW, "Atomic Transport in Heavily Defective Solids," *Philos. Mag. A*, 64, 5, 1011–1024 (1991); see also P. VARGAS, L. MIRANDA, L. RODRIGUEZ, M. LAGOS, and J. ROGAN, "Quantum Diffusion in Transition Metals," *J. Less-Common Met.*, 172–174, 557 (1991).

51. B. M. KLEIN and R. E. COHEN, "Anharmonicity and the Inverse Isotope Effect in the Palladium-Hydrogen System," *Phys. Rev. B*, 45, *21*, 405 (1992); see also E. WICKE and H. BRODOWSKY, "Hydrogen in Palladium and Palladium Alloys," *Hydrogen in Metals II*, G. ALEFIELD and J. VOLKL, Eds., Springer, Berlin (1978).

52. D. A. PAPACONSTANTOPOULOS et al., "Band Structure and Superconductivity of PdD_x and PdH_x," *Phys. Rev.*, 17, *1*, 141150 (1977).

53. M. R. SWARTZ, "Quasi-One-Dimensional Model of Electrochemical Loading of Isotopic Fuel into a Metal," *Fusion Technol.*, 22, 296 (1992).

54. M. R. SWARTZ, "Isotopic Fuel Loading Coupled to Reactions at an Electrode," *Trans. Fusion Technol.*, 26, *4T*, Part 2, 74 (1994).

55. M. R. SWARTZ, "Generalized Isotopic Fuel Loading Equations," *Cold Fusion Source Book, International Symposium on Cold Fusion and Advanced Energy Systems*, H. FOX, Ed., Minsk, Belarus (May 1994).

56. M. R. SWARTZ, "The Minimal Photon Energy for *Ab Initio* π-Meson Fusion Activation," *Phys. Lett. A* (submitted for publication).

Mitchell R. Swartz [ScD, Massachusetts Institute of Technology (MIT), 1984; MD, Harvard University, 1978; EE, MS, and BS, MIT, 1971] is a senior research scientist at JET Energy Technology, where he is responsible for the development of quality-control procedures in calorimetric analyses and electrode and material fabrication. His research interests are the interaction of radiation and matter, and his current research investigations probe phonon spectra, material changes during loading, and engineering aspects of energy transfer during the reactions.

LETTERS TO THE EDITOR

THE RELATIVE IMPACT OF THERMAL STRATIFICATION OF THE AIR SURROUNDING A CALORIMETER

Mitchell R. Swartz[1]

Last month there were several responses to the paper entitled "Potential for Positional Variation in Flow Calorimetric Systems" which discussed a theoretical examination [1] of heat and mass flow [2] with inclusion of the Bernard instability [3].

"I've been thinking about another problem that could be plaguing the Cravens-style vertical flow calorimetry ... thermal stratification in the air space outside the cell. In at least one of the public demos Cravens put on, he enclosed the cell in an insulated chamber made with two Dewars placed mouth-to-mouth. This created a more-or-less dead airspace around the cell and, since the cell was operated at a temperature significantly above ambient, I would expect a considerable temperature gradient to exist in this air space, hottest at the top and cool at the bottom. With the very slow flows he used (14 ml/min is ~0.7cm/sec flow velocity in 1/4" ID tubing), the temperature sensors could be significantly affected by simple conduction through the walls of his fittings. Such a problem would cause the upper temp sensor, which is the outlet sensor, to be hotter than the lower sensor ... resulting in a false positive indication. Because the airspace stratification is "driven" by the heat of the cell, this false positive indication should become larger when the cell temperature is raised...."

[Scott Little (little@eden.com)]

Several issues appear to be involved.
1) Could thermal stratification of the air physically located outside of the electrolytic cell influence the thermal leakage from the cell by changes in the net thermal conductance?
2) Does thermal conduction through mechanical fittings effect the reading of a temperature sensor?
3) Could such a thermal air thermal stratification effect also alter the temperature sensors through the fitting effect (described at #2)?

The following is the semiquantitative estimate of the impact of the phenomenon discussed in question #1. Instead of a simple mean temperature of outside air of 30°C, in this gendanken experiment assume the air is varied over the temperature range from 20 to 40°Centigrade. Assume there does not exist any variation in the air or calorimeter conditions with respect to time or external mass transport. The enthalpic losses to the local "ambient" environment from the cell include conduction, radiation (with the 4th power temperature term in the Stefan-Boltzmann equation), and convection losses of two types — both flow incurred and thermal induced [4,5]. To qualitatively determine the impact, let us model the calorimeter in a single dimension and as a linear system. We will ignore for simplicity spatial- or time-variation of the material factors, boundary effects [6], and other isothermal effects.

Changing the air by thermal stratification probably would mainly alter the thermal conduction term. That thermal conduction loss is in "series" with the thermal conduction term through the calorimeter wall itself. The thermal conductance of the two compartments — consisting of the air and the outer wall of the calorimeter — could be modeled as

$$K_{equiv} = \frac{K_{wall} * K_{air}}{K_{wall} + K_{air}} \quad [\ \text{cal/(sec-cm}^2\text{)(degC/cm)}\ ].$$

The equation is derived similar to the corresponding electrical system with the thermal resistances added in series, after converting the thermal barriers (resistances such as R_{wall}) to thermal conductance ($R_{wall} = 1/K_{wall}$).

How much could such thermal stratification — physically located outside of the electrolytic cell — influence the net thermal conductance loss of the calorimeter and thus alter the measured result of a calorimeter? These thermal

[1]JET Energy Technology, P.O. Box 81135, Wellesley Hills, MA 02181

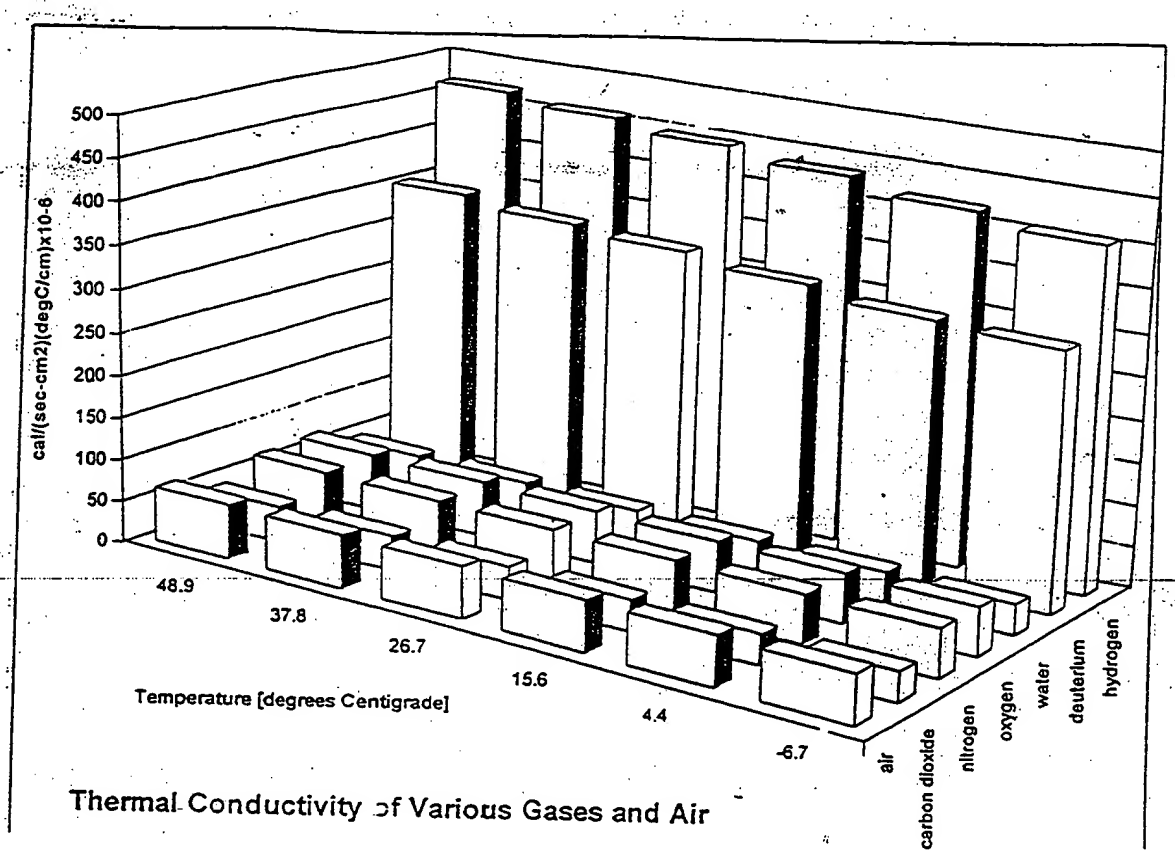

Temp. (C)	air	carbon dioxide	nitrogen	oxygen	water	deuterium
-6.7	56.2	33.7	56.2	57.2	36.8	305.8
4.4	58.3	35.6	58.3	59.4	38.9	310
15.6	60.3	37.6	60.3	61.6	40.5	322.3
26.7	62.2	39.7	62.4	63.6	42.6	334.7
37.8	64.2	41.7	64.1	65.9	44.6	343
48.9	66	43.8	65.7	68.2	46.7	355.4

Fig. 1 — Thermal Conductivity of Gases
The hydrogen isotopes show markedly greater thermal conductivity than other, higher molecular weight, gases. This 3D bar graph demonstrates thermal conductivity (cal/(sec-cm^2)(degC/cm) x 10^{-6} as a function of temperature (-7 to 49 degrees Centigrade) for air, carbon dioxide, deuterium (D_2), hydrogen (H_2), nitrogen (N_2), oxygen (O_2), and water (data after Handbook of Chemistry and Physics (Chemical Rubber Co., 1973).

conduction changes are based upon relatively small differences in thermal conductivity of the gases surrounding the calorimeter. The thermal conductivity of air varies from 42 to 45 cal/(sec-cm^2)(degC/cm) x 10^{-6} between 20 and 40°C. In this example, this difference in thermal conductivity amounts to a 6% change, ± 3% around the mean. Furthermore, the variation's impact might, if it varies linearly with temperature, just balance when integrated over the entire wall. The impact, based upon convention models of heat and mass transfer [4,5,6], is that if the spatial distribution of temperature is even and linearly distributed, there will be no significant changes upon calorimeter calibration. It appears that only when there is a nonlinear variation of the air's thermal conductance-temperature curve, that there accrues significant deviation from the calibration. To calculate the impact of the effect, let us assume the nonlinear asymmetry is quite significant and results in a 2% variation. With equation (1), it is possible to actually substitute number. If K_{air} is a tenth that of the wall, $K_{air} = 0.1\ K_{wall}$, then a hypothetical 2% asymmetric stratification change in air conductivity will alter the total conductivity by about ± 1.8%. If K_{air} is $\sim K_{wall}$ ($10\ K_{wall}$), a hypothetical 2% asymmetric stratification change in air conductivity will alter the total conductivity by about ± 1.0% (± 0.2% respectively).

Most importantly, as shown in Fig. 1, the thermal conductivity effects generated by the stratification are quantitatively small, compared to the impact of the "hydrogen gas displacement effect" which might exist in some electrolysis systems. So what is the impact of possible thermal stratification of gas external to a calorimeter? The overall impact of such a distribution upon the overall system thermal conductance is small. This is reasonable because it must be less than a few % change from expected, and furthermore — only those changes deviating from linearity will produce a net change. Finally, any putative change from such thermal stratification is insignificant compared to the "hydrogen gas airspace effect" which occurs when the air around the electrochemical cell is replaced by hydrogen (or deuterium in heavy water experiments) which thereby markedly increase the thermal conductance of the system (Fig. 1). Most significantly, the hydrogen gas effect has the impact of making calculations of putative excess energy a lower limit to that which may have actually occurred if such systems have such an unanticipated hydrogen volume in the gas space.

In summary, temperature gradients in the vicinal air surrounding a calorimeter can exist for several reasons. For this to be significant there must be either a nonlinear or an asymmetric thermal air stratification. Even then the impact is small and probably not significant when compared to the quantitatively larger hydrogen gas airspace effect.

REFERENCES

1. M. Swartz, "Potential for Positional Variation in Flow Calorimetric Systems," *J. New Energy*, vol. 1, no 1, pp 126-130 (1996).
2. J. Melcher, Continuum Electromechanics, MIT Press, Cambridge, 10.13-10.18 (1981).
3. S. Chandrasekhar, Hydrodynamic and Hydromagnetic Stability, Clarendon Press, Oxford, 9-75 (1961).
4. M. Jakob, , G.A. Hawkins, Elements of Heat Transfer and Insulation, John Wiley, New York, (1950).
5. A.I. Brown, S.M. Marco, Introduction to Heat Transfer, McGraw-Hill Book Co (1958).
6. H. Schlichting, D.J. Kestin, Boundary Layer Theory, Pergamon Press, New York (1951).

CONSISTENCY OF THE BIPHASIC NATURE OF EXCESS ENTHALPY IN SOLID-STATE ANOMALOUS PHENOMENA WITH THE QUASI-ONE-DIMENSIONAL MODEL OF ISOTOPE LOADING INTO A MATERIAL

NUCLEAR REACTIONS IN SOLIDS

KEYWORDS: *quality control, light water electrolysis, biphasic thermal response*

MITCHELL R. SWARTZ *JET Energy Technology, Inc.*
P.O. Box 81135, Wellesley Hills, Massachusetts 02181

Received June 11, 1995
Accepted for Publication February 4, 1996

Electrochemical experiments, using nickel cathodes in light water solutions, were used to examine the enthalpy generated by electrically driving each electrode pair compared with ohmic controls contained within the same solution. For nickel wire cathodes, the peak power amplification (π_{Ni}) was in the range of $1.44^{\pm 0.58}$. For spiral-wound nickel cathodes with platinum foil anodes, π_{Ni} was $2.27^{\pm 1.02}$. By contrast, neither iron nor aluminum cathodes demonstrated excess heat.

Driving these nickel samples beyond several volts, however, produced an exponential falloff of the power gain. This biphasic response to increasing input power may be consistent with the quasi-one-dimensional model of isotope loading and may contribute to the difficulty of reproducing these phenomena.

INTRODUCTION

Nickel cathodes can produce excess enthalpy (heat) during electrolysis of light water solutions.[1-8] Although not all of the putative isotopic fuel (protium or deuterium) enters the metal, the degree of loading is critical.[9-11] Unfortunately, there has been insufficient (or no) mention of the amount of filling (loading) achieved in many previous "negative result" studies and research papers in this field. The loading has been analyzed through the quasi-one-dimensional (Q1D) model of isotopic loading using the isotope diffusivity and electrophoretic mobility. This has provided insight into the competing gas-evolving reactions at the surfaces of the to-be-loaded electrode. At such a metal surface (possibly the 110 surface for nickel,[12] effected by many materials[13]), the loading flux into the bulk volume of the electrode must be distinguished from the gas evolving flux,[9] which is controlled by ζ [the electric order/thermal disorder ratio[11] involving the applied electric field energy to thermal energy ($k_B * T$)]. This paper continues to confirm the observations of excess enthalpy for nickel cathodes, clarifies the role of the input power, and extends the Q1D model of isotopic fuel loading to conform with these observations.

Conventional[14] and multiring calorimetry[8,15] can eliminate several sources of erroneous false positive "excess heat," including nickel colloid generation and recombination. Electrochemical experiments, using nickel, aluminum, iron, and platinum cathodes with platinum or gold[16] comprising the anode in light water solutions, examined the enthalpy generated by electrically driving each electrode pair under varying input power levels,[8] compared to ohmic controls contained within the same solution. Samples of straight, spiral-wound,[8] and woven[16] nickel cathodes under controlled low-to-moderate current density cathodic conditions produced excess enthalpy.

An optimum "notch" or plateau is observed using a multiring calorimeter, in the power gain curve relative to either input power for low current density drive conditions ($\sim 2 \times 10^{-5}$ to 10^{-2} A/cm^2) (Ref. 8). At the notch, the peak power ratio (π_{Ni}) in the range of 2.5 to 3 was typical; characterized with a falloff under increasing input

power or current levels back toward a ratio of <1. Such biphasic behavior of the observed excess heat[8] is important because—combined with the rarity of adequately loaded and properly prepared electrodes—it may account for some of the difficulty in reproducing these phenomena.

EXPERIMENTS

A multiring calorimetric system, containing dual feedback control loops,[8] was used to both measure the electrical power and energy delivered during each sequence and to compare them to the power and energy released by either or both the ohmic and the electrolytic power source. Several compartments (or rings, each composed of several materials and barriers) were used, beginning with the inner (source) ring and ending at the environment outside of the chamber. The thermal barriers ("rings") serve to thermally isolate the cell from the environment by a series of concentric envelopes, which allow redundant measurement of heat storage and transport, and enable the addition of terms to the equations, which enable waveform reconstruction.[15,16] Figure 1 shows a schematic diagram of the five-ring calorimeter with a Peltier heating/cooling device. The electrochemical cell was completely contained in the first (inner) ring, which also included a control ohmic resistor (or two), a thermistor, and on some occasions iron or aluminum in place as an alternate cathode. The second ring was a closed system containing a large area of the platinum as a recombiner. This ring, the larger of the first two rings, also included an *in situ* pump motor. The pump enabled examination of the effect of stirring water in the second compartment during a few of the initial control experiments where an additional thermal heater was used in the second compartment. The barrier between rings 1 and 2 was gas permeable. It was arranged so that the majority of the recombination would occur in ring 2, thereby eventually draining ring 1 of light water over several days after each fill (depending on the electrolysis rate, temperature, and pressure in ring 1). For most experiments, the barrier between rings 2 and 3 was completely sealed. For simplicity, not shown in the figure, are the pump motor in compartment 2, two of the ohmic thermal sources (enthalpic controls), the gas outlet tube (closed for these experiments, except for Fig. 3) located in ring 2, and the humidity detectors and other sensors in rings 3 and 4.

The inner two rings were monitored for temperatures (±0.1 K) using groups of matched thermistors

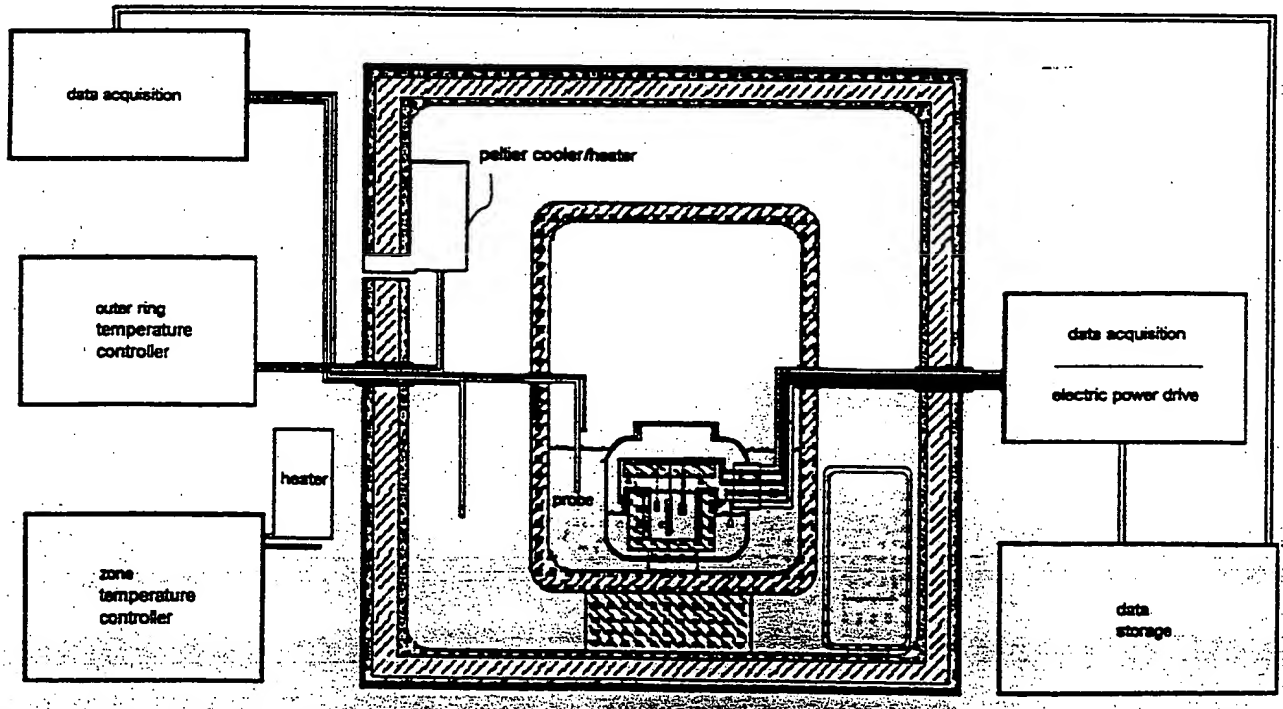

Fig. 1. Multiring calorimeter. This is a schematic diagram of a five-ring calorimeter. The figure presents the rings and barriers as located from the source-ring (inner ring containing electrodes, ohmic control, and thermistor) to the environment outside of the chamber. For simplicity, not shown are the pump motor, ohmic thermal sources, other thermistors or temperature sensors, or gas outlet tube (closed for all of these experiments) in ring 2, the humidity detector in ring 3, or the Styrofoam or wooden thermal isolation supports and water ballast in rings 4 and 5 (Ref. 8).

These included Omega precision thermistors (44034 and 44006 series with additional Teflon insulation) and Boone thermistors (STH02 with in-line voltage and temperature compensation, each covered with insulation of molded epoxy). Rings 3, 4, and 5 were monitored for temperature using Omega Engineering OMEGA 250 and Vaisala HMI32 temperature (and humidity) sensors. Other temperature measurements were made, to corroborate the former, with a Simpson dual temperature system, a UDElectronics temperature system, an Omega 8020 pyrometer, a Honeywell recording relative humidity/temperature system, and Omega mercury thermometers (where accessible and possible). Feedback control of temperature of either ring 3 or 4 was maintained by a Yellow Spring Thermal Controller Model 72 (bandwidth 0.1 K; second loop). Feedback control of temperature in ring 5 was maintained by Honeywell water circulation zone control heating (±3.5 K; first loop).

For the spiral cathodes, Johnson Matthey brand wire (0.49-mm diameter, cold drawn, protected from contamination by polyethylene) was carefully wound closely packed down on a sterile wood shaft of the desired diameter. This shaft was removed prior to the experiment with separation of the wire and increased availability of the surface area. The iron cathodes were commercial grade.[a] All nickel cathodes were handled and cathode assemblies fashioned using sterile techniques to minimize organic and solvent contamination. The nickel colloid was collected and spundown with a ClayAdams Windsor 0131 centrifuge. The anodes were constructed either from wire matched to the cathode, from platinum wire protruding through Teflon tubing, or from paired platinum foils held within an acrylic holder as previously described.[17] The parallel paired platinum foil electrodes located on each side the of the spiral nickel cathode enabled electrolysis to continue with constant path length during the experiment (Fig. 1). The electrical path length was 0.5 cm to the center of the spiral in the midline at the axis. The use of platinum foil enabled relatively large area anodes (2.5-cm^2 peak). The electrochemical cell constant [L/A (1/cm)] was 0.76. Ohmic 1% precision resistors were carefully prepared with multiple layers of Cole-flex irradiated polyolefin heat shrink tubing (ST221) to minimize their contact with the solution. They were washed in distilled water and air dried, as were all electrodes prior to use. The loading was with either distilled water (CVS) or ordinary water (stored at sodium 1 milliequivalent per litre, potassium 0.3 milliequivalent per litre, TCO_2- < 5 mmol/ℓ, chloride 12 milliequivalents per litre, and pH 7.4).[b] Other materials in the inner two rings included polyethylene, polypropylene, methyl methacrylate, and Parafilm. Teflon tubing and tape[c] were used for seals. A rubber stopper was used in the second ring, located above the water level. Neither silicates nor glasses were used. The outer ring in the calorimeter included both Styrofoam and an Igloo thermal box, supported by a wooden and Styrofoam structure to minimize thermal conduction.

Electrical voltage sources included a LAMBDA 340A, LAMBDA LQ51, Kepco JMK 055, Regtron 050, and a Hewlet Packard HP722 AR. Current sources included a Keithley 225 and JET Technology 1280 and 1200 Electrophotodynamic Drivers®, with transsample potentials of peak voltages of 107, 20, and 15 V, respectively. Electrical currents (±1%) ranged from 1 nA to 3 A and were monitored with a Keithley 480 picoammeter. Voltages (±0.5%) were measured with a Keithley 610C Electrometer, Keithley 179 TRMS digital multimeter, and Keithley 160B digital multimeter, or HP 412 vacuum tube voltmeter for the reactor. An Amprobe-4B, an Amprobe 9, or a Triplet 3550 multimeter was used for the other electrical ports and to cross check electrical parameters. All alternating current measurements were made with a Tektronix 7403N oscilloscope, a Princeton Applied Research Model 121 Lock-in Amplifier, and a Microdot F280A programmable waveform generator. The power source used for the pump motor in the second ring was a Heathkit regulated power supply 1P-1B, delivering about 49 mW heat when in use. Lumped parameter impedances of all components [including the open electrolytic cells when dry and leads to the electrochemical cell (range 0.4 to 1.8 Ω)] were measured and used to derive corrected values of V_{cell} from $V_{applied}$. The ohmic resistance controls (heaters) were in the range of 15 to 2500 Ω. The lumped parameter electrical resistivity of the aqueous solution was 1667 Ω·cm; however, controlled bubbling results in calculated impedances as high as ~12 000 Ω·cm. The derived lumped parameter resistivity is artificial because of the low dielectric constant layers in front of the electrodes, which change the electric field distribution between electrodes. The electrical setup included buffering of data acquisition signals by a high-impedance system, and cross checking. Data acquisition used four systems, a Computer Boards PPIO-AI8 board,[d] an ezAD measureport 105 analog-to-digital (A/D) converter[e] with modules for three differential inputs, a JET Technology 1280/D112, and a Keithley DAS-TC/B.[f] The PPIO system has 12-bit resolution, sample and hold acquisition times of 15 μs to 0.01%, and 0.01% (±1 bit) accuracy (input impedance 10 MΩ).

The Keithley system was superior at almost 16 bit resolution for 16 differential inputs with CJC compensation (temperature accuracy ± 1.0°C, precision <0.5°C). The matched Boone thermistors had excellent accuracy

[a]From Mallinckrodt.
[b]Hitachi/Boehringer 911 autoanalyzer and Radiometer 28.
[c]Chicago Specialty Manufacturing Company; Teflon Thread Seal Tape (0.5 in., No. 6241).
[d]Mansfield, Massachusetts.
[e]Boone Technologies, Inc., Virginia.
[f]Keithley MetraByte, Taunton, Massachusetts.

when correlated with output with the Vaisala system. Their temperature detection had a rated accuracy of ±0.8 K over 223 to 383 K, a precision of 0.1 K (at 298 K, see the following), with a sensor time constant of 75 s in air. Temperature-dependent computed junction compensation was included to correct for junction potentials at the data acquisition location. With such A/D conversion and data storage, the calibrated precision is <0.1 K resolution (298 K). The thermocouples, thermistors, and other probes were compared in preliminary studies as part of an ongoing thermometry study. Only the best probes were chosen for the experiments based upon those initial tests.

Samples were taken at rates of 1 Hz or greater to circumvent possible sampling error in all cases of computed data acquisition. The computed input was taken with a 68000 series microprocessor (Commodore Amiga 2000, 2500, or 4000) with a sampling rate of 1 to 100 Hz, and a 386 series microprocessor (Zenith Turbosport 386, sampling rate circa 1 to 3 Hz). After storage on BERNOULLI Multidisk (2 to 5 megabytes per channel day), preprocessing of the data was achieved by sliding-gate time average[18–20] over times ranging from 1 to 5 min to significantly improve performance[8,15] of the final processing computer system.[g,h]

In the absence of pump use, there was negligible electromagnetic interference (EMI) of any significance relative to the excess power levels under consideration and reported here. This was directly measured with an oscilloscope (to 1 MHz) and a Holaday 1501 microwave survey meter (2450 MHz) to be <0.01 μV/cm. In control experiments, peak induced voltages were <50 mV, which would imply peak available power levels (if the EMI was able to couple to the electrode-cable system and was then impedance matched to the radiation resistance of the nickel-electrolyte-platinum system) of 10 μW. This power is two orders of magnitude below the lowest noise levels here and is of no significance. With the electrical cables in parallel and with solution impedances of 1000 to 9000 Ω, even less EMI-contributed power would be available than in these control experiments where no effort was made to minimize the area subtended by the leads.

The experiments were conducted in the dark when possible. The enthalpy of visible and infrared electromagnetic radiation has not been previously discussed, although it may be significant. Therefore it was excluded from these studies. The incident visible illumination was monitored continuously within the chamber by a photodetection system in ring 4, comprising a photovoltaic cell subtending nearly one entire wall of the chamber comprising that ring. There was no significant input from this source for these investigations.

[g]U.S. LOGIC Pentium-60.
[h]Hewlitt Packard 7170.

Current calorimetry to examine the enthalpic behavior of current systems is simple, but the problems are formidable. These include the difficult determination of excess energy using the total heat produced and the input electrical energy. It is customary to use Newton's method and assume a linear time-invariant system. The output power is determined from the temperature rise, that is $T_1 - T_{bath}$ (= $\Delta\theta$). However, the best calorimetric analyses[14] include additional terms involving thermal transfer by radiation (see Nomenclature on p. 72):

$$C_{P,H_2O,l} M^0 * \frac{d\Delta\theta}{dt} = [V_{cell}(t) - V_{thermoneutral,bath}] * I - \frac{3I}{4F} * \frac{P}{P_{ambient} - P} \times [(C_{P,H_2O,g} - C_{P,H_2O,l}) * \Delta\theta + L_{H_2O}] + P_x(t) + P_h * [u_{-1}(t) - u_{-1}(t - \tau)] + k_R * [(\theta_{bath} + \Delta\theta)^4 - \theta_{bath}^4] . \quad (1)$$

The left term is the increase in enthalpy within the calorimeter. The terms on the right side are the enthalpy input from the electrolysis, the enthalpy content leaving with the electrolysis gas stream, the putative excess power (if any), the heater calibration pulse (with the Heaviside functions), and the radiative energy transfer to the water bath. There are some major problems, however, with this equation.[8,15] First, the increase in enthalpy within the calorimeter is actually composed of several terms, and some of them are not a function of $\Delta\theta$. For example, the barriers between rings have $T_1 + T_2$ terms. Three other problems with the equation have been discussed using a more advanced model that includes thermal conduction as well as those terms in the heat and mass transfer equations that are not a function of the differential temperature $\Delta\theta$ (Ref. 8).

Many of these issues are corrected here. In this more inclusive model, thermal conduction is included.[15] The other errors corrected here include the compartmental model of the rings, which enables consideration of enthalpic uptake by each barrier. Thus, the terms comprising the nonwater portions of the calorimeter are explicitly separated out as the materials (reflected as the summation term in the following discussion) in each compartment. The value $\Delta\theta$ is not used here simply because it is equal to $T_1 - T_2$ but more importantly because there is additional data that can be derived by the use of the additional rings. Because successive rings are involved and used, additional information [enthalpy to ring 2 (previously "bath")] is not lost. It can be added in for each level. This analysis enables inclusion of those terms in the heat and mass transfer equations that are not a function of the differential temperature $\Delta\theta$. Some of the

materials constitute barriers between rings, and hence the energy terms have $T_1 + T_2$ terms as opposed to only $T_1 - T_2$ terms.

Briefly, the mathematical solution to the power and energy flow equations is derived from a Q1D model of heat and mass transfer in a calorimeter. This should not be confused with the Q1D model of isotope loading[9–11] of the cathode from the solution. In the calculations, account was taken of the specific heat and mass of all barriers, although inhomogeneities in the barriers were not considered. Given that there were no sudden changes in thermal diffusion and ignoring the inhomogeneities and anisotropies, the barriers 1, 2, 3, 4, and 5 remain spatially fixed, thereby making the mathematical solution amenable to the Q1D heat transfer analysis.[9–11]

The boundary conditions are the first ring (containing the electrochemical cuvette and monitored as T_1), the feedback-controlled midrings (T_3 or T_4), and the zone-controlled room temperature. The heat and mass transfer equations between each set of rings determines the excess heater power (both as an incremental term and amplification rate) and excess energy, if any.

There remains some confusion as to the definition of input power and excess heat.[21] However, the electrochemistry considers the thermodynamics by simply assuming the steady state is achieved.[22,23] Even though the theoretical decomposition voltage of water is 1.23 V, it is the thermoneutral potential V_{therm} that is subtracted from the cell voltage to derive the electrochemical "input power" where the voltage is $V_{cell} - V_{therm}$. The thermoneutral potential, based on the standard free enthalpy of water, is 1.48 V for light water (1.54 heavy water), which is the potential that produces gas without a local temperature change. Although most calorimetry in the field is directed towards utilization of the thermoneutral potential, it is simply not respected universally. The major reasons are the lack of thermodynamic equilibrium, the use of this number ($V_{cell} - V_{therm}$) in a denominator, and the lack of evidence that this system is isothermal.[21]

This paper uses power and energy in the manner defined as follows. Because of the previous discussion and because power in electrical and power engineering[24,25] is defined as $V * I$, input power for these experiments is defined as $V * I$, and *does not* include reduction of the transsample potential by the thermoneutral potential (1.48 V for light water).[21] The output parameters derived from P_{out} (the output power in watts) include the power amplification factor π_{Ni} (nondimensional), which is defined as $P_{out}/P_{in} = \pi_{Ni}$ and the incremental excess power [$= P_x$ (watts)], defined as $P_{out} - P_{in}$. For these experiments, it was also important to separate power from energy because storage and other mechanisms of "negative" power can create false positives of excess heat, not supported by the total energetic computations[8,16,21].

$$\left[C_{P,H_2O,l}M^0 + \sum_i (C_{P,i}M^i)\right] \times \frac{dT_1}{dt} + \left[\frac{(C_{P,Z_{12}} * M_{Z_{12}})}{2} * \frac{d(T_1 + T_2)}{dt}\right]$$
$$= [(V_{cell}) - V_{thermoneutral}] \times I - \frac{3I}{4F} * \frac{P}{P_{ambient} - P}$$
$$\times \{[(C_{P,H_2O,g} - C_{P,H_2O,l}) * (T_1 - T_2)] + L_{H_2O}\} + P_x(t) + P_h * \{[u_{-1}(t)] - [u_{-1}(t - \tau)]\}$$
$$+ k_{R_{12}} * (T_1^4 - T_2^4) + k_{C_{12}} * [(T_1 - T_2)] \quad (2)$$

We correct Eq. (2) with an electrical input that is uniquely and more easily defined because the thermoneutral potential is not used.[8,15] Furthermore, the use of a small number in the denominator is avoided.[21] The final two terms match the final term of Eq. (1) and the conduction term previously omitted.[14] As discussed elsewhere, using waveform reconstruction techniques, both power and energy are monitored so as to rule out energy storage and other false positives of excess heat.[8,15,16]

RESULTS

The multiring calorimeter was sensitive and stable under the conditions described elsewhere[8,15] and enabled significant short experimental time constants after very long settling times (settling time and thermal noise decrease of ~1 mW/h). The best choice of barriers and thermal masses has been those chosen to provide a short time constant between the first and second rings thereby enabling many experiments during each sequence. Close examination of the heat transfer coefficient within the multiring system has heralded that delta-T/power input may not be a constant. This is consistent with the nonlinear terms in the heat transfer equation. By the use of differential (and integral) equations, generated powers and energies in the ring system have been derivable anyway. Following minimization of the background noise, this system ruled out false indications of excess heat allowing us to focus on purportedly active samples of nickel under controlled low-to-moderate current density conditions.

When careful observation is made of some samples of nickel under controlled low-to-moderate current density, cathodic conditions excess heat is observed. Figure 2 shows the output for a reactor containing a platinum foil anode and a spiral nickel cathode [ordinary water (H_2O)]. The input and output power and energies of the calorimeter are shown. The step-like functions are the energy curves (read off the right y axis). The input and measured output powers (including thermal background)

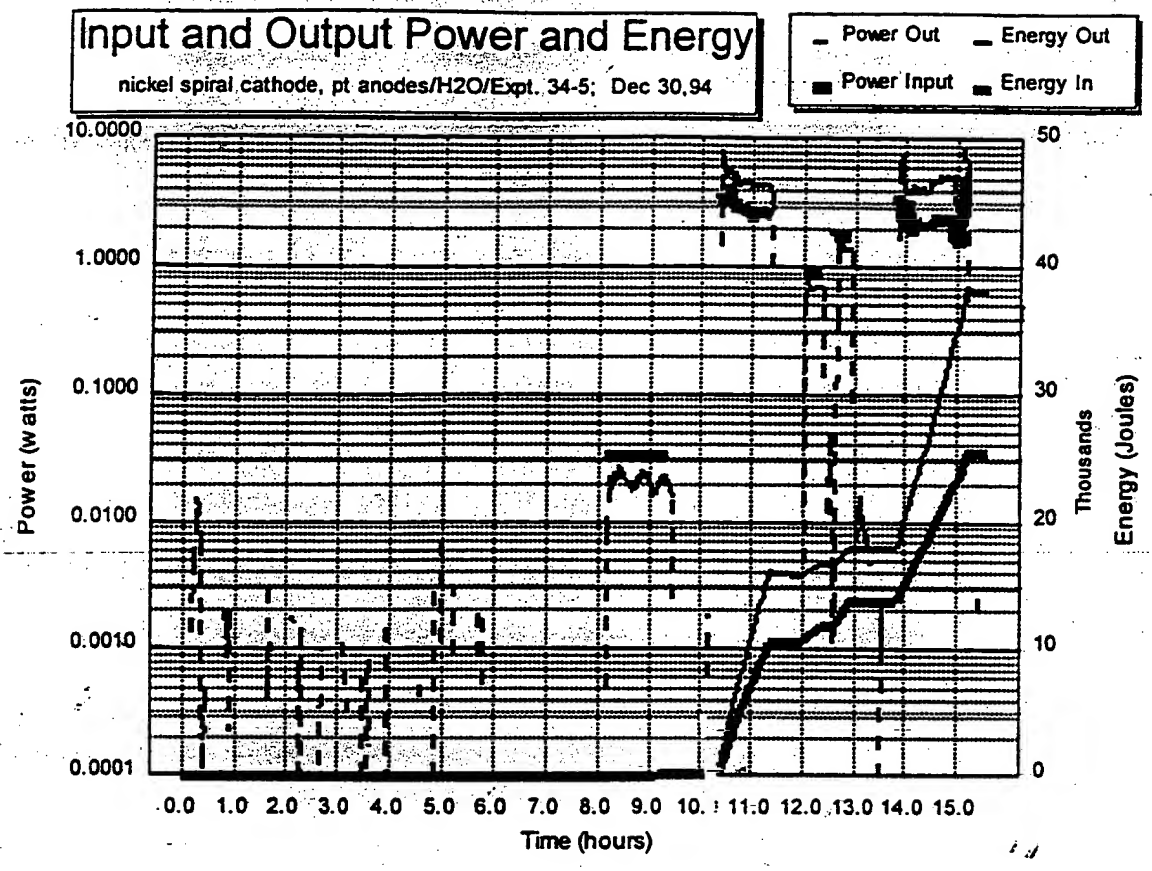

Fig. 2. Thermal spectrogram. The input and output power and energies of a platinum foil anode (4.0-cm^2 area) and spiral nickel cathode (4.8-cm^2 area, 0.059-cm^3 volume) in ordinary light water (H_2O) are shown. The step-like functions are the energy curves (read off the right y axis). The powers (thermal background, input, and output) are the remainder of the curves and have a logarithmic scale (left y axis). To the lower left is shown thermal noise (background for this experiment) ranging from 100 to a few milliwatts and extending until the first input (control) pulse at ~8 h.

are the remainder of the curves and have a logarithmic scale (left y axis). Figure 3 shows the output for a second reactor containing six spiral nickel cathodes (combined 28-cm^2 cathodic area, 0.35-cm^3 volume). To the lower left is shown the settling time and thermal noise (background for this experiment) ranging from 60 to 90 mW and extending until the first input (control) pulse at ~12 h. These figures show that these systems are characterized by excess heats in greater amounts than that which occurred for the ohmic controls.

When platinum foil was used as the anode, at intermediate power inputs, a repeatable excess heat for certain conditions was obtained. There was more excess heat and more clean postreaction reactors (measured by the absence of both corrosion and colloid products) in wide area platinum anode reactor systems. For matched nickel wire as the anode, there was power amplification [π_{Ni}] in the range of $1.44^{\pm 0.58}$ if the transsample potential (V_{cell}) was below 5 V. For nickel spiral cathodes with platinum foil anodes, the power amplification was in the range of $2.27^{\pm 1.02}$ for transsample potentials <5 V. Peak power outputs have been in excess of 2 W, with power densities (nickel) of more than $7^{\pm 4.3}$ W/cm^3 or 0.088 ± 0.053 W/cm^2. The peak energy ratios E_{out}/E_{in} have been in the range of 1.3 to 1.9 (maximum 2.4).

For controls, ohmic resistors (as thermal heaters) were included in the reactor and with each experiment provided metachronous bracketing of the reactor response to the electrical energy input pulses (Figs. 2 through 5). Neither the iron nor aluminum as cathodes had evidence of excess heat, but instead demonstrated recovered power ratios of less than one. These power amplifications for open systems were as low as $\pi_{Fe} \sim 0.71^{\pm 0.1}$ and $\pi_{Al} \sim 0.75^{\pm 0.1}$, respectively. Platinum, examined in the presence of nickel, did not show any compelling evidence of power gain either. As a control, in those reactors with two platinum anodes, the platinum anode-platinum cathode system, with the nickel electrode open circuited between the platinum electrodes, had recovered power ratios differing from 1.0 by levels comparable to noise at the low input electrical power levels tested ($\pi_{Pt} \sim 1.19^{\pm 0.37}$).

A biphasic response to input electric power was observed to characterize the generation of excess heat from nickel using light water (Figs. 4 and 5). In conditions

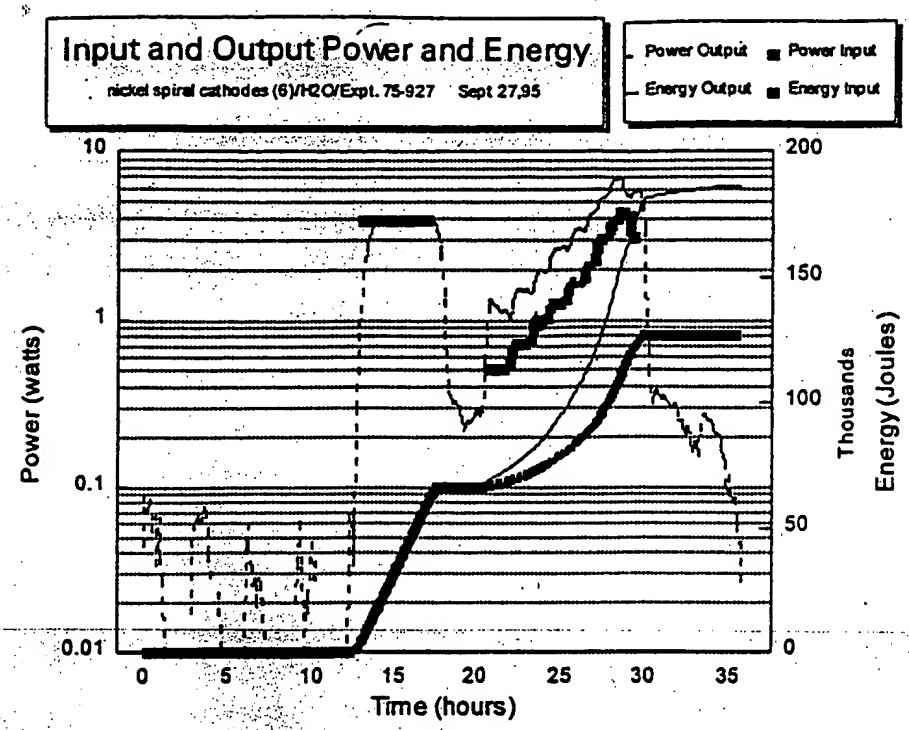

Fig. 3. Thermal spectrogram. The input and output power and energies of a similar system as in Fig. 2, located within a four-ring calorimetric system. Six spiral nickel cathodes (28-cm^2 combined cathodic area, 0.35-cm^3 volume) were driven in distilled H_2O. The step-like functions are the energy curves (right y axis). The powers (thermal background, input, and output) are the remainder of the curves and have a logarithmic scale (left y axis). To the lower left is shown thermal noise (background for this experiment) ranging from 60 to 90 mW and extending until the first input (control) pulse at ~12 h.

where stability and sensitivity of the multiring calorimeter were maximized, an optimum notch or peak was observed in the curve of power gain versus input power, current, and voltage under low current density conditions. At the notch, the peak power ratio π_{Ni} of 2.5 to 3 was typical with a falloff under increasing input power or current levels toward a ratio of 1. Figure 3 is a graph showing the biphasic character of the power amplification factor [π_{Ni} (nondimensional) defined as P_{out}/P_{in}] as a function of current. Figure 4 is a graph showing the output of the nickel cathodes and a control as a function of logarithmic applied voltage.

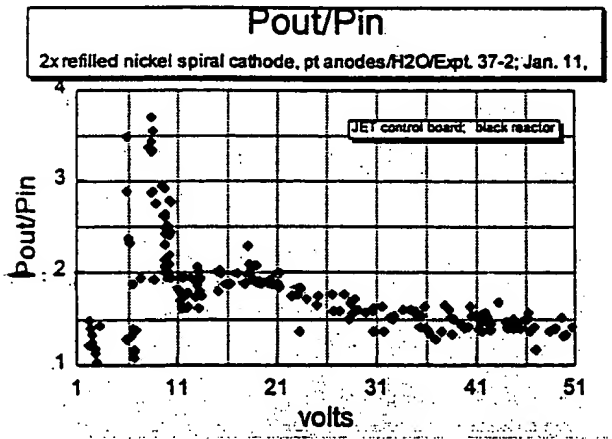

Fig. 4. Biphasic character of power amplification factor (H_2O). The biphasic character of power amplification ($\pi_{Ni} = P_{out}/P_{in}$) as a function of applied transsample potential in an experiment using a platinum foil anode (4.0-cm^2 area) and a spiral nickel cathode (4.8-cm^2 area, 0.059-cm^3 volume) in light water (H_2O).

INTERPRETATION

The results of excess power in this loaded electrode system are consistent with reports in some of the literature for nickel light water,[1–7] heavy water,[26–29] and other[30–32] systems. Given the π-notch results reported here, these results might even be consistent with some of the observed negative findings involving electric drive at either extrema. The observations of biphasic behavior may also be consistent with some of the negative experiments if such experiments were actually conducted in a region outside of the notch. Such biphasic behavior of the materials may account for some of the widespread difficulties in observing the phenomena π_{Ni} outside of the notch manifold.

False positives have been considered and ruled out in this investigation. As discussed elsewhere, nickel

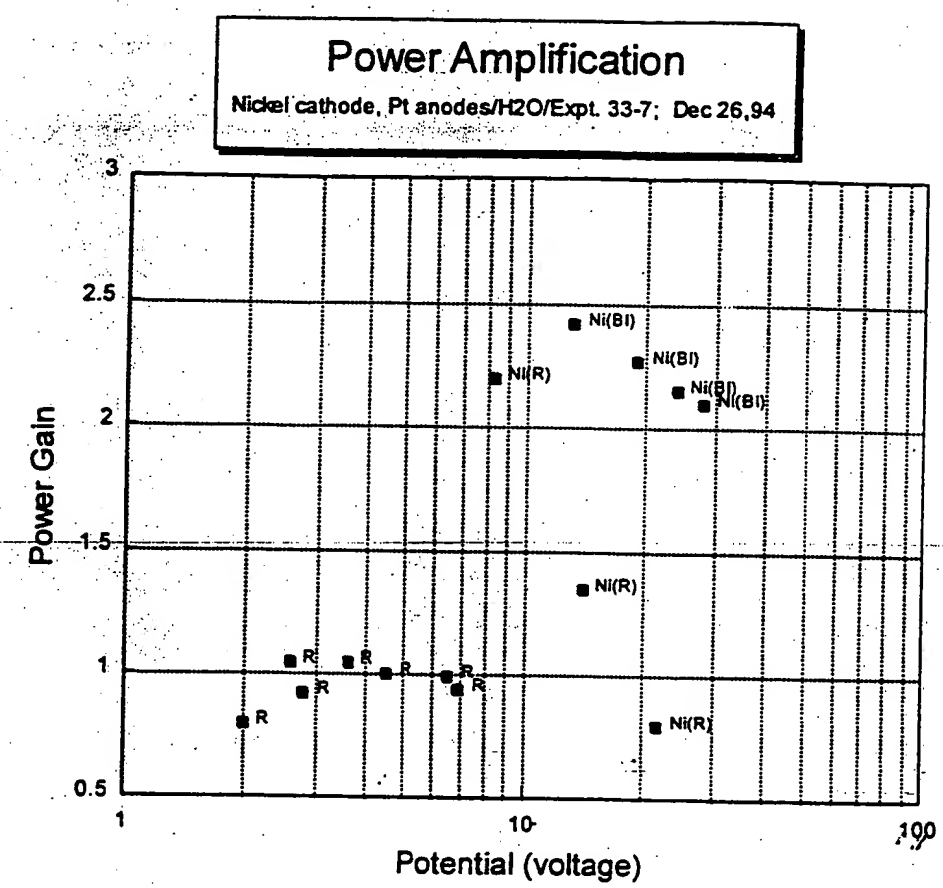

Fig. 5. Power amplification for platinum foil anode–spiral nickel cathode (H_2O). The power amplification as a function of the transsample potential is shown. The power amplification is seen to be ~1 for the ohmic controls (labeled R). Ni(BI) refers to one platinum foil-spiral nickel cathode system. Ni(R) refers to a second platinum foil—the nickel cathode experiment differing only by a diminished area over a portion of the solution path length.

colloid generation, recombination, and sampling errors are capable of generating false positives. A light green-colored nickel colloid (which settles over hours) was observed to follow anodic polarization of the nickel electrodes. By allowing anodic polarization to continue for days, this voluminous gel, possibly consistent with nickel oxide and/or nickel hydroxide,[33] was collected. This colloid material is capable of interfering with measurements because it may be able to store electrochemical energy and may contribute additional conduction polarization[34] and other[35] effects. Because anodic polarization has been recommended in the literature,[1-3] the presence of this nickel colloid material should be ruled out in those cases where anodic polarization may have occurred, to eliminate any possible incremental electrical storage contribution. Further investigations are underway because reported measurements of excess heat ought to exclude any incremental increase due to such material or note its presence.

Recombination has been reported to levels of milliwatts but is not a problem here for several reasons. First, this is a closed system. Second, and most importantly, any error due to recombination was definitively ruled out by taking the input power as $V * I$, defined by Poynting's vector.[24,25] Third, many of the excess power levels are more than an order of magnitude greater than those provided by recombination. Fourth, since $V * I$ is used to define the electrical input, then to the degree that any recombination does not occur, the measured outputs and derived excess heats are a lower limit to that which actually is present.[21,36]

Contaminants do not appear to be responsible for the excess heat in these experiments. Silicate deposition has been hypothesized to create a false positive of excess heat; elementary analysis reveals that it can provide heat but not excess heat under normal conditions, and furthermore, silicates were not present here. Lithium deposition has also been hypothesized to create a false positive of excess heat by depositing on the cathode, covering it with a surface to prevent reaction with water, and then suddenly converting the cathode to an anode, which then becomes the site of oxidation. The lack of added lithium here and the lack of anodic polarization in most of the experiments rules out this unlikely scenario.

The reported result of the electrical resistance effects of the leads is important but, in any case, could not account for the observed calibrated excess heat in these experiments using nickel. This is because the contacts and leads were measured for these experiments, and their resistances were arranged to be much less compared with the ohmic controls. Errors in power input calculations are unlikely because they were significantly reduced by sampling at 1 to 10 Hz, using precision current sources and visual indicators when any maximum available voltage was reached.

Given the documentation of the excess enthalpy now observed, it is important to take a closer look. Figure 5 demonstrates the effective activity of one spiral nickel sample as a function of the logarithm of the applied voltage. For the active nickel, the power amplification factor π_{Ni} has a significantly high initial peak Π_{Ni} and an exponential falloff, which on the logarithmic plot of Fig. 5 appears as a straight line. There appears to be a "peak activity Π_{Ni}," and a "drop-off." Thus, this might be modeled by an activity that does have exponential (κ_1 and κ_2) as well as the preexponential Π_{Ni} term. The power amplification factor thus becomes

$$\pi_{Ni} = \Pi_{Ni} * \exp[\kappa_1 * (V - \kappa_2)] . \quad (3)$$

The preexponential term, the peak activity Π_{Ni}, characterizes the material comprising the electrode. For controls this (cf., Fig. 4) preexponential term is equal to unity, and there was no observed enthalpic postdrive behavior. The solution and its response to the applied electric field intensity, the geometry of the electrochemical cell, and even the lead electrical impedances may account for the "shift" by altering the effective voltage actually available for a useful electric field intensity in the vicinity of the active fully loaded material. Experiments are currently underway separating out the influence of these parameters.

Futhermore, other materials like palladium (loaded electrolytically from heavy water) may demonstrate such biphasic curves characterized by a considerable "shift to the right" because of their own rapid internal redistribution of loaded isotopic fuels, and so may not demonstrate the biphasic notch until much higher drive levels able to achieve adequate loading.[i]

Also important, these experiments have demonstrated that λ_{Ni} is not a constant. The falloff with increasing power input is also consistent with the Q1D model of isotope loading[9-11] especially where λ_{Ni} (the loading ratio) decreases with increasing power input. With the model written in general terms of hydrogen (which could be deuterons or protons), the solution to the partial differential equation is separable into five terms after separation of variables. The result is determined by three nondimensional factors: λ_{Ni}, the loading flux ratio[9]; Ψ_{fus}, the fractional amount of intranickel hydrogen that actually contributes to the desired reactions[11]; and ζ, the electric order/thermal disorder ratio[10,11]:

$$J_{fus} = \frac{[B_H * [H^+]]}{L_c} * \frac{2\lambda_{Ni}}{(2\lambda_{Ni} + 1)} \times \frac{1}{\left[\exp\left(\frac{q * V}{k_B * T}\right) - 1\right]} * \left[\frac{(q * V)^2}{(k_B * T)^2}\right] * \Psi_{fus} \quad (4)$$

The first term results from material and geometric factors. The second term is composed of gas evolution terms. The next two terms reflect the applied electric field intensity and k_BT and are dominated by the ratio of the applied electrical energy that is organizing the distribution of hydrogen to the energy available for its random thermal disorganization.

As a result of the actual observations, this fusion equation was modified by correcting the second term to account for the observed increasing probability of gas evolution with increasing transsample potential. An attempt was made to approximately analyze this by defining the loading as an exponential involving the ratio of the applied electric field intensity and the thermal disorder. Taking into account that there is a known threshold to gas evolution, the loading factor might then be defined as

$$\lambda_{Ni} = \lambda_{Ni,0} * \left\{\exp\left[-\Theta_{\lambda,Ni} * \left(\frac{q * \Delta V}{k_B * T}\right)\right]\right\} \quad (5a)$$

and

$$\Delta V = V - V_{threshold} , \quad (5b)$$

where $V_{threshold}$ is the threshold voltage where hydrogen gas evolution first occurs. The value $\lambda_{Ni,0}$ is the preexponential factor. The value $\Theta_{\lambda,Ni}$ is the exponential factor relating the order/disorder ratio to the observed loading ratio. In this zeroth order approximation, $\Theta_{\lambda,Ni}$ is independent of the threshold voltage, although they may be linked.

Figure 6 shows the corrected fusion rate, using Eq. (5) in substitution, for the Q1D model of loading. Shown here for various $\Theta_{\lambda,Ni}$ are a series of parametric curves that demonstrate the relative fusion flux rate as a function of the ordering parameter. Figure 6 should be compared to Fig. 4. This observation of similar curves may be consistent with the fact that the Q1D model is valid as regards the loading at moderate-to-large applied voltages.

SUMMARY AND CONCLUSION

This paper reports comparison tests of nickel versus aluminum and iron cathodes with platinum used as the anode in light water (H_2O) solutions. Several sources of erroneous false positive excess heat, which can occur

[i]At the ILENR2 Conference, Dr. George Miley suggested that reported transmutations might proceed in the region beyond the π-notch.

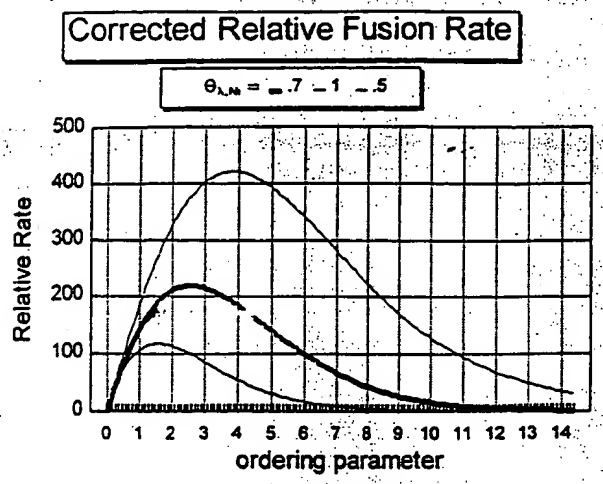

Fig. 6. Biphasic character of power amplification factor and the Q1D model of loading. These curves show the corrected expected fusion rate derived by the Q1D model of loading. Various loading parameters were examined (Θ_{Ni}), and there results a series of parametric curves. These curves demonstrate a biphasic output in the relative rate of the expected reaction as function of the ordering parameter [proportional to the voltage (V_{cell}) if all other factors are equal].

under uncontrolled conditions, including nickel colloid generation, recombination, and analytic errors, have been ruled out. When careful observation is made of some samples of nickel under controlled low-to-moderate current density, cathodic conditions excess heat is observed. When nickel wire was used as the cathode, there was power amplification in the range of $1.44^{\pm 0.58}$. When cold worked nickel spiral cathodes with platinum foil anodes was used, the power amplification was in the range of $2.27^{\pm 1.02}$. Neither iron nor aluminum demonstrated excess heat.

A notch or plateau is observed in the curve of power gain versus power input and is important because it may account for some of the wide-spread difficulties in observing the phenomena. The exponential falloff of the output with increasing electric potential may be consistent with the Q1D model of isotope loading. Although the Q1D model of isotope loading does not explain exactly the nature of these reactions, it—and the observed π-notch—begin to explain when these reactions will not occur.

ACKNOWLEDGMENTS

The author thanks J. Driscoll, S. Olasky, S. Baer, and K. Johnson for some of the nickel samples and the gracious loan of some equipment to make these experiments possible. Also, I. Straus, G. Dash, P. Hagelstein, K. Johnson, T. Stolper, M. Zahn, S. Baer, A. Kleiner, R. Kurzweil, L. Smullin, and especially G. Verner have continued to make very helpful comments, encouragement, and suggestions throughout this work and the development of this model. Their support is greatly appreciated.

NOMENCLATURE

A	= area (cm^2)
B_D	= diffusivity (cm^2/s)
C_{P,H_2O}	= specific heat water, light water [J/(K·mol)]
$[D]$	= deuteron concentration (mol/cm^3)
$[D]_i$	= initial deuteron concentration (mol/cm^3)
E	= energy (J)
E	= electric field intensity (V/m)
$E_{out} - E_{in}$	= incremental energy (J)
E_{out}/E_{in}	= relative energy gain (nondimensional)
F	= Faraday (96484.56 C/mol)
I	= electrical current (A)
J_e	= deuterons entering cathode [$mol/(cm^2 \cdot s)$]
J_f	= deuterons crossing surface to participate in fusion reactions [$mol/(cm^2 \cdot s)$]
J_g	= deuterons evolving to gas [$mol/(cm^2 \cdot s)$]
k_B	= Boltzmann constant (J/K)
k_C	= thermal conductive coefficient [$J/(cm^2 \cdot s \cdot K)$]
k_R	= radiative conductive coefficient [$J/(cm^2 \cdot s \cdot K^4)$]
L	= length (cm)
L_{H_2O}	= enthalpy of evaporation for water (J/mol)
$\sum M^i$	= mass of all sensors, probes, leads, etc.
M_0	= mass of solution in compartment 1
M_{Z12}	= mass of barrier between rings 1,2 (g)
$P_{ambient}$	= ambient partial pressure (Torr)
$P_{electrolysis}$	= ohmic control heat (W)
P_h	= heater power (W)
P_{H_2O}	= partial pressure of water (Torr)
P_{in}	= input power ($= V * I$) (W)
$P_{out} - P_{in}$	= incremental power (W)
P_{out}/P_{in}	= power amplification (nondimensional)
P_x	= excess enthalpy = P_{excess} (W)
q	= electric charge (C)
T	= temperature (K)
T_1	= temperature inner ring (K)
T_2	= temperature second ring (K)

$u_{-1}(t)$ = Heaviside function (nondimensional)

V_{cell} = potential across electrochemical cell (V)

$V_{thermoneutral}$ = thermoneutral potential (1.48 V)

Y_{12} = combined thermal coefficient (conductive and linearized radiative) [J/(cm^2·s·K)]

Greek

α_1 = increased thermal capacity in first ring due to electrodes, etc. [J/(K·mol)]

$\Delta\theta$ = $T_1 - T_2$ = delta-T (K)

$\Delta F^0(H_2O)$ = standard free enthalpy water (J)

$\Delta G^0(H_2O)$ = standard free energy water (J)

ΔT = change in T during Δt (K)

Δt = increment in time (s)

γ_{12} = thermal capacity of barrier between rings 1 and 2 [J/(K·mol)]

ζ = electrical order/thermal disorder ratio (nondimensional)

θ = used in some calorimetric equations for temperature (K)

$\vartheta_{\lambda,Ni}$ = loading potential characteristic (1/V)

κ_1 = first exponential factor for π_{Ni}

κ_2 = second exponential factor for π_{Ni}

λ_{Ni} = loading ratio (nondimensional)

μ_D = electrophoretic mobility [cm^2/(V·s)]

Π_{Ni} = peak power amplification factor (nondimensional)

π_{Ni} = power amplification factor (nondimensional)

σ_{SB} = Stefan-Boltzmann constant [J/(cm^2·s·K^4)]

Φ = potential = −V (volts)

Ψ_{fus} = deuterons involved (nondimensional)

REFERENCES

1. R. L. MILLS and S. P. KNEIZYS, "Excess Heat Production by the Electrolysis of an Aqueous Potassium Carbonate Electrolyte and the Implications for Cold Fusion," *Fusion Technol.*, **20**, 65 (1991).

2. V. C. NONINSKI, "Excess Heat During the Electrolysis of a Light Water Solution of K_2CO_3 with a Nickel Cathode," *Fusion Technol.* (1991).

3. R. NOTOYA, Y. NOYA, and T. OHNISHI, "Tritium Generation and Large Excess Heat Evolution by Electrolysis in Light and Heavy Water-Potassium Carbonate Solutions with Nickel Electrodes," *Fusion Technol.*, **26**, 179 (1993); see also R. NOTOYA, "Alkali-Hydrogen Cold Fusion Accompanied by Tritium Production on Nickel," *Trans. Fusion Technol.*, **26**, *4T*, Part 2, 205 (1994).

4. T. OHMORI and M. ENYO, "Excess Heat Evolution During Electrolysis of H_2O with Nickel, Gold, Silver, and Tin Cathodes," *Fusion Technol.*, **24**, 293 (1993).

5. T. MATSUMOTO, "Cold Fusion Observed with Ordinary Water," *Fusion Technol.*, **17**, 490 (1990); see also T. MATSUMOTO, "Cold Fusion Experiments with Ordinary Water and Thin Nickel Foil," *Fusion Technol.*, **24**, 296 (1993).

6. R. T. BUSH and R. D. EAGLETON, "Evidence for Electrolytically Induced Transmutation and Radioactivity Correlated with Excess Heat in Electrolytic Cells with Light Water Rubidium Salt Electrolytes," *Trans. Fusion Technol.*, **26**, *4T*, Part 2, 431 (1994); see also R. T. BUSH, "A Unifying Model for Cold Fusion," *Trans. Fusion Technol.*, **26**, *4T*, Part 2, 431 (1994).

7. M. SRINIVASAN et al., "Tritium and Excess Heat Generation During Electrolysis of Aqueous Solutions of Alkali Salts with Nickel Cathode," *Frontiers of Cold Fusion*; see also H. IKEGAMI, Ed., *Proc. 3rd Int. Conf. Cold Fusion*, Tokyo, Japan, October 21–25, 1992, p. 123, Universal Academy Press (1992).

8. M. SWARTZ, "The Relationship Between Input Power and Enthalpic Behavior of Nickel Cathodes During Light Water Electrolysis," *Fusion Technol.* (submitted for publication).

9. M. SWARTZ, "Quasi-One-Dimensional Model of Electrochemical Loading of Isotopic Fuel into a Metal," *Fusion Technol.*, **22**, 296 (1992).

10. M. SWARTZ, "Generalized Isotopic fuel Loading Equations," *Cold Fusion Source Book: Int. Symp. Cold Fusion and Advanced Energy Systems*, H. FOX, Ed., Minsk, Belarus, May 1994 (1994).

11. M. SWARTZ, "Isotopic Fuel Loading Coupled to Reactions at an Electrode," *Trans. Fusion Technol.*, **26**, *4T*, Part 2, 74 (1994).

12. K. JOHNSON, "Jahn-Teller Symmetry Breaking and Hydrogen Energy in PdD 'COLD FUSION' as Storage of the Latent Heat of Water," *Trans. Fusion Technol.*, **26**, *4T*, Part 2, 427 (1994); see also B. M. KLEIN and R. E. COHEN, "Anharmonicity and the Inverse Isotope Effect in the Palladium-Hydrogen System," *Phys. Rev. B*, **45**, *21*, 405 (1992).

13. A. KIMURA and H. K. BIRNBAUM, "Effect of Adsorbed Surface Poisons on the Loss of Hydrogen from Nickel," *Acta Metall. Mater.*, **39**, *3*, 295 (1991).

14. M. FLEISCHMANN and S. PONS, "Calorimetry of the Pd-D_2O System: From Simplicity Via Complications to Simplicity," *Phys. Lett. A*, **176**, 118 (1993); see also M. FLEISCHMANN and S. PONS, "Some Comments on the Paper

'Analysis of Experiments on Calorimetry of LiOD/D_2O Electrochemical Cells,'" *J. Electroanal. Chem.*, **332**, 1 (1992); *J. Electroanal. Chem.*, **332**, 33 (1992).

15. M. SWARTZ, "Thermal Conduction and Non-Differential Temperature Corrections to the Enthalpic Flow Equation," *Phys. Lett. A* (submitted for publication).

16. M. SWARTZ, "Possible Deuterium Production from Light Water Excess Enthalpy Experiments Using Nickel Cathodes," *J. New Energy*, **1**, *3* (1996).

17. M. R. SWARTZ, L. SCHNIPPER, A. LEWIN, and C. CRUMPACKER "Inactivation of Herpes Simplex Viruses with Methylene Blue, Light and Electricity," *Proc. Soc. Experimental Biology and Medicine*, **161**, 204 (1979).

18. M. SWARTZ, "A Method to Improve Algorithms Used to Detect Steady State Excess Enthalpy," *Trans. Fusion Technol.*, **26**, *4T*, Part 2, 369 (1994).

19. M. MELICH and W. N. HANSEN, "Some Lessons from 3 Years of Electrochemical Calorimetry," *Proc. 4th Int. Conf. Cold Fusion*, Maui, Hawaii, December 6–9, 1993 (1993).

20. M. SWARTZ, "Some Lessons from Optical Examination of the PFC Phase-II Calorimetric Curve," *Proc. 4th Int. Conf. Cold Fusion*, Maui, Hawaii, December 6–9, 1993, Vol. 2 (1993).

21. M. SWARTZ, "Definitions of Power Amplification Factor Used to Describe Enthalpy Production," *J. New Energy*, **1**, 2, 54 (1996).

22. H. H. UHLIG, *Corrosion and Corrosion Control*, Wiley, New York (1971).

23. J. O'M. BOCKRIS and K. N. REDDY, *Modern Electrochemistry*, Plenum Press, New York (1970).

24. R. B. ADLER, R. M. FANO, and L. J. CHU, *Electromagnetic Energy Transmission and Radiation*, Wiley, New York (1966).

25. R. M. FANO, L. J. CHU, and R. B. ADLER, *Electromagnetic Fields, Energy, and Forces*, Wiley, New York (1967).

26. M. FLEISCHMANN and S. PONS, "Electrochemically Induced Nuclear Fusion of Deuterium," *J. Electroanal. Chem.*, **261**, 301, and Erratum, **263**, 187 (1989); see also M. FLEISCHMANN, S. PONS, M. W. ANDERSON, L. J. LI, and M. HAWKINS, "Calorimetry of the Palladium-Deuterium-Heavy Water System," *J. Electroanal. Chem.*, **287**, 293 (1990).

27. M. H. MILES, R. A. HOLLINS, B. F. BUSH, J. J. LAGOWSKI, and R. E. MILES, "Correlation of Excess Power and Helium Production During D_2O and H_2O Electrolysis Using Palladium Cathodes," *J. Electroanal. Chem.*, **346**, 99 (1993); see also M. H. MILES and B. F. BUSH, "Heat and Helium Measurements in Deuterated Palladium," *Trans. Fusion Technol.*, **26**, *4T*, Part 2, 156 (1994).

28. F. G. WILL, K. CEDZYNSKA, and D. C. LINTON, "Tritium Generation in Palladium Cathodes with High Deuterium Loading," *Trans. Fusion Technol.*, **26**, *4T*, Part 2, 209 (1994); see also "Reproducible Tritium Generation in Electrochemical Cells Employing Palladium Cathodes with High Deuterium Loading," *J. Electroanal. Chem.*, **360**, 161 (1993).

29. E. STORMS and C. TALCOTT, "Electrolytic Tritium Production," *Fusion Technol.*, **17**, 680 (1990).

30. P. GRANEAU, "The Role of Ampère Forces in Nuclear Fusion," *Phys. Lett. A*, **165**, 1 (1992); see also P. GRANEAU, "The Role of Ampère Forces in Nuclear Fusion," *Phys. Lett. A*, **165**, 1 (1992).

31. I. B. SAVVATIMOVA, Ya. R. KUCHEROV, and A. B. KARABUT, "Cathode Material Change After Deuterium Glow Discharge Experiments," *Trans. Fusion Technol.*, **26**, *4T*, Part 2, 389 (1994).

32. X. Z. LI, G. S. HUANG, D. W. MO, and B. Y. LIAW, "The Analysis of the Neutron Emission from the Glow Discharge in Deuterium Gas Tube and the Gas Loading in Palladium," *Trans. Fusion Technol.*, **26**, *4T*, Part 2, 384 (1994).

33. F. A. COTTON and G. WILKINSON, *Advanced Inorganic Chemistry*, Interscience Publishers, New York (1972).

34. A. VON HIPPEL, *Dielectric Materials and Applications*, The MIT Press, Cambridge, Massachusetts (1954); see also A. VON HIPPEL, D. B. KNOLL, and W. B. WESTPHAL, "Transfer of Protons Through 'Pure' Ice I_h Single Crystals," *J. Chem. Phys.*, **54**, *134*, 145 (1971).

35. J. R. MELCHER, *Continuum Electromechanics*, The MIT Press, Cambridge, Massachusetts (1981).

36. M. SWARTZ, "The Relative Impact of Thermal Stratification of the Air Surrounding a Calorimeter," *J. New Energy*, 1, 2, 141 (1996).

Mitchell R. Swartz [BS and MS, electrical engineering, Massachusetts Institute of Technology (MIT), 1971; MD, Harvard, 1978; ScD, MIT, 1984] is a senior research scientist at JET Energy Technology, Inc., where he is responsible for the development of quality-control procedures in calorimetric analysis and material fabrication. His specialties include the interaction of radiation and matter, and his current research interests investigate phonon spectra and material changes during loading.

COLD "FUSION": THE TRANSMISSION RESONANCE MODEL FITS DATA ON EXCESS HEAT, PREDICTS OPTIMAL "TRIGGER" POINTS, AND SUGGESTS NUCLEAR-REACTION SCENARIOS

MITCHELL R. SWARTZ, M.D.
16 PEMBROKE ROAD
[illegible]TON, MASS. 02193

Robert T. Bush
Physics Department
California State Polytechnic University
3801 West Temple Avenue
Pomona, CA 91768

Abstract: The transmission resonance model (TRM) previously introduced is now combined with some electrochemistry of the cathode surface and found to provide a good fit to new data on excess heat. For the first time, a model for cold fusion not only fits calorimetric data, but also predicts optimal "trigger" points. This suggests both that the model is meaningful and that the excess heat phenomenon claimed by Pons and Fleischmann is genuine. A crucial role is suggested for the "overpotential" and, in particular, for the "concentration overpotential"; i.e., the "hydrogen overvoltage". "Self-similar geometry", or "scale invariance", i.e., a "fractal" nature, is revealed by the relative excess power function. Heat "bursts" are predicted with a scale invariance in time, suggesting a link between the TRM and Chaos Theory. The model describes a near-surface phenomenon with an estimated excess power yield of about 1kW per cm^3 of palladium, as compared to 50W per cm^3 of reactor core for a good fission reactor. TRINT (Transmission resonance-induced nuclear transmutation), a new type of nuclear reaction, is strongly suggested with two types emphasized: Trint (transmission resonance-induced neutron transfer) reactions yielding essentially the same end result as Teller's hypothesized "catalytic neutron transfer", and a three-body reaction promoted by standing de Broglie waves. The cross-section, σ, for the nuclear reaction that is the ultimate source of the excess heat is estimated to satisfy $10^{-29}\ cm^2 \lesssim \sigma \lesssim 10^{-20}\ cm^2$. Suggestions for the "anomalous" production of heat, particles, and radiation are given. A "polarization conjecture" leads to a derivation of a branching ratio of 1.64×10^{-9} for the D-on-D reaction in electrolytic cold "fusion" in favor of tritium over neutrons. The model can account for the Bockris curve, in which a lower-level production of tritium mirrors that of excess heat. Heat production without tritium is also accounted for, as well as the possibility of tritium production without heat. Thus, the TRM has a high probability for unifying most, if not all, of the seemingly-anomalous effects associated with cold "fusion".

Letters

"Superbug" Evidence

We are writing with concern about the tone of the article "Superbug attacks California crops" by Elizabeth Culotta (News & Comment, 6 Dec., p. 1445), which dealt with the new strain of the sweet potato whitefly, *Bemisia tabaci* (Gennadius). While we are in sympathy with the growers in California's Imperial Valley because they certainly suffered significant crop losses during the fall of 1991, we are not convinced that all the statements being made about the whitefly's biology are well grounded in fact, nor are we certain that these losses are attributable entirely to the presence of a new whitefly strain.

Our principal concern is that the distinction between hypothesis and fact be made clear. There have been reports of "increased" polyphagy, but no experimental tests have yet been published on the degree of polyphagy of either strain. It is an exaggeration to cite "over 500 plants . . ." as a host range for the poinsettia strain of the whitefly when this represents the total published feeding records for the entire species worldwide over the last 100 years. Furthermore, the cropping system in the southwest desert valleys of the United States is dominated by approximately a dozen cultivated plant species, so the matter of absolute degree of polyphagy appears to have little to do with the current problem. In particular, references to a narrow degree of polyphagy in the "cotton" strain in comparison to a wider degree of polyphagy in a "poinsettia" strain are unsubstantiated by published experimental evidence.

Such hyperbole places at risk the measured assessment and reporting of the species' biology by allowing readers to believe that we already know more than we do. The promotion of a "Paul Bunyanesque" mythical insect of the Old West that is sucking the Southland dry and carries away entire melons to feed its young does not advance our understanding of the situation. We know that changes are taking place, but we need to carefully examine what those changes are.

DAVID N. BYRNE
Department of Entomology, University of Arizona, Tucson, AZ 85721
THOMAS S. BELLOWS
Department of Entomology, University of California, Riverside, CA 92521

Response: My article clearly stated that the crucial next step is to verify the identity of the whitefly problem strain. The article's tone reflects the atmosphere of crisis surrounding the whitefly. The pest triggered a state-of-emergency declaration in two California counties and has cost $118 million to date in those counties, according to the California Department of Food and Agriculture. To say merely that there are "changes" in the whitefly situation does not reflect what most scientists in California agriculture consider a very serious problem.

—ELIZABETH CULOTTA

Free-Electron Laser

The effort to demonstrate the applicability of free-electron lasers (FELs) to lithography described in the item "From star wars to chip wars" (ScienceScope, 22 Nov., p. 1099) is a collaboration between Los Alamos National Laboratory, Motorola, and Texas Instruments; Sandia National Laboratory is not involved. However, Los Alamos and Sandia *are* working together to explore the utility of a broadly based Department of Energy laboratory–industry collaboration to develop some of the manufacturing tools and technologies that the "Microtech 2000" study recommends. The goal of "Microtech 2000" is to develop the set of manufacturing technologies needed by industry by the year 2000 and is not limited to light source technology for chip production (which isn't perceived to be the greatest challenge). To have the FEL described as being "politically well connected" surprises us, but we take it as a compliment from those who are. Matters of commercial viability are yet to be determined for all of the newer approaches to microlithography.

SIDNEY SINGER
Program Director, Directed Energy Science Technology, Los Alamos National Laboratory, Los Alamos, NM 87545

Cold Fusion: China Lake Results

Gary Taubes, in his article about Martin Fleischmann's cold fusion seminar at the California Institute of Technology (News & Comment, 13 Dec., p. 1582), states that "researchers working with the China Lake group have said that those observations . . . could be explained by helium-4 contamination from the ambient atmosphere." We are basically a two-man group with respect to cold fusion research at China Lake and neither of us h such a statement. To my knowle ther has anyone else at China La any such statement.

Regarding our report of time-c measurements of excess heat an (*1*), the simple yes-or-no detectio um-4 in eight of eight experiment ing excess heat and the absence of in six of six control experiments ducing excess heat (one in D_2C H_2O) implies a chance probabilit $(1/2)^{14}$ = 1/16,384 or 0.00619 attributing our results to atmosph tamination should try to flip a c they obtain a predetermined seq volving 14 tosses. Furthermore, t iments at China Lake producing er amounts of excess enthalpy yi larger amounts of helium-4. Ou experiments show that atmosph tamination is a highly unlikely ex for our results.

MELVIN
Weapons
Naval Air Warfa
China Lake,

REFERENCES

1. B. F. Bush *et al.*, *J. Electroanal. Che* (1991).

Museums: Storehouses of DN

Traditional museum collection brates and other organisms incre being viewed by molecular bi valuable storehouses of DNA (*1*) ifying that new uses have been fo specimens; however, the privile pling specimens is accompanied sponsibility of supporting the m and growth of museums.

Removing fragments of tis bone, or feathers from museum for DNA analysis is destructive. focus on the phylogeny and characteristics of rare and exti exacerbates the problem because of these species, once destroyed be replaced. For example, if pre continue, museum holdings of cies (for example, Hawaiian h ers) will be gradually picked t researchers. Museum specime only be sampled when fresh truly unavailable or when mus mens can add a legitimate h perspective. Fresh tissue should ed and used in molecular resear er possible because it yields h DNA that is much less prone to

J. Electroanal. Chem., 332 (1992) 33–53
Elsevier Sequoia S.A., Lausanne
JEC 02250

Some comments on the paper Analysis of Experiments on Calorimetry of $LiOD/D_2O$ Electrochemical Cells, R.H. Wilson et al., J. Electroanal. Chem., 332 (1992) 1 *

M. Fleischmann

Department of Chemistry, University of Southampton, Highfield, Southampton, SO9 5NH (UK)

S. Pons

Department of Chemistry, University of Utah, Salt Lake City, UT 84112 (USA)

(Received 26 March 1992; accepted 1 May 1992)

Abstract

We comment here on the title paper and find that it is a series of misconceptions and misrepresentations of previous reports by Fleischmann, Pons and co-workers. It is shown that the conclusions reached by the authors lead to gross errors in the prediction of the observed responses of the electrochemical calorimeters described in the original work and that the correct methods of analyses are indeed those we originally described as well as those which have been outlined in subsequent publications. We find that the authors have not validated their own methods and have not provided sufficient information to allow assessment of their work.

INTRODUCTION

In our major paper on the calorimetry of Pd cathodes polarized in D_2O [2] we used two methods of evaluating the excess enthalpy generated in these systems (above that which can be attributed to the enthalpy input) that designated:

"Approximate specific Q_{excess}/W cm^{-3}" (Method 1)

"Specific Q_{excess} from regression analysis/W cm^{-3}" (Method 2).

* Ref. 1.

In two further papers on the subject [3–6] we have used additionally:

'Point by point evaluation of Q_{excess}" (Method 3)

'Kalman filtering" (Method 4)

ınd Kalman filtering has also been used in an independent evaluation of some of he data which we collected at the National Cold Fusion Institute (NCFI), Salt ake City [7]; see also ref. 8.

The major claim made in the paper by Wilson et al. [1] is that the calibration of ıur calorimeters as used in Method 1 was in error and, in particular, that we ıverestimated the heat transfer coefficients of the cells and therefore also Q_{excess}. n making this claim, the authors have devised a further method of data treatment vhich we will designate:

'General Electric (GE) approximate method of data analysis" (Method 5)

ınd for the purposes of this paper, we will also designate a further method which s based on the estimation of a lower bound of k'_R:

'Complete distrust of all methods of calibration" (Method 6).

The authors further report that they have made extensive sets of calorimetric neasurements and that these did not give excess enthalpies for any of their xperiments.

In the present comment we show that the GE method (Method 5) and our own pproximate method (Method 1) are, in fact, equivalent although they estimate the hermal balance at different times along the temperature ($\Delta\vartheta$)–time (t) profile. loth are based on the application of the "steady-state hypothesis" to the differen- ial equations which model the calorimeters. This approach is known to give results f only limited accuracy in other fields of research (although Method 1 would be xpected to be somewhat more accurate than Method 5). We show here again :ompare refs. 2–10) that accurate estimates of the heat transfer coefficients and f the excess enthalpy (as well as of the other parameters of the models) must be ased on the comparison of the integrated forms of the differential equations with ıe experimental data, and we comment on some other issues raised in the critique 1]; more detailed comments will be given elsewhere [9].

HE DESIGN AND MODELLING OF THE CALORIMETERS

In the experiments which we carried out up to October 1989 (and which formed ıe basis of our first full-length publication [2]) we used a range of Dewar-type lectrochemical cells of various sizes so as to achieve a range of heat transfer rates. Ve no longer have the full range of these cells to hand but drawings approximately) scale of cells close to the smallest and largest of those made in 1988 are shown ı Figs. 1(A) and (B). The cells were designed to allow accurate measurements to e made at enthalpy inputs lying in the range 0.1–4 W. However, because of ıadequate evacuation of the "vacuum gap" the heat transfer rates were up to ouble those predicted from the Stefan Boltzmann coefficient and the radiant ırface area, as has also been noted by the group at GE [1], i.e. these rates lay in

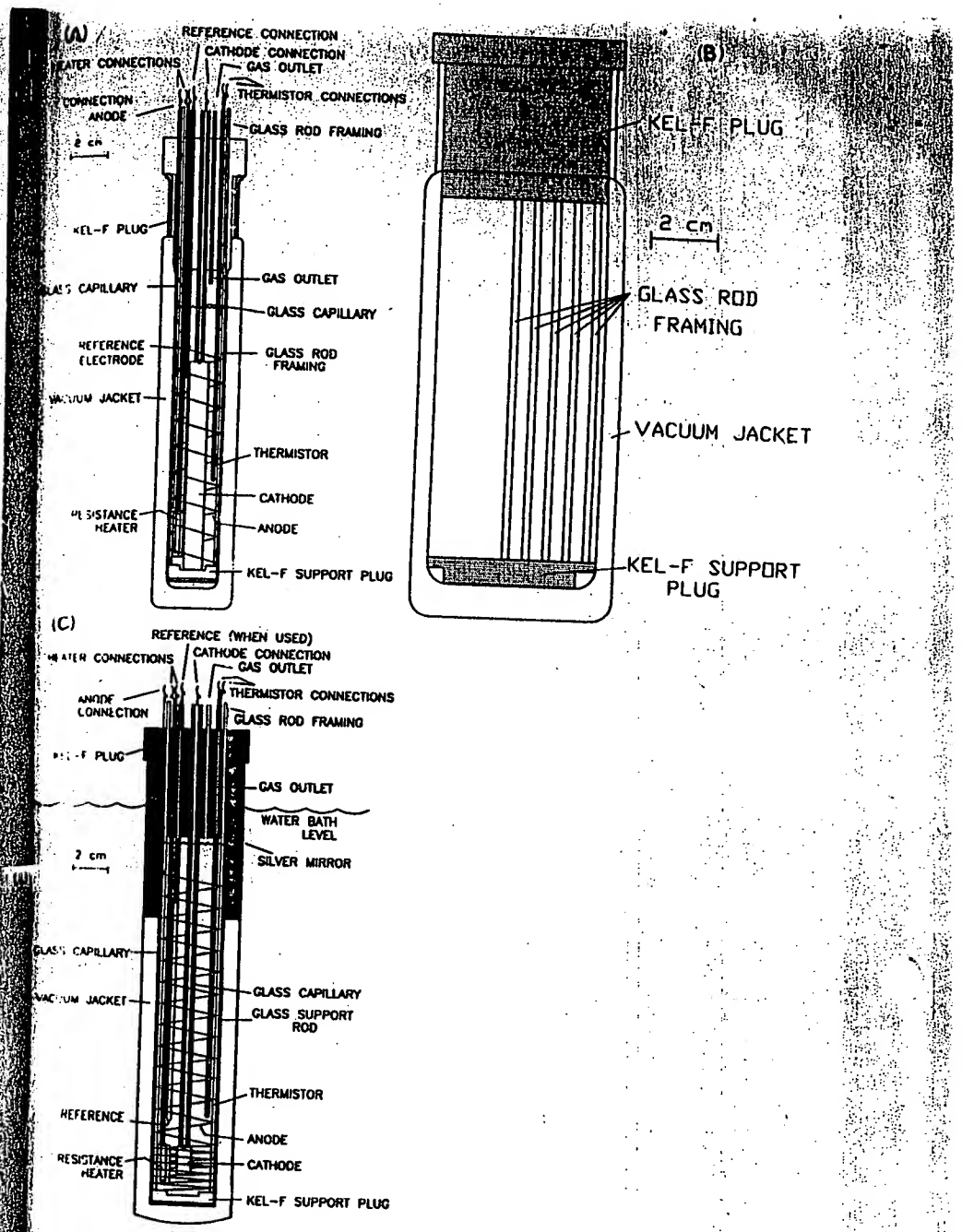

Fig. 1. Single compartment vacuum Dewar calorimeter cells used in 1988 and 1989. (A) small and (B) arge calorimeters with mixed conductive and radiative heat transfer; (C) silvered calorimeter character- ed by radiative heat transfer.

the range 0.2–8 W. Our specification of "accurate measurements" was that all measured changes in temperature should exceed 2°C when these temperatures were measured to ±0.01°C and that the cell temperatures should not exceed 50°C when that of the surrounding water baths was 30°C. The lowering of the thermostat temperature to 15°C or 5°C allowed us to achieve enthalpy inputs up to 19 W while still restricting the cell temperature to 50°C.

In practice, the projected performance had to be somewhat degraded because the pressure of events at that time (and since then also!) forced us to restrict measurements to the lower end of the size range of our cells. This in turn meant that we had to accept data collected at cell temperatures up to 60°C for parts of the work reported in ref. 2.

In our experiments carried out since October 1989 we have made a simple modification to some of our cells; this is shown in Fig. 1(C). Although this change is simple, it has a marked effect on the modelling: the silvering of the top section of the Dewars ensures that heat transfer is confined mainly to the lower, unsilvered, portion; the time dependence of the heat transfer rates found with cells of the type shown in Figs. 1(A) and (B) (due to the progressive electrolysis of the contents of the Dewars) is thereby markedly reduced. This has allowed the development and application of a particularly simple model which contains no arbitrary parameters [3–7,10]. At the same time, the more effective evacuation of the Dewar gap has given cells whose heat transfer coefficients have been lowered to values close to those predicted for radiation alone. This, combined with the use of Pd-alloy electrodes showing high Q_{excess}, has led to the operation of cells up to the boiling point. The evaporation of the solvent has therefore had to be taken into account in a more detailed manner [3–7,10] than in the earlier work [2] (compare eqns. (1) and (2) with eqn. (3) below).

The models for the various calorimeters can be represented conveniently by the appropriate differential equations predicting the changes with time (t/s) of the difference in temperature ($\Delta\vartheta$/K) between the cell contents and the thermostat bath. Thus, in our work up to October 1989 we have used:

$$\underbrace{C_{P,D_2O,l}M^\circ\left[1-\frac{(1+\beta)It}{2FM^\circ}\right]\frac{d\,\Delta\vartheta}{dt}-C_{P,D_2O,l}M^\circ\frac{(1+\beta)I\,\Delta\vartheta}{2FM^\circ}}_{\text{change in the enthalpy content of the calorimeter}}$$

$$=\underbrace{[E_{cell}(t)-E_{thermoneutral,cell}]I}_{\text{enthalpy input due to electrolysis}}$$

$$-\frac{I}{F}\left\{\underbrace{\left[0.5C_{P,D_2}+0.25C_{P,O_2}+0.75\left(\frac{P}{P^*-P}\right)C_{P,D_2O,g}\right]\Delta\vartheta+0.75\left(\frac{P}{P^*-P}\right)L}_{\text{enthalpy content of the gas stream}}\right\}$$

$$+\underbrace{Q_f(t)}_{\text{excess enthalpy}}+\underbrace{\Delta QH[t-t_1]-\Delta QH[t-t_2]}_{\text{calibration pulse}}$$

$$-\underbrace{k_R^0\vartheta_{bath}^3\left[1-\left(\frac{(1+\lambda)It}{2FM^\circ}\right)\right]}_{\substack{\text{time dependent}\\ \text{heat transfer coefficient}}}\left\{\underbrace{\left[\frac{(\vartheta_{bath}+\Delta\vartheta)^4-\vartheta_{bath}^4}{\vartheta_{bath}^3}\right]}_{\text{effect of radiation}}+\underbrace{4\Phi\,\Delta\vartheta}_{\text{effect of conduction}}\right\} \quad (1)$$

(A3.7 of ref. 2)

Such an equation is naturally already based on a number of inbuilt assumptions, e.g. here the fact that heat transfer across any given element of the calorimeter surface is in a quasi-steady state and that the current efficiency for gas production is unity. Such points do not appear to be at issue. However, Wilson et al. [1] have modified the modelling somewhat by introducing second order small quantities which subsequently they show to be of such second order small character.

In eqn. (1) the term $[1-(1+\beta)It/2FM^\circ]$ allows for the change of the heavy water equivalent of the calorimeter with time: the system is "open" so that the cell contents decrease progressively with time. The term β was introduced to allow for a more rapid decrease than would be given by electrolysis alone (exposure of solid components of the cell contents, D_2O vapour carried off in the gas stream) but, as expected, the effects of β on Q_f and k_R^0 could be neglected for temperatures below ≈ 60°C. Similarly, the term $[1-((1+\lambda)It/2FM^\circ)]$ allows for the decrease in the radiant surface area with time. In this case, the term λ must be retained, again as expected.

We take note here also of a further approximation which we have used throughout our work. We have set the term Φ, which accounts for the heat loss from the calorimeters by conduction equal to zero and have increased the radiative heat transfer coefficient k_R^0 to k_R' to allow for this assumption. In Appendix 2 [2] we showed that this leads to a small systematic underestimate of $Q_f(t)$. At the same time the random errors of the estimations are decreased markedly because the number of parameters to be fitted is reduced by one and because we do not need to make separate estimates of the radiative and conductive terms from the calibration pulse $\Delta QH(t-t_1)-\Delta QH(t-t_2)$. We note here that the system is normally calibrated using this pulse although it is also possible to do this using the perturbation produced by the "topping up" of the cells with D_2O to make up the losses due to electrolysis and evaporation [3–7,10] (this term has not been included in any of the equations used here).

We have also used throughout the thermoneutral potential at the temperature of the water bath as the reference value and we arrive at the differential equation which we used extensively in our work up to October 1989:

$$C_{P,D_2O,l}M^\circ\left[1-\frac{It}{2FM^\circ}\right]\frac{d\,\Delta\vartheta}{dt}$$

$$=[E_{cell}(t)-E_{thermoneutral,bath}]I+Q_f(t)+\Delta QH[t-t_1]$$

$$-\Delta QH[t-t_2]-\frac{3I}{4F}\left[\frac{P}{P^*-P}\right]\left[(C_{P,D_2O,g}-C_{P,D_2O,l})\Delta\vartheta+L\right]$$

$$-k_R'\left[1-\frac{(1+\lambda)It}{2FM^\circ}\right]\left[(\vartheta_{bath}+\Delta\vartheta)^4-\vartheta_{bath}^4\right] \quad (2)$$

We point out that this equation is not to be found in ref. 2 as we have there introduced some further steps in going from eqn. (A3.7) to eqn. (A5.1).

The use of the calorimeter illustrated in Fig. 1(C) allows us to assume that the heat transfer coefficients are independent of time at the first level of approximation. We have also allowed in greater detail for the D_2O vapour carried off in the gas stream (since these cells have been used at temperatures up to the boiling point) and we have formulated the behaviour in terms of an equation which contains no arbitrary parameters:

$$C_{P,D_2O,l}\left[M^\circ - \frac{I}{4F}\int_0^t\left(\frac{2P^* + P}{P^* - P}\right)\mathrm{d}t\right]\frac{\mathrm{d}\,\Delta\vartheta}{\mathrm{d}t}$$
$$= [E_{cell}(t) - E_{thermoneutral,bath}]I + Q_f(t) + \Delta QH[t - t_1] - \Delta QH[t - t_2]$$
$$- \frac{3I}{4F}\left(\frac{P}{P^* - P}\right)\left[(C_{P,D_2O,g} - C_{P,D_2O,l})\,\Delta\vartheta + L\right] - k'_R\left[(\vartheta_{bath} + \Delta\vartheta)^4 - \vartheta^4_{bath}\right]$$

(3)(A2.3 of ref. 3)

However, although the major effect of the "sloping base line" has been markedly reduced, it is still present to some extent. We have therefore also used the equation with k'_R replaced by $k'_R[1 - (1 + \lambda)It/2FM^\circ]$ (see eqn. (A4.1) of ref. 3).

METHODS OF DATA EVALUATION

The central assumption in the paper by Wilson et al. [1] is that one can assume the systems to be in a steady state at the point in time at which they are calibrated (25 990 s for the simulations given in Fig. 2) and at which the values of Q_f are to be evaluated. In point of fact there is no such steady state (neither for $\Delta\vartheta$ nor for E_{cell}) as can be seen from Fig. 2 and from Fig. 1 of the paper by Wilson et al. [1] (this figure is the same as Fig. 3A of our main paper [2]). The magnitudes of terms $M^\circ C_{P,D_2O,l}(\mathrm{d}\,\Delta\vartheta/\mathrm{d}t)$ are in fact comparable to those of the corrections to ΔQ introduced in deriving the heat transfer coefficients $(k'_R)_1$, $(k'_R)_2$, and $(k'_R)_3$ (see below).

It is well known in many fields of research that accurate values of the parameters of the differential equations which model the systems can only be obtained by comparing the integrated forms of the equations with the experimental data. An example of such a field is that of chemical kinetics where the "steady state approximation" has frequently been used to obtain approximate values of rate constants. However, these values are well recognized as being approximate and it is also recognized that it is not feasible then to use these values to make accurate determinations of the constant terms appearing in the equations. The analogy to the application of equations (1)–(3) will be apparent.

It can be seen therefore that we need to compare the integrated forms of these differential equations with the experimental data in order to obtain accurate values of Q_f. The difficulty which presents itself immediately is that the equations are non-linear and inhomogeneous; furthermore P is a non-linear function of ϑ and

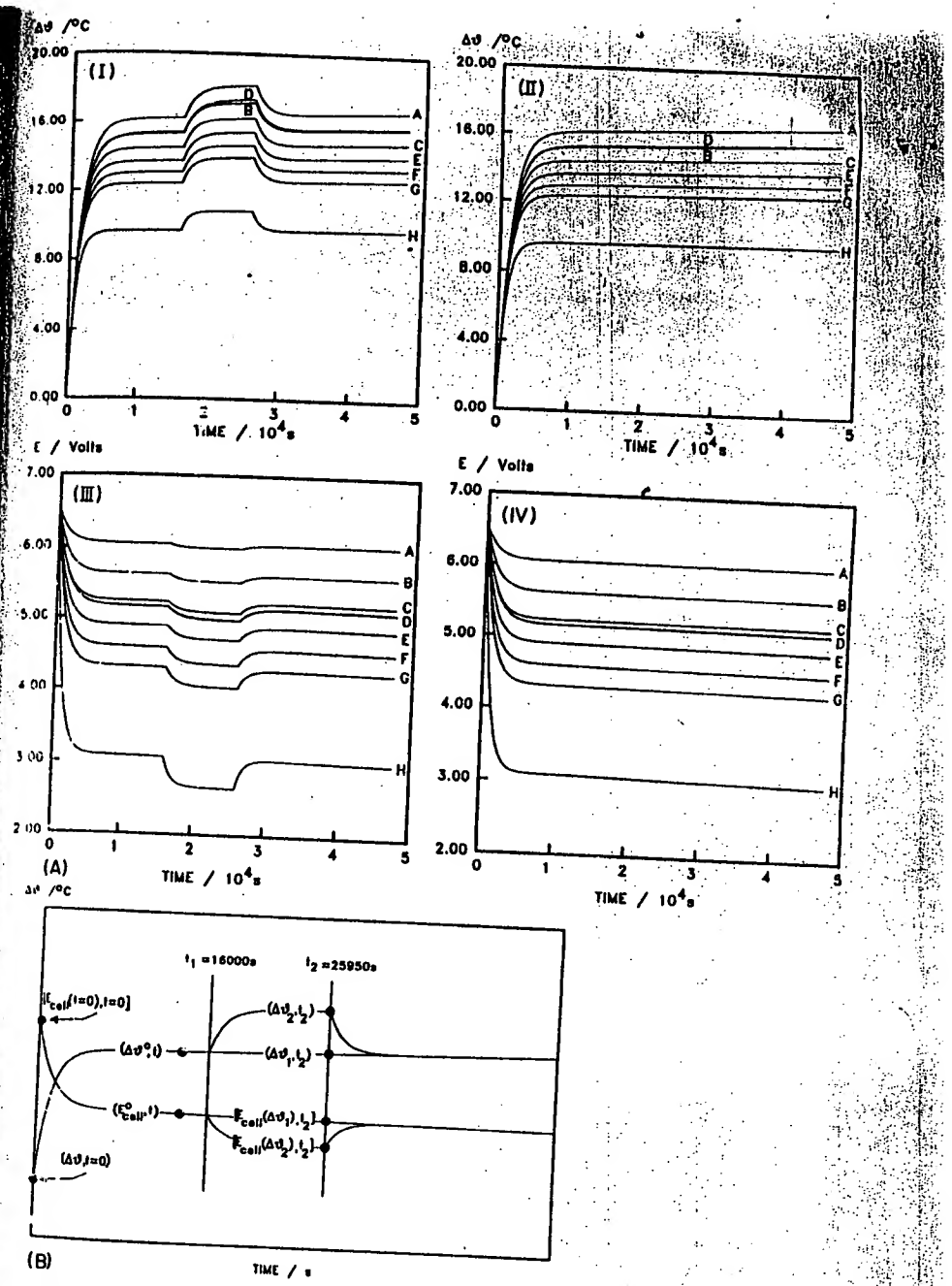

Fig. 2. (A) Simulated temperature–time and potential–time plots with and without a heater calibration pulse as a function of ψ/ϑ_{bath}: plots A = 0.03, plots B = 0.06, plots C = 0.09, plots D = 0.09 (using a linearized heat transfer coefficient), plots E = 0.12, plots F = 0.15, plots G = 0.18, plots H = 0.36. (B) Schematic diagram of the methodology used for the calculations. The points $(\Delta\vartheta_2, t_2)$; $(\Delta\vartheta_1, t_2)$; $[E_{cell}(\Delta\vartheta_1, t_2)]$; $[E_{cell}(\Delta\vartheta_2, t_2)]$; $(\Delta\vartheta = 0, t = 0)$; $[E_{cell}(t = 0), t = 0]$ were used for the calculations in Table 1 and the points $(\Delta\vartheta^\circ, t)$, (E°_{cell}, t) were used for the calculations in Appendix 4 of ref. 2.

$E_{cell}(t)$ is an unknown function of time, t. It is therefore next to impossible to develop analytical solutions of these equations (see further below and Appendices 3 and 4 of ref. 2). We have therefore used three strategies to develop "exact" methods of data evaluation:

first and foremost the comparisons of the numerical integrals of eqns. (1)–(3) with the experimental data using non-linear regression [2–6,10] (Method 2);

secondly, Kalman filtering of the data [4,6] which is also the basis of an independent evaluation of some of our data [7] (Method 4);

thirdly, point-by-point evaluation of Q_{excess} using heat transfer coefficients determined with Methods 2 and 4 [3–6,10] (Method 3).

Of these methods, 2 and 4 are undoubtedly more accurate than 3 but they do require the assumption that Q_f is constant during any given measurement cycle, a restriction which is lifted for Method 3. We note here that our preferred method of data processing is low pass filtering (such as Method 4), for reasons which will be given elsewhere [9]; we also note that some of our current work is concerned with the development of filters which allow the evaluation of the time dependence of Q_f in relaxation measurements.

Wilson et al. [1] do not deal with any of these evaluations: they regard Method 2, which was outlined in Appendix 5 of ref. 2 as "very complicated and very difficult to follow in detail". However, this method, together with low pass filtering, using, for example, the Kalman filter, is the standard method of modern data processing. The Kalman filters which have been used have been based on eqn. (3) (as well as on eqn. (A4.1) of ref. 3) which take full account of the evaporation of the solvent to within a few tenths of a percent: the assertion that we did not take this into account [1] can be seen to be incorrect; these terms were omitted in the evaluation of the results given in ref. 2 because of the restriction of the cell temperatures in those experiments (see further below). We observe that the results of the independent investigation using Kalman filtering [7] were presented to the group at GE during 1991; their omission of reference to this work shows that they also reject this method of data processing in addition to Method 2.

We are therefore reduced to examining the claim that the method put forward by Wilson et al. [1], Method 5, provides an accurate means of evaluating Q_f. The authors imply that as the results obtained by their Method 5 differ from those obtained by our own approximate method, Method 1, it is our method which must be judged to be incorrect. It is therefore necessary to make a comparison of these two techniques and we do this using simulated data. Moreover, as the results of Methods 1 and 2 can be seen to be in close accord at low and intermediate values of the input enthalpy (see Table 3 of ref. 2 and also further below) Wilson et al. [1] also cast doubts on the validity of the application of non-linear regression methods. It is therefore necessary for us to make a comparison of our own approximate and exact Methods 1 and 2 and this comparison arises naturally from the interpretation of the simulated $\Delta\vartheta$–t plots.

We have used eqn. (2) as the starting point and have assumed that the cell temperatures are sufficiently low that we can neglect the heat flow due to evaporation of the solvent; the neglect of this term raises no new issue of principle. We have already pointed out above that the time dependence of E_{cell} cannot be specified a priori. We have therefore used the same approximation as that used in ref. 2, namely that we can carry out a Taylor series expansion of $E_{cell}(t)$ to give $E_{cell}(\vartheta)$. In order to simplify the problem as far as possible and to enhance the effects, we have here chosen this temperature to be ϑ_{bath} so that we can write

$$E_{cell}(t) = E_{cell}(t=0) + \psi/\vartheta_{bath}\,\Delta\vartheta \tag{4}$$

We point out, however, that in our earlier work this temperature was chosen to lie just before the application of the heater calibration $\Delta QH(t-t_1)$: $t_1 = 16000$ s in Fig. 2. We have also chosen the following simple values so that our calculations can readily be checked even with a pocket calculator:

$C_{P,D_2O,l} = 75\ \mathrm{J\ K^{-1}\ mol^{-1}}$
$M^\circ = 4$ mol
$E_{cell}(t=0) - E_{thermoneutral,bath} = 5$ V
$I = 0.4$ A
$Q_f = 1$ W
$\Delta Q = 0.36$ W
$k'_R = 1.5 \times 10^{-9}\ \mathrm{W\ K^{-4}}$
$\lambda = 1$
$\vartheta_{bath} = 300$ K
$E_{thermoneutral,batn} = 1.54$ V

and we designate Q_1 by

$$Q_1 = (E_{cell}(t=0) - E_{thermoneutral,bath})I + Q_f$$

and Q_5 by

$$Q_5 = (E_{cell}(t=t_2) - E_{thermoneutral,bath})I + Q_f$$

so that eqn. (2) becomes in standard form

$$\frac{\mathrm{d}\,\Delta\vartheta}{\mathrm{d}t} = \frac{10^{-2}}{1-(5\times10^{-2}t/F)} + \frac{0.36[H(t-t_1)-H(t-t_2)]}{1-(5\times10^{-2}t/F)} - \left\{\frac{10^{-4}\,\Delta\vartheta + 5\times10^{-12}[1-(10^{-1}t/F)]\left[(300+\Delta\vartheta)^4-(300)^4\right]}{1-(5\times10^{-2}t/F)}\right\} \tag{5}$$

for $\psi/\vartheta_{bath} = 0.03$.

Simulated plots of $\Delta\vartheta$ and E_{cell} vs. t are given in Fig. 2(A) for a range of values of ψ/ϑ_{bath} and it can be seen that eqn. (5) gives results which resemble quite closely the experimental data of Figs. 3 and 4 of ref. 2. We point out here that the values of ψ/ϑ_{bath} which apply to the experimental data are near the bottom of the range shown in Table 1. Some of the key values of $\Delta\vartheta$ and E_{cell} used in the later evaluations are given in the table.

We observe next that as far as Methods 1 and 5 are concerned we can define four heat transfer coefficients measured close to the time t_2 on Fig. 2(B) depending on the following particular assumptions [3–6,10]:

TABLE 1

Simulations of eqns. (5) and (10) and the derived values of $(k'_R)_1$, $(k'_R)_5$, $\dot{Q}_1$ and $\dot{Q}_5$

$-\psi I/\vartheta_{bath}$ /K^{-1}	Eqn. (10)	Eqn. (5)					
	0.09	0.03	0.06	0.09	0.12	0.15	0.18	0.36
$(k'_R)_{simulation}$ /W K^{-1}	0.162	n.a.	n.a.	n.a.	n.a.	n.a.	n.a.	n.a.
$(k'_R)_{simulation}$ /W K^{-4}	n.a.	1.5×10^{-9}	1.5×10^{-9}	1.5×10^{-9}	1.5×10^{-9}	1.5×10^{-9}	1.5×10^{-9}	1.5×10^{-9}
$\Delta\vartheta_2$ /K	17.327	18.178	17.148	16.221	15.383	14.624	13.932	10.820
$\Delta\vartheta_1$ /K	15.473	16.368	15.426	14.581	13.819	13.129	12.501	9.690
E_2 /V	4.981	5.995	5.511	5.080	4.694	4.346	4.032	2.645
E_1 /V	5.147	6.049	5.614	5.228	4.882	4.571	4.290	3.052
$(k'_R)_5\times10^9$ /W K^{-1}	0.1584	–	–	n.a.	–	–	–	–
$(k'_R)_1\times10^9$ /W K^{-1}	0.1942	–	–	n.a.	–	–	–	–
$(k'_R)_{1,predicted}$ $\times10^9$/W K^{-1}	0.1944	–	–	n.a.	–	–	–	–
$(k'_R)_5\times10^9$ /W K^{-4}	n.a.	1.4635	1.4627	1.4614	1.4620	1.4601	1.4600	1.4609
$(k'_R)_1\times10^9$ /W K^{-4}	n.a.	1.5569	1.6518	1.7491	1.8481	1.9468	2.0468	2.6669
$(k'_R)_{1,predicted}$ $\times10^9$/W K^{-1}	n.a.	1.5939	1.6896	1.7868	1.8854	1.9851	2.0858	2.7054
$\dot{Q}_1$ /W	3.005	2.9857	2.9716	2.9618	2.9547	2.9470	2.9410	2.9290
$\dot{Q}_{1,predicted}$ /W	3.0000	3.0000	3.0000	3.0000	3.0000	3.0000	3.0000	3.0000
$\dot{Q}_5$ /W	2.4509	2.8066	2.6315	2.4746	2.3374	2.2102	2.0978	1.6045
$\dot{Q}_{5,predicted}$ /W	2.4428	2.8036	2.6296	2.4752	2.3368	2.2124	2.1000	1.6048

if we allow for the change in the electrical energy input during the calibration cycle

$$(k'_R)_1 = \frac{\Delta Q - \left(\left[E_{cell}(\Delta\vartheta)_1\right]_{t_2} - \left[E_{cell}\left[(\Delta\vartheta)_2\right]\right]_{t_2}\right) I}{\left[(\vartheta_{bath}+\Delta\vartheta_2)^4 - (\vartheta_{bath}+\Delta\vartheta_1)^4\right]} \tag{6}$$

if we allow additionally for the change in the enthalpy of evaporation of the solvent during this cycle

$$(k'_R)_2 = \frac{\Delta Q - \left(\left[E_{cell}(\Delta\vartheta)_1\right]_{t_2} - \left[E_{cell}\left[(\Delta\vartheta)_2\right]\right]_{t_2}\right) I - \frac{3I}{4F}\left\{\left(\frac{P_2}{P^*-P_2}\right)\left[(C_{P,D_2O,g} - C_{P,D_2O,l})\,\Delta\vartheta_2 + L\right] - \left(\frac{P_1}{P^*-P_1}\right)\left[(C_{P,D_2O,g} - C_{P,D_2O,l})\,\Delta\vartheta_1 + L\right]\right\}}{\left[(\vartheta_{bath}+\Delta\vartheta_2)^4 - (\vartheta_{bath}+\Delta\vartheta_1)^4\right]} \tag{7}$$

if we neglect the changes in both the electrical energy input and enthalpy of evaporation of the solvent

$$(k'_R)_3 = \frac{\Delta Q}{\left[(\vartheta_{bath}+\Delta\vartheta_2)^4 - (\vartheta_{bath}+\Delta\vartheta_1)^4\right]} \tag{8}$$

and, finally, if we neglect the changes in the electrical energy input but include those for the enthalpy of evaporation of the solvent

$$(k'_R)_4 = \frac{\Delta Q - \frac{3I}{4F}\left\{\left(\frac{P_2}{P^*-P_2}\right)\left[(C_{P,D_2O,g} - C_{P,D_2O,l})\,\Delta\vartheta_2 + L\right] - \left(\frac{P_1}{P^*-P_1}\right)\left[(C_{P,D_2O,g} - C_{P,D_2O,l})\,\Delta\vartheta_1 + L\right]\right\}}{\left[(\vartheta_{bath}+\Delta\vartheta_2)^4 - (\vartheta_{bath}+\Delta\vartheta_1)^4\right]} \tag{9}$$

As far as the present discussion is concerned, we need to use $(k'_R)_2$ for Method 5 and to examine the significance of $(k'_R)_3$ in the evaluations based on Method 1. We will also refer to the heat transfer coefficient by Method 2 which we have designated by $(k'_R)_5$ [3–6,10] and to that determined by Method 6 as $(k'_R)_6$.

It is important to realize at the outside that Methods 1 and 5 are not the same as they lead to evaluations of the thermal balance at different times of the $\Delta\vartheta-t$ transient. This should have been apparent from a comparison of Appendices 2 and 4 of ref. 2 but Wilson et al. do not refer to the latter Appendix in their paper [11].

As in that Appendix, this point can be appreciated most immediately by using the linearized form of eqn. (5):

$$\frac{d\,\Delta\vartheta}{dt} = \frac{10^{-2}}{1-(5\times10^{-2}t/F)} + \frac{0.36[H(t-t_1)-H(t-t_2)]}{1-(5\times10^{-2}t/F)} - \left\{\frac{10^{-4}+0.162[1-(10^{-1}t/F)]}{1-(5\times10^{-2}t/F)}\right\}\Delta\vartheta \qquad (10)$$

The results from a simulation based on eqn. (10) are given in the first column of Table 1: Method 5 predicts an approximate value of $(k'_R)_1$ while Method 1 predicts $((k'_R)_1 - \psi I/\vartheta_{bath})$ as was pointed out in Appendix 4 of ref. 2: needless to say, Method 1 also gives only approximate values of this parameter.

A set of data based on eqn. (5) and using a range of values $\psi I/\vartheta_{bath}$ is also given in Table 1. As can be seen, $(k'_R)_1$ is constant while $(k'_R)_6$ has the predicted values. It is important to point out here that the small deviations between the derived and predicted values of $(k'_R)_1$ and $(k'_R)_5$ are artefacts of the simulation procedure; we have used only the simplest possible forward integration method.

Values of Q_1 and Q_5 predicted using $(k'_R)_1$ and $(k'_R)_5$ are also shown in Table 1. The most immediately obvious point is that Q_5 applies to the point $t = t_2$ in Fig. 2(B) while Q_1 is evaluated at $t = 0$.

We conclude that Methods 1 and 5 are comparable but they give the thermal balance at different parts of the $\Delta\vartheta$–t transient. If Q_f is essentially constant during a measurement cycle (including the value zero for blank experiments) then it is not at all surprising that Methods 1 and 2 should give closely similar results contrary to the views expressed by Wilson et al. [1].

ERRORS AND OTHER ISSUES RAISED BY WILSON ET AL. [1]

Both our own approximate method evaluation, Method 1 [2] and that of Wilson et al., [1] Method 5, rely on making a thermal balance at a single point, t_2 in Fig. 2(B). They are therefore inevitably subject to the errors inherent in adopting such a strategy. At first sight the errors inherent in Method 1 would be expected to be dominated by the measurement of two absolute temperatures whereas Method 5 requires in addition the measurement of two cell voltages and would therefore be expected to be somewhat less accurate than Method 1.

This supposition is incorrect however because Method 1 is subject in the main to systematic errors unless due care is taken in controlling the level of electrolyte in the cells at the point at which the measurements are taken; by implication, Method 5 will be subject to the same systematic errors. We illustrate this point by the results of 33 sets of calibration cycles, shown in Fig. 3(A), a typical cycle being shown in Fig. 3(B) (Fig. 5A of ref. 2; Fig. 3(A) was not given in ref. 2). This variability has been recognized by other authors e.g. refs. 11 and 12 and Wilson et al. [1] reiterate the assertion that measurements can only be made to 5%–10%

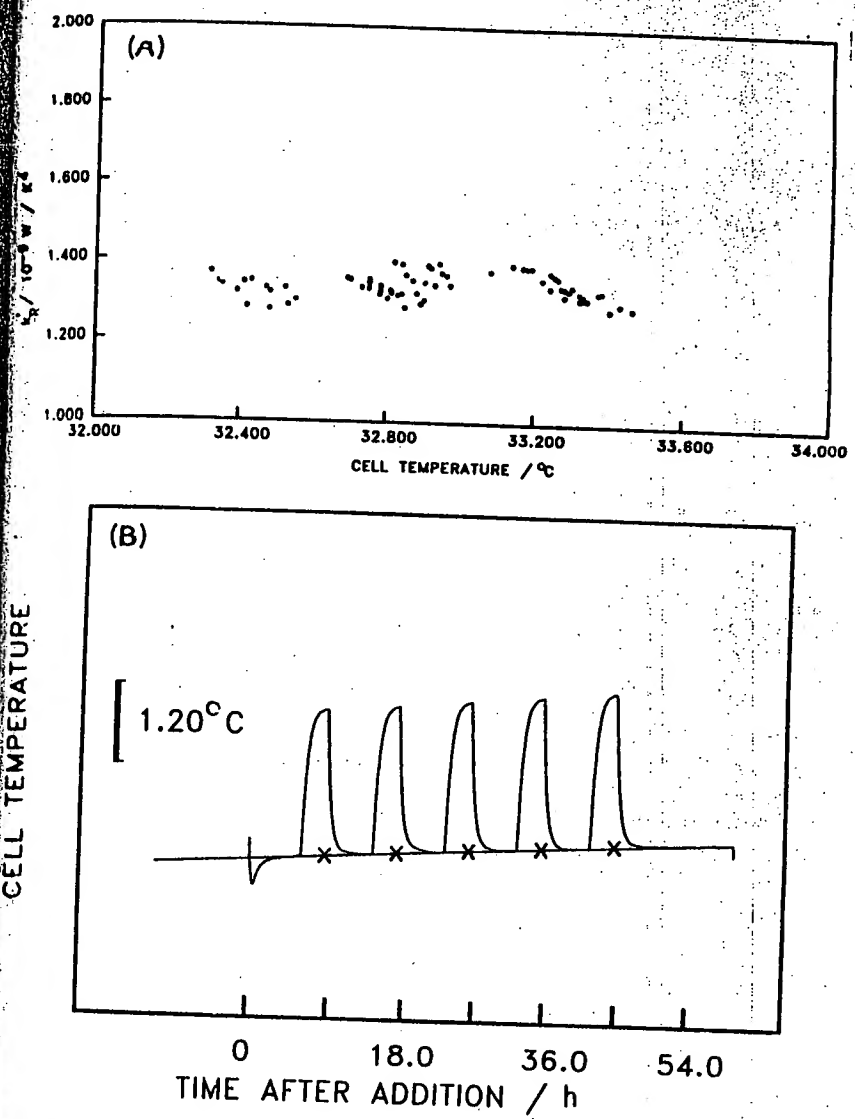

Fig. 3. (A) Plot of the heat transfer coefficients for multiple sets of calibration cycle experiments as a function of cell temperature. (B) A typical set of calorimeter calibration cycles made at 9, 18, 27, 36 and 45 h after the addition of D_2O (0.1 × 10 cm Pd electrode polarized at 0.1 M LiOD at a current density of 64 mA cm^{-2}). (C) The derived heat transfer coefficients for 14 calibration cycles as a function of time after the addition of D_2O. (D) Superposition of 165 derived heat transfer coefficients determined in 33 sets of calibration cycles for a single cell. The superposition was made at the 27 h calibration point and demonstrates the precision of $\sigma_R = 0.155\%$ in determining the actual coefficient at the remaining points.

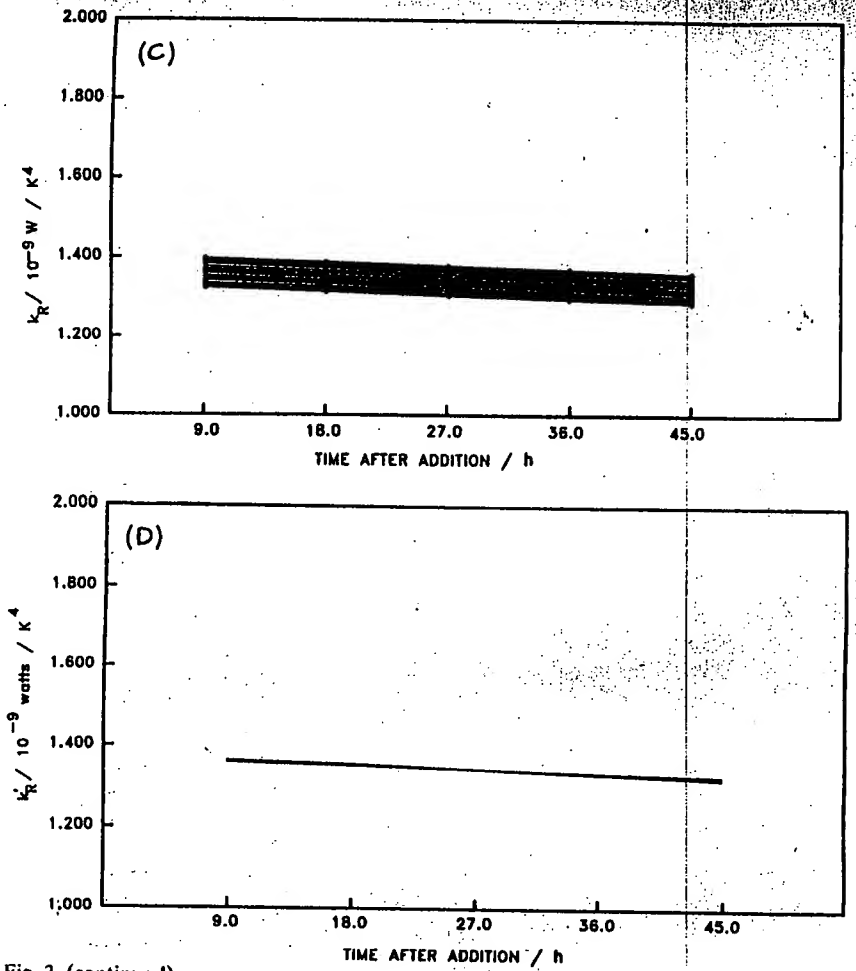

Fig. 3. (continued).

precision with this type of calorimetric technique. It is well known that isoperibolic calorimetry is capable of an accuracy of 1%–2% even without paying special attention to problems which limit the accuracy; we contend that we have taken special steps in this regard.

That the variability that we have observed in our measurements is systematic rather than random is shown by Fig. 3(C) (Fig. 5C of ref. 2); superposition of these plots at the central calibration point shows that the residual standard deviation is only 0.155%, see Fig. 3(D) (Fig. 5D of ref. 2).

The variability is due to changes in the level of electrolyte in the calorimeters, i.e. of the term $[1-(1+\lambda)It/2FM^{\circ}]$ in eqn. (5) and the related equations and must be taken into account in accurate methods of data analysis. The cause of the variability has also been correctly identified by others [11] but, to the best of our knowledge, has so far only been allowed for in the work reported by us, e.g. in ref. 2.

The question naturally is how can such an objective be achieved? The precise control of the level of electrolyte in routine work is hardly feasible (but, naturally, such precise control needs to be achieved for measurement cycles which are to be evaluated in detail). The answer lies in making the term $[1-(1+\lambda)It/2FM^{\circ}]$ (or of other equivalent parameters) part of the evaluation and this in itself dictates the strategy that the whole of the $\Delta\vartheta$–t and E_{cell}–t transients be fitted to the integrated forms of the differential equations which model the calorimeters i.e. it dictates the use of methods such as Methods 2 and 4. It is not surprising that such methods can give precise results as a matter of routine.

The information on this issue which was contained in our original paper [2] and in the related papers has been ignored by Wilson et al. [1]. They have also ignored the fact that we showed that it is possible to achieve at least 99% heat accuracy the methods we have used (Table 2 of ref. 2); we have never claimed an accuracy of better than 1% or 1 mW, whichever is the greater. They also do not discuss the fact that even on the basis of their own evaluations the excess enthalpy for a 0.2 cm diameter × 10 cm length Pd cathode polarized at 128 mA cm^{-2} has reached ≈ 50% of the enthalpy input after 15 days of polarization (data taken from Fig. 4C of ref. 2). Presumably they believe that the errors have now reached 50% to explain away these effects? It should be noted that these enthalpy outputs are of the order 4 W cm^{-3} or ≈ 42 W mol^{-1} of Pd and that over the duration of the experiment shown the total enthalpy released is of the order 4 MJ cm^{-3} or 42 MJ mol^{-1} of Pd, which hardly lies in the province of Chemistry.

Wilson et al. should have set out their scheme of calculation for this series of experiments set out in Figs. 4A, B and C of our paper [2]. Of this series, Fig. 4C would have been the most reasonable choice (excess enthalpy in the middle range of those reported in ref. 2; cell temperature in the acceptable range). The excess enthalpies generated in the experiments described by Figs. 3A, B and and C (and which have been used by Wilson et al. for part of their analysis leading to Table of ref. 1) are too low to allow reliable calculations to be made from data points read from these graphs (these graphs and the data diskettes have been claimed as the property of, and are in the hands of, NCFI and the University of Utah). This set of figures was included to illustrate the behaviour of the systems at the low end of excess enthalpy generation. It was an unfortunate choice; the example should have been for the polarization at the same current density (64 mA cm^{-1}) either of shorter electrodes in the same calorimeter or of the given electrode (0.4 cm diameter × 10 cm length) in a calorimeter of larger diameter. As it is, the temperatures are too high to allow the application of methods such as 1 and 5. We observe that Wilson et al. [1] have chosen the most unsuitable example for their detailed calculation, namely Fig. 3A of ref. 2 (low excess enthalpy, high cell temperature) and their scheme of calculation inevitably magnifies the errors (multiplication and division by the differences between two large quantities).

TABLE 2

Comparisons of the values of the heat transfer coefficient calculated by Wilson et al. [1] with the lower bound $(k'_R)_6$ for the data in Figs. 3A–C of ref. 2; comparison of Q_f in ref. 1 with that derived using the lower bound $(k'_R)_6$ and the values in ref. 2

Fig. in ref. 2	$k'_R \times 10^9$/W K^{-4}	Q_f/W	$(k'_R)_6 \times 10^9$ /W K^{-4} (lower bound)	Q_f/W	Q_f/W [2]
	Wilson et al. [1]		This paper		
3A	0.81	−0.43	0.94	0 (assumed)	0.158
3B	(0.96?) [a]	(−0.48?) [a]	n.a.	0.100	0.178
3C	0.92	−0.37	n.a.	0.528	0.372

[a] Note to the Editor: these values are illegible on the copy of the draft paper in our possession.

That the analysis of Wilson et al. [1] is incorrect, quite apart from its lack of accuracy (it leads to double subtraction errors, see below), can be seen by comparing their calculation of k'_R with that of $(k'_R)_6$ using Method 6. In this method we assume that $Q_f = 0$ at the time just before the application of the calibration pulse (Fig. 1 of ref. 1 or Fig. 3A of ref. 2). We ignore completely the use of this pulse and use eqn. (2) to estimate $(k'_R)_6$; as can be seen from Table 2 this lower bound for k'_R is in fact much larger than the value deduced by Wilson et al. [1], which shows that their calculation is subject to a gross error. The use of this value of $(k'_R)_6$ for the data in Figs. 3B and 3C of our paper [2] gives the excess enthalpies shown in Table 2, not the negative enthalpies derived by Wilson et al. [1] (which contravene the laws of thermodynamics). We point out, however, that in the absence of a proper calibration these values of the excess enthalpies are inevitably inaccurate. We point out furthermore that a somewhat similar calculation in the independent evaluation of a different data set (but based on the application of Kalman filtering and using eqn. (3) [7]) has also given excess enthalpy which increases progressively with time. We emphasize again that a proper analysis must rely on the comparison of the integrated equations with the experimental data sets (such as Methods 2 and 4) and these comparisons must be based on the differential equations which take full account of evaporative cooling, for example eqn. (3) (see further below). As we have noted above, we restricted exact calculations in ref. 2 to those cases where the details of evaporative cooling could be neglected and the values of Q_f quoted for Figs. 3A–C and Figs. 4A–C remained estimates rather than exact values.

We note here that we agree with the discussion by Wilson et al. [1] of the effects of evaporative cooling and our own calculations of these effects (based on readings taken from the published figures [2]) are given in columns 6–8 of Table 3.

We draw attention here to the fact that the E_{cell}–t plots in Figs. 3 and 4 of ref. 1 have been displaced by one data point (300 s) to longer times than the $\Delta\vartheta$–t plots by the plotting routines used to generate these figures. We have corrected for

TABLE 3

Corrections to the data in Figs. 3A–C and Figs. 4A–C of ref. 2 to allow for changes in the evaporative cooling terms in eqn. (7) due to the resistive heater calibration pulse; corrections to Q_f to allow for the use of $(k'_R)_1$ or $(k'_R)_3$ as well as for the heat flows due to evaporation and the heating of the cell contents

Fig. in ref. 2	$\Delta\vartheta_2$ /K	$\Delta\vartheta_1$ /K	P_2 /bar	P_1 /bar	Evaporative heat flow at $\Delta\vartheta_2$ /W	Evaporative heat flow at $\Delta\vartheta_1$ /W	Correction to Q_f to allow for the use of $(k'_R)_2$ /W	Credit to allow for heating of cell contents /W	Q_f given in ref. 2 /W	Corrected Q_f /W
3A	333.51	331.82	0.193	0.178	−0.077	−0.070	−0.103	+0.014	0.158	0.139
3B	335.67	334.04	0.212	0.197	−0.087	−0.079	−0.131	+0.014	0.178	0.140
3C	341.37	339.74	0.272	0.254	−0.124	−0.112	−0.228	+0.018	0.372	0.274
4A	323.09	321.17	0.118	0.113	−0.042	−0.040	−0.032	+0.011	0.736	0.755
4B	325.33	323.44	0.132	0.121	−0.048	−0.044	−0.039	+0.013	0.888	0.906
4C	327.70	325.84	0.148	0.135	−0.055	−0.050	−0.055	+0.014	1.534	1.543

...placement in drawing up Tables 2 and 3. We also draw attention to the need to correct for the heating of the cell contents (the term $C_{P,D_2O,l}[1 - It/2FM^\circ](d\,\Delta\vartheta_1/dt)_{t=t_2}$ in column 9 of Table 3) when the smaller terms in the estimation of Q_f are taken into account. The difference $C_{P,D_2O,l}[1 - It/2FM^\circ][(d\,\Delta\vartheta_2/dt)_{t=t_2} - (d\,\Delta\vartheta_1/dt)_{t=t_2}]$, although detectable, is too small to be taken into account in evaluating the heat transfer coefficients using Methods 1 or 5.

The major correction term estimated by Wilson et al. [1], that due to their correction of ΔQ due to the change induced by the heater pulse on the cell potential, is, however, not applicable. As we have shown above and in Appendix 4 of ref. 2, that term has already been taken into account in estimating Q_f using $(k'_R)_3$ as given by Method 1. The scheme of calculation adopted by Wilson et al. [1] therefore leads to a double correction of k'_R for the effects of changes of the cell potential. It is not surprising therefore that the magnitudes of the corrections to Q_f calculated by Wilson et al. [1] are precisely of the order expected for such a double subtraction. The values of k'_R derived are too low (as the authors themselves remark) and the authors also conclude that the cells are markedly endothermic for the conditions represented by Fig. 3A of ref. 2, a condition which evidently contravenes the laws of thermodynamics.

That the conclusions reached by Wilson et al. are untenable is shown by the simulation of the $\Delta\vartheta$–t curves using their derived parameters in eqn. (2) (Fig. 4). These simulations demonstrate clearly the inadequacy of using a single point calculation to predict the observed response of these calorimeters; it is pointed out again here that one must use the fully integrated form of the differential equations for such predictions. We regard it as being most important that such checks be made routinely in any further development of the calorimetry of electrode reactions and note that Method 4, Kalman filtering, has a special advantage in that it produces comparisons of the experimental data and of the simulation using the derived parameters as an intermediate step in the calculations.

Instead of exploring the causes of their conclusions, Wilson et al. [1] discuss the validity of our "blank" experiments and their discussion is again largely based on their misinterpretation of our Method 1. They maintain quite correctly that this method could not be expected to give results in close accord with those of Method at high enthalpy inputs. This is indeed apparent from our own results for Pd cathodes polarized in D_2O, given in Table 3 of ref. 2. The explanation is that the "blank" experiments have been incorrectly described in the footnotes of Table 4. It was our uniform practice at that time to reduce the lengths of our cathodes to 25 cm at high enthalpy inputs (e.g. Table 3 of ref. 2). For these blank experiments we still followed the manner of presentation first given in our preliminary publication [13] of subsequently rescaling the results to electrodes of 10 cm length. The erroneous results of cells operating above the boiling point is explained by this rescaling of the data.

We return finally to the question of the applicability of the various heat transfer coefficients $(k'_R)_1$–$(k'_R)_5$ described above. We have found in our more recent work

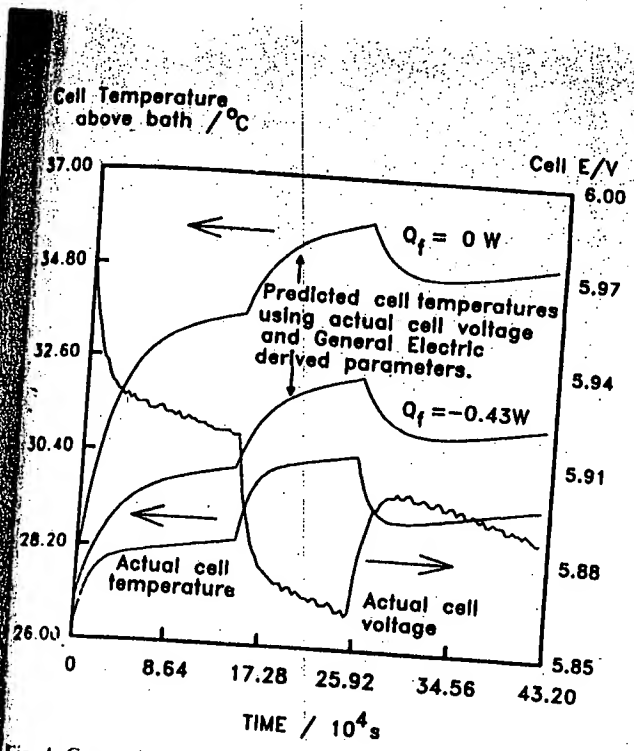

Fig. 4. Comparison of the data shown in Fig. 3A of ref. 1 (two lower plots) with simulations of the temperature response using the given cell voltage and the parameters derived by Wilson et al. [1]: k'_R = 0.81×10^{-9} W K^{-4}, ΔQ = 0.24 W; and (top plot) Q_f = 0.0 W or (bottom plot) Q_f = −0.43 W.

using cells of the type shown in Fig. 1(C) that a long term balance of the enthalpy generated in "blank" experiments (Pt cathodes polarized in H_2O or D_2O; Pd cathodes polarized in H_2O) is only achieved when using the heat transfer coefficients derived by non-linear regression fitting, Method 2 [3–6,10]. It is of interest that these heat transfer coefficients are closely similar to those derived by Kalman filtering, Method 4. The use of $(k'_R)_1$ or $(k'_R)_2$, eqns. (6) and (7), indicates endothermic operation of these cells, which is clearly impossible. It is also of interest that, notwithstanding the endothermic operation of these cells when using $(k'_R)_1$ or $(k'_R)_2$, the use of these coefficients nevertheless shows that Pd-alloy cathodes polarized in D_2O generate excess enthalpy. The fact that the heat transfer coefficients $(k'_R)_1$ and $(k'_R)_2$ are evidently too small indicates that the steady state approximation is inapplicable for reasons which we do not as yet understand. It is certain, however, that the inapplicability of the approximation leads to some further forms of "double subtraction error". However, we have not investigated this because precise methods of data evaluation are available; for the work reported in ref. 2 we used $(k'_R)_3$ as an initial value in the non-linear regression procedure which leads to precise values of Q_f.

CONCLUSION

The critique presented by Wilson et al. [1] is based largely on a misreading and misrepresentation of the information contained in ref. 2. We are unable to make any judgement of the authors' own work on the subject since the paper contains no experimental details or results. We observe that some of our own work has now been subjected to an independent analysis [7] and indeed we made it a condition of our continuing work on this topic after October 1989 that this should be done. It would be useful if the experimental work of Wilson et al. [1] could be made available for such independent scrutiny. This would allow the application of advanced data processing methods to the results, and, at the very least, lead to a clear definition of the experiments carried out.

GLOSSARY

$C_{\ldots,g}$	Heat capacity of O_2, J K^{-1} mol^{-1}.
$C_{\ldots,g}$	Heat capacity of D_2, J K^{-1} mol^{-1}.
$C_{P,D_2O,l}$	Heat capacity of liquid D_2O, J K^{-1} mol^{-1}.
$C_{P,D_2O,v}$	Heat capacity of D_2O vapour, J K^{-1} mol^{-1}.
E_{cell}	Measured cell potential, V.
$E_{cell,t=0}$	Measured cell potential at the time when the initial values of the parameters are evaluated, V.
$E_{thermoneutral,bath}$	Potential equivalent of the enthalpy of reaction for the dissociation of heavy water at the bath temperature, V.
F	Faraday constant, 96484.56 C mol^{-1}.
g	Gas phase.
H	Heaviside unity function.
I	Cell current, A.
k_R	Heat transfer coefficient due to radiation at a chosen time origin, W K^{-4}.
$k'_R)$	Effective heat transfer coefficient due to radiation, W K^{-4}.
l	Liquid phase.
r_0	Enthalpy of evaporation, J K^{-1} mol^{-1}.
	Heavy water equivalent of the calorimeter at a chosen time origin, mol.
x	Partial pressure, Pa; product species.
	Atmospheric pressure, Pa.
(t)	Rate of generation of excess enthalpy, W.
	Time dependent rate of generation of excess enthalpy, W.
t	Time, s.
	Rate of heat dissipation of calibration heater, W.
	Difference in cell and bath temperature, K.
	Difference in cell and bath make-up stream temperature, K.
	Absolute temperature, K.
T_{bath}	Bath temperature, K.
T_0	Cell temperature at $t = 0$, K.
λ	Slope of the change in the heat transfer coefficient with time.
Φ	Proportionality constant relating conductive heat transfer to the radiative heat transfer term.
ψ	Slope of the change of cell potential with temperature, V K^{-1}.

REFERENCES

1 R.H. Wilson, J.W. Bray, P.G. Kosky, H.B. Vakil and F.G. Will, J. Electroanal. Chem., 332 (1992) 1.
2 M. Fleischmann, S. Pons, M.W. Anderson, L.J. Li and M. Hawkins, J. Electroanal. Chem., 287 (1990) 293.
3 M. Fleischmann, S. Pons, M. Wadsworth, S. Guruswamy, R. Rajamani, J.L. Li, X. Xu, Y. Qian and J. Pons, The Calorimetry of Electrode Reactions, submitted to NCFI September 1990.
4 M. Fleischmann, S. Pons, J.L. Li, X. Xu, Y. Qian and J. Pons, The Calorimetry of Electrode Reactions, revised text of ref. 3 now submitted for publication.
5 S. Pons, M. Fleischmann, M. Wadsworth, S. Guruswamy, R. Rajamani, J.L. Li, X. Xu, Y. Qian and J. Pons, Excess Enthalpy Generation in Palladium Alloy Cathodes Polarized in Heavy Water, submitted to NCFI September 1990.
6 S. Pons, M. Fleischmann, J.L. Li, X. Xu, Y. Qian and J. Pons, Excess Enthalpy Generation in Palladium Alloy Cathodes Polarized in Heavy Water, revised text of ref. 5 now submitted for publication.
7 W. Hansen, Report to the Utah State Fusion Energy Council on the Analysis of Selected Pons–Fleischmann Calorimetric Data, in T. Bressani, E. Del Giudice and G. Preparata (Eds.), The Science of Cold Fusion: Proceedings of the II Annual Conference on Cold Fusion, Vol. 33 of the Conference Proceedings, The Italian Physical Society, Bologna, 1992, p. 491, ISBN-887794-045-X.
8 Reports on II Annual Conference on Cold Fusion, 21st Century Science Associates, Washington, DC, Autumn 1991 Issue, p. 25.
9 M. Fleischmann and S. Pons, to be published.
10 S. Pons and M. Fleischmann, in T. Bressani, E. Del Giudice and G. Preparata (Eds.), The Science of Cold Fusion: Proceedings of the II Annual Conference on Cold Fusion, Vol. 33 of the Conference Proceedings, The Italian Physical Society, Bologna, 1992, p. 349, ISBN-887794-045-X.
11 N.S. Lewis, C.A. Barnes, M.J.Heben, A. Kumar, S.R. Lunt, G.E. McManis, G.M. Miskelly, R.M. Penner, M.J. Sailor, P.G. Santangelo, G.A. Shreve, B.J. Tufts, M.G. Youngquist, R.W. Kavanaugh, S.E. Kellog, R.G. Vogelaar, T.R. Wang, R. Kondrat and R. New, Nature, 340 (1989) 525.
12 D.E. Williams, D.J.S. Findlay, D.W. Craston, M.R. Sene, M. Bailey, S. Croft, B.W. Hooton, C.P. Jones, A.R.J. Kucernak, J.A. Mason and R.I. Taylor, Nature, 342 (1989) 375.
13 M. Fleischmann, S. Pons and M. Hawkins, J. Electroanal. Chem., 261 (1989) 301–308, err., J. Electroanal. Chem., 263 (1989) 187–188.

ELECTROCHEMICAL CHARGING OF Pd RODS

S. Szpak and C. J. Gabriel

Naval Ocean Systems Center, San Diego, CA 92152-5000

J. J. Smith

Department of Energy, Washington, DC 20545

R. J. Nowak

Office of Naval Research, Arlington, VA 22217-5000

Abstract

A model describing the electrochemical charging of *Pd* rods is presented. The essential feature of this model is the coupling of the interfacial processes with the transport of interstitials in the electrode interior. It is shown that boundary conditions arise from the solution of equations governing the elementary adsorption-desorption and adsorption-absorption steps and the symmetry of the electrode. Effects of the choice of rate constants of the elementary steps and the charging current on the surface coverage, the electrode potential and the time required to complete electrode charging are examined.

1.0 Introduction.

In a recent effort(1) to account for the long charging time needed to initiate the effects reported by Fleischmann and Pons(2), in a Pd rod, certain assumptions concerning the concentration of deuterium at the electrode surface, the nature of the interaction between the diffusing deuterium and the Pd lattice and the homogeneity of the medium were made. The condition of zero flux at the center of Pd rod, used by Jorne(1), is evident; however, the condition of constant deuterium concentration at the electrode surface, although appropriate for charging from the gas phase, is open to question because, to be physically realistic, the boundary conditions must consider all processes that determine the concentration, or the flux, of the diffusing substance at the point where the influence of the interphase ceases. The nature of the interactions of diffusing hydrogen and, to a lesser degree deuterium, with the Pd lattice, has been examined in considerable detail(3-11). To account for these interactions by a simple, first order irreversible chemical reaction may not be applicable. Moreover, a polycrystalline Pd rod can be treated as a homogeneous medium, but only under restrictive conditions.

The purpose of this work was to examine the problems associated with the charging of the palladium lattice. The charging of metals by hydrogen/deuterium by itself is a technologically important issue aside from the interest generated by the recently described extraordinary behavior of deuterium charged Pd rods(2).

2.0 Model.

Prior to developing the mathematics of the electrochemical charging of Pd rods, we review those aspects that tend to control the penetration of deuterium. In particular, we examine the structure of the electrolyte/electrode interphase, the deuterium evolution reaction, interactions between the interstitials and the host lattice, and the effect of grain boundaries in the polycrystalline material. This qualitative discussion provides the basis for the formulation of simplified governing equations in which we ignore the distinction between α/β phases and employ a simple diffusion coefficient for the purpose of modeling the con-

pling between surface and transport (bulk) processes.

2.1 Concept of an interphase / Charging fluxes.

Two homogeneous phases that are in contact with each other are separated by an interphase region. This region may be viewed as made up of several laminae each of which is treated as a very thin homogeneous phase(12). Often, to simplify the treatment, an appropriately defined single homogeneous phase may be substituted(13). The structure of the electrolyte portion of the interphase was treated by van Ryssel-berghe(14); here, the structure on the metal side, with respect to transport, will be identified and examined.

Four fluxes are involved in charging the *Pd* metal from the gas phase. They are the adsorption and desorption fluxes, j_2 and j_{-2}, and the absorption-desorption fluxes consisting of the exchange between the species present in the metal interior and the surface, j_3 and j_{-3}, respectively. In reality, the dynamics of the surface processes is more complex(15,16). In the case of electrochemical charging, Fig. 1, the structure is further complicated because the applied overpotential and charge transfer result in two additional fluxes, j_1 and j_{-1}. The effect of the applied potential on the transport of interstitials becomes negligible at a point close to the metal surface where diffusion is initiated.

2.2 Deuterium evolution reaction.

The reaction path for the deuterium evolution is essentially the same as that for hydrogen(2,17), Eqs. (I) to (III)

$$D_2O + e^- \rightarrow D(a) + OD^- ;\ k_1 , k_{-1} , \eta \qquad \text{(I)}$$

followed by either

$$D_2O + D(a) + e^- \rightarrow D_2(s) + OD^- ;\ k_2 , k_{-2} , \eta \qquad \text{(II)}$$

or

$$D(a) + D(a) \rightarrow D_2(s) ;\ k_3 , k_{-3} \qquad \text{(III)}$$

where (a) and (s) denote species present in an adsorbed state and in solution, respectively. Potential dependent surface coverage for special cases, *e.g.*, the steady state condition with an *a priori* specified rate determining step (rds), in the absence of absorption, was examined by Gileadi and Conway(18). They found that highest surface coverages are obtained when Eq. (III) is the rds, *i.e.*, is proceeding more rapidly than Eq. (II), but morre slowly than Eq (I). Furthermore, if Eq. (II) is the rds, *i.e.*, is proceeding more rapidly than Eq. (III), but more slowly than Eq. (I), the surface coverage exhibits a limiting value, determined by the ratio k_2/k_1 ; the smaller this ratio, the higher the surface coverage.

The absorption into the lattice of electrochemically generated deuterium is given by Eq. (IV)

$$D(a) \rightarrow D(l)\,;\; k_4\,,\, k_{-4} \qquad \text{(IV)}$$

where (l) denotes species in the lattice. The hydrogen analog of Eq. (IV) was investigated to a limited extent by Iyer *et al.* (19). The inclusion of diffusional transport necessitates the separation of the interphase region from the diffusion space. The characteristic feature of the Iyer *et al.* model is the interdependence of the diffusion flux and the interphase reactions.

2.3 Molecular interactions related to transport.

There is ample experimental evidence of interactions between the interstitials and the host Pd lattice. During the transport of hydrogen as well as deuterium, a change from the α phase to the β phase occurs. This change manifests itself by the lattice expansion which is larger in the α phase than in the β phase(6). The expansion of the Pd lattice creates localized highly stressed conditions that affect the diffusional transport(10). This deviation from ideality occurs even at very low hydrogen concentration with the process becoming more exothermic as the concentration of $H(l)$ increases. However, once the β phase has formed, the process becomes less exothermic. The rate of absorption increases exponentially with the increase in $H(l)$ concentration and is attributed to an expansion of the lattice.

Quantum mechanical treatment requires that the motion of interstitials occurs by a hopping mechan-

ism(9). The energies of activation for the H/D species are of an order of magnitude less than for other interstitials, while the values of their diffusion coefficients are many orders of magnitude higher indicating the importance of the pre-exponential factor. The jump frequencies for H interstitials are comparable to the highest frequency of the host lattice. Of interest is the fact that the isotope effect enters through the exponential factor, *i.e.*, contrary to the prediction based on the classical absolute rate theory(15).

2.4 Forms of diffusion coefficient.

Here, we review the various interpretation of the diffusion coefficient to underscore the importance of interactions between the interstitials and the host lattice on their transport. Starting with the Fick's first law, Eq. (1)

$$j = -\mathrm{D}\frac{\partial c}{\partial x} \tag{1}$$

we note that in this formulation, D is a proportionality constant relating the flux, j, to the driving force, $\partial c/\partial x$. However, as written, Eq. (1) is valid only for non-interacting solute/solvent systems. Substituting the activity for concentration, $a = c\phi$, we transform Eq. (1) into an equivalent form

$$j = -\frac{c\mathrm{D}}{RT}\frac{\partial \mu}{\partial x}\ ; \quad \mu = \mu^0 + \mathrm{RT}\ \ln a \tag{2}$$

Defining $v = j/c$ as the average linear velocity of the diffusing particles, we have for the Nernst-Einstein formulation

$$f(x)dx = B^{-1}vdx\ ;\ B = \mathrm{D}/\mathrm{RT} \tag{3}$$

i.e., the diffusing particles behave as if they were acted upon with the force $f(x)$ against the viscous resistance. If additional forces are affecting diffusional transport, *e.g.*, lattice expansion, it is necessary to add the appropriate terms to the balance eqation, Eq. (3), *e.g.*, Eq. (4)

$$f(x)dx = B^{-1}vdx + \sum_i dw_i \tag{4}$$

Comparing Eqs. (3)/(4) and (2) we note that $f(x) = -\partial\mu/\partial x$ while the comparison of Eqs. (1) and (2)

yields the diffusion coefficient of the form

$$\mathbf{D} = D_0 \exp\left[-\frac{1}{RT}\int (f(x) - \sum_i dw_i/dx)dx \right] \tag{5}$$

Equation (5) implies that the diffusion coefficient reflects specific features associated with the transport. For example, Barrer and Jost(20) found that the transport of $H(l)$ in the Pd lattice belongs to the "zeolitic diffusion", where the probability of migration is proportional to the probability of finding an unoccupied site. The diffusion coefficient involving the possibility of jumps of length λ over several sites has the form

$$D_n = (n\lambda)^2(1-\zeta)^n \ \nu \exp(-E_n/RT) \tag{6}$$

where ν is the oscillation frequency , $(1-\zeta)^n$ is the probability of finding a vacant neighboring site n times in succession and E_n is the energy of activation, most likely a slowly varying function of n. The "effective" diffusion coefficient D_{eff} is the normalized sum of individual coefficients. Evidently, for small ζ, the $n-$ fold jumps contribute substantially while for large ζ only the first term is significant.

Kuballa and Baranowski(21), examining the transport properties at high concentration of hydrogen through the $\beta - Pd$ lattice, employed the diffusion coefficient formulated on the basis of absolute rate theory, Eq. (7)

$$\mathbf{D} = \kappa\, f\, \frac{\lambda^2}{6}\, z\, \nu \exp\left(\frac{S_m + S_f}{k}\right) \exp\left(-\frac{E_m + E_m}{kT}\right) \tag{7}$$

where κ is the transmission coefficient, f is the correlation factor, λ is the jump distance in the lattice, z the coordination number, ν the vibration frequency in the potential well, S the entropy and E the energy. The subscripts f and m, respectively, identify the formation of a neighboring vacancy and the motion from one site to another. They concluded that within the α phase, the diffusion coefficient is independent of concentration. However, at higher concentrations, many neighboring sites are occupied and both the entropy and the energy of vacancy formation must be included. The formation of new sites is associated

with the mechanical distortion of the lattice, thus sharply increasing the vibrational frequency of the diffusing particle. As the concentration of hydrogen increases there is continuous change in the mechanism of transport, most likely involving the tetrahedral sites.

In yet another example, the effect of mechanical distortion on transport was examined by Voelkl(10). Results were expressed in terms of changes of the electrochemical potential, *i.e.* a factor appearing in the exponent of the diffusion coefficient.

2.5 Effect of grain boundaries.

Grain boundaries represent the locations of a high density of lattice imperfections. In effect, they may be viewed as internal surfaces where an exchange process, similar to adsorption-desorption, can occur. The interaction of an interstitial with a lattice defect is energetically quite different from its interaction with the undisturbed lattice. Consequently, by Eq. (5), transport properties should differ in polycrystalline material as compared with those in a single crystal. Yet, measurements of the steady state permeation of hydrogen indicate no influence of grain boundaries. This apparent discrepancy is attributed to the absence of trap-to-trap hopping of interstitials and the filling of all traps during steady state transport (22). By creating sinks, the tendency of interstitials to accumulate in the lattice defects modifies their transport before the steady state is realized.

2.6 H(a)/H(l)-Pd *vs* D(a)/D(l)-Pd interphase behavior.

Common reaction paths for the hydrogen evolution reaction and deuterium evolution reaction, reported by Schuldiner and Hoare(17), do not assure identical rates of the elementary processes comprising the charging of palladium rods. Qualitative observations show considerable difference in the behavior of the interfacial region between hydrogen and deuterium, notably in the rate of absorption-desorption. Rolison and Trzaskoma(23) reported a significant difference in the rate of escape of absorbed hydrogen and deuterium upon termination of the charging current. Szpak *et al.* (24) found similar behavior by an *in situ* examination of the penetration of deuterium and hydrogen by a single grain in a specially designed cell

using Nomarski optics.

3.0 Formulation of charging equations.

Davenport *et al.* (25) considered absorption from the gas phase into a thin metallic film. We extend their treatment to consider a much larger solid body immersed in an electrolyte. This body is taken to consists of N layers; the $i-$ th layer having a volume V_i and the area of the dividing surface between it and the $i+1-$ th layer is $S_{i,i+1}$. In general: $V_i \neq V_{i+1}$ and $S_{i-1,i} \neq S_{i,i+1}$. The diffusion of deuterium in the bulk of the solid body is then considered as a process of jumping from one layer to an adjacent layer with a rate that is proportional to the interfacial area between the layers, as well as, to the number of occupied sites in the initial layer and the number of vacant sites in the final layer. Consequently, we write for the time rate of change in the fractional number per unit volume of occupied sites, ς_i in the $i-$ th layer within the bulk

$$\frac{d\varsigma_i}{dt} = \frac{k_d Z_m}{V_i}\Big\{S_{i-1,i}[\varsigma_{i-1}(1-\varsigma_i) - \varsigma_i(1-\varsigma_{i-1})] - S_{i,i+1}[\varsigma_i(1-\varsigma_{i+1}) - \varsigma_{i+1}(1-\varsigma_i)]\Big\}; \; i = 1,2,3,\ldots,N \tag{8}$$

where k_d is the jump rate constant and Z_m is the maximum number of available sites per unit volume.

The boundary conditions for this set of equations are determined by the physical considerations of events occurring at the first and $N-$ th layers. The reactions (I) through (IV) set the boundary conditions at the first layer in terms of corresponding fluxes. Defining the anodic current as the positive current (*i.e.*, the flow of electrons from the working electrode to the power supply), we obtain for the charge transfer reaction, Eq. (I)

$$\frac{i_1}{\Gamma_m F} = k_{-1}[OD^-]\,\theta\exp\left(\frac{\alpha F\eta}{RT}\right) - k_1[D_2O]\,(1-\theta)\exp\left[\frac{-(1-\alpha)F\eta}{RT}\right] \tag{9}$$

where Γ_m, is the maximum number of sites per unit area and θ is the fractional surface coverage. Analo-

gously, for the charge transfer reaction Eq. (II)

$$\frac{i_2}{\Gamma_m F} = k_{-2}[D_2(s)][OD^-](1-\theta)\exp(\frac{\beta F\eta}{RT}) - k_2[D_2O]\theta\exp[\frac{-(1-\beta)F\eta}{RT}] \tag{10}$$

While reactions (III) and (IV) do not directly pass electrons through the interface, it is convenient to define equivalent charge transfer currents, Eqs. (11) and (12), respectively

$$\frac{i_3}{\Gamma_m{}^2 F} = 2k_{-3}[D_2(s)](1-\theta)^2 - 2k_3\theta^2 \tag{11}$$

$$\frac{i_4}{\Gamma_m Z_m F} = k_{-4}\varsigma_1(1-\theta) - k_4\theta(1-\varsigma_1) \tag{12}$$

In terms of these currents, the time rate of change of adsorbed deuterium is given by Eqs. (13)

θ = % surface coverage

$\sim \frac{d\theta}{dt}$

$$\Gamma_m F\frac{d\theta}{dt} = -i_1 + i_2 + i_3 + i_4 \tag{13}$$

and the applied current, i, is given by Eq. (14)

$$i = i_1 + i_2 + C\frac{d\eta}{dt} \tag{14}$$

where the last term in Eq. (14) gives the charging current for the interfacial layer in terms of its effective capacitance C and the time rate of change of the overpotential. The time rate of change of the absorbed deuterium in the interfacial layer between the bulk Pd and the electrolyte is governed by both the flux through the surface given in terms of the equivalent current i_4 and diffusion into the bulk, which generates the flux: $k_d\ Z_m{}^2\ S_{1,2}[\varsigma_1(1-\varsigma_2) - \varsigma_2(1-\varsigma_1)]$, so that the time rate of change of the fractional occupation of sites in the interfacial layer is given by Eq. (15)

$\frac{d(\theta_0 S_i)}{dt}$

$$V_1\ Z_m\ \frac{d\varsigma_1}{dt} = -\ S_{0,1}\ \frac{i_4}{F} - k_d\ Z_{max}^2\ S_{1,2}\ (\varsigma_1 - \varsigma_2) \tag{15}$$

Deut. jump rate; # avail sites (max) vol.

Equations (13), (14) and (15), in effect, specify the boundary conditions for Eq. (8) at the interfacial layer. The boundary condition at the $N-$ th layer depends on the physical arrangement; *e.g.*, with reflection symmetry at that location, the flux passing beyond the $N-$ th layer would be zero.

The jump rate constant k_d introduced in Eq. (8) can be related to the diffusion constant by observing that, if the number of layers is large and each layer is thin, then Eq. (8), which in cartesian coordinates becomes

$$\frac{d\varsigma_i}{dt} = \frac{k_d\, Z_m}{\delta}\left(\varsigma_{i-1} - 2\,\varsigma_i + \varsigma_{i+1}\right) \tag{16}$$

where δ is the thickness of the layers, can be compared with the finite difference approximation to the diffusion equation indicating that the diffusion constant $D = k_d Z_m \delta$.

3.1 Charging of Pd rods; numerical solutions.

For a rod (cylindrical symmetry) divided into annular layers of thickness Δr numbered from surface to center (1 to N), Eq. (8) becomes Eq. (17) (see Appendix A)

$$\frac{d\varsigma_i}{dt} = \frac{k_d\, Z_m}{\Delta r}\left(\frac{2\,r_i}{r_i + r_{i+1}}\right)\left[\varsigma_{i-1} - \left(2 - \frac{\Delta r}{r_i}\right)\varsigma_i + \left(1 - \frac{\Delta r}{r_i}\right)\varsigma_{i+1}\right]$$
$$i = 2,3,4,\ldots N \tag{17}$$

where $r_i = (N - i + 1)\Delta r$ and $\varsigma_{N+1} = \varsigma_N$ in order to insure the condition of zero flux at the center of the rod as required by symmetry considerations. Similarly, for the interfacial layer between the electrolyte and the bulk, Eq. (15) becomes Eq. (18)

$$\frac{d\varsigma_1}{dt} = -\left(\frac{2r_0}{2r_0 - \Delta r}\right)\left\{\frac{\Gamma_m}{\Delta r}\left[k_{-4}\varsigma_1(1-\theta) - k_4\,\theta\,(1-\varsigma_1)\right] + \frac{k_d\, Z_m}{\Delta r}\left(\frac{r_0 - \Delta r}{r_0}\right)(\varsigma_1 - \varsigma_2)\right\} \tag{18}$$

where $r_0 = N\Delta r$ is the radius of the rod.

Equations (13), (14), (17) and (18) form a set of stiff ordinary differential equations that can be solved using *e.g.* the method of Kaps-Rentrop described by Press and Teukolsky(27) with suitable modifications to take advantage of the tridiagonal nature of the Jacobi matrix.

4.0 Results and discussion.

A propopsed requirement for the initiation of the effect reported by Fleischmann and Pons is that a set of conditions must be met to "switch-on" the Pd electrode. Due to a large number of these conditions it is difficult, if not impossible at the present time, to identify a dominant factor although a high degree of loading has been assumed to be one of the necessary conditions. High overpotentials and/or charging currents have also been proposed. In the context of the present discussion, we accept the correctness of the reaction path, Eqs. (I) - (IV). However, because of the lack of the rate constant data for the deuterium evolution reaction, the discussion is essentially reduced to the examination of the behavior of the set of coupled equations describing the charging process.

4.1 Construction of solution; input data

The numerical solution of Eqs. (13), (14), (17) and (18) requires three types of input parameters. The first is associated with the electrode/electrolyte system, the second characterizes the initial conditions, and the third comprises the rate constants whose effect on charging process is examined. The electrode/electrolyte system consists of two regions: (i) the bulk material characterized with regard to transport by the density of available bulk sites, Z_m, and the diffusion coefficient D; (ii) the electrode/electrolyte interface described by the density of available surface sites, Γ_m, and the rate constants for all processes including the exchange reaction, Eq. (IV). The assumption employed here of concentration independent parameters represents a first approximation only, but can be easily extended to incorporate concentration dependences, if they are known.

To initiate calculations, we assume that, prior to the application of a charging current, equilibrium has been reached so that the time rate of change of η, θ , and ς_i , $i = 1,2,3...,N$ will be zero; in addition, we require that the time rate of change of the evolution of $D_2(s)$ also be zero. The latter requirement imposes the condition that $i_2 + i_3 = 0$. Consequently, the equilibrium condition becomes $i_j = 0$; $j = 1,2,3,4$. Equilibrium is characterized by the values of the three variables: η , θ , $\varsigma = \varsigma_i$; $i = 1,2,3,...N$ and deter-

mined by four equations. It follows, therefore, that an equilibrium condition may not exist for arbitrarily chosen sets of rate constants for the four reactions, Eqs. (I) - (IV). For this reason, it is convenient to choose equilibrium values for θ and ς with $\eta = 0$, *viz.*, $\theta = \theta_0$, $\varsigma = \varsigma_0$ and use these values to provide the following relationships among the rate constants, Eqs. (19) - (22)

$$k_{-1}\,[OD^-]\theta_0 = k_1[D_2O]\,(1-\theta_0) \tag{19}$$

$$k_{-2}[D_2(s)][OD^-](1-\theta_0) = k_2[D_2O]\theta_0 \tag{20}$$

$$k_{-3}[D_2(s)](1-\theta_0)^2 = k_3\theta_0^2 \tag{21}$$

$$k_{-4}\varsigma_0(1-\theta_0) = k_4(1-\varsigma_0)\theta_0 \tag{22}$$

Table I lists the values of the parameters used in the computations described here unless noted otherwise.

4.2. Electrode charging.

To relate the charging process to observable quantities and to evaluate the driving force, we calculated the surface coverage, the electrode overpotential and the amount of absorbed material. In particular, the surface coverage was selected because the operating driving force for the charging process is the chemical potential difference between the relevant species in an adsorbed state and those residing in the lattice. For the charging process to occur we require that the inequality, Eq. (23)

$$\mu(a,t) - \mu(l,t) > 0 \tag{23}$$

be fulfilled at all times. But, since $\mu(a,t) = f_1(\theta)$ and $\mu(l,t) = f_2(\varsigma)$, it follows that the charging process may be conveniently examined in terms of the surface coverage which is determined by the participating processes responding to the applied charging current. The amount of material incorporated into the electrode interior and its distribution was calculated to determine whether or not a threshold value for loading has been reached and to provide information on the efficiency of the charging process.

An example of an electrode charging is shown in Fig. 2 where two time intervals are delineated. The first, of a short duration, *eg*, less than 0.1 second, during which the processes within the interphase dominate. This period terminates when these processes become stationary, *ie* as $\theta(t) \rightarrow \theta_{lim}$ and $\eta(t) \rightarrow \eta_{lim}$. The second time interval, of a considerable length, is that during which actual charging of the electrode interior occurs, *ie*, the fraction of available sites occupied $Q(t) \rightarrow Q_{lim}$.

4.2.1 Electrode initial response to current flow.

The assumed model, Fig. 1, provides for position dependent elementary processes, *ie.*, it suggests the separation of processes occurring within the interphase from those within the electrode interior. It follows that the electrode charging and the effect of rate constants can be examined within well defined time intervals, as illustrated in Fig. 2, of which the first time interval consists of three distinct time periods: the first, $0 < t < \tau_1$, represents the charging of the double layer; the second, $\tau_1 < t < \tau_2$, covers the period needed for the attainment of a quasi-stationary state; and the third $t > \tau_2$ is the time during which the electrode begins to accept intersttials, Fig. 3. For different choices of rate constants, the regions may be less distinct and the time dependence of the surface coverage and overpotential can have somewhat different forms. The amount of the interstitial material absorbed during the attainment of the quasi-steady state of surface coverage is insignificant under all conditions examined (*eg*, on the order of 0.0001% above the assumed equilibrium value).

As expected, an elementary process that controls the overall reaction also controls the time dependence of both the surface coverage and overpotential. In particular, Fig. 4 illustrates the effect of an emerging rds. Here, the pairs of curves, respectively, a - a', b - b', etc are the $\theta(t)$ and $\eta(t)$ that represent changes in the surface coverage and overpotential with the changing ratios of k_2/k_1 and k_3/k_1. Clearly, as these ratios are decreased, the quasi-steady state surface coverage, θ_{lim}, increases due to enhanced adsorption and reaches a limiting value of one. Further decrease in this ratio, after $\theta_{lim} = 1.0$, causes the knee of the $\theta(t)$ curve to move to earlier times, cf. curves c and d. It is noted that within the time period examined, the

amount of absorption is insignificant; consequently, as expected, an agreement with the earlier work of Gileadi and Conway(18) is evident.

A somewhat different behavior is seen as the rds is changed from the recombination reaction, Fig. 5 curve a, to electrodesorption, Fig. 5 curve b. The effect, which is minimal in the $\theta(t)$ curve, is associated with a more negative overpotential, decreased by *ca* 200 mV and a longer time required to attain the quasi-staedy state. This is likely connected with the fact that the recombination reaction does not involve charge transfer.

Intuitively, the present model ascribes a dominant role to the rate of absorption, *viz.*, the higher the rate, the faster the charging of the electrode. However, due to coupling between the surface processes, no such clear conclusion should be drawn unless the interphase (j_3, j_{-3}) controls the overall event. In general, an increase in the rate of absorption shifts the attainment of the quasi-steady state to somewhat longer times, as illustrated in Fig. 6. Also, the lower the rate of absorption, the greater the tendency to develop a maximum in the $\theta(t)$ curve, Fig. 6, curve a.

The coupling effect of the interphase processes on the surface coverage and overpotential as a function of charging current, suggested by Eqs. (13) and (14), is illustrated in Figs. 7 - 9. Here, three cases are illustrated, *viz.*, with the electrodesorption reaction as the rds, θ_{lim} increases with an increase in the charging current, Fig. 7 ; with a less clearly defined rds, θ_{lim} first increases, goes through a maximum and then decreases, Fig. 8; and with recombination/adsorption as a rather weak rds, θ_{lim} always decreases with an increase in the charging current, Fig. 9.

4.2.2 Charging of electrode interior.

A threshold phenomenon has been proposed to initiate the effects reported by Fleischmann and Pons, *ie*, contingent on achieving a degree of loading exceeding a certain critical value within a reasonably short period of time. In this section, we illustrate the interphase control *vs* bulk transport control and show that

an increase in the charging currents need not increase the level of electrode loading.

The coupling between interfacial processes and bulk transport admits, in principle, two modes of charging control. This is illustrated in Figs. 10 and 11. To demonstrate the transition from interphase to transport control, we calculated the time dependences $\theta(t)$,$\eta(t)$ and the normalised amount of absorbed deuterium in terms of $Q(t) = \sum_{i=1}^{N} V_i \varsigma_i(t) \; / \; \sum_{i=1}^{N} V_i$ for the values of the diffusion coefficient differing by several orders of magnitude. As expected and illustrated in Fig. 10, the initial electrode response is independent of the diffusion coefficient. The quasi-steady state was established within 0.5 second. However, as soon as the build-up of absorbed deuterium has begun, θ and Q vary almost linearly with time. For an unrealistic value of the diffusion coefficient, (*eg*, $D = 10^{-4}\ cm^2 s^{-1}$), θ and Q reached almost simultaneously their limiting values. This is consistent with interphase control. The transition to transport control, however, is not sharp and the electrode exhibits a mixed control for a substantial range of diffusion coefficients, *eg*, $10^{-6} < D < 10^{-8}\ cm^2 s^{-1}$. In particular, for the set of input parameters in the example illustrated in Fig. 10, the electrode charging is under diffusion control only when $D = 10^{-8},\ cm^2 s^{-1}$ or less. This transition from interphase to diffusion control manifests itself by an increase in the slope $d\theta/dt$ and a substantial delay in the achievement of full saturation of the electrode interior. The distribution of the filling of the available sites, Fig. 11, further illustrates the transition from the interphase to bulk diffusion control.

Another example of the effect of the complex interplay between the interphase processes at two charging current densities is shown in Fig. 12. Contrary to intuitive expectations that an increase in the charging currents should increase loading, the model predicts that, with a specific set of rate constants, a lower level of loading can result with no reduction in charging time observed.

5.0 Concluding remarks.

Qualitatively, the model reflects the complicated nature of the charging process. It indicates that difficulties may be encountered in controlling the charging process because of the large number of factors that

may affect one or more of the interphase processes. Quantitative analysis could not be carried out because the relevant data were not available and the use of kinetic parameters associated with the hydrogen evolution reaction cannot be justified in view of recent results(23). Other simplifications, *eg*, the constancy of input parameters can be corrected (for example, a concentration dependent diffusion coefficient could be included). A more serious deficiency is the employment of the simplest interphase when, in fact, a supercharged region exists.

Acknowledgement

The authors wish to thank Professors Fleischmann and Pons for helpful comments.

References

1. J. Jorne, J. Electrochem. Soc., **137** (1990) 369

2. M. Fleischmann and S. Pons, J. Electroanal. Chem., **261** (1989) 301

3. C. Wagner, Z. phys. Chem., **A159** (1932) 459; ibid., **A193** (1944) 386

4. R. Fowler and E. A. Guggenhein, Statistical Thermodynamics, Cambridge Univ. Press, 1949

5. H.-G. Fritsche, Z. Naturforsch., **38a** (1983) 1118

6. M. v. Stackelberg and P. Ludwig, Z. Naturforsch., **19a** (1964) 93

7. B. Dandapani and M. Fleischmann, J. Electroanal. Chem., **39** (1972) 323

8. H. Brodowsky, Z. phys. Chem.,N. F.,**44** (1965) 9

9. R. M. Stoneham, Ber. Bunsenges.,**76** (1972) 816

10. J. Voelkl, ibid., **76** (1972) 797

11. E. Wicke and G. H. Nernst, ibid., **68** (1964) 224

12. R. Defay, I. Prigogine, A. Bellamans and D. H. Everett, Surface Tension and Adsorption, Longmans, Green and Co, Ltd., London, 1966

13. H.-D. Ohlenbusch, Z. Elektrochem., **60** (1955) 603

14. P. van Rysselberghe, in Moderns Aspects of Electrochemistry, (J. O'M. Bockris and B. E. Conway,

eds.), Plenum Press, New York

15. W. Auer and H. J. Grabke, Ber. Bunsenges., **78** (1974) 58

16. E. Fromm, H. Uchida and B. Chelluri, ibid., **87** (1983) 410

17. S. Schuldiner and J. P. Hoare, J. Electrochem. Soc., **105** (1958) 278

18. E. Gileadi and B. E. Conway, J. Chem. Phys., **39** (1963) 3420

19. R. N. Iyer, H. W. Pickering and M. Zamanzadeh, J. Electrochem. Soc., **136** (1989) 2463

20. R. M. Barrer and W. Jost, Trans. Far. Soc., **45** (1949) 928

21. M. Kuballa and B. Baranowski, Ber. Bunsenges., **78** (1974) 335

22. G. Sicking, M. Glugla and B. Huber, ibid., **76** (1972) 418

23. D. Rolison and P. P. Trzaskoma, J. electroanal. Chem., in press

24. S. Szpak, P. A. Mosier-Boss and J. J. Smith, unpublished results (1990)

25. J. W. Davenport, G. J. Dienes and R. A. Johnson, Phys. Rev., **25** (1982) 2165

26. W. H. Press and S. A. Teukolsky, Computers in Physics, May/June issue, 1989, p. 88

Appendix: Derivation of Eqs. (17) and (18).

The cross section of the rod of length L and radius r_0 is partitioned into N anular layers of thickness Δr. With the layers labeled from 1 to N from the outer surface to the center, respectively, the volume V_i of the $i-$ th layer and the interface surface $S_{i,i+1}$ between the $i-$ th and $i+1-$ th layers are:

$$V_i = \pi(r_i^2 - r_{i+1}^2)L \tag{1A}$$

$$S_{i,i+1} = 2\pi r_{i+1}L \tag{2A}$$

where $r_i = (N - i + 1)\Delta r$. Consequently, the relevant surface to volume ratios are

$$\frac{S_{i-1,i}}{V_i} = \frac{2r_i}{r_i^2 - r_{i+1}^2} = \left(\frac{2r_i}{r_i + r_{i+1}}\right)\frac{1}{\Delta r} \tag{3A}$$

and

$$\frac{S_{i,i+1}}{V_i} = \frac{2r_{i+1}}{r_i^2 - r_{i+1}^2} = \frac{2r_i}{r_i + r_{i+1}}\left(1 - \frac{\Delta r}{r_i}\right)\frac{1}{\Delta r} \tag{4A}$$

Subsitutions of these ratios into Eq. (8) yields

$$\frac{d\varsigma_i}{dt} = k_d Z_m \Delta r \left(\frac{2r_i}{r_i + r_{i+1}}\right)\left[\frac{\varsigma_{i-1} - 2\varsigma_i + \varsigma_{i+1}}{\Delta r^2} + \frac{1}{r_i}\left(\frac{\varsigma_i - \varsigma_{i+1}}{\Delta r}\right)\right] \tag{5A}$$

which, upon rearrangement becomes Eq. (19). The ratios given in Eqs. (3A) and (4A) become, for $i = 1$

$$\frac{S_{0,1}}{V_1} = \left(\frac{2r_0}{2r_0 - \Delta r}\right)\frac{1}{\Delta r} \tag{6A}$$

and

$$\frac{S_{1,2}}{V_1} = \frac{2r_0}{2r_0 - \Delta r}\left(1 - \frac{\Delta r}{r_0}\right)\frac{1}{\Delta r} \tag{7A}$$

since $r_1 = r_0$ and $r_2 = r_0 - \Delta r$. Substitution of Eqs. (6A) and (7A) into Eq. (17) yields Eq. (18).

The form of Eq. (5A) shows the relationship of Eq. (5A) to the diffusion equation written in cylindrical coordinates and approximated by finite differences. Generally, $k_d Z_m \Delta r$ would be identified with the diffu-

sion coefficient and the ratio $2r_i/(r_i + r_{i+1})$ set equal to one as, in the limit, Δr approaches zero. However, here we retain the ratio as Δr is not necessarily small enough to take the limit, but do identify the diffusion coefficient as $k_d Z_m \Delta r$.

Figure captions

Fig. 1 - Schematic representation of an interphase (fluxes included).

a - adsorption plane; t - charge transfer plane; l - lattice

Fig. 2 - Evolution of surface coverage, overpotential and concentration of interstitial in the course of electrode charging.

Fig. 3. - Surface coverage and overpotential as a function of time. Initial period: charging of the double layer, $0 < t < \tau_1$; un-steady state, $\tau_1 < t < \tau_2$; quasi-steady state, $t > \tau_2$.

Charging current: $-40 \cdot 10^{-3}\ A/cm^2$;

Rate constants:

$k_1 = 10^3\ cm^3/mole-s$; $k_2 = 10 cm^3/mole-s$;

$k_3 = 10^3 cm^2/mole-s$; $k_4 = 2.0 \cdot 10^5 cm^3/mole-s$.

Fig. 4. - Surface coverage and overpotential as a function of time. Effect of an emerging rds.

Charging current: $-40 \cdot 10^{-3}\ A/cm^2$;.

Rate constants:

$k_2 = 1.0 cm^3/mole-s$, $k_3 = 0.1 cm^2/mole-s$, $k_4 = 3 \cdot 10^6\ cm^3/mole-s$;

$k_1 = 10^2$, 10^3 , 10^4 , $10^5\ cm^3/mole-s$ curves a, b, c and d, respectively.

Fig. 5 - Surface coverage and overpotential as a function of time. Effect of changing the rds.

Charging current: $-40 \cdot 10^{-3}\ A/cm^2$; $\theta_0 = 0.1$; $\zeta_0 = 0.08$.

Rate constants: $k_1 = 10^6\ cm^3/mole-s$, $k_4 = 2.0 \cdot 10^7\ cm^3/mole-s$.

curve a - $k_2 = 1.0\ cm^3/mole-s$, $k_3 = 10^3\ cm^2/mole-s$

curve b - $k_2 = 10^3\ cm^3/mole-s$, $k_3 = 1.0\ cm^2/mole-s$.

Fig. 6 - Surface coverage and overpotential as a function of time. Effect of adsorption-absorption exchange

rate.

Charging current: $-40{\cdot}10^{-3}\ A/cm^2$.

Rate constants: $k_1 = 10^5\ cm^3/mole{-}s$, $k_2 = 100 cm^3/mole{-}s$, $k_3 = 0.1\ cm^2/mole{-}s$.

curve a - $k_4 = 3.0{\cdot}10^4\ cm^3/mole{-}s$

curve b - $k_4 = 3.0{\cdot}10^5\ cm^3/mole{-}s$

curve c - $k_4 = 3.0{\cdot}10^6\ cm^3/mole{-}s$

curve d - $k_4 = 3.0{\cdot}10^7\ cm^3/mole{-}s$

Fig. 7 - Surface coverage and overpotential as a function of time: Effect of charging current.

Rate constants: $k_1 = 10^5 cm^3/mole{-}s$, $k_2 = 10^3\ cm^3/mole{-}s$,

$k_3 = 1.0\ cm^2/mole{-}s$, $k_4 = 2.0{\cdot}10^7\ cm^3/mole{-}s$.

curve a - $-4.0{\cdot}10^{-3}\ A/cm^2$

curve b - $-10.0{\cdot}10^{-3}\ A/cm^2$

curve c - $-40.0\ 10^{-3}\ A/cm^2$

curve d - $-80{\cdot}10^{-3}\ A/cm^2$

Fig. 8 - Surface coverage and overpotential as a function of time: Effect of charging current. Rate constants: as in Fig. 6 except for $k_3 = 10.0\ cm^2/mole{-}s$.

curve a - $-10.0{\cdot}10^{-3}\ A/cm^2$

curve b - $-40.0{\cdot}10^{-3}\ A/cm^2$

curve c - $-80.0{\cdot}10^{-3}\ A/cm^2$

curve d - $-160.0{\cdot}10^{-3}\ A/cm^2$

curve e - $-800.0{\cdot}10^{-3}\ A/cm^2$

Fig. 9 - Surface coverage and overpotential as a function of time: Effect of charging current. Rate constants:

$k_1 = 1000 cm^3/mole{-}s$, $k_2 = 10 cm^3/mole{-}s$, $k_3 = 1000 cm^2/mole{-}s$, $k_4 = 2.0{\cdot}10^5\ cm^3/mole{-}s$.

curve a - $-4.0 \cdot 10^{-3}\ A/cm^2$

curve b - $-10.0 \cdot 10^{-3}\ A/cm^2$

curve c - $-40.0 \cdot 10^{-3}\ A/cm^2$

curve d - $-80.0 \cdot 10^{-3}\ A/cm^2$

curve e - $-800.0 \cdot 10^{-3}\ A/cm^2$

Fig. 10 - Time dependent overpotential, η, surface coverage, θ, and normalized amount of absorption as a function of diffusion coefficient.

curve a: $10^{-4}\ cm^2/s$; b : $10^{-8}\ cm^2/s$; c : $10^{-10}\ cm^2/s$

charging current: $0.1\ A/cm^2$

rate constants:

$k_1 = 10^3\ cm^3/mole-s$, $k_2 = 10\ cm^3/mole-s$

$k_3 = 10^3\ cm^2/mole-s$, $k_4 = 2 \cdot 10^5\ cm^3/mole-s$

Fig. 11 - Normalized amount of absorbed material as a function of distance.

Diffusion coefficients (in cm^2/s) indicated; Other data as in Fig. 10

Fig. 12 - Effect of charging current on electrode loading.

curve: a- $0.05\ A/cm^2$; b- $0.1\ A/cm^2$

rate constants -

$k_1 = 10^3\ cm^3/mole-s$; $k_2 = 10\ cm^3/mole-s$

$k_3 = 10^3\ cm^2/mole-s$; $k_4 = 2 \cdot 10^5\ cm^3/mole-s$

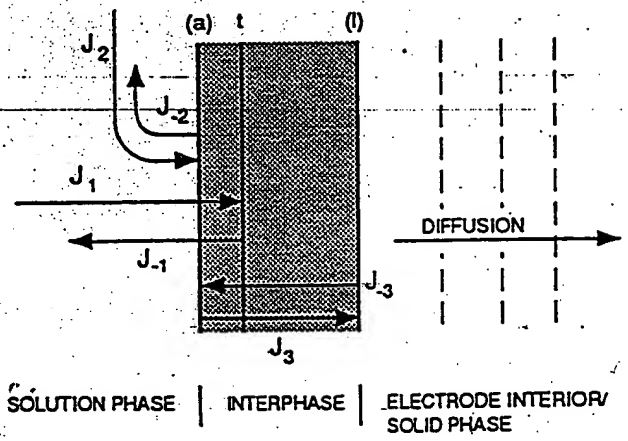
(a)
t
(l)
J_2
J_{-2}
J_1
J_{-1}
J_{-3}
J_3
DIFFUSION
SOLUTION PHASE
INTERPHASE
ELECTRODE INTERIOR/
SOLID PHASE

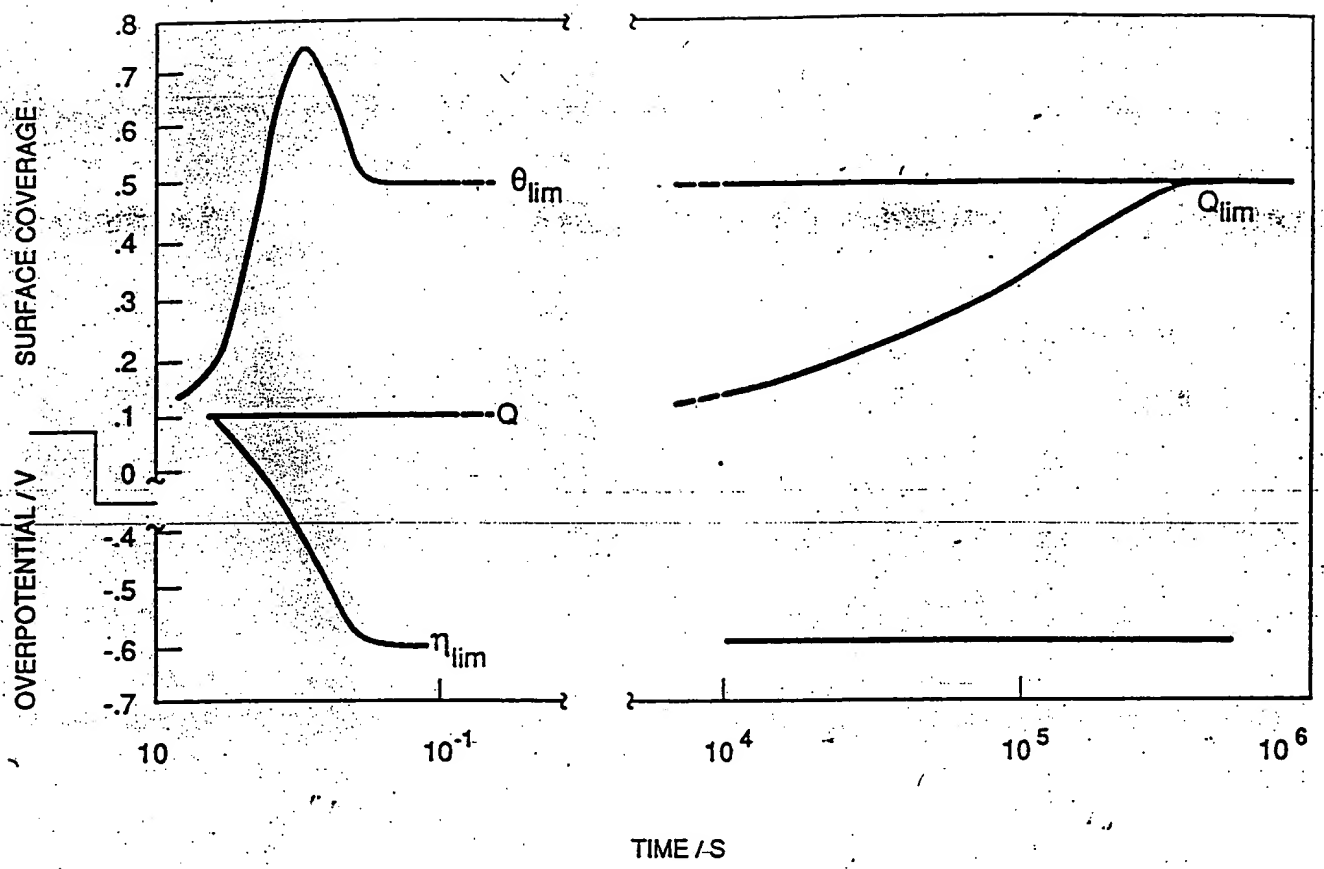
SURFACE COVERAGE
OVERPOTENTIAL / V
.8
.7
.6
.5
.4
.3
.2
.1
0
-.4
-.5
-.6
-.7
θ_{lim}
Q
η_{lim}
Q_{lim}
10
10^{-1}
10^4
10^5
10^6
TIME / S

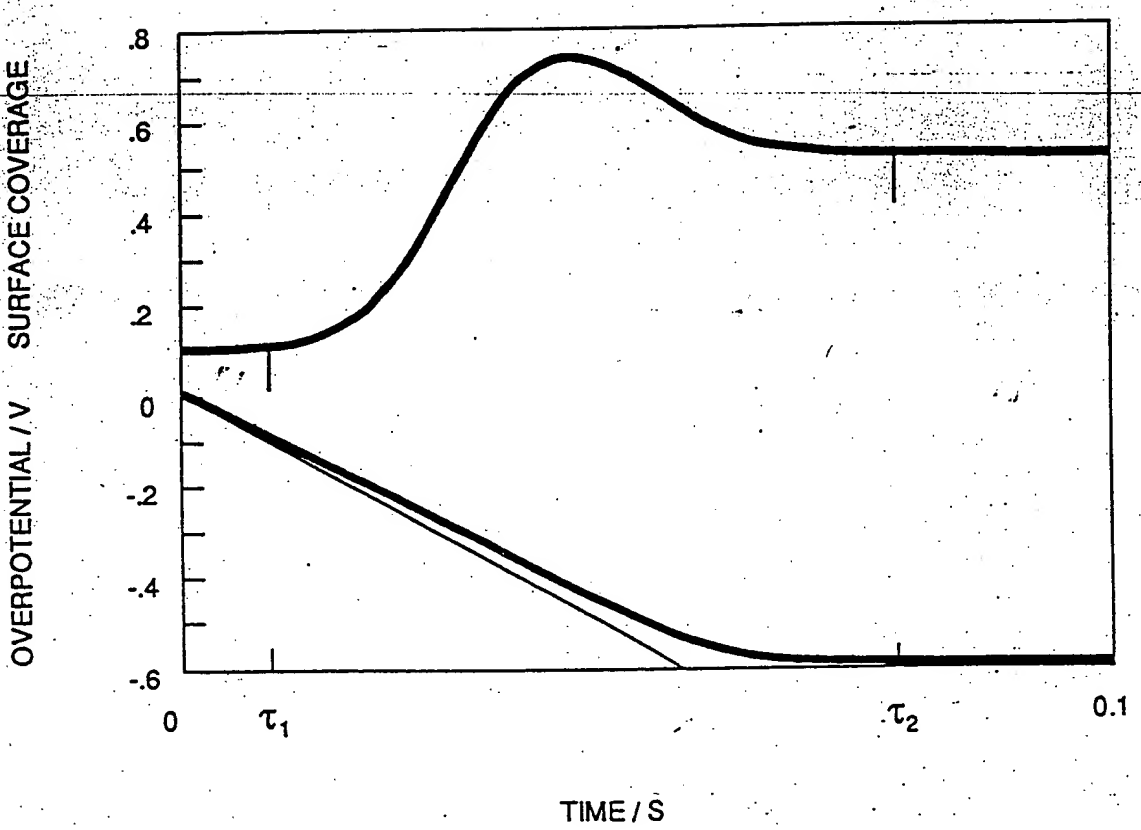
OVERPOTENTIAL / V
SURFACE COVERAGE
.8
.6
.4
.2
0
-.2
-.4
-.6
0
τ_1
τ_2
0.1
TIME / S

Figure 3

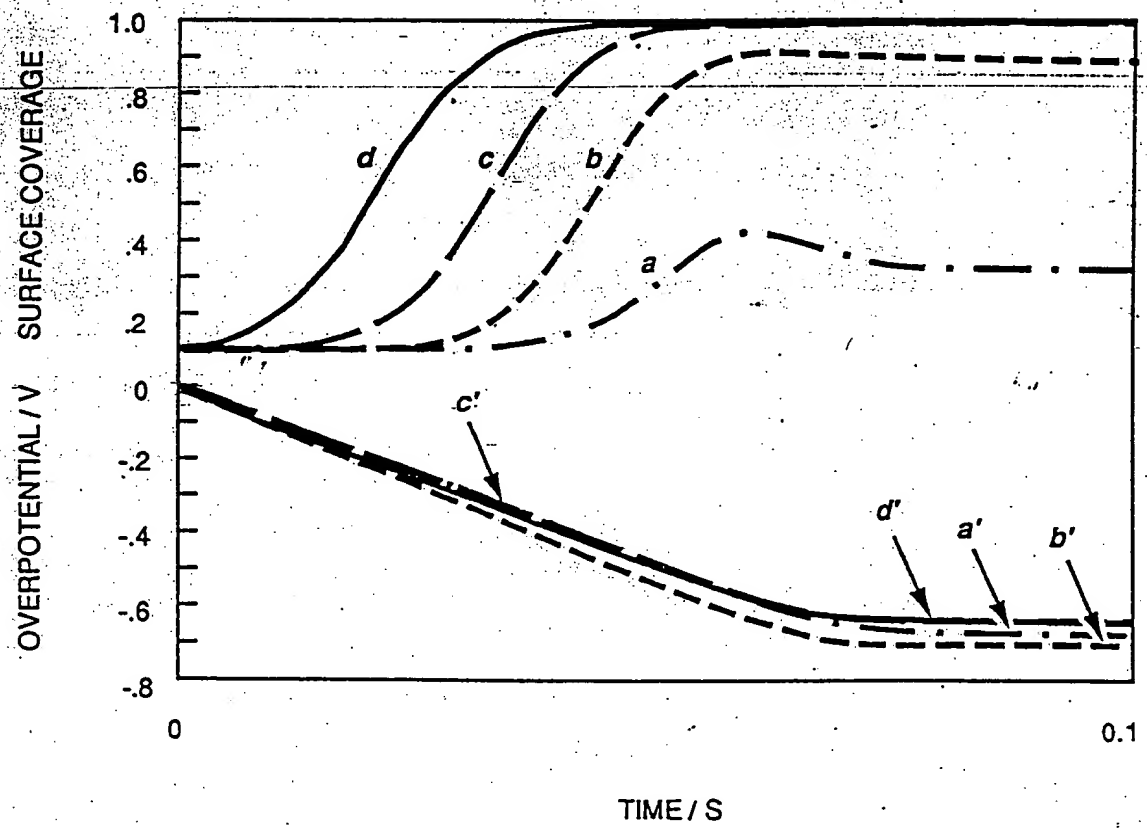
SURFACE COVERAGE
OVERPOTENTIAL / V
1.0
.8
.6
.4
.2
0
-.2
-.4
-.6
-.8
d
c
b
a
c'
d'
a'
b'
0
0.1
TIME / S

Figure 4

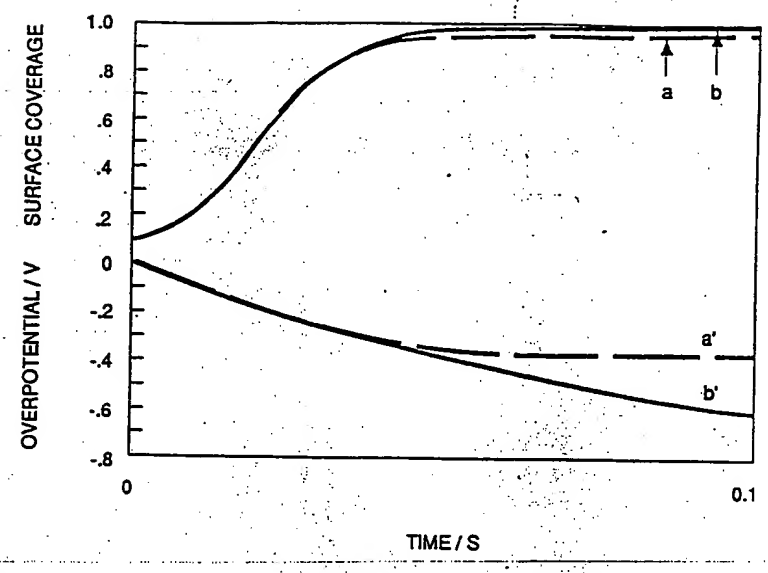
OVERPOTENTIAL / V SURFACE COVERAGE
1.0
.8
.6
.4
.2
0
-.2
-.4
-.6
-.8
a
b
a'
b'
0
0.1
TIME / S

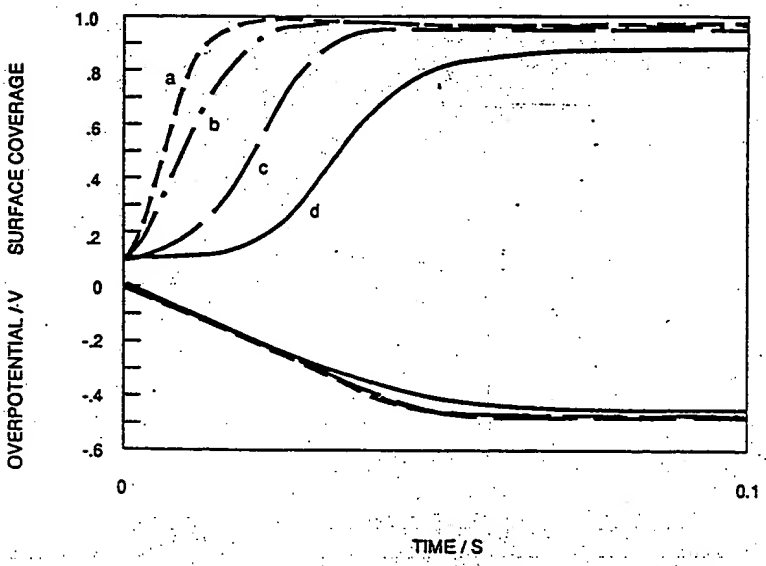
OVERPOTENTIAL /V SURFACE COVERAGE
1.0
.8
.6
.4
.2
0
-.2
-.4
-.6
a
b
c
d
0
0.1
TIME / S

9-13 April, 1995
ICCF5 ©1995

Radioactivity of the Cathode Samples after Glow Discharge.

SAVVATIMOVA I.B, KARABUT A.B.
Scientific Industrial Association "Lutch"
142100 Podolsk, Moscow Region, 24 Zhelesnodorozhnaya St. Russian Federation
Phone:(7-095) 137-9258; Fax:(7-095) 137-93-84;
E-mail: postmaster@npoluch.msk.su

We registered the residual radioactivity of the cathode foils (Pd, Ag, Nb and other materials) after irradiation at the glow discharge. The samples were irradiated by proton, deuteron and argon, xenon ions with low energy. We consider that main activity is beta emission from samples after experiments /1/. Samples were placed in the contact with X-ray films. Semiquantitative radiographic method with measurement of the degree of blackening x-ray films by micro photometer was used. We made the estimate of beta activity of the samples . The x-ray film was calibratec with use of a tritium beta source with activity of $4.1 \cdot 10^9 \beta.s^{-1}$ (Ti implanted). The characteristic curve from this film was gotten in vacuum chamber. The high energy radiation was compared with 90Sr radiation ($E\beta$ ~546 keV). Within ~103 s after discharge termination the second x-ray film exposure corresponds to equivalent dose of $(1.5\text{-}4.5) \cdot 1010\ \beta/cm^2$ from 90Sr. Activity of the isotope(s) with high radiation energy is estimated as corresponding to 90Sr activity of $\sim(2\text{-}5) \cdot 10^4\ \beta/(cm^2 \cdot s)$.

Earlier we said that there were at least two isotopes with different energy: first < 20 keV and second (0.1...0.5) MeV /2/. Now we would like to note that activity was not observed for ion irradiated zones some times, when high ion's density was at the experiments with compound cathode samples (put together. of the 2-7 foils from different materials). In this case high energy activity isotope was observed only in the second layer of the X-ray film.

Activity of the irradiated surface in comparison with non irradiated surface was less to 2-10 times (Fig.1,2). Encrease of the radioactive isotopes energy were registered after experiment only during 2-4 hours (Fig. 3).

When we took other cathodes (Ag, Nb, Ti... instead of Pd), its activity was less Pd to 10-100 times under equal conditions of the experiments. Activity Ag,Nb, Ti was less $10^2\text{-}10^4 cm^{-2}s^{-1}$.

Activity of the Pd films under Ag, Nb and others was more to 10^5-10^6 $cm^{-2}s^{-1}$ (Fig.2).

We observed increase of the sample radioactivity during the first several hours after experiment and its decreasing later. It means, that radioactive chains of the nuclear decay was regestrated.

We did not observe activity of the Ag cathode after deuterium ions and watched the Pd cathodes' activity after Ar, Xe ions under other equal conditions of the experiment. Thus we registered the irradiation in the resuit of the blackening films that was not the result of the formation tritium or chemical interaction H, D, T with X-ray films.

We have to note the following main results:

- increase of the sample radioactivity during the first several hours after experiment and its decreasing later;
- presence of the radioactive nucleus with different energy from units to hundreds keV on the cathode ;
- radioactivity of the samples after Ar, Xe irradiation presence.

As the result we can suppose that we observed radioactive chains of the nuclear decay. It means that we have more universal phenomenon than reactions in the system Pd-D (passing nuclear process during and after irradiated low energy ions).

References:

1. I.Savvatimova, Ya.Kucherov and A. Karabut, "Cathode Material Change after Deuterium Glow Discharge Experiments," Transactions of Fusion Technology, v.26:1994, pp. 389-394, Fourth Int. Conf. on Cold Fusion, Dec. 6-9,1993, Hawaii.

2. A.Karabut, Ya.Kucherov, I.Savvatimova "Nuclear product ratio for glow discharge in deuterium". Physics Letters A, 170, 1992, 265-272 .

3. A.Karabut, Ya.Kucherov, I.Savvatimova "Possible Nuclear Reactions mechanisms at Glow Discharge in Deuterium," Proc.of the Third the Int. Conf, on Cold Fusion, Nagoya, Japan October 21-25,1992, pp. 165-168.

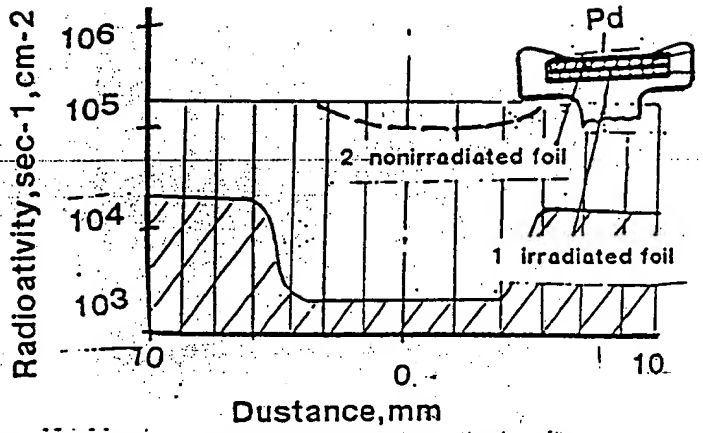

Fig. 1 Activity of the foils of the complite cathode after experiment in the deuterium (Pd+Pd)

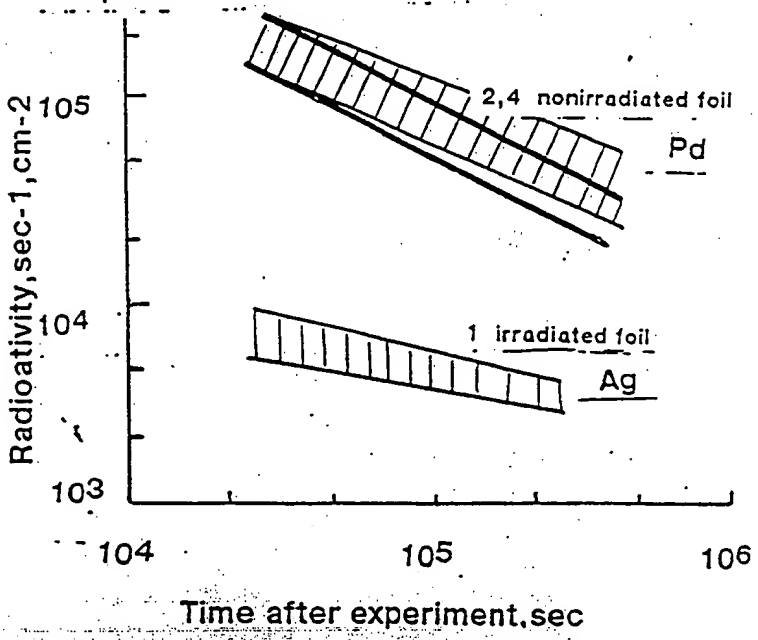

Fig. 2 Activity of the foils of the complite cathode after experiment in the deuterium (Ag+Pd+Ag+Pd)

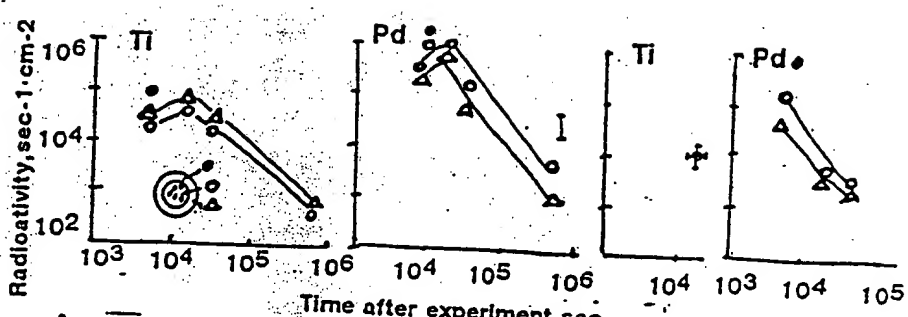

a

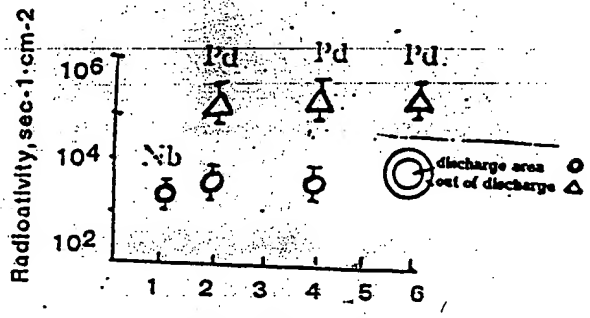

b

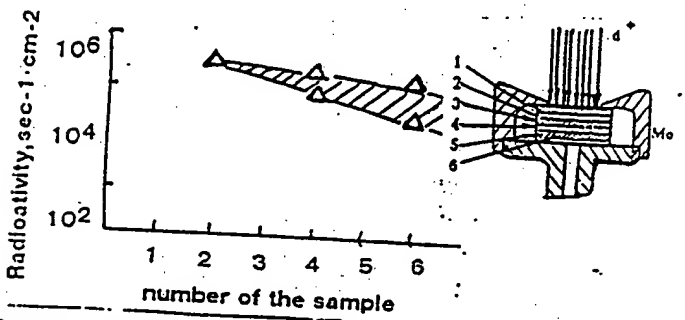

c

Fig 3 Activity of the foils of the complite cathode after experiment in the deuterium (Ti+Pd+Ti+Pd)

1-Ti; 2-Pd; 3-Ti; 4-Pd. ● specks ○ center of the sample △ under screen area

(Nb-Pd-Nb-Pd-Nb-Pd)

1 - irradiated foil, 2,3,4,5,6 - nonirradiated foil

1,3,5 - Nb; 2,4,6 - Pd

○ - discharge area, △ - out of discharge

b - $2.3 \cdot 10^4$ cccond after experiment,

C - $4.5 \cdot 10^4$ second after experiment,

9-13 April, 1995 - Monte Carlo, Monaco
ICCF5 ©1995

Solving the Puzzle of Excess Heat without Strong Nuclear Radiation

Xing Zhong LI*
Department of Physics, Tsinghua University
Beijing 100084, CHINA
*Current address: Dept. of Chem., Univ. of Hawaii, Honolulu, HI 96822-2275, USA

Abstract

Five experimental evidences show that the excess heat is from a nuclear source with a life-time of 10^4 seconds. This life-time is shown to be related to the barrier penetration number, θ, in terms of the resonance penetration theory. The boson nature of the deuteron ion (D^+), and the deuteron energy band structure in lattice play the critical roles in filling the corresponding narrow resonance energy level. Prof. J. Huizenga's challenge of three miracles[1] is answered, and "excess heat" without strong nuclear radiation is a reasonable phenomenon. It predicts: (1) there must be a critical loading ratio; (2) the greater the grain size and the activation energy are, the better the reproducibility.

1. Introduction

After six years of studies on the "cold fusion" phenomenon, two facts are established: (1) Under certain conditions there is "excess heat" of several watts per cubic centimeter of palladium; (2) There are no commensurate neutrons, tritons, or γ-radiation in parallel with the "excess heat" which is of non-chemical origin. The regression is that: instead of using the neutron signal to convince people to believe there is any nuclear reaction, we attempt to explain that these two facts are due to the existence of a long life-time nuclear resonance state inside a lattice.

Early in 1928, Gamow proved that the life-time of an α-radiation nuclide, τ_α, was determined by the Coulomb barrier penetration number, θ.[2] At that time the α-particle after disintegration was a free-moving particle , and $\tau_\alpha \propto \theta^{-2}$. Now the penetration of the Coulomb barrier happens in a reverse direction and in a different environment: the lattice confined deuteron penetrates the Coulomb barrier and enters a resonance state. The life-time of this resonance state, τ_{xh}, is determined by the θ again, but $\tau_{xh} \propto \theta$. Now τ_{xh} is linearly proportional to the θ due to the discrete nature of the energy level of the lattice confined deuteron which is different from the continuum of the free-moving deuteron.

We will start from the experimental evidences of this long life-time state (section 2); then, we calculate this life-time based on the nuclear resonance theory (section 3). In order to fill this resonance state, this theory requires a critical loading ratio which is another well-established experimental fact in the past five years (section 4). Finally, we discuss the famous challenge of three miracles (section 5), and the conclusion (section 6).

2. Evidences for Long Life-time State

The strongest evidence is from the "heat after death".[3] The boiling-to-dry electrolytic cell was kept at about 100 °C for three hours without any power input. It clearly showed that the "excess heat" source was inside the palladium deuteride. The reliable calorimetric calculation proved that the energy released in this 3 hours was 20 times greater than the heat of combustion possibly released by the deuterium stored in this system. This was a nuclear active state with a life-time of 10^4 seconds.

The second evidence is from the "heat after life".[4] The SRI electrolytic cell was a closed cell. It was not driven to boil. However, when the electrolysis was shut down, and input power was zero, the system did not cool down as a source-free system. The flow-calorimeter clearly recorded that there was an energy source inside the system. The first peak of the "excess power" was about 100 mW (the accuracy and the precision of that experiment was ±10 mW), and the width of that peak was about 3 hours again. The energy released in these three hours was also about 10 times greater than the heat of combustion possibly released by the deuterium available in the palladium electrode. This was again a nuclear active state with a life-time of 10^4 seconds.

During the ICCF-5, J.P. Biberian's "excess heat" data [5] showed that after the shut down of the input power, the "excess heat" continued for 3–4 hours. Although there was no palladium lattice, an $AlLaO_3$ single crystal provided the lattice confined deuterons. Once again the life-time of that "excess heat" source was of the order of 10^4 seconds.

In the "Critical Review of the 'Cold Fusion' Effect",[6] E.Storms talked about the replacing time of the palladium deuteride. When he put the deuteron-loaded electrode into the light water cell, he observed the "excess heat" continuing for the first several hours. He called this time the replacing time, because he considered that when the deuteride was replaced by hydride, the "excess heat" was supposed to stop. From another point of view, this showed that the life-time of the nuclear active state was again of the order of 10^4 seconds.

After my talk in ICCF-5, M.Eisner of the University of Houston was so kind as to give me his 1989 data for the "excess heat".[7] It clearly showed that the width of the first "excess power" peak after the shut down of the electrolysis was once again of the order of 10^4 seconds.

It was not realized that the answer to Prof. J.Huizenga's challenge of three miracles has been indeed implied in this long life-time of nuclear active state.

3. Theory of Resonance Penetration for Lattice Confined Ions

The life-time of a quantum mechanical state, τ, is related to the width of its energy level, Γ, by the uncertainty principle:

$$\tau \approx \frac{\hbar}{\Gamma} \tag{1}$$

The width of the energy level can be expressed by the imaginary part of the wave number, k^I, through the identity:

$$\Gamma = \mathrm{Im}U \equiv \frac{\hbar^2}{m} k^r k^I \tag{2}$$

Here $\mathrm{Im}U$ is the imaginary part of the potential well U, k^r and k^I are the real and imaginary part of the wave number k, respectively. $k^2 \equiv \frac{2m}{\hbar^2}(E-U)$. E is the total energy of the relative motion of the two deuterons. When the energy E coincides with the energy level inside the nuclear well, $(k^r a) \approx O(1)$. Here a is the size of the nuclear well. However

$$\left|k^I a\right| \approx O(\theta^{-1}) \tag{3}$$

for this resonance. Here θ is defined as

$$\theta \equiv \exp[\int_a^b \sqrt{\frac{2m}{\hbar^2}(U-E)}dr] \tag{4}$$

and θ^{-2} is just the famous Gamow barrier penetration factor. Equation (3) has been rigorously proved for the square well case, [8] and for the arbitrary potential configuration.[9] Here we just explain why the imaginary part of the wave number, k^I, should be such a small number in order to have a resonance penetration. As we know, when $k^I < 0$, k^I determines the damping of the wave function. The wave $e^{-ik^r r}$ will be damped by a factor of $\exp[-\left|k^I a\right|]$ when the wave propagates through a length of a. On the other hand the Coulomb barrier suppresses the amplitude of the penetrating wave function by a factor of θ^{-1}. In order to use the resonance effect to build-up the wave amplitude to its initial value in terms of the constructive interference between the reverberating wave and the penetrating wave, we need at least θ-times reverberation before the wave is damped. So we need $\left|k^I(\theta a)\right| \le O(1)$, or $\left|k^I a\right| \le O(\theta^{-1})$.

Consequently, sustituting k^r and k^i in eq.(1) and (2), we have the life-time for "excess heat"

$$\tau_{xh} \approx \frac{ma^2}{\hbar}\theta \tag{5}$$

For the d+d interaction, m≈10^{-24}g., $a \approx 10^{-13}$ cm, $\theta \approx 10^{27}$, [10,11] we have $\tau_{xh} \approx 10^4$ sec. The theory just gives the correct order of magnitude of the life-time of the nuclear active state.

4. Bose Condensation and the Critical Loading Ratio

Such a long life-time state corresponds to a very narrow energy level in the order of 10^{-19} eV. This is the reason why we could not observe this resonance level in any low energy beam-target experiment.[12] Because the beam energy distribution is much wider than the width of the resonance energy level, it is an analogy to using a screw driver to detect a tiny crack in a brick wall. The crystal lattice assists in observing this narrow resonance in two ways: (1) the trapped deuteron ion in the lattice well is sitting on a discrete energy level with very narrow width also; (2) the periodical structure of the lattice well creates an energy band for the trapped deuteron ions. Then, we have a bunch of needles to detect the single tiny crack on the brick wall. The number of the energy levels (needles) in this band is determined by the grain size, L (i.e. the size of the periodical structure, or the coherent length), and the size of the primitive cell in the palladium lattice, δ (i.e. the size of the PdD molecule). When $\delta \approx 3\text{Å}$, L≈ 60μ, we have roughly $(L/\delta)^3 \approx 10^{16}$ energy levels inside a deuteron energy band. On the other hand the deuteron energy band width, Γ_B, is determined by the size of the primitive cell as:

$$\Gamma_B \le \frac{\hbar^2}{2m}\left(\frac{1}{\delta}\right)^2 \approx 10^{-3}\,\text{eV} \tag{6}$$

Thus, the energy difference between each neighboring energy level inside the band is about 10^{-19} eV. Hence, if the whole band is occupied by the deuterons; then, the whole population has the chance to be in resonance penetration of Coulomb barrier, as long as the energy band is adjusted to a level in resonance with the nuclear energy level. When $(L/\delta)^3 << 10^{16}$, we have much less chance to have resonance penetration of the Coulomb barrier due to the difficulty in matching the narrow nuclear energy level with the lattice energy level.

Now the question is: how can we populate the deuterons into this energy band ? We need the Bose-Einstein condensation. Experiment has shown that hydrogen solved in palladium acts like an ion,[13] so deuteron should act like a boson. If the deuterons are totally free-moving particles like a gas inside the palladium; then, the critical density for Bose-Einstein condensation is about[14]

$$n_c = 2.612\left(\frac{mk_BT}{2\pi\hbar^2}\right)^{3/2} \approx 8.5\times10^{24}\ \text{cm}^{-3} \tag{7}$$

It is much higher than the maximum possible deuteron density inside the palladium ($\approx 6.8\times10^{22}$ cm^{-3}). However, the experiment has also shown that the hydrogen solved in palladium is not a free-moving gas. In order to explain the anomalous diffusion behavior of the hydrogen in the palladium, we must assume that there is a component of trapped hydrogen ions (localized).[15] If we assume an energy spectrum as that in Fig.1,

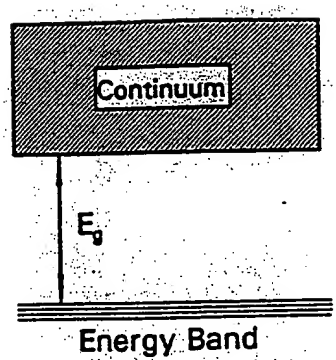

Fig.1 Energy Band Structure in Palladium Deuteride lattice

then the critical density for Bose-Einstein condensation would be

$$n_{cg} = n_c \exp(-\frac{E_g}{k_BT}) \tag{8}$$

Using $n_{cg}\approx 6.8\times10^{22}$ cm^{-3} (corresponding to critical loading ratio≈1), T=300 K, we have

$$E_g = -k_BT\log(\frac{n_{cg}}{n_c}) \approx 125\ \text{meV} \tag{9}$$

this number is very close to the activation energy for hydrogen in palladium.[15]

In fact this condensation model gives a good reason for the critical loading ratio. If the deuteron density is lower than this critical density n_{cg}, then, there will be no enough population in the low lying energy band, and less chance for resonance penetration.

5. Nuclear Surface Absorption and $0^+\rightarrow0^+$ Forbidden Transition

The low energy beam-target experiments have established a fact that the strong interaction will annihilate the penetrating deuteron wave after several reverberations. When one assumes the reaction rate

$$\Lambda = A|\Psi(0)|^2 \tag{10}$$

low energy experimental data show that $A = 1.5\times10^{-16}\text{cm}^3\,\text{sec}^{-1}$.[16] Considering that the volume of the deuteron-deuteron nuclear interaction is the order of 10^{-39} cm^3, we know that the life-time of the deuteron-deuteron strong interacting system is the order of 10^{-23} sec, i.e. the order of the reverberation time. Then, one may ask the reason why the built-up wave function in the resonance case is not annihilated by this strong interaction.

In fact, the strong absorption in the nuclear well is concentrated on the surface region as suggested by the nuclear optical model.[17] The reaction "constant", λ, is not a constant inside the nuclear well; hence, the reaction rate, Λ, should be

$$\Lambda = \int \lambda(r)\left|\Psi(r)\right|^2 d^3\vec{r} = \int \lambda_v(r)\left|\Psi_v(r)\right|^2 d^3\vec{r} + \int \lambda_s(r)\left|\Psi_s(r)\right|^2 d^3\vec{r} \qquad (11)$$

Here, the subscripts, V and S, denote the volume and surface, respectively. $\lambda_v(r)$ is much smaller than $\lambda_s(r)$ by a factor of θ^{-1}. When there is no resonance, $\left|\Psi_v(r)\right| \approx \left|\Psi_s(r)\right|$; then, the reaction happens mainly in the surface region of the nuclear well, and the life-time is the order of the reverberation time. When the energy reaches the resonance level, the wave function, $\Psi_v(r)$, builds up due to the constructive interference between the penetrating wave and the reverberating wave. $\left|\Psi_v(r)\right| \approx \theta\left|\Psi_s(r)\right| >> \left|\Psi_s(r)\right|$ .Hence,

$$\int \lambda_v(r)\left|\Psi_v(r)\right|^2 d^3\vec{r} \approx \int \frac{1}{\theta}\lambda_s(r)\left|\theta\Psi_s(r)\right|^2 d^3\vec{r} >> \int \lambda_s(r)\left|\Psi_s(r)\right|^2 d^3\vec{r} \qquad (12)$$

The life-time of the state is determined by the core part of the wave function, and is greater than the reverberation time by a factor of θ.

In other words, the strong interaction annihilates only the deuteron wave near the nuclear surface. The deuteron wave function can still be built up inside the core of the nuclear well where the absorption due to strong interaction is weak. Physically, the absorption (i.e. deuteron loses its identity) only happens in the region where the nuclear force (the derivative of the nuclear potential) is large. Inside the nuclear core, although the nuclear well is deep, the nuclear force is weak there. So the deuteron wave can survive inside the core of the nuclear well.

In contrast to the short range of the nuclear force, the electromagnetic interaction is a kind of long range force. One may ask the reason why the electromagnetic force does not annihilate the long life-time state . This is due to the symmetry of the system. The symmetry of the wave function of the d+d system is determined by their orbital motion and their spin motion. At the low incident energy, only the S-wave (orbital angular momentum l = 0) is dominant inside the core of the nuclear well. So the symmetry for the orbital motion is symmetric about the exchange of the two deuterons. Then, the spin motion part of the wave function should be symmetric also in order to keep the symmetry of the total wave function which is necessary for a boson-boson indistinguishable particle system. The spin for each deuteron is 1, the resultant angular momentum may be 0,1, or 2. Since the state of resultant spin 1 is anti-symmetric about the exchange of the two deuterons, it is not an allowable state. The resultant spin should be 0 or 2.[18] Consequently, the possible total angular momentum and parity for the d+d system is 0^+, or 2^+. If the resonance state takes the 0^+; then, it should be stable against the electromagnetic interaction. Because the ground state for d+d system is 0^+ (helium-4), and the spin for photon (the electromagnetic quantum) is 1,

it is forbidden to have a $0^+ \rightarrow 0^+$ electromagnetic transition due to the conservation of the angular momentum.

What we have to figure out is the mechanism through which the excited d+d system transfers the energy to the lattice system in a slow time scale.

6. Conclusion: Thunder without Lightning is OK

Based on above-mentioned discussion, we have seen that the long life-time nuclear active state may be created after the resonance penetration of Coulomb barrier in the d+d system in terms of the lattice confined deuterons. This is a resonance state which cannot be observed in a low energy beam-target experiment. This resonance state will not emit strong nuclear radiation (neutron, triton, or γ radiation). This is just the answer to Professor J.Huizenga's challenge of three miracles. Only the chemists have a better chance to discover this nuclear active state in terms of calorimeter, because there is no strong nuclear radiation.

Although it is a long life-time slow reaction, it is still a practically useful energy source. Even if only one thousandth of the deuterons inside the palladium are involved in this state, the "excess power" is of the order of 1 kW per cubic centimeter of the palladium. This is about the same as that in a fuel rod of a fast fission breeder reactor.

In these two meanings, we say that thunder without lightning is O.K. This theory predicts that if we could produce the palladium with greater grain size and greater activation energy, it should be easier to reproduce the "excess heat" experiment.

Acknowledgments

This work is under the project of the State Commission of Science & Technology, and the Natural Science Foundation of China. Many thanks to Mr. Karl Chang, the co-founder of the VeriFone Inc., for his generous support, and to Professors D.Yount, G.Andermann, B.Liebert, and Dr. B.Liaw for their hospitality during author's visit to the Univ. of Hawaii. Professor M.Fleischmann's personal contribution is critical for this work to be presented at ICCF-5.

List of Symbols

a=size of the nuclear well, cm

A=experimental bulk reaction constant, $cm^3 sec^{-1}$

b=classical turning point of Coulomb barrier, cm

d=deuteron

E=total energy of relative motion, erg.

$\hbar$=Planck constant divided by 2π, erg·sec

k, k' and k''=wave number, its imaginary and real part, cm^{-1}

k_B=Boltzmann constant, erg·K

L=grain size in crystal, cm

m=mass of deuteron, g

n_c=critical density for Bose condensation of free-moving particles, cm^{-3}

n_{cg}= critical density for Bose condensation of particles with energy gap in spectrum, cm^{-3}

r =radial coordiante, cm

T=temperature, K

U=potential energy, erg

ImU=imaginary part of the potential energy, erg

Γ= width of energy level, erg

Γ_B=width of energy band, erg
δ=size of the primitive cell of a crystal, cm
λ=reaction constant, sec^{-1}
λ_V=reaction constant in core region of the nuclear well, sec^{-1}
λ_S=reaction constant in surface region of the nuclear well, sec^{-1}
Λ=reaction rate, sec^{-1}
θ=square root of the reciprocal of Gamow factor
τ=life-time of an energy level, sec
τ_{xh}=life-time of the resonance state releasing "excess heat"
Ψ=wave function, $cm^{-3/2}$

References

1.J.R.Huizenga, "*Cold Fusion: The Scientific Fiasco of the Century*", p.112,University of Rochester Press (1992).
2.G.Gamow, "Zur Quantentheorie des Atomkernes." *Zeitschrift fur Physik*, 51, 204 (1928).
3.S.Pons & M.Fleischmann, "Heat after death", *Proceedings: Fourth International Conference on Cold Fusion*,Decmber 6-9,1993, Lahaina, USA, Vol.2, p.8-1(1994).
4.M.C.H.McKubre, et al.,"Loading, Calorimetry, and Nuclear Investigation of the D/Pd System", *Proceedings: Fourth International Conference on Cold Fusion*, Decmber 6-9,1993, Lahaina, USA,Vol.1, p.5-26(1994).
5.J.P.Biberian,"Excess Heat Measurement in $AlLaO_3$ Doped with Deuterium", ICCF-5, paper No.205(1995).
6.E.Storms,"A Critical Overview of Cold Fusion", ICCF-5, paper No.101(1995).
7.M.Eisner,"The Serendipitous Design and Execution of an Early Experiment which Confirmed Heat in the Fleischmann-Pons Effect",ICCF-5, paper No.212(1995).
8.X.Z.Li, "Tunneling the Coulomb Barrier via Lattice Confined Ions", submitted to *Physics Letters A*,(1995).
9.X.Z.Li, "Revisit to Gamow Factor", ICCF-5, paper No.403,(preprint,1995).
10. S.E.Koonin, and M.Nauenberg, "Calculated Fusion Rates in Isotopic Hydrogen Molecules." *Nature*, 339, 690(1989).
11.Ya. B. Zel'dovich, S.S.Gershtein, "Nuclear Reactions in Cold Hydrogen, I. Mesonic Catalysis", *Soviet Phys. Usp.* 3, 593 (1961).
12. F.E.Cecil, and G.M.Hale, "Measurement of d-d and d-^{6}Li Nuclear Reactions at Very Low Energies." in the "*The Science of Cold Fusion.*" Edited by T.Bressani, E.Del Giudice and G.Preparata, SIF, Bologna, p.271 (1991).
13.A.H.Verbruggen, et al., *Phys. Rev. Lett.* 52, 1625 (1984).
14.C.Kittel, and H.Kroemer, "*Thermal Physics*", 2-nd ed., p.281, Freenman, New York (1980).
15.Y.Fukai, "*The Metal-Hydrogen System*", p.212, Springer Verlag, Berlin (1993).
16.F.W.Fowler, G.R.Caughlan, & B.A. Zimmerman, *A. Rev. Astr. Astrophys.* 5, 525-570 (1967).
17.H.Feshbach, "*Theoretical Nuclear Physics*", Wiley & Sons, Inc.,Boston, p.488(1992)
18. D.M.Brink, and G.R.Satchler, "*Angular Momentum*", 3-rd ed., p.35, Oxford Science Publications (1993).

Fifth International Conference on Cold Fusion
9-13 April, 1995 - Monte Carlo, Monaco
ICCF5 ©1995

Cold Fusion and anomalous effects in deuteron conductors during non-stationary high-temperature electrolysis

Samgin A.L., Finodeyev O.*, Tsvetkov S.A.,
Andreev V.S., Khokhlov V.A., Filatov E.S.,
Murygin I.V., Gorelov V.P., Vakarin S.V.
Institute of High-Temperature Electrochemistry,
Russian Academy of Sciences
S.Kovalevskaya 20
620219 Ekaterinburg, RUSSIA
*ENECO
391-B Chipeta Way
Salt Lake City, Utah 84108, USA

Abstract

The studies were conducted with the perovskite-type solid electrolytes based on the strontium and barium cerates under hydrogen and deuterium atmosphere. Anomalous effects were found manifesting themselves in the overbackground neutron bursts, excess heat release, phase composition and crystal lattice parameter changes. At 200-750° C the regions of the temperature were identified which accompained by significant heat evolution that was greater in the deuteron conductors than in the proton conductors.

1. Intoduction

It is known /1,2/ that the hydrogen and deuterium absorption and transfer induced electrochemically in the solid oxide electrolytes is affended with the "excess" heat evolution. In specific cases excess heat power has been ranged up to several tens of percent. Meanwhile the poor reproducibility of these experiments was observed. As a result there is no escape from the correct conclusion concerning the causes of anomalous heat liberation. The calculation of the power balance has been pointed to the possibility of the processes associated with overstoichiometrical hydrogen and deuterium concentration in the crystal lattice resulting in the cold fusion or other anomalous phenomena.

In order to obtain the valid data about the reasons of the phenomena observed we carried out the complex investigation of solid electrolytes involving the careful measurements of heat and radiation, the correct determination of above temperature regions, the thorough research of the structure and phase transformations.

In this paper the results of calorimetric and radiometric experiments with samples of $Sr(Ba)CeO_3$-type proton (deuterium) conductors doped by Dy- and Nd-oxides during high temperature non-stationary electrolysis under D_2 or H_2 atmosphere is presented.

2. Methods

Samples was produced as a tablet 10 mm of diameter and 1-2 mm in thickness with Pd- or Pt-electrodes applied. The design of electrochemical cell used is showed in Fig. 1. As calorimeter the metall cylinder was used. Two hole was bored through its walls for fixing the termocouples. The inner plane heater was placed under sample studied for calibrating calorimeter and providing the temperature gradient through the tablet. The fixed temperature was supported with the outer calorimeter heater. The electrochemical cell was connected with the gas system. It was housed in two-ring neutron detector /3/. Multiple measurements of the neutron background during 1-2 day period showed that the maximum background counts did not exeed 8 pulses for the inner detector ring and 9 pulses for outer detector ring per 16,77 s.

Before the measurements the cell was evacuated with the vacuum pump, then it was heated up to initial working temperature the heat losses being compensated. After this operation the gas was admitted into cell. The heating regime provided a means for the establishment of initial constant temperature. Then the calorimeter calibration was carried out at the several fixed power loads (50, 100, 150 and 200 mW) on the inner heater. The calibrating curve is approximated by equation W=f(dT) where W and dT are the heat power of the inner heater and the after temperature of the calorimeter. In all cases the same order of the principle steps in the experimental procedure was used.

I. After achievment of constant temperature over the cell the invariable electrical potential was applied to the electrodes for producing the electrolytic process. Within a few hours heat quasiequilibrium have been established.

II. Then the electrolysis was continued with the periodic sign-variable /reversible/ electrical potential supplied.

III. When fixed thermal steady-state condition the sample was sharply heated up to the cycling temperature Tcycl, the reverse electrolysis being contineed.

IV. Further thermal cycling was conducted by means of the inner and outer heaters in the range of temperature from 200 ° C to Tcycl. For the same sample all above experimental stages has been repeated a few times. Troughout the whole experiment the calorimeter temperature and that of sample surface was being steadely recorded as well as the time distribution of the neutron counte rate with digitization time of detection of 4 microseconds. By means of crate CAMAC all the data is stored in PC memory for subsequent processing. The heat power was determined with the calibrating curves found for both stationary conditions and non-steady-state ones. The typical examples of dT-t and W-dT dependences are presentad in Fig. 2 and 3.

A wariety of ceramic samples with the Pt- and Pd- electrodes was examined under different gas atmosphere. It was recently shown / 4/ that the perovskite-type

oxide electrolytes with about the same chemical composition as the ones stadied by us has been transformated to the proton conductors under the influence of H_2-gas or H_2O-vapour medium. Therefore in the subsequent discussion we shall use the terms "protonconducting" and "deuteronconducting" ceramic samples with respect to the ones researched under H_2 or D_2 gas atmosphere.

Besides the additional investigations of heat releasing processes during the electrolysis under hydrogen and deuterium atmosphere were carried out using the scanning Calvet-microcalorimeter with the constant heating rate in the temperature range from 200 to 750°C.

3.Results and Discussion

Deuteronconducting electrolyte (No.1).

Many-day experiment was being conducted in above consequence. Under heating and cooling dopped $SrCeO_3$-sample the unknown phase transition was found at the 445°C. All fortscoming operations involving current reversing and heat cycling was conducted with special attention to the temperature changes and neutron flashes close to the phase transition point. The runs were broken when the current density at constant electrical potential sharpy diminished. This fact was evidence of scaling electrodes off the oxide tablet.

Anomalous heat effects and overbackground neutron bursts were found in this experiment. They were observed with supplied constant electrical potential about 10V. The heat power released exceeded one expended for producing electrolytic process by 10-1000% depending on way of electrical current loading. Within 18 hours the six events emitting neutrons as the individual bursts out the experimental errors were observed.

Deuteronconducting electrolyte (No.2).

In this run with unlike sample of deuteronconducting ceramics we were deciding the problem to obtain additional information on the heat evolution under non-steady-state heating or cooling regime as well as to fix temperature in situ. Only distinction from the run No.1 was the dynamical dT-t curves was recording for every heat power given up to the stationary temperature. Besides, inner surface of two-ring neutron detector was controlled thermostatically.

The results of these examinations were used to calculate excess heat liberated during electrolysis. To do this the value of heat power released (W_{libr}) compared with one expended (W_{exp}). When electrolyzing without thermocycling

$W_{exp}=W_{outer\ heater}+W_{electr}$ while when electrolyzing with thermocycling

$W_{exp}=W_{outer\ heater}+W_{electr}+W_{inner\ heater}$ Then the relative excess heat effect is

$$\frac{W_{libr}-W_{exp}}{W_{electr}} \times 100\%.$$

Table 4. The electrolysis with reversing electrical load and thermocycling

t, min	$W_{outer\ heater}$, W	$W_{inner\ heater}$, W	W_{electr} (max), W	W_{exp}, W	W_{libr}, W	$\frac{W_{libr} - W_{exp}}{W_{electr}}$, %
N1 5	14.686	23.994	2.11	40.800	43.300	118
N1 10	14.686	23.994	1.057	39.737	40.400	62.7
N2 5	14.686	24.108	1.283	40.071	41.100	80.2
N2 10	14.686	24.222	0.585	39.490	39.600	18.8

Total errors in finding heat power are ± 10,5mW for electrolyzing regime without thermocycling and ± 154 mW for one with thermocycling. The overbackground neutron bursts of duration of 100 microseconds were observed in ten hours from beginning the electro lysis. The eight exceeding events (Count number is greater than 10) were registated within time interval 16.7 s during 32 hours. A half of them was found for direct electrolisis, while the others were measured for reverse electrolisis.

Protonconducting electrolyte

According to the above procedure the experiments were carried-out with the same ceramic probe under H_2-atmosphere. The thermal treatment and evacuation were brought about to remove residual D_2-gas from the sample.

After control calibrating calorimetr and establishing heat steady-state condition the experiment was continued. The calculation showed the heat power released was lower than one for deuteronconducting sample. The excess heat effect was not found in the case of the electrolysis with direct electrical supply while one was fixed under reverse electrolyzing and thermocycling. The last fell down for a short time the natural neutron background was not exceeded.

Microcalorimetric investigation

The studies showed three temperature regions with the anomalous thermal effects for the both deuteron and proton conductors in the temperature range from 200 to 750 ° C (See fig.4). The heat evolution for deuteron conductor is greater than proton one. One can suppose the phase transition (I) are occured. The cathastrofic change of the heat liberation can be associated to some processes at phase transitions in the systems of ceramics - isotopic hydrogen. To elucidate these phenomena the additional investigations ough to conduct.

The X-ray diffraction studies.

The X-ray examination with deuteron conducting solid electrolytes fixed change of the phase composition and crystal lattice parameters after electrolysis. In particular, for the samples with the significant excess heat release two separate phase was found including $SrCeO_3$-type phase and CeO_2-type one. As a rule for the samples under thermocycling the crack formation was clearly observed.

References

1. A.Samgin, A.Baraboshkin, I.Murigin, S.Tsvetkov, V.Andreev, S.Vakarin "The influence of conductivity on neutron generation process in proton conducting solid electrolytes". *Proc Fourth International Conference on Cold Fusion*, Hawaii, December 6-9, 1993, 3, p.5-1, EPRI, Palo Alto, USA (1994).

2. T.Mizuno, M.Enio, T.Akimoto, K.Azumi "Anomalous Heat Evolution from SrCeO3-type Proton Conductors during Absorption/Desorption of Deuterium in Alternate Electric Field". *Proc. Fourth International Conference on Cold Fusion*, Hawaii, December 6-9, 1993, 2, p.14-1, EPRI, Palo Alto, USA (1994).

3. A.Samgin, V.Andreev. S.Tsvetkov, A.Cherepanov "Electrolysis of solid deuteron conducting electrolytes in deuterium atmosphere: microsecond structure analysis of neutron pulses by means of two-ring detector". Cold Fusion source book (Minsk Cold Fusion conference proceedings, May 21-26, 1994), USA (1994).

4. N.V.Arestova, V.P.Gorelov "Electroconductivity and ionic transport in the $BaCeNdO_3$-type perovskite", *Electrochemistry*, 30, 988 (1994) (In Russian).

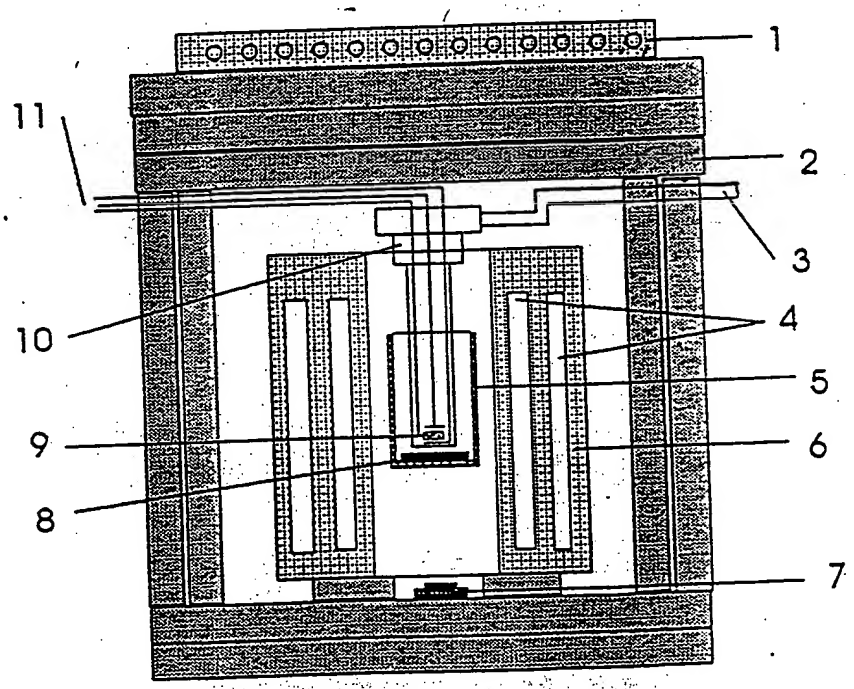

fig. 1.

1 - Block of detectors SI-19N.
2 - Neutron protective wall (3% boron).
3 - Vacuum-pumping system tube.
4 - Two rings of detectors SNMO-5.
5 - Heat shield.
6 - Moderator.
7 - Ventilator.
8 - The heater.
9 - The sample.
10 - The working cell.
11 - Two current conductors and thermocouple.

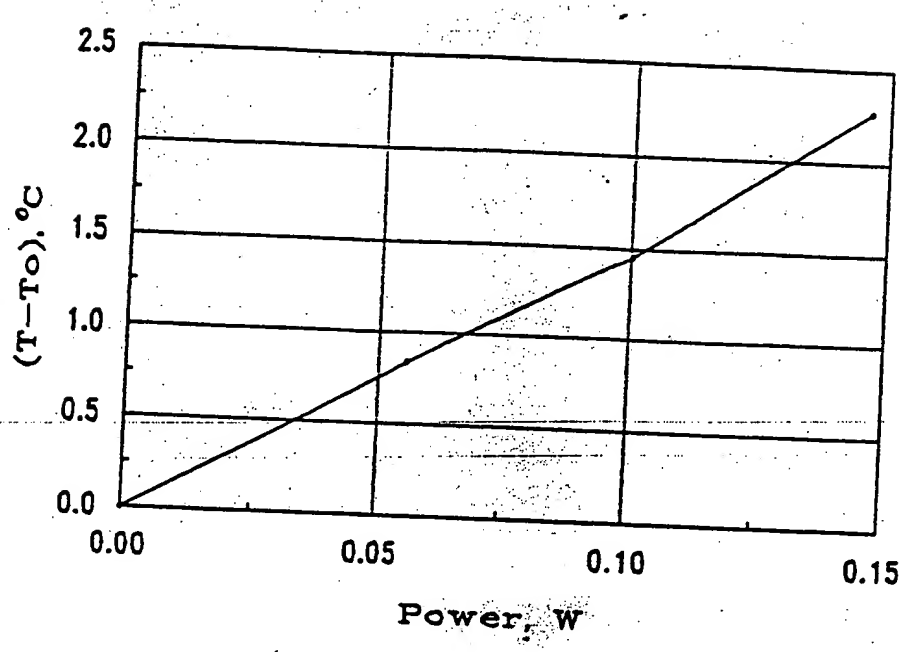
2.5
2.0
1.5
1.0
0.5
0.0
(T−To), °C
0.00
0.05
0.10
0.15
Power, W

Fig.3

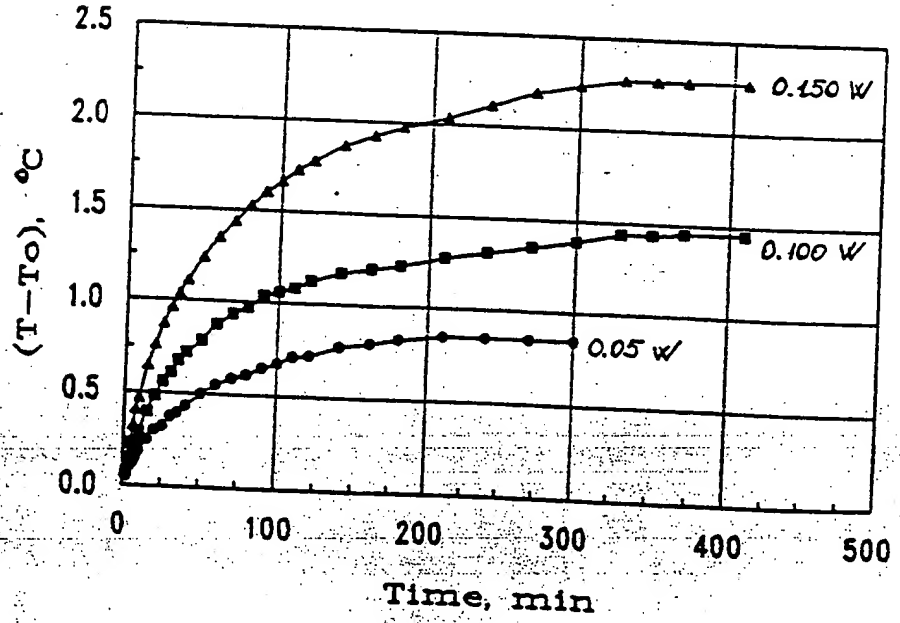
2.5
2.0
1.5
1.0
0.5
0.0
(T−To), °C
0.150 W
0.100 W
0.05 W
0
100
200
300
400
500
Time, min

Fig.2

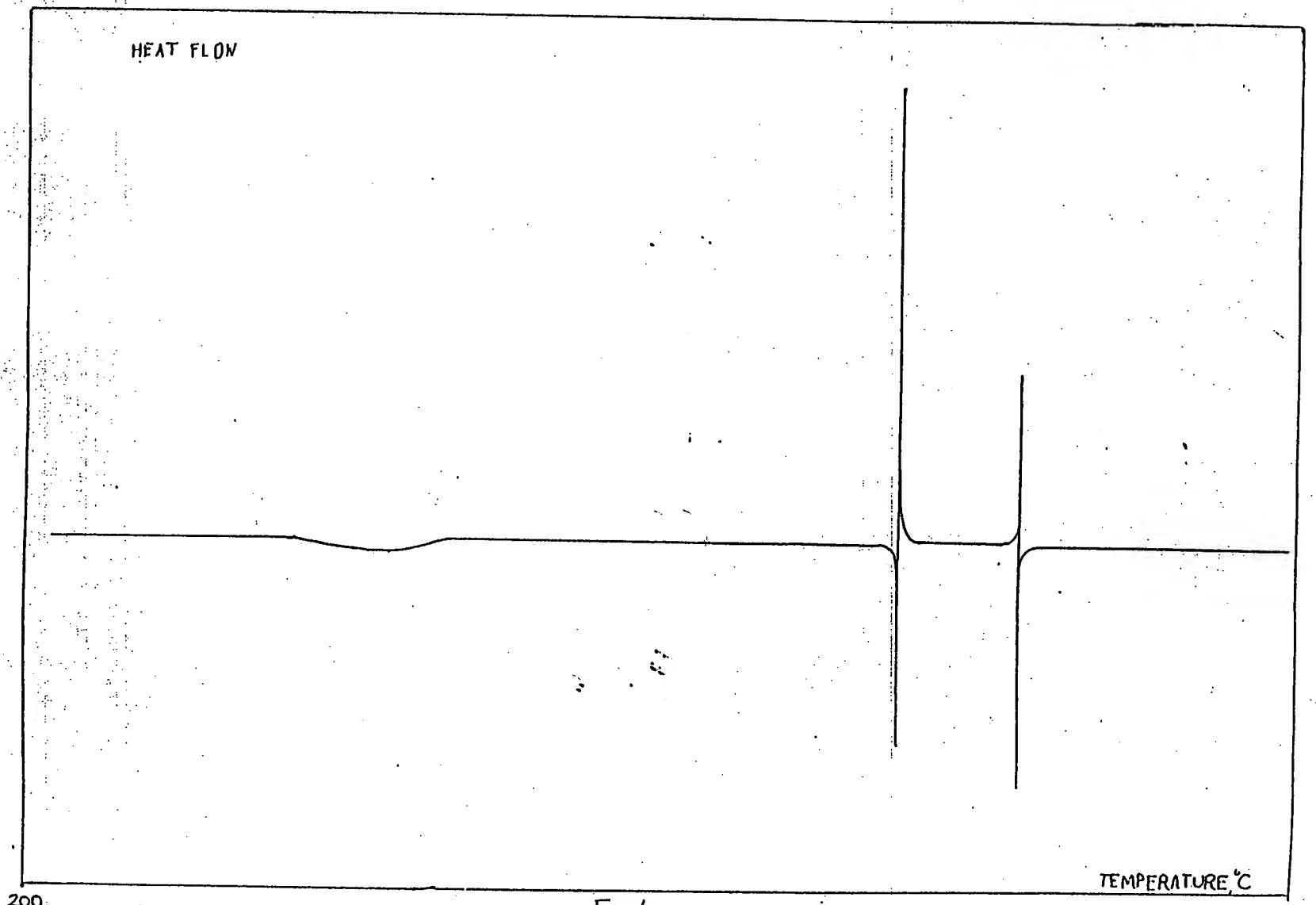

Fig. 4.

9-13 April, 1995 - Monte Carlo, Monaco
ICCF5 ©1995

Status of "Cold Fusion"

Edmund STORMS
270 Hyde Park Estates
Santa Fe, NM 87501

Abstract

A selection of experimental evidence supporting the "cold fusion" effect is evaluated. In addition, an effort is made to show why these observations can be considered real and correct. The total evidence set strongly demonstrates a new phenomenon worthy of potential technological development.

1. Introduction

Six years have passed since the modern era of chemically assisted nuclear reactions (aka "cold fusion") was started by Profs. Stanley Pons and Martin Fleischmann (then at the University of Utah)[1]. During this time, criticisms made by skeptics have been taken seriously, errors have been reduced or eliminated, and a wide variety of studies have been done using modern equipment in many countries.[2] As a result, the early problem of reproducing the effect has been largely eliminated, a rich assortment of nuclear products has been found, and theoretical explanations are blossoming like flowers after a long delayed rain. Ten different methods are known to initiate nuclear reactions of various types in a variety of chemical environments. The boundaries of a new field of science are gradually being extended into territory guaranteed to challenge the imagination.

The problem now is more psychological than scientific. In spite of this new and improved information, general skepticism about the effect continues within the scientific community. This attitude has limited the availability of financial support, reduced publication options, and required excessive effort to demonstrate the reality of the effect. In addition, resolution of the many conflicting explanations requires a consensus about what is known to be true and correct. I will show what I believe is known about a few selected aspects of the field. Hopefully, this will lead a discussion toward agreement about what is actually known rather than what fits a particular explanation or what provides justification for rejecting the phenomenon.

Only work reported before ICCF-5 is included. Papers at ICCF-5 show how several of the ongoing studies are maturing toward an understanding that will eventually produce an acceptable explanation and make commercialization possible. Although information is still inadequate, it is safe to conclude that conventional theo-

ries are no longer adequate to explain the observations and that a clean and inexhaustible source of potentially useful energy has been discovered.

2. Anomalous Claims

Table 1 lists the major indicators of what is normally called "Cold Fusion". Note the wide variety of manifestations and wide range of implied nuclear reaction rates. The first three manifestations clearly have the greater rates and, therefore, greater technological importance. Items 4, 5, and 6 are important to demonstrate a variety of possible nuclear reactions and to understand the nuclear mechanisms. While the observed quantities are too small to explain the excess energy, few if any measurements have been done while significant energy was being generated. Neutron emission, the 7th item, is very insignificant even during energy generation. While we can be thankful that the various radiation fluxes are small, the use of such measurements for diagnostic purposes has been frustrating and unconvincing to some people.

These manifestations do not appear to be strongly coupled because they frequently occur at different times and under different conditions. Therefore, different chemical environments apparently trigger different nuclear reactions. This important realization complicates any explanation.

TABLE 1

INDICATORS OF THE "Cold Fusion" EFFECT
Estimated rate of implied nuclear reaction shown

1. Excess energy (10^{10}-10^{14} /sec)
2. Helium (0.5-1.0 x energy rate)
3. Tritium (10^{7}-10^{8}/sec)

4. Nonradioactive isotopes
5. Charged particles including strange particles
6. Prompt and delayed gamma
7. Neutron (10-100/sec excluding bursts)

Because fusion is only one of the apparent nuclear reactions, the phenomenon is overdue for a name change. Table 2 lists a number of suggestions. It is still too early to achieve universal agreement. The name listed last, normally used by skeptics, is no longer appropriate because many characteristics of this value judgment are no longer operating. The phenomenon is becoming more reproducible and is growing in magnitude as techniques are improved. This term is appropriate only when the opposite experience is encountered.

3. Discussion

Before discussing the first three indicators listed in Table 1, it is worth discussing neutron emission.

3.1 Neutron Emission

Over 300 attempts to measure neutron emission have been published. About 1/3 have claimed a signal sufficient to be considered significant. Regardless of expectations based on experience obtained from hot fusion environments, very few neutrons are generated during cold fusion. A few of these neutrons appear to

---

TABLE 2

"Cold Fusion" aka

Chemically Assisted Nuclear Reactions (CANR)
Lattice Assisted Nuclear Transformations (LANT)
Lattice Induced Nuclear Chemistry (LINC)
Nuclear Energy in an Atomic Lattice (NEAL)
Catalyzed Nuclear Reactions (CNR)
Solid-State Nuclear Reactions (SSNR)
New Hydrogen Energy (NHE)
Pathological Science (PS)

---

have energy near 2.5 MeV [3; 4; 5; 6; 7; 8; 9], a value consistent with a fusion origin. A few others have energies up to about 7 MeV[10; 11; 12; 13] which require a more exotic explanation. Occasionally, bursts of neutrons are seen having a high average rate but containing a relatively small number of particles. These bursts might result from rare fractofusion events.[14]

Although the complete data set strongly suggests the existence of neutron producing reactions, the numbers are too small to have any important relationship to energy or tritium production. This experience does not preclude novel neutron transfer reactions, but it does show that important neutron generating reactions are not part of the general "cold fusion" effect.

3.2 Tritium

Of those products giving evidence for the existence of significant nuclear reaction, tritium stands well above the rest in magnitude and in the number of successful studies. Tritium is produced in quantities that are well outside of any conventional explanation, and that are occasionally well above levels that could be caused by potential contamination. Production rates of 10^7-10^8 atoms/sec have been achieved in small, laboratory-sized cells, giving as many as 10^{15} atoms before the experiment was terminated. At least 6 different methods have succeeded as shown in Table 3.

There is no reason to believe these are the only methods or that this rate is the upper limit. If a method could be scaled-up to generate 10^{12} atoms/sec, such tritium production would become very cost effective without having to deal with the many radioactive products associated with present techniques.

Tritium production occurs in different chemical/physical environments than does heat production. This fact is very important in demonstrating the broad range of possible nuclear-active conditions (NAC) and in arriving at a correct explanation for the general effect.

Failure to detect 14 MeV neutrons from secondary fusion during tritium generation has caused uncertainty as to how the tritium can be produced at energies less than the required ≈25 keV needed to avoid this reaction. Proposed solutions to this

TABLE 3

METHODS USED TO PRODUCE TRITIUM

Pd as a cathode in D_2O-based electrolyte.[15; 16; 17; 18; 19; 20]
Ni as a cathode in H_2O-based electrolyte.[21; 22]
Low-voltage discharge involving Pd electrodes in low pressure D_2.[23]
Low-voltage discharge involving Pd electrodes in high pressure D_2.[23]
Rapid gas release from Pd upon heating.[23]
Gas loading of Ti with high pressure D_2 followed by temperature change.[24; 25]

problem still do not have universal agreement although plausible theories are now being developed.

Why should we believe such tritium has been produced by "cold fusion"? Only two errors are possible. Either the presence of tritium is misdiagnosed or it is present but results from contamination. Five different methods have been used to detect tritium, all giving positive evidence in different studies. Most skeptics now admit that anomalous tritium is present. The next question is, Where does the tritium come from? Two sources are possible; either from the environment or from tritium dissolved in the palladium cathode. Let's examine environmental tritium first.

Although an open cell can absorb tritium-water from the surrounding atmosphere, this option is not available to sealed cells in which tritium has also been found. In addition, large amounts of tritium-water are not normally present in the environment. Even tritium laboratories work very hard to keep the tritium level low. However, if it is present, its entry into the cell would have a constant rate determined by the size of the opening in the container and the ambient concentration. The mechanism is well understood from much general experience, and it has been applied to the cold fusion configuration by exposing a typical cell to a high-tritium environment.[26]

Tritium has yet to be detected in commercial palladium.[27] Nevertheless, tritium that might be present has well-known characteristics.[28] Such tritium quick-

ly leaves the metal and appears in the evolving gas during normal cathodic electrolysis. It does not enter the electrolyte where anomalous tritium is found, in this case only after a long delay. This behavior not only demonstrates that anomalous tritium does not result from previously-dissolved tritium, but it also shows that the nuclear-active environment is not within the bulk material when the electrolytic method is used. In addition, tritium has been produced by gas-loading various metals followed by a temperature change. The nature of the metal has a large effect on this process.[23; 29] These considerations will be addressed using an electrolytic study as an example.

Chien et al. [15] at Texas A& M electrolyzed two cells at the same time, in the same room, using the same construction materials. One cell produced tritium in the electrolyte and the other did not. Both pieces of palladium were prepurified. The early behavior is shown in Fig. 1. At each current-voltage increase, the tritium production rate increased to a new, constant value. This behavior can not be explained by assuming the presence of environmental tritium or contaminated palladium for the following reasons.

For the sake of argument, we will first assume the tritium came from the environment. Environmental tritium could have entered the open cell along with the observed normal-water uptake. Measurements of the normal-water content of the cell allow calculation of the tritium concentration in the air required to produce the observed tritium increase in the cell. Within a factor of three, 20 $\mu Ci/m^3$ would be required in the surrounding air to produce the maximum apparent generation rate of 1×10^8 atoms/sec within the cell. This concentration triggers the evacuation alarms in the tritium laboratories at LANL. Skeptics would have us believe that this concentration exists at Texas A & M, that it fluctuates in concert with current changes, and that it enters only one cell while ignoring the other one.

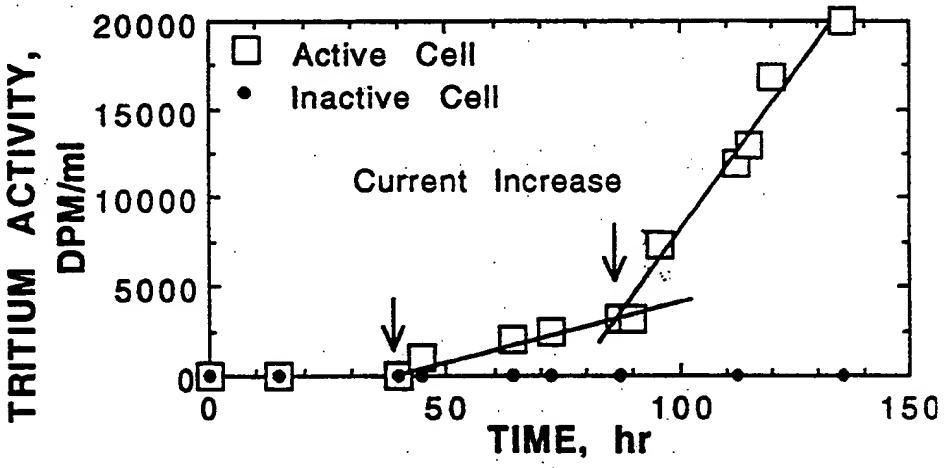

FIGURE 1. Change in tritium content of D_2O electrolyte caused by change in cell current/voltage during electrolysis during early part of study. Tritium concentration is given as disintegrations per minute (DPM). Background is 20 DPM.

Possible tritium in the palladium was eliminated by pre-analyzing the metal. This was done by sweeping any tritium out during anodic electrolysis (a process known to remove tritium along with all other hydrogen isotopes[28]) and by analyzing the palladium for ^3He, the tritium decay product. The absence of ^3He shows that the anomalous tritium was not present in the palladium during prior years. The absence of tritium after anodic electrolysis shows that it was not dissolved in the palladium immediately before the experiment. Only pre-analyzed, hence pre-purified, palladium was used for the experiment.

If the tritium found in this cell, or that claimed in more than ten other well-documented studies, can not be rationally explained as contamination, the existence of a completely unexpected nuclear reaction must be acknowledged.

3.3 Helium Production

Of the nuclear products, only ^4He has been found in sufficient quantity to roughly account for the observed excess energy. Most helium is found in the gas with lesser amounts being retained by the metal.[15; 30; 31; 32; 33; 34; 35] Charged particles similar to energetic helium emission (α-particles) have also been detected when suitable detectors were in place.[36; 37; 38; 39; 40; 41] Therefore, this product appears to be a major part or perhaps all of the sought for nuclear ash required to explain energy production.

Two studies stand out in demonstrating the helium/energy relationship.[42; 43] Space limitations allow the showing of only one. The first measurement of helium in the evolved gas is provided by Miles and Bush[42]. Eight gas samples taken in Pyrex flasks during heat production were found to contain helium while six control cells showed no helium. Because glass was used to contain the gas, the results might have resulted from diffusion of helium through the glass. In response to these concerns, the investigators measured the diffusion rate of helium through glass, When corrections were made, excess helium remained in the flasks. Another study was launched using metal flasks. These results are shown in Figure 2. Although the errors are large, the measured helium is close to that expected from the $d + d = {}^4He +$ 23.8 MeV fusion reaction and well above measurements made using a H_2O-based electrolyte in a control study. A study recently reported by Bush et al.[44], done at SRI (Stanford Research International), shows the same trend.

Possible errors include helium that might leak into the system along with air. If all of the collected gas were replaced by normal air, a helium concentration of 6 ppm would be expected. Even though such total replacement is impossible, a large random variation in measured values would be expected if a leak had been present. Absence of helium during the control studies and the absence of these large random variations during active measurements strongly indicate that the measured helium does not result from a leak.

Many other studies have shown that helium observed in the gas does not reside initially in the palladium. Even if helium were present, electrolytic action would not remove it.[45] This fact is important to the understanding of where the helium-producing region might be located. Clearly this region is not within the bulk

material and must be much less than 10 μm from a surface.[45] Otherwise, most of the helium would be retained by the palladium, which is contrary to experience. Other factors such as local heating by the nuclear reaction or presently unknown properties of the nuclear-active environment might also contribute to a greater than expected helium release.

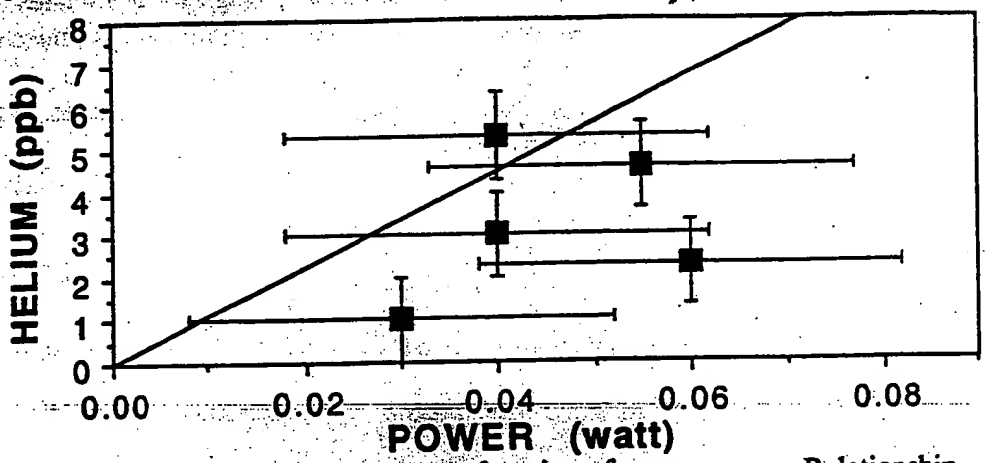

FIGURE 2. Helium produced as a function of excess power. Relationship based on d+d=He+23.8 MeV shown as line. The helium concentration results from a constant current of 500 ma held for a constant time. Collection was done using a metal system.

3.4 Excess Energy Production

More than 120 studies of energy production have been published, with about 1/3 being successful. Table 4 lists the claimed successful methods. These can be grouped into four major categories: Gas Reaction, Electrolytic Reaction, Ion Discharge, and Bubble Generation. Only a few of many possible citations are listed for the first two items listed in the table. McKubre et al. at SRI have made the most complete study of the first method.

TABLE 4

METHODS CLAIMED TO PRODUCE EXCESS ENERGY

1. Electrolysis of D_2O-based electrolyte using a Pd cathode.[46]
2. Electrolysis of H_2O-based electrolyte using a Ni cathode.[47; 48]
3. Electrolysis of KCl-LiCl+ D electrolyte using a Pd anode.[49]
4. Current passed through $Sr(CeNbY)O_3$ in D_2.[50]
5. Gas discharge using Pd electrodes in hydrogen.[51]
6. Gas discharge using Pd electrodes in deuterium.[52; 40]
7. Gas reaction with Ni under special conditions.[53]
8. Enhanced reaction involving D_2O using an acoustic field.[35]
9. Enhanced reaction in H_2O using microbubble formation.[54]
10. Gas-loading of finely divided palladium.[55]

Of these techniques, electrolysis of D_2O using a palladium cathode—the so-called Pons-Fleischmann Effect—has been given the greater attention. Table 5 summarizes the results and how often a particular experimental approach was used. All cases included in this table claim power production rates well above the stated error and sensitivity of the respective calorimeter. Use of closed, sealed cells or testing for recombination eliminates uncertain recombination as an error in 19 cases. Six studies were calibrated using electrolytic power as well as Joule heat supplied by an internal resistor. This dual method effectively tests the calorimeter using a known chemical reaction, eliminates most suggested errors, and demonstrates that the calorimeter does not have an unexpected bias.

TABLE 5

SUMMARY OF RESULTS FOR THE PONS-FLEISCHMANN EFFECT

Measured Excess Values Shown
Power Range: 0.015 to 130 Watt
Energy Range: 0.06 to 200 MJ

Number of cells of the following type:
Closed and sealed: 12
Checked for recombination: 7
Used blank: 2
Stirred or not needed: 13
Dual calibration: 6

Several important variables required to initiate the Pons-Fleischmann Effect have been found. Figure 3 shows how cell current affects power production. A critical current generally between 100 and 200 ma/cm^2 is required to initiate the effect. Once initiated, power production increases in an apparently linear fashion as the current is increased. Increased current causes a larger average deuterium concentration in the palladium because the unavoidable loss from cracks is overcome to a greater extent. In general, a larger D/Pd ratio results in a greater heat production rate because, perhaps, a greater fraction of the hydride has been converted to the nuclear-active state (NAS).

A combination of observations have suggested the location of the nuclear-active sites. Studies using thin (≈5 μm) palladium hydride films on silver[56] show a similar energy production rate compared to bulk hydride. Simple diffusion theory combined with the observed dynamic loading process[28] show that the highest D/Pd ratio exists at the electrolyzing surface. Therefore, this region is proposed to be the site of the heat-producing reaction. Because most of the helium is found in the gas rather than in the cathode, the helium-producing reaction must also be very near the surface.

It is important to realize that it is the current, not the voltage that creates the measured average composition. The observed overvoltage is created by the resulting surface composition required to maintain the average.

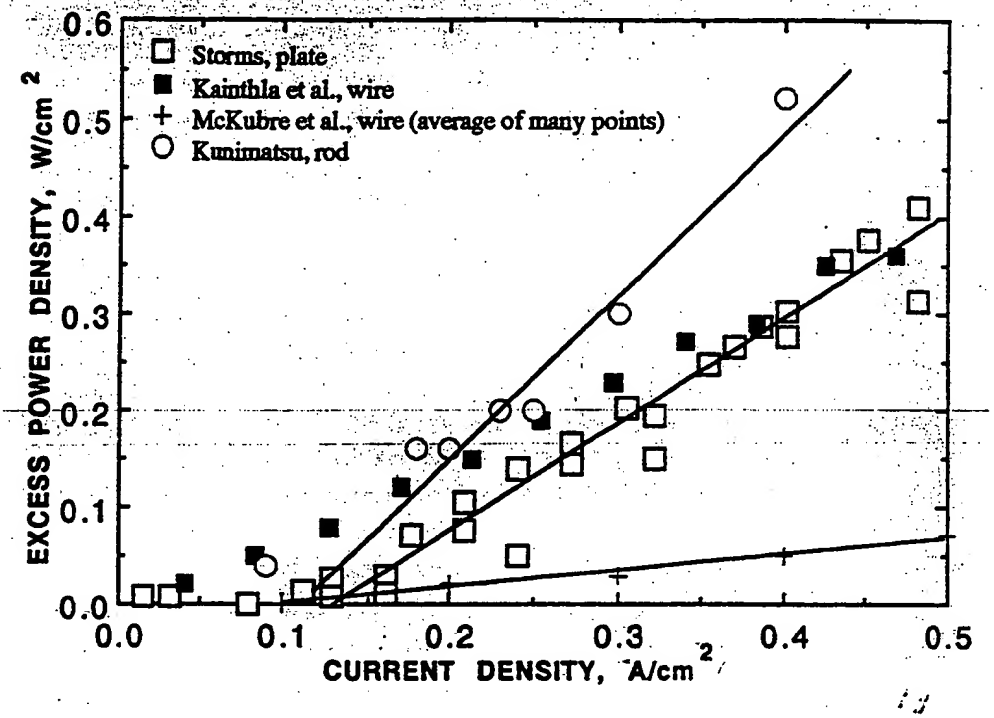

FIGURE 3. Comparison between excess power production and applied current.

In addition to a high D/Pd ratio, other, less well-defined conditions must be met.[57] Creation of these conditions generally requires many hours after a suitable composition has been achieved. One of these conditions seems to be the introduction of sufficient energy, from various sources, into the lattice.[58] The situation suggests the need to initiate an endothermic phase change in order to achieve the NAS. Regardless of the explanation, difficulty in creating this special environment has caused acceptance to be limited and has slowed technological and theoretical progress. Therefore, the mechanism for creating the NAS as well as the resulting crystal structure need to be better understood.

Several other, less well understood methods should be acknowledged. Bubbles that collapse next to a metal surface are possibly a common factor involved in several energy generation methods. Stringham and George[35] use an ultrasonic generator (20 kHz) to produce bubbles in D_2O that, when collapsed against palladium or titanium, generate significant heat and helium. Griggs[54] generates bubbles in H_2O using a special aluminum rotor driven by a 100 hp motor. Although large amounts of excess energy are produced in the latter study, no nuclear products have yet been identified. This search needs to be intensified.

Arata et al.[55] have generated significant energy after exposing finely divid-

ed palladium (palladium-black) to pressurized deuterium gas generated by electrolysis. This technique has the potential to be very useful and needs further study.

A few (at least 9) studies have claimed excess energy by electrolyzing H_2O containing various carbonate salts, mainly K_2CO_3, using a high-surface-area nickel cathode.[2; 47] Evidence for a transmutation reaction involving a proton addition to the nucleus of the electrolytic salt has been published.[21; 48] These claims indicate that the coulomb barrier is not as formidable as claimed by conventional theories.

4. Conclusions

The number of methods claimed to generate energy and nuclear products is growing along with the magnitude of effects. While some of the claims are hard to believe or inadequately supported, an objective evaluation of all claims clearly shows the occurrence of a new phenomenon having enormous potential.

Technological development and a clear understanding are handicapped by the difficulty in creating the special, nuclear-active state (NAS). Therefore, this problem needs special attention. The NAS in the Pd-D system appears not to include the normal β-PdD phase, but another structure requiring energy for its formation. Furthermore, the NAC is located only in a very narrow layer near the electrolyzing surface when it is formed by electrolysis. Its formation is controlled by the applied current and energy from various sources, with the electrode over-voltage being determined by the resulting composition of the surface. This environment must be better understood before an explanation can be accepted or total reproducibility can be achieved.

The large variety of observed nuclear reactions involving high-Z elements strongly suggests the presence of a very efficient process for overcoming the coulomb barrier. Therefore, theoreticians need to concentrate on the general process rather than trying to explain only the fusion reaction in palladium. Absence of significant high-energy radiation, both X-ray and γ-ray, strongly suggests a novel process for coupling energy to the lattice.

5. Acknowledgments

The author would like to thank ENECO for supporting the effort required to make this paper possible.

Reference

[1] Fleischmann, M., S. Pons and M. Hawkins "Electrochemically Induced Nuclear Fusion of Deuterium", *J. Electroanal. Chem.*, 261, 301 (1989) : see also *ibid* 263, 187 (1989).

[2] Storms, E. K., "Critical Review of the 'Cold Fusion' Effect", Submitted to *Phys. Rev. B* (1995).

[3] Arata, Y., and Y.C. Zhang, "Achievement of Intense 'Cold' Fusion Reaction", *Japan Acad. Ser. B* 66, 1 (1990); *Fusion Technol.* 18 , 95 (1990). See also: ibid, ""Cold" Fusion in a Complex Cathode", *Frontiers of Cold Fusion*, Nagoya Japan, October 21-25, 1992, p. 441. Universal Academy Press, Inc.,Tokyo (1993).

[4] Bertin, A., M. Bruschi, M. Capponi, S. DeCastro, U. Marconi, C. Moroni, M. Piccinini, N. Semprini-Cesari, A. Trombini, A. Vitale, A. Zoccoli, S.E. Jones, J.B. Czirr, G.L. Jensen, and E.P. Palmer, "Experi-

mental Evidence of Cold Nuclear Fusion in a Measurement Under the Gran Sasso Massif", *Il Nuovo Cimento* 101, 997 (1989). See also: Bertin, A., M. Bruschi, M. Capponi, S. De Castro, U. Marconi, C. Moroni, M. Piccinini, N. Semprini-Cesari, A. Trombini, A. Vitale, A. Zoccoli, S.E. Jones, J.B. Czirr, G.L. Jensen, and E.P. Palmer, "First Experimental Results at the Gran Sasso Laboratory on Cold Nuclear Fusion in Titanium Electrodes", *J. Fusion Energy* 9 [2], 209 (1990).

[5] Bittner, M. , A. Meister, D. Seeliger, R. Schwierz and P. Wüstner, "Observation of d-d Fusion Neutrons During Degassing of Deuterium-Loaded Palladium", *Fusion Technol.* 23 , 346 (1993).

[6] Agnello, M. E. Botta, T. Bressani, D. Calvo, A. Feliciello, P. Gianotti, F. Iazzi, C. Lamberti, B. Minetti, and A. Zecchina, "Measurement of 2.5 MeV Neutron Emission from Ti/D and Pd/D Systems", *Frontiers of Cold Fusion*, Nagoya Japan, October 21-25, 1992, p. 433. Universal Academy Press, Inc., Tokyo (1993).

[7] Jones, S. E., E. P. Palmer, J. B. Czirr, D. L. Decker, G. L. Jensen, J. M. Thorne, S. F. Taylor and J. Rafelski, "Observation of Cold Nuclear Fusion in Condensed Matter", *Nature* 338, 737 (1989).

[8] Hongyu, Z., W. Chenlin, R. Yanin, F. Guoying, Y. Hua, Z. Weidong, W. Dachun, H. Ming, L. Shuzen, H. Zhuen, W. Zhongda, Y. Runhu, L, Zhenghao, and R. Guoxiao, "Some Results on Cold Fusion Research", *The Science of Cold Fusion*, Vol. 33, Como, Italy, June 29–July 4, 1991, p. 49. Societa Italiana di Fisica, Bologna (1991).

[9] Shani, G., C. Cohen, A. Grayevsky, and A Brokman, "Evidence for a Background Neutron Enhanced Fusion in Deuterium Absorbed Palladium", *Solid State Comm.* 72 [1], 53 (1989).

[10] McKee, J. S. C., G. R. Smith, J. J. G. Durocher, C. B. Kwok, H. L. Johnston, M. S. Mathur, J. K. Mayer, A. Mirzai, Y. H. Yeo, K. S. Sharma, and G. Williams, "Neutron Emission from Low-Energy Deuteron Injection of Deuteron-Implanted Metal Foils (Pd, Ti, and In)", *Anomalous Nuclear Effects in Deuterium/Solid Systems*, Provo, UT, Oct. 22-23, 1990, p. 275. American Institute of Physics, NY (1991).

[11] Nakada, M., T. Kusunoki, and Okamoto, "Energy of the Neutrons Emitted in Heavy Water Electrolysis", *Frontiers of Cold Fusion*, Nagoya Japan, October 21-25, 1992, p. 173. Universal Academy Press, Inc.,Tokyo (1993).

[12] Okamoto, M., Y. Yoshinaga, M. Aida, and T. Kusunoki, "Excess Heat Generation, Voltage Deviation, and Neutron Emission in D_2O-LiOD Systems", *Proc. Fourth International Conference on Cold Fusion*,(EPRI TR-104188-V2), Lahaina, Maui, Dec. 6-9, 1993, p. 3. Electric Power Research Institute, Palo Alto (1994).

[13] Takahashi, A., T. Takeuchi, T. Iida, and M. Watanabe, "Neutron Spectra from D_2O-Pd Cells with Pulsed Electrolysis", *Anomalous Nuclear Effects in Deuterium/Solid Systems*, Provo, UT, Oct. 22-23, 1990, p. 323. American Institute of Physics, NY (1991). *Ibid*, "Short Note; Emission of 2.45 MeV and Higher Energy Neutrons from D_2O-Pd Cell Under Biased-Pulse Electrolysis", *J. Nucl. Sci. Tech.* 27, 663 (1990); Takahashi, A., T. Iida, T. Takeuchi, A. Mega, S. Yoshida, and M. Watanabe, "Neutron Spectra and Controllability by PdD/electrolysis Cell With Low-High Current Pulse Operation", *The Science of Cold Fusion*, Vol. 33, Como, Italy, June 29–July 4, 1991, p. 93. Societa Italiana di Fisica, Bologna (1991).

[14] AbuTaha, A. F., "Cold Fusion-The Heat Mechanism", *J. Fusion Energy* 9 [3], 345 (1990).
Bagnulo, L. H., "Crack-fusion: a Plausible Explanation of Cold Fusion", *The Science of Cold Fusion*, Vol. 33, Como, Italy, June 29–July 4, 1991, p. 267. Societa Italiana di Fisica, Bologna (1991).
Chechin, V. A., V. A. Tsarev, P. I. Golubnichyi, A. D. Philonenko, and A. A. Tsarik, "Fracto-Acceleration Model of Cold Nuclear Fusion", *Anomalous Nuclear Effects in Deuterium/Solid Systems*, Provo, UT, Oct. 22-23, 1990, p.686. American Institute of Physics, NY (1991).

O - 044

REPRODUCTION OF FLEISCHMANN AND PONS EXPERIMENTS

G. Lonchampt, CEREM/CENG, Avenue des Martyrs, 38054 Grenoble Cedex 9, France
L. Bonnetain, P. Hicter, ENSEEG, BP 75, 38402 Saint Martin d'Hères, France

The French Atomic Energy Commission, in association with the ENSEEG (Ecole Nationale Supérieure d'Electrochimie et d'Electrométallurgie de Grenoble) started in 1993 a program of verification of the results of "cold fusion" published in 1993 by Fleischmann and Pons ([1]). Experiments have been performed in calorimeters identical to the ones used by Fleischmann and Pons ([1]).

We point out here that these types of experiments can be analysed in three temperature domains :

- At low temperatures, below 70°C, excess enthalpy is the difference between the heat radiated to the water bath, and the enthalpy input due to electrolysis.
- At intermediate temperatures, between 70°C and 99°C, excess enthalpy is the difference between the heat radiated towards the water bath plus the enthalpy contents of the gas stream, plus the variation of enthalpy of the contents of the calorimeter (because of the fast temperature variation observed) and the introduced electrical enthalpy.
- In the boiling regime (without condensation), excess enthalpy is calculated from the difference between the total amount of water contained in the calorimeter evaporated and the theoretical quantity of water that should be evaporated by the energy introduced in the calorimeter (i.e. the enthalpy input due to electrolysis minus radiated enthalpy at boiling temperature).

Six calibration runs with platinum cathodes and 17 runs with different palladium type cathodes have been performed.

At low temperature, 8 experiments have produced an excess energy rate between 1 and 5 %.

In the intermediate regime, the water vapor carried away by the gases of the electrolysis are large, and cannot be evaluated precisely. This makes the analysis difficult, and has not been carried out fully yet. We discuss this point in detail.

At boiling, three positive experiments have been successful, giving excess enthalpies rates of 80 % to 150 %.

We present the results obtained with different types of cathode materials : pure, annealed and cold worked palladium and alloys (Pd-Rh and Pd-Ce).

In conclusion, we confirm the results published by Fleischmann and Pons ([1]), more particularly in the boiling regime.

([1]) M. Fleischmann and S. Pons, Phys. Lett. A 176, 118(1993)

TS - 003

ISOTOPIC DISTRIBUTION FOR THE ELEMENTS EVOLVED IN PALLADIUM CATHODE AFTER ELECTROLYSIS IN D_2O SOLUTION

T. Mizuno, T.Ohmori, T.Akimoto, K.Kurokawa, M.Kitaichi, K.Inoda, K.Azumi, S.Simokawa and M. Enyo*, Hokkaido University, * National College of Technology, Japan

It was confirmed by several analytic methods that reaction products with mass number ranging from 2 to 82 are produced in palladium cathodes subjected to electrolysis in a heavy water solution at high pressure, high temperature, and high current density for one month. Isotopic distributions were radically different from the natural ones. The anomalous isotopic distribution of these elements shows they do not come from contamination. For example, natural copper is 70% Cu-63, and 30% Cu-65. But the copper found in the cathode was 100% Cu-63, with no detectable levels of Cu-65. Natural isotopic distribution varies by less than 0.001% for copper.

Electrolysis experiments were performed at a current density of 0.2 A/cm^2 or total current of 5.6 A to 33 cm^2 surface area for 2.76 x 10^6 s (32 days). The sample electrodes were analyzed for element detection by energy dispersive X-ray spectroscopy (EDX), Auger electron spectroscopy (AES), secondary ion mass spectroscopy (SIMS) and electron probe microanalyzer (EPMA). Thus, the presence of Ca, Ti, Cr, Mn, Fe, Co, Cu, Zn, Cd, Sn, Pt and Pb was confirmed. AES and SIMS measurements were also made after bombardment by O_2^- ions, thus removing surface layers, but the element concentrations at 1 micro m below the electrode surface were almost the same as at the surface. The SIMS analysis showed other elements; As, Ga, Sb, Te, I, Hf, Re, Ir, Br and Xe. These elements, except Xe, are difficult to detect by AES and EDX because the peaks are very close to each other, or lower than the limits of detection. Xe is naturally difficult to detect by EDX because it is in the gas state. The SIMS count numbers ranged from 10^3 to 10^6 where the background counts were as low as ~10. The intensity of Xe was 10 times larger than Pd; it may be that the gas was released by bombarding with O_2^- ions which caused a temperature rise at the sample. Large differences in isotopic distributions compared with the natural distributions were observed by the SIMS method for Cu, Zn, Br, Xe, Pd, Cd, Hf, Re, Pt, Ir and Hg. Especially notable was the fact that no Cu-65 peak was observed. Except for a few cases; in generally the isotope abundances are higher for odd mass numbers and lower for even ones, as compared with the natural ratios. It must be admitted that these reactions have no solid, detailed theoretical basis yet, but in broad terms this can explain most of the elements which were observed. One may also imagine that as such transmutation reactions were presumably taking place during the electrochemical process.

TS-004

Production of heavy metal elements and the anomalous surface structure of the electrode produced during the light water electrolysis on Au electrode

T. Ohmori[a], T. Mizuno[b] and M. Enyo[c]

a Catalysis Research Center, Hokkaido University, Kita-ku Sapporo 060 Japan.
b Faculty of Engineering, Hokkaido University, Kita-ku Sapporo 060 Japan.
c Hakodate National College of technology, Tokura-cho Hakodate 042 Japan.

Porous black deposits of 0.3 - 1 mg were obtained during the cathodic electrolysis on Au electrode in 0.5 M Na_2SO_4 or Na_2CO_3 light water solutions at a current density of 200 - 300 mA/cm^2 for 7 days. It was found by SIMS analysis that the deposits are composed of Hg, Au, Pt, Os, Hf, Zn, Fe, etc. and the atomic abundances of these elements other than Au are evidently different from those of natural values. The production of these elements with intrinsically different isotopic abundances suggests the occurrence of some nuclear reactions during the electrolysis.

SEM images of the Au electrode surface after the electrolysis showed formation of a number of micro craters with various sizes. The size of the largest one reaches ca. 30 μm diam. and 30 μm height. They look like volcanoes. The outside walls were made of very porous substances and the inside walls very fine porous substance and fine hexagonal crystals (200 - 400 nm). The structure of the porous substance is very much alike to that of the deposits mentioned above. Therefore, it would be natural to consider that the deposits are spewed out from these craters which are created by a micro-explosion occurred locally on Au surface, perhaps due to some nuclear reactions. The hexagonal crystals are considered to be Au(111) formed by recrystallization, the presence of which suggests that high temperature was evolved when these craters were created. From the SEM images it is seen that the craters were formed along the scraped lines on the Au electrode. It is then likely that the lattice defects play an important role to cause this reaction.

From the elements detected here, we can consider the following reaction scheme. Firstly, Hg is produced by

$$_{79}Au^{197} + {}_{1}H^{1} \longrightarrow {}_{80}Hg^{198}$$

which would then convert into Pt, Os, and Hf by

$$_{80}Hg^{198} \longrightarrow {}_{78}Pt^{194} + {}_{2}He^{4}$$

$$_{78}Pt^{194} \longrightarrow {}_{76}Os^{190} + {}_{2}He^{4}$$

$$_{76}Os^{190} \longrightarrow {}_{72}Hf^{180} + 2\,{}_{2}He^{4}$$

The production of other elements would be more complicated.

O-036

A CONFIRMATION OF ANOMALOUS THERMAL POWER GENERATION FROM A PROTON-CONDUCTING OXIDE

R.A. Oriani, Corrosion Research Center, Department of Chemical Engineering and Materials Science, University of Minnesota, 221 Church St. SE, Minneapolis, MN 55455, U.S.A.

The claims of Mizuno and collaborators, and the earlier claims of Biberian and Forrat, that excess thermal power can be developed by proton-conducting oxides held in deuterium gas at elevated temperatures are important because thermal power generated at high temperatures can be converted to other forms of power with greater Carnot efficiency than thermal power at lower temperatures. Therefore a Seebeck calorimeter operating at 400°C was constructed to attempt to verify these claims. This calorimeter, whose operation is independent of the spatial distribution of power sources and of the thermal conductivity of the gas, is described.

The calorimeter was used with specimens of nominal composition $SrCe_{0.9}Y_{0.08}Nb_{0.02}O_{2.97}$ supplied by Dr. T. Mizuno. Two of these specimens produced positive deviations from the calibration curve by more than four standard deviations so that thermal power was produced that was greater than the d.c. power of alternating polarity supplied to the specimen. In several episodes excess power was produced without supplying any d.c. power.

Verification of the claims has been achieved. It remains to increase the reproducibility and the power output of the technique, as well as to achieve understanding of the underlying mechanism of the phenomenon.

Fifth International Conference on Cold Fusion
9-13 April, 1995 - Monte Carlo, Monaco
ICCF5 ©1995

Excess Heat Measurement in AlLaO3 Doped with Deuterium

Jean-Paul BIBERIAN
Département de Physique, Faculté des Sciences de Luminy,
70 Route Léon Lachamp,
13288 Marseilles Cédex 9, France

Abstract:

We show evidence that solid state electrolytes can be used successfully in "cold fusion" experiments. We describe in this work that LaAlO3 single crystals loaded with deuterium produce excess heat up to 10 times the amount of electrical power applied. No significant amount of neutrons has been detected.

1. Introduction

Since the public announcement of the discovery of "cold fusion" in 1989 by Fleischmann et al. ([1]), most of the experimental research work has been done in liquid electrolytes. However, as soon as 1989, Forrat ([2]) patented a solid state electrolytic device, with the reaction in the electrolyte. He proposes a process catalyzed by nascent muonic like atoms in polyvalent vacancies compensated by H^+ or D^+ ions in refractory oxides. Mizuno et al. ([3]) have shown that large quantities of excess heat could be generated in perovskite ceramics in deuterium atmosphere when a slowly varying current is passed through the sample.

It is the purpose of this work to repeat this early work, and to determine the characteristics of the reaction in a better controlled environment.

2. Theoretical point of view

Oxides with the perovskite structure are excellent proton conductors, when metal atoms are replaced by protons ([4,5]). They are therefore a good choice for "cold fusion" experiments. In this work we have used LaAlO3 single crystals. Figure 1a shows the unit cell of the stoichiometric lanthanum aluminum oxide. The structure is composed of a lanthanum atom at each corner of the cubic unit cell, an aluminum atom at the center, and an oxygen atom at the center of each face. An alternative description is shown in figure 1b, with an aluminum atom at each corner, a lanthanum atom at the center, and oxygen atoms in the middle of each side.

If a lanthanum vacancy is created (V center or p type semiconductor), the unit cell is shown in figure 1c. Since lanthanum is trivalent, three protons (or deuterons) can replace one lanthanum ion as shown in figure 1d. When a negative voltage is applied, more protons (deuterons) are attracted and can fill up the vacancy.

Figure 1e shows the structure of the cell with interstitial deuterium. Five protons can be placed in a single lanthanum vacancy. The density of deuterons is then close to that of liquid deuterium.

Intrinsic lanthanum aluminum is transparent. When lanthanum vacancies are present, it becomes red (the maximum vacancy concentration being 5%). When vacancies are filled with deuterium, the crystal becomes transparent again [4,5].

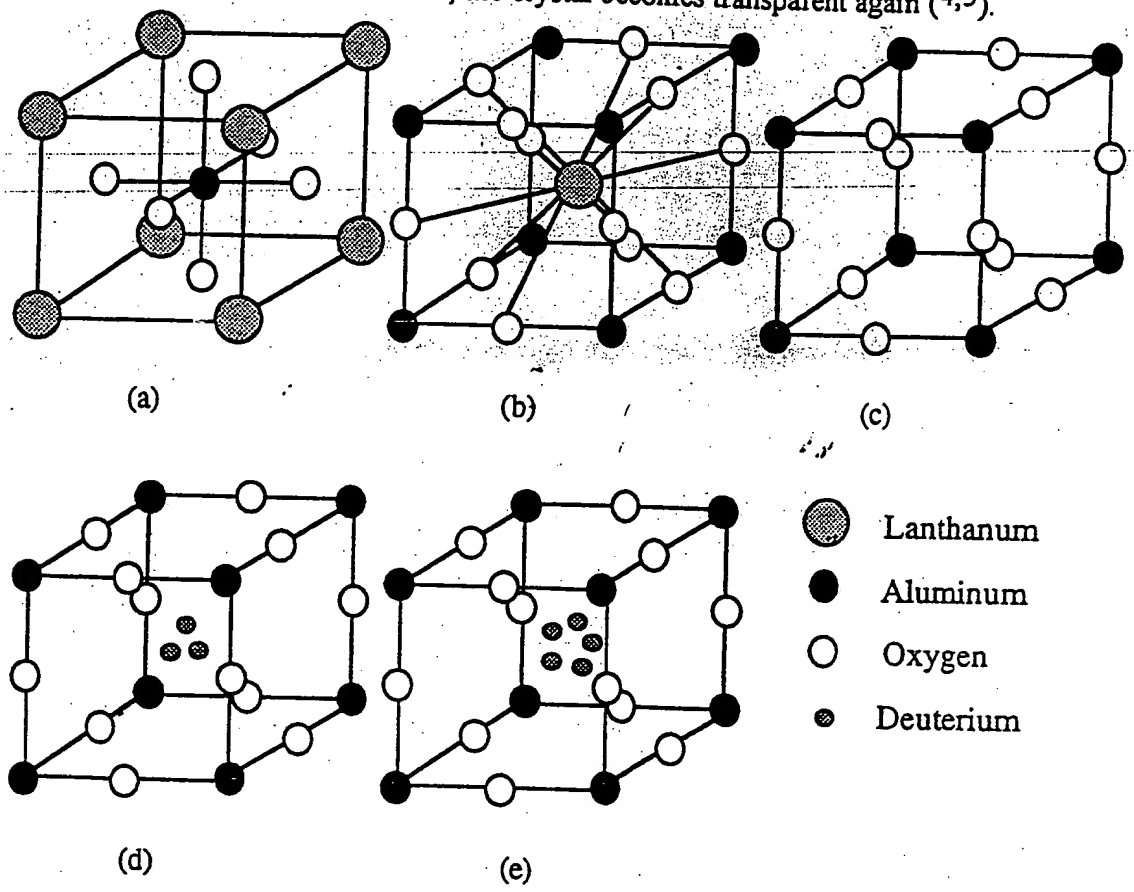

Figure 1

The $LaAlO_3$ perovskite type unit cell. a) The intrinsic unit cell with Lanthanum atoms at the corners and Aluminum at center. b) Same cell with Aluminum at corners and Lanthanum at center. c) Cell with Lanthanum missing creating a V center. d) Cell with Lanthanum replaced by 3 deuterons to compensate vacancies. e) Cell with Lanthanum replaced by 5 deuterons forming F centers.

When the crystal is heated in an hydrogen (deuterium) atmosphere, protons (deuterons) diffuse in the crystal. If a voltage is applied on two faces of the crystal, protons (deuterons) diffuse towards the cathode. Three zones develop, as shown in figure 2. The cathode side has excess-interstitial deuterium, so that it becomes blue, (F centers), as described in figure 1e. The middle section is white, because it is stoichiometric, the lanthanum vacancies have been filled by three hydrogen (deuterium) atoms as in figure 1d. The anode side is red because it has lanthanum vacancies as in figure 1c (V centers).

Numerous such crystals can be used as proton conductors, however rare earth aluminates are very well suited because aluminum and lanthanum are both solely trivalent. $AlLaO_3$ proton conductivity has been extensively studied for fuel cell applications ([4]).

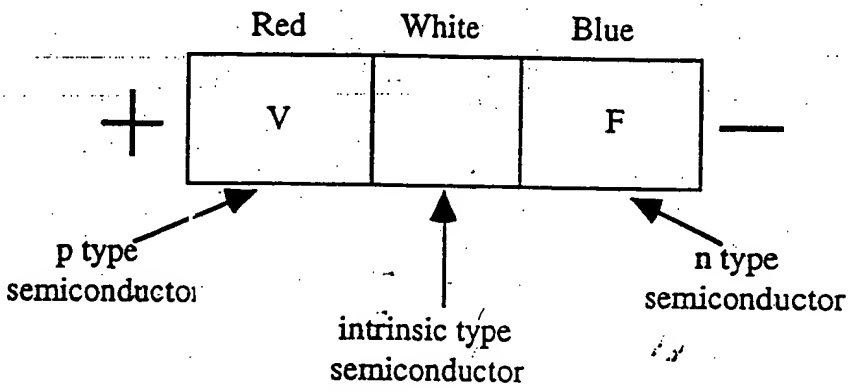

Figure 2

When a voltage is applied through the sample at high temperature in an hydrogen (deuterium) atmosphere, the anode becomes red, because of depletion in proton (deuteron) contents, the cathode becomes blue due to proton (deuteron) enrichment, and the middle returns white because the vacancies are neutralized by the protons (deuterons).

The structure of the intrinsic aluminum lanthanate is:

$$Al^{3+}La^{3+}O_3^{6-}$$

and the crystal appears white.

A crystal with 5% vacancies will be red and will have the following structure:

$$Al^{3+}La_{0.95}^{2.85+}O_3^{5.85-}$$

When the crystal is heated in a deuterium or hydrogen atmosphere, ions diffuse in the sample and vacancies are occupied by the deuterium ions, and consequently the crystal recovers its intrinsic white color. The structure of the crystal is now:

$$Al^{3+}La_{0.95}^{2.85+}D_{0.15}^{0.15}O_3^{6-}$$

After application of a voltage an F zone appears at the cathode with the composition:

$$Al^{3+}La^{2.85+}D^{0.2}O_3^{6.05-}$$

Therefore, when a voltage is applied through the sample at high temperature in an hydrogen (deuterium) atmosphere, the anode becomes red, because of depletion in proton (deuteron) contents, the cathode becomes blue due to proton (deuteron) enrichment, and the middle returns white because the vacancies are neutralized by the protons (deuterons) as shown in figure 2.

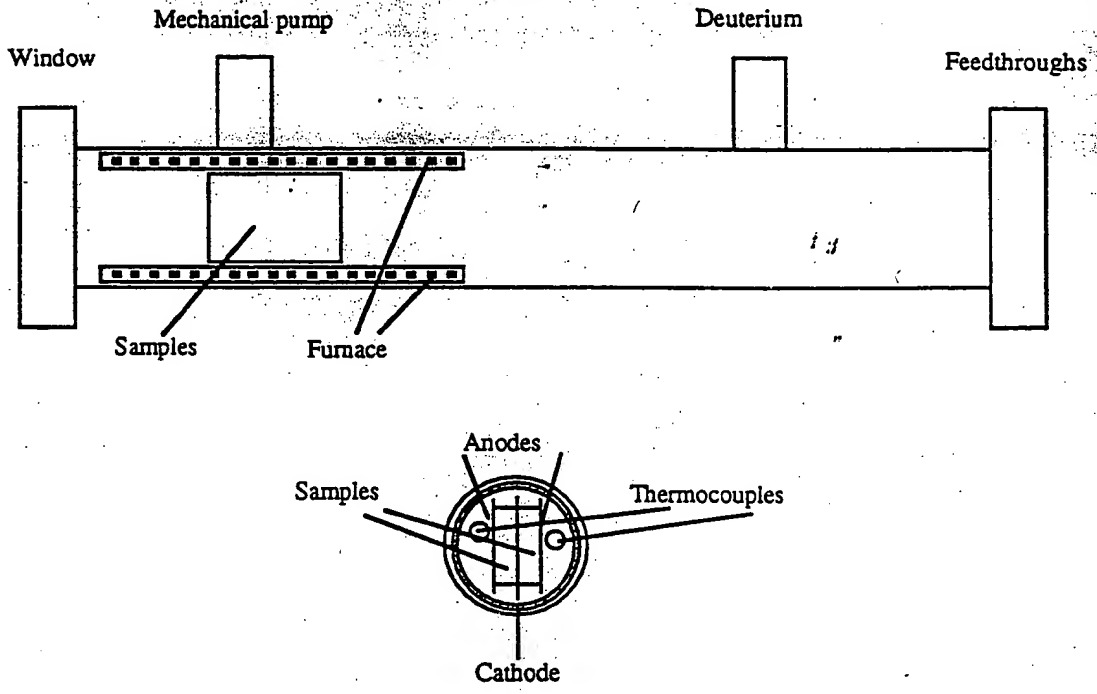

Figure 3

Schematic of the experimental setup. The samples are sandwiched between two palladium foils. They are heated by a cylindrical furnace. Two thermocouples measure temperatures near the sample. A glass window allows viewing of the sample, and a gauge monitors pressure. The cylindrical chamber is 35 mm in diameter and 300 mm long.

3. Experimental set up

The samples we have used are $LaAlO_3$ single crystals with unknown amounts of vacancies, but probably less than 5 %, and in some cases doped with rare earth metals. They have been prepared in the sixties by the flame fusion process. They are cut with a diamond saw: 4 cm^2 in area and 3 mm thick. The first experiments have been conducted with a thin film of gold sputtered on each side. In one occurrence, when the crystal has been heated at high temperature (500-600 C), the gold layer dissolved in the crystal, so later bare crystals were used successfully.

Figure 3 shows a schematic of the experimental set-up. The system is a 300 mm stainless steel tube 35 mm in diameter, positioned horizontally The crystals are sandwiched with 100 µm thick palladium foils. Two chromel-alumel thermocouples measure the ambient temperature near the sample. A window at the other end of the tube allows viewing the sample. A gauge is used for crude measurement of the pressure in the chamber.

The sample is positioned at 250 mm from the flange, so that the feedthroughs do not warm up significantly. A palladium foil is used as cathode between two identical wafers cut from the same crystal rod. Two palladium foils used as anodes are then placed symmetrically on the other faces of the crystals. These two anodes are hold together by a molybdenum clamp. The symmetric design has the advantage of eliminating the problem of the mechanical attachment of the electrodes without producing a short circuit.

Temperature is measured two ways: on one hand, two chromel-alumel thermocouples are positioned in the ambient deuterium gas surrounding the crystal. And on the other hand temperature is deduced from measuring the resistivity of the tungsten wire used in the furnace heater. This resistance has been first calibrated against the two thermocouples, and shown to behave linearly with temperature in the whole temperature range. The advantage of using this second type of temperature measurement is that it is an average temperature and not a local measurement as with thermocouples.

All measurements are made with a PC based data acquisition system. The heating power of the furnace is maintained constant by regulating the applied voltage.

A helium-3 neutron detector is positioned 30 cm from the sample, and its measurements are recorded at all times. An internal source inside the detector produces a signal at a frequency of 0.534. Therefore any neutron emission from the sample should add to this signal.

4. Experimental procedure

The crystals are first heated in air to remove any hydrogen present. After that crystals are red indicating the presence of lanthanum vacancies. It is then heated in deuterium for several hours at about 800 °C. At this point crystals turn white.

Crystals are placed in pairs in order to simplify the attachment as described in the above section. The stainless steel chamber is evacuated using a mechanical pump down to a pressure of 10^{-2} torr. Deuterium is subsequently introduced at about atmospheric pressure. Power of the furnace is raised slowly, without passing current through the crystals. After a few hours, when the desired temperature is reached, and remains stable,

a voltage is applied through the crystal. This is done with four 120 Volts power supplies mounted in series. To avoid any power surge in the crystal when the current is applied, we use the current limitation mode.

Blank experiments have been performed in a similar way, but with a virgin crystal, without any deuterium. We can therefore compare directly data obtained with samples loaded with deuterium and blanks experiments.

5. Experimental results

A blank experiment is shown in figure 4. Sample temperature is deduced from the measurement of the resistance of the furnace. The furnace power is 150 Watts, producing a sample temperature of 545 °C. The electrochemical power is 250 mW (250 V, 1 mA). The temperature rise is 0.5 K.

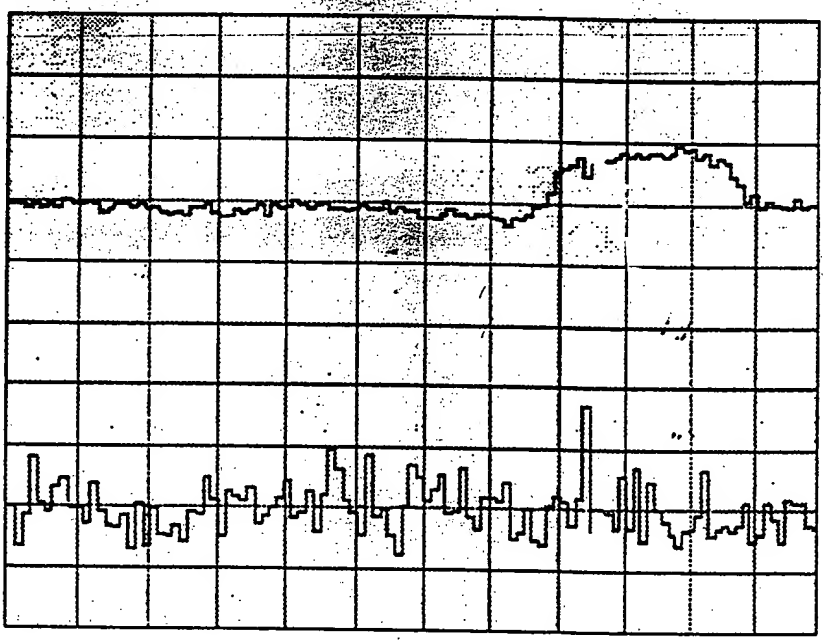

Figure 4
Blank experiment. Top curve: temperature, bottom curve: neutron counter.
Time: full scale 120 minutes. Temperature: full range 5 K.

Figure 5 shows similar curves, but the crystals are doped with an unknown amount of praseodymium, and loaded with deuterium. The furnace power is 150 Watts, and the electrochemical power is 50 mW (250 V, 0.2 mA). The temperature rise is 1 K, and corresponds to 500 mW. The excess energy gain is therefore 10.

The lower curves in figures 4 and 5 represent the neutron counts, and show no sign of increase. However in one occasion a very slight increase 0.1 counts/sec has been measured. We cannot exclude that this signal is due to noise, because further experimentation has shown that the detector is very sensitive to noise.

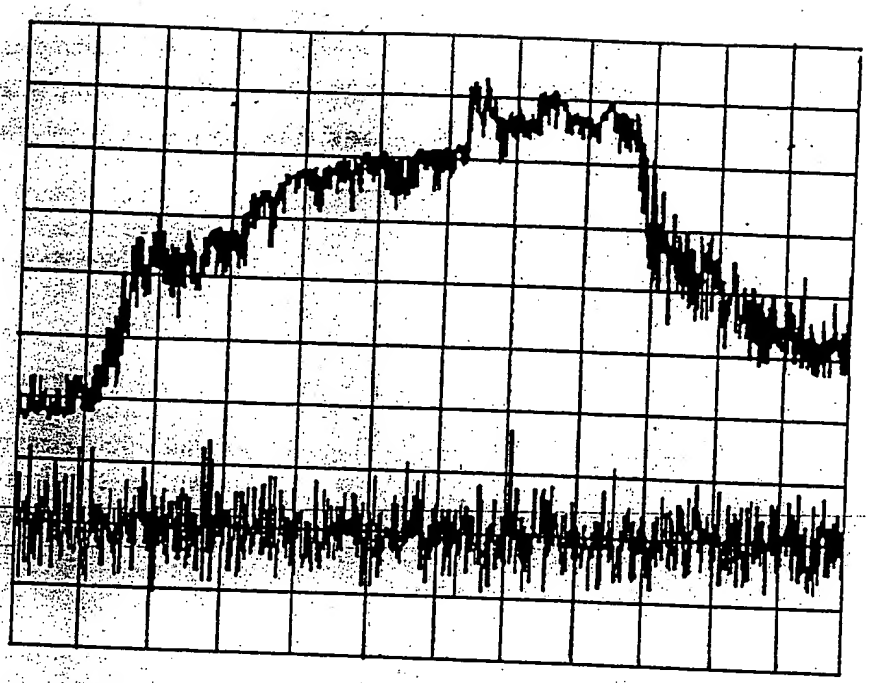

Figure 5
Experiment in deuterium. Top curve: temperature, bottom curve: neutron counter. Time: full scale 18 hours. Temperature: full range 5 K.

An interesting observation is the potential difference between anode and cathode when the voltage generator is disconnected. Values of up to 1.9 Volts have been measured. This indicates that upon application of the initial voltage through the crystal, there is a non-uniform distribution of the deuterium inside the crystal. This voltage decreases with a time constant in the 5 to 10 minutes range.

6. Discussion

A comparison between temperature curves of figure 4 and 5 shows that in the blank experiment, temperature increase is achieved in 3 or 4 minutes, whereas with the active sample the temperature rise happens after at least one hour. This indicates that during the process of passing current through the sample, there is probably diffusion of deuterium inside the crystals.

Experiments have been carried out in a closed cell. So if we assume that all the deuterium molecules have reacted somehow, we obtain an energy of 10 eV per molecule. This is not possible because after the experiment is stopped, there is still plenty of deuterium.

We therefore believe that the reaction mechanism is either nuclear in origin, (in which case it corresponds to unknown reactions since observed fusion ashes lie below the threshold needed to explain the observed heat) or to a new quantum chemistry.

Mizuno et al. (3) have observed similar effects with a SrCeO3 ceramics , that have the same perovskite structure. However, they observe a much larger excess heat of

the order of 10^4, at 300 to 400 °C! The main difference is probably the structure of the sample. We have used a single crystal , whereas Mizuno et al. have used a ceramic that has a polycrystalline structure with grain boundaries.

7. Conclusion

We have shown that excess heat is observed when a current is passed through a lanthanum aluminum oxide crystal with lanthanum vacancies in a deuterium atmosphere. The amount of excess heat has been determined to be up to 10 times the electric power passed through the sample.

We cannot exclude low level neutron emission, but at this point noise can still be the cause of the small signal increase observed.

Solid state electrolytes are excellent candidates for future applications because they operate at much higher temperature than liquid electrolytes. This should make it much easier to generate electricity. Also because of the closed cell configuration, and the possibility of working at low deuterium pressure, it would be possible to measure helium-4 production with an excellent accuracy.

Acknowledgments

I would like to thanks: Yves Grange now at the Commissariat a l'Energie Atomique in France for providing me with the samples, Francis Forrat for all the support he gave me to understand and succeed in this work, Huntington Laboratories for their technical support, and my children Mélanie and Gabriel in collecting data during the first successful experiment.

References

1. M. Fleischmann, S. Pons and M. Hawkins,
   J. Electroanal. Chem. 261 (1989) 301.

2. F. Forrat,
   Patents numbers: F 89 07703 and F 90 08360

3 T. Mizuno, M. Enyo, T. Akimoto and K. Azumi, I
   ICCF-4, Maui, Hawaii, 1993.

4- F. Forrat, G. Dauge, P. Trévoux, G. Danner and M. Christen,
   C.R. Acad. Sc. Paris, 259 (1964) 2813.

5 F. Forrat, R. Jansen, P. Trévoux,
   C.R. Acad. Sc. Paris, 256 (1963) 1271.

O-031

TRITIUM PRODUCTION FROM PALLADIUM AND PALLADIUM ALLOYS

T. N. Claytor, M. J. Schwab and D. G. Tuggle, Los Alamos National Laboratory
Los Alamos, NM 87545

A number (22) of pure palladium samples and palladium alloys have been loaded with a deuterium or hydrogen plasma in a system that allows the instantaneous measurement of tritium. By carefully controlling the high pressure plasma conditions, the plasma can be constrained to only contact palladium surfaces and to only lightly sputter the palladium. Long run times (up to 200 h) result in an integration of the tritium and this, coupled with the high intrinsic sensitivity of the system(~ 0.1nCi/l), enables the significance of the tritium measurement to be many sigma (>10). In addition to the real time tritium measurement, the deuterium gas can be combined with oxygen, at the end of a run, resulting in water samples that were counted in a scintillation counter. The results of these confirmatory measurements of the tritium in these water samples agree quantitatively with the decrease in tritium as measured by the ion sensor. However, surprising concentrations (up to 1.5×10^6 dpm/ml) of tritium were found in several samples that had been exposed to a hydride inhibitor. We have continued to investigate the effect of hydrogen additions on the output of tritium in these types of experiments and find that hydrogen additions always suppress tritium production. We will show the difference in tritium generation rates between batches of annealed palladium, as received palladium and the palladium alloys (Rh, Co, Cu, Ni, Be, B, Li, Hf, Hg and Fe) of various concentrations to illustrate that tritium generation rate can vary greatly from alloy to alloy as well as within a specific alloy, dependent on concentration. Other metals (Pt, Hf, Ni, Nb, Ta, V, W, Zr) have also been run in the system as background samples or to determine if tritium could be detected in the gas analysis system. In nearly all cases they have produced results very close to background drift rates.

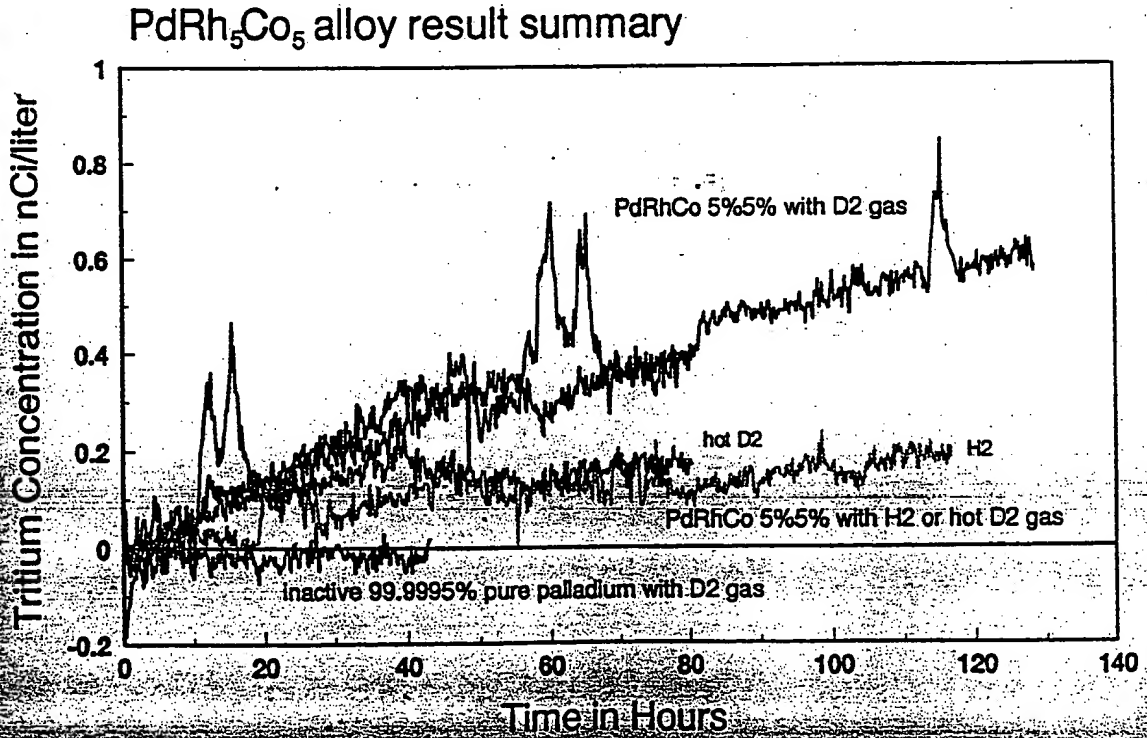

MEASUREMENTS OF EXCESS HEAT FROM A PONS-FLEISCHMANN–TYPE ELECTROLYTIC CELL USING PALLADIUM SHEET

COLD FUSION

TECHNICAL NOTE

KEYWORDS: *excess heat measurement, calorimetry, palladium*

EDMUND STORMS *Los Alamos National Laboratory*
NMT Division, Los Alamos, New Mexico 87545

Received July 27, 1992
Accepted for Publication September 28, 1992

Two pieces of palladium sheet similar to that used by Takahashi were loaded with deuterium in a Pons-Fleischmann–type electrolytic cell, and heat production was measured. One sheet produced a steady increase in excess power that reached 7.5 W (20% of input power) before the study was interrupted. A second similar sheet from a different batch of palladium did not produce any measurable excess power. There were differences in the loading behavior, the maximum stoichiometry, and the presence of excess volume in the deuteride made from these materials. The first sheet contained 0.8% excess volume after having been deloaded from its maximum deuterium/palladium (D/Pd) ratio of 0.82 to 0.73, and the second sheet contained 13.5% excess volume while at its maximum ratio of 0.75. The high excess volume in the latter case is an indication of internal escape paths that reduce the required high D/Pd ratio.

I. INTRODUCTION

A computer-controlled, sealed, isoperibol-type calorimeter has been constructed to study the Pons-Fleischmann effect. This device will be used to study a variety of cathode materials, but its first use was the study of palladium sheets supplied by Tanaka Kikinzoku Kogyo K. K. to A. Takahashi of Osaka University. Single samples of palladium sheet from two different batches were studied.[a]

Takahashi reported[1] the production of excess power that exceeded 100 W/cm^3 (average of 1.7 × input power) from a Pons-Fleischmann–type electrolytic cell using this material. In addition to this extraordinary energy production, low-level neutron emission was measured that was roughly proportional to the magnitude of heat production when the cell current was changed, and it decreased with time.

In addition to using this unique palladium, Takahashi has suggested two procedures for success. The arrangement between the cathode and anode should produce uniform loading of the palladium sheet with deuterium, and the cathode should be subjected to periodic changes in cell current. He reports that excess energy increased with time when these procedures were used.

In addition to this recent success, excess heat production has also been reported in a significant number of studies[2–28] using a variety of procedures and calorimeter designs; these studies found, in most cases, many positive results. Palladium rods were studied in most of this work, in contrast to the plate-shaped cathode used here.

Because relatively large amounts of excess heat are expected, a calorimeter design having a relatively low sensitivity but a high upper power limit was chosen. In addition, a design having simplicity of operation and calibration was used in order to reduce the various objections raised by critics of the cold fusion effect. Active stirring and temperature readings at two levels within the cell were used to eliminate the effect of possible temperature gradients. Four different calibration procedures were used, and these were applied before, during, and after the production of excess energy. The primary calibration used electrolytic heating of the LiOD electrolyte with a platinum cathode and anode. Except for chemical heat that might be associated with palladium, this method had the same bubble pattern, heat distribution, and chemical effects within the electrolyte as would be found in the cold fusion cell. In addition, this method produced a calibration constant similar to that determined when "dead" palladium was used as the cathode. Consequently, most of the objections raised to discount excess heat production are eliminated because they are canceled out by the calibration procedure. Because the calorimeter contained a recombiner, it could be completely sealed and pressurized with deuterium gas, and the internal pressure could be monitored. In this way, no material entered or left the cell under normal conditions. Significant excess heat was observed using these methods.

This technical note concentrates on the verification of excess heat and the measurement of various physical and chemical factors that are thought to be associated with excess energy production. No data or theories are presented about the possible source of heat or associated nuclear products other than to note that no tritium was produced.

II. EXPERIMENTAL

II.A. Palladium Characterization

The palladium sheets were weighed (±0.0001 g), the dimensions were measured (±0.002 cm), and the sheets were

[a]The palladium sheets were transferred through R. George and E. Mallove.

TABLE I

Result of Physical Measurements Made Before the Study

	Weight (g)	Area (cm^2)	Volume (cm^3)	Density (g/cm^3)	Surface
Palladium sheet 1	3.9186	6.643	0.3358	11.670	Smooth
Palladium sheet 2	3.8915	6.575	0.3273	11.889	Fine parallel lines

washed with acetone. When the metal had to be removed from the electrolytic cell for extended periods, it was placed in liquid nitrogen. Table I lists the physical measurements made before the calorimeter study.

II.B. Calorimeter Description

Figure 1 shows a cross section of the closed Pyrex glass calorimeter. A Teflon plug is held into a standard taper by a spring that allows pressure release should the internal pressure rise above 1.5 atm. Holes through this plug give access for various probes. The calorimeter is attached to a sealed gas-handling system that maintains an overpressure of D_2 and allows the pressure to be monitored. An additional sheet of platinum (counterelectrode) within the electrolyte provided the means to calibrate the cell without disturbing the palladium and to conduct heat generated at the recombiner into the electrolyte. Later in the study, this feature was eliminated

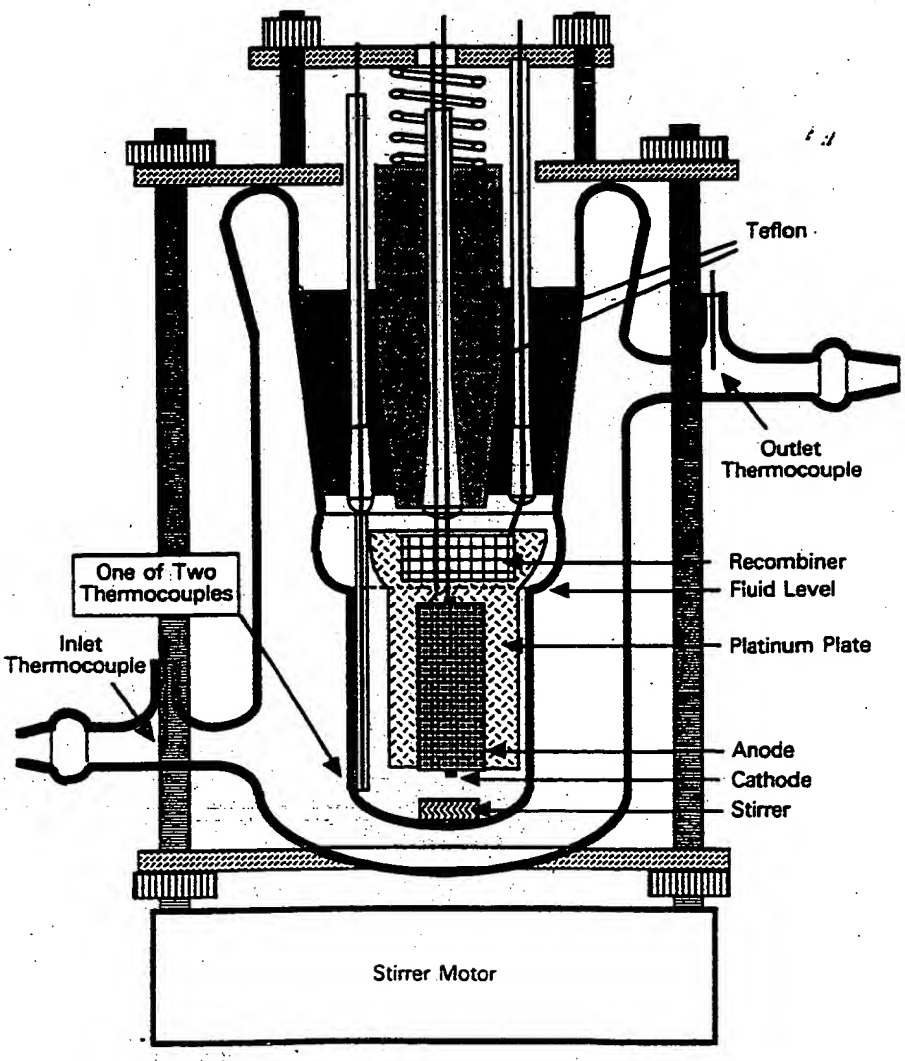

Fig. 1. Cross section of the calorimeter.

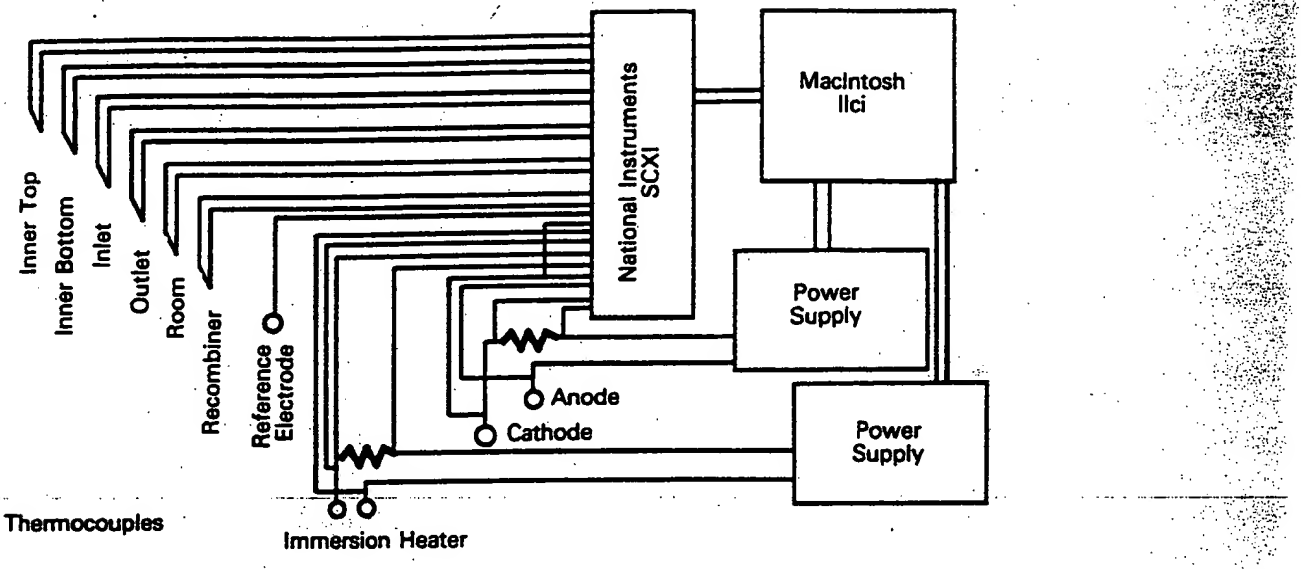

Fig. 2. Electrical connections to the data acquisition system.

without producing a change in the calibration constant. The recombiner is carbon cloth impregnated with Teflon and platinum. A Teflon-covered magnet is used for active stirring.

Figure 2 shows the electrical connections to the data acquisition system, and Fig. 3 shows the position of the various access probes into the calorimeter. Two thermocouples monitor the top and bottom of the electrolyte, a glass-encased Joule heater is used for calibration, and a capillary, placed within 0.5 mm of the cathode surface, monitors the voltage between the cathode and an external platinum electrode (reference electrode).

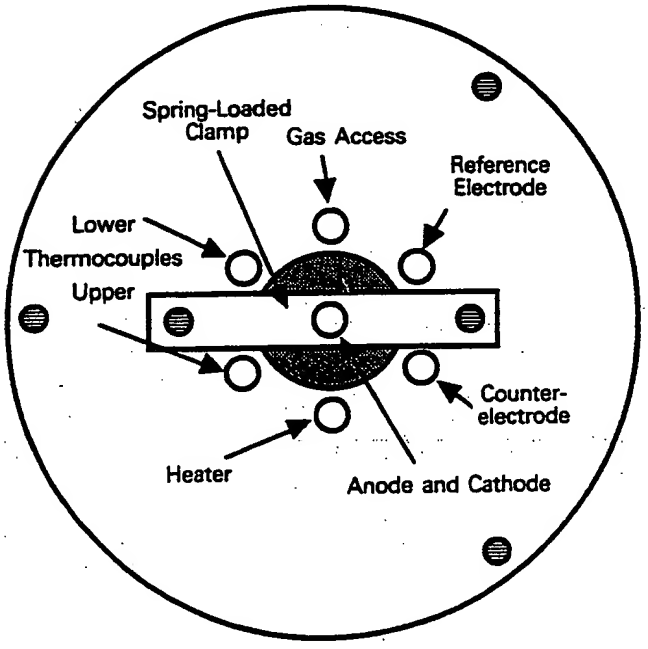

Fig. 3. Top view of probe positions. The reference electrode is an electrolyte bridge from the cathode to an exterior platinum electrode. The counter electrode is a piece of platinum immersed in the electrolyte.

II.B.1. Anode-Cathode Relationship

Uniform charging of the palladium with deuterium is generally agreed to be an essential feature for successful excess heat production. Because a plate is studied, a coplanar arrangement is used. A cross section of the anode-cathode assembly is shown in Fig. 4. The anode is platinum gauze having seventeen 0.006-in. wires per centimetre that are wrapped around Teflon posts. These posts center the cathode in the assembly with 9-mm spacing between the anode and the cathode. A heavy platinum wire makes electrical contact along one edge of the anode to transmit uniform charging current to the anode.

II.B.2. Electrolyte

The electrolyte used in these studies is double-distilled D_2O containing 99.76 mol% D_2O and 0.3 *M* LiOD (natural lithium). The liquid is stored in a plastic bottle. Because of chemical interactions of lithium with oxygen in the electrolyte and with carbon in the recombiner, the concentration of lithium in the cell solution slowly decreases as Li_2CO_3 is formed on the recombiner. In addition, the solution gradually becomes saturated with CO_2.

II.B.3. Temperature Measurement

Temperature is measured by thermocouples at two levels within the inner region and at the inlet and outlet of the surrounding water jacket. The temperature difference across the cell wall is used to measure heat production. This difference is calculated by subtracting the average of the inlet and outlet jacket temperatures from the average of the inner top and inner bottom temperature readings.

All thermocouples (type T) are compared with a calibrated mercury thermometer traceable to the National Institute of Standards and Technology and corrected to within ±0.1°C. However, the absolute error in an individual temperature is at least ±1°C because of uncertainty in the temperature

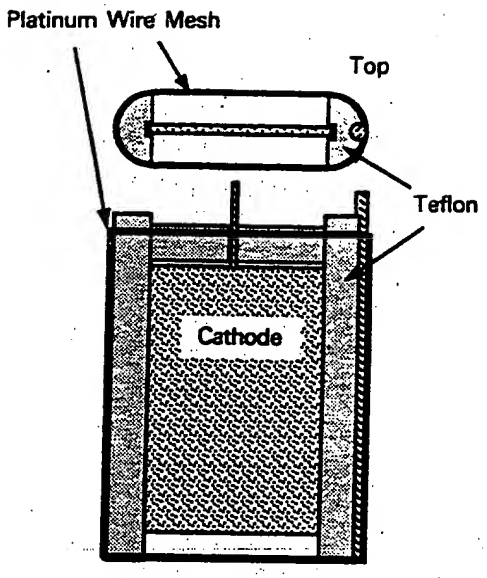

Fig. 4. View of the cathode-anode assembly.

compensating circuit. It is important to note that this uncertainty is removed when ΔT is determined. The standard deviation from the mean of individual ΔT measurements at constant power is ±0.02°C when zero power is applied to the cell and ±0.07°C when 0.42 A/cm^2 (2.8 A) is applied.

Room temperature and, later, the temperature of an external recombiner catalyst located in the gas handling system are also monitored. Heat generation at this location is an indication that the internal catalyst has failed to recombine all of the generated oxygen. This catalyst also prevents the unintentional buildup of an explosive mixture of O_2 and D_2.

II.B.4. Calibration

Calibration is done by four methods:

1. Current is passed through an internal, glass-covered immersion heater to give simple Joule heat.

2. A platinum sheet is substituted for the palladium cathode, and electrolytic heat is created using the normal anode-cathode configuration.

3. Electrolytic current is passed between the normal platinum anode and a platinum sheet that holds the recombiner.

4. The current is cycled between two values over an extended period of time using either a platinum cathode or an inactive palladium cathode. This technique is called "bivalue" in subsequent discussion.

Several of these methods contribute heat to different positions within the cell, thus testing the effect of potential temperature gradients. The time stability of the calibration is tested by the bivalue mode. A comparison between electrolytic and Joule heat tests the effect of heat being produced at the recombiner in the former case. It is important to note that method 2 has the same heat distribution, bubble pattern, and recombiner heat when palladium is studied. This method is used to calibrate the cell before and after each cell modification. Method 1 is used to detect changes in the calibration constant while palladium is being electrolyzed but is not used to provide an absolute calibration because of a small heat loss through the wires. A small charging current is applied to the palladium electrode during this calibration to prevent loss of deuterium. This additional power is taken into account. Method 4 tests the effects of the recommended bivalue mode of charging on the calibration constant. Platinum is used as the cathode, or when excess heat is not being produced, palladium is used. However, this calibration method is less accurate when palladium is used because fewer points must be taken in order not to alter the charging conditions too much.

Calibration using methods 1, 2, and 3 is accomplished by automatically sequencing the current through two cycles consisting of current steps up to a maximum then down to zero. The cell is allowed to equilibrate for 12 min, the time needed to reach >99% of the final value, after each current change before measurements of temperature, current, and voltage are made and recorded. A total of 72 values are normally taken to define a linear least-squares equation. These data show no curvature within the measurement range up to 50 W. The slope of the line through the data is the calibration constant that, when multiplied by the measured ΔT across the cell wall, gives the number of watts of power P_T being developed within the electrolyte. The constant term in the least-squares equation is caused by a small temperature offset due to slight differences in the various thermocouples. Excess power is determined by subtracting the applied power, obtained by multiplying the cell current by the applied voltage, from the measured total power P_T.

Voltage is measured at the point where the current enters the active region of the calorimeter. The voltage circuits of the LabView data acquisition system (National Instruments SCXI and NB-MIO-16H systems for the Macintosh IIci) are calibrated to an accuracy of ±0.001 V, and the resistor used for current measurement is calibrated to an accuracy of ±0.1%. Two HP-6038A power supplies under computer control supply regulated current to the cell and the immersion heater.

Figure 5 compares calibrations made with the normal electrolytic configuration using a platinum cathode and with the immersion heater. Table II lists the values for the calibration equations and the standard deviation of the applied power (in watts) from the respective equation. The applied power is the product of the current times the voltage, and the standard deviation is obtained from the difference between the calculated watts using the calibration equation and the applied watts at each point. Although the average standard deviation is about ±0.4 W, there are variations between calibration runs that make the power uncertain by about ±1 W at 40 W of applied power and ±0.3 W near zero applied power. This results in an absolute uncertainty in the measured power of ~5%. On the other hand, the calorimeter is sensitive to changes in power at the 0.2% level if a sufficient number of data points are averaged.

A slight difference between the constant obtained using the immersion heater and that using normal electrolysis is apparent. This difference is caused by a slight loss of heat from the heater through the connecting copper wires and through the air above the oil that surrounds the nichrome heater wire within the glass enclosure.

Figure 6 compares the calibration constant obtained from individual fits with the data shown in Fig. 5, but as a function of jacket temperature. The line shown in the figure is obtained from a linear least-squares fit and results in the equation

$$B = 3.7 + 0.015T_J \ , \qquad (1)$$

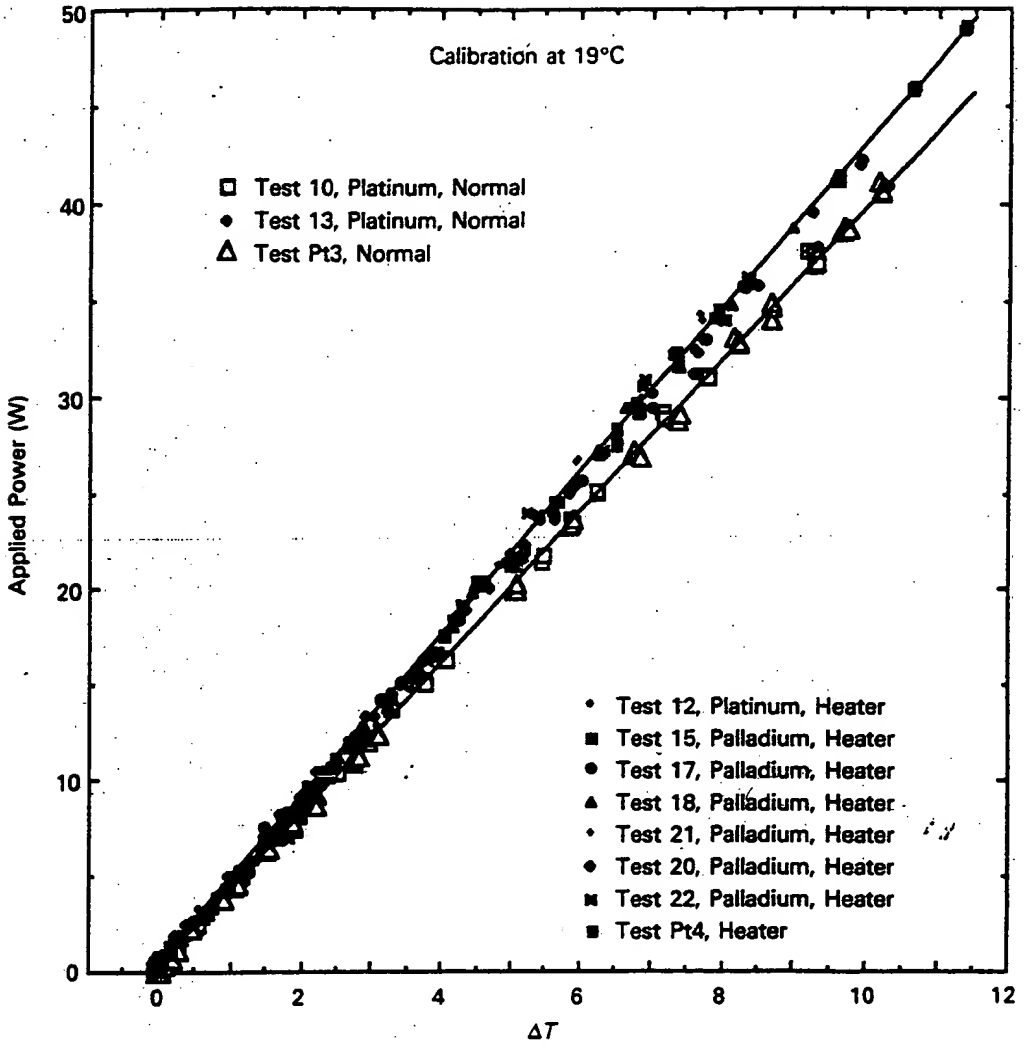

Fig. 5. Comparison between calibrations using normal electrolysis with a platinum cathode and with the immersion heater. Linear least-squares fits to the data are shown. The jacket temperature is near 19°C, and the electrolyte is 0.3 *N* LiOD.

in which B is the calibration constant and T_J is the jacket temperature in degrees Celsius. Because most studies are made at jacket temperatures near 20°C, an exact knowledge of the effect of jacket temperature is not necessary. An average calibration equation of

$$\text{developed power (W)} = 0.36 + (3.7 + 0.015T_J)\Delta T \quad (2)$$

is used during the study of the first palladium sample.

II.B.5. Factors Affecting Accuracy of Heat Measurement

Because bivalue charging of the palladium cathode is used, this mode is studied by using platinum electrodes in order to determine the amount of scatter introduced. Figure 7 shows that the scatter in the apparent excess power is about ±1 W at a current that deposits 35 W in the cell and ±0.3 W at low current. This scatter is caused by local variations in the temperature within the cell as well as by rapid changes in cell voltage caused by bubble action. While a detailed statistical analysis might reveal excess heat at lower levels, the production of excess heat is not claimed unless the measured average value exceeds this scatter (±1 W).

During excess heat production, the temperature of the electrolyte is above room temperature. Consequently, to the extent that heat could be exchanged with the room, excess heat is underestimated.

When apparent excess heat is observed, various tests are made to determine whether it might be an artifact of the measurement. Two artifacts are observed: (a) an abrupt 2-V negative error in the measured cell voltage when the value rises above 14 V and (b) a very unstable temperature reading when the cell voltage rises above 20 V. These defects do not affect the data reported here.

Concerns have been expressed in the past about the introduction of error by temperature gradients within the cell. Although active stirring is used at all times, small gradients are observed between the top and bottom temperature probes, as can be seen in Fig. 8. The reason for this behavior can easily be understood by watching the bubble pattern during electrolysis. Stirring action pulls liquid down past the anode, up the outer wall, and past the temperature probes. Because the

TABLE II

Comparison of Coefficients in Least-Squares Equations

Date	Test Number	T_J (°C)	Condition	watts = $A + B * \Delta T$		Standard Deviation (W)	Remarks
				A	B		
Platinum cathode							
May 2, 1992	10	19.1	Normal	0.2069	3.9748	0.26	
May 3, 1992	11	19.1	Exterior	0.7821	4.2611	0.28	
May 4, 1992	13	19.2	Normal	0.8994	4.0091	0.49	
May 4, 1992	14		Bivalue[a]	0.5400	4.0870		
Palladium sample 1 cathode							
May 5, 1992	15	19.2	Heater	0.2178	4.2991	0.22	Before charging
Recombiner changed							
May 13, 1992	17	19.3	Heater[b]	0.2687	4.2518	0.26	193 to 197 h
May 14, 1992	18	19.4	Heater[c]	0.1732	4.2881	0.27	208 to 212 h
May 18, 1992	20	19.5	Heater[c]	0.5794	4.1888	0.22	304 to 309 h
Recombiner changed							
May 19, 1992	21	19.0	Heater[d]	0.6319	4.2803	0.32	332 to 337 h
Recombiner changed, palladium weighed, and connections repaired							
May 21, 1992	22	17.2	Heater[e]	0.1115	4.3020	0.45	382 to 386 h
Recombiner changed and moved, exterior electrode removed							
Platinum cathode							
May 22, 1992	Pt1	9.7	Normal	0.0104	3.8340	0.26	
May 23, 1992	Pt2	9.7	Heater	−0.1159	4.0103	0.58	
May 23, 1992	Pt3	20.8	Normal	0.1261	3.9649	0.22	
May 24, 1992	Pt4	20.7	Heater	0.0451	4.2919	0.29	
May 24, 1992	Pt5	20.7	Bivalue[a]	0.1100	4.0500		
Palladium cathode							
May 25, 1992	Cal1	19.7	Heater[e]	0.1248	4.2808	0.28	
Platinum cathode							
New electrolyte, recombiner, and inner thermocouples							
June 2, 1992	Pt6	18.9	Normal	0.2668	3.9682	0.41	
June 3, 1992	Pt7	20.5	Normal	−1.5050	2.9222	1.04	
June 3, 1992	Pt8	20.4	Heater	−0.2295	4.2477	0.32	No stirring
June 4, 1992	Pt9	20.4	Normal	0.0396	4.0125	0.34	
June 4, 1992	Pt10	20.4	Bivalue[a]	−0.400	3.9850	0.43	

[a]Using values at 0.13 and 2.77 A.
[b]0.25-A electrolysis current applied along with heater power.
[c]1.0-A electrolysis current applied along with heater power.
[d]0.5-A electrolysis current applied along with heater power.
[e]0.3-A electrolysis current applied along with heater power.
[f]0.13-A electrolysis current applied along with heater power

bottom probe sees the flowing liquid first, it becomes slightly warmer than the top probe as electrolytic power is increased. Because the cathode is less affected by this stirring action, much of its heat goes to the top of the cell. Consequently, a change in this temperature gradient at constant applied power is a sensitive indicator of a change in where heat is being produced. A tendency for the top probe to become hotter than the bottom would indicate that heat production at the cathode has increased relative to the anode. In the absence of stirring, a warmer top is observed as expected.

When the immersion heater is used, there is a slight gradient of <0.1°C at 40 W, and the top is hotter than the bottom. This behavior is expected because the immersion heater deposits heat uniformly with depth, while normal upward convection tends to slightly favor the top. Variations in the placement of the anode-cathode assembly change the gradient

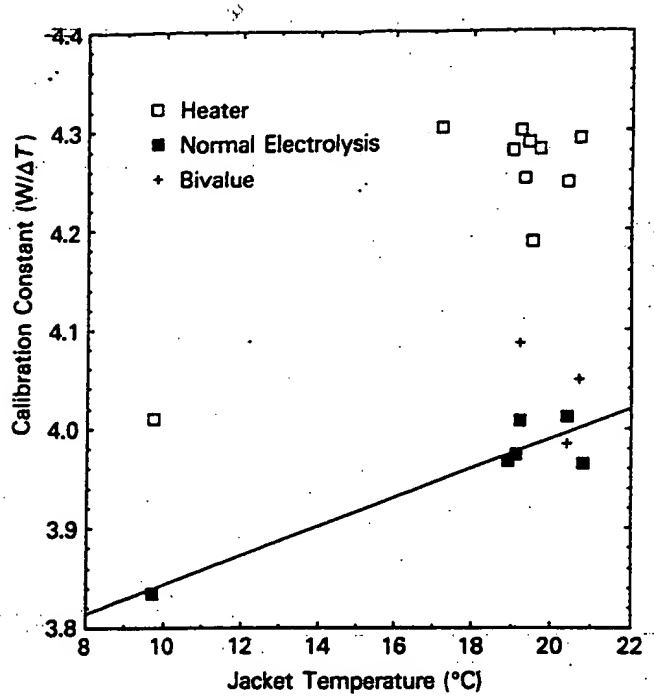

Fig. 6. Effect of jacket temperature on the calibration constant when calibration is done using the immersion heater and normal electrolysis with a platinum cathode.

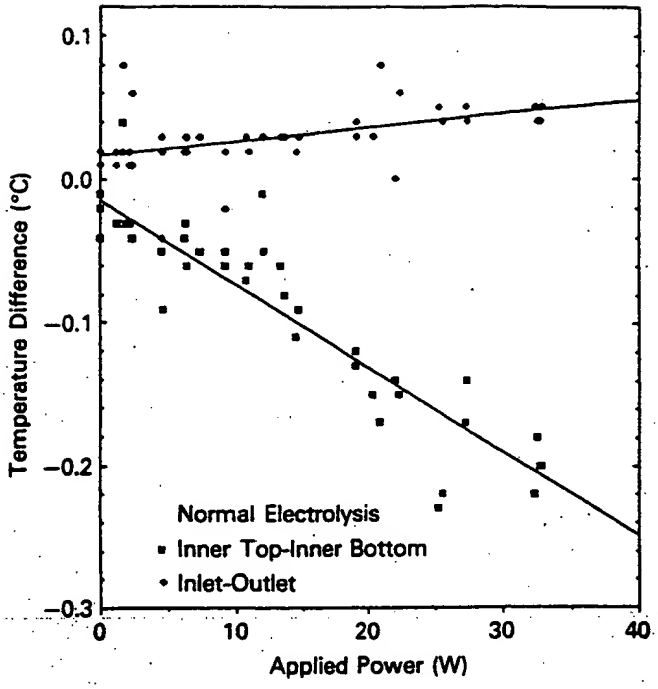

Fig. 8. Effect of applied power on the temperature difference within the electrolyte and through the flowing water in the jacket. A platinum cathode is used.

pattern without having any significant effect on the calibration constant. Consequently, these small gradients do not have an important affect on heat measurements in this calorimeter.

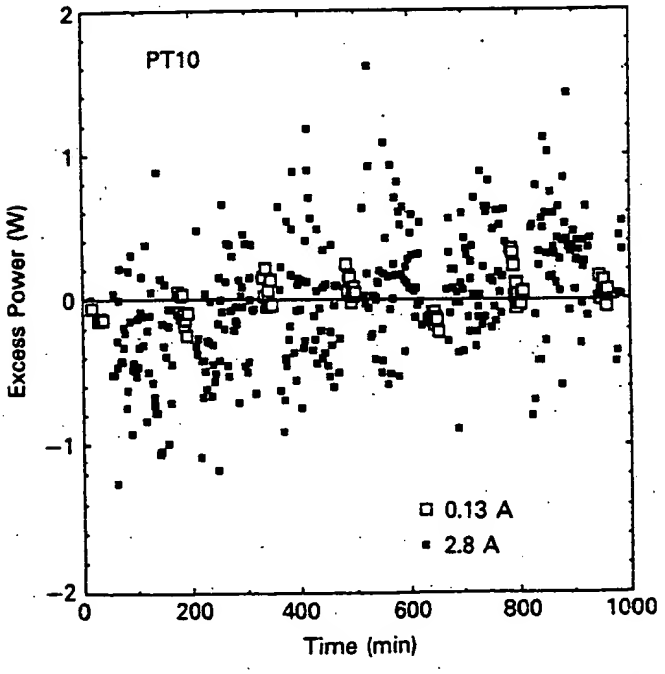

Fig. 7. Apparent excess power determined by subjecting a platinum cathode to bivalued charging at 0.13 and 2.8 A.

Flow through the jacket is so rapid that little temperature difference exists between the inlet and outlet, even at the highest power level, as shown in Fig. 8. Consequently, the fixed bath temperature is not affected by power production within the cell. However, there are abrupt fluctuations of about ±0.3°C in the bath temperature due to limitations in the bath temperature controller. These occasional fluctuations do introduce some scatter in the ΔT measurements and appear to be the major cause of outliers.

When stirring is stopped, the top temperature tends to increase slightly (<0.4°C) with respect to the bottom, and the calibration constant decreases significantly. Although bubble action alone prevents serious temperature gradients from developing, apparently the stagnant liquid barrier at the glass surface is not altered as it is when active mechanical stirring is used. Consequently, if stirring action should decrease during a run, the resulting temperature increase could be interpreted as excess heat.

II.C. Additional Measurements

The ambient deuterium pressure in the calorimeter and the cathode potential, referenced to a platinum electrode, are measured to reveal changes in the deuterium/palladium (D/Pd) ratio of the cathode bulk and surface, respectively.

II.C.1. Deuterium Pressure Measurement

A Baratron pressure transducer (±0.1% full scale, 0 to 1000 mm) is used to measure the D_2 pressure within the system. Changes in this pressure combined with the known volume of the gas system allow the amount of deuterium taken up by the palladium to be determined. This pressure is corrected for changes in room temperature. When determined in this manner, the D/Pd ratio is accurate to ±0.005 during

the first few days. However, there is a gradual increase in pressure over time that is proposed to be caused by interaction between oxygen and carbon in the catalyst to form CO_2, thereby leaving behind excessive deuterium. Consequently, after a few days, the pressure cannot be used to obtain an absolute D/Pd ratio, although short-term relative changes can be seen. A weight measurement at 405 h gives a D/Pd ratio that agrees within ±0.002 with the D/Pd ratio obtained from a pressure measurement made at 10 h.

II.C.2. Cathode Surface Potential Measurement

A capillary probe is placed within ~0.5 mm of the cathode surface, and the voltage between the cathode and an activated platinum sheet immersed in the electrolyte outside the cell is measured. This voltage has no absolute meaning because the reference electrode was not calibrated. On the other hand, relative changes in this voltage at constant cell current are significant and are used as an indication of changes in the surface D/Pd ratio. This voltage is also sensitive to the deposition of impurities on the surface, to the dissolution of lithium in the palladium, and to changes in electrolyte resistivity. However, these processes are relatively slow compared with changes in deuterium content, at least during initial charging.

III. STUDY OF PALLADIUM

III.A. Initial Loading of Palladium Sample 1

After assembly, the calorimeter is evacuated several times and backfilled with D_2 gas at an initial pressure of 692 mm. Calibration using the immersion heater is done, giving the result shown in Table II. Because there are no significant differences between this calibration and the ones done previously, all the calibrations are combined as described previously to give Eq. (2) and applied to the first part of the study.

III.B. Initial Charging of Palladium Sample 1

Initial loading is done at a constant current of 0.13 A (0.02 A/cm^2). Figure 9 compares the measured D/Pd ratio with the ideal ratio, assuming that all deuterium atoms produced by electrolysis are dissolved in the metal. For the first 150 min, essentially all of the deuterium dissolves. Once a ratio of 0.82 is achieved, loading is stopped. The following slight indication of deuterium loss is not thought to be meaningful. There is no subsequent indication, to the extent that uncertainties allow, that higher bulk D/Pd ratios are achieved during subsequent treatments. A later measurement of weight change indicated a D/Pd ratio of 0.82.

Both the voltage at the capillary probe and the cell voltage show a similar relationship to the D/Pd ratio during this time, as shown for the probe voltage in Fig. 10. Changes in slope correspond to previously reported compositions of the equilibrium phase boundaries at 1 atm D_2 and 25°C. This agreement with previous equilibrium measurements suggests that the composition gradient within the palladium is small at this loading current.

During charging, the excess power is equal to zero within the uncertainty of the measurement. Table III summarizes the history of palladium sample 1. This detail is included because the importance of charging history is not known at this time. During the first 17.2 h, the sample is loaded at constant current. For the next 65.4 h, the current is ramped in steps beginning at the lower current and extending to the upper current limit, then the current is abruptly returned to the lower current, as recommended by Takahashi. This cycle is repeated at the intervals noted in the table. Periodically during this treatment, the current is fixed at the lower current, and measurements of excess heat are made. There is no indication during this time that excess heat is being produced at 0.13 A. Because the calorimeter is not in equilibrium during the ramp

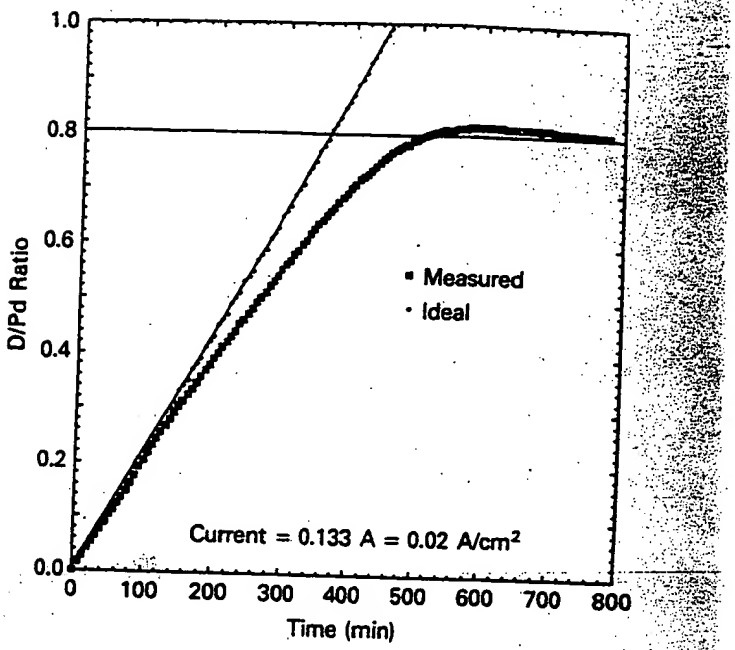

Fig. 9. The D/Pd ratio as a function of time during the initial charging of palladium sample 1.

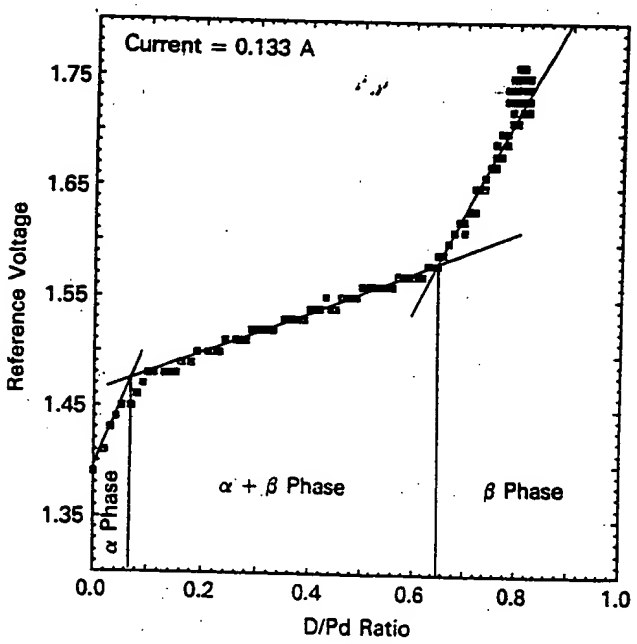

Fig. 10. Relationship between probe voltage and D/Pd ratio when charging palladium sample 1 at constant current.

TABLE III

Charging History of Palladium Sheet 1

Data Set	Time (h)	Treatment
May 5, 1992		
Test 15		Calibrated using heater
Pd1	0 to 17.2	Charged at 0.13 A
Pd2	17.2 to 17.5	Ramped from 0.13 to 2.77 A
	17.5 to 18.0	Held at 0.13 A
	18.0 to 25.4	Ramped from 0.13 to 2.77 A every 18 min
Pd3	25.4 to 26.3	Controlled at 0.13 A
	26.3 to 39.1	Ramped from 0.13 to 2.77 A every 6 min
Pd4	39.1 to 39.8	Controlled at 0.13 A
	39.8 to 47.2	Ramped from 0.13 to 2.77 A over 6 min
Pd5	47.2 to 48.7	Controlled at 0.13 A
	48.7 to 64.3	Ramped from 0.13 to 2.77 A over 6 min
Pd6	64.3 to 65.4	Controlled at 0.13 A
	65.4 to 90.1	Cycled between 0.13 and 2.77 A each 20 min
Pd7	90.1 to 98.1	Cycled between 0.13 and 2.77 A each 30 min
Pd8	98.1 to 114	Cycled and held at 0.13 A for 30 min and 2.77 A for 60 min
Pd9	114 to 122	Cycled and held at 0.13 A for 30 min and 2.00 A for 60 min
Pd10	122 to 136	Cycled and held at 0.13 A for 30 min and 2.50 A for 60 min
Pd11	136 to 146	Cycled and held at 0.13 A for 30 min and 2.80 A for 60 min
Pd12	146 to 159	Cycled and held at 0.13 A for 30 min and 0.5 A for 60 min; 6 ml D_2O added
	159 to 160	Cell turned off and recombiner replaced; cathode in air for most of the time (47 min)
Pd13	160 to 170	Controlled at 0.13 A
	170 to 186	Controlled at 0.25 A; recombiner thermocouple installed
Test 17	186 to 208	Calibrated while electrolyzing at 0.25 A using heater
Test 18	208 to 216	Calibrated while electrolyzing at 1.0 A using heater
	216 to 232	Controlled at 0.25 A
Pd14	232 to 238	Cycled and held at 0.25 A for 30 min and 2.8 A for 60 min
	238 to 258	Cycled and held at 0.40 A for 30 min and 2.8 A for 180 min
Pd15	258 to 267	Cycled and held at 1.0 A for 30 min and 2.8 A for 180 min
Pd16	267 to 270	Controlled at 2.0 A
	270 to 289	Cycled and held at 1.0 A for 30 min and 2.8 A for 180 min
Pd17	289 to 304	Controlled at 2.8 A
Test 20	304 to 312	Calibrated while electrolyzing at 1.0 A using heater
Pd18	312 to 331	Cycled and held at 0.5 A for 30 min and 2.8 A for 180 min
	331 to 332	Recombiner replaced; 6 ml D_2O added + 1.0 ml electrolyte; cathode in air
Test 21	332 to 337	Calibrated while electrolyzing at 0.5 A using heater; cell resistance dropped from 7.5 to 3 Ω; no bubbles
Pd19 and 20	337 to 381	Controlled at 20 V, ≈0.7 A; poor electrical contact in cell
	381 to 382	Cell opened and connection repaired; palladium washed with acetone, weighed, and placed in liquid nitrogen; 2 ml electrolyte added; new recombiner
Test 22	382 to 387	Calibrated while electrolyzing at 0.3 A using heater
Pd21	387 to 401	Cycled and held at 0.3 A for 30 min and 2.8 A for 180 min; bath controller failed; $T = 5°C$
	401 to 405	Electrical connection to anode broke; no bubbles; palladium washed with acetone,
	405	weighed, and placed in liquid nitrogen

(Continued)

TABLE III (Continued)

Data Set	Time (h)	Treatment
May 22, 1992		
The following changes were made in the cell:		
1. The exterior electrode was removed, and its electrical connector was attached to the anode. This caused the anode-cathode structure to be moved off center.		
2. The recombiner was placed on a platinum screen at the top of the gas space.		
3. The electrolyte was replaced.		
4. A platinum cathode was installed.		
Pt1		Calibration using normal electrolysis
Pt2		Calibration using internal heater
Pt3		Calibration using normal electrolysis
Pt4		Calibration using internal heater
Pt5		Cycled and held at 0.13 A for 30 min and 2.8 A for 180 min
May 25, 1992		
The palladium cathode was returned to cell, and the electrolyte was replaced.		
Cal1	477 to 482	Calibrated using internal heater + 0.13-A electrolysis
Pd22	482 to 505	Held at 0.13 A Cycled and held at 0.5 A for 30 min and 2.8 A for 180 min
Pd23	505 to 522	Held at 2.8 A
Pd24	522 to 543	Cycled and held at 1.0 A for 30 min and 2.8 A for 180 min

mode, it is not possible to know whether excess heat is being made at the other currents. This limitation is overcome by using a bivalue current mode that allows the calorimeter to stabilize before the current is again changed.

III.C. Excess Heat Production

A bivalue mode is used starting at 65.4 h with the times and upper current values listed in Table III. Once this mode is adopted, excess energy is observed, as shown in Fig. 11. An indication of excess power is first observed after 90 h, and this fluctuates between 0 and 2 W at 2.8 and 2.5 A throughout the study. No excess is observed at 2.0, 0.5, and 0.13 A.

Unfortunately, the cell is observed to lose fluid, and water begins to appear in the gas system at the external recombiner. Thus, at some time during this study, but after calibration, the recombiner within the cell has stopped recombining most of the released oxygen. The exact time is unknown because the temperature of the external recombiner was not yet being recorded. Consequently, the excess heat values are lower limits to the actual heat produced. The remaining energy leaves the cell as oxygen.

At 159 h, the cell is opened, and the recombiner is replaced. This operation requires that the cathode be exposed to air for ~47 min with a resulting slight loss of deuterium. After reassembly, the cell is calibrated, and the bivalue mode is resumed. The resulting excess heat is plotted in Fig. 12. After ~5 h, a small burst of heat is observed, followed by a steady increase over the next 55 h. A calibration using the immersion heater is run between 304 and 312 h while 1.0 A of current is applied to the cathode. Periodically, excess power measurements are made at various lower currents. Not only is the excess absent at 2.0 A and below, but these periodic interruptions do not seem to alter the steady rise once 2.8 A is resumed. At 295 h, the recombiner begins to fail again, and the measured excess power begins to decrease. This failure can be seen in the temperature rise at the external recombiner shown in Fig. 13. If no oxygen were being recombined in the cell at 330 h, 4.3 W (2.8 A × 1.54 V) would have to be added to the measured excess to give the actual value. When this is done, the value falls on the upward trend created by the earlier data. Thus, the upward trend in power generation apparently continues to the point when the cell is again turned off.

While excess power is being produced, the normal temperature gradient in the cell changes. Although the effect shown in Fig. 14 is rather scattered, the least-squares line suggests a trend toward an increase in the top temperature relative to the bottom as excess power increased. This trend is opposite to that found when electrolytic power is increased without the production of excess power, as shown by Figs. 15 and 8. Figure 15 shows the effect of applied power at currents below those producing excess power during this phase, while Fig. 8 shows the effect when platinum was used as the cathode. This difference suggests that the excess heat is originating from a different position in the cell than does electrolytic heat. This position is proposed to be the palladium cathode, a region that deposits its heat mainly at the top of the cell.

At 331 h, the cell is shut down again for 78 min to replace the recombiner. When the current is again turned on, a poor electrical connection is found within the cell. The cell is again opened, and the palladium is washed with acetone, weighed,

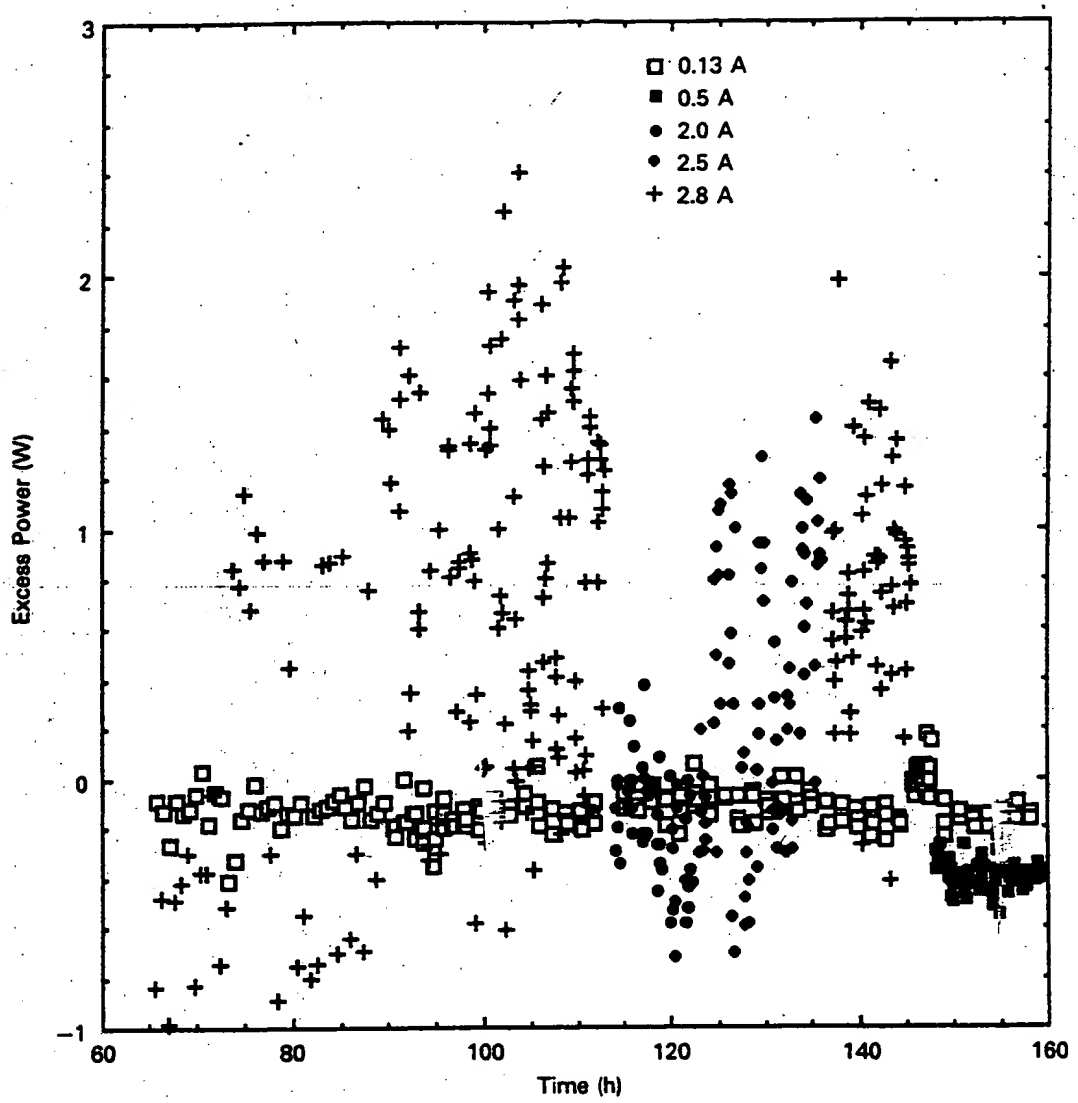

Fig. 11. Excess power for the high- and low-current modes as a function of time during phase 1. The current values are indicated.

and placed in liquid nitrogen. The D/Pd ratio is 0.818 based on the weight. At 382 h, the cell is assembled and calibrated using the immersion heater while electrolyzing at 0.3 A. A small excess power production resumes when the current is raised to 2.8 A, as shown in Fig. 16.

At 397 h, a sharp drop in room temperature causes failure of the bath temperature controller. The jacket temperature drops to ≈5°C, and any quantitative measure of excess heat is lost. At 401 h, electrical connection to the cathode breaks, and the metal is without charging current for 4 h. The D/Pd ratio drops to 0.73 based on the weight. The metal is placed in liquid nitrogen while repairs are made, calibrations are done, and palladium sample 2 is studied. Before palladium sample 1 is returned to the calorimeter, the lower halves of both sides are sanded with 600-grit SiC paper until bright. This material is studied for 314 h at various currents up to 3.5 A and at temperatures between 10 and 30°C. At the end of the study, the D/Pd ratio is 0.64, and most of the outgassing is occurring from the region that had been sanded. These efforts fail to show further excess heat production.

III.D. Excess Volume Measurement

When palladium loads with hydrogen, stresses that develop when the α phase converts to the β phase can introduce cracks and dislocations and cause excess volume. This excess volume reduces the ability of palladium to achieve an average, high D/Pd ratio.[29] A comparison between the physical volume measured before reacting with deuterium and a similar measurement when the D/Pd ratio is equal to 0.73 shows that the material is within 0.8% of the expected volume. The excess volume increases to 1.7% at D/Pd = 0.64 after the second part of the study using this palladium.

III.E. Initial Loading and Study of Palladium Sample 2

Initial loading is done at 0.020 A/cm^2. A small gas leak in the system, although corrected for, makes a measurement of the absolute D/Pd ratio somewhat uncertain. This problem has a less important effect on the shape of the loading curve. As can be seen in Fig. 17, the shape of the loading behavior is very different from that in palladium sample 1

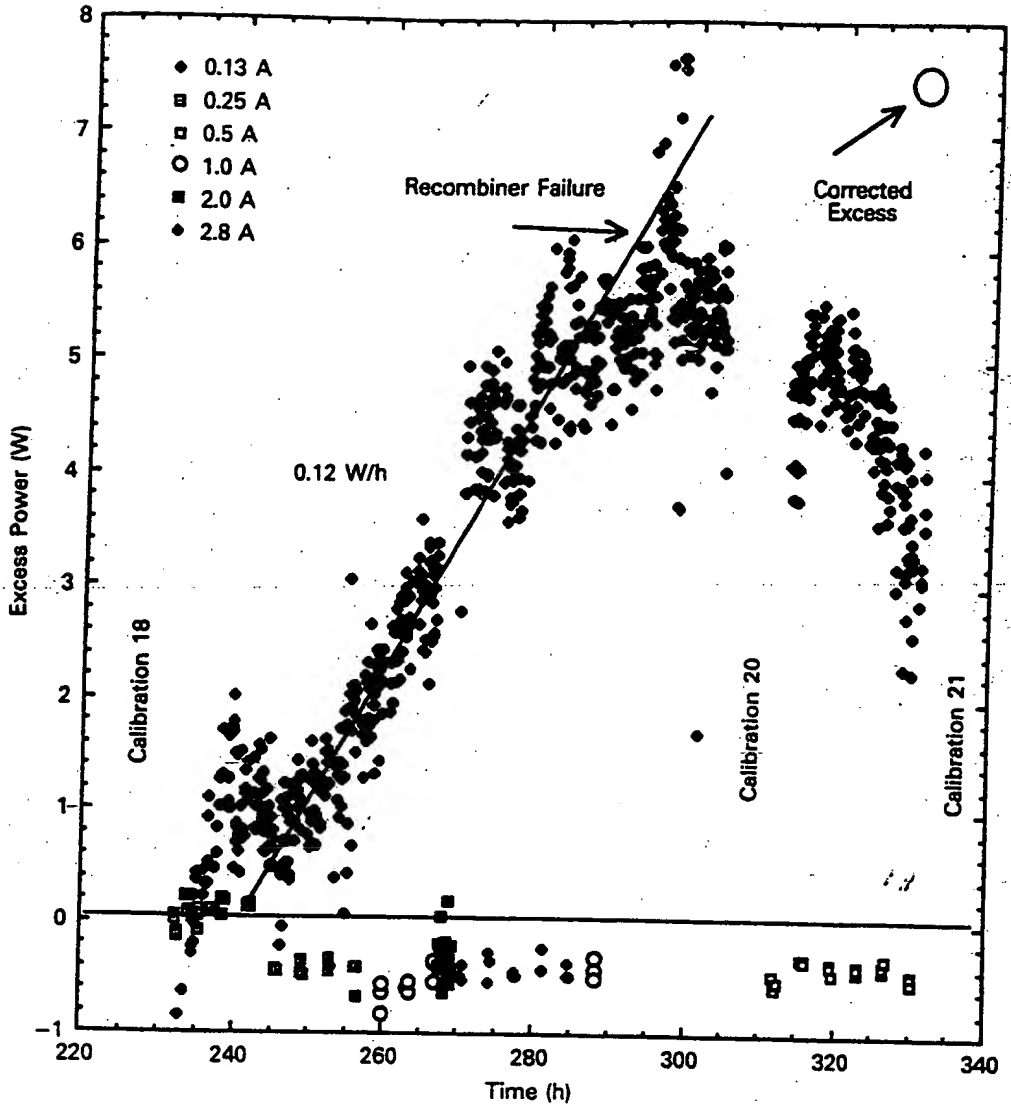

Fig. 12. Excess power at various cell currents during phase 2. The "corrected excess" value is the maximum excess power expected if the recombiner had worked properly.

(Fig. 9). This palladium was treated to charging conditions similar to those used for palladium sample 1. When no excess heat is observed during 76 h, the cell is opened, and the palladium is weighed. The D/Pd ratio, based on the weight, is 0.75.

A volume measurement shows that the palladium is 13.5% larger than expected based on the deuterium content.

IV. CONCLUSION

Two pieces of palladium sheet from different batches were studied. One produced excess power for a while, and the other did not.

Excess power has been produced in an electrolytic cell using palladium similar to that used by Takahashi. During the first 330 h of the study, excess power levels that reached ≈20% of applied power (≈7.5 W) were measured before the study had to be interrupted. This power increased with time while the palladium was electrolyzed at 0.42 A/cm^2. No measurable excess power was seen below 0.38 A/cm^2. This excess is ~75% of the amount expected at 0.42 A/cm^2 as proposed by Storms[30] based on a variety of calorimetric measurements.

The excess heat originated from a different position within the cell than did electrolytic heat. This position is proposed to be the palladium cathode. The palladium produced heat in spite of being exposed to air after loading with deuterium and being placed in liquid nitrogen for a short time and despite the electrolyte being saturated with CO_2. However, no excess was produced after deloading to D/Pd = 0.73. The bivalue mode of charging, as used by Takahashi, does not appear to be a requirement for continued heat production once production starts.

The palladium sheet that produced excess heat was loaded to D/Pd = 0.82, and the deuteride contained no significant excess volume. On the other hand, the palladium sheet that failed to show excess power was loaded to only D/Pd = 0.75 and had 13.5% excess volume. One explanation is that the second piece of palladium contained internal defects that

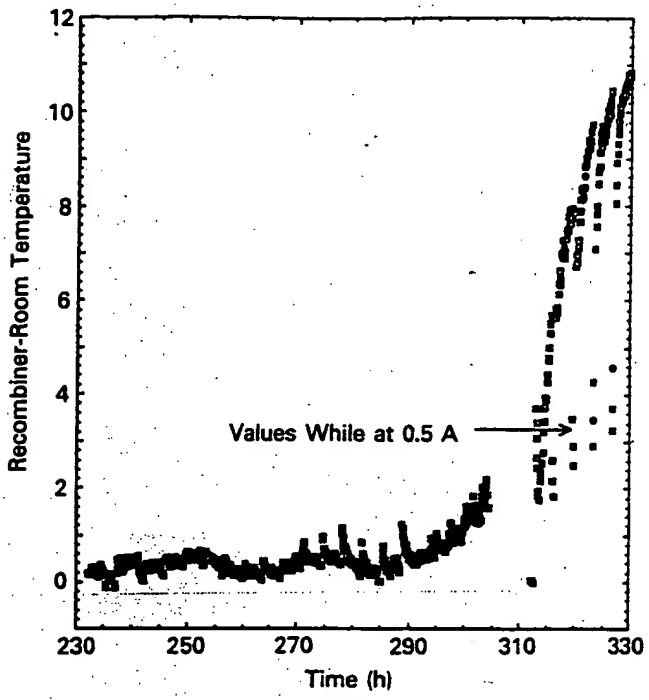

Fig. 13. Temperature difference between the external recombiner and room temperature as a function of time.

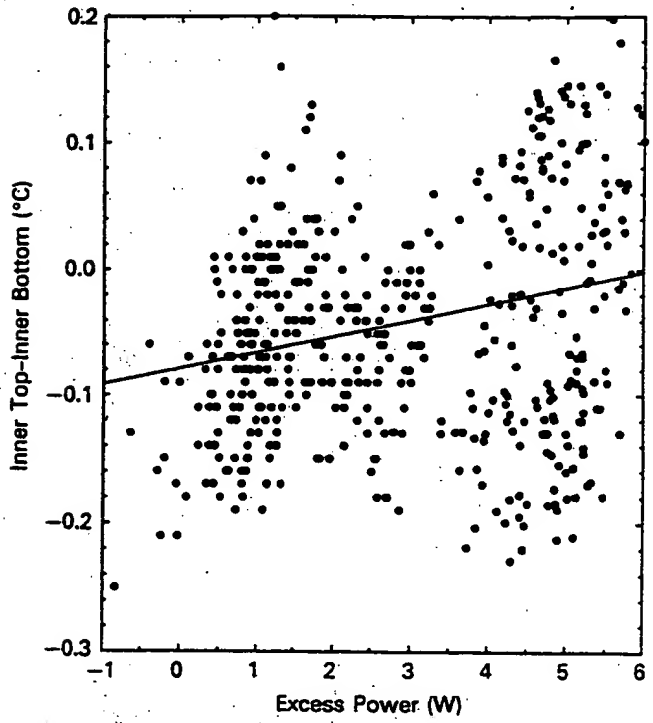

Fig. 14. Relationship between excess power and inner temperature gradient when 2.8 A (38.4 W) is applied. The line is a linear least-squares fit to the data.

caused the formation of cracks during loading with the result that a high D/Pd ratio could not be achieved. On the other hand, sanding of the first palladium sheet prevented high loading even though no significant excess volume was created.

It is generally agreed that the production of excess energy requires high local concentrations of deuterium. To achieve high concentrations, a high rate of deuterium dissolution at the surface must occur as well as a low rate of loss from the interior through escape paths. The ability to dissolve deuterium rapidly at the surface depends in part on using a high applied current, having the absence of certain impurities but the presence of others, and having a uniform current density. No matter how fast the deuterium is loaded into the palladium, if the deuterium can escape more rapidly from the interior, a high stoichiometry cannot be achieved. Escape paths form when defects or cracks are present in the metal or when the metal is cycled between the α and β phases. A routine measurement of the palladium volume during a study would help give a partial understanding of why some materials work and others do not.

Once electrolysis is started, a concentration gradient with respect to deuterium forms within the cathode. The magnitude of this gradient is determined by the relative competition among deuterium uptake, deuterium loss, and the diffusion constant. The diffusion constant is influenced by temperature and the dissolution of impurities such as lithium. The lower the temperature is, the smaller the diffusion constant and the steeper the gradient are. In any case, the highest concentration of deuterium must exist at the surface. Therefore, to the extent that the deuterium concentration is important, the heat-producing reaction will be localized at the surface. A greater fraction of the volume might become involved as electrolysis continues to raise more of the gradient above the critical composition, but this will be a slow process. Consequently, reporting heat production on the basis of the cathode volume not only conflicts with this expected behavior but also gives the false impression of a much higher heat-producing rate than was actually observed when the usual

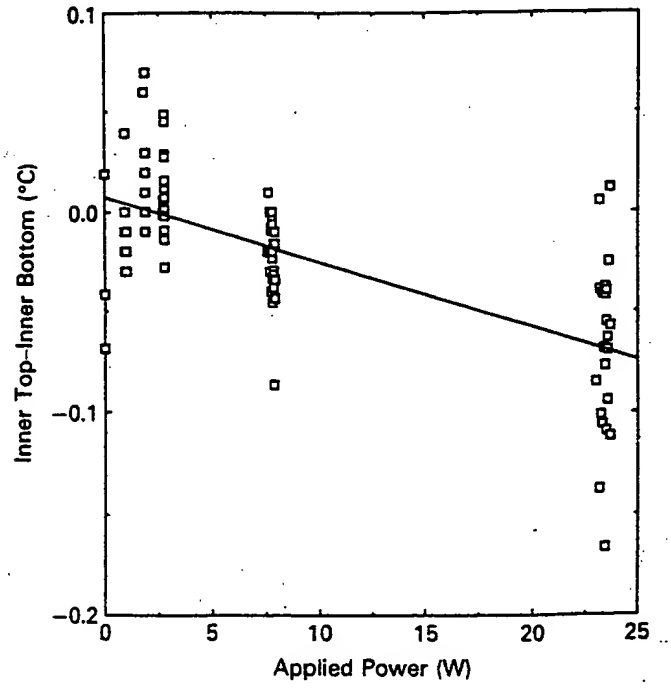

Fig. 15. Effect of applied power on the inner top and bottom temperature at power levels below where excess power is observed during phase 2.

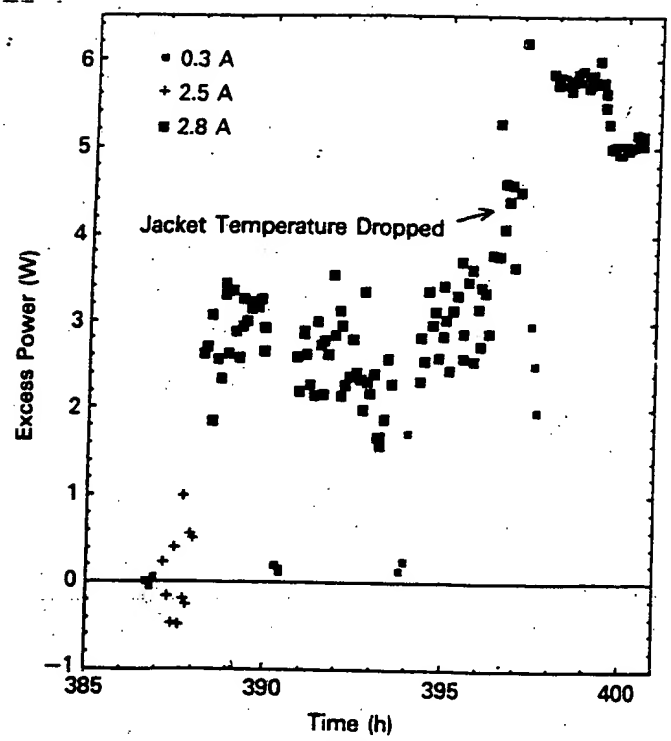

Fig. 16. Excess heat production during phase 3.

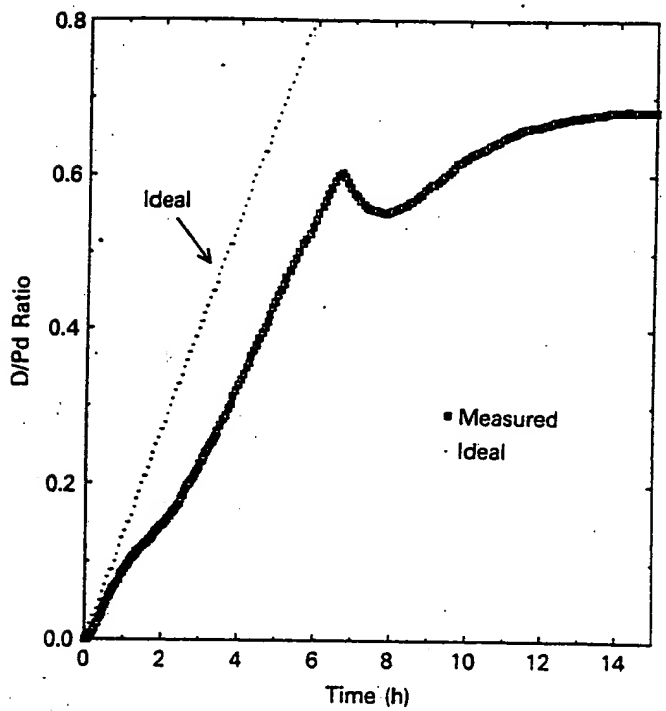

Fig. 17. Charging behavior of palladium sample 2. The ideal curve shows the expected D/Pd ratio if all deuterium produced by electrolysis were dissolved in the palladium.

small samples were used. Based on the thin film studies by Bush and Eagleton,[26] the reaction is within 5 μm of the surface, and the power densities are much higher than those reported using the total cathode volume.

Changes in heat production produced by changes in current cannot be attributed to the current change alone. When the current is changed, the applied power changes, and this causes the temperature of the cathode to change. In the calorimeter used here, a change in current from 0.02 to 0.4 A/cm^2 causes the temperature of the electrolyte to change by 10°C. While this does not appear to be a large amount, changes in the diffusion constant for deuterium or changes in the other processes that affect the chemical environment may be significant.

ACKNOWLEDGMENTS

The author wishes to thank D. Harbur and W. Stark for their open-minded support of this work, R. Logsdon for making the glass parts of the calorimeter, and R. Bush and R. Eagleton (California State Polytechnic University) for sharing their experience using a calorimeter of similar design.

REFERENCES

1. A. TAKAHASHI, T. IIDA, T. TAKEUCHI, and A. MEGA, "Excess Heat and Nuclear Products by D_2O Electrolysis and Multibody Fusion," submitted to *Appl. Electromag. Mater.* (1992).

2. M. FLEISCHMANN and S. PONS, "Electrochemically Induced Nuclear Fusion of Deuterium," *J. Electroanal. Chem.*, **261**, 301 (1989); see also M. FLEISCHMANN and S. PONS, Errata, *J. Electroanal. Chem.*, **263**, 187 (1989); see also S. PONS and M. FLEISCHMANN, "Calorimetric Measurements of the Palladium/Deuterium System: Fact and Fiction," *Fusion Technol.*, **17**, 669 (1990); see also S. PONS and M. FLEISCHMANN, "Calorimetry of Palladium-Deuterium Systems," *Proc. 1st Annual Conf. Cold Fusion*, Salt Lake City, Utah, March 28–31, 1990, p. 1, National Cold Fusion Institute (1990); see also M. FLEISCHMANN, S. PONS, M. W. ANDERSON, L. J. LI, and M. HAWKINS, "Calorimetry of the Palladium-Heavy Water System," *J. Electroanal. Chem.*, **298**, 293 (1990); see also S. PONS and M. FLEISCHMANN, "The Calorimetry of Electrode Reactions and Measurements of Excess Enthalpy Generation in the Electrolysis of D_2O Using Pd-Based Electrodes," *Proc. 2nd Annual Conf. Cold Fusion*, Como, Italy, June 29–July 4, 1991, p. 349.

3. L. L. ZAHM, A. C. KLEIN, S. E. BINNEY, J. N. REYES, Jr., J. F. HIGGINBOTHAM, and A. H. ROBINSON, "Experimental Investigations of the Electrolysis of D_2O Using Palladium Cathodes and Platinum Anodes," *J. Electroanal. Chem.*, **281**, 313 (1990); see also A. C. KLEIN et al., "Anomalous Heat Output from Pd Cathodes without Detectable Nuclear Products," *Proc. Anomalous Nuclear Effects in Deuterium/Solid Systems*, Provo, Utah, October 22–23 1990.

4. M. C. H. McKUBRE, R. C. ROCHA-FILHO, S. SMEDLEY, F. TANZELLA, J. CHAO, B. CHEXAL, T. PASSELL, and J. SANTUCCI, "Calorimetry and Electrochemistry in the D/Pd System," *Proc. 1st Annual Conf. Cold Fusion*, Salt Lake City, Utah, March 28–31, 1990, p. 20, National Cold Fusion Institute (1990); see also J. CHAO, W. LAYMEN, C. M. KANG, T. GUR, M. SCHREIBER, R. HUGGINS, G. LUCIER, and J. FERRANTE, "Three-Dimensional Computer Simulation of an Isoperibolic Calorimeter for Cold Fusion Experiments," *Proc. 1st Annual Conf. Cold Fusion*, Salt Lake City, Utah, March 28–31, 1990, p. 308, National Cold Fusion Institute (1990); see also M. C. H. McKUBRE, R. ROCHA-FILHO, S. T. SMEDLEY, F. L. TANZELLA, S. CROUCH-BAKER, T. O. PASSELL, and J. SANTUCCI, "Isothermal Flow Calorimetric Investigations of the D/Pd System," *Proc. 2nd Annual Conf. Cold Fusion*, Como, Italy, June 29–July 4, 1991, p. 349.

5. A. J. APPLEBY, Y. J. KIM, O. J. MURPHY, and S. SRINIVASAN, "Anomalous Calorimetric Results During Long-Term Evolution of Deuterium on Palladium from Alkaline Deuteroxide Electrolyte," *Proc. 1st Annual Conf. Cold Fusion*, Salt Lake City, Utah, March 28–31, 1990, p. 32, National Cold Fusion Institute (1990); see also S. SRINIVASAN, Y. J. KIM, O. J. MURPHY, C. R. MARTIN, and A. J. APPLEBY, "Evidence for Excess Heat Generation Rates During Electrolysis of D_2O in LiOD Using a Palladium Cathode: A Microcalorimetric Study," presented at Workshop on Cold Fusion Phenomena, Santa Fe, New Mexico, May 23–25, 1989, LA-11686-C, Los Alamos National Laboratory (1989).

6. D. P. HUTCHINSON, C. A. BENNETT, R. K. RICHARDS, J. BULLOCK IV, and G. L. POWELL, "Initial Calorimetry Experiments in the Physics Division at ORNL," *Proc. 1st Annual Conf. Cold Fusion*, Salt Lake City, Utah, March 28–31, 1990, National Cold Fusion Institute (1990); see also ORNL/TM-11356 and #Y/DZ-490, Oak Ridge National Laboratory; see also G. L. POWELL, J. S. BULLOCK IV, R. L. HALLMAN, P. J. HORTON, and D. P. HUTCHINSON, "The Preparation of Palladium for Cold Fusion Experiments," *J. Fusion Energy*, **9**, 355 (1990).

7. M. SCHREIBER, T. M. GUR, G. LUCIER, J. A. FERRANTE, J. CHAO and R. A. HUGGINS, "Recent Measurements of Excess Energy Production in Electrochemical Cells Containing Heavy Water and Palladium," *Proc. 1st Annual Conf. Cold Fusion*, Salt Lake City, Utah, March 28–31, 1990, p. 44, National Cold Fusion Institute (1990); see also M. SCHREIBER, T. M. GUR, G. LUCIER, J. A. FERRANTE, and R. A. HUGGINS, "Recent Experimental Results on the Thermal Behavior of Electrochemical Cells in the Hydrogen-Palladium and Deuterium-Palladium Systems," *Proc. Cold Fusion Symp., 8th World Hydrogen Energy Conf.*, Honolulu, Hawaii, July 22–27, 1990, p. 71, University of Hawaii; see also T. M. GUR, M. SCHREIBER, G. LUCIER, J. A. FERRANTE, J. CHAO, and R. A. HUGGINS, "Experimental Considerations in Electrochemical Isoperibolic Calorimetry," *Proc. 1st Annual Conf. Cold Fusion*, Salt Lake City, Utah, March 28–31, 1990, p. 82, National Cold Fusion Institute (1990); see also A. BELZNER, U. BISCHLER, S. CROUCH-BAKER, T. M. GUR, M. SCHREIBER, and R. A. HUGGINS, "Two Fast Mixed Conductor Systems: Deuterium and Hydrogen and Palladium—Thermal Measurements and Experimental Considerations," presented at Workshop on Cold Fusion Phenomena, Santa Fe, New Mexico, May 23–25, 1989, and published in LA-11686-C, Los Alamos National Laboratory (1989), *J. Fusion Energy*, **9**, 219 (1990), and *Solid State Ionics*, **40/41**, 519 (1990).

8. C. D. SCOTT, J. E. MROCHEK, T. C. SCOTT, G. E. MICHAELS, E. NEWMAN, and M. PETEK, "Measurement of Excess Heat and Apparent Coincident Increases in the Neutron and Gamma-Ray Count Rates During the Electrolysis of Heavy Water," *Fusion Technol.*, **18**, 103 (1990); see also C. D. SCOTT, J. E. MROCHEK, T. C. SCOTT, G. E. MICHAELS, E. NEWMAN, and M. PETEK, "Initiation of Excess Power and Possible Products of Nuclear Interactions During the Electrolysis of Heavy Water," *Proc. 1st Annual Conf. Cold Fusion*, Salt Lake City, Utah, March 28–31, 1990, p. 164, National Cold Fusion Institute (1990) and TM-11322, Oak Ridge National Laboratory; see also C. D. SCOTT, E. GREENBAUM, G. E. MICHAELS, J. E. MROCHEK, E. NEWMAN, M. PETEK, and T. C. SCOTT, "Preliminary Investigation of Possible Low Temperature Fusion," presented at Workshop on Cold Fusion Phenomena, Santa Fe, New Mexico, May 23–25, 1989, and published in LA-11686-C, Los Alamos National Laboratory (1989), and *J. Fusion Energy*, **9**, 115 (1990).

9. L. J. DROEGE and T. F. DROEGE, "A Zero Gradient Calorimeter for the Measurement of Anomalous Heat from the Electrolysis of Deuterated Metals," *Proc. 1st Annual Conf. Cold Fusion*, Salt Lake City, Utah, March 28–31, 1990, p. 229, National Cold Fusion Institute (1990); see also T. F. DROEGE, "A Discussion of an H_2O Run Which Followed Operation with D_2O," SMATN-90-2, Environmental Optics Corporation, Batavia, Illinois (Apr. 1990).

10. D. GOZZI, P.L. CIGNINI, L. PETRUCCI, M. TOMELLINI, and G. DE MARIA, "Evidences for Associated Heat Generation and Nuclear Products Release in Palladium Heavy-Water Electrolysis," presented at Workshop on Cold Fusion Phenomena, Santa Fe, New Mexico, May 23–25, 1989, and published in LA-11686-C, Los Alamos National Laboratory (1989), and *Nuovo Cimento*, **103**, 143 (1990); see also D. GOZZI, P. L. CIGNINI, L. PETRUCCI, M. TOMELLINI, G. DE MARIA, S. FRULLANI, F. GARIBALDI, F. GHIO, M. JODICE, and E. TABET, "Nuclear and Thermal Effects During Electrolytic Reduction of Deuterium at Palladium Cathode," *J. Fusion Energy*, **9**, 241 (1990); see also D. GOZZI, P. L. CIGNINI, and M. TOMELLINI, "Multicell Experiments for Searching Time-Related Events in Cold Fusion," *Proc. 2nd Annual Conf. Cold Fusion*, Como, Italy, June 29–July 4, 1991, p. 21.

11. R. C. KAINTHLA, O. A. VELEV, L. KABA, G. H. LIN, N. PACKHAM, J. BOCKRIS, M. SKLARZYK, and J. WASS, "Sporadic Observation of the Fleischmann-Pons Effect," *Electrochim. Acta*, **34**, 1315 (1989); see also O. A. VELEV and R. C. KAINTHLA, "Heat Flow Calorimeter with a Personal-Computer-Based Data Acquisition System," *Fusion Technol.*, **18**, 351 (1990).

12. R. T. BUSH, "Cold 'Fusion': The Transmission Resonance Model Fits Data on Excess Heat, Predicts Optimal 'Trigger' Points, and Suggests Nuclear-Reaction Scenarios," *Fusion Technol.*, **19**, 313 (1991); see also R. T. BUSH, "The TRM (Transmission Resonance Model) for Cold 'Fusion' Fits Calorimetric Data on the Pons-Fleischmann Effect and Suggests Solutions to Nuclear 'Anomalies,'" *Proc. Cold Fusion Symp., 8th World Hydrogen Energy Conf.*, Honolulu, Hawaii, July 22–27, 1990, University of Hawaii; see also R. D. EAGLETON and R. T. BUSH, "Design Considerations on Electrodes as Suggested by a Deuterium Cluster Model for Cold Nuclear Fusion," *J. Fusion Energy*, **9**, 359 (1990); see also R. T. BUSH and R. D. EAGLETON, "'Cold Nuclear Fusion': A Hypothetical Model to Probe an Elusive Phenomenon," *J. Fusion Energy*, **9**, 397 (1990).

13. B. Y. LIAW, P.-L. TAO, P. TURNER, and B. E. LIEBERT, "Elevation Temperature Excess Heat Production Using Molten Salt Electrochemical Techniques," *Proc. Cold Fusion Symp., 8th World Hydrogen Energy Conf.*, Honolulu, Hawaii, July 22–27, 1990, University of Hawaii; see also B. Y. LIAW, P.-L. TAO, P. TURNER, and B. E. LIEBERT, "Elevated-Temperature Excess Heat Production in a Pd-D System," *J. Electroanal. Chem.*, **319**,161 (1991); see also B. Y. LIAW, P.-L. TAO, and B. E. LIEBERT, "Recent Progress on Cold Fusion Research Using Molten Salt Techniques," *Proc. 2nd Annual Conf. Cold Fusion*, Como, Italy, June 29–July 4, 1991, p. 55.

14. C. S. YANG, C. Y. LIANG, T. P. PERNG, L. J. YUAN, C. M. WAN, and C. C. WAN, "Observations of Excess Heat and Tritium on Electrolysis of D_2O," *Proc. Cold Fusion Symp., 8th World Hydrogen Energy Conf.*, Honolulu, Hawaii, July 22–27, 1990, p. 95, University of Hawaii.

15. A. B. KARABUT, Ya. R. KUCHEROV, and I. B. SAVATIMOVA, "Cold Fusion Observations at Gas-Discharge Device Cathode," presented at Specialists' Conf. Nuclear Power Engineering in Space, Obninsk, USSR, May 15–19, 1990.

16. V. C. NONINSKI and C. I. NONINSKI, "Determination of the Excess Energy Obtained During the Electrolysis of Heavy Water," *Fusion Technol.*, **19**, 364 (1991).

17. R. A. ORIANI, J. C. NELSON, S. LEE, and J. H. BROADHURST, "Calorimetric Measurements of Excess Power Output During the Cathodic Charging of Deuterium into Palladium," *Fusion Technol.*, **18**, 652 (1990).

18. K. S. V. SANTHANAM, J. RANGARAJAN, O'N. BRAGANZA, S. K. HARAM, N. M. LIMAYE, and K. C. MANDAL, "Electrochemically Initiated Cold Fusion of Deuterium," *Indian J. Technol.*, **27**, 175 (1989).

19. M. H. MILES, K. H. PARK, and D. E. STILWELL, "Electrochemical Calorimetric Evidence for Cold Fusion in the Palladium-Deuterium System," *J. Electroanal. Chem.*, **296**, 241 (1990); see also B. F. BUSH, J. J. LAGOWSKI, M. H. MILES, and G. S. OSTROM, "Helium Production During the Electrolysis of D_2O in Cold Fusion," *J. Electroanal. Chem.*, **304**, 271 (1991); see also M. H. MILES, B. F. BUSH, G. S. OSTROM, and J. J. LAGOWSKI, "Heat and Helium Productions in Cold Fusion Experiments," *Proc. 2nd Annual Conf. Cold Fusion*, Como, Italy, June 29–July 4, 1991, p. 363.

20. Y. ARATA and Y. ZHANG, "Achievement of an Intense Cold Fusion Reaction," *Fusion Technol.*, **18**, 95 (1990), and *Proc. Jpn. Acad. B*, **66**, 1 (1990); see also Y. ARATA and Y. ZHANG, "Cold Fusion Caused by a Weak 'On-Off' Effect," *Proc. Jpn. Acad. B*, **66**, 33 (1990).

21. D. LEWIS and K. SKÖLD, "A Phenomenological Study of the Fleischmann-Pons Effect," *J. Electroanal. Chem.*, **294**, 275 (1990).

22. S. GURUSWAMY and M. E. WADSWORTH, "Metallurgical Aspects in Cold Fusion Experiments," *Proc. 1st Annual Conf. Cold Fusion*, Salt Lake City, Utah, March 28–31, 1990, p. 314, National Cold Fusion Institute (1990).

23. S. SZPAK, P. A. MOSIER-BOSS, and J. J. SMITH, "On the Behavior of Pd Deposited in the Presence of Evolving Deuterium," *J. Electroanal. Chem.*, **302**, 255 (1991).

24. N. HUANG, Q. H. GAO, B. Y. LIAW, and B. E. LIEBERT, "A Flow Calorimeter Used in Duplication of 'Cold Fusion,'" presented at Special Session Cold Fusion, Electrochemical Society Mtg., Hollywood, Florida, October 20, 1989.

25. R. D. EAGLETON and R. T. BUSH, "Calorimetric Experiments Supporting the Transmission Resonance Model for Cold Fusion," *Fusion Technol.*, **20**, 239 (1991).

26. R. T. BUSH, "Excess Heat Production from a Cold Fusion Cell Using a Cathode of Silver Coated with a Thin Layer of Palladium," California State Polytechnic University, Private Communication (1991).

27. H. IKEGAMI, "Cold Fusion Research in Japan," *Proc. 2nd Annual Conf. Cold Fusion*, Como, Italy, June 29–July 4, 1991, p. 297.

28. F. G. WILL, K. CEDZYNSKA, M.-C. YANG, J. R. PETERSON, J. E. BERGESON, S. C. BARROWES, W. J. WEST, and D. C. LINTON, "Studies of Electrolytic and Gas Phase Loading of Palladium with Deuterium," *Proc. 2nd Annual Conf. Cold Fusion*, Como, Italy, June 29–July 4, 1991, p. 297.

29. E. STORMS and C. TALCOTT-STORMS, "The Effect of Hydriding on the Physical Structure of Palladium and on the Release of Contained Tritium," *Proc. Anomalous Nuclear Effects in Deuterium/Solid Systems*, Provo, Utah, October 22–23, 1990 and *Fusion Technol.*, **20**, 246 (1991).

30. E. STORMS, "Review of Experimental Observations About the Cold Fusion Effect," *Fusion Technol.*, **20**, 433 (1991).

OBSERVATION OF ANOMALOUS NUCLEAR EFFECTS IN D_2-Pd SYSTEM

Yasuhiro Iwamura, Takehiko Itoh and Ichiro Toyoda

Advanced Technology Research Center,
Mitsubishi Heavy Industries, Ltd.
1-8-1, Sachiura, Kanazawa-ku, Yokohama, 236, Japan
81-45-771-1316

ABSTRACT

Gas loading experiments have been performed with a method of heating deuterated palladium metals in a vacuum chamber to induce anomalous nuclear effects. Neutron emissions and tritium productions were observed in some cases when deuterium gas was released from the deuterated palladium samples with heating. It shows anomalous and unexpected phenomena occur in D_2-Pd system as reported in many papers on cold fusion.

I. INTRODUCTION

Research on cold fusion began in 1989 with the announcement of Dr. Fleishman and Pons[1]. Since cold fusion phenomena have possibility of being a new energy technology, considerable efforts have been paid to confirm their experimental results that nuclear reactions are electrochemically induced in D_2-Pd system[2-4]. However, we still have much uncertainty on the nature of cold fusion phenomena.

The authors started the research on cold fusion from the begging of 1993, in order to clarify the nature of cold fusion phenomena and investigate its potentiality as a new energy source. In this paper, we performed gas loading type experiments in D_2-Pd system, and could observe neutron and tritium production several times.

II. EXPERIMENTAL METHODS

A. Preparation of Deuterated Palladium

Palladium samples loaded with deuterium gas were prepared as follows. Palladium sheets (25x25x1mm; Tanaka Kikinzoku Kogyo K.K.) were washed with acetone in a supersonic cleaning device and heated in th air at 573K for an hour to remove organic contaminan from the surface. After that, we cooled down the sample to room temperature (~ 298K) in deuterium gas. Afte loading (D/Pd ~ 0.66), we kept the deuterated palladiur samples in liquid nitrogen temperature (77K) for seve:a hours. Usually it takes more than a week to fir's loading. We estimate a loading ratio (D/Pd) by measur a mass change of a palladium sample caused by absorptio of deuterium gas. Loading ratio we obtain in 1 atm i about 0.66. The samples were bring back to roon temperature environment, and then gold or aluminum thin film was vapor deposited onto both surfaces of th deuterated palladium in order to reduce the rate o deuterium gas release. We tried many kinds of pre treatment methods. Some samples were heated in the ai at 900K for two hours and were quenched in pure wate instead of cooling the samples in liquid nitrogen.

B. Experimental System

The sample is introduced into a vacuum chamber an set on a heater located in it. Figure 1 shows a schemati view of experimental devices. The chamber is equippe with two He-3 neutron detectors (EG&G Ortec: RS-P4 0803-235), a NaI scintillation counter (Bicron: 2M2/2) fo gamma-ray spectroscopy, a silicon surface barrier detecto (EG&G Ortec: CU-020-450-300) for charged particl spectroscopy and a high-resolution quadrupole mas spectrometer (Ulvac: HIRESOM-2SM) for gas analysis.

Neutron detectors surrounded with polyethylen modulators are used only for neutron counting. Countin system consists of preamplifiers (EG&G Ortec 142PC) amplifier and single channel analyzers (EG&G Ortec 590A) and counters (EG&G Ortec 996) which ar connected to a personal computer by GPIB interface. A to gamma-ray spectroscopy system, we use a preamplifier

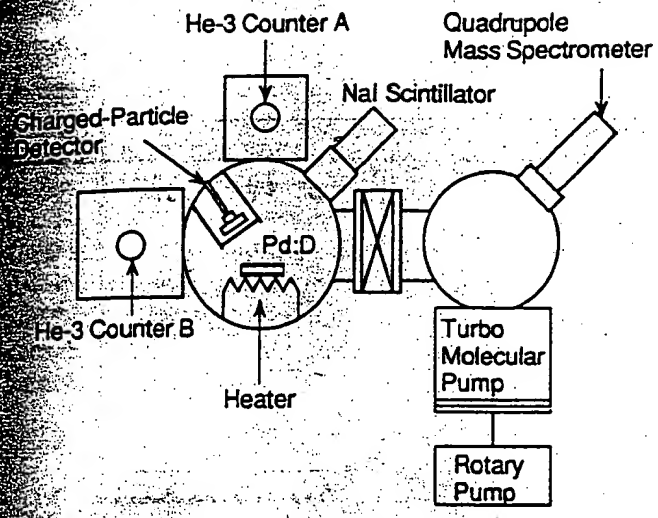

Figure 1 Schematic View of Experimental Devices

(EG&G Ortec : 276), an amplifier (EG&G Ortec : 575A) and a multi-channel analyzer (SEIKO EG&G : MCA4100, 4200). Charged particle spectroscopy system consists of a preamplifier (EG&G Ortec : 142B), an amplifier (EG&G Ortec : 570) and a multi-channel analyzer (SEIKO EG&G MCA4100, 4200).

All these devices are located in a clean-room where temperature and humidity are always controlled at constant levels (23°C±1°C, 40%±5%) in order to prevent contamination and false counts induced by humidity in the air. We always monitor electrical signals from these detectors by digital storage oscilloscopes to confirm that the signals originate from true nuclear events.

C. Experimental Procedure

As a way to induce anomalous nuclear effects, we heat the sample and make deuterium in the palladium metal released out. The reason is that the authors consider that anomalous nuclear effects occur in deuterium diffusion process or recombination process on the surface. If we heat the deuterated palladium sample kept at room temperature up to about 400K, deuterium atoms contained in the palladium metal move toward the gold or aluminum thin-film surfaces of the sample and then release out as deuterium gas. We observed neutron, tritium and charged particle emissions several times during deuterium gas desorption from the samples by heating.

Experimental procedure is as follows.

(1) Pre-treatment of a palladium sample (washing and annealing)
(2) Loading
(3) Calculation of D/Pd ratio
(4) Surface modification (gold or aluminum vapor deposition)
(5) Set the deuterated sample into the vacuum chamber.
(6) Evacuating the chamber (~10^{-6} Torr)
(7) Begin to measure neutron, gamma-ray, charged particle, pressure in the chamber, temperature of the heater and start up the quadrupole mass spectrometer
(8) Heating the sample up to 400K
(9) Observation
(10) Heater off

III. RESULTS AND DISCUSSION

A. Neutron Emission

Figure 2 shows an example of experimental results on neutron emission. This sample has gold thin film on it, and D/Pd is 0.66. In this experiment, we had only a single neutron counting line.

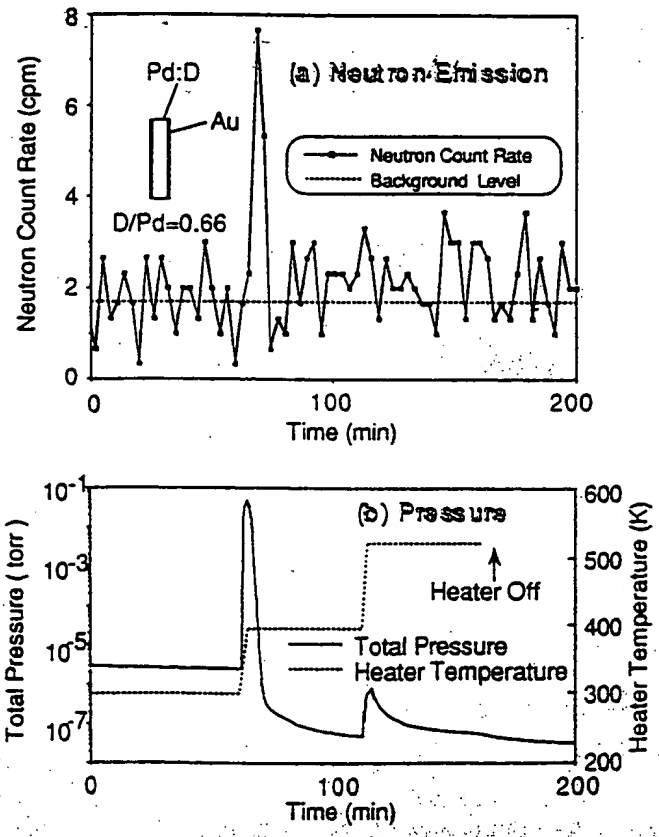

Figure 2 Neutron Emission

At the beginning, heater temperature equals to room temperature, then we can see only background neutron counting. With heating the sample up to 400K, we can see in Fig.(b) that total pressure in the vacuum chamber increases and decreases rapidly. Simultaneously a clear and prominent neutron emission peak is observed as shown in Fig.(a). After heating up to 520K, we cannot see any peak in Fig.(b). It is considered that in the case of heating up to 520K, the release rate of deuterium gas, which is closely related with diffusion process of deuterium atom in palladium lattice and recombination process on the sample surface, is not adequate to induce neutron emission. However, the reason why neutron emission occurs is not clear. The emission rate is estimated $4.0X10^{2}$ (neutron/sec) by using a Cf-252 calibration source, and that corresponds to the rate of $3.0X10^{-20}$ (event/sec/d-d pair).

B. Tritium Production

An experimental result of mass spectrometric analysis of released gas from a sample is shown in Fig.3. D/Pd of this sample with gold thin film is 0.65. Since the resolution (M/DM) of this measurement is low (M/DM=60M), both signals shown in this figure are composed of DT(5.030 amu) and DDH(5.036 amu). The signal for mass number 5 (DT+DDH) after heating reaches about 6 times as large as loading D2 gas.

In order to distinguish DT signal from DDH, the released gas from the sample and D_2 gas used for loading were analyzed with high resolution(M/DM=250M). Figure 4 shows a result of the high resolution measurement. Mass difference between the peak for released gas and the peak for loading gas is 0.006 amu. These peaks for released and loading gas correspond to DT and DDH, respectively. We can see that DT signal was about 50 times as large as DDH signal. Therefore it demonstrates that DT is dominant in the released gas around mass number 5. We can say that certain tritium production mechanism exits in our experimental process.

It is possible to consider that signal of mass number 5 after heating in Fig.3 is also attributed to DT. Although we can distinguish DT from DDH by high resolution operation, there is a demerit that we lose sensitivity instead of obtaining high resolution. Therefore we chose to monitor mass number 5 with low resolution and high sensitivity, since the sensitivity was important for measurement of time evolution of DT.

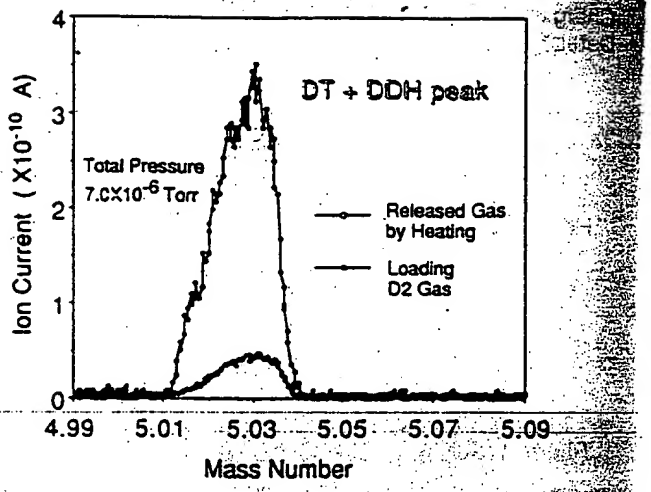

Figure 3 Mass Spectrum for Released Gas

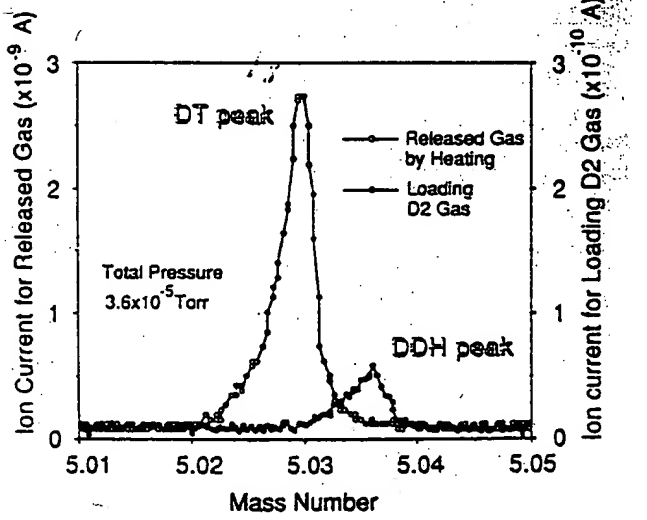

Figure 4 Separation of DT and DDH

C. Neutron and tritium production

An experimental result on neutron and tritium production with time evolution of total pressure in the vacuum chamber is shown in Fig.5. The atomic ratio D/Pd of this sample, which has aluminum thin film, is 0.66.

Two independent He-3 counters are used to improve neutron counting reliability. Concerning tritium production, we measured only peak value of the signal for mass number 5 detected by the mass spectrometer. We define DT+DDH breeding ratio as shown in the figure, and it is normalized by the measured value of loading D_2 gas. If DT+DDH breeding ratio is larger than 1.0, it means that the released gas from the sample contains more DT and DDH than D2 gas used for loading. Furthermore, it is considered that most of the released gas consists of DT as we described before.

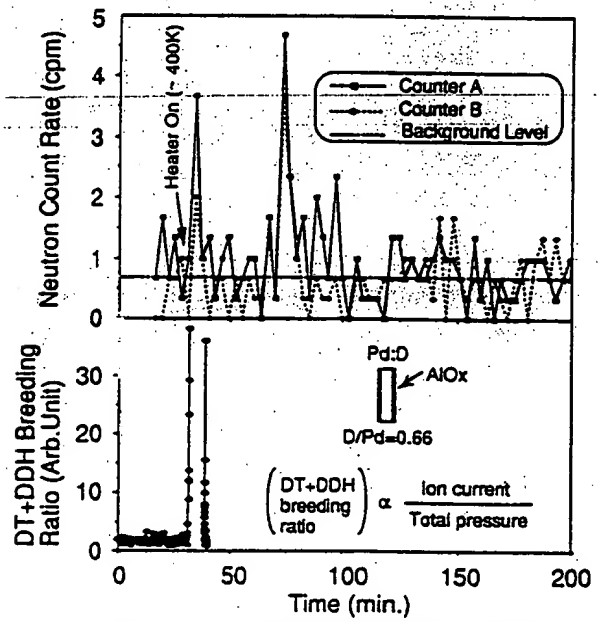

(i) Time vs. Neutron and Tritium production

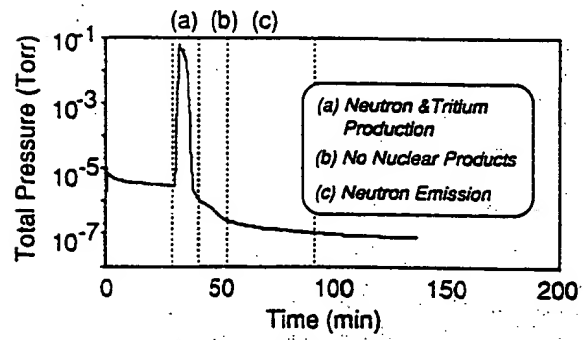

(ii) Time vs. Total Pressure in Vacuum Chamber

Figure 5 Neutron and Tritium Production

After heating the sample up to 400K, we can see sudden increases of total pressure, neutron count rate and DT+DDH breeding ratio simultaneously.
It shows that both neutron and tritium are generated with deuterium gas release from the sample. Coincidence of neutron and tritium production with deuterium gas release has been observed several times.

A larger neutron emission peak can be seen after about 40 minutes of the first neutron emission. We also experienced to observe similar phenomena in the other samples. The authors consider that these phenomena are related with the diffusion process of deuterium atom, since the time for diffusion through 1mm thick palladium metal at 400K is about several ten minutes[5-6] and it corresponds to the delay time of the second neutron emission.

D. The other Nuclear Products

Up to the present, gamma-rays which would emitted from deuterated palladium samples have never been detected. However, we observed charged particle spectra several times during deuterium gas release from some quenched samples covered with aluminum thin-film. Mass number of charged particles can not be specified at present, since only one detector for charged particle is available. Therefore the authors will show the spectra after specifying what type of charged particles are produced in the samples.

E. Reproducibility

Reproducibility on neutron emission and tritium production is summarized in the table 1.The number of total samples is about 50. Criteria for neutron emission and tritium production are also shown in the table. We experienced that some deuterated palladium samples did not show any nuclear effects with the same experimental procedure. It suggests that the nuclear effects we observed depend on the hidden condition of the sample.

With regard to neutron emission, only 15% of total samples emitted statistically significant neutrons if we choose the criteria shown in the table. Reproducibility of tritium production is better than neutron emission, however, it is desirable to measure DT gas only by β-ray counting to decide quantitative tritium production rate. It is a next work to be done.

Table 1 Reproducibility

	Neutron	Tritium
A	6%	3%
B	9%	60%
C	85%	37%

Criteria	Neutron emission statistical significance	DT+DDH Breeding Ratio
A	$>5\sigma$	$>10^2$
B	3σ–5σ	$10 \sim 10^2$
C	$< 3\sigma$	<10

Reproducibility of our experiments is not good as it is shown in the table. Since the nature of cold fusion phenomena is still unclear, we cannot control macroscopic experimental factors in order to cause anomalous nuclear effects that must be dominated by uncertain microscopic factors. It is necessary to investigate much more about cold fusion phenomena to establish this new field of science.

IV. CONCLUSION

We heated deuterated palladium metals in the vacuum chamber and made deuterium gas in the samples released out, assuming that anomalous nuclear effects occur in deuterium diffusion process or recombination process on the surface. As a result of it, neutron emission and tritium production induced by deuterium gas release have been observed several times. Coincident neutron emission with tritium production has been also observed. However, reproducibility of our experiments is not good at present. It is considered that these anomalous nuclear effects in D_2-Pd system are attributed to cold fusion phenomena reported in many papers.

REFERENCES

1. M. Fleishmann and S. Pons, *J.Electroanal. Chem.* **261**, 301 (1989).
2. A. Takahashi et al., *Int. J. Appl. Electromag. Materials*, **106**,1 (1992).
3. J. Kasagi et al., *Proc. of ICCF-3*, Nagoya, 209 (1993).
4. E. Yamaguchi and T. Nishioka, *Proc. of ICCF-3*, Nagoya, 179 (1993).
5. F. A. Lewis, *The Palladium Hydrogen System*, Academic Press (1967).
6. Y. Fukai, *The Metal-Hydrogen System*, Springer-Verlag (1993).

OMB No. 0704-0188

1. AGENCY USE ONLY *(Leave blank)*	2. REPORT DATE	3. REPORT TYPE AND DATES COVERED
	September 1996	Final, Jan 92-Sep 95

4. TITLE AND SUBTITLE

Anomalous Effects in Deuterated Systems

5. FUNDING NUMBERS

PE 061153N
Project R1306
R&T Project Code
313z001srp06

6. AUTHORS

Melvin H. Miles, Benjamin F. Bush, and Kendall B. Johnson

7. PERFORMING ORGANIZATION NAME(S) AND ADDRESS(ES)

Naval Air Warfare Center Weapons Division
China Lake, CA 93555-6100

8. PERFORMING ORGANIZATION REPORT NUMBER

NAWCWPNS TP 8302

9. SPONSORING/MONITORING AGENCY NAMES(S) AND ADDRESS(ES)

Office of Naval Research
800 North Quincy
Arlington, VA 22207-5660

10. SPONSORING/MONITORING AGENCY REPORT NUMBER

11. SUPPLEMENTARY NOTES

12a. DISTRIBUTION /AVAILABILITY STATEMENT

A Statement; public release; distribution unlimited.

12b. DISTRIBUTION CODE

13. ABSTRACT *(Maximum 200 words)*

(U) Excess power was measured in 28 out of 94 electrochemical experiments conducted using palladium or palladium-alloy cathodes in heavy water. Reproducibility continues to be the major problem in this controversial research area. Based on our experiments, this lack of reproducibility stems from unknown variables in the palladium metal. The best reproducibility for excess power was obtained using palladium-boron materials supplied by the Naval Research Laboratory. Our basic isoperibolic calorimeters were capable of measuring excess power with a sensitivity of ±1% of the input power or ±20 mW, whichever was larger. Calorimeters that are capable of detecting excess power levels of 1 watt per cubic centimeter of palladium are essential for research in this field. Results from our laboratory indicate that helium-4 is the missing nuclear product accompanying the excess heat. Thirty out of 33 experiments showed a correlation between either excess power and helium production or no excess power and no excess helium. The collection of the electrolysis gases in both glass and metal flasks place the helium-4 production rate at 10^{11} to 10^{12} atoms per second per watt of excess power. This is the correct magnitude for typical deuteron fusion reactions that yield helium-4 as a product. Anomalous radiation was detected in some experiments by the use of X-ray films, Geiger-Mueller counters, and by the use of sodium iodide detectors. There was never any significant production of tritium in any of our experiments.

14. SUBJECT TERMS	15. NUMBER OF PAGES
Calorimetry, Deuterium, Electrolysis, Excess Power, Helium-4, Radiation, Tritium	98
	16. PRICE CODE

17. SECURITY CLASSIFICATION OF REPORT	18. SECURITY CLASSIFICATION OF THIS PAGE	19. SECURITY CLASSIFICATION OF ABSTRACT	20. LIMITATION OF ABSTRACT
UNCLASSIFIED	UNCLASSIFIED	UNCLASSIFIED	UL

P - 079

NUCLEAR PRODUCTS ASSOCIATED WITH THE PONS AND FLEISCHMANN EFFECT; HELIUM COMMENSURATE TO HEAT GENERATION, CALORIMETRY, AND RADIATION.

B. F. Bush and J. J. Lagowski, University of Texas, Dept. of Chem., Austin, TX 78712, USA.
M. H. Miles, Naval Air Warfare Center, Weapons Division, China Lake, CA 93555, USA

The nature of the nuclear phenomena associated with the Pons and Fleischmann effect remains largely unexplored. The phenomena are reproducible, but the processes lack controllability. The circumstances of the electrolysis experiments do not produce the same nuclear product distribution as that expected during hot plasma D + D fusion experiments.

From our earliest qualitative heat versus helium nuclear products analyses (J. Electroanal. Chem., 304, 271 (1991)) to our more recent quantitative helium analyses; the utmost care has been exercised with respect to the scientific rigor of our work. The correlation between the production of helium and the generation of excess heat has been reproduced in different laboratories and under different experimental protocols. Preliminary results are shown in the Figure:

The quantitative correlation between the amount of energy generated and the helium produced is at the level that is expected for a high energy nuclear reaction, such as fusion. These results are underwritten by extensive ^{3}He:^{4}He:^{20}Ne control experiments, which will be described in the presentation.

Calorimetric quality is the foundation of this work. In our early work, isoperibolic calorimetry was used successfully. In our later work as depicted in the Figure, high performance Calvet calorimetry is used. This is the most rigorous method of calorimetry known, amounting to an integrated measurement of the total thermal flux. Electrolysis off-gas production rates were measured to determine the Coulombic efficiency of the electrolysis. Atmospheric helium contamination was precluded by use of all-metal sampling flasks and all-metal gas collection equipment with helium leak-tight Cajon VCR metal seals.

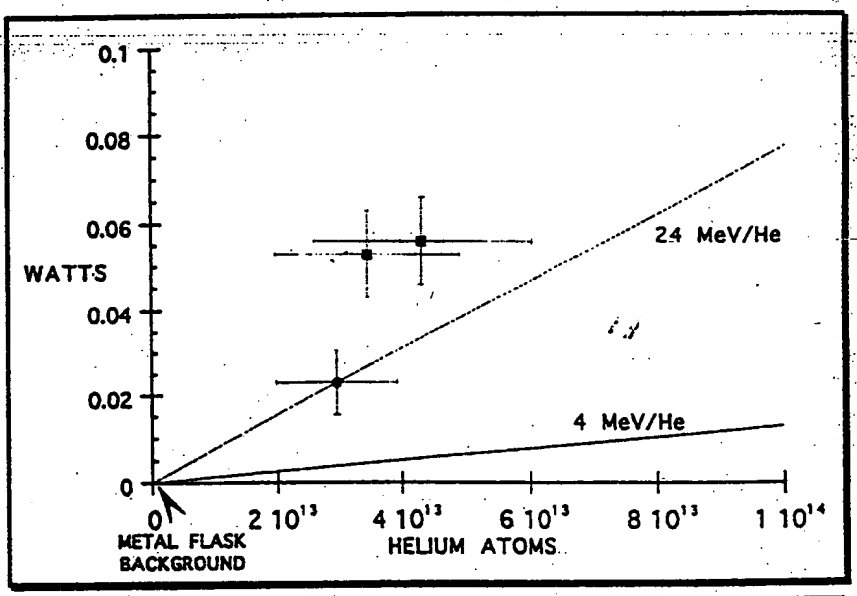

Figure. D + D → ^{4}He + 24 MeV is the most energetic reaction known. The heat *versus* helium analysis can be used to attempt to identify the nuclear reaction pathway by comparing the quantity of helium produced to the amount of energy generated. Thus, the most energetic reaction known would generate 24 MeV/^{4}He, as shown depicted by the line in the plot. Likewise, the 4 MeV/^{4}He line is included to add perspective. These results were obtained with all-metal apparatus shown to be capable of eliminating atmospheric contamination.

Radiation monitoring suggested the presence of a weak source of high energy γ-radiation. The weakness of the source tended to confound the analysis because of the statistics of the minimum detectable activity associated with various radiation detectors. The cathodes used in these experiments were palladium electroplated on gold-flashed copper. No calorimetry was associated with these radiation experiments.

The technical aspects of the nuclear products analysis will be described as it was reproduced under various protocols. The ultimate goal of this effort is to identify explicitly which nuclear reactions result in the Pons and Fleischmann effect.

NEW EXPERIMENTAL RESULTS OF ANOMALOUS NUCLEAR EFFECT IN DEUTERIUM / METAL SYSTEMS

Long He-Qing, Yin Wen
Institute of Sichuan Material and Technology
P.O.Box 538-14 Chengdu 610007, PRC

Zhang Xin-Wei, Wu Jun, Zhang Wu-Shou
Institute of Applied Physics and Computational Mathematics
P.O. Box 8009 Beijing 100088, PRC

Tang Hong-Qing, Li Ze, Shen Guan-Ren, Zhou Zu-ying
Qi Bu-Jia, Liu Yong-Hui, Wang Xiao-Zhong, Yang Yi
China Institute of Atomic Energy
P.O. Box 275, Beijing 102413, PRC

ABSTRACT

Counts and energy spectrum of anomalous neutron and possible anomalous X-rays have been measured in Deuterium / Metal gas discharge Systems. Electrodes made of Nb, Ta, WTh_x, Pd, Ni or other metals were fixed to both ends of a glass reaction bulb, the voltage of applied alternating current was 2.7-18 KV (50Hz). 2.45MeV neutrons have been measured on condition of dynamic low pressure (<100Pa) deuterium gas glow discharge, neutrons of other energy over background have not been detected. The ratios of experimental neutron yield to theoretical one were much greater than 1 when low voltage was applied; the ratio >8 in D / WTh_x system when U=4.7KV; the ratio >46 in D / Ta system when U=4.1KV; the ratio >170 in D / Nb system when U=2.7KV. The neutron emission was stable, reproducible and controllable.

Comparing with air discharge, there were indications that anomalous X-rays have been produced in D / Pd system. The X-ray spectrum (Ex <20KeV) were similar to the Bremsstrublung spectrum but not any spectrum of which low energy X-rays had been absorbed mostly by the glass wall (about 2mm thick) of reaction bulb.

I. INTRODUCTION

Since the announcement of cold fusion by Fleishmann and Pons[1] and Jones et al[2], a lot of experiments have been carried out in the field. Most of the researches are concentrated on the low energy process such as the electrolysis of heavy water, absorbing and degassing deuterium gas. The luckwarm fusion on the charged $(D_2O)_n^+$ molecules cluster (E=200-325Kev, n=10-100) impinging on the deuterium targets has been reported by Beuhler et al.[3] There have been few results of conditions between cold fusion and luckwarmfusion in the world.[4-6] The gas discharge method which will be introduced below is the very situation.

The apparatus used for the fusion studies was discribed in the preceding publications.[5,6] The values of voltage mentioned below are virtual ones.

II. NEUTRON MEASUREMENTS

The neutron detector is composed of a liquid scintillator (ST-451, 10.5 cm in diamter and 5 cm thick) and a photo multiplier tube XP-2041, an n-γ pulseshape discriminator modular (CANBERRA 2160A) is used. The detector efficiency is calibrated with n-p scattering experiments and Monte-Carlo calculation.[7] The detector is calibrated by 2.5 MeV neutrons produced in a standard neutron source. The electrodes used in the neutron measurements are rods of Ta, Nb, Ni, WTh_x, Pd....

Neutron spectrum are obtained with different metals at various voltage, the recoil-proton spectra of D / Ta system at 7.1 KV is shown in Fig.1. Neutron

spectra corresponding to Fig.1 is shown in Fig.2, there are 2.45 MeV neutrons and we conclude that $D(d,n)^3He$ reactions have taken place in the gas discharge process.

The recoil–proton spectrum of three different D / M systems at 9.1 KV are shown in Fig.3, the energy of neutrons is 2.45 MeV as well.

Last year, we reported that we had measured lower and higher energy neutrons,[5,6] but we have not detected them in the present experiment. We think there were too high errors in the detectors used before, so we had obtained wrong informations.

For gas discharge method, the main problem is whether the neutrons are normal beam–target neutrons or anomalous ones. For distinguishing them, we compare the experimental results with the theory.

Experimental and theoretical works of high–voltage / low–pressure discharge had been established by McClure.[8,9] As a result of calculation, we find that the beam–target neutrons are produced major in the cathod fall region between the electrodes instead of the cathod targets interior, the gas pressure and distance of electrodes have few effects on the neutron yields. The neutron yields are inversely proportional to the secondary emmission coefficients γ (: number of secondary electrons rleased from the cathode by positive ion and fast neutral atom impact), i.e. neutron yields $\propto \frac{1}{\gamma(\gamma+1)}$. There are different γ values for different materials, various configurations and surface conditions of cathodes. The γ tends to a constant when the energy of impinging particles (D_2, D_2^+, D, D^+) goes up. Therefore, the ratios of the neutron yields for different cathodes at a fixed voltage are constants. In Fig.4, there are ratios of experimental neutron yields for three sortsof electrodes to theoretical neutron yields for a reference conditions taken from ref. 8, From Fig.4, we find that when $U > 7-9$ KV, the ratios are roughly constants in 4 times order, but when $U < 7-9$ KV, the experimental results are much greater than that of theories. the maximum discrepancy reaches 10^2 flod. When U= 11–15KV, there are small peaks which are very lower than those of low voltage, it is difficult to understand. We have regulated theoretical parameters but the considerable discrepancy at low voltage (5 – 7 KV) and small discrepany at 11–15KV couldn't be eliminated. We can draw a conclusion that there are anomalous neutrons at low voltages at least in D / M discharge systems.

It seems that the neutron yields depend on the gas pressure.

Ⅲ. X–RAY MEASUREMENTS

The measurement system is composed of a Ge(Li) detector (GMX200) made in ORTEC company of U.S.A., a pulse shape analyser (CANBERRA,2160A) and a IBM–PC / XT computer. The detector sensitive volume is 102 cm^3, the measuring range is 5 KeV to 1.64 MeV, the relative efficiency is 20%. The Ge(Li) detector is placed in a lead shielded cabin so that the background is 11 counts / sec within 20 to 1024 channels (the background is decreased to 1 / 20, compared to the ones before shielded).

The electrodes used for X–ray measurements are in shape of Pd plate. The thickness of the glass wall of the reaction bulb is 2.0± 0.2mm.

The theoretical spectrum of X–ray are calculated with calssical Bremsstrablung formula[10]:

$$\frac{dN}{dE_r} = N_0 \frac{1}{E_r} \int_{E_r/eV_0}^{1} \ln\left[\frac{\left(\sqrt{x}+\sqrt{x-E_r/eV_0}\right)^2}{E_r/eV_0}\right] \frac{dx}{\sqrt{1-x^2}}$$

and empirical formula

$$\int E_r dN = 1.1 \times 10^{-9} ZV(IV)$$

Where E_r is energy of X–ray, Z is atom number of target metal, e is magnitude of electron charge, V_0 and V are the maximum and virtual voltage in a period respectively. The glass wall and absorbing plates of Al, Cu etc. are concerned at the same time.

In Fig.5, the experimental and theoretical spectrum of air discharge at 11.8 KV are shown, they are consistent very well.

The Fig.6 shows the spectrum of D / Pd and air / Pd system under the glow discharge condition of 8.0 KV voltage and 0.05cm thick absorbing plate (Cu). We can see that the spectra of air discharge is close to the background due to the thick absorbing plates, and the spectra of deuterium discharge is similar to the emission spectra of Bremsstrablung instead of a spectra through the absorbing plate. That means the measured X–rays of D / Pd system are formed at the outside of the reaction bulb instead of the inside.

When the reaction bulb and the detector are coaxial, we think the X–ray spectra of D / Pd system is close to the background due to the thick plate electrode absorbing, but there is still emission spectra and which is shown in Fig.7.

In Fig.8, there are spectrum of D / Pd system when the collimator hole of the detector aims at the reaction bulb or diverges it. It seems that the emission spectra is not caused by the electromagnetic interference.

The photons caused by neutrons are less than 10^2 / sec under this condition by estimate but we have measured about 10^4 photons / sec behind the shield of absorbing plates. It could not be interpreted by the classical theory.

IV. CONCLUSION

1. 2.45MeV neutrons are produced in D / M discharge system when the voltage is greater than 2.7KV.
2. when the applied voltages are less than 7 to 9 KV, the neutron yields are much greater than the theoretical results, the discrepancy reaches 10^2 at 2.7 KV.
3. the anomalous X–rays have been measured, they should be produced at the outside of the reaction bulb, it seems to be secondary X–rays.
4. the anomalous X–ray phenomena should be confirmed further in the future.

ACKNOWLEDGEMENT

This work is supported by the Natural Science Foundation of China. The authors express their thanks to professors Wang Ganchang, Chen Nengkuan, Qian Shaojun, Xie Renshou, Wu Sheng, Wu DongZhou, Liu Hongqun, Sun Sihai and Wang Dalun.

REFERENCE

1. M. Fleishmann et al., "Electrochemically Induced Nuclear Fusion of Deuterium," *J. Electronal. Chem.* **261**, 301, (1989)
2. S. E. Jones et al., "Observation of Cold Nuclea Fusion in Condensed Matter," *Nature*, **338**, 737, (1989)
3. R. J. Beuhler et al., "Deuteron–Deuteron Fusio by Impact of Heavy–Water Clusters on Deutera ed Surfaces," *J.Phys.Chem.* **94**, 7665, (1990)
4. A. B. Karabut et al., "Nuclear Product Ratio for Glow Discharge in Deuterium," *Physics Lett.* **170**, 265, (1992)
5. Long Heqing, Zhang Xiwei et al., "Anomalou Effects in Deuterium / Metal System," *Frontiers o Cold Fusion, Proceedings of the Third Internation al Conference on Cold Fusion, October 21–25, 1992, Nagoya,"* H. Ikegami, ed. pp447, Univer sal Academy Press, Inc., Tokyo, 1993
6. Long Heqing, Zhang Xiwei et al., "The Anoma lous Nuclear Effects inducing by the Dynamic Low Pressure Gas Discharge in Deuterium / Palladium System," *Frontiers of Col Fusion, Proceedings of the Third Internationa Conference on Cold Fusion, October 21–25, 1992, Nagoya,"* H. Ikegami, ed. pp455, Univer sal Academy Press, Inc., Tokyo, 1993
7. G. Dietze and H. Klein, PTB–Report ND–22 Braunschweig, Oct., 1982
8. G. W. McClure, " High– Voltage Glow Discharges in D_2 Gas. I . Diagnosti Measurements," *Phys. Rev.* **124**, 969, (1961)
9. G. W. McClure et al.," High– Voltage Glow Discharges in D_2 Gas. II . Cathode Fal Theory," *Phys. Rev.* **125**, 1792, (1962)
10. J. D. Jackson, *Classical Electrodynamics*, *Chapter 15*, John Wiley & Sons, Inc., New York, 1976

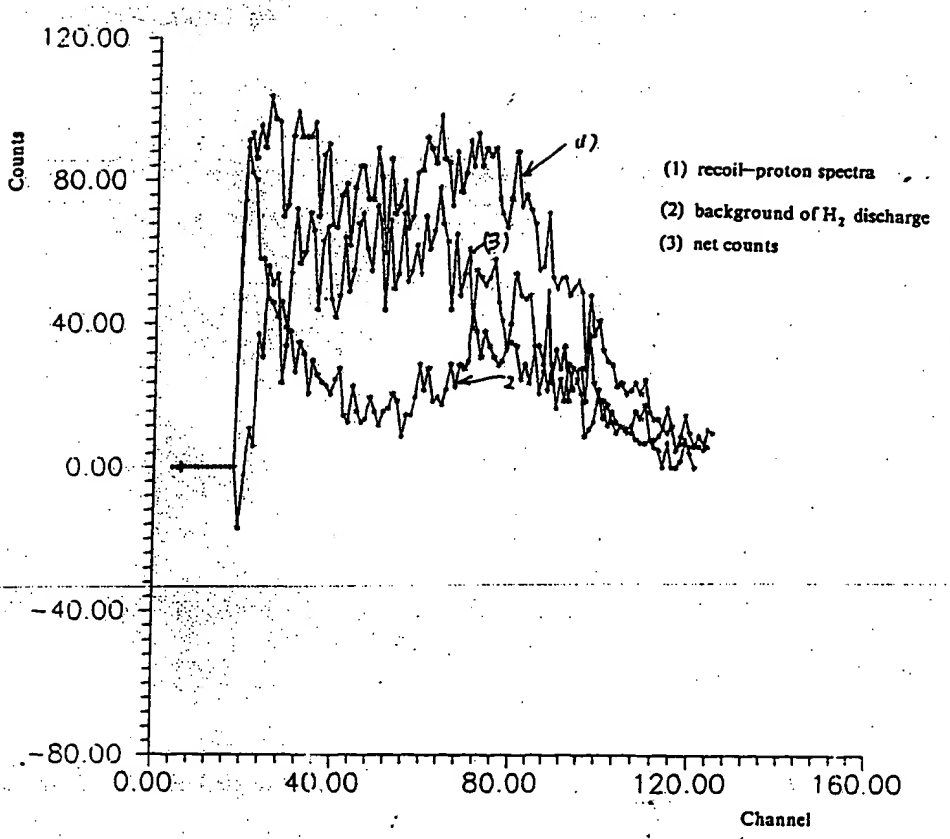

Fig. 1 Recoil–proton spectra of D / Ta, 7.1KV, 22mA

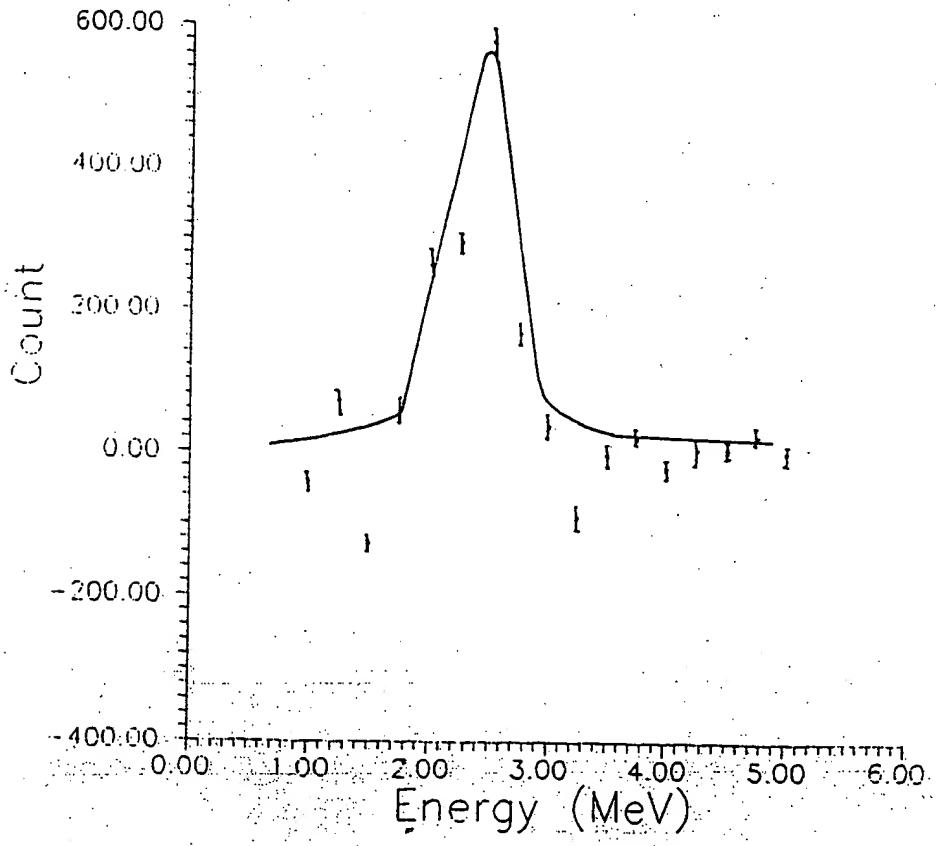

Fig.2 Neutron spectra corresponding to Fig.1

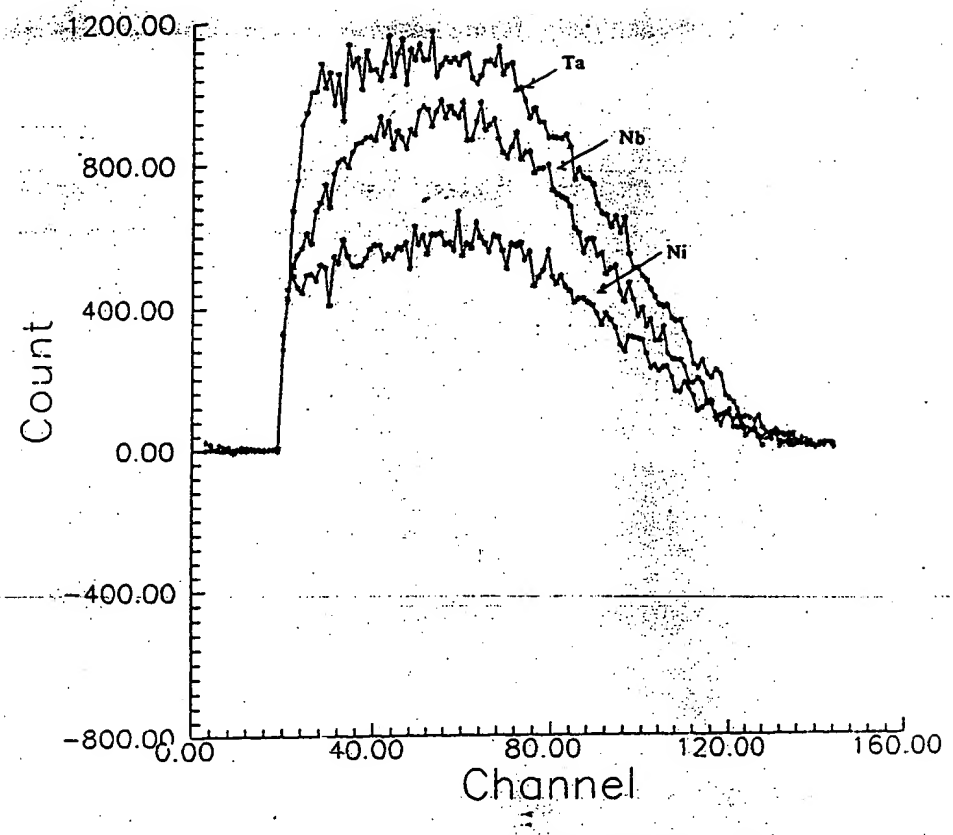

Fig. 3 Rec ..il—proton spectrum of different electrodes, 9.1KV, 10mA

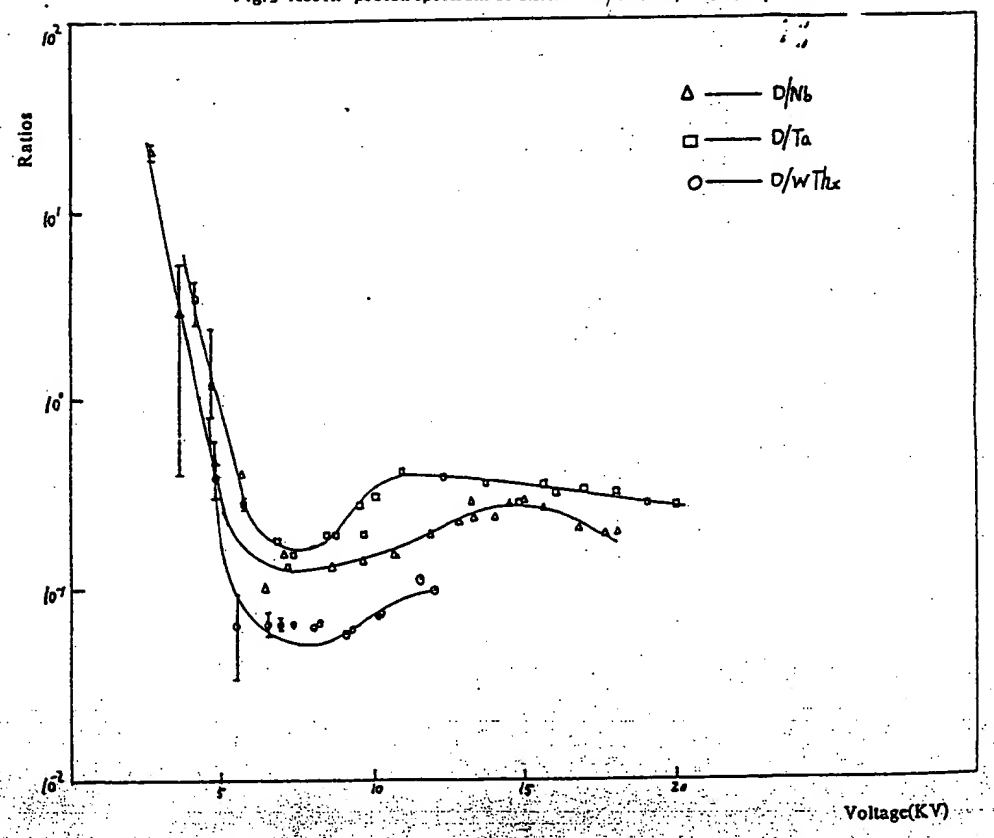

Fig.4. Ratios of experimental neutron yields for three kinds of electrodes to theoretical neutron yields for a reference condition.

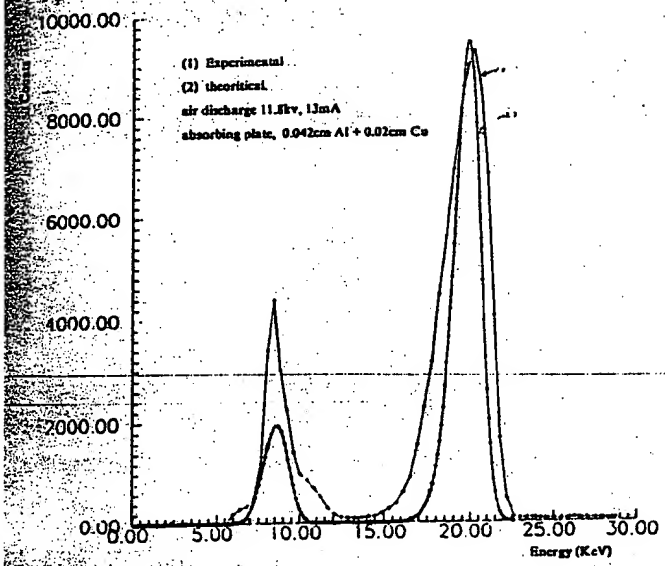

Fig.5 Results of X-ray spectra of experiment and theories

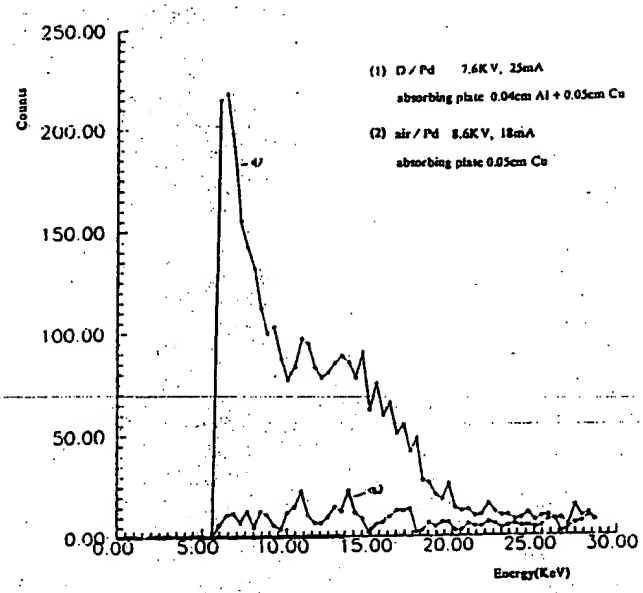

Fig.6 Comparing the X-ray Spectra of D / Pd with air / Pd

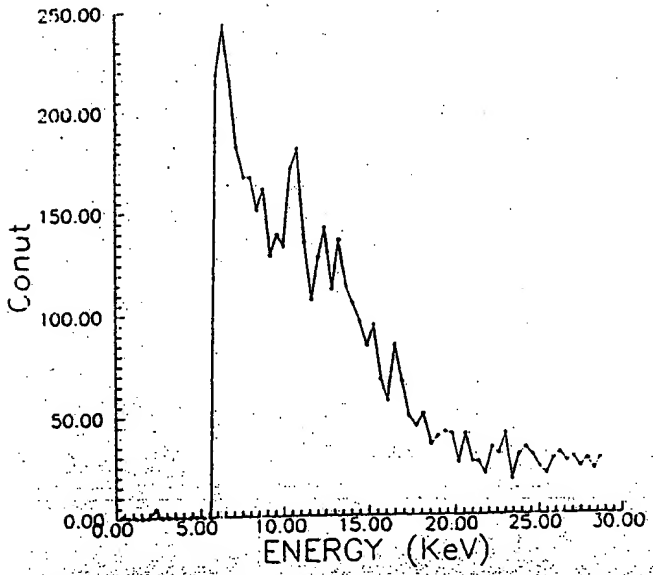

Fig.7 X-ray spectra of D / Pd, reaction bulb and detector are coaxial. 7.25KV, 24.5mA.

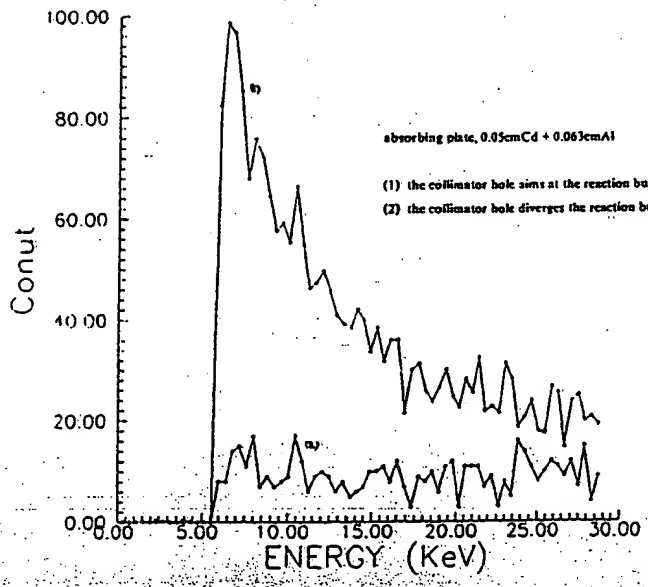

Fig.8 X-ray spectra of D / Pd 8.9-11.5KV, 26-35mA

***

POSSIBLE DEUTERIUM PRODUCTION FROM LIGHT WATER EXCESS ENTHALPY EXPERIMENTS USING NICKEL CATHODES

Mitchell Swartz
JET Energy Technology, Inc. [1]

ABSTRACT

Nickel cathodes that produced excess enthalpy during the electrolysis of light water solutions were examined serveral weeks later (metachronously) by electron emission spectroscopy. The absence of an obvious significant emitting ash might be consistent with a short-lived product, loss of the product, self-absorption, or low signal to noise, or a new fusion pathway leading to a stable ash. The latter may contribute to the excess heat as well as other researchers' reported transmutation reactions through a portion of the pathway leading to the production of *de novo* deuterons. If deuterium is a product of these reactions then its production levels, the inevitable separation factors, and present detection thresholds pose a significant challenge for its unambiguous identification.

INTRODUCTION -- EXPLANATIONS NEEDED

The deuteron is rarely, if ever, considered a possible product of cold fusion systems. Although examination of a large subset of the cold fusion literature (>840 abstracts [1]) revealed eighteen papers concerning tritium or triton production [2-19], a similar search revealed none discussing deuterium or deuteron production. This absence exists even though a pathway to its production might also explain the excess heat [20-27] and reported transmutations [3,25,26,28-30]. There must be a reasonable explanation for the excess heat and transmutation reactions. In light water nickel cold fusion systems, even purported transmutated products do not appear to be proportional to the expected ash required for the observed excess enthalpy. The anomalous branching ratio remains as problematic as the excess heat, and the lack of a theoretical model has been a major cause of the knee-jerk dismissal of this scientific field.

The coulomb barrier approach has been examined by many hypotheses but screening factors alone may not be sufficient to explain the observations, and thus the reaction pathway probably does not involve the classic collision of two particles. Several hypotheses exist including "shrunken" hydrogen [20], positron emission [31], and possible deuteron production [2]. In the case of helium produced from deuterium-loaded palladium, the Phuson theory [33] has been developed describing the multi-body reactions involving the loaded deuterons within the lattice of the fully loaded Group VIII transition metal electrode cathodically driven to ~1 kilomolar electron density. In the Phuson theory, the phonon clusters distribute energy between the excited state and the ground state, thereby conserving momentum within the palladium.

Because there does not exist a similar theory for nickel, due to the excess heat observed and the lack of a clear electron emission in these metachronous experiments, we elected to look more closely at deuterium, its production, its spin structure, and its possible role in these phenomena. This paper introduces a pathway that could yield *de novo* deuterons and explain the observed transmutation reactions. The hypothesis suggests that

---

energy may be transferred to the lattice through a phonon cloud (Phuson) as a non-bound virtual deuteron state collapses to the ground state configuration.

BACKGROUND -- DEUTERON STRUCTURE AND SEPARATION

Chemically, the hydrogen isotopes slightly differ in their equilibrium constants, enabling the difficult separation of deuterium oxide from ordinary water (Table 1). Although hydrogen was isolated as a distinct substance in 1766 by Cavendish, deuterium was separated electrolytically in 1932 by Urey, Brickwedde and Murphy after its spectroscopic identification one year earlier. The actual situation is complicated because of tritium and the fractional species (e.g., DTO). The fragile deuteron decomposes at temperatures cooler than our sun's core (~ million degrees Kelvin). So even though interstellar clouds and protostars contain deuterium (abundance D/H = ~1.9 {+/-0.5} 10^{-4}) evolved stars have essentially none [34-36]. Therefore, deuterium oxide (D_2O), although ubiquitous (D/H = ~1.5 10^{-4}) *in situ* within ordinary water, must be commercially refined and purified at considerable difficulty to obtain the several megaliters per year required for its use as a moderator for some nuclear reactors. The difficulty in refining deuterium arises for several reasons. The separation of the deuterium is highly endothermic, and most of the separation factors are small (Fig. 1). Deuterium is generally refined electrolytically following cascaded refiners using the slight difference in the free energies of formation of different hydrogen, nitrogen, or sulfer compounds (e.g., ammonia-hydrogen exchange and the Girdler-Sulfide system) [37].

In a deuteron, the constituent neutron and proton have an exceptionally large internucleon separation. The importance is the deuteron binding energy is only ~2.2 MeV in a well of about ~40-50 MeV. As a corollary, the deuteron has no bound excited states [38,39]. Since each nucleon has isospin +1/2, the deuteron has total isospin of either 0 or 1, and so there are four possible triplet and singlet states [40]. The deuteron ground nuclear state is the triplet $^3S_1$ state with the nuclear orbital angular momentum = 0, and the nuclear spins parallel. States with any nuclear orbital angular momentum of >0 show no signs of binding. The actual structure, and energy, of the deuteron ground state results from its three form factors (electric monopole {charge}, magnetic dipole, and electric quadrupole moments). The magnetic moment of the deuteron ($\mu_D = 0.8574$) is not exactly the sum of its component parts (μ_H and μ_N), and the slight difference -- and the unusual electric quadrupole moment (Q = 0.282 e-fm^2) -- are both consistent with a more complex mixture of nuclear spin states in the deuteron ground state (suggested by Rarita and Schwinger) such as inclusion of some $^3D_1$ state [41,42]. There is a virtual ($^1S_0$) state located above the zero binding energy at +30 keV which has been confirmed by nuclear photoeffects and other phenomena [43].

EXPERIMENTAL - ABSENCE OF METACHRONOUS BETA EMISSION

Nickel cathodes produce excess enthalpy (heat) during electrolysis of light water solutions [27]. As a result of competing reactions [44-46], an optimum "notch" occurs in the power gain curve relative to input power [27]. Nickel electrodes were driven within their π-notch using ordinary water in combination with either platinum or gold anodes. We examined several electrodes that had demonstrated episodes of excess heat for their metachronous electron emission, at 12 to 24 weeks, using a modified Maestro-EEG system with solid state detector. Fig. 2 shows the control, the background, and the background subtracted from the sample's emission spectrum. There was apparently insignificant metachronous electron or ionizing radiation emission from the previously-driven nickel cathodes to herald an explanation for the excess enthalpy. The absence of an obvious emission signature to declare ash might be consistent with a short-lived product, or with inadvertant removal of the isotope from the surface during the interval between driving and examination of the samples, or with unintentional self-absorption of the emission signal, or with loss of the signal in the noise background, or even with an unconsidered pathway yielding a stable final product. Given the recent results of Lin [47] and Bockris, and Mizuno, it may be that the delay of several months prior to the metachronous measurement was far too long

and that emissons may have been in the range of 15-25 keV. Studies are underway to reexamine this experimentally. Nonetheless, we considered the latter possibility.

INTERPRETATION -- POSSIBLE PATHWAY

When the possible pathway mentioned above is considered, it is noted that it might contribute to the excess heat and to other researchers' reported transmutation reactions, through the production of *de novo* deuterons. We suggest a multistep pathway leading to deuteron production with the generation of an excited intermediate state (a virtual deuteron in light water with nickel, and -- as presented elsewhere -- an excited helium-4 nucleus in heavy water with palladium systems). Fig. 3 shows some of the relevant nuclear states.

The first step is the corollary of well-known neutron decomposition. Free neutrons have a theoretical lifetime of ~10 minutes but are observed to decay within circa three minutes via interaction with a proton. Taking the neutron lifetime as 918 seconds, we rewrite the basic beta decay equation, using backwards time, to give a proton and electron opportunity to react to an extremely rare occurance in a fully loaded, one kilomolar electron-loaded, fully-hydrided alloy. This gives a thermal neutron and neutrino.

$$p^+ + e^- \rightarrow n^0 + \nu^e$$

Could there actually be sufficient quantities of such putative ephemeral thermal neutrons available? Of the estimated 5×10^{21} nickel atoms in the cathode, perhaps the relatively active portion may extend to a depth yielding ~0.04% of the nickel lattice sites which actually are able to have a role and contribute. This constitutes about ~4 micromoles of nickel contributing lattice sites within the cathode. Thus, assuming full local hydridation, the amount of protons available is also in the range of 2×10^{18}. Given the neutron lifetime, there is a statistical likelihood of only 0.000987 contributing at any point in each second. With the putative active sites available, this would give ~2×10^{15} potential virtual neutrons per second. This does exceed the required event rate described below.

The second step, similar to the Phuson mechanism proposed for deuteron-laden palladium, involves a hypothesized intermediate precursor-product excited state. Here, the critical excited (and virtual) nuclear state (D^*) is energetically located above the non-bonding axis. The ground-state deuteron forms through a simultaneous cooperative reaction involving a cluster of phonons (the Phuson) linking the de-excitation of the excited virtual deuteron state. These phonons are critical because they account for the coupling, for the focusing of energy into the critical sites, and possibly even for the positive feedback that permits the reactions. The D^* deexcitation enables the vicinal phonon ensemble to compete effectively and permit fusion reactions to proceed in the fully loaded metals with energy transfer to the phonon cloud. If such nuclear-phonon cloud pathway was not available then the tiny population of D^* would saturate and end all such reactions. Only in the fully loaded material are the virtual levels continuously drained leading to their replenishment. When nuclear-phonon cloud pathways are not available then the tiny population of D^* immediately saturates to an insignificant level.

Our calculations suggest that in order to conserve momentum and energy not all the ~2.2 MeV binding energy would be available. The four-vector relates the momenta (p_i; i = x,y,z) and energy (E), and begins in the center of mass frame-of-reference at the primary reaction site within the hydrided metal. Although several approximations have been made, the energy of the reaction actually available to the Phuson cluster appears to be closer to 1.4 MeV per transition; somewhat less than the binding energy. Because each watt requires ~6.24 10^{12} MeV per second, one impact of this correction is that this putative pathway would require 2.8-4.5 10^{12} events per second (Fig. 4).

Assuming a distribution of phonon energies in the range of 30-50 eV, there would be 2.8-7.3 x 10^7 phonons in the phuson cluster (the cooperative phonon group linked to the excited state). Thus, this would require the involvement of about 5-44 million lattice sites, and therefore about ~170-350 lattice sites in any direction radial from the prime reaction site. Now, any putative deuteron production releases energy on the ~1-2 MeV scale at a single location, but with a possibility for spreading the released energy among these lattice sites that can be coupled during the deexcitation time of D^*. The interaction radius [r_{DE}] is determined by the speed of light, c, so the number of lattice cells involved in a single event, coupled through the Phuson deexcitation pathway, assuming isotropicity, is

$$N_{sites}(r_{DE}) = \frac{[c * \tau_{DE}]^3}{[V_{unitcell}]}$$

The uncertainty principle can estimate the lifetime based upon the "energy bandwidth" of the energy involved. For the excited state of deuterium located at +30 keV, the energy width of the virtual state must be on the order of a fraction of that, which would be consistent with an adequate lifetime of the excited state. The ensemble of phonons, with consideration of the available lattice sites, is thus sufficient to account for energy transfer to the lattice during the deexcitation D^*.

LIMITS OF DEUTERON DETECTION

Several experiments are suggested based upon the Phuson theory. First, if deuterium is an ash, and if there are no secondary reactions (e.g., to convert the generated deuterium to helium-4), then there will be an ultimate limit to the amount of energy which can be obtained by loading nickel with a fixed volume of light water. Per mole of hydrogen converted (in ~9 cubic centimeters of ordinary water) this would theoretically generate a maximum energy of ~10^{11} joules. Second, if the putative thermal neutron production does occur, then there is a maximum excess rate of heat production available based upon that factor, too. This would limit the rate of generation of the desired product. The observed π-notches could be consistent with this.

Third, the rate of generation of *de novo* deuterium per megajoule, if any, is miniscule and would create only a few percentage change in a background of ordinary water (Fig. 4). Such small production levels, and the inevitable separation factors (Fig. 1) refining further possibly already present deuterium, together pose significant challenges for the unambiguous identification of deuterium. Reexamination of vibrational spectroscopic data [48] (Fig. 5) indicates that small amounts of deuteron production remain below the present selectivity and sensitivity of the system. However, other spectroscopies that may offer potential for *in situ* examination include infrared absorption analysis, neutron reflectometry and, nuclear resonance broadening (NRB) and elastic-recoil-detection-analytic (ERDA) techniques. Some techniques penetrate subsurface structures to examine the magnetic properties of, and the impact of nonequivalent occupied sites within, the hydrided metal.

Fourth, if Phusons are involved, then given the requirement for sufficient lattice recruitment, any observed isotopic changes in transmutation systems may occur in greatest amounts below the lattice surface, and at depths which are the order of the interaction radius. Fifth, if the putative thermal neutron pathway exists, then there may also be the potential for nickel (and other elements) to be transmutated to higher isotopes of the same element with the unstable isotopes becoming, for the nickel, the stable isotopes of copper and cobalt.

ACKNOWLEDGMENTS

The author is grateful to Drs. Michael Staker, Peter Hagelstein and Russ George for their discussions involving the possibility of deuteron production in some of these reactions, to Prof. Louis Smullin who performed the β-

emission collections, and also to Jeff Driscoll, Steven Olasky, Dr. Stephen Baer, and Prof. Keith Johnson for some of the equipment used to make these experiments possible, and to Gayle Verner and JET Energy Technology and its staff for their support and assistance during this study, and to the staff at Fusion Information Center for their assistance with the preparation of this manuscript.

REFERENCES

1. D. Britz, "*CNF bibliography updates and archive retrieval*", URL http://www.kemi.aau.dk/~britz. Of the eighteen papers dealing with tritium production, four were theoretical, and fourteen were experimental. Of the experimental papers, 78% were positive, although because of repeated authors this should be ~72%. 2. V.A. Alekseev, et al., *Tech. Phys. Lett.*, vol 21, p 231 (1995).
3. R.T. Bush, R.D. Eagleton, *J. Fusion Energy*, vol 9, p 397 (1990).
4. J. Chene, A.M. Brass, *J. Electroanal. Chem.*, vol 280, p 199 (1990).
5. C-C. Chien, D. Hodko, Z. Minevski, J.O'M. Bockris, *J. Electroanal. Chem.*, vol 338, p 189 (1992).
6. C-C. Chien, T.C. Huang, *Fusion Technol.*, vol 22, p 391 (1992).
7. T.N. Claytor, D.D. Jackson, D.G. Tuggle, "Tritium Production from Low Voltage Deuterium Discharge on Palladium," *Cold Fusion Times*, vol 4, p 3 (1996).
8. M. Fleischmann, S. Pons, G. Preparata, *Nuovo Cimento*, vol 107 A, p 143 (1994).
9. D. Hodko, J.O'M. Bockris, *J. Electroanal. Chem.*, vol 353 (1993).
10. Y.E. Kim, *Fusion Technol.*, vol 19, p 558 (1991).
11. G.H. Lin, R.C. Kainthla, N.J.C. Packham, O. Velev, J.O'M. Bockris, *Int. J. Hydrogen Energy*, vol 15, p 537 (1990).
12. G. Mengoli, et al., *J. Electroanal. Chem.*, vol 304, p 279 (1991).
13. G. Mengoli, et al., *J. Electroanal. Chem.*, vol 322, p 107 (1992).
14. S.R. Rajagopalan, *Curr. Sci.*, vol 58, p 1059 (1989).
15. K.A. Ritley, et al., *Fusion Technol.*, vol 19, p 192 (1991).
16. C.D. Scott, et al., *Fusion Technol.*, vol 18, p 103 (1990).
17. E. Storms, C. Talcott, *Fusion Technol.*, vol 17, p 680 (1990).
18. H. Wiesmann, *Fusion Technol.*, vol 17, p 350 (1990).
19. L.L. Zahm, et al., *J. Electroanal. Chem.*, vol 281 (1990).
20. R.L. Mills, S.P. Kneizys, "Excess Heat during the Electrolysis of an Aqueous Potassium Carbonate electrolyte and the implications for cold fusion," *Fusion Technol.*, vol 20, pp 65-81, (Aug. 1991).
21. V.C. Noninski, "Excess Heat during the Electrolysis of a Light Water Solution of K_2CO_3 with a nickel cathode," *Fusion Technol.*, vol 163 (1991).
22. R. Notoya, Y. Noya, T. Ohnishi, "Tritium Generation and Large Excess Heat Evolution by Electrolysis in Light and Heavy Water-potassium Carbonate solutions with Nickel Electrodes," *Fusion Technol.*, vol 26, pp 179-183 (1993); R. Notoya, "Alkali-Hydrogen Cold Fusion Accompanied by Tritium Production on Nickel," *Transactions of Fusion Technol.*, vol 26, pp 205-208 (Dec. 1994).
23. T. Ohmori, M. Enyo, "Excess Heat Evolution During Electrolysis of H_2O with Nickel, Gold, Silver, and Tin Cathodes," *Fusion Technol.*, vol 24, no 3, pp 293-295 (1993).
24. T. Matsumoto, "Cold Fusion Observed with Ordinary Water," *Fusion Technol.*, vol 17, pp 490-492 (1990); T. Matsumoto, "Cold Fusion Experiments with Ordinary Water and Thin Nickel Foil," *Fusion Technol.*, vol 24, pp 296-306 (1993).
25. R T. Bush, R D. Eagleton, "Evidence for Electrolytically Induced Transmutation and Radioactivity Correlated with Excess Heat in Electrolytic Cells with Light Water Rubidium Salt Electrolytes," *Transactions of Fusion Technol.*, vol 26, pp 431-441, (Dec. 1994); Robert T. Bush, "A Unifying Model for Cold Fusion," *Transactions of Fusion Technol.*, vol 26, pp 434-354 (Dec. 1994).
26. M. Srinivasan, A. Shyam, T.K. Shankarnarayanan, M.B. Bajpai, H. Ramamurthy, U.K. Mukherjee, M.S. Krishnan, M.G. Nayar and Y. Naik, "Tritium and Excess Heat Generation During Electrolysis of Aqueous Solutions of Alkali Salts with Nickel Cathode," Frontiers of Cold Fusion, Ed. by H. Ikegami, *Proceedings of the Third International Conference on Cold Fusion*, October 21-25, 1992, Universal Academy Press, Tokyo, pp 123-138 (1992).
27. M. Swartz, "Consistancy of the Biphasic Nature of Excess Enthalpy in Solid State Anomalous Phenomena with the Quasi-1-Dimensional Model of Isotope Loading into a Material", accepted in *Fusion Technol.*, for January 1997 issue.

28. T. Ohmori, T. Mizuno, M. Enyo, "Production of Heavy Metal Elements and the Anomalous Surface Structure of the Electrode Produced During the Light Water Electrolysis of Gold Electrode," 6th Int'l. Conf. on Cold Fusion, Oct. 1996, Toya, Hokkaido, Japan.
29. R. Notoya, T. Ohnishi, Y. Noya, "Nuclear Reactions Caused by Electrolysis in Light and Heavy Water Solutions," 6th Int'l. Conf. on Cold Fusion, Oct. 1996, Toya, Hokkaido, Japan.
30. B.F. Bush, J.J. Lagowski, M.H. Miles, "Nuclear Products Associated with the Pons and Fleischmann Effect: Helium Commensurate to Heat Generation, Calorimetry, and Radiation," 6th Int'l. Conf. on Cold Fusion, Oct. 1996, Toya, Hokkaido, Japan.
31. Russ George, personal communication.
32. Michael Staker, personal communication.
33. M. Swartz, "Phusons in Nuclear Reactions in Solids", accepted in *Fusion Technol.* for March 1997 issue.
34. J. Craig, D.N. Schramm, M.S. Turner, "Big Bang Nucleosynthesis and a New Approach to Galactic Chemical Evolution," *Astrophysics Journal*, vol 459, pp L95-98 (1996).
35. M. Rugers, C.J. Hogan, "Confirmation of High Deterium Abundance in Quasar Absorbers," *Astrophysics Journal*, vol 459 (1996).
36. Following the Big Bang (τ = ~1 second into the expansion), the temperature lowered to a few hundred MeV, and nucleons (baryons or ordinary matter) generated other elements, mainly helium ($24^{+/-1}$% throughout the universe at that time, and ~30% in our sun now, where additional helium has since been created). Although nucleosynthesis forms helium efficiently at high baryon density, the less efficient pathways generate deuterium. The D/H ratio then becomes the best indicator of initial baryon density. As a result of the destructionof deuterons due to their relative fragility, back corrections have been made to deduce an initial pregalactic deuterium abundance of 0.01% percent relative to protons.
37. This heavy water distillation machinery for commercial deuterium production involves towers of 35 meters height with a 9 meter diameter operating in countercurrent exchange mode. These towers must perform at high pressure in anticipated severely corrosive environments (> 6 mm allowance). In the GS system, hot hydrogen sulfide (70% H_2S) rises through falling water in a series of cascades; providing enrichments of ~30-40%. The GS system uses final enrichment of electrolytic means so as to produce 99.75-99.8% deuterium oxide (reactor grade heavy water). The ammonia hydrogen exchange system requires an additional catalyst. The high temperature is used since the forward reactions toward material deuteration (from the contamination levels in the water) are then favored. These reactors contain toxic, flammable, and corrosive substances. (Cf. H.K. Rae,
"Separation of Hydrogen Isotopes," ACS Symposium, Series 68, Washington D.C., 1978.)
38. A.I. Akhiezer, A.G. Sitenko, Tartakovskii, V.K., Nuclear Electrodynamics, Springer-Verlag (1993).
39. Byron. P. Roe, *Particle Physics at the New Millenium*, Springer (1996).
40. M.A. Preston, P.K. Bhaduri, Structure of the Nucleus, Addison-Wesley Publishing Co., Reading, MA (1975).
41. Povh, Rith, Scholz, Zetsche, Particles and Nuclei, ISBN 3-540-59439-6, Springer (1995); Kaplan, Irving, Nuclear Physics, Addison-Wesley, MA (1962); H. Kopfermann, E.E. Schneider, Nuclear Moments, Academic Press (1958).
42. Some use the Sachs formula to reveal several possible states, and other analyses (Feshback-Lomon) indicate a mixing of 4.3% or slightly more D state. The electric form factor of the deuteron suggests a 6-7% D-state contribution, but additional meson-exchange current to make this slightly less, ~4.3-5%. The meson exchange current enables electromagnetic transitions between T = 0 and T = 1 states, such as in the photodisintegration of the deuteron. Although the mixture is only a few per cent, the tensor force further contributes to the total binding energy of ~2.23 MeV.
43. G.A. Jones, The Properties of Nuclei, Clarendon Press, Oxford (1987); Nilsson, S.G., Ragnarsson, I., Shapes and Shells in Nuclear Structure, Cambridge U. Press (1987).
44. M. Swartz, "Quasi-One-Dimensional Model of Electrochemical Loading of Isotopic Fuel into a Metal", *Fusion Technol.*, vol 22, no 2, pp 296-300 (1992).
45. M. Swartz, "Generalized Isotopic Fuel Loading Equations," Cold fusion Source Book, International Symposium on Cold Fusion and Advanced Energy Systems, Ed. Hal Fox, Minsk, Belarus (May 1994).
46. M. Swartz, "Isotopic Fuel Loading Coupled to Reactions at an Electrode," Proceedings: Fourth International Conference on Cold Fusion, Vol 4, p 33 (1994); Swartz, M., "Isotopic Fuel Loading Coupled to Reactions at an Electrode," *Fusion Technol.*, vol 26, no 4T, pp 74-77 (December 1994).
47. G.H. Lin, Bockris, J. O'M., "Anomalous Radioactivity and Unexpected Elements Upon Heating Inorganic Mixtures," *Cold Fusion Times*, vol 4, no 4 (1996); Mizuno, T., Ohmori, T., Enyo, M., "Anomalous Isotopic Distribution in Palladium Cathodes after Electrolysis," *Cold Fusion Times*, vol 4, no 4 (1996).
48. M. Swartz, "Systems to Monitor and Accelerate Electrochemically Induced Nuclear Fusion Reactions," U.S. Patent Application 07/371,937 (June 27, 1989).

49. Compilations, including Handbook of Chemistry and Physics, C. Hodgeman et al. CRC (1961, 1973); S. Parker, "Encyclopedia of Science and Technology, McGraw Hill, NY; R.B. Heslop, P.L. Robinson, Inorganic Chemistry, Elsevier, Ampsterdam, 1967; and T. Claytor (personal communication).

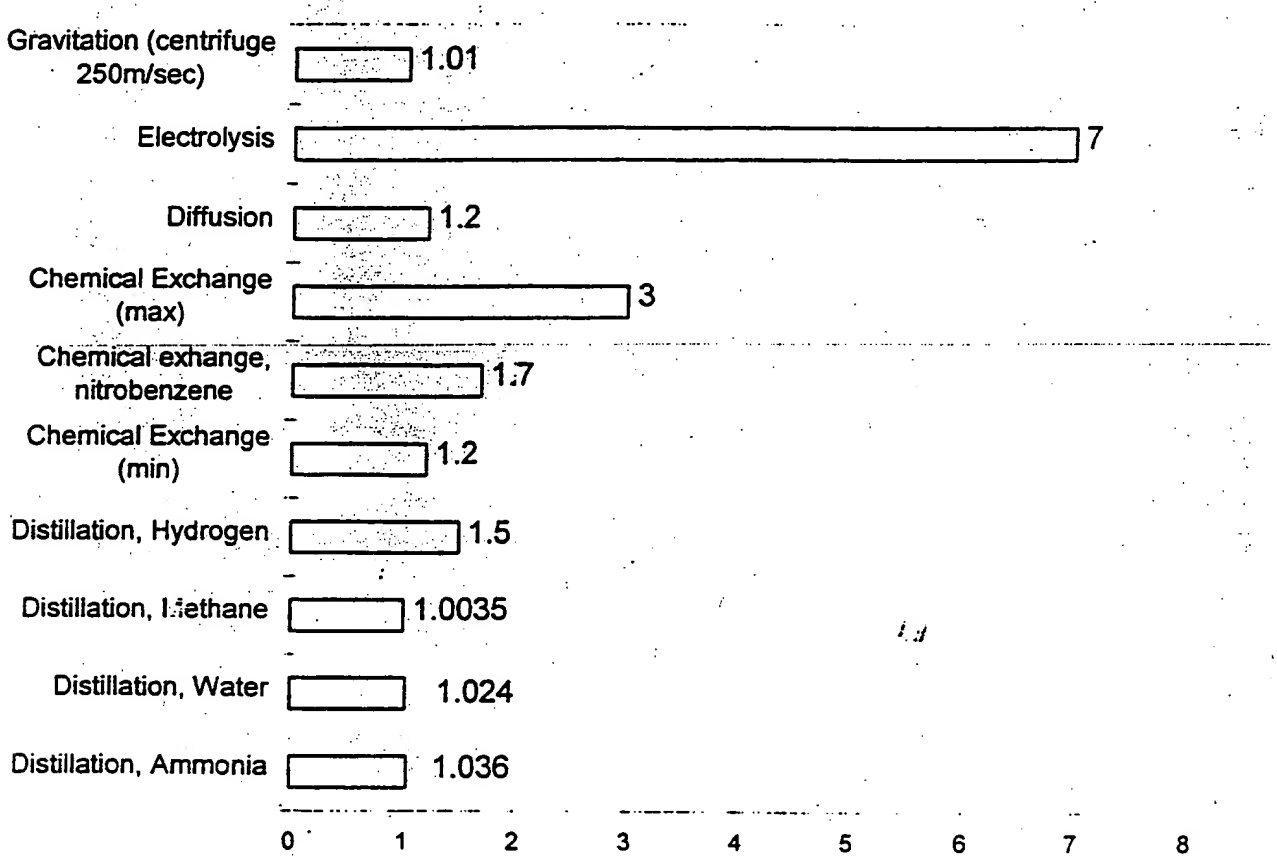

Fig. 1. Common Separation Factors for Deuterium Production

This Figure shows the separation factors for refining deuterium from ordinary water. The values range from a maximum for electrolysis to those values characteristic of evaporation or centrifugation.

Table I

HYDROGEN ISOTOPE PROPERTIES (ref. 49)			
Baryon/Nucleon	Proton	Deuteron	Triton
Mass (amu)	1.0078	2.0142	3.0160
Electric monopole charge	1+	1+	1+
Magnetic dipole moment	2.7928	0.8574	2.9789
Electric quadrupole moment (nuclear magnetons)	0	0.282 e-fm^2	0
Isospin (parity) J	1/2+	1+	1/2+
Binding energy	0	2.224 MeV	6.461 MeV
Lifetime	stable	stable, fragile	12.3y
Decomposition product	not applicable	not applicable	18.59 keV beta
Diatomic gas	Hydrogen	Deuterium	Tritium
Molar volume of solid cm^3	28.3	23.5	
Triple Point (deg K)	13.92 K - 13.96 K	18.58 K - 18.72 K	20.6 K
Heat of vaporization at triple point Joules/mole	910.9	1268.2	
Melting point (deg K)	13.95	18.65	
Boiling point (deg K)	20.38 - 20.4	23.5	
Latent heat of fusion (melt) Joules/mole	117.2	197 - 217	
Heat of dissociation KJoules/mole	437.5	439.2	
Water (ignores HDO, HTO, etc.)	H_2O	D_2O	T_2O
Background concentration	1	0.000156	1/10^{17}
Molecular weight (C^{12} scale)	18.015	20.028	
Surface tension (20C)	72.75 dynes/cm	67.8 dynes/cm	
Temperature of Maximum density	3.98 C	11.23 - 11.6 C	
Dielectric constant (25 C)	78.54	78.25	
Absolute viscosity (20 C)	10.09 millipoises	12.6 millipoises	
Melting point (deg C)	0	3.82	
Boiling point (deg C)	100.00	101.42	
Specific gravity (20 deg C)	0.9982	1.106	
Heat of fusion Joules/mole	6008.2	6317.8	
Heat of vaporization Joules/mole	43,840	44,936	
Solubility NaCl (25 C) gms/100 g	35.9	30.9	
Autopyrolysis constant $[D_3O+]$ $\{OH-\}$ 25 C	1.00 10^{-14}	3.00 10^{-15}	
pH	7.00	7.26	
Cost	rain, snow	1$/L(gas) $100 - $1000/L (liq)	~ $30 K/gm
World production	-	~ 1-3 10^6 L/year	< 10^2 Ci/yr
World capacity	-	10^{13} tons on surface	

Fig. 3. Metachronous Emission of Nickel Cathodes

This Figure shows Emission Spectrograms of a control, of the background, and of a nickel cathode which had previously demonstrated excess heat (~52 kilojoules, 0.35 cm^3, 28 cm^2, 15 weeks prior to examination).

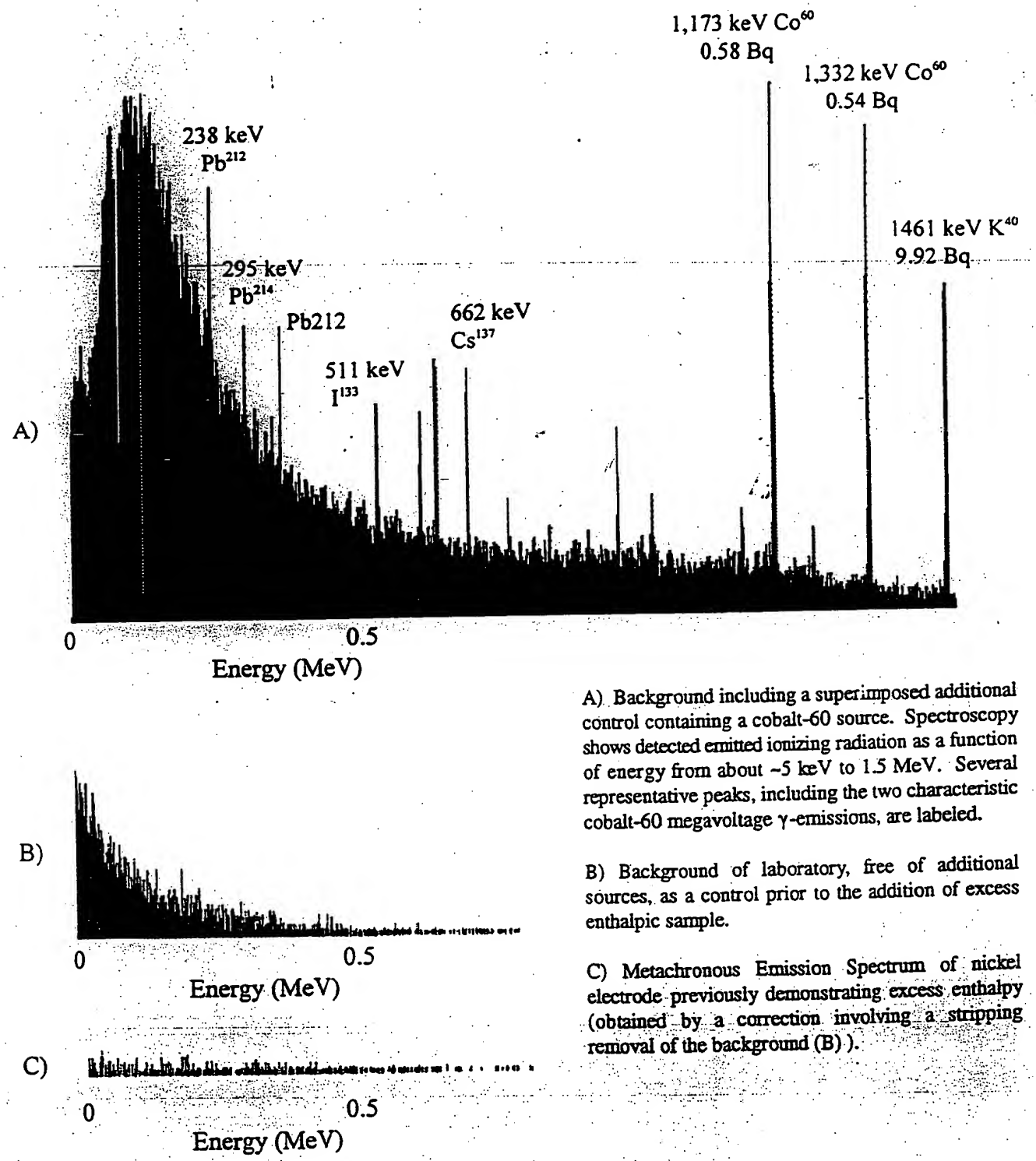

A) Background including a superimposed additional control containing a cobalt-60 source. Spectroscopy shows detected emitted ionizing radiation as a function of energy from about ~5 keV to 1.5 MeV. Several representative peaks, including the two characteristic cobalt-60 megavoltage γ-emissions, are labeled.

B) Background of laboratory, free of additional sources, as a control prior to the addition of excess enthalpic sample.

C) Metachronous Emission Spectrum of nickel electrode previously demonstrating excess enthalpy (obtained by a correction involving a stripping removal of the background (B)).

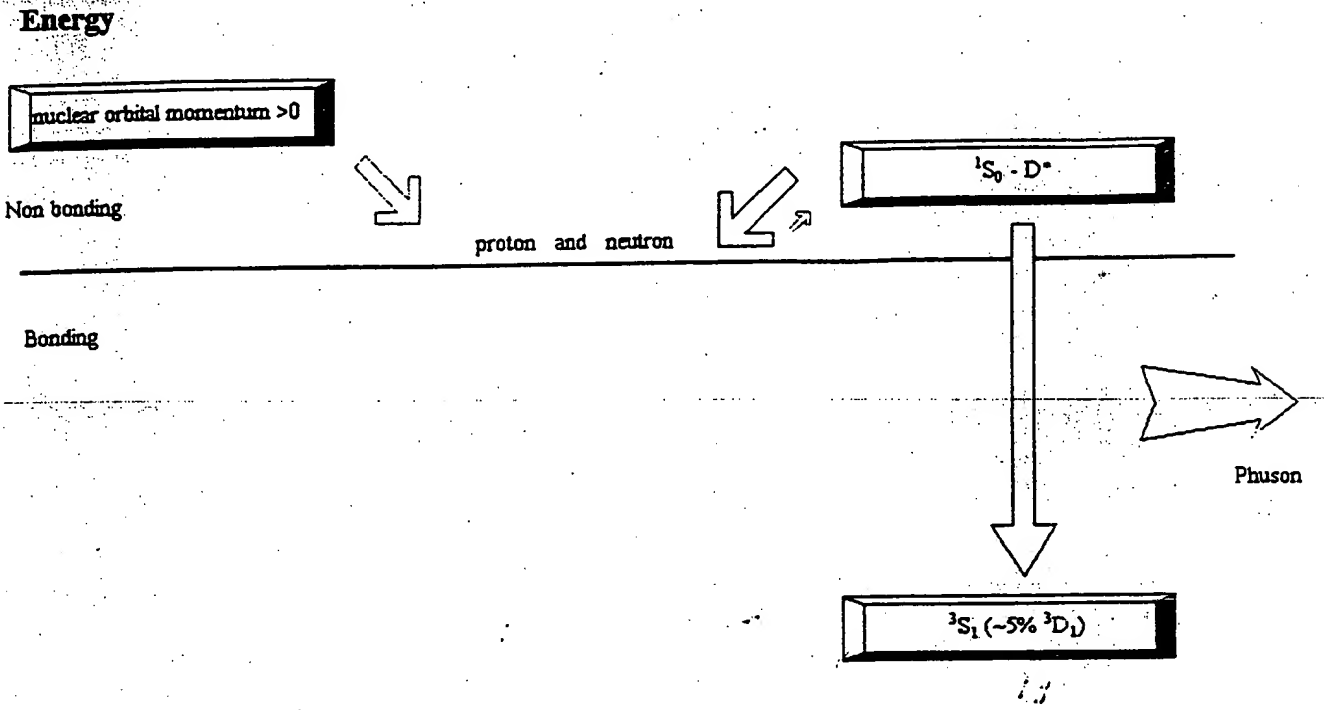

Fig. 3. Spin Manifolds of the Deuteron

This Figure shows the pathway leading to possible deuterium production. It does not include the preceeding generation of the neutron as discussed in the text. Shown are three of the "states" available to an interacting proton and neutron. The vertical axis is energy and is not quantitative. If there is any nuclear orbital angular momentum then the non-binding "state" on the upper left is not achieved for reasons discussed in the text. If the nuclear orbital angular momentum is zero, the manifold on the right can be entered. The singlet state above the axis (~30 keV) is a virtual state observed in incident beam studies. The state on the bottom right is the well-known ground state of the deuteron, which is mainly a $^3S_1$ state. The hypothesis is that there may be leakage from the virtual state to the ground state with Phuson coupling to the solid hydrided lattice cathodically loaded with electrons.

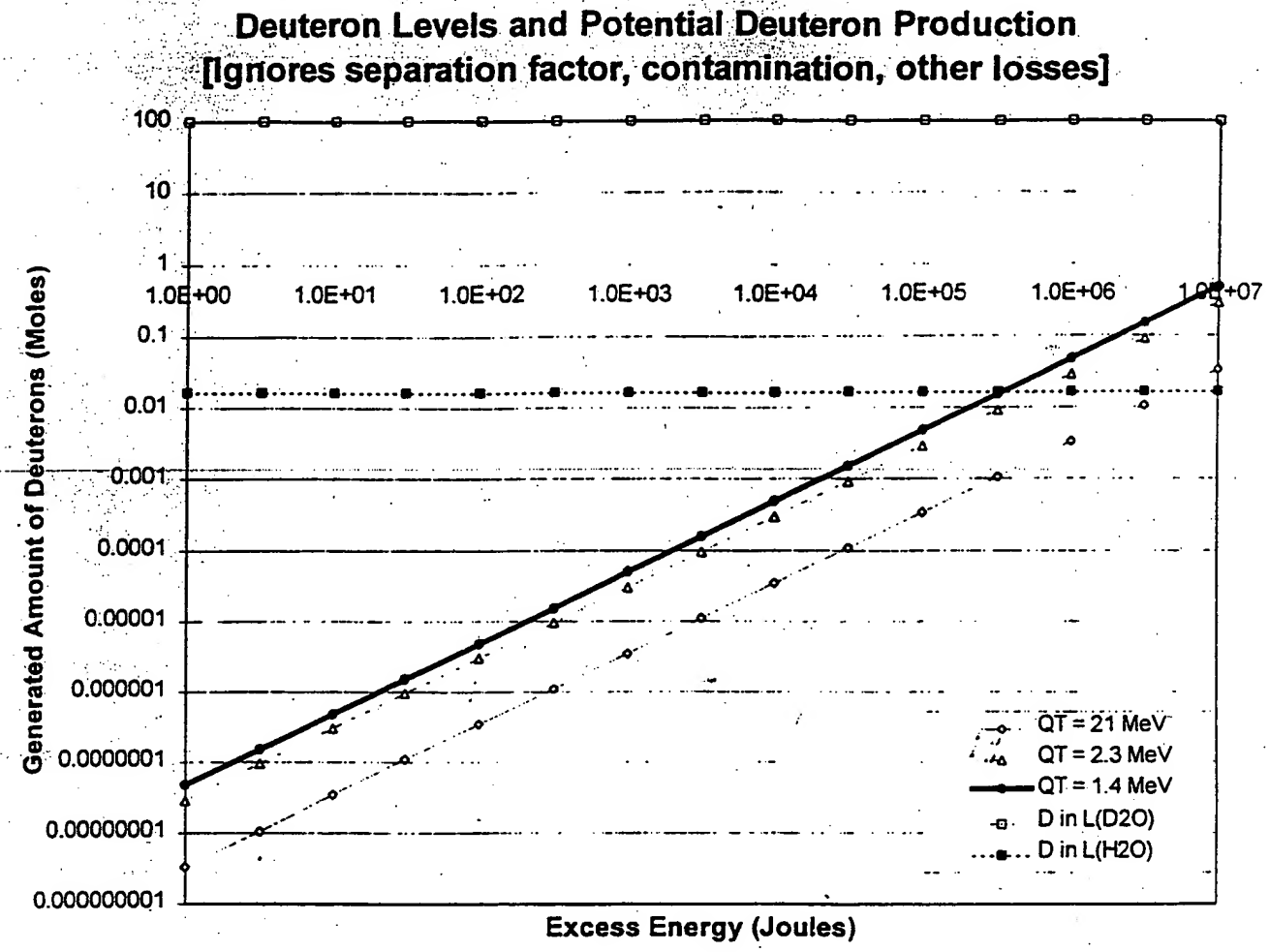

Fig. 4 Putative Production Rates of Deuterium Would Present Detection Challenges

This Figure shows the quantity of deuterium present in, or generated *de novo* in, water as a function of excess energy. The three rising curves show the amount of expected deuteron ash which would be produced if that reaction did occur and did only account for the observed excess heat. Each curve represents a different derived energy for each single event nuclear reaction. The event (binding) energy of 21 MeV does not hold for deuterium, but is representative of what occurs for other final states such as helium. Q_T of 2.3 is what might be expected for the binding energy of the deuteron. The curve representing "Q_T" of 1.4 (thick diagonal line) is derived from the calculations which correct for momentum transfer to the Phuson cluster (see text). Also shown for comparison is the quantity of deuterons contained in a liter of light, and heavy, water.

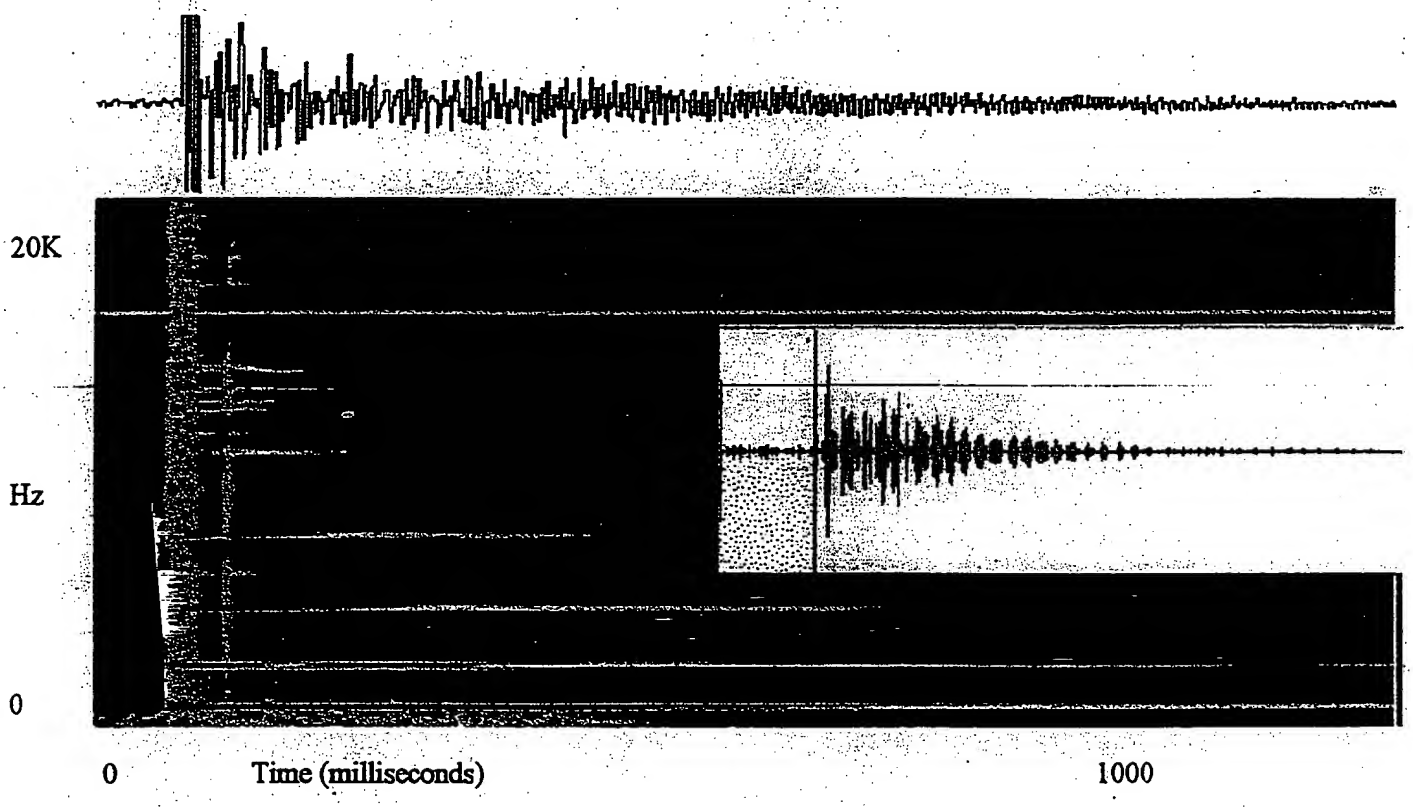

Fig. 5. Vibration Spectroscopy of Nickel Cathode

This figure shows a Vibration Spectrogram of a loaded nickel cathode. The cathode (Sample 92-505b/Ni-B2) surrounded with 20 ml of ordinary water, during its electrical polarization with a platinum anode, is struck with a single mechanical pulse at t = 0. The vibrational modes of the electrode, and their damping, can be used to determine loading, but because of separation issues may be insensitive to any putative deuteron production. Two recorders were used to pickup the data (top and inset), and the fast fourier transform is also shown as a frequency versus time plot. The solid bar three-quarters of the way up the calibration signal at $17{,}390^{+/-53\ Hz}$. The lowest evanescent normal mode, the most irregular of the group, is believed to be a circular mode around the relatively large annular electrode. The sampling rate was ~100 kHertz.

FUSIONfacts

A Monthly Newsletter Providing Factual Reports on Cold Fusion Developments

ISSN 1051-8738 Offices located in the University of Utah Research Park

--Since 1989--

Fusion Facts Now Reports on Both Cold Fusion and Other Enhanced Energy Devices.

VOLUME 8 NUMBER 3 SEPTEMBER 1996

CONTENTS FOR SEPTEMBER 1996

This issue of *Fusion Facts* provides its readers with abstracts of papers presented at LENR conference. The Proceedings will be published within the next two weeks as Volume 1, Number 3, Fall Issue, of the *Journal of New Energy*.

IF YOU DO NOT HAVE A SUBSCRIPTION, ORDER NOW!

Single copies $45. Four issues for $150 sent postpaid airmail anywhere on earth.

A. SUMMARY OF THE SECOND LOW ENERGY NUCLEAR REACTIONS CONFERENCE

By Hal Fox

Fifty scientists, engineers, and interested business leaders attended the Second Conference on Low-Energy Nuclear Reactions. This important conference was held at the Holiday Inn, College Station, Texas on September 13-14, 1996. The conference was not held on the campus of Texas A&M because 12 out of 12 members of the Department of Chemistry voted no to the request by Distinguished Professor of Chemistry, John O'M. Bockris to hold the meeting on campus. The vote was an example of a democratic process. The choice was an example of pathological skepticism.

Papers presented in all conferences range in importance, however, this conference must be considered as being of special importance because the issue of low-energy transmutation was directly addressed with reports of several new sets of experimental data from prestigious scientists. Here are some examples:

George Miley presented "Nuclear Reactions in Palladium-Hydrogen System." This paper is especially important because it is the first paper to explore the nuclear reactions occurring in the thin-film layers of nickel-palladium-nickel coated on small beads. This work was supported by CETI (Clean Energy Technologies, Inc.).

Mitchell Swartz presented an excellent paper discussing the cold fusion work using light water and nickel cells. Swartz made an excellent point about using data from the noise level when making claims for excess heat. Swartz also

indicated that all of his data is conservative because it does not subtract for the power consumed in electrolyzing the water. Swartz reported three to six times as much energy out as input into the cells. It appears that Swartz has accomplished some of the most effective work with the nickel-light water cold fusion. Swartz has not observed elemental changes.

Kenneth Shoulders presented an excellent paper on the possible effects of high-density charge clusters in promoting nuclear reactions in metal lattices. Shoulders has examined a variety of cathodes used in cold fusion work and has found evidence for numerous metal lattice damage sites caused not just by the strike of a high-density charge cluster (EVs) but apparently from nuclear effects caused by the highly-energetic EVs. To Shoulders, with his familiarity with EVs, the nuclear results are clearly evident. Shoulders has labeled such high-density charge clusters as NEVs or nuclear electrum validums. He suggests that the primary cause of nuclear reactions in cold fusion occurs by creating a brittle metal by hydrogen loading, causing cracks which produce EVs, and the energetic EVs cause nuclear reactions. Ken presented SIMs analysis of typical EV-reaction spots to show that the palladium had been transmuted into other elements. The concepts presented by Shoulders were not readily appreciated, as shown by a vote of two out of about fifty who thought that this process was an explanation of heat production in cold fusion cells. We believe that the number of believers will increase as they further examine their cathodes. However, no one is saying that this is the only source of excess heat in cold fusion reactions.

The first-ever paper on the Neal-Gleeson Process was presented. This was not a scientific paper in the sense that a full disclosure of the process was not made. However, it was announced that third-party verification was being planned for the near future. From the preliminary data (taken from over 100 experiments) it was suggested that radioactivity could be reduced fifty percent or more in a one-pass operation taking only one to four hours. The paper strongly suggests that if replicated by noted scientists this process has great potential for ameliorating radioactive slurries, such as the 66 million gallons stored in over 170 tanks at the Hanford Site, Washington. (Note: The inventors are Rod Neal and Stan Gleeson who have been previously referred to as "the Cincinnati Group".)

John Dash (Portland State University) presented a paper extending his successes with heavy water and palladium to include the use of titanium electrodes. With each successful experiment that produces excess heat, there are shown to be low-energy nuclear reactions involved. His procedures are sufficiently reproducible that he brings in quality high-school students each summer to get them involved in this new technology of cold fusion. John Dash has offered to share his procedures with anyone that is interested.

T. Mizuno (Hokkaido Univ.); Z. Minevski (Lynntech); Russ George (E-Quest Sciences); Guang Lin (Texas A&M); R. Monti & E. Bauer (Burns Development); G. Rabzi (Ukrainian Int'l Academy of Original Ideas); Thomas Claytor (LANL); and T. Ohmori (Univ. of Hokkaido) all presented additional data on transmutation in their papers.

In summary: Drs. Bockris and Lin of Texas A&M University should be congratulated for a successful and important conference. All authors were asked to provide copies of their papers immediately after the conference so that these important papers can be published in the **Proceedings** immediately. We have already received 13 of the 21 papers presented. These papers will be published as Volume 1, Number 3, of the *Journal of New Energy*.

We are pleased to announce that articles published in the *Journal of New Energy* will be abstracted in *Chemical Abstracts, Engineering Index Monthly,* and *Metal Abstracts.* Scientists, engineers, and students world-wide will have access to the excellent papers given at this important conference. The same staff that publishes this newsletter also publish the *Journal of New Energy.* The same policy of rapid communication is a constant goal of this organization. To keep current on the latest developments in this exciting new science, you will want to subscribe to this new journal.

THE SECOND INTERNATIONAL LOW ENERGY NUCLEAR REACTIONS CONFERENCE

Abstracts of Presented Papers
(received by press time)

Basic Experimental Studies Sessions

Tadahiko Mizuno (Dept. of Nuclear Eng., Hokkaido Univ., Japan), Tadayoshi Ohmori (Catalysis Res. Cntr., Hokkaido Univ., Japan), Michio Enyo (Hakodate Natl. College of Tech., Japan), **"Isotopic Changes of the Reaction Products Induced by Cathodic Electrolysis in Pd."**

AUTHORS' ABSTRACT

It was confirmed by several analytic methods that reaction products with mass number ranging from 6 to 220 are deposited on palladium cathodes subjected to electrolysis in a heavy water solution at high pressure, high temperature, and high current density for one month. These masses were composed of many elements ranging from hydrogen to lead. Isotopic distribution for the produced elements were radically different from the natural ones.

S. Szpak and P.A. Mosier-Boss (Naval Command, Control and Ocean Surveillance Center RDT & E Division, San Diego, CA), **"Nuclear and Thermal Events Associated with Pd + D Codeposition."**

AUTHORS' ABSTRACT

In the Pd + D codeposition process, palladium is electrodeposited in the presence of evolving deuterium. This process favors the initiation and propagation of nuclear and thermal events through a rapid absorption of deuterium to yield high D/Pd atomic ratios. This process results in the formation of non-equilibrium electrode structures that become the seat for localized gradients. Evidence for tritium production, X-ray emanation and generation of localized heat sources, with emphasis on experimental methodology, is provided. The active role of the electrode/electrolyte interphase in the development of these events is examined.

Mitchell Swartz (JET Energy Technology, Inc., Weston, MA), **"Deuterium Production and Light Water Excess Enthalpy Experiments using Nickel Cathodes."**

AUTHOR'S ABSTRACT

Select nickel cathodes can produce excess enthalpy (heat during the electrolysis of light water solutions. A multi body reaction involving two protons within the lattice of th fully loaded Group VIII transition metal cathodically drive to a ~1 kilmolar electron density, is proposed to account fo the excess heat by the production of deuterons. Th reactions occur through an intermediate excited nuclea state of a deuteron formed (D^*), which then de-excites wit the generation of a cloud of phonons. The excess heat i driven by the reconfiguration of the intermediate state to th more tightly bound deuteron ground state.

The phonons are linked to the de-excitation (a Phonon) an are critical both because they enable a pathway permittin further penetration of the coulomb barrier and also becaus they focus energy and interstitial into optical sites, thereb creating feedback mechanisms which can further fuel th desired reactions. The observed temperature rise occurs a disequilibrium as the well-mixed acoustical and optica phonons are unable to carry off all the local momentum an excess energy of the reactions. Special relativisti considerations indicate the phonon cloud in nickel subtend ~200 unit cells. Four-vector analysis indicates that thes hypothesized reactions are consistent with conservation o energy.

Robert Bass, Rod Neal, Stan Gleeson, & Hal Fox **"Electro-Nuclear Transmutations: Low-Energy Nuclea Reactions in an Electrolytic Cell."**

AUTHORS' ABSTRACT

A special electrolytic cell and power supply have bee designed to promote low-energy nuclear reaction (electro-nuclear transmutations). Using electrical pow ranging up to 1,000 watts, it has been experimentall determined that various high-mass parent elements can b fissioned into somewhat equal daughter products. Th experimental evidence for nuclear reactions is based on th difference between input samples and processed samples determined by commercial mass-spectrometer analysis an by gamma-ray emission spectroscopy.

Although other new elements are produced, the bulk of th fission elements appear to be mass fractions consistent wit the conservation of the initial elemental atomic numbe For example, tungsten can be fissioned into cadmium an iron. Thorium has been fissioned into mercury and neo Up to seventy percent of a parent element has bee

fissioned with a few hours of processing time. Further development work is planned, especially for application to the stabilization of radioactive slurries. It is important that these preliminary results be independently replicated and verified.

David J. Nagel (Naval Res. Lab., Washington, DC), **"Cold Fusion Experiments, Theory, & Management at the Naval Research Laboratory."**

AUTHOR'S ABSTRACT

As a matter of responsibility to the public, which ultimately funds it, the Naval Research Laboratory has actively conducted and monitored attempts to make "cold fusion" phenomena reproducible and understandable. This presentation will survey these activities.

Experiments: We performed six different experiments, either new or copies of others, explicitly aimed at "cold fusion' and related phenomena. These will be summarized and some views of others reported "cold fusion" experiments will be presented.

Theories: NRL and associated scientists have published theoretical work on two "cold fusion" motivated studies, namely ion band states and phonon-driven hydrogen isotope diffusion. A broad review of "cold fusion" theories is now underway,

Management: Numerous presentations have been made by the author to government agencies and other groups to provide information and stimulate programs, These include the OSTP, DARPA, DSWA, (ex-DNA), ONR, IDA, and the Philosophical Society of Washington. Results of these interactions will be summarized briefly.

T.N. Claytor, M.J. Schwab and D.G. Tuggle (Los Alamos Natl. Lab., Los Alamos, NM). **"Tritium Production from Palladium and Palladium Alloys."**

AUTHORS' ABSTRACT

A number (22) of pure palladium samples and palladium alloys have been loaded with a deuterium or hydrogen plasma is a system that allows the instantaneous measurement of tritium. By carefully controlling the high pressure plasma conditions, the plasma can be constrained to only contact palladium surfaces and to only lightly sputter the palladium. Long run times (up to 200 h) result is an integration of the tritium and this, coupled with the high intrinsic sensitivity of the system (~0.1 nCi/1), enables the significance of the tritium measurement to be many sigma (>10). In addition to the real time tritium measurement, the deuterium gas can be combined with oxygen, at the end of a run, resulting in water samples that were counted in a scintillation counter. The results of these confirmatory measurement of the tritium in these water samples agree quantitatively with the decrease in tritium as measured by the ion sensor. However, surprising concentrations (up to 1.5 X 10_6 dpm/ml) of tritium were found in several samples that had been exposed to a hydride inhibitor. We have continued to investigate the effects of hydrogen additions on the output of tritium in these types of experiments and find that hydrogen additions always suppress tritium production. We will show the difference in tritium generation rates between batches of annealed palladium, as received palladium and the palladium alloys (Cu, Ni, Be, Li, Hf, Hg and Fe) of various concentrations to illustrate that tritium generation rate can vary greatly from alloy to alloy as well as within a specific alloy, dependent on concentration. Other metals (Pt. Hf, Ni, Nb, Ta, V, W, Zr) have also been run in the system as background samples or to determine if tritium could be detected in the gas analysis system. In nearly all cases they have produced results very close to background drift rates.

T. Ohmori (Catalysis Res. Cntr., Hokkaido Univ., Sapporo, Japan), T. Mizuno (Faculty of Eng., Hokkaido Univ., Sapporo, Japan) and M. Enyo (Hakodate Natl. College of Tech., Hakodate, Japan), **"Isotopic Distributions of Heavy Metal Elements Produced During the Light Water Electrolysis on Gold Electrode."**

AUTHORS' ABSTRACT

Some 100 μ g of fine black porous deposits comprising mainly of Au, Hg, Pt, Fe, Si and F were obtained during the cathodic electrolysis on Au electrodes in 0.5 M Na_2SO_4 and Na_2CO_3 light water solutions for 20-30 days at a current densities >300 mA/cm^2. The isotopic distributions of these elements other than Au, Pt and F determined by SIMS analysis were found to deviate from their natural isotopic abundance. The structure of Au electrode surface after the electrolysis revealed very unusual aspects.

Thoretical Models Session

Yeong E. Kim and Alexander L. Zubarev (Dept. of Phys. Purdue Univ., West Lafayette, Indiana), **"Nuclear Physics**

Mechanisms for Gamow Factor Cancellation in Low-Energy Nuclear Reactions."

AUTHORS' ABSTRACT

In our recent paper [1], we showed that a Gamow factor cancellation (GFC) can occur for nuclear fusion reactions if the imaginary part of the effective nuclear interaction in the elastic channel (ENIEC) has a small component of a finite long-range interaction (FLRI), but we could not prove nor rule out theoretically the existence of such a FLRI component in the imaginary part of ENIEC. In another recent paper [2], we demonstrated (without a rigorous derivation) a possibility of the existence of FLRI components if the target nucleus has a weakly bound excited state ("halo" nuclear state). Most recently, we have succeeded to derive rigorously a new type of FLRI interaction in the imaginary part of ENIEC for the case in which one of the final-state nuclei has an excited halo nuclear state [3]. We have obtained a separable form factor for the imaginary part of ENIEC which at large distances behaves as $cos(k_o r - \eta ln2k_o r + \delta)\Psi_n(r)/r^4$, where k_o, η, δ, and $\phi_n(r)$ are the final state wave number, the Sommerfeld parameter, the phase shift, and the wave function for the excited p-wave halo nuclear state, respectively. Consequences and implications of our results for the cold fusion phenomena are described. GFC due to effects of excited halo nuclear state for low-energy radiative nuclear fusion reactions are also described using a three-body formulation [4].

[1] Y.E. Kim and A.L. Zubarev, *Nuovo Cimento*, vol 108A, pg 1009-1025 (1995).

[2] Y.E. Kim and A.L. Zubarev, *Genshikaku Kenkyu*, vol 40, no 5, (1995), pp. 27-36.

[3] Y.E. Kim and A.L. Zubarev, "Excited Halo Nuclear State and Long Range Interaction in Nuclear Reactions," to be published in *Physical Review C*. (Oct. 1996)

[4] Y.E. Kim and A.L. Zubarev, "Low-Energy Radiative Nuclear Reactions Involving Weakly Bound States," submitted to *Fusion Technology*.

Albert Cau (A.R.T., Paris, France), **"Natural Nuclear Synthesis of Superheavy Elements (SHE)."**

AUTHOR'S ABSTRACT

As soon as nuclear scientists became convinced that some superheavy elements (SHE) could exist with atomic numbers around 114 and 126, numerous attempts have been made to detect them in natural samples and to synthesize them in heavy ion accelerators. No positive results have been obtained until now since no element higher than 101 have been isolated for chemical study.

A new direction to the research of SHE is taken. The source of the present work is old alchemy as described in old treatises written prior to 1850. It appears that the key material used by alchemists was pitchblende. The hypothesis that SHEs could be peculiar elements but only stable in the form or fluorides is discussed.

The mechanism conducive to the production of SHE, in a chemical medium is studied. The main point is that SHE are necessarily produced via *soft fusion*, a synergism of exoenergetic nuclear reactions (proton absorption) and endoenergetic nuclear reactions (light element fusion) — a mechanism that allows the creation of macroscopic amount of SHE fluoride under mild conditions.

The nuclear reactivity of natural mixtures containing uranium and light elements is described. A 1986 experiment showed an unexpected nuclear activity characterized by very intense neutron bursts. The 1996 experiment shows increases of gamma activity upon heating and the production of a peak around 50 KeV.

Shang-Xian Jin and Hal Fox (Fusion Information Cntr., Inc., Salt Lake City, Utah), **"Possible Palladium-Related Nuclear Reactions."**

AUTHORS' ABSTRACT

The recent discoveries by Bockris and Minevski and by Mizuno et al. of apparent numerous low-temperature nuclear reactions has challenged current atomic models. By making the assumption that standard conservation laws for nuclear reactions would be preserved, a large variety of possible nuclear reactions have been proposed and checked for obeying conservation rules. The purpose of this paper is to present a list of some possible nuclear reactions between palladium isotopes and the following single particles: deuterons, protons, neutrons, and alpha particles.

Innovative Approaches Session

G.H. Lin and J. O'M. Bockris (Dept. of Chem., Texas A&M Univ. TX), **"Anomalous Radioactivity and Unexpected Elements as a Result of Heating Inorganic Mixtures."**

AUTHORS' ABSTRACT

This paper reports on anomalous radioactivity and unexpected elements observed in 1992 at the Texas A&M University as a result of igniting a mixture of inorganic compounds. The details of the experiments and the analysis in our laboratory and other private laboratories are presented.

T. Grotz (Wireless Engineering, Inc., Craig, CO) **"Investigation of Reports of the Synthesis of Iron via Arc Discharge through Carbon Compounds."**

AUTHOR'S ABSTRACT

Recent research has investigated the transformation of carbon to iron under certain experimental conditions. Reports by Pulver and Oshawa of iron formation in carbon by exposure to an electric arc are the subject of this report. Iron formation was originally proposed as a result of the reaction of carbon and oxygen to form silicon, then nickel and finally iron as follows;

$$2_6C^{12} + 2_8O^{16} \rightarrow 2_{14}Si^{28} \rightarrow {}_{28}Ni^{58} \rightarrow {}_{26}Fe^{56}$$

Particles of magnetic material attracted to a magnet were given as proof of a transformation. Duplication of this experiment under more controlled conditions with analysis of the iron content of the of the carbon sample before exposure to an electric arc discharge lead to the conclusion that the iron found in the sample may be due to other factors than originally proposed.

Ken Shoulders and Steve Shoulders (Bodega, CA), **"Observations on the Role of Charge Clusters in Nuclear Cluster Reactions."**

AUTHORS' ABSTRACT

Deuterium-loaded palladium foils, produced by both electrolytic and ultrasonic processing, have been micro-analyzed for nuclear reactions. The characteristic strike marks of charge clusters, known as EVs, have been found to occur concurrently with nuclear reactions in micrometer-sized areas. In the electrolytic case, the reaction is attributed to charge clusters generated from mechanical energy, first stored and then suddenly released, from a brittle metal lattice through the mechanism of fracto-emission of electrons. For the acoustic case, EVs are generated by charge separation in a collapsing bubble. When areas previously free of low energy nuclear reactions are bombarded in either vacuum or air by externally generated charge clusters, nuclear reactions are produced at the bombardment site. Charge clusters are considered to function as a collective accelerator capable of injecting a large group of nuclei into a target with sufficient energy density to promote the nuclear cluster reactions observed.

Roberto A. Monti, **"Low Energy Nuclear Reactions: Experimental Evidence for the Alpha Extended Model of the Atom."**

AUTHOR'S SUMMARY

An up to date list of experimental tests constituting, in my opinion, a good validation for the alpha-extended model of the atom, is presented.

A. Michrowski (President, P.A.C.E., Inc., Canada), **"Advanced Transmutation Processes and Their Application for the Decontamination of Radioactive Nuclear Wastes."**

AUTHOR'S ABSTRACT

There are deviations to the standard model of radioactive atomic nuclei decay reported in the literature. These include persistent effects of chemical states and physical environment and the natural, low-energy transmutation phenomena associated with the vegetation processes of plants. The theory of neutral currents is proposed by Nobelist O. Costa de Beauregard, to account for the observed natural transmutations, also known as the Kervran reaction. "Cold fusion" researchers have also reported anomalies in the formation of new elements in cathodes. This body of knowledge provides the rationale for the observed, successful, and developed advanced transmutation processes for the disposal of nuclear waste developed by Yul Brown involving a gas, developed by him, with a stoichiometric mixture of ionic hydrogen and ionic oxygen compressed up to 100 psi. Another procedure, still in experimental stages, involves the environmental interaction

2-20-23 Takanawa
Minato-ku Tokyo 108 JAPAN
Tel: +81(0)3-3442-7521
Fax: +81(0)3-3442-7651

For academic information contact:
Dr. Shiuji Inomata
2-2-2 Sekigawa-cho
Arai-shi
Niigata-944, JAPAN
Tel/Fax: +81(0)255-72-0558

ICCF6
Sixth International Conference on Cold Fusion
will be held 13-17 October 1996
Hotel Apex Toya, Hokkaido, Japan
Conference Secretariat:
Tel +81-3-3508-8901
Fax +81-3-3508-8902
E-mail mac@iae.or.jp

The conference will consist of both oral and poster sessions covering experimental work and theory on the following topics:

- Excess Energy Phenomena in D_2/Metal Systems
- Correlation Between Excess Energy and Nuclear Products
- Nuclear Physics Approaches
- Material Science Studies
- Innovative Approaches (Miscellaneous Phenomena)

Registration fee of ¥40,000 (about $400) includes a banquet and proceedings. A technical tour to the NHE lab is scheduled on Oct. 18, along with other professional and social events.

History shows us that science progress permanently has been retarded by the overbearing influences favoring particular concepts and impelling their acceptance as dogma. Thus, it has become necessary from time to time to return to first principles, which may be used without constraint.

— DeBroglie

Commercial Column

The following companies (listed alphabetically) are commercializing cold fusion or other enhanced energy devices:

COMPANY: PRODUCT

American Pure Fusion Engineering and Supply: Information and troubleshooting for the fusion research and development industry. Developing "Fullerene Fusion Fuel™." Salem, Oregon. The president, Warren Cooley, can be reached at 1-800-789-7109 or 503-585-6746. Email to: Coolwar@aol.com

CETI (Clean Energy Technologies, Inc.): Developers of the Patterson Power Cell™. Dallas, Texas. Voice 214-982-8340, FAX 214-982-8349.

Clustron Sciences Corp.: New energy research consulting and information. Contact: Ron Brightsen, 703-476-8731.

ENECO: Portfolio of intellectual property including over thirty patents issued or pending in cold nuclear fusion and other enhanced energy devices. Salt Lake City, Utah. Contact Fred Jaeger, Voice 801-583-2000, Fax 801-583-6245.

E-Quest Sciences: Exploring The Micro-Fusion™ process. Seeking qualified research partners for their sonoluminesence program. Contact Russ George, FAX 415-851-8489.

Fusion Information Center (FIC): Research and development of new energy systems. The world's most complete resource depository for cold fusion research information, as well as other new energy research including zero-point energy; space energy research; electronic, electromagnetic, and mechanical over unity devices and more. We are the publishers for *Fusion Facts*, *New Energy News*, and *the Journal of New Energy*. Voice 801-583-6232, Fax 801-583-2963.

Holotec AG: Clean Energy Technology, contact André Waser, Gen. Mgr., Bireggstrasse 14, CH-6003, Luzern, Switzerland. Phone 011 41-41 360 4485, or Fax 011 41-41 360 4486.

Hydro Dynamics, Inc.: Hydrosonic Pump, heat-producing systems using electrical input with thermal efficiencies of 110 to 125 percent. Rome, Georgia. Contact James Griggs, Voice 706-234-4111 Fax 706-234-0702.

JET Energy Technology, Inc.: Design and manufacture of π-electrode systems, calorimeters, and associated equipment and systems. Consulting regarding radiation, materials, and other scientific and engineering issues. Weston, MA. Contact Dr. Mitchell Swartz, Voice 617-237-3625. Fax 617-237-3625.

Labofex, Experimental and Applied Plasma Physics: R&D of PAGD (Pulsed Abnormal Glow Discharge) plasma technology.

Applications under development include protable power supplies, electric vehicles and autonomous housing. Licensing. Ontario, Canada. Contact Dr. Paulo N. Correa. Tel 905-660-1040 Fax 905-738-8427

Magnetic Power Inc.: Supermagnets and supermotors; Solid-state, heat to electric transducers, for temperatures up to 300°F (cold fusion, waste heat, etc.). Featuring Ultraconductors™ under development by ROOTS, a subsidiary. Sebastapol, CA. Contact Mark Goldes, voice 707-829-9391, Fax 707-829-1002.

Nova Resources Group, Inc.: Design and manufacture ETC (Electrolytic Thermal Cell); EG (commercial power cogeneration module); and IE (integrated electrolytic system). Denver, CO. Call Chip Ransford, Phone 303-433-5582.

UV Enhanced Ultrasound: Cold Fusion Principle being used for an ultrasonic water purifier. Hong Kong. FAX 852-2338-3057.

"YUSMAR"- Scientific-Commercial Company: manufacture, licensing, research and development of water-based generators: thermal (5 sizes), electrothermal (up to 2 MW), and 'quantum' types. President: Dr. Yuri S. Potapov, 277012 Kishinev, Moldova. Phone and Fax 011-3732-233318.

Zenergy Corporation: Founded in 1996 to facilitate the introduction of commercially viable energy alternatives. 390 South Robins Way, Chandler, AZ 85225. Contact Reed Huish: 602-814-7865, Fax 602-821-0967, e-mail: info@zenergy.com

Note: The Fusion Information Center has been acting as an information source to many of these companies. We expect to augment our international service to provide contacts, information, and business opportunities to companies considering an entry into the enhanced energy market.

INFORMATION SOURCES

Academy for New Energy (ANE) is a subsidiary organization to the International Association for New Science, which has specific goals directed toward the field of alternative and "New" energy research. 1304 S. College Ave., Fort Collins, CO 80524. Tel. 970-482-3731

ANE Newsletter, quarterly publication of ANE, providing an open forum for discussion, and disseminating newsworthy and inspirational information on invention and new energy. Edited by Robert Emmerich.

Advanced Energy Network Newsletter, quarterly, a reprint of articles and papers from other energy publications, with book reviews and worldwide conference list. Advanced Energy Network, P.O. Box 691, Rondebosch 7700 Capetown, Rep. South Africa.

"Cold Fusion", monthly newsletter, edited by Wayne Green, 70 Route 202N, Petersborough, NH 03458.

Cold Fusion Times, quarterly newsletter published by Dr. Mitchell Swartz, P.O. Box 81135, Wellesley Hills MA 02181. Home Page: http://world.std.com/~mica/cft.html

Cycles, a R&D newsletter, published by Dieter Soegemeier, Editor, GPO Box 269, Brisbane, QLD.4001, Australia. Phone/Fax: +61 (0)7 3809 3257.

Electric Spacecraft Journal, quarterly, edited by Charles A. Yost, 73 Sunlight Drive, Leicester, NC 28748.

***Fusion Facts* monthly newsletter.** Salt Lake City, UT. 801-583-6232, also publishes Cold Fusion Impact and Cold Fusion Source Book. Plans on-line database access.

Fusion Technology, Journal of the American Nuclear Society, edited by Dr. George Miley, publishes some papers on cold nuclear fusion. 555 N. Kensington Ave., La Grange Park, IL 60525.

Infinite Energy, new bi-monthly newsletter edited by Dr. Eugene Mallove (author of Fire from Ice), P.O. Box 2816, Concord, NH 03302-2816. Voice: 603-228-4516. Fax: 603-224-5975 E-mail 76570.2270@compuserve.com

Institute for New Energy (INE), organization to promote and help find funding for new energy research. Home Page: www.padrak.com/ine/ contains many important scientific papers and current reports on all areas of research. E-mail: ine@padrak.com Salt Lake City, Utah. Voice 801-583-6232, Fax 801-583-2963.

New Energy News monthly newsletter for INE, highlighting the research and development in the worldwide new energy arena. Edited by Hal Fox.

Journal of New Energy, quarterly, presenting papers representing the new areas of energy research, leading-edge ideas in the development of new energy technology, and the theories behind them. Published by the Fusion Information Center, Inc. Editor: Hal Fox.

KeelyNet BBS - Science and health oriented information exchange that specializes in nonstandard research, much of it on new energy. Jerry Decker, 214-324-3501 Internet: www.keelynet.com E-mail: jdecker@keelynet.com

Planetary Association for Clean Energy Newsletter, quarterly, edited by Dr. Andrew Michrowski. 100 Bronson Ave, # 1001, Ottawa, Ontario K1R 6G8, Canada.

Now available: *Clean Energy Review*, a technical and scientific discussion on nuclear fuel wastes disposal. Discusses transmutation as one possible solution. $5 U.S. and Canadian, $7.50 other countries.

Space Energy Journal, quarterly, edited by Jim Kettner & Don Kelly, P.O. Box 1136, Clearwater, FL 34617-1136.

The above list of commercial and information sources will be growing. New listings will be added as information is received. Send information to *NEN*, P.O. Box 58639, Salt Lake City, UT, 84158.

OBSERVATION OF HEAVY ELEMENTS PRODUCED DURING EXPLOSIVE COLD FUSION

TAKAAKI MATSUMOTO and KAZUYA KUROKAWA
Hokkaido University, Sapporo 060, Japan

COLD FUSION

TECHNICAL NOTE

KEYWORDS: *explosive cold fusion, many-body fusion reaction, element production*

Received March 19, 1991
Accepted for Publication May 6, 1991

Many-body fusion reactions may take place during cold fusion. Heavy elements are observed that might have been produced by such reactions during electrolysis of heavy water. Elements such as sodium, magnesium, aluminum, and zinc are observed inside grain-shaped defects in a palladium rod used in a cold fusion experiment.

INTRODUCTION

This technical note describes two subjects: (a) an attempt to cause explosive cold fusion by moving hydrogen through metal and (b) the observation of heavy elements produced by many-body fusion reactions.

Reference 1 indicates that cold fusion takes place in the grain boundaries of a host metal by hydrogen chain reactions. If the concentration of hydrogen exceeds a critical value, direct cold fusion chain reactions can be ignited locally in bursts. When hydrogen atoms are forced to move in metal, they might be stored in layers between media with different structures or properties, and the concentration of hydrogen atoms in those places could be increased far beyond the critical value. Thus, the hydrogen might be burned in bursts or very rapidly, i.e., explosively.

On the other hand, the Nattoh model[2] has indicated that three- and four-body fusion reactions that produce lithium and beryllium, respectively, can take place during cold fusion. Furthermore, many-body fusion reactions that produce much heavier elements could occur under suitable conditions. Microscopic observations of palladium metal used for a cold fusion experiment[3] have shown that as cold fusion proceeds, tiny spot defects grow into grain-shaped defects in which materials disappear by extraordinary burning. The formation processes of the grain-shaped defects seem complicated, but it is highly probable that many-body fusion reactions take place to produce heavy elements.

In the grain-shaped defects, two processes may occur by which heavier elements, rather than direct fusion products such as helium, might be produced during cold fusion: (a) a many-body fusion reaction of hydrogen atoms or (b) transmutation of the host element. The first process produces heavy elements from light hydrogen atoms instantaneously by many-body fusion reactions or sequentially by absorbing hydrogen atoms or electrons. This is similar to processes that take place to form cold stars such as the Earth. The second process produces elements with masses similar to that of the host metal by absorbing hydrogen atoms or electrons.

EXPLOSIVE COLD FUSION EXPERIMENT

An effort to produce explosive cold fusion has been attempted by moving hydrogen atoms inside palladium metal, and the production of heavy elements has been examined.

Hydrogen atoms were charged into palladium metal by electrolyzing heavy water (mixed with 3% NaCl). A palladium rod (5-mm diam × 46.4 mm long) was used as the cathode with a helical wire for the anode. The current was 0.8 to 1.0 A with a 5-V bias. Figure 1 shows the arrangement of the palladium in the cell. After hydrogen was heavily accumulated in the metal, the level of water was decreased to uncover the top of the palladium metal so that hydrogen could easily escape from the top of the palladium metal and an upward flow of hydrogen could be induced. This procedure was performed after a 19-day hydrogen charging period. A small-scale explosion occurred several hours later. (The same procedure had been tried twice earlier but with no explosion because insufficient hydrogen had been accumulated.) As a result of the explosion, an upper plug and a cell cap flew out. This explosion was caused by a hydrogen chemical reaction; it is shown later that cold fusion contributed to heat generation.

The palladium metal used for this experiment was examined by an optical microscope, a scanning electron microscope (SEM), energy dispersive X-ray spectroscopy (EDX), and radioactive analysis. Gas in the metal also was analyzed by mass spectroscopy.

RESULTS

Figure 2 shows a flowchart of the experiment. The palladium metal also underwent radioactive analysis; the results are reported in Ref. 4.

Figure 3 shows an optical microscopy picture of a longitudinal cross section of the palladium metal. It clearly shows that cold fusion has taken place violently near the surface of

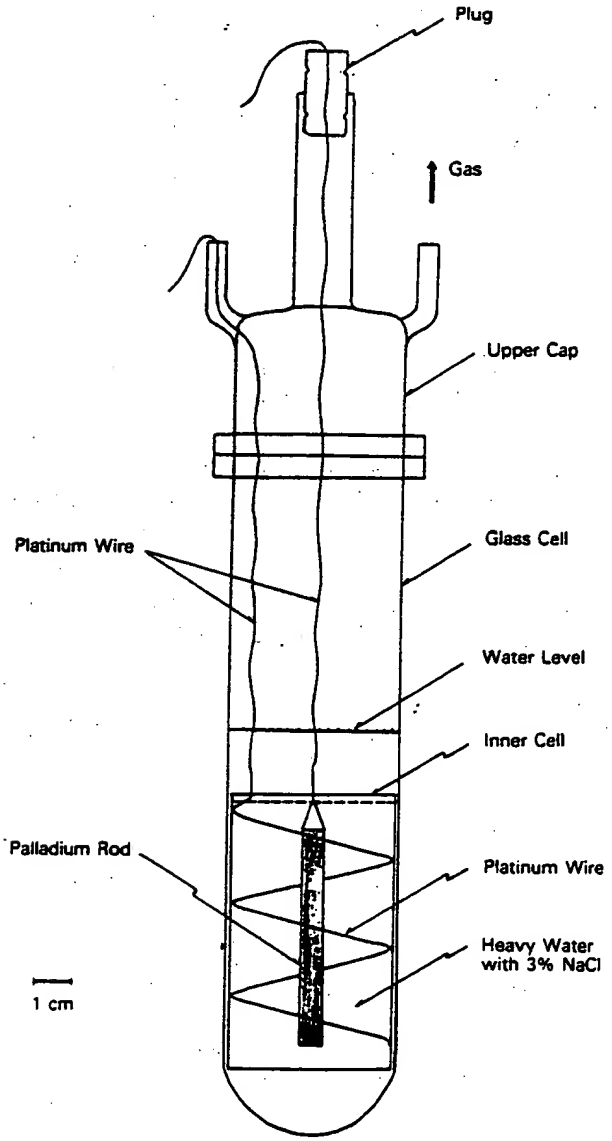

Fig. 1. Arrangement of cell.

the palladium. The surface layers seem to have acted as barriers against hydrogen escape so that hydrogen is heavily concentrated under the surface. Figure 4 shows an interesting burn pattern: A series of grain-shaped defects are arranged along an inclined layer that might have prevented the upward flow of hydrogen.

The gas contained in the metal was analyzed by mass spectroscopy before and after the electrolysis experiment. Before the experiment, gas was discharged by keeping the palladium metal at 800°C in vacuum for >10 h. It has been confirmed that the mass spectrum gives no signal except flat background. Figure 5 shows the mass spectra after the experiment, measured while increasing the temperature from room temperature to 775°C and keeping it at 775°C. Figure 5a shows the spectrum measured at 175°C while increasing the temperature; several remarkable peaks can be seen at masses 2, 3, 4, and 6 in the light region and masses 17, 18, 19, and 20 in the heavy region. Figure 5b shows the spectrum at 775°C measured ~1 h later; the peak for mass 6 disappears. Figure 5c shows the spectrum at 775°C ~2 h later still; only the peaks of masses 2, 3, and 4 remain.

Figure 6 is a SEM picture of a longitudinal cross section showing grain-shaped defects produced near the surface of the metal. The right side is a palladium region, and the left side is a copper region plated on to clarify the boundary of the surface. Pointlike analyses were made by EDX with SEM. Figure 7 shows an EDX spectrum at point A in Fig. 6. The two main peaks at 2.84 and 3.00 keV correspond to characteristic X rays emitted from palladium. In addition to the host element, the very heavy elements of ruthenium and indium can be clearly seen at the energies of 2.56, 3.30, and 3.50 keV, respectively. Reference 4 shows that the ruthenium and indium are produced by transmutation of palladium. This energy spectrum is standard here; similar patterns have been observed elsewhere over palladium metal. For example, the energy spectra at points of B, C, and D in Fig. 6 are almost the same.

Figure 8 is an SEM picture of a grain-shaped defect in which the materials are left somewhat unburned. Figure 9 shows an EDX spectrum at point E in Fig. 8. The energy spectrum is different from the standard one. It is remarkable that elements such as silicon, sulfur, and calcium exist among the materials remaining inside the grain-shaped defects.

Figure 10 shows a SEM picture of another grain-shaped defect. Figure 11 shows an EDX spectrum at point F. The elements sodium, magnesium, aluminum, silicon, calcium, and copper can be recognized.

Figures 12 and 13 show SEM pictures of a radial cross section. Figure 14 shows an EDX spectrum of point G in Fig. 12. Figures 15, 16, and 17 show EDX spectra at points H, I, and J, respectively. The EDX spectrum depends not only on the grain-shaped defects but also on their position.

Finally, the weight of the palladium metal was measured by an electric balance before and after the experiment; the values were 11.3497 and 11.3506 g, respectively, which are very similar. The latter value was obtained after gas discharging; before gas discharging, the value was 11.53 g.

DISCUSSIONS

Explosive cold fusion was easily performed by moving hydrogen in palladium metal, and experimental evidence suggesting the occurrence of explosive cold fusion was observed. Although the explosion was caused mainly by a chemical reaction of the mixed hydrogen and oxygen gas, it is reasonable to consider that fusion energy has also contributed to the explosion by decomposing water. It is not clear how much fusion energy has been consumed to decompose water to hydrogen and oxygen. Not only grain boundaries but also layers between media with different structures or properties could store hydrogen to induce explosive cold fusion. Multilayer materials might be more effective in increasing the power density. Explosive cold fusion might be available as an effective engine for vehicles such as automobiles.

Cold fusion products have been sought using mass spectroscopy, SEM, and EDX. It is remarkable that heavy elements have been observed by EDX inside grain-shaped defects. The elements that have been recognized are neon, sodium, magnesium, aluminum, silicon, phosphorus, sulfur, chlorine, argon, potassium, calcium, titanium, chromium, iron, nickel, copper, and zinc. It is difficult to consider these

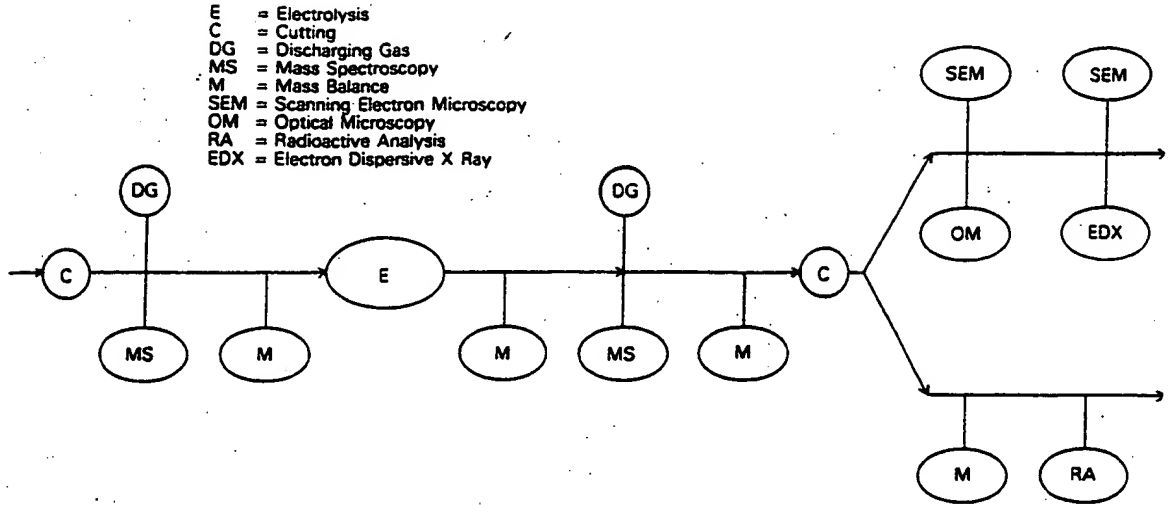

Fig. 2. Flowchart of experiment.

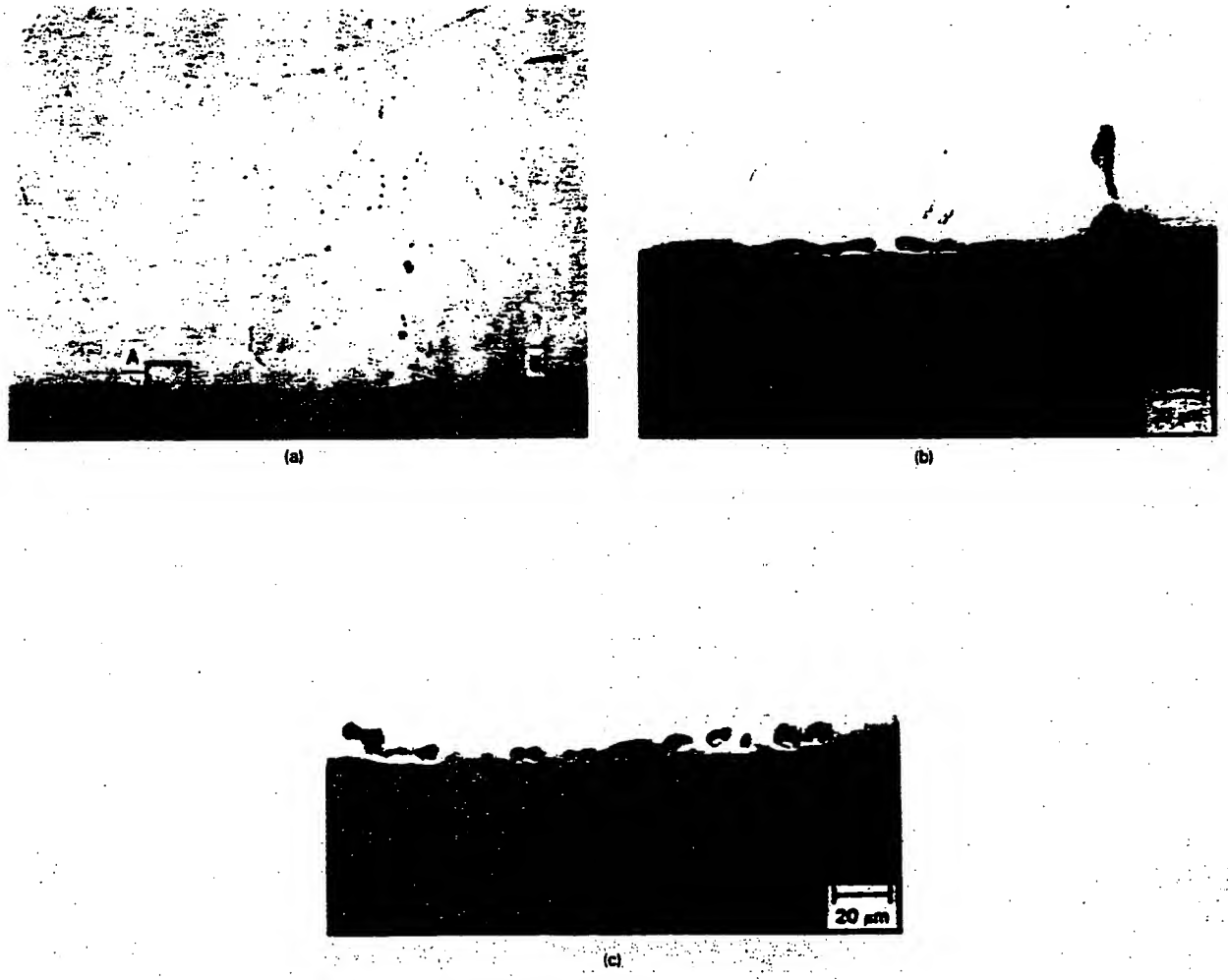

Fig. 3. Optical microscopy picture of the top region of the palladium rod: (a) magnified 38.5 times, (b) expanded at point A, and (c) expanded at point B.

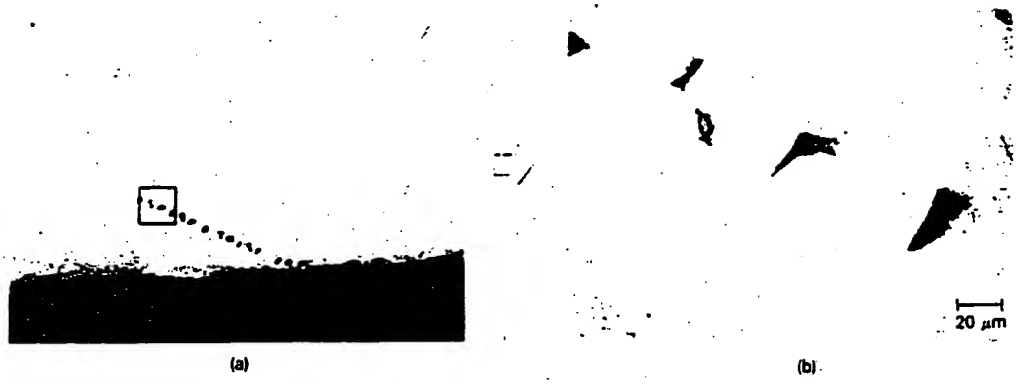

Fig. 4. Optical microscopy picture of grain-shaped defects: (a) magnified 28.5 times and (b) expansion of area indicated in the square.

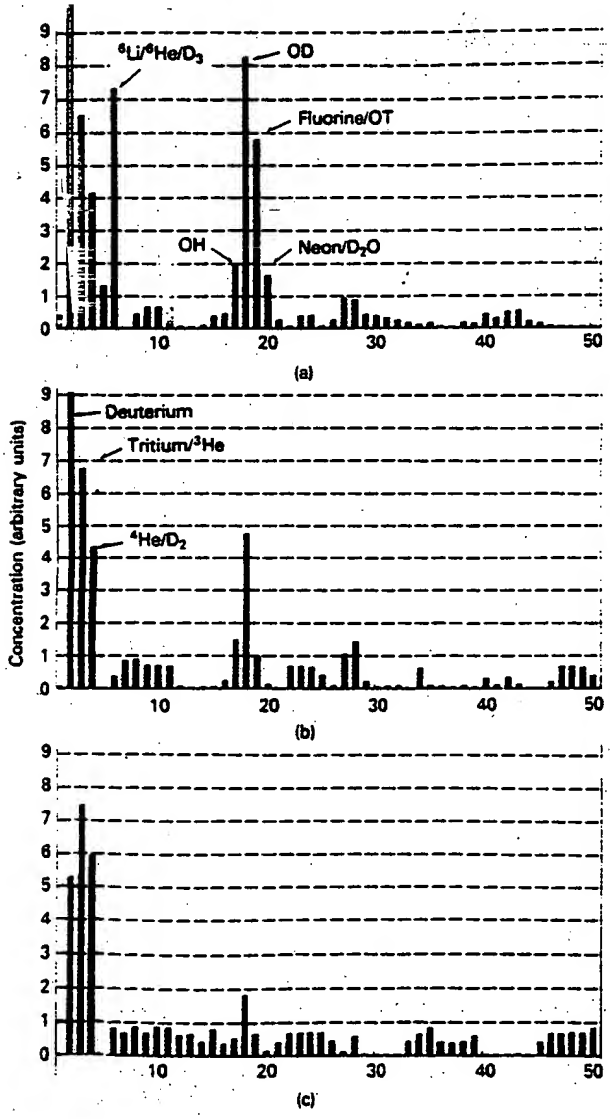

Fig. 5. Mass spectrum of discharged gas: (a) at 175°C, (b) at 775°C −1 h later, and (c) at 775°C −2 h later still.

Fig. 6. SEM picture of a longitudinal cross section (297.5×).

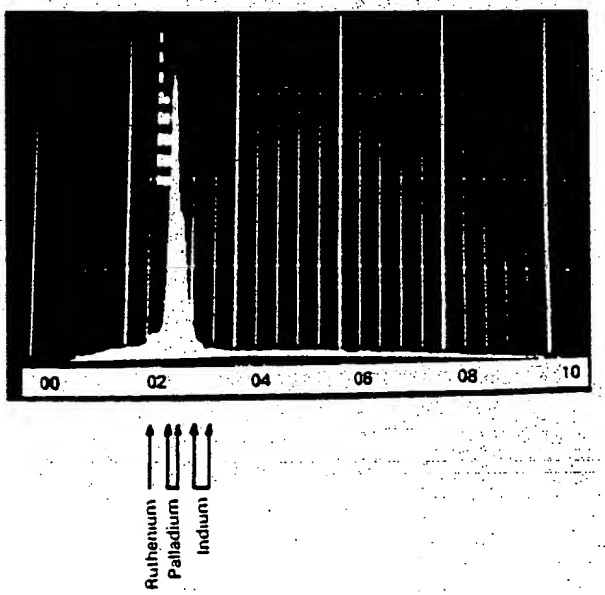

Fig. 7. EDX spectrum for point A in Fig. 6.

Fig. 8. SEM picture of a grain-shaped defect (935×).

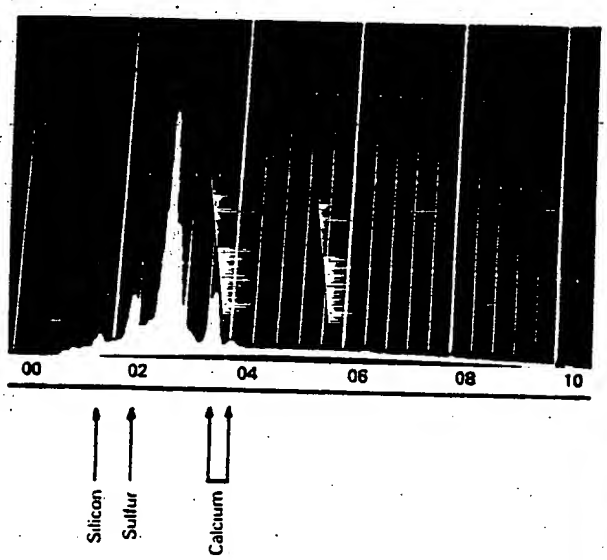

Fig. 9. EDX spectrum for point E of Fig. 8.

Fig. 10. SEM picture of another grain-shaped defect (595×).

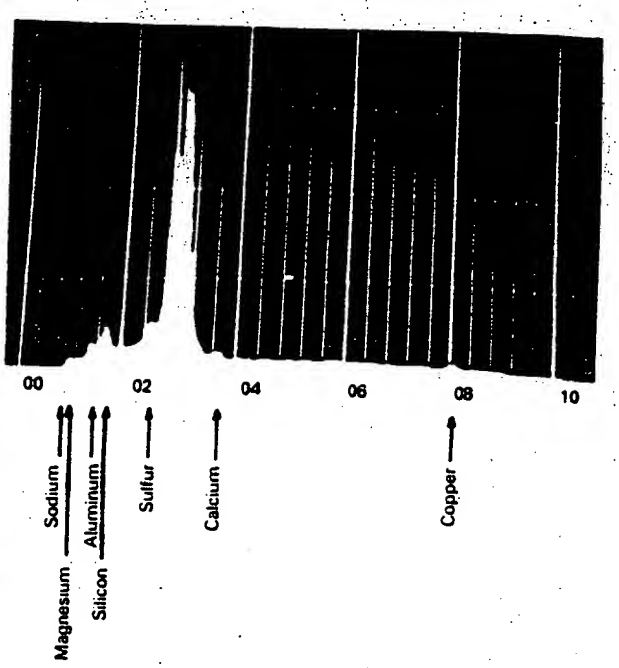

Fig. 11. EDX spectrum for point F.

Fig. 12. SEM picture of a radial cross section (1800×, unpolished).

Fig. 13. Another SEM picture of a radial cross section (1800×, unpolished).

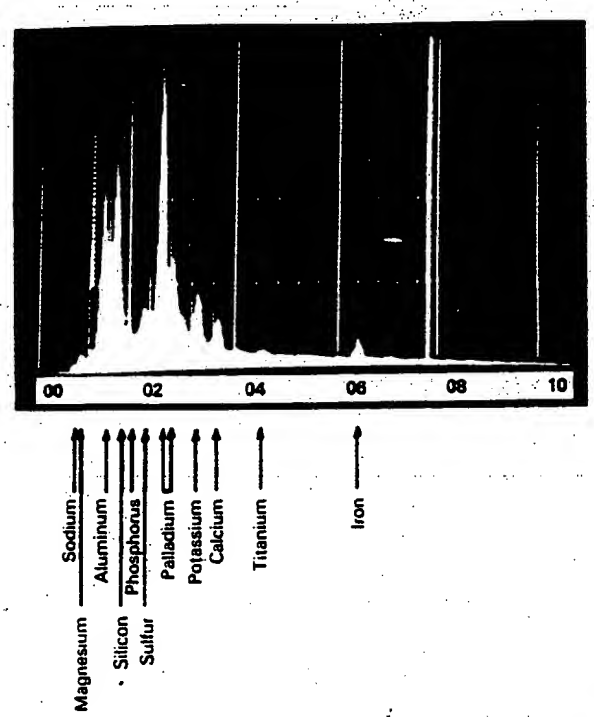

Fig. 14. EDX spectrum of point G.

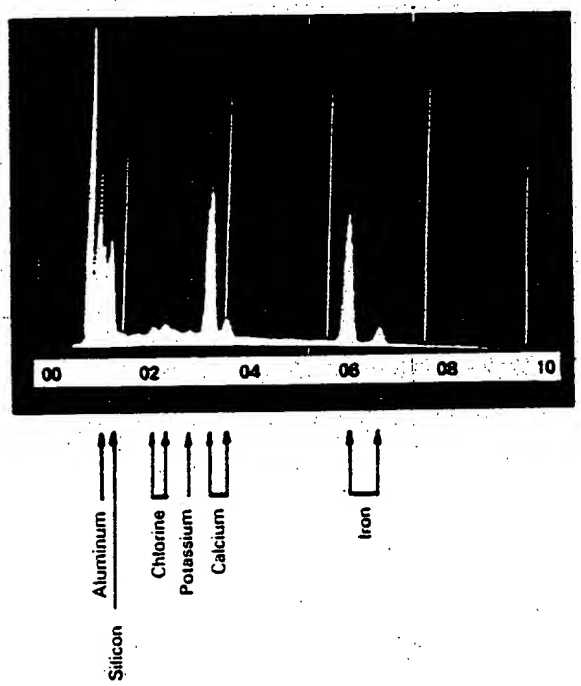

Fig. 15. EDX spectrum of point H.

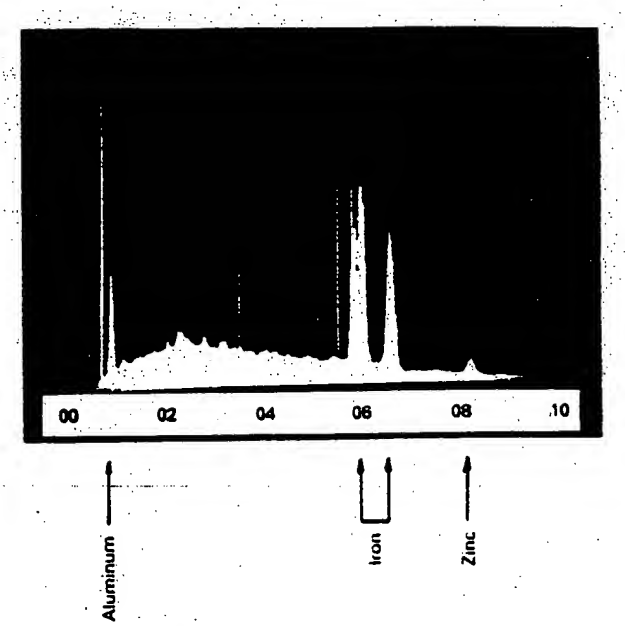

Fig. 16. EDX spectrum of point I.

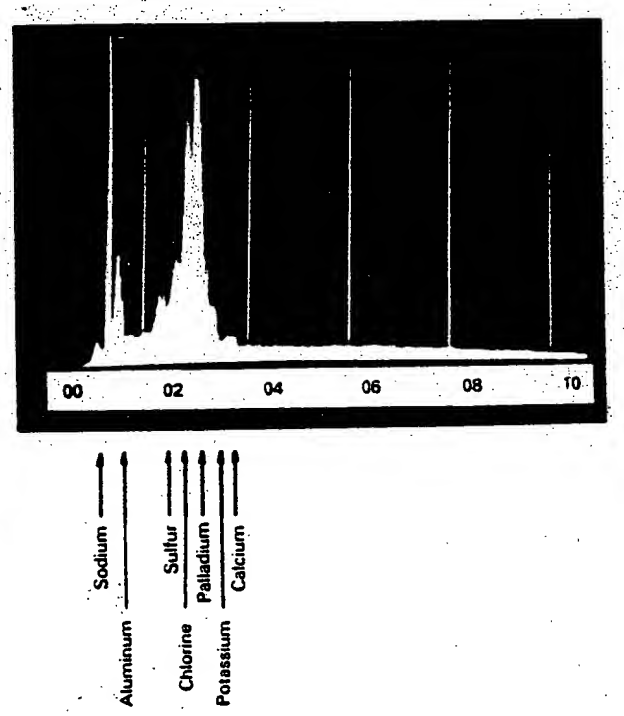

Fig. 17. EDX spectrum of point J.

elements to be impurities. It can be concluded that these elements have been produced by many-body fusion reactions instantaneously or sequentially, as predicted by the Nattoh model.[2] The materials remaining inside grain-shaped defects have extremely different mass distributions, which suggests that the distribution might depend on how much many-body fusion reactions have occurred. No elements heavier than zinc have been observed up to the present. Since fusion reactions that produce heavier elements have negative reaction energies, it is difficult to produce them at a high rate. It needs a higher burning rate.

Strange petals have been observed around the grain-shaped defects, as shown in Figs. 6, 8, and 10. These had not been seen in earlier observations[4]; the etching process applied might have washed them out. The petals might consist of elements lighter than sodium because the EDX system used here cannot be applied to elements lighter than sodium.

Mass spectroscopy of discharged gas shows that light elements or molecules of mass 2, 3, 4, 6, 17, 18, 19, and 20 have been produced. These can be classified into two groups: (a) those with masses of 2, 3, and 4 and (b) those with masses of 6, 17, 18, 19, and 20. The former have been produced inside the metal and the latter near the surface. The probable identifications are shown in Fig. 5. However, all these identifications are not definite as there are multiple candidates. An EDX analysis applicable to those light elements is now planned.

Although clarifications are still needed in the light element region, it has been verified that heavy elements such as titanium, iron, and copper can be produced directly by electrolyzing seawater. These materials are by-products of energy production; thus, industrial nuclear alchemy can be expected in the future.

ACKNOWLEDGMENT

The authors thank Y. Hayashi of the Nuclear Fuel Development Company, Ltd., for his useful discussions on the defects inside the metal.

REFERENCES

1. T. MATSUMOTO, "Progresses of the Nattoh Model and New Particles Emitted During Cold Fusion," *Proc. Int. Conf. Anomalous Nuclear Effects in Deuterium/Solid Systems*, Provo, Utah, October 22–24, 1990.

2. T. MATSUMOTO, "'NATTOH' Model for Cold Fusion," *Fusion Technol.*, **16**, 532 (1989).

3. T. MATSUMOTO, "Microscopic Observation of Palladium Used for Cold Fusion," *Fusion Technol.*, 19, 567 (1990).

4. T. MATSUMOTO and K. KOBAYASHI, "Radioactive Analysis of Palladium Used for Explosive Cold Fusion," to be submitted to *Fusion Technol.*

Fifth International Conference on Cold Fusion
9-13 April, 1995 - Monte Carlo, Monaco
ICCF5 ©1995

Concerning Reproducibility of Excess Power Production

M. C. H. McKUBRE, S. CROUCH-BAKER, A. K. HAUSER,
S. I. SMEDLEY, F. L. TANZELLA, M. S. WILLIAMS, S. S. WING
SRI INTERNATIONAL
Menlo Park, CA 94025 (USA)

Abstract

An apparent irreproducibility in the production of an, as yet, anomalous excess power from Pd cathodes electrochemically loaded with D can be associated with irreproducibility in the attainment of several necessary starting conditions. Of these, the threshold loading (D/Pd atomic ratio) has received the most attention. A statistical analysis is presented of the results of 176 experiments intended to test the means of establishing reproducible control over D/Pd loading. A set of variables are examined, and procedures identified which permit the attainment of loading above the threshold necessary for excess heat production.

Calorimetric results from two experiments are presented and analyzed. A mathematical function is identified which correlates closely with the time evolution of excess power. An important element of this correlation is the measured rate of change of the cathode resistivity. We have interpreted the resistance change as indicating the presence of an oscillation or "breathing" of the cathode loading induced by a flux of deuterons through the cathode/electrolyte interface.

The observed functionality of excess power with deuteron flux above a loading threshold, conforms closely with theoretical predictions.

1. Introduction

Six years have passed since publication of the defining paper of Fleischmann, Pons and Hawkins.[1] In this time, scientific progress has been made to resolve issues that were quickly, and easily, anticipated. The resolution of some important issues has been accompanied by a slow, somewhat unsteady, but certain growth in the field of science which has come to be called "cold fusion".

At the time of that publication, few would have suspected after six years of study, that the field revealed would have survived, but not thrived. This surprising situation has come about because, in restraint of progress, stand two technically challenging problems:

i) Irreproducibility. This is not, as some have argued, an irreproducibility of results. It is a difficulty in achieving reproducible starting conditions for comparative experiments.

ii) Scarcity of energetic (nuclear) products. It is quite clear that the nuclear product(s) quantitatively associated with excess heat, if there is one, is not an energetic particle, or penetrating radiation, or a radioactive isotope; this makes the search very difficult.

In this paper, an attempt is made to address the first of these difficulties, with specific attention to the reproducible attainment of positive heat excess in the D/Pd system, under electrochemical conditions.

2. Necessary Conditions

We need first to identify the experimental starting condition thought, or observed, to be associated the phenomenon under study. In a series of papers SRI[2-7] and others[8,9] have attempted to define and quantify the variables associated with apparent excess heat production. These are:

i) Loading. The D/Pd loading seemed, at the outset, to be a likely controlling variable; this has clearly been shown to be the case. The loading is relatively easily measured; the attainment and maintenance of high loading (D/Pd $\geq$ 0.9), is not easily controlled. Independent experiments at SRI[4] and IMRA-Japan[8] have demonstrated a roughly parabolic functionality between excess power and loading above a loading threshold of D/Pd ~ 0.84 $\pm$ 0.02. In order to achieve appreciable (and measurable) power excess, loadings much higher than the threshold are needed (D/Pd $\geq$ 0.9 and preferably $\geq$ 0.95). Several other factors also are necessary.

ii) Current Density. In an electrochemical experiment, current density affects loading. In addition to this expected, but complex, functionality, the interfacial current density also directly affects the rate of excess heat production. In experiments performed under nearly isothermal conditions at nearly constant loading, a linear dependence of excess power is observed with increasing current density above the threshold value. Unlike the loading threshold, the current density threshold displays considerable variability ranging from ~ 100 to ~ 400 mA cm^{-2} in different experiments, or in the same experiments, at different times.

iii) Initiation. Many authors have reported a delay in the onset of excess heat production. Even after the loading and current density thresholds have been usefully exceeded, excess heat is (generally) not observed until a significant time has elapsed, on the order of 300 h for 1-4 mm dia. Pd wires. It is apparent that some initiation process must occur, presumably within the Pd lattice. At this stage, the origin is unclear.

iv) Disequilibrium. It has long been suspected that a flux of deuterium atoms through the interface is needed in addition to high deuterium atom loading, to produce measurable excess power. Recently theoretical arguments have been advanced to support the conjecture that flux, combined with high loading are necessary for excess heat or nuclear product formation. In this paper, we present experimental evidence of this, and attempt to quantify the role of deuterium interfacial flux in excess power production.

3. Loading

The attainment of high D/Pd loading is critical to the appearance of excess power. We previously have presented evidence[2-7] that, in every case that we have observed in a calorimeter, where a cathode achieved a maximum loading of D/Pd ≥ 0.95 while meeting criteria (ii) and (iii) above, excess power was measured ($P_{xs} > 0$). For cathodes achieving maximum loadings $0.90 \leq D/Pd < 0.95$, approximately half exhibited $P_{xs} > 0$. In only one case for which the maximum loading was less than 0.90, have we observed $P_{xs} > 0$. This case will be discussed later in this paper, as it is instructive.

Attainment of these high loadings, while clearly critical, is neither usual, nor can it be achieved reproducibly. An analysis is presented here of the results of 214 experiments, both loading and calorimetric, representing 200,416 hours of experiment operation (or 23 experiment-years). All experiments employed Pd cathodes, and loading was measured using a four terminal resistance method.[3,7,10]

From this set of 214 experiments, the data from 38 have been excluded by reason of poor resistance measurement, premature failure, or suspected compromise, leaving 177,640 hours of reliable data, (20 experiment-years). The following Tables show the material sources, electrolytes and additives employed.

Table 1. Metal Sources

Engelhard			Various		
E1	32*	Engelhard Lot #1	AE	1	AECL**
E2	24	Engelhard Lot #2	AM	4	Aithaca Metals
E3	38	Engelhard Lot #3	IB	4	Ingot Block - cast
E4	4	Engelhard Lot #4	JM	40	Johnson Matthey
E5	15	Engelhard Lot #5	NL	5	NRL†
E-	6	Engelhard 1mm	ZR	1	Zone Refined

* Number of experiments

** AECL Atomic Energy of Canada Ltd (Cast, High Purity)

†NRL Naval Research Laboratories (High Purity). 30 and 600 μ grain sizes.

Table 2. Electrolytes, Additives and Variables

Electrolytes			Additives††		Variables
3	0.5 D_2SO_4	D	71	None	Additive
6	0.5 Li_2SO_4	D	68	Al	Annealing
158	1.0 LiOD	D	10	Ni†††	Cathode machining
2	0.3 M LiCl	D	6	B	Diameter
1	0.1 M LiOD	D	6	Cu	Experiment length
1	0.5 Li_2SO_4	H	6	Poison*	Metal source
4	1.0 LiOH	H	3	Si**	
1	0.1 M LiOH	H	2	Be	

* Additional series of experiments were performed specifically to test the effects of classical hydrogen recombination poisons and the effect of their concentrations. The results of these have not been included in this data set.

** All experiments were performed in quartz vessels and/or with quartz structures in the electrolyte. Si, was therefore present in increasing amounts as this element dissolved. For these three cases, additional Si was added as SiO_2 dissolved in electrolyte.

†† For the 176 cases analyzed here, when present, additive concentrations were ~ 200 ppm.

††† These 10 experiments employed Ni anodes not additives.

Each experiment has been characterized by the maximum loading attained by the cathode, at any time during the experiment (the average experiment length was 1009 hours). Twelve approximately equal groups were defined, according to the mean loadings shown in Table 3. An exhaustive analysis of these results is presented elsewhere.[11] The purpose here is to focus attention on those variables that strongly influence loading; this we can do with a relatively simple analysis.

The results in Table 3 show great dispersion, with a significant number of experiments achieving a maximum loading of only 0.74 (just beyond the maximum in R/R°), while an equal number apparently exceed 1.0 (R/R° ≤ 1.5 on the right hand side of the maximum). At this point, it is worth remembering that the experiments analyzed here represent our "best efforts" to attain high loading; 57% of all experiments reported in Table 3 achieved our stated target of 0.9.

Table 3. Maximum Loading

Group	Mean	#	Quartile	Group	Mean	#	Quartile
1	0.74	14	4	7	0.92	13	2
2	0.75	13	4	8	0.93	1	2
3	0.83	18	4	9	0.94	15	2
4	0.87	14	3	10	0.95	13	1
5	0.89	13	3	11	0.96	16	1
6	0.90	16	3	12	1.02	14	1

We are interested in the variables, of those examined, which affect the attainment of high loading. We have divided the results into quartiles. Very roughly, we are interested in the correlation between the experimental variables, and attainment of the first (preferably) or first and second quartiles. In Table 4 we indicate the variable, the number of experiments in that set, the percentage attaining the first quartile, and the percentage attaining the first or second quartile.

Table 4. Variables Affecting Loading Quartiles

	#	First	First or Second
Pd Lot Variation:			
E1	32	53%	78%
E2	24	29%	67%
E3	38	26%	42%
Not {E1,E2,E3}	82	12%	38%
E5	15	13%	80%
JM	40	18%	35%
Additives:			
Al	68	34%	57%
Ni	10	0%	0%
None	71	17%	48%
Physical Variables:			
Machined	39	36%	77%
d<0.25 cm	42	14%	26%
t>1009 h	70	34%	63%

Table 4 reveals a striking variation between Pd samples, even in lots from the same manufacturer. For Engelhard Lot#1 (E1), 53 % loaded into the first quartile while 78 % reached the first two quartiles. Whatever property this material had (or, critical flaw it did not have), there was less of it in subsequent lots, which exhibited generally inferior behavior.

For various samples from Johnson Matthey (JM), the pattern is not so clear. On average, these materials performed poorly (although better than other samples in the not {E1, E2, E3} set). The distribution for all JM samples is, however, bimodal, exhibiting a peak in Group 5 and another in Group 12.

For the effect of additives, only Al and Ni were sampled in statistically significant numbers. For Al, the effect is moderately strong and positive; for Ni (in this cases as an anode, not an additive) the effect is strong and deleterious. The set with no additives {None} loaded less well, on average, than those with deliberate additives.

In the final category, strong effects are seen for machining, cathode diameter, and experiment duration. "Machined" refers to those cathodes for which the outer surface was removed mechanically, by a cutting tool, in a lathe. In this process, the radius (of a 1/8" or 3mm diameter) cathode was reduced by ~ 0.1mm (respectively to 3mm or 2.8mm diameter), in a single pass of the cutting tool. This process appears to be beneficial in removing surface inclusions and mechanical defects, and in promoting loading.

In our experiments, smaller diameter wires ($d < 0.25$ cm) have not loaded, on average, as well as cathode 2.8 mm in diameter and larger. It should be noted that none of the smaller diameter wires were machined prior to electrolysis.

The final variable, duration of experiment, needs to be interpreted with care. Experiments longer than average ($t > 1009$ h) correlate with high loading. This reflects two factors. Cathodes which initially load poorly (fourth quartile) tend not to respond with better loading following anodic stripping or chemical addition, and these experiments often were terminated early. Cathodes which initially load at least into the third quartile, often display increased loading after anodic stripping cycles with or without chemical addition. This improvement may continue in several sequential loading cycles, each of which may require 200-400 hours. Such experiments tend to be longer than average and to result in better than average loading.

4. Metallurgical Variables in Loading

It is clear from Table 4, that the metal, itself, plays a role in determining the maximum loading. One might propose, as a hypothesis, that a difficulty in attaining reproducible starting conditions, in this case threshold loading, is due in large part to an uncontrolled variable contained within the Pd stock. Anticipating this possibility, the 176 cathodes analyzed in this paper were all prepared from moderate to high purity Pd. All were subjected to a similar annealing process (800-850°C for 2-3 hours, in low O_2 Ar, vacuum, or D_2 gas). With only one or two exceptions, all were etched with aqua regia (appropriately light or heavy) after machining and annealing. These procedures were intended to assert a uniform bulk and surface condition on the cathodes; nevertheless, significant variability was encountered between and within Pd lots.

Several important questions are raised in this analysis:

i) What is the characteristic of a "good" material?
ii) What is the uncontrolled parameter?
iii) How can we control this parameter to yield consistently high loading?
iv) How can we maximize the loading for a "good" Pd sample?
v) Does this procedure work to optimize loading in "poor" Pd samples?

We can begin to answer some of these questions by further analysis of our loading data base. Examining Table 4 we see that the parameters associated with the attainment of high loading are: Metal Source; Machining; {Annealing}; {Etching}; {1M LiOD} + Al addition. { } is a parameter employed, but not tested statistically. At this point, it is worth noting that a significant variable, the presence of dissolved silicate in solution, has also not been tested in this data set. Previous experiments[12] have indicated that Si is critical for the attainment of high loading. In all of the experiments described here this species was provided adventitiously by dissolution of quartz components of the electrochemical cell.

We can therefore propose a "best" procedure to achieve loading, based on the set of parameters examined. In this procedure one would:

[0) Select a suitable material]
1) Machine the outer surface to remove surface inclusions and damage.
2) Anneal at low oxygen partial pressure, in the temperature range 800-850°C, for 2-3 hours.
3) Etch cathode (plus Pt contact wires) in freshly prepared (heavy) aqua regia, for 5-10 seconds.
4) Electrolyze in 1 M LiOD, freshly prepared (in a H_2O free environment), by the reaction of D_2O with high purity Li.
5) After electrolyte preparation, and shortly before electrolysis, include in the electrolyte a small piece of high purity Al foil, sufficient to yield 200 ppm when dissolved.

The results are shown in Table 5 for experiments in which this enumerated procedure was followed.

Table 5. "Best Procedure" for Loading

	#	Quartiles	
Procedures 1-4 (No additive)		**First**	**First or Second**
E1	11	27%	55%
E2-4	6	33%	83%
Other	10	10%	80%
All	27	23%	69%
Procedures 1-5 (Al additive)			
E1	8	88%	100%
E2-4	4	100%	100%
Other	9	22%	78%
All	21	62%	90%
Procedures 2-5 (No machine)			
E2-4	26	23%	50%

While the selection constraints are severe, and the numbers in each category are small, a clear pattern emerges. Without the addition of Al, Procedures 1-4 show a small benefit for the Engelhard samples but no significant effect for other samples. In the presence of Al, however, following Procedures 1-5 yields a striking and useful result for Engelhard samples, and a beneficial effect for all metal samples.

We cannot generally assess the influence of machining as all E1 samples were machined before use. Procedures 2-5 (with Al, no machining), results in no significant improvement in maximum loading for the set of Engelhard samples {E2-4}.

From the analysis presented here, one may conclude that surface machining, and the addition of Al to the electrolyte both are important in concert, but that neither has a strong influence, alone. This concerted action, or synergism, benefits both the "good" loading materials, specifically early Engelhard Lots, and other generally more difficult to load Pd samples. In the light of this discovery, we must focus attention on the underlying mechanisms of loading, in order to reveal the hidden variable which influences the reproducibility of loading.

5. Other Issues of Reproducibility

The D/Pd loading is clearly a critical element in attaining the conditions that have been shown to be necessary for excess heat production. In the past six years, the issue of loading, and its reproducible attainment for both the D/Pd and H/Pd systems, has been studied extensively and with renewed vigor. Our understanding, however, remains poor. Furthermore, other parameters have been shown to be critical for the reproducible attainment of excess power: interfacial current density; time delay or initiation. In neither case is the role of these variables, or the process(es) that they engender, understood. Either may contribute significantly to an (apparent) irreproducibility of effect.

Recent experimental results have indicated a significant mathematical correlation between the rate of excess heat production, and the rate of change of the Pd cathode resistance. This effect, if not monitored, may constitute another important factor in (apparent) irreproducibility. If monitored and understood this phenomenon may yield information about fundamental processes and the underlying mechanism of excess heat production.

We measure cathode resistance, using a four-terminal method[3,7,10], to monitor D/Pd loading. Two parameters importantly control the resistance of palladium: hydrogen isotope loading, and temperature. In the experiments to be discussed, we observed a periodic variation in Pd resistance with fundamental period ~ 2 hours ($\sim 10^{-4}$ Hz), the amplitude of which appeared to correlate directly with the magnitude of the excess power being measured simultaneously in a mass flow calorimeter.[6,7]

If we accept that R/R° and P_{xs} both are measured accurately, then, as an explanation for this correlation we offer two hypotheses:

i) The observed excess heat is sourced at one or more small regions within the cathode. Because of the small volumes, local heating of the cathode produces resistance fluctuations which are observed at effectively constant loading. In this hypothesis, the excess power is the "cause", and the resistance the "effect". Periodicity of the resistance (perhaps induced by local de-loading following local heating) should be

associated in this model with a periodicity in excess power with the same frequency. Such an effect is indeed, observed.

ii) One can propose an alternative hypothesis in which resistance fluctuations reflect the "cause" with excess power the "effect". Unless the source of excess heat is extremely localized, at the levels of average excess power observed (1-5 W cm^{-3}) one would expect changes in local temperature insufficient to cause a detectable resistance variation. In which case one must look to a change in loading to cause a change in resistance. Bulk loading changes by adsorption/desorption processes at the cathode/electrolyte interface; this is accompanied by a flux of deuterons orthogonal to, and through the interface. The rate of change of average loading ($\delta x/\delta t$) is thus related to the deuteron flux.

There has been a suggestion[13] that, above a critical loading threshold, the rate of excess heat production should be related to the deuteron flux (*i.e.* ~ $\delta x/\delta t$). For this reason we have chosen to analyze our data in terms of hypothesis (ii). It should, however, be remembered that an alternative hypothesis exists which is consistent with the experimental evidence so far obtained.

6. Results

Figure 1 presents the current density, loading and excess power, measured by the methods previously described,[2-7] for a 1 mm dia., 10 cm long Pd cathode. The palladium was obtained from Johnson Matthey, and was formed into the shape of a horizontal "lasso", and annealed by our normal procedure.[7] The electrolyte was 1.0M LiOD containing 200 ppm Al at the outset. Sufficient Cu was added, dissolved in LiOD, 156 hours before the data shown in Figure 1, to make the concentration ~ 3 ppm in the electrolyte.

Figure 1 shows, initially, the normal response of a cell producing excess power: P_{xs} rising with increasing current density and loading above threshold values. After ~ 2 days, however, the characteristic of P_{xs} at constant current density and (generally) decreasing loading, is unexpectedly dynamic. Furthermore excess power was observed in this cell at an unusually low maximum loading (D/Pd ≈ 0.88).

Examining closely the loading plotted in Figure 1 we see that this too is unexpectedly dynamic. For the first and last 24 hours shown, the amplitude of the variation in x is small, in the period around 608 h intermediate, but for the rest of the time the average loading shows a significant variation about the mean, with standard deviation ~ ± 0.002. These periods of greater dynamism in x correlate with those for which $P_{xs} > 0$.

Figure 1b shows in detail the period of transition between low and modest excess power after 608 hours of electrolysis. While the frequency of the oscillation in loading does not change significantly, during the time of increasing P_{xs} (at t > 620h), the amplitude of this oscillation increases by a factor of 3 or more. When converted to a flux the rate of change of net loading could be accommodated by an adsorption and desorption current density, of ~ 0.1 - 1 mA cm^{-2}.

Understanding that considerable approximation is involved, we will propose a simplified predictive function for P_{xs}, and test this against the time series data. Figure 2 shows the excess power data from Figure 1a compared to the test function,

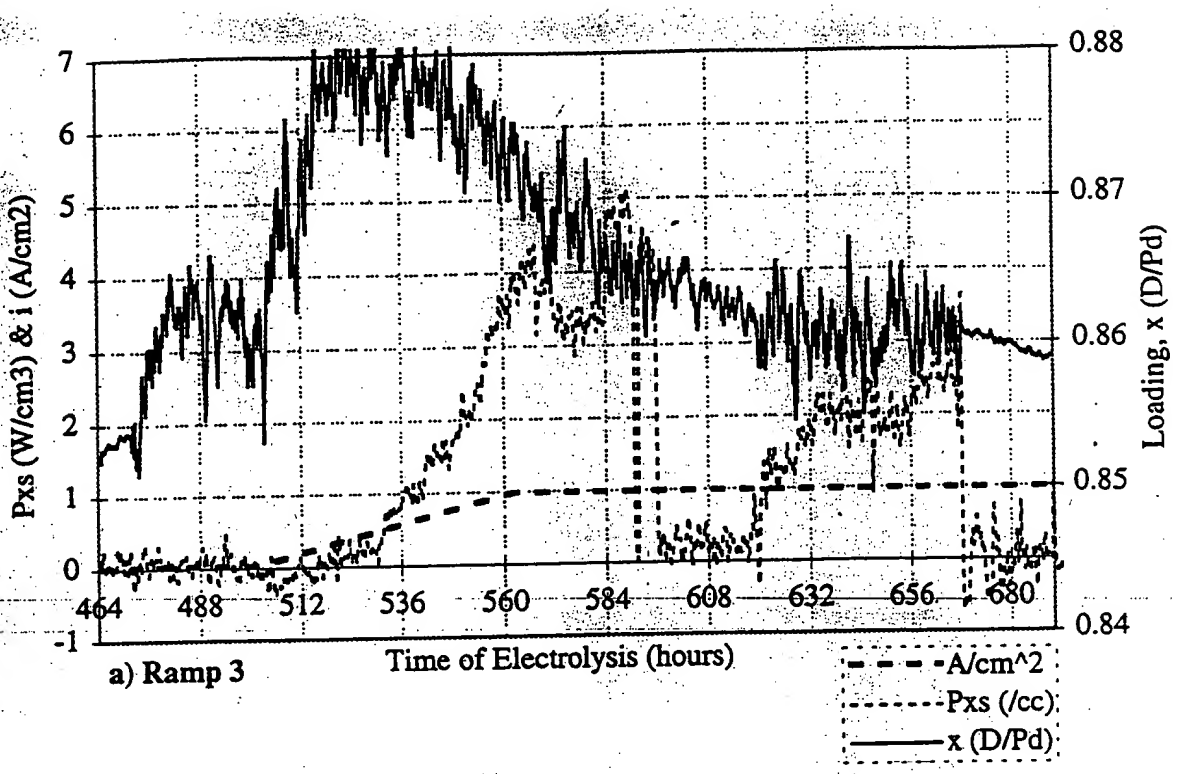

a) Ramp 3

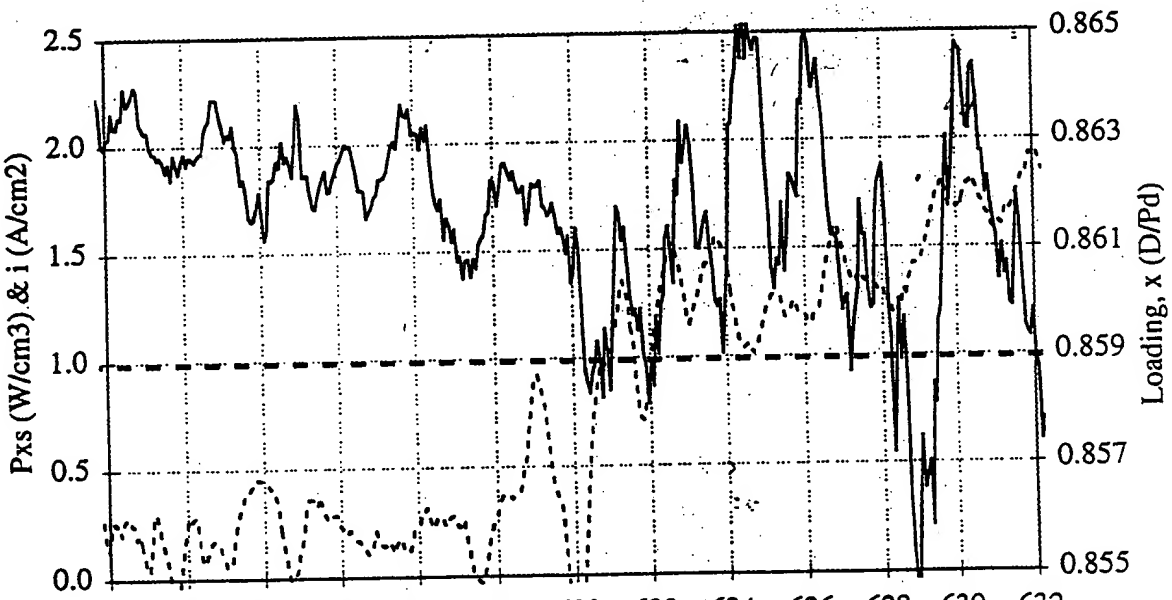

b) Detail

Figure 1 M4 Excess Power Current Density and Loading

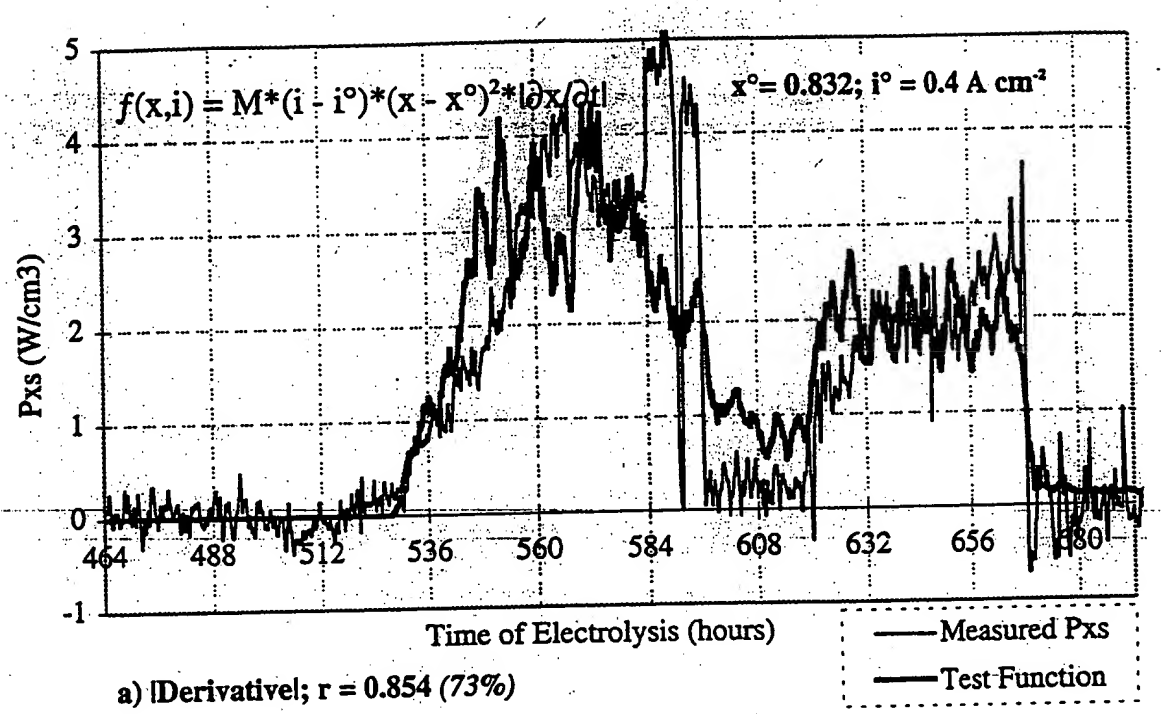

a) |Derivative|; r = 0.854 *(73%)*

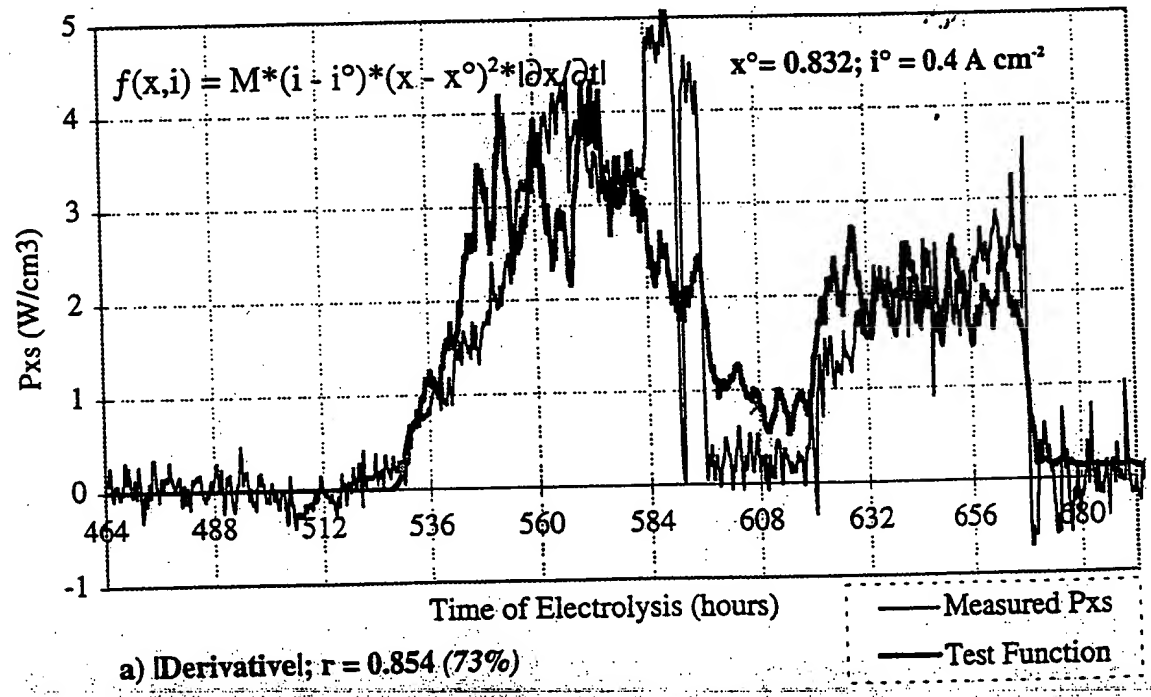

a) |Derivative|; r = 0.854 *(73%)*

Figure 2 M4 Excess Power and Fit Functions

$$P_{xs.test} = M\,(i - i^\circ)\,(x - x^\circ)^2\,|\delta x/\delta t|$$

The term $|\delta x/\delta t|$ assumes the importance of flux to be independent of sign, and gives no weight to a steady state flux. The proportionality constant, M, was determined to be 2.33×10^5 in order to set the two functions $P_{xs}(t)$ and $P_{xs.test}(t)$ to equal energy. The threshold values, x° and i° were determined by maximizing the correlation between these two functions. For the two data sets shown in Figure 2, the correlation coefficient, r = 0.854, with $x^\circ = 0.832$ and $i^\circ = 0.4$ A cm^{-2}

A value of 0.854 indicates that ~ 73% of the excess power is related linearly to our test function. Other variables may be involved (the test function is not complete) or the coefficients may not be precisely right or the component variables strictly independent (the test function is not completely correct); this is nevertheless a remarkable degree of correlation when the approximations and implications involved in generating the test function are considered.

A factor not taken into account in the simple correlation function is the possibility of temporal displacement between the two data sets. If one imagines that the test function is a generating function and the measured excess power is the response (that our test function is causal) then one might expect $P_{xs}(t)$ to be delayed with respect to $P_{xs.test}(t)$, and to have large amplitude (high frequency) features somewhat smoothed. Close inspection of Figure 2 reveals that this may indeed be the case; an analysis of the cross correlation function will be presented elsewhere, together with a more rigorous description of the treatment of the variable $|\delta x/\delta t|$.

Important questions are raised by the apparent success of our test function:

i) how generally applicable is this function?
ii) is the function predictive or responsive to other (possibly hidden) variables?
iii) can the function be used to explain the appearance of excess power in some experiments and its non-appearance in others.
iv) can the function variables be used to induce controllable excess power?
v) what can this function teach us about the phenomenon under test?

On the question of general applicability, we are limited in our choice of comparative experiments. It would be desirable to select reference experiments having the same cathode geometry and dimension as the M4 cathode. Very few of our experiments have been performed with 1 mm wires, and none, previously, with the "lasso" geometry employed in M4. In practice, we are more constrained in our choice by the need for high data quality in resistance measurements, so that random measurement errors are not introduced into the values of $\delta x/\delta t$. Simply because the signal-to-noise ratio for 1 mm wires is better than the 3 or 4 mm diameter wires more typically (and successfully) employed, we are reduced in our selection of comparative experiments to one only: C1.

Experiment C1 has been described previously.[4] Figure 3a presents the loading and current density data for the first current ramp of C1. As for M4, the loading inferred from the measured resistance initially shows little perturbation, first decreasing with time at low current density, then increasing with the current ramp. Some time after initiation of the current ramp, an oscillation appears in x, which builds in amplitude. Figure 3b

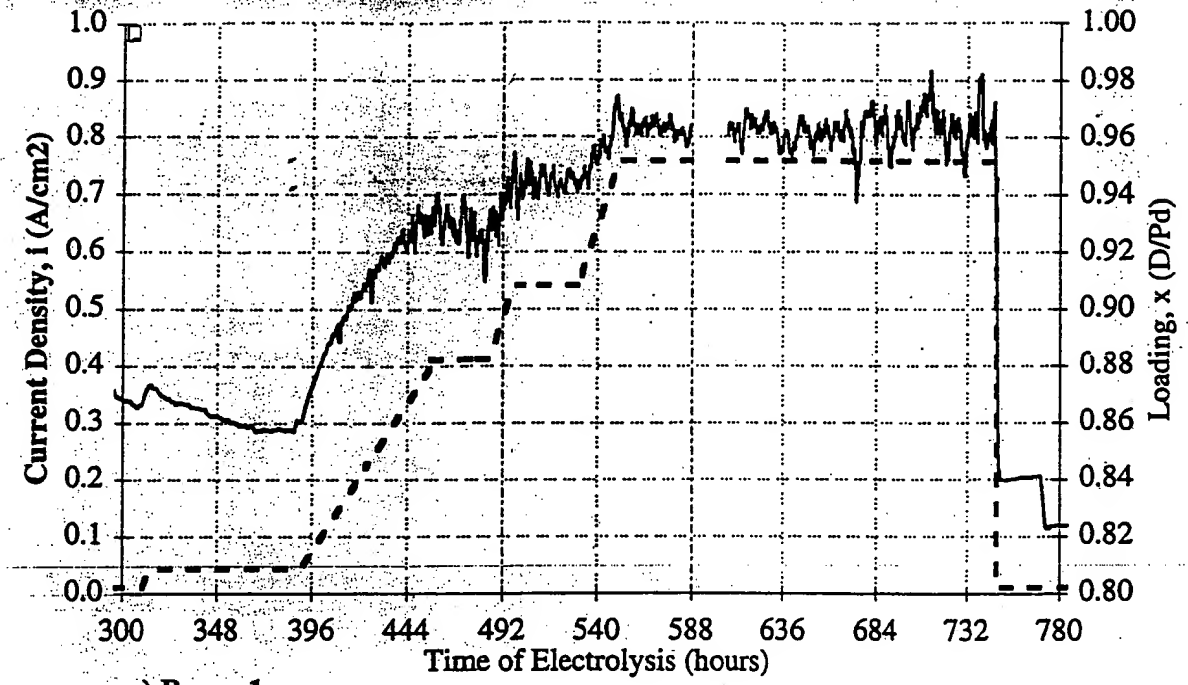

a) Ramp 1

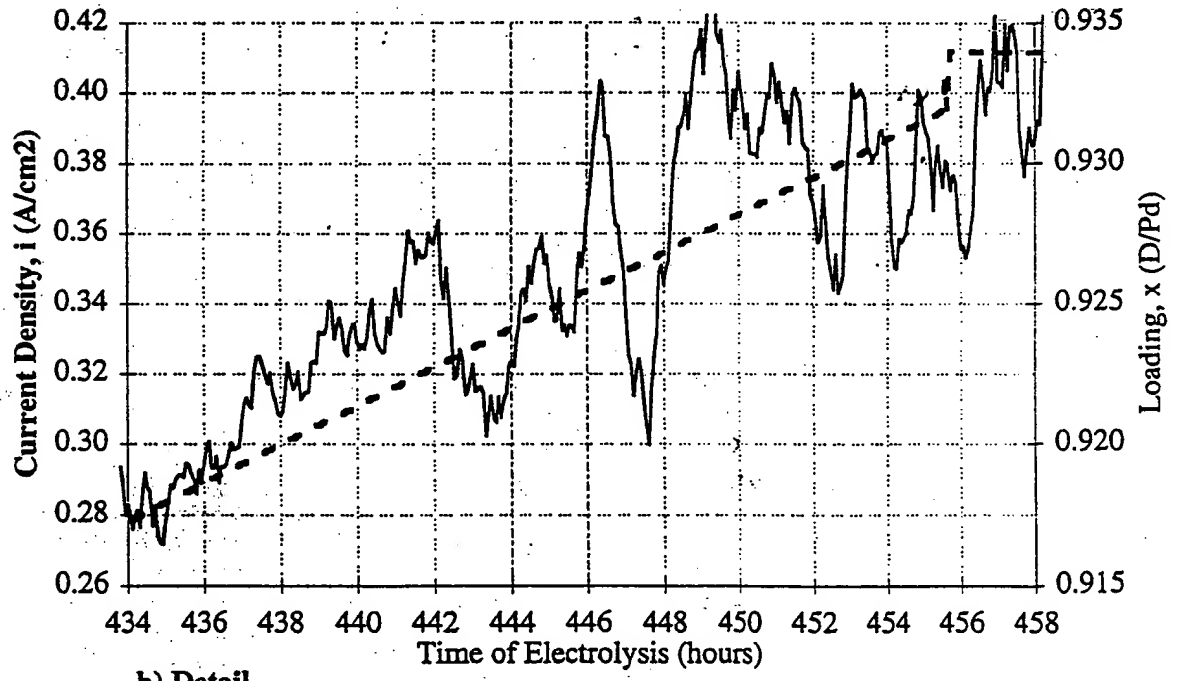

b) Detail

Figure 3 C1 Current Density (A/cm2) & Loading (D/Pd)

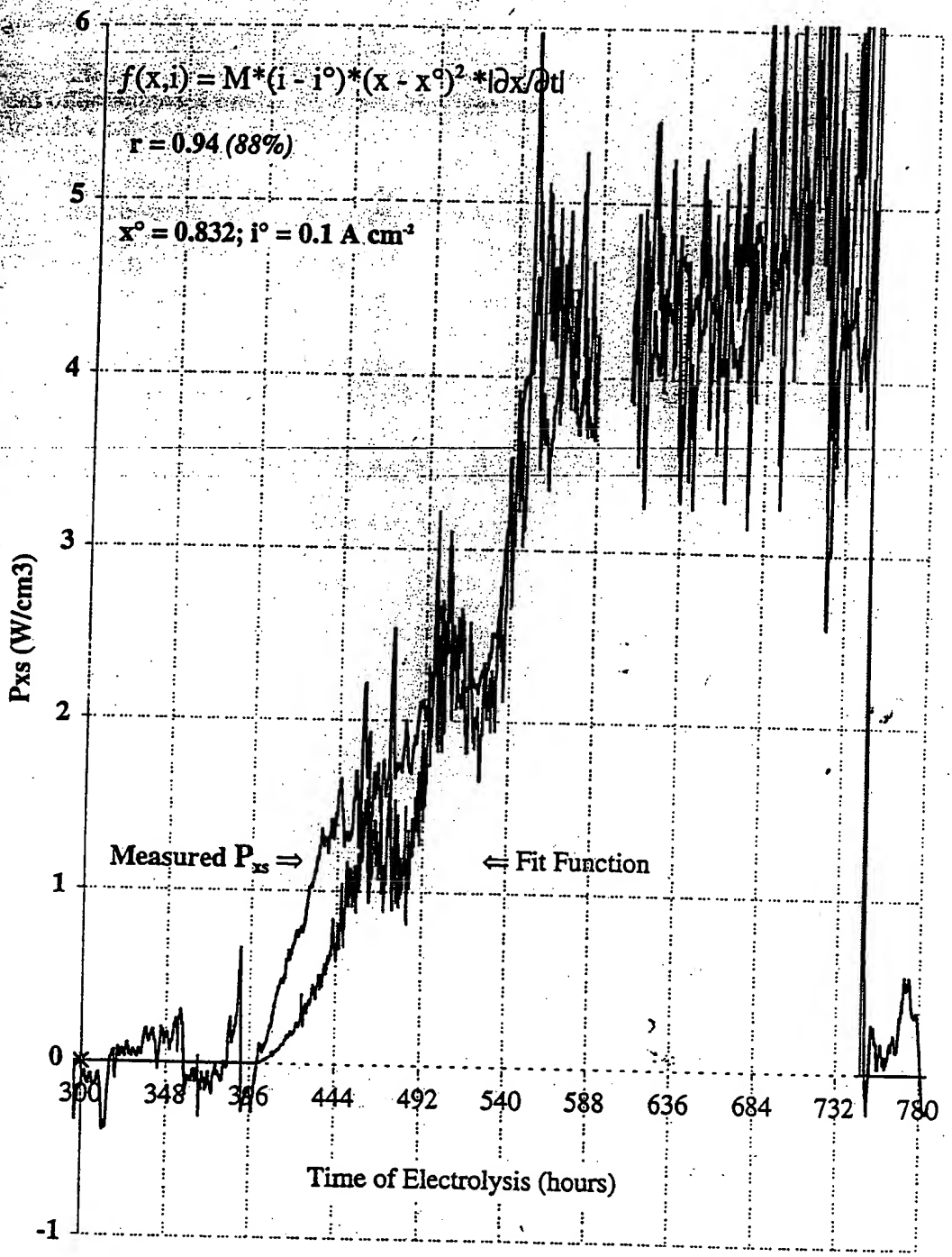

Figure 4 C1 Excess Power and Fit Function

shows a 24 hour detail in the vicinity of 444 h. While generally increasing with increasing current density, before 442 h the loading shows small fluctuation. After ~ 442h the loading exhibits a superimposed somewhat sinusoidal oscillation of period ~2h, as seen for M4. Perhaps significantly, the rate of increase in loading with increasing current density decreases at this point, suggesting the initiation of a transient de-loading (desorption) process, superimposed on the steady state loading.

Figure 4 shows the excess power measured during C1; ramp 1, compared to the test function employed previously for the M4 data (Figure 2). In this case, the value of x° was chosen to be the same as previously used for the M4 data (0.832); this value is also consistent with the number found by direct regression of P_{xs} vs. $(x - x^\circ)^2$. The maximum correlation is, however, found with a significantly lower current density threshold for C1 (0.1 A cm^{-2}) than for M4 (0.4 A cm^{-2}). For the two data sets shown in Figure 4, the correlation coefficient $r = 0.94$, with $x^\circ = 0.832$ and $i^\circ = 0.100$ A cm^{-2}. This correlation suggests that 88% of the function $P_{xs.test}(t)$ is reflected linearly in $P_{xs}(t)$.

7. Discussions and Conclusions

We have demonstrated a mathematical correlation between excess power and the product of three variables: the excess current density, $(i-i^\circ)$; the excess loading, squared, $(x-x^\circ)^2$; the rate of change of the Pd cathode resistance. While we have demonstrated this correlation only for two experiments, M4 and C1, we have no reason to suppose that this correlation is not general. In one of two possible interpretations we have associated the rate of change of resistance with the rate of change of cathode deuterium loading, $\delta x/\delta t$, at constant temperature.

In terms of the "excess" parameters, there is little difference in the maximum value, $(i_{max} - i^\circ)$ between experiments M4 and C1. Although the threshold value for M4 is much higher, the current density obtained in experiment M4; ramp 3, also was higher, and the exponent of 1 makes this not a strong variable. A significant difference does exist in the maximum "excess loading" variable, $(x_{max} - x^\circ)^2$. Due to the higher loading attained, this variable for C1 exceeded that for M4 by nearly an order of magnitude.

This latter observation is exceedingly important. Assuming that we can, as seems reasonable, use our test function as a predictor or, at least diagnostic for P_{xs}, then we need to pay close attention to the variables which give rise to large increases in the magnitude of the test function. An order of magnitude is the difference between indiscernible levels of excess power (~ 50 mW), and an interesting effect. This focuses attention on the need to obtain loadings as high as possible, above the threshold, as the parabolic dependence has greater power in amplifying the effect.

In the M4 and C1 experiments, the observed excess power densities and excess current densities were very similar. In order to achieve this result in terms of our multiplicative test function, the order of magnitude lower excess loading in M4 must be compensated for by a similar increase in the flux variable, $\delta x/\delta t$. In terms of hypothesis (ii), therefore, it is only the adventitious presence of a large deuteron flux that has promoted the excess power in experiment M4 from an insubstantial level at the low maximum loading achieved, to significant levels.

It is important to recognize that in neither experiment, M4 or C1, was an attempt made to maximize $\delta x/\delta t$. Quite the contrary. Both experiments were operated at constant (or slowly changing) currents, temperatures, and gas pressures; the three variables most

likely to influence loading. What fluctuation in loading did occur, and in both cases it was significant and varied, occurred apparently spontaneously; we observed the effect, we did not control it.

Nevertheless, if our hypothesis is correct, it may prove advantageous to understand the role of deuteron flux, and the means by which this can be stimulated without net de-loading, as a means to understand the phenomenon of excess power generation.

To this point we have treated the data statistically, and empirically. The functionality of our excess power test function can, however, be discussed in terms of at least one of the theories proposed for "cold fusion" phenomena. Hagelstein[13] has proposed that a phonon laser operates to initiate solid state neutron transfer, and to couple the nuclear energy produced, to the lattice, as heat. The details of this model are presented in Reference 13, and in preceding papers cited therein. This model makes two predictions that are relevant in the discussion:

i) No excess power will be observed at deuterium loadings below that at which the partial molar enthalpy change for desorption becomes exothermic.

ii) The rate of excess heat release (excess power) will increase with the desorption flux.

The first (threshold) criterion establishes the point at which a phonon laser may begin to operate. In an accompanying paper[14] we have attempted to define the position of this loading threshold based on literature data for the Pd-D system. By extrapolating the literature data at lower loadings, we estimate that the threshold value for the exothermic desorption of deuterium from palladium to be $0.83 \leq x^{\circ} \leq 0.85$. A value closely in accord with our observed value of $x^{\circ} \approx 0.832$.

The second (flux) criterion is associated with the rate of phonon excitation. This flux can be measured as the rate of change of the average loading; in the Hagelstein model only the desorption flux plays a role. In our empirical function we have employed $|\delta x/\delta t|$. For a symmetric loading/de-loading cycle (*i.e.* no dc term) the average value of $|\delta x/\delta t|$ is simply twice the average value of the desorption component alone, so that our observed correlation would be unchanged, and consistent with the Hagelstein model prediction.

A great deal more needs to be said about our results, the correlation analysis, and the relationship of these to the Hagelstein model predictions. We need to consider the time-scales of the various processes, the relationship of the observed transient net flux to the atomic scale process of a heterogeneous surface, and any possible role that a steady state flux may play. A related topic of importance is the relationship between the endothermic/exothermic transition surveyed by Crouch-Baker[14] to the phonon laser threshold predicted by Hagelstein[13], particularly as these affect the onset of thermal positive feedback, observed calorimetrically by Pons and Fleischmann.[15]

Despite our incomplete understanding, we are encouraged to see, perhaps for the first time in this field, the suggestion of a synthesis and consensus of theory and experiment.

Acknowledgments

The financial support provided by the Institute of Applied Energy and the New Energy and Industrial Technology Development Organization (Japan) and the Electric Power Research Institute (U.S.A.) is gratefully acknowledged.

References

1. M. Fleischmann, S. Pons and M. Hawkins, "Electrochemically Induced Nuclear Fusion of Deuterium", *J. Electroanalytical Chem*, **261** p. 301-308, (1989).

2. M. McKubre, R. Rocha-Filho, S. Smedley, F. Tanzella, J. Chao, B. Chexal, T. Passell, and J. Santucci "Calorimetry and Electrochemistry in the D/Pd System" in *Proceedings of the First Annual Conference on Cold Fusion*, National Cold Fusion Institute, Salt Lake City, UT, 1990, p. 20.

3. M. McKubre, R. Rocha-Filho, S. Smedley, F. Tanzella, S. Crouch-Baker, T. Passell, and J. Santucci "Isothermal Flow Calorimetric Investigations of the D/Pd System" in *The Science of Cold Fusion*,, Eds. T. Bressani, E. Del Giudice, and G. Preparata, Conference Proceedings Vol. 33, Italian Physical Society, Bologna, 1992, p. 419

4. M. McKubre, S. Crouch-Baker, A. Riley, S. Smedley and F. Tanzella "Excess Power Observations in Electrochemical Studies of the D/Pd System: Proceedings of 3rd International Conference on Cold Fusion, *"Frontiers of Cold Fusion"*, ed. H. Ikegami, Universal Academy Press, Inc., Tokyo p. 139 (1993).

5. M. McKubre, S. Crouch-Baker, S. Smedley and F. Tanzella, "An Overview of Calorimetric Studies on the D/Pd System, at SRI; May 1989 to October 1993. Proceedings of the Russian Conference on Cold Fusion (RCCF), Abrau Durso, September 1993.

6. M. McKubre, S. Crouch-Baker, A. Hauser, N. Jevtic, S. Smedley, M. Srinivasan, T. Passell and F. Tanzella, "Loading, Calorimetric and Nuclear Investigation of the D/Pd System", Presented at the Fourth International Conference on Cold Fusion, Maui Hawaii (1993).

7. M. McKubre, S. Crouch-Baker, R. Rocha-Filho, S. Smedley, F. Tanzella, T. Passell, and J. Santucci "Isothermal Flow Calorimetric Investigations of the D/Pd System" *J. Electroanalytical. Chem.*, **368** (1994) p. 55

8. K. Kunimatsu, "Deuterium Loading Ratio and Excess Heat Generation", Proceedings of 3rd International Conference on Cold Fusion, *"Frontiers of Cold Fusion"*, ed. H. Ikegami, Universal Academy Press, Inc., Tokyo p. 139 (1993).

9. N. Hasegawa and N. Hayakawa, "Observation of Excess Heat During Electrolysis of 1M LiOD in a Fuel Cell Type Closed Cell", Proceedings of the 4th International Conference on Cold Fusion, Maui Hawaii (1993).

10. D. Macdonald, M. McKubre, A. Scott and P. Wentrcek, "Continuous *In-Situ* Method for the Measurement of Dissolved Hydrogen in High Temperature Aqueous Systems", I&EC Fundamentals **20**, p. 290, (1981).

11. M. McKubre, S. Crouch-Baker, A. Hauser, N. Jevtic, S. I. Smedley, F. L. Tanzella, M. Williams, S. Wing, "Development of Energy Production Systems from Heat Produced in Deuterated Metals", Final Report on EPRI Contract 3170-23, (1995).

12. M. McKubre, S. Crouch-Baker, S. Smedley, F. Tanzella, M. Maly-Schreiber, R. Rocha-Filho, P. Searson, J. Pronko and D. Kohler, "Development of Advanced Concepts for Nuclear Processes in Deuterated Metals", Final Report on EPRI Contract 3170-01, (1994).

13. P. Hagelstein, "An Update on Neutron Transfer Reactions", Proceedings of the Fifth International Conference on Cold Fusion, Monte Carlo (1995).

14. S. Crouch-Baker, M. McKubre, and F. Tanzella, "Some Thermodynamic Properties of the H(D)-Pd System", Proceedings of the Fifth International Conference on Cold Fusion, Monte Carlo (1995).

15. S. Pons and M. Fleischmann, "More About Positive Feedback, More About Boiling", Proceedings of the Fifth International Conference on Cold Fusion, Monte Carlo (1995).